Structural Optimisation of Multi-storey Buildings

A thesis submitted in fulfilment of the requirements for the degree of

Doctor of Philosophy

Harshavardhan V. Ranade

Bachelor of Engineering (Civil), Master of Information Technology

School of Civil, Environmental and Chemical Engineering

Science, Engineering and Technology Portfolio

RMIT University

November 2006

DECLARATION

I certify that except where due acknowledgement has been made, the work is that of the author alone; the work has not been submitted previously, in whole or in part, to qualify for any other academic award; the content of the thesis is the result of work which has been carried out since the official commencement date of the approved research program; and, any editorial work, paid or unpaid, carried out by a third party is acknowledged.

Harshavardhan V. Ranade

Date: 8 Nov 2006

ACKNOWLEDGEMENTS

I would like to thank Prof. Yi Min (Mike) Xie for... everything. He has been a constant source of encouragement and inspiration throughout the duration of this research work. An extremely good teacher, his discussions and suggestions are always sincerely appreciated. I have learnt a lot just by observing Mike and feel privileged to have been associated with him over the past three years. This thesis would not have been possible without his valuable guidance.

This project was funded by the Australian Research Council (ARC) under the ARC Linkage scheme with Felicetti Pty. Ltd as the industry based partner. I was supported by an Australian Postgraduate Award - Industry (APA-I). This financial support is gratefully acknowledged.

I would also like to thank Mr. Peter Felicetti, Director, Felicetti. Pty. Ltd. for providing guidance on the practical and technical aspects of this project. His suggestions, discussions, advice, and time are sincerely appreciated. The enthusiasm he has shown for this research work right from the beginning and throughout the duration of this project is gratefully acknowledged. I will be joining Felicetti Pty. Ltd. as a Research Engineer on completion of this thesis, and I appreciate the opportunity to apply the techniques I have developed in this thesis to several commercial projects of real buildings currently being designed by Felicetti Pty. Ltd.

Thank you to my family, first and foremost my parents for.....everything.....that words just can't describe. Thank you for the emotional support, initially and later, as always encouraging me to study further as much as I could. You are my strength and I sorely missed your presence in these three years. I would also like to thank my elder brother, Yogesh V. Ranade and his wife, for their enthusiasm, advice and constant support. In spite of your busy schedule, thank you for always being available bro. Your advice always kept my motivation levels up and helped me focus on my work. Thank you to my wife, Supriya Ranade, for her moral support and encouragement. Coming home late from the university almost every night was always met with a smile. Thank your for always being there. I would also like to express my gratitude to my uncles Dr. A.C. Ranade and Dr. A.P. Kulkarni for inspiring me to study towards a PhD in the first place.

Finally, thank you to all the staff in the School of Civil, Environmental and Chemical Engineering at RMIT University, and the post-graduate students for their kind assistance. I thank Dr. Abbas Mohajerani and Dr. Indubhushan Patnaikuni for their encouragement. Thank you RMIT University for giving me the opportunity to study for a PhD.

Last but not the least, I would also like to thank my few friends here in Melbourne for their company and being good mates.

Harshavardhan V. Ranade
November 2006, Melbourne

CONTENTS

	Page
Title	i
Declaration	ii
Acknowledgements	iii
Contents	v
List of Figures	xvi
List of Tables	xxvii
Summary	xxix
Chapter 1 Introduction	1-1
1.1 Introduction to Structural Optimisation	1-1
1.2 Aims and Scope of This Research Work	1-4
1.3 Layout of This Thesis	1-6
Chapter 2 Literature Review	2-1
2.1 Introduction	2-1
2.2 Main Approaches to Structural Optimisation	2-1
2.2.1 Mathematical Programming Methods	
2.2.2 Optimality Criteria Methods	
2.3 Evolutionary Structural Optimisation (ESO) Method	2-3
2.4 Structural Optimisation of Multi-storey buildings	2-5
2.4.1 Topology and Shape Optimisation of Frames	2-5
2.4.2 Discrete Variable Structural Optimisation	2-7
2.4.2.1 Linked Discrete Variables	2-8
2.4.2.2 Single Variable Approaches with Approximations	2-9
2.4.2.3 Single Variable Approaches without Approximations	2-11
2.4.2.4 Mixed Single and Multiple Variable Approaches	2-12
2.4.2.5 Rounding-Off Methods	2-12

2.4.3 Conceptual Design Optimisation of Engineering Structures 2-13

2.4.4 Recent Advances in Optimal Structural Design of Multi-storey Buildings 2-16

2.5 Comments on Current Research and Applications 2-19

Chapter 3 Thickness Optimisation of Structural Walls in Multi-storey Buildings 3-1

3.1 Introduction 3-1

3.2 Structural Wall Systems 3-1

3.3 Scope of the Work in This Chapter 3-2

3.4 Assumptions and Limitations of the Work in This Chapter 3-3

3.5 Optimisation Problem Formulation 3-4

3.6 Proposed element sizing criteria 3-4
3.6.1 Element-wise Optimisation 3-5
3.6.2 Sizing Algorithms 3-6
3.6.3 Panel-wise Optimisation 3-8
3.6.4 Comments on the Proposed Approach for Sizing Elements/Groups 3-11

3.7 Comparison of Algorithms 3-14
3.7.1 Finite Element Model for Comparison Purposes 3-15
3.7.2 Panel-wise Optimisation 3-15
3.7.2.1 Panel-wise Optimisation Using Forced Zones Algorithm 3-17
3.7.2.2 Panel-wise Optimisation Using 'Ratios' Algorithm 3-18
3.7.2.3 Discussion of Results 3-19
3.7.3 Element-wise Optimisation 3-20

3.7.3.1 Element-wise Optimisation Using Forced Zones Algorithm 3-20
3.7.3.2 Element-wise Optimisation Using 'Ratios' Algorithm 3-21
3.7.3.3 Discussion of Results 3-22

3.8 Examples 3-22
3.8.1 Example 1 - Wall A – Panel-wise Optimisation 3-22
3.8.2 Example 2 – Wall D – Panel-wise Optimisation 3-25
3.8.3 Example 3 - Wall A – Element-wise Optimisation 3-28
3.8.4 Example 4 - Wall D – Element-wise Optimisation 3-30
3.8.5 Comparison of Results for Wall A and Wall D Using Both Methods 3-34
3.8.6 Ten Storey 3D Structure (Panel-wise Optimisation Using "Ratios" Algorithm) 3-35
3.8.7 Ten Storey 3D Structure (Element-wise Optimisation Using "Ratios" Algorithm) 3-41

3.9 Examples of Structural Walls in Multi-storey Buildings 3-47
3.9.1 "Shear Wall – Slab" Type Structural System (Thickness Optimisation of Shear Walls and Internal Core) 3-47
3.9.2 Thickness Optimisation of Core Walls for a 40 Storey Symmetric "Tube-In-Tube" (Hull-Core) Structural System 3-55

3.10 Conclusions 3-61

Chapter 4 Layout Design for Infill Walls and Bracing Systems in Multi-storey Buildings

4.1 Introduction 4-1

4.2 Assumptions and Limitations of the Work of this Chapter 4-1

4.3 Optimisation Problem Formulation 4-2

4.4 Proposed Element Sizing and Removal criteria 4-2

4.5 Examples 4-6
4.5.1 Requirement for Infill Walls in a "Shear Wall – Slab" Type Structural System 4-6
4.5.2 Conceptual design of Bracing Systems 4-12
4.5.2.1 Introduction 4-12
4.5.2.2 Continuum Design Domain with a Single Lateral Load at the Top 4-12
4.5.2.3 Optimal Bracing Pattern for a Multi-storey Building 4-15

4.6 Discussions and Conclusion 4-21

Chapter 5: Review of Conventional Reinforced Concrete Flat Slab Design

5.1 Introduction 5-1

5.2 Flat Slab Systems 5-1

5.2.1 Literature Review of Finite Element Application to Reinforced Concrete Slab Design 5-2
5.2.1.1 Design based on Linear Finite Element Analysis 5-4
5.2.1.2 Design based on Non-linear Finite Element Analysis 5-7
5.2.1.3 Further comments 5-9

5.3 Limitations of Finite Element Analysis 5-9

5.4 General AS 3600 Requirements for Reinforced Concrete Design 5-11
5.4.1 Analysis Requirements 5-12
5.4.2 Flexural Strength Requirements 5-13
5.4.3 Ultimate Flexural Capacity 5-14
5.4.4 Minimum Flexural Reinforcement 5-18
5.4.5 Shear Strength Requirements 5-19
5.4.5.1 Punching Shear with No Moment Transfer 5-21
5.4.5.2 Moment Transfer Shear 5-22

5.4.7 Serviceability Requirements 5-26

5.4.8 Detailing of Reinforcement 5-27

5.5 The Simplified Method of Slab Design 5-27

5.6 The Idealised Frame Method 5-30

5.7 Yield Line Method 5-33

5.8 Strip Design Technique 5-36

Chapter 6 Flat Slab Modelling Issues

6.1 Introduction 6-1

6.1.1 General Modelling Requirements 6-1

6.1.2 Assumptions in Reinforced Concrete Flat Slab FEA 6-2

6.1.3 Modelling of Boundary Conditions for Flat Slab Systems 6-4

6.2 Conventional Techniques for Flat Slab Design using FEA Results 6-10

6.2.1 Design Using Average Stress Resultants 6-10

6.2.1.1 Computation of Element Stress Resultants

6.2.2 Design Procedure Using Bending Moment Resultants 6-12

6.2.2.1 Nodal Integration of Moments in SAFE

6.2.2.2 Wood-Armer Integration Scheme

6.2.2.3 Bending Moment Integration in SLABS (Inducta Engineering)

6.2.2.4 Moments Calculated in SAP2000

6.2.3 Design Using Element Forces 6-14

6.2.3.1 Computation of Element Forces

6.2.3.2 Computation of Resultant Design Moment Using Element Forces

6.2.4 Approach Adopted in This Study 6-15

6.3 Slab-to-Column Connection Issues 6-16
6.3.1 Effects of Inaccurate Modelling of Slab-to-Column Connections 6-16
6.3.2 Plate Constraint in SAP2000 6-19

6.4 Concluding Remarks 6-19

Chapter 7: Optimal Conceptual Design of Slabs for Flexure 7-1

7.1 Introduction 7-1

7.2 Scope of the Work in This Chapter 7-1
7.2.1 Significance of This Research 7-2
7.2.2 Assumptions and Limitations of This Work 7-3

7.3 Optimisation Problem Formulation 7-3

7.4 Element Sizing Criteria 7-4

7.5 Development of Conceptual Design Techniques and the Corresponding Computer Programs 7-5
7.5.1 Implementation 7-6
7.5.2 Algorithm 7-13
7.5.3 Validation of Design Data Input by the User 7-17

7.6 Simple Examples 7-19
7.6.1 Seeking Optimal Depths in a Single Span One-way slab 7-19
7.6.2 Effect of Load on Convergence 7-21
7.6.3 Effect of Steel Quantity on Results 7-26
7.6.4 Effect of a Further Increased Load on Results 7-28
7.6.5 Comparison of Examples 7-31

7.6.6 Continuous One-way Slab - Design using Technique 1 7-32
7.6.7 Continuous One-Way Slab – Design Using Technique 2 7-34
7.6.7.1 Case A: Less Steel 7-34

7.6.7.2 Case B: More Steel 7-37
7.6.8 Continuous One-Way Slab – Design Using Technique 3 7-41

7.7 Flat Slabs 7-45
7.7.1 Need for Integrating Element Level ESO Optimisation and Group ESO Optimisation 7-45
7.7.1.1 A Typical Flat Slab Model 7-45
7.7.1.2 Effect of Column Size (i.e. Mesh Size) and Steel Quantity on Results 7-51
A. Smaller Column Size (Finer Mesh) 7-51
B. Bigger Column Size (Coarse Mesh) 7-55
7.7.1.3 Proposed Approach to Modelling Flat Slabs in SAP2000. 7-57

7.7.2 Numerical Studies 7-58
7.7.2.1 Symmetrical and Asymmetrical Results 7-58
7.7.2.2 Oscillating Solutions due to Different Effective Depths 7-69
7.7.2.3 Moment Difference Approach 7-73
7.7.2.4 Moment Relaxation 7-77
7.7.2.4.1 Design Using Technique 1 7-78
7.7.2.4.2 Design Using Technique 2 7-80
7.7.2.4.3 Design Using Technique 2 – More Steel Quantity 7-83
7.7.2.4.4 "Average" of Smoothed Maximum Nodal Moment Values 7-87

7.7.3 Example of a Symmetrical Flat Slab with UDL Using All Three Techniques 7-88
7.7.3.1 Technique 1 7-89
7.7.3.2 Technique 1 (Min-Max Steel) 7-90
7.7.3.3 Technique 2 7-91
7.7.3.4 Technique 3: Comparison With and Without Economy 7-95

7.8 Case Studies 7-102
7.8.1 Industry Partner's 8.4m x 8.4m Model 7-102
7.8.1.1 Ends Fixed – Technique 3 7-102

7.8.1.2 Ends Free – Technique 3 7-105
7.8.1.3 Comparison with Industry Partner's Final Design based on Conventional Approach 7-110
7.8.2 Q2 Project with Drop Panels 7-115
7.8.2.1 Technique 1 7-116
7.8.2.2 Technique 2 7-118
7.8.2.3 Technique 3 7-121
7.8.2.4 Comparison with Industry Partner's Final Design based on Conventional Approach 7-124
7.8.3 Q2 Project with Band Beams 7-127
7.8.3.1 Design using Technique 3 7-127
7.8.3.2 Comparison with Industry Partner's Final Design 7-128
7.8.4 Q2 Project with Band Beams – Different Initial Model 7-131
7.8.4.1 Design using Technique 3 7-131
7.8.5 Q2 Project with Atrium 7-134
7.8.5.1 Design using Technique 1 7-134
7.8.5.2 Design using Technique 2 7-137
7.8.5.3 Design using Technique 3 7-140
7.8.6 SAFE Example 7-143
7.8.6.1 Design using Technique 3 7-145
7.8.6.2 Comparison with SAFE Design 7-149

7.9 Concluding Remarks 7-154

Chapter 8: Optimal Conceptual Design of Slabs for Flexure, Punching Shear and Transverse Shear 8-1

8.1 Introduction 8-1

8.2 Scope of the Work in This Chapter 8-2

8.3 Optimisation Problem Formulation 8-2

8.4 Element Sizing Criteria 8-3

8.5 Optimisation Procedure 8-5

8.5.1 Algorithm 8-5
8.5.2 Punching Shear Design 8-7
8.5.2.1 Labelling Schema 8-10
8.5.3 Normal Beam Shear/Transverse Shear 8-12
8.5.4 Shell Element in SAP2000 8-13
8.5.5 Flowchart for Flexural and Shear Design Optimisation of Flat Slabs 8-18

8.6 Examples 8-19
8.6.1 Comparison between Bending Moment and Shear plus Bending Moment as Constraints 8-19
8.6.2 Calculation of Moment Difference between Column Faces for Punching Shear 8-21
8.6.2.1 Design using Technique 1
8.6.2.2 Design using Technique 2
8.6.2.3 Design using Technique 3
8.6.2.4 Recommendation 8-25
8.6.3 Transverse Shear Performance 8-26
8.6.3.1 Comparison of Designs With and Without Transverse Shear Constraint
8.6.3.2 Design Using Technique 3
8.6.4 Industry Partner's 8.4m x 8.4m model - Design using Technique 3 8-31

8.7 Concluding Remarks 8-33

Chapter 9: Conclusions and (Recommendations for) Further Work

9.1 Conclusions 9-1
9.2 Further Work 9-4

Appendix A

Appendix B

References

LIST OF FIGURES

Chapter 1

Fig. 1.1. Choice of design window and "optimal design"

Chapter 3

Fig. 3.1. Finite Element Model for Comparison Purposes

Fig. 3.2. 1st Iteration of Panel-wise Optimisation Using Forced Zones Algorithm

Fig. 3.3. Panel Thicknesses Assigned to All Four Walls after 1st Iteration

Fig. 3.4. 1st Iteration of Panel-wise Optimisation Using Ratios Algorithm

Fig. 3.5. Panel Thicknesses Assigned to All Four Walls after 1st Iteration

Fig. 3.6. 1st Iteration of Element-wise Optimisation Using Forced Zones Algorithm

Fig. 3.7. Thicknesses Assigned to Elements on All Four Walls after 1st Iteration

Fig. 3.8: 1st Iteration of Element-wise Optimisation Using Ratios Algorithm

Fig. 3.9. Thicknesses Assigned to Elements on All Four Walls after 1st Iteration

Fig. 3.10. Initial FE Model of Planar Wall Loaded In-plane for Panel-wise Optimisation

Fig. 3.11. Design Solutions for Wall Loaded In-plane using Panel-wise Optimisation

Fig. 3.12. Top Deflection History of Wall Loaded In-plane using Panel-wise Optimisation

Fig. 3.13. History of Weight Reduction for Wall Loaded In-plane using Panel-wise Optimisation

Fig. 3.14. Initial FE Model of Planar Wall Loaded Out-of-plane for Panel-wise Optimisation

Fig. 3.15. Design Solutions for Wall Loaded Out-of-plane-plane using Panel-wise Optimisation

Fig. 3.16. Top Deflection History of Wall Loaded Out-of-plane using Panel-wise Optimisation

Fig. 3.17. History of Weight Reduction for Wall Loaded Out-of-plane using Panel-wise Optimisation

Fig. 3.18. Initial FE Model of Planar Wall Loaded In-plane for Element-wise Optimisation

Fig. 3.19. Design Solutions for Wall Loaded In-plane-plane using Element-wise Optimisation

Fig. 3.20. Top Deflection History of Wall Loaded In-plane using Element-wise Optimisation

Fig. 3.21. History of Weight Reduction for Wall Loaded In-plane using Element-wise Optimisation

Fig. 3.22. Initial FE Model of Planar Wall Loaded Out-of-plane for Element-wise Optimisation

Fig. 3.23. Design Solutions for Wall Loaded Out-of-plane-plane using Element-wise Optimisation
Fig. 3.24. Top Deflection History of Wall Loaded Out-of-plane using Element-wise Optimisation
Fig. 3.25. History of Weight Reduction for Wall Loaded Out-of-plane using Element-wise Optimisation

Fig. 3.26. Initial FE Model of 10-Storey 3D Structure
Fig. 3.27. Design Solutions for 10-Storey 3D Structure using Panel-wise Optimisation
Fig. 3.28. Top Deflection History of 10-Storey 3D Structure using Panel-wise Optimisation
Fig. 3.29. History of Weight Reduction for 10-Storey 3D Structure using Panel-wise Optimisation
Fig.3.30. Panel Wise Optimal Solution for *building model*
Fig. 3.31 Panel Wise Optimal solution for *Planar Wall* (Wall A)

Fig. 3.32. Initial FE Model of 10-Storey 3D Structure
Fig. 3.33. Design Solutions for 10-Storey 3D Structure using Element-wise Optimisation
Fig. 3.34. Top Deflection History of 10-Storey 3D Structure using Element-wise Optimisation
Fig. 3.35. History of Weight Reduction for 10-Storey 3D Structure using Element-wise Optimisation
Fig.3.36. Panel Wise Optimal Solution for *building model*
Fig.3.37. Element Wise Optimal Solution for *building model* (single element lying in the region of the middle panel of Wall A at the bottom storey)

Fig 3.38. Element Wise optimal solution for *Planar Wall* A.
Fig 3.39. Panel Wise optimal solution for *Planar Wall* A

Fig. 3.40. Initial FE Model and Plan of *Shear Wall – Slab* type structural system
Fig. 3.41. Behaviour of laterally loaded coupled shear walls
Fig. 3.42. Design Solutions for Core Wall Loaded In-plane
Fig. 3.43. Design Solutions for Core Wall Loaded In-plane
Fig. 3.44. Design Solutions for Core Wall Loaded Out-of-plane
Fig. 3.45. Design Solutions for Core Wall Loaded Out-of-plane
Fig. 3.46. Design Solutions for Side Shear Walls Loaded In-plane
Fig. 3.47. Design Solutions for Side Shear Walls Loaded In-plane
Fig. 3.48. Design Solutions for Side Shear Walls Loaded Out-of-plane
Fig. 3.49. Design Solutions for Side Shear Walls Loaded Out-of-plane

Fig. 3.50. Top Deflection History of *Shear Wall – Slab* type structure using Element-wise Optimisation
Fig. 3.51. History of Weight Reduction for *Shear Wall – Slab* type structure using Element-wise Optimisation

Fig. 3.52. Initial FE Model and Plan of 40-Storey Symmetric Tube-In-Tube (Hull-Core) Structural System
Fig. 3.53. Shear wall – frame interaction
Fig. 3.54. Design Solutions for Wall Loaded In-plane
Fig. 3.55. Design Solutions for Wall Loaded In-plane
Fig. 3.56. Design Solutions for Wall Loaded Out-of-plane
Fig. 3.57. Design Solutions for Wall Loaded Out-of-plane
Fig. 3.58. Top Deflection History of *40-Storey Hull-Core Structural System* using Element-wise Optimisation
Fig. 3.59. History of Weight Reduction for *40-Storey Hull-Core Structural System* using Element-wise Optimisation

Chapter 4

Fig. 4.1. Physical Behaviour of Infill Walls
Fig. 4.2. Interactive Behaviour of Frame and Infills
Fig. 4.3. Modes of Infill Failure and Frame Failure
Fig. 4.4. Initial FE Model of Infill Walls in a *Shear Wall – Slab* Type Structural System
Fig. 4.5. ESO Optimisation Parameters for element removal
Fig. 4.6. Design Solutions for Infill Wall Loaded In-plane
Fig. 4.7. Design Solutions for Infill Wall Loaded Out-of-plane
Fig. 4.8. Optimal Design Solution for Infill Wall in a Shear Wall – Slab Type Structure subjected to a Single Lateral Load Case

Fig. 4.9. Initial FE Model of 2D Continuum Design Domain
Fig. 4.10. ESO Optimisation Parameters
Fig. 4.11. Topology History of Material Layout and Thickness for a Single Horizontal Load at the Top Left Corner
Fig. 4.12. History of Weight Reduction for the 2D Continuum example
Fig. 4.13. Top Deflection History of the 2D Continuum Example

Fig. 4.14. Initial FE Model for seeking Optimal Bracing Pattern: 3D and Planar View

Fig. 4.15. ESO Optimisation Parameters

Fig. 4.16. Topology History of Evolving Bracing Pattern to resist In-plane Horizontal Loading

Fig. 4.17. Topology History of Continuum Loaded Out-of-plane

Fig. 4.18. 3D View of Optimal Topology of Bracing Pattern

Fig. 4.19. Enlarged View of Optimal Topology of Bracing Pattern

Fig. 4.20. History of Weight Reduction

Fig. 4.21. Top Deflection History

Chapter 5

Fig 5.1. A typical flat slab structure

Fig. 5.2. Cracked Section Behaviour

Fig 5.3. Compressive stresses at failure

Fig. 5.4 Span Lengths

Fig. 5.5. Widths of strips for two-way slab systems

Fig. 5.6. Slab Beam Layout and Dimensions

Fig. 5.7. Moment Diagrams for Flat Slabs

Fig 5.8. Plane frame analytical model for the equivalent column method

Fig. 5.9. Equivalent column with attached torsional member

Fig. 5.10. Yield line patterns for distributed loads

Fig. 5.11. Example strip design layout

Chapter 6

Fig. 6.1 (a). Frame element is used as a column

Fig. 6.1 (b). Solid Element is used as a column

Fig. 6.2 (a). Columns modelled using Frame Elements – M_{11} distribution near central column (*No Plate Constraint)*

Fig. 6.2 (b). Columns modelled using Solid Elements - M_{11} distribution near central column (*No Plate Constraint*)

Fig. 6.3. Element stress resultants at a node

Fig. 6.4 Element forces at a node. (a) Plate Bending Element (b) Plate Element

Fig.6.5. Element force resultant from nodal forces along a cut.

Fig. 6.6. Design Data for Technique 2.

Fig. 6.7. FEA Results for a Symmetrical Slab

Fig. 6.8. Design Solution at first iteration

Fig. 6.9. Close-up view of depths around a central column

Chapter 7

Fig. 7.1. WinBatch "Message Boxes"
Fig. 7.2. Flowchart Of Control Process During Optimisation
Fig. 7.3. Graphical User Interfaces (GUI) developed in Compaq Visual Fortran: (a) GUI 1
Fig. 7.3. Graphical User Interfaces (GUI) developed in Compaq Visual Fortran: (b) GUI 2
Fig. 7.3. Graphical User Interfaces (GUI) developed in Compaq Visual Fortran: (c) GUI 3
Fig. 7.3. Graphical User Interfaces (GUI) developed in Compaq Visual Fortran: (d) GUI 4
Fig. 7.3. Graphical User Interfaces (GUI) developed in Compaq Visual Fortran: (e) GUI 5
Fig. 7.3. Graphical User Interfaces (GUI) developed in Compaq Visual Fortran: (f) GUI 6
Fig. 7.4. Flowchart for Moment-based Optimisation of Slabs

Fig. 7.5. Design Data for Technique 2.
Fig. 7.6. Design Solutions for One-Way Slab using Technique 2
Fig. 7.7. History of Reduction in Concrete Weight for One-Way Slab using Technique 2 Optimisation

Fig. 7.8. Design Data for Technique 2
Fig. 7.9. Technique 2 Design Solutions for One-Way Slab Subjected to Increased Loading
Fig. 7.10. Convergence Information
Fig. 7.11. History of Reduction in Concrete Weight for One-Way Slab Subjected to Increased Loading using Technique 2 Optimisation

Fig. 7.12. Design Data for Technique 2
Fig. 7.13. Technique 2 Design Solutions for One-Way Slab with More Steel
Fig. 7.14. History of Reduction in Concrete Weight for One-Way Slab with More Steel using Technique 2 Optimisation

Fig. 7.15. Design Data for Technique 2
Fig. 7.16. Technique 2 Design Solutions for One-Way Slab Subjected to Further Increased Loading
Fig. 7.17. History of Reduction in Concrete Weight for One-Way Slab Subjected to Further Increased Loading using Technique 2 Optimisation

Fig. 7.18. Initial Model of Continuous One-Way Slab
Fig. 7.19. Design Data for Technique 1

Fig. 7.20. Technique 1 Design Solution showing Main Steel Layout
Fig. 7.21. Technique 1 Design Solution showing Transverse Steel Layout

Fig. 7.22. Design Data for Technique 2
Fig. 7.23. Technique 2 Design Solutions for Continuous One-Way Slab
Fig. 7.24. Design Data for Technique 2
Fig. 7.25. Technique 2 Design Solutions for Continuous One-Way Slab Using More Steel
Fig. 7.26. Design Data for Technique 3
Fig. 7.27. Technique 3 Design Solutions for Continuous One-Way Slab

Fig. 7.28. Design Data for Technique 2
Fig. 7.29. Initial Model of Flat Slab
Fig. 7.30. Element Level Design Solutions for Flat Slab using Technique 2
Fig. 7.31. Enlarged Views showing Element level Design Solution near Column Supports Using Technique 2

Fig. 7.32. Design Data for Technique 2 with 4-Y16 bars
Fig. 7.33. Design Data for Technique 2 with 5-Y16 bars
Fig. 7.34. Comparison between Element Level Design Solutions for a Finely Meshed Flat Slab Using Technique 2 with Different Quantities of Steel Specified

Fig. 7.35. Design Data for Technique 2 with 4-Y16 bars
Fig. 7.36. Design Data for Technique 2 with 5-Y16 bars
Fig. 7.37. Comparison between Element Level Design Solutions for a Coarsely Meshed Flat Slab Using Technique 2 with Different Quantities of Steel Specified

Fig. 7.38. Effective Depths
Fig. 7.39. Design Data for Technique 2
Fig. 7.40. Initial Model
Fig. 7.41. Technique 2 Design Solutions using Different Effective Depths in both directions

Fig. 7.42. Design Data for Technique 2
Fig. 7.43. Initial Model
Fig. 7.44. Technique 2 Design Solutions using Different Effective Depths in both directions
Fig. 7.45. History of Concrete Weight Reduction

Fig. 7.46. Design Data for Technique 2
Fig. 7.47. Initial Model
Fig. 7.48. Technique 2 Design Solutions using the Average Effective Depth in both directions
Fig. 7.49. History of Concrete Weight Reduction

Fig. 7.50. Design Data for Technique 2
Fig. 7.51. Initial Model
Fig. 7.52. Technique 2 Design Solutions showing Oscillations due to Different Effective Depths in both directions

Fig. 7.53. Design Data for Technique 2
Fig. 7.54. Technique 2 Design Solutions Using the 'Moment Difference' Approach for a Continuous One-way Slab
Fig. 7.55. History of Concrete Weight Reduction
Fig. 7.56. History of Maximum Slab Deflection

Fig. 7.57. Design Data for Technique 1
Fig. 7.58. Comparison of Technique 1 Design Solutions showing Steel in X direction
Fig. 7.59. Comparison of Technique 1 Design Solutions showing Steel in Y direction

Fig. 7.60. Design Data for Technique 2
Fig. 7.61. Initial Model
Fig. 7.62. Comparison With and Without Moment Relaxation between Technique 2 Design Solutions

Fig. 7.63. Design Data for Technique 2
Fig. 7.64. Comparison With and Without Moment Relaxation between Technique 2 Design Solutions using More Steel

Fig. 7.65. Design Data for Technique 2
Fig. 7.66. Initial Model
Fig. 7.67. Result when the Average of the Maximum Nodal Moment Values in the Panel is Chosen

Fig. 7.68. Design Data for Technique 1
Fig. 7.69. Initial Model
Fig. 7.70. Technique 1 Design Solution showing Steel in X direction
Fig. 7.71. Technique 1 Design Solution showing Steel in Y direction

Fig. 7.72. Design Data for Technique 1 - Using Min. Steel (4-Y16)
Fig. 7.73. Technique 1 Design Solution showing Steel in X direction
Fig. 7.74. Technique 1 Design Solution showing Steel in Y direction

Fig. 7.75. Design Data for Technique 2
Fig. 7.76. Initial Model
Fig. 7.77. Technique 2 Design Solutions
Fig. 7.78. History of Concrete Weight Reduction

Fig. 7.79. Design Data for Technique 3 – No Economy
Fig. 7.80. Design Data for Technique 3 – Economy
Fig. 7.81. Comparison between Economical and Uneconomical Technique 3 Designs

Fig. 7.82. Design Data for Technique 3
Fig. 7.83. Initial Model
Fig. 7.84. Technique 3 Design Solutions

Fig. 7.85. New Initial Model
Fig. 7.86. Design Data for Technique 3
Fig. 7.87. Technique 3 Design Solutions
Fig. 7.88. Optimal Solution (at 12^{th} iteration)
Fig. 7.89. Industry Partner's Conventional Design showing Top Steel
Fig. 7.90. Industry Partner's Conventional Design showing Bottom Steel
Fig. 7.91. Comparison between Optimal Solution Obtained using Technique 3 and Industry Partner's Design Obtained using Conventional Approach

Fig. 7.92. Typical Floor Plan of Q2 Project
Fig. 7.93. 3D View of a Single Floor Level of Q2 Project
Fig. 7.94. Design Data for Technique 1
Fig. 7.95. Technique 1 Design Solution showing Steel in X direction
Fig. 7.96. 3D View of Technique 1 Design Solution showing Steel in X direction
Fig. 7.97. Technique 1 Design Solution showing Steel in Y direction
Fig. 7.98. 3D View of Technique 1 Design Solution showing Steel in Y direction

Fig. 7.99. Design Data for Technique 2

Fig. 7.100. Technique 2 Design Solutions

Fig. 7.101. Design Data for Technique 3
Fig. 7.102. Initial Model
Fig. 7.103. Technique 3 Design Solutions
Fig. 7.104. Industry Partner's Conventional Design for Q2 Project showing Top Steel
Fig. 7.105. Industry Partner's Conventional Design for Q2 Project showing Bottom Steel

Fig. 7.106. Design Data for Technique 3
Fig. 7.107. Initial Model of Q2 Project with Band Beams
Fig. 7.108. Technique 3 Design Solutions for Q2 Project with Band Beams

Fig. 7.109. Design Data for Technique 3
Fig. 7.110. Different Initial Model of Q2 Project with Band Beams
Fig. 7.111. Technique 3 Design Solutions for Q2 Project with Different Band Beams

Fig. 7.112. Design Data for Technique 1
Fig. 7.113. Initial Model of Q2 Project with Atrium
Fig. 7.114. 3D View of Initial Model of Q2 Project with Atrium
Fig. 7.115. Technique 1 Design Solution showing Steel in X direction
Fig. 7.116. 3D View of Technique 1 Design Solution showing Steel in X direction
Fig. 7.117. Technique 1 Design Solution showing Steel in Y direction
Fig. 7.118. 3D View of Technique 1 Design Solution showing Steel in Y direction

Fig. 7.119. Initial Model of Q2 Project with Atrium
Fig. 7.120. Design Data for Technique 2
Fig. 7.121. Technique 2 Design Solutions for Q2 Project with Atrium

Fig. 7.122. Design Data for Technique 3
Fig. 7.123. Initial Model of Q2 Project with Atrium
Fig. 7.124. Technique 3 Design Solutions for Q2 Project with Atrium

Fig. 7.125. Plan View of Initial Model of SAFE Example
Fig. 7.126 Frontal 3D View of Initial Model of SAFE Example
Fig. 7.127. Backside 3D View of Initial Model of SAFE Example
Fig. 7.128. Plan Dimensions of Initial Model of SAFE Example

Fig. 7.129. Design Data for Technique 3

Fig. 7.130. Technique 3 Design Solutions for SAFE Example

Fig. 7.131. Optimal Design Solution using Technique 3 for SAFE Example

Fig. 7.132. Initial Model created in SAFE

Fig. 7.133. Reinforcement required in X-strip direction (Shows rebar area required in $inches^2$)

Fig. 7.134. Reinforcement required in Y-strip direction (Shows rebar area required in $inches^2$)

Chapter 8

Fig. 8.1. Labelling Scheme for Columns and Drop Panels

Fig. 8.2. Labelling Schema For Frames Modelled As Columns

Fig. 8.3. Calculation of Internal Force F_{11} in SAP2000

Fig. 8.4. Positive Directions for Shell Element Internal Forces in SAP2000

Fig. 8.5. Positive Direction for Shell Element Principal Forces in SAP2000

Fig. 8.6. Shell Element Stress Resultants - Moments in SAP2000

Fig. 8.7. Positive Direction for Shell Element Principal Moments in SAP2000

Fig. 8.8. Flowchart for Flexural and Shear Design Optimisation of Slabs

Fig. 8.9. Design Data for Technique 2

Fig. 8.10. Initial Model of Symmetrical Flat Slab

Fig. 8.11. Comparison between Only Bending Moment and Bending Moment with Shear as Design Constraints

Fig. 8.12. Design Data for Technique 1

Fig. 8.13. Initial Model of Symmetrical Flat Slab

Fig. 8.14. Technique 1 Design Solutions showing Steel Required in Global X direction

Fig. 8.15. Technique 1 Design Solutions showing Steel Required in Global Y direction

Fig. 8.16. Design Data for Technique 2

Fig. 8.17. Initial Model of Symmetrical Flat Slab

Fig. 8.18. Technique 2 Design Solutions at 1st Iteration

Fig. 8.19. Design Data for Technique 3

Fig. 8.20. Initial Model of Flat Slab

Fig. 8.21. Technique 3 Design Solutions at 1st Iteration

Fig. 8.22. Initial Model for Comparison With and without Transverse Shear Constraint

Fig. 8.23. Design Data for Technique 3

Fig. 8.24. Comparison Between Design Solutions Obtained for only Bending Moment Constraints and Bending Moment with Shear Constraints

Fig. 8.25. Design Data for Technique 3

Fig. 8.26. Initial Model for Bending Moment and Transverse Shear Design

Fig. 8.27. Technique 3 Design Solutions for Bending Moment and Transverse Shear Constraints

Fig. 8.28. Design Data for Technique 3

Fig. 8.29. Initial Model using 3D solids to Model Columns

Fig. 8.30. Initial Model using Single Frame Members to Model Columns

Fig. 8.31. Comparison between Technique 3 Design Solutions for only Bending Moment and Bending Moment with Punching Shear and Transverse Shear Constraints.

Fig. 8.32. 3D-View of Optimal Solution

LIST OF TABLES

Chapter 1

Table 1.1. General Solution Procedure for an Optimisation Task

Chapter 3

Table 3.1. Results of Panel-wise Optimisation for Wall Loaded In-plane

Table 3.2. Results of Panel-wise Optimisation for Wall Loaded Out-of-plane

Table 3.3. Results of Element-wise Optimisation for Wall Loaded In-plane

Table 3.4. Results of Element-wise Optimisation for Wall Loaded Out-of-plane

Table 3.5. Comparison of Top Deflection Reduction between Element-wise optimisation and Panel-wise optimisation for Wall Loaded In-plane and for Wall Loaded Out-of-plane

Table 3.6. Comparison of Concrete Weight Reduction between Element-wise optimisation and Panel-wise optimisation for Wall Loaded In-plane and for Wall Loaded Out-of-plane

Table 3.7. Results of Panel-wise Optimisation for 10-Storey 3D Structure

Table 3.8. Results of Element-wise Optimisation for 10-Storey 3D Structure

Table 3.9. Results of Element-wise Optimisation for *Shear Wall – Slab* Type Structural System

Table 3.10. Results of Element-wise Optimisation for 40-Storey Symmetric Tube-In-Tube (Hull-Core) Structural System

Chapter 7

Table 7.1. Design Optimisation Results of One-Way Slab using Technique 2

Table 7.2. Design Optimisation Results using Technique 2 for One-Way Slab Subjected to Increased Loading

Table 7.3. Design Optimisation Results using Technique 2 for One-Way Slab with More Steel

Table 7.4. Design Optimisation Results using Technique 2 for One-Way Slab Subjected to Further Increased Loading

Table 7.5. Comparison of Examples in Sections 7.6.1 to Section 7.6.4

Table 7.6. Design Optimisation Results using Technique 2 for Continuous One-Way Slab

Table 7.7. Design Optimisation Results using Technique 2 for Continuous One-Way Slab with More

Steel

Table 7.8. Design Optimisation Results using Technique 3 for Continuous One-Way Slab

Table 7.9. Technique 2 Design Optimisation Results using Different Effective Depths for Flat Slab

Table 7.10. Technique 2 Design Optimisation Results using Different Effective Depths for Flat Slab

Table 7.10a. Table comparing M_{11}, M_{22} with the Moment Capacities of the Two Design Sections used for the Oscillating Elements

Table 7.11. Technique 2 Design Optimisation Results Using the 'Moment Difference' Approach for the Continuous One-way Slab

Table 7.12. Technique 2 Design Optimisation Results for the Symmetrical Flat Slab with UDL

Table 7.13. Technique 3 Design Optimisation Results for Economy

Table 7.14. Technique 3 Design Optimisation Results without Economical Considerations

Table 7.15. Technique 3 Design Optimisation Results

Table 7.16. Technique 3 Design Optimisation Results

Table 7.17. Technique 2 Design Optimisation Results

Table 7.18. Technique 3 Design Optimisation Results

Table 7.19. Technique 3 Design Optimisation Results for Q2 Project with Band Beams

Table 7.20. Technique 3 Design Optimisation Results for Q2 Project with Different Band Beams

Table 7.21. Technique 2 Design Optimisation Results for Q2 Project with Atrium

Table 7.22. Technique 3 Design Optimisation Results for Q2 Project with Atrium

Table 7.23. Technique 3 Design Optimisation Results for SAFE Example

SUMMARY

Topology optimisation of continuum structures has gained important industrial relevance in recent years. Size optimisation, although used widely in practice and in research environments, has generally been developed to an advanced stage for optimisation of discrete elements such as frames and trusses. Size optimisation of continuum elements on the other hand has generally focussed on not more than a few design variables such as thickness or Young's modulus. As a result, size optimisation of continuum elements has not found its way in design practice for civil structures such as floor slabs and structural walls.

The work in this thesis presents the development of a practice-oriented approach and the corresponding computer programs for the flexural and shear design of floor slabs in buildings. Thickness optimisation of structural walls and layout design of bracing systems in multi-storey buildings are also investigated.

New techniques have been developed in the course of this work and novel solutions have been obtained that satisfy practical design code requirements and demonstrate economic benefits. The new tools developed are to be used at the conceptual and preliminary stages of design. The basic concepts of Evolutionary Structural Optimisation (ESO) method of structural optimisation are employed and extended for element removal and sizing operations. The focus of this work therefore is on applying the ESO method of structural optimisation to the design of continuum elements such as floor slabs and structural walls in real 3D multi-storey buildings.

The optimal solutions for floor slabs are obtained by repeated finite element analysis and element sizing till all the constraints are satisfied or no further improvement can be achieved. Rather than using few simple examples to demonstrate the validity and effectiveness of the proposed techniques, the work in this thesis is mostly example-oriented to comprehensively demonstrate the applicability and benefit of the proposed techniques in a wide variety of situations and building models.

The potential benefits of using the new design tools are demonstrated by design and cost comparisons of the optimal solutions with the industry partner's conventional, non-optimised designs for his real projects.

Chapter 1: Introduction

1.1 Introduction to Structural Optimisation

It is generally accepted that the design procedure of any technical product is done in cycles, which may often take years with the intention to improve the quality of the product. It is a matter of debate whether by this procedure an everlasting optimal state may be reached or, if so, may be maintained. A first observation of the many years of active work in the field of structural optimisation states that an optimal state can usually be obtained only at a certain time and is defined within a personal context. The abstraction or modelling of the structural problem determines the result. This may sound trivial but cannot be emphasized strongly enough. It is important to realise that an optimal solution is found only within the prescribed context (Kroll 2001). To illustrate this point, consider Figure 1.1 below.

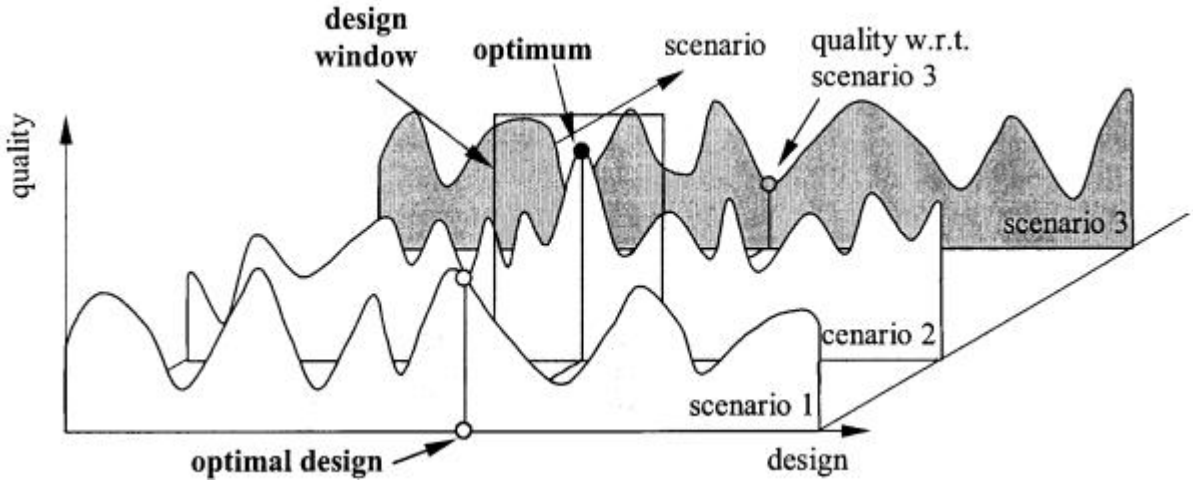

Fig. 1.1. Choice of design window and "optimal design" (Kroll 2001)

According to Kroll (2001), a design window as is seen in Figure 1.1 above, can be thought of as a small region that cuts out a little well-defined scenario from the complex reality. The challenging engineering task is to adjust this window with respect to the characteristics of the real problem while deciding about allowable simplifications. This means that the results obtained within a chosen design window always have to be checked against other scenarios.

In structural optimisation parlance, we have terms such as design objectives, constraints and optimisation or design variables. Design objectives as means to measure the design quality can be, for example, minimal construction cost, minimum life cycle cost, minimum weight, maximum stiffness or many others. Typically, the design is limited by constraints, e.g. the choice of material, feasible strength, displacements, eigen-frequencies, loading, support

condition, and other constraints such as the kind and sizes of available structural members and cross sections etc. Also, the engineer needs to decide about what is allowed to be modified during optimisation, which relates to the selection of optimisation or design variables.

In the context of structural optimisation we distinguish between sizing, shape optimal design and topology optimisation with respect to increasing complexity of the optimisation task.

Once the shape of the structure and type of cross sections is decided, sizing optimisation is concerned with the determination of cross section size. In shape optimisation, the geometry of the structure has to be determined for the given connectivity of structural elements. In topology optimisation, a selection from various structural types can be made. In general, topology optimisation is a question of combinatorial optimisation. As the effort required to solve these questions is enormous, topology optimisation is restricted in practice to problems that can be efficiently solved, e.g. the optimal member assembly in truss design or to the design of optimal numbers and positions of holes in continuous 2D and 3D structures. The latter has gained important industrial relevance in recent years.

Since optimisation requires quantitative comparisons of simulation results to choose the best solution amongst others, accurate simulation plays an important part in the optimisation process. Mathematical optimisation theory is the backbone of structural optimisation. According to Kroll (2001), prerequisites of structural optimisation are therefore:

- The whole problem must be formulated by mathematical means.
- Appropriate algorithms for all concerned disciplines.
- Knowledge in numerical methods, mathematics and mechanics and optimisation theory.

The general outline of an optimisation task can be said to consist of the following two major steps:

1. Problem formulation
2. Problem solution

The solution procedure is arranged as shown in Table 1.1:

Table 1.1. General Solution Procedure for an Optimisation Task (Kroll 2001)

	Project	Customer's general definition of the problem	
	Disciplines	Selection of concerned disciplines	
	Design window	Set up of appropriate scenarios, selection of a design window, characterized by: -objective -constraints -variables	Problem Formulation
→	Optimisation		
	Discretization and models	Set up of models and interactions	Problem Solution
	Solver	Solution	
	Repeated analysis	By directive of mathematical optimisation procedure (e.g.non-linear programming)	

If many different disciplines are involved the procedure is also called *multidisciplinary optimisation*. Particularly in aerospace, automotive and even in civil engineering, multidisciplinary optimisation is becoming increasingly important, as these structures have to satisfy various requirements of strength, stiffness, dynamic behaviour, economics, aesthetics etc. at the same time.

A mathematical statement for a general optimisation problem can be given as:

Find the set x that will

$$\begin{aligned} &\text{Minimize} && f(x) \\ &\text{Subject to} && g_j(x) \le 0 && (j = 1, m) \\ & && x_i^L \le x_i \le x_i^U && (i = 1, n) \end{aligned} \tag{1.1}$$

where $f(x)$ – objective function

$g_j(x)$ – constraint functions

$x = \{x_1, \ldots x_n\}$ – design variables

x_i^L and x_i^U – lower and upper limits for x_i

The constraints may be given in the form of equality or inequality conditions. The additional constraints of lower and upper limits imposed on the design variables are called side constraints. The objective and constraint functions can be either linear or non-linear functions of design variables. When all the objective and constraint functions are linear functions, the problem is a *linear optimisation problem*. When at least one of them is a non-linear function of design variables, the problem becomes a *non-linear optimisation problem*. Most structural optimisation problems are highly non-linear where the objective and/or constraint functions are implicit functions of design variables. When the objective and constraint functions are expressed as a sum of functions, and each is a function of only one design variable, i.e.

$$f(X) = \sum_{i=1}^{n} f_i(x_i) \tag{1.2}$$

$$g_j(X) = \sum_{i=1}^{n} g_{ij}(x_i) \tag{1.3}$$

they are separable functions and the problem is referred to as a *separable optimisation problem*. Separability is an important feature in derivation of the optimality criteria for optimisation problems (Chu 1997).

If one or more objective or constraint functions are a function of more than one design variable, then the problem is referred to as a *non separable optimisation problem*.

When all design variables are continuous, i.e. they can have any value between the given lower and upper limits, the problem is called as a *continuous variable problem*. If one or more design variables can have only certain values from a set of discrete values, the problem is referred to as a *discrete variable problem* (Chu 1997).

Design variables can be any quantity relating to description of the geometry of the structure (nodal coordinates), or member cross-sectional dimensions, or member cross-sectional properties, or member material properties or topology (the pattern of connection to nodes by members or member connectivities), which are required to be determined in the solution process. A different type of design variable may require a different mathematical approach. We shall discuss briefly the different approaches in the next chapter.

1.2 Aims and Scope of This Research Work

This work aims to explore possible benefits from, and develop algorithms for, incorporating size and topological optimisation techniques in the conceptual and preliminary design of continuum elements in multi-storey building structures. It will be seen from the literature review in the next chapter that most of the past research on structural optimisation of multi-storey buildings has

focussed on sizing frame structures. Sizing optimisation or topological optimisation of continuum elements in real 3D multi-storey buildings on the other hand has received scant attention. The structural aspects of sizing or topological optimisation of continuum elements has generally been applied to rather trivial problems (compared to the mathematical aspects) to demonstrate the successful application of a particular optimisation algorithm. Moreover, very little work has been carried out on design optimisation of structural systems that are represented as "objects" in the building structure. For example, building structures and more importantly, structural systems, can now be represented as collections of slab objects, beam objects, wall objects etc. SAP2000 (Computers and Structures Inc., 2002) is a finite element analysis and design software that uses object-oriented representation in which each component (such as beam, slab etc) is treated as an object. The design optimisation algorithms developed in this work modify the properties of these objects during the course of iterations. A broad spectrum of applications is covered in this work ranging from thickness optimisation of structural walls in multi-storey buildings, optimisation of bracing patterns for multi-storey buildings, determining the requirement and location of infill walls in buildings, to design optimisation of slabs, particularly the flat slab type of floor system. Thus all the continuum elements in the building superstructure are given attention for optimisation. Optimisation of frame and discrete elements is not treated in this work. The objective of this work therefore is to propose and validate new design techniques for continuum elements in multi-storey buildings and apply these techniques to real buildings to achieve improved designs.As this project is funded jointly by the industry partner, an objective that has been emphasized throughout this study is to develop a conceptual and/or preliminary design tool that can be directly used by the structural designer in the design office. With this in mind, the slab design optimisation algorithms developed in this work follow specifications given in the Australian Standard, AS3600 (AS 3600 – 2001).

Apart from the theoretical work on proposing and validating new techniques, the practical deliverables from this work include:

1. A structural optimisation computer code incorporating the ESO method for optimal design of structural walls and slabs will be developed and validated. The code can be readily linked to the commercial finite element analysis software package SAP2000. The combined software environment will provide a new design tool, which enables design optimisation of walls and slabs to be carried out for any type of multi-storey building structure. It can be used for practical applications as well as for further research and development.

2. Documented results from several case studies of real multi-storey buildings will demonstrate the potential economic benefits and possible architectural innovations from using the new design tool.

Depending on the type of structure to be optimised, the type of elements can be beams, plate or bricks. This study focuses on continuum structures (both 2D and 3D) modelled using plate/shell elements such as walls and slabs. It is assumed that all materials behave within the linear elastic range. As continuum structures are highly statically indeterminate, the capacity for force redistribution is very high. This enhances opportunities for optimisation as well as increases the complexities involved.

1.3 Layout of this thesis

The thesis consists of nine chapters and a list of references. A literature review on structural optimisation, with a particular emphasis on structural optimisation of multi-storey buildings is provided in Chapter 2.

Chapter 3 presents stress-based thickness optimisation of structural walls in multi-storey buildings. A simple approach to redistributing material in the walls is proposed and the pros-and-cons of using the proposed approach at an element level and at a group level are investigated. A variety of examples are presented that demonstrate the benefit of using the proposed method as a conceptual design tool for the structural engineer. Implementation details and the effect of algorithmic choices on design solutions are discussed.

Chapter 4 builds on the work in Chapter 3 and employs the soft-kill option of element removal together with thickness optimisation to obtain efficient layouts for different models. Different problems are investigated and optimal topologies sought for each case. This chapter focuses on layout design for infill walls and bracing systems in multi-storey buildings. The objective of the work in this chapter is to seek the optimal topology and the thickness pattern in the resulting topology at the same time.

In Chapter 5 we turn our attention to slab systems in multi-storey buildings. The current state-of-practice of reinforced concrete slab design is reviewed. The principles of the various methods of slab design along with a critical evaluation of their applicability and limitations are presented. Additionally, the current state of the art of slab design based on finite element analysis results is presented, along with various modelling techniques. Several design methodologies are reviewed such as the Wood and Armer approach (based on element stress resultants), and the resultant force approach (based on element forces).

Chapter 6 examines flat slab modelling issues and identifies possible pitfalls in numerical modelling of slab structures. Accurate modelling of slab-to-column connections and of boundary conditions is emphasized. The effects of stress singularity at the slab-to-column connections are discussed.

Chapter 7 presents three new techniques developed for flexural design of slabs in SAP2000. The goal is to satisfy the 'yield condition' or 'plastic moment condition' requirement in all areas of the slab. Three techniques, each with a different objective, are formulated and optimal solutions are sought. The first technique designs for the steel requirement in various regions of the slab with the slab thickness being kept constant. No optimisation is involved in this technique. It follows conventional slab design processes. In Technique 2, the steel in the slab is kept constant throughout the slab and the depths or thicknesses are varied in different regions of the slab. In Technique 3, both the steel and the slab depths are varied in different regions of the slab. The chapter also discusses the user interfaces and the software system developed for implementing the design optimisation algorithms. Techniques to mitigate the effects of stress singularity at the slab-to-column connections are also discussed and numerical studies carried out. The need for integrating Element level ESO optimisation and Group ESO optimisation together, in order to achieve converged solutions for flat slabs is demonstrated. Several examples and case studies are presented and benefits from design improvements are demonstrated by comparing with the industry partner's slab design obtained using conventional design process for real commercial projects.

Chapter 8 extends the design optimisation algorithms of all three techniques developed in Chapter 7 to include punching shear and transverse shear as additional constraints in the optimisation procedure. The goal of the optimisation then is to seek the optimal slab design that satisfies bending requirements in two orthogonal directions, punching shear requirements at column supports and transverse shear requirements. Examples are presented at the end of the chapter that demonstrate the need to include these requirements in addition to flexure.

Chapter 9 presents the conclusions of this study and suggests areas for further investigation

CHAPTER 2: LITERATURE REVIEW

2.1 Introduction

A brief introduction to structural optimisation in general has been provided in the previous chapter. In this chapter we review some of the past research work carried out on structural optimisation with emphasis on aspects of and applications to multi-storey buildings. We begin first by discussing briefly the two main and popular approaches to structural optimisation in general viz. the mathematical programming methods and optimality criteria methods. As the work in this thesis is based mostly on the ESO method, we discuss this method concisely and review its recent developments briefly. We then narrow our focus to structural optimisation of multi-storey buildings and review some of the past work carried out in this area. The literature review carried out in this chapter is by no means exhaustive as the body of knowledge available on structural optimisation of multi-storey buildings is huge and covering each and every activity would be beyond the scope and aim of this chapter. This literature review examines past work in two broad categories, viz (1) Size optimisation of skeletal structures such as frames in buildings and (2) Size optimisation of continuum elements such as walls and slabs in buildings. Topological optimisation in multi-storey buildings is also very briefly covered. As practical structural optimisation of multi-storey buildings generally involves discrete variable structural optimisation, one section is devoted to reviewing work in this regard. We then look at conceptual design optimisation of engineering structures. Some of the recent advances (in the last 5-10 years) in structural optimisation of multi-storey buildings are covered in Section 2.4.4. Finally, comments are drawn on the current body of knowledge available in research literature and a motivation for a finite element based discrete structural design optimisation of continuum elements in 3D multi-storey building structures is presented. In the next section we begin first by introducing the main approaches to structural optimisation.

2.2 Main Approaches to Structural Optimisation

The main approaches to structural optimisation are mathematical programming and optimality criteria methods.

2.2.1 Mathematical Programming Methods

Mathematical programming methods include techniques such as linear programming, penalty function method, feasible direction method, sequential linear programming and sequential non-linear approximate optimisation. These methods require calculation of derivatives of objective and constraint functions with respect to all design variables, which is referred to as sensitivity

analysis. Repeated finite element analyses are usually performed to carry out the sensitivity analysis, which is very costly for large problems. The computational time for sensitivity analysis sometimes becomes prohibitively high. Many approximation methods and techniques have been developed and employed, to improve the efficiency of the sensitivity analysis and optimisation algorithms (Chu 1997).

2.2.2 Optimality Criteria Methods

In optimality criteria methods, a prior criterion is derived before the optimisation process and the optimal result is reached when that criterion is satisfied. Whereas in mathematical programming methods, the objective function is optimised directly until the convergent condition is satisfied by one of several numerical search techniques. Prager *et al.* first introduced the optimality criteria methods in the 1960s. The earliest intuitive optimality criteria approach for strength optimisation of structural systems is the fully stressed design approach. In the simplest procedure, the design variables, for example a member cross sectional area (x), is scaled by the ratio of the element stress to the allowable stress using Eq. 2.1

$$x_i^{new} = x_i^{old}\left(\frac{\sigma_i}{\sigma_a}\right) \tag{2.1}$$

where σ_i is the stress of the i^{th} element and σ_a is the allowable stress. $\left(\frac{\sigma_i}{\sigma_a}\right)$ is called the *stress ratio*. An iterative process of analysis and design rationing may result in a structure where all members, except those that are at the minimum gauges, are fully stressed, i.e. their stresses are at an allowable level.

Fully stressed design procedures are very attractive and efficient in the sense that the iterative process usually converges in few iterations. The disadvantage is that it cannot necessarily give minimum weight designs due to the fact that no objective is involved. It has been pointed out by researchers that the fully stressed design method can give minimum weight designs only for statically determinate structures under a single loading condition with equal allowable stresses on tension and compression. However, because of its effectiveness, this method is still used to get a starting point for more rigorous optimisation procedures (Chu 1997).

The rigorous optimality criteria methods try to satisfy the Kuhn-Tucker necessary conditions of optima. A common criterion is that the strain energy density in each member of the structure should be uniform. A recursive formula is derived which leads to the desired solution using iterative process. Fleury (1980) pointed out that mathematical programming and optimality criteria methods have a common basis in the duality of the original problem statement.

Optimality criteria are valid for a mathematically separable problem. Researchers have shown the optimality criteria approach to be quite effective as a design tool. Its major advantage is the ability to be programmed easily for the computer. It is also relatively independent of problem size and usually provides a near optimum design with relatively smaller number of structural analyses compared with mathematical programming methods (Vanderplaats 1981).

The details of the optimality criteria method and its implementation are not discussed in this section as the focus of this chapter is on reviewing structural optimisation of multi-storey buildings.

There are also other modern approaches to structural optimisation such as Genetic Algorithms (GA) (Holland 1975, Hajela *et al.* 1993), homogenisation method (Bendsoe and Kikuchi 1988, Cheng and Olhoff 1982), ESO method (Xie and Steven 1997) etc. A brief discussion of the ESO method is presented in the following section:

2.3 Evolutionary Structural Optimisation (ESO) Method

The evolutionary structural optimisation method, developed by Xie and Steven (1993), is based on the simple concept of gradually removing inefficient material from a structure, thereby evolving the residual shape of the structure towards an optimum. The original idea of the ESO method was developed for topology and shape design of continuum structures based on fully stressed design. In the initial work, ESO was also employed to optimise structural frequencies and buckling loads. The frequency of a structure can be shifted in a desired direction by removing material from the design domain based on a sensitivity analysis. Since then the ESO method has been extended for a number of constraints such as overall stiffness, displacement at a single point, displacement at multiple points and for design dependent loading, dynamic loading, single and multiple load cases etc., thus making it suitable for a variety of situations. It is relatively easy to program the ESO method using standard finite element codes to achieve structural shape and layout optimisation. To date, a wide range of examples have been presented in the literature by Xie and Steven to demonstrate the capabilities of such an evolutionary procedure for solving structural shape and layout optimisation of continuum structures. They have shown that this method is capable of reproducing many existing solutions obtained by other mathematically more complex methods (Xie and Steven 1997). A bi-directional evolutionary structural optimisation (BESO) method was developed by Yang (1999). In the BESO method, elements can be removed from as well as added to the model to obtain the optimum. Although the BESO method starts with the simplest initial design connecting the load and supports, the maximum design domain in which the structure is allowed to occupy or grow must also be defined, i.e., these elements are stored in the database but they do not physically

exist as part of the structure in the initial design. Both the ESO and BESO methods possess their respective advantages and disadvantages but like every other structural optimisation method, they are not without their limitations. A performance-based procedure using the ESO method was developed by Liang (2001) in which after element elimination the process uses scaling technique at the end of each iteration to monitor and determine the optimal topology. This method has proved reliable for 2D continuum structures in which the global stiffness matrix is a linear function in terms of design variables. However, for structures with a combination of discrete and continuum elements, Liang's performance index is no longer valid. Nonetheless, it was an important advancement in terms of measuring or quantifying the performance of each topology generated in the solution process. The extension of the ESO method for discrete sizing problems was investigated first by Chu (1997) and later by Manickerajah (1998) in which the thickness of elements is changed to values specified in a discrete set provided by the user. Instead of removing elements, the thickness is changed according to the objective function and constraints specified. The sizing of members in Manickerajah's work (1998) aimed at increasing the buckling load factor while keeping the weight unchanged. Chu (1997) on the other hand has demonstrated the capability of the ESO method for discrete sizing optimisation by performing:

- Minimum weight design subject to displacement constraints
- Minimum displacement design subject to weight constraints
- Maximum stiffness (minimum strain energy) design subject to a weight constraint.

Later, a modification to the ESO method known as the Group ESO method was proposed by Lencus *et al.* (1999). Group ESO is a modification of the ESO method that is used effectively to constrain the ESO method to only produce manufacturable results. There exist four variations of ESO, namely Binary ESO, Morphing ESO, Binary GESO and Morphing GESO. Descriptions of the methodology, use and examples of these methods can be found in Lencus *et al.* (1999), Steven and Xie (1993) and Querin (1997). The design variables that are operated on by Binary ESO are the existence or absence of elements in an FE model. Binary ESO treats each design variable in a binary fashion, an element may exist or it may not. When an element is considered unfit by ESO, it is removed. The design variables used in Morphing ESO are the thickness of elements. Morphing ESO alters the thickness of unfit elements based on a discrete user-defined set of thicknesses. This method can also remove elements after the smallest thickness is reached. The two GESO methods are parallels of the two ESO methods, except that the design variables are not limited to single elements, but user-defined groups of elements. Comprehensive information on the Group ESO method and its applications is available in the literature and the reader is referred to Lencus *et al.* (1999), Steven and Xie (1993) and Querin (1997) cited in this thesis.

It is thus seen that a lot of work has been done on making the ESO method a robust design tool and applying it in a variety of situations on different examples. In addition to it being a well-established and sound approach, the attractiveness of the ESO method for practical structural optimization problems (which usually involve different objectives and multiple constraints) and its simplicity to program with existing finite element codes (compared to other structural optimization methods such as the Homogenization Method) make it a suitable choice of basis on which to implement new techniques and algorithms (developed in this work) for specific real-world design situations. Moreover, ESO based designs give a clear, interpretable pattern of material required in a structure (and usually do not necessitate further image processing techniques for interpretation). The work in this thesis therefore makes direct use of the ESO method and modifies it for optimising components such as structural walls and slabs in real buildings. It will be shown that the ESO method can be used as an efficient and robust design tool in the structural designer's office for performing design optimisation of continuum elements in building structures. At this point, we now turn our attention to specifically review past research carried out on structural optimisation of multi-storey buildings in general.

2.4 Structural Optimisation of Multi-storey Buildings

In general, the role structural optimisation plays in the design of multi-storey buildings (whether at the conceptual, preliminary or detailed design stage) is broadly divided into two categories in research literature:

- Optimisation of the discrete elements in frames and trusses
- Optimisation of continuum elements such as slabs and walls in a building structure.

Significant research is reported in literature for the former case above compared to the latter. As the focus of work in this thesis is on structural optimisation of continuum elements in buildings based on the ESO method, we review past work on both the categories above to study what has been done and what remains to be achieved. It should be noted though that a vast body of knowledge is available for the former category mentioned above and it is not possible to cover each and every aspect of research conducted on optimising discrete elements in multi-storey buildings. Optimisation of frames and trusses with multiple constraints such as size, stress, displacement and buckling have been studied by various people using either mathematical programming methods or optimality criteria methods (Michell 1904, Maxwell 1894, Hemp 1973, Kirsch 1989, Rozvany 1976, 1989, 1997).

2.4.1 Topology and Shape Optimisation of Frames

As mentioned previously, there are two broad classes of techniques that can be applied to optimise the size, shape and topology of a structural system early on in the design process:

- Discrete optimisation of the structural system
- Continuum optimisation of the structural system

In the discrete optimisation methods, the structure is generally modelled with discrete truss and/or beam-column elements, whereas in continuum methods, the structure is modelled as a continuum (using plate and brick elements). Both methods have undergone extensive research and development in the past two decades, and both have their strengths and weaknesses. We review here the application of both methods in the context of building structures. According to Ohsaki cited in Burns (2002), the initial design of discrete structures such as trusses and frames can be broken down into the selection of nodal (or joint) locations, and design of the connectivity of structural elements. The former process is referred to as *geometry optimisation* or *configuration optimisation or shape optimisation*, and the latter is called *topology optimisation*. Both processes sometimes include sizing optimisation or traditional optimum design where the cross-sectional properties are optimised. Simultaneous optimisation of topology and shape may be referred to as *layout optimisation*.

The *ground structure approach* is a widely used numerical approach for topology optimisation. In this approach, unnecessary members are removed from a highly connected *ground structure* while the nodal locations are fixed (Kirsch 1989, Topping 1992). Many methods have been presented based on this *ground structure approach*. The main research topics in this field include the difficulties for the cases with constraints on stresses and local buckling (Ohsaki cited in Burns 2002). Development of efficient computational algorithms for optimising large-scale practical structures is also an important subject.

In shape optimisation of discrete structures, the nodal coordinates are considered as continuous design variables, and the optimal solutions may be found by using appropriate methods of mathematical programming. In this process, side constraints are usually given for the nodal coordinates to prevent existence of short members, or intersection of members. Therefore, topology cannot be optimised and simultaneous optimisation of topology and shape is a very difficult problem that cannot be a simple extension to either topology optimisation or shape optimisation (Ohsaki cited in Burns 2002).

Topology optimisation problem is virtually a combinatorial optimisation problem with 0-1 variables for absence or existence of members. If the cross-sectional areas of the existing members are also to be optimised then the problem becomes a mixed-variable problem. In the traditional *ground structure approach*, optimal solutions are found by considering the cross-sectional areas as continuous design variables, and the members with vanishing cross-sectional areas are removed to obtain the optimal topology.

Grierson and Pak (1993) have successfully applied Genetic Algorithm (GA) method to frame topology optimisation problems, where the lists of topologies, cross-sectional properties and nodal locations are encoded into binary strings. The null cross-sectional area is also included in the list to enable the removal of members.

Continuum structural topology optimisation is quite different from discrete structural optimisation, in that the structure is modelled as a solid continuum of variable topology rather than as a finite system of fully fixed, partially restrained or pin-jointed frame elements. This yields solutions fundamentally different in nature than those of discrete optimisation methods. While discrete frame techniques deal with a finite number of frame elements each having well-defined length and cross-sectional characteristics, continuum techniques deal instead with spatial arrangements of materials that might be difficult to interpret as a system of discrete structural elements having well defined length and cross-sectional characteristics. For large-scale structural systems, however, the structure must actually be constructed as a system of discrete structural elements that are joined together. Thus when applied to large scale structures, the arrangements of materials from continuum topology optimisation must be "interpreted" as a system of discrete structural elements, whose cross-sectional properties can subsequently be optimised (Ohsaki cited in Burns 2002).

It should be noted that for large-scale civil structures such as multi-storey buildings, continuum topology design problems are typically formulated without stress constraints. The reason is that the stresses in the final structure will depend on the cross-sectional properties of the members chosen. In this sense, continuum topology design really only tells the designer what the overall form of the structure should be, and where the structural elements should be positioned. However, actual selection of member cross-sections remains to be determined with discrete sizing optimisation techniques.

2.4.2 Discrete Variable Structural Optimisation

Discrete design variables are met with in most practical engineering design applications. There are many promising optimisation methods that can treat such design variables in their solution

process. Some of these methods will be reviewed in the following pages. Often, the selection of a solution method depends on the type of discrete design variables, and cost and constraint functions for the problem. In practical applications of optimisation, Arora cited in Burns (2002) mentions the natural occurrence of discrete design variables in the problem formulation. He provides the following as examples:

- Structural members must be selected from commercially available ones;
- Plate thickness that must be selected from the available ones;
- Number of rebars in an RC member must be an integer;
- Diameter of rebars must be selected from the available ones;
- Number of bolts must be an integer;
- Size of the RC members must correspond to the available formwork;
- Material properties must correspond to the available materials.

Such variables need to be treated properly in procedures for optimum design of systems. It should be noted that discrete variable optimisation problems usually require considerably more computational effort compared to the continuous variable problems. This is true even though the number of feasible points with discrete variables is finite and they are infinite with continuous variables. Literature pertaining to the application of discrete variable optimisation to design optimisation of building structural systems is now reviewed.

2.4.2.1 Linked Discrete Variables

According to Arora cited in Burns (2002), a *linked discrete variable* is defined as a variable whose value specifies the values for a group of parameters related to it. There are many design applications where such linked discrete variables are encountered. Framed structural systems in multi-storey buildings are applications of structural optimisation problems with linked discrete design variables. These are called linked-discrete variable NLP problems designated as LD-NLP problems (linked discrete variable, non-linear programming problems). As an example of linked discrete variables, consider the use of standard steel sections available in the AISC (American Institute of Steel Construction) manual for design of steel frames. The section number, section area, moment of inertia, or any other section property can be designated as a discrete design variable for a frame member. Once a value for such a discrete variable is specified from the AISC table, each of its linked variables (properties) also needs to be assigned the unique value. These properties affect values of the cost and constraint functions for the problem. A certain value for a particular property (variable) can only be used when appropriate values for other properties (variables) are also assigned. Sometimes, relationships among such variables and their linked properties cannot be expressed analytically, and so a gradient-based optimisation method may be applicable only after some approximations. It is not possible to use one of the

properties as the only design variable because other section properties cannot be calculated using just that property. Also, if each property were treated as an independent design variable, the final solution would generally be unacceptable since the variables would have values that do not co-exist (Arora cited in Burns 2002). Linked discrete variables are employed in the optimisation procedures developed for flexural and shear design of slabs in Chapters 7 and 8.

Design variables for optimisation problems with linked discrete variables, such as design of steel frames using commercial sections, have in the past been defined in several ways leading to different solution approaches. Most approaches are based on defining only one design variable for each member. Some approaches have also been developed using multiple design variables for each member. A significant amount of research has been carried out on design optimisation (sizing design) of frames, especially steel frames. Burns (2002) provides an excellent source of information on this subject.

According to Arora cited in Burns (2002), solution approaches for ND-LNP problems can be divided into four broad categories based on how the problem is formulated and solved. The first two approaches use only one design variable for each member of the structure, the third one uses mixed-single and multiple design variable formulations, and the fourth one uses a continuous variable formulation along with a rounding-off procedure. Two phases are used in most of the solution approaches to obtain the final discrete solution. In the first phase, the LD-NLP problem is formulated as a standard NLP problem where all the variables are treated as continuous. This is also true for many of the solution procedures for MD-NLP (mixed discrete, non-linear programming) problems (Arora *et al.* 1994). The problem is then solved using any one of the many available NLP methods. In the second phase, the continuous solution is manipulated using a discrete variable optimisation method to obtain the final solution.

2.4.2.2 Single Variable approaches with Approximations

This has been the most popular approach in literature for optimisation of steel structures using available sections. In this approach, one of the section properties (e.g., area or moment of inertia) is treated as a continuous design variable for each member and other properties are *approximately* linked to it. It is difficult to use multiple properties (such as section area, moment of inertia I_x and I_y, and section moduli S_x and S_y) for each member, as independent design variables as it could so happen that the section area of a beam will reach its lower bound to minimise the weight, and the section modulus S_x will be driven upward to satisfy the bending stress constraints. This will result in a member that is not close to any of the available sections.

Many researchers use section area as the sole design variable (continuous) and approximate other properties using the following relationships:

$$I_x, I_y, S_x or S_y = A^{ri} \tag{2.2}$$

where r_i for each property is determined using a curve fitting procedure.

The advantages and disadvantages of this approach are discussed in detail by Arora cited in Burns (2002).

Grierson and co-workers have extensively developed and demonstrated procedures for discrete variable optimisation based on the above approach. Using the section area as the only design variable and by relating the moment of inertia and the extreme fibre distance to it by employing the relationships based on eq. (2.2) above, Grierson and Lee (1984) have formulated their problem of optimal design of 2D frameworks. They have extensively analysed a database of available sections and divided it into several data sets. For each data set, the constants that relate moment of inertia and fibre distance to the section area are calculated in such a way to have more accurate relationship in eq. (2.2). They divide members of the structure into three groups: axial force members, pure flexural members and combined axial and flexural members. The data sets of the available sections are also identified for each type of the member. These data sets are re-arranged into selection tables in the ascending order of key member property which is the section area for each axial or axial-flexural member and moment of inertia for each flexural member. The entire optimisation procedure consists of two phases. Phase 1 uses three iterations of a continuous variable optimisation method (based on an optimality criterion). In Phase 2, a discrete solution is sought using a dual algorithm (Fleury 1980). There are a few drawbacks noted for the adopted procedure, one of which is that any new section must be analysed for inclusion in appropriate data sets.

Grierson and Lee (1986) have extended the above work to include constraints under ultimate load conditions. Grierson and Cameron (1989) describe features of a computer program required for practical applications in design of steel frameworks. Imposed constraints include strength/stability of members and stiffness of the structure. Member buckling constraints are treated by adjusting the allowable stress limits. The effective length factors are automatically calculated for buckling strength calculations. A two-phase optimal design procedure using available discrete sections is presented and demonstrated for a 2D building framework. No formal optimisation is performed in the first phase, wherein a member-by-member procedure is used to assign sections based on the current analysis results only. In the second phase, a continuous variable optimisation is performed using the section area as the only design variable. The problem is linearized using Taylor's expansions for all the constraints and the cost

functions. The two phases are executed in sequence until no changes occur in the weight of the structure. Cameron *et al.* (1991) have extended this work to design of 3D frameworks.

Chan (1992) and Chan *et al.* (1995) have developed a procedure for optimal design of tall building steel frameworks using available sections. The procedure is demonstrated by an example of a 3D unsymmetrical frame. The section area of members is treated as the only design variable; all other section properties are related to the area through regression analyses. Structural members are grouped together to reduce the total number of design variables. The entire solution process, consisting of several phases, is nicely summarized in a section entitled "Overall Design Procedure" by Chan *et al.* (1995). Initially, the largest available sections are chosen for all members. Assuming the member internal forces to remain unchanged, explicit approximate expressions for the two drift constraints (drift in two directions for 3D frames) are obtained. Using these expressions, the members are re-sized to satisfy the constraints approximately. The structure is then analysed to check the member strength requirements. The lower limits on the member sizes are adjusted to satisfy the strength requirements. In the next phase, all the inter-storey drift constraints are considered, and an optimality criterion method is used to obtain a continuous variable optimum solution. The last phase of the solution process involves final discrete member specification. After obtaining the continuous variable optimum solution, penalty on the structural weight for each member to be specified a higher available section is calculated. A few members that have least penalty on the weight are assigned discrete available sections, and continuous variable optimisation is performed again with the reduced set of design variables. According to Arora cited in Burns (2002), this adaptive member selection procedure seems to work quite well and is similar to the one proposed by Arora (1989).

A simulated annealing (SA) method for optimum design of 3D steel frameworks using available sections has been implemented by Balling (1991). An unsymmetrical 3D six-storey frame subjected to three loading conditions is considered. Details of the approach and results are discussed by Arora cited in Burns (2002). May and Balling (1991, 1992) have developed a filter for the SA strategy as they observed it generates poor designs that are quite heavy or infeasible.

2.4.2.3 Single Variable Approaches without Approximations

According to Arora cited in Burns (2002), the table containing data for all the AISC sections can be used directly in structural optimisation instead of using eq. (2.2) above. The cross sectional area A can be used as the sole discrete design variable and when structural analysis is required, the table can be searched to obtain proper values of other section properties corresponding to the current value of A. This, he suggests, would make the mixed-variable optimisation for steel structural design problem into a more general form represented in the problem for LD-NLP in

which other properties are related to the sole design variable via a table in the catalogue of available sections. However, he also mentions that this relationship is not continuously differentiable and hence a gradient-based method cannot be used. Huang (1995) and Huang and Arora (1997) have used the above approach of tabular search during Phase 2 of a solution process for optimisation of steel frames with available sections where a branch and bound method is employed.

Another approach, says Arora in Burns (2002), is to use the available section number as the integer design variable for each member of the structure. Once the section number is specified, all its properties can be obtained from the appropriate row of the table and used in all the calculations. He cites the example of Liebman *et al.* (1981) who have used this approach for optimal design of steel frames and have solved three example problems: two framed structures and a reinforced concrete beam. In their approach, the constrained optimisation problem is transformed to an unconstrained one using an integer gradient method. The table of available sections has to be re-arranged in ascending order for section areas. All the design constraints can be explicitly imposed. An initial feasible point is needed to start the search process that may be difficult to obtain in some applications (Elwakeil and Arora 1995). Arora suggests that this method is quite simple to implement, but points out that it can be quite time consuming on computer because integer-gradient evaluation as well as step size calculation can require a large number of analyses. The penalty function approach to impose the constraints too can be time consuming, he explains.

Research work has been carried out on stochastic methods, such as simulated annealing and genetic algorithm. These methods can also be used to solve problems with linked discrete variables, formulated as LD-NLP. Burns (2002) is a good source of information on this topic. The main disadvantage of these methods is that they are extremely time consuming when the number of design variables is large and the number of available sections for each member is large. They have however been used with other methods to reduce the computational cost.

2.4.2.4 Mixed Single and Multiple Variable Approaches

An additional approach to deal with dependent design variables is to treat some of them as independent design variables. However, this often results in an impractical design. The application of this approach to 2D frames has been studied by Hager and Balling (1988) and their strategy is extended by Balling and Fonseca (1989) to 3D frames. Recently, Huang and Arora (1997b) have developed three procedures for design of planar steel frames using the AISC standard sections. Burns (2002) presents the details of the methods developed in each of these works.

2.4.2.5 Rounding-Off Methods

Rounding-off all of the design variables' values obtained at the continuous optimum is the simplest and fastest way to obtain a discrete solution. The problem should first be formulated and solved with continuous design variables and the optimum design variables are then rounded to their nearest discrete values. It often produces a more conservative design, especially for structural design problems and in some cases; the resulting discrete solution may violate some of the constraints too. One technique is to increase only some variables to their upper discrete neighbours and decrease others to their lower neighbours. The main difficulty with this is to decide which variables to be increased and which variables to be decreased. Several researchers have sought to overcome this problem. Huang and Arora (1995, 1997b) describe a dynamic rounding-up method which increases only *one* variable to its upper discrete neighbour at a time. The selected variable is then fixed at the discrete value and the problem is optimised again, allowing other variables to change. This process is repeated until all variables are selected and fixed to discrete values. Arora explains that this method still does not guarantee a feasible discrete solution but the cost function value is usually smaller than a simple rounding-off method. Another approach has been presented by Al-Saadoun and Arora (1989) to optimise framed structures using AISC sections in which four design variables are chosen for each I-section viz., flange width, flange thickness, height of the section and web thickness. The problem is formulated as a continuous variable optimisation problem to minimise the weight. The Sequential Quadratic Programming (SQP) method is used to solve the problem. Once the final solution from SQP is obtained, each member is selected from the available ones according to two criteria: a) selection based on optimum depth and section modulus, and b) selection based on optimum section modulus and minimum area of cross-section.

Chan *et al.* (1995) also use a similar procedure for optimal design of tall steel building frameworks. In their approach, once a continuous solution is obtained (using an optimality criterion method), a member that gives the least penalty for the cost function due to discrete specification, is selected from the available sections. The problem is then re-optimised using the continuous variable method while keeping the selected members as fixed. This process is continued until all members have been selected from the available sections. The dynamic rounding up procedure along with the optimality criterion approach is used to obtain a discrete solution.

2.4.3 Conceptual Design Optimisation of Engineering Structures

This section focuses on reviewing conceptual design optimisation of engineering structures. Conceptual design is the earliest phase of the design process and commences with a set of initial

concepts. There are many factors that affect the design of a project such as construction cost, operation cost, structural efficiency, quality and comfort of the built project, and the potential for revenue generation. The need to determine the relative benefits of all of these various quantities and qualities makes the design process quite complex. In fact, there is generally no design solution having optimal performance with respect to all requirements because the objective criteria are often conflicting, and designers must evaluate different competing criteria with the view to achieving a good compromise design. The selection of a suitable design concept thus involves making informed compromises between conflicting objective criteria. This is an important activity because decisions made at this stage have significant influence on the overall financial feasibility of a project.

This section provides a brief review of past work highlighting only important issues. A conceptual structural design system that determines compatible structural and architectural configurations and types which provide the basis for subsequent analysis and optimisations to find 'best' solutions has been attempted by Baker and Fenves (1989).

Haber and Karshenas (1990) describe an expert system for conceptual structural design based on a model of the process by which a human expert arrives at a conceptual design for a building.

El-Sayed *et al.* (1989) have used goal-programming techniques to present a method for solving non-linear structural optimisation problems, which can also be used as a conceptual design tool since it removes the difficulty of having to define one criterion as the objective function and the rest as constraints.

Yau *et al.* (1991) have described a prototype tool that is built using an object-oriented environment and focuses on mid-rise building construction. It integrates the processes of design, scheduling and cost estimating and performs, among other activities, a conceptual design to generate structural components from a set of given project parameters.

Hajela *et al.* (1991) have examined applications of adaptive resonance theory using neural networks to the automated conceptual design of beam and frame structural systems for minimum weight and maximum load carrying capacity.

Brokowski *et al.* (1991) emphasize the significance of conceptual decisions taken during the preliminary design of structures, and the need for Artificial Intelligence (AI) based computer techniques to support such decisions in the areas of access to previous design experience stored

in databases, automatic generation and comparison of possible alternatives, and the acquisition of new knowledge through algorithmic structural optimisation.

For the optimisation of concrete structures at the conceptual design stage, Reddy *et al.* (1993) discuss the use of informal methods such as heuristics based on designers' expertise and derived cost functions for estimating the optimum sizes of members.

A shape-annealing approach to the creative design of structures is presented by Cagan and Mitchell (1993), in which they discuss how shape grammars and the simulated annealing stochastic optimisation technique can be used to model structural engineering problems during the conceptual design phase.

Fuyama *et al.* (1993) have described the computerization of the conceptual structural design stage for moment resisting steel frame structures, for the specified loading conditions and building configuration.

Fruchter (1993) has described a methodology for deriving alternative structural modifications for lateral load resisting frame structures based on qualitative interpretation at the conceptual design stage.

Fuyama *et al.* (1993) focus on object-oriented representation and reasoning schemes to elaborate on their earlier attempt of producing an interactive computer-assisted system for conceptual structural design of steel buildings. The development of a computer-based facility for conducting conceptual design using emergent self-organizing computing paradigms, such as genetic algorithms and neural networks, is presented by Grierson (1994). The objective of this work is to seek 'best-concept' solutions through simulated evolution and artificial learning.

Domeshek *et al.* (1994) sought to improve the conceptual design process for complex artefacts such as buildings by creating an on-line hypermedia library. This online library offers designers access to evaluations of existing projects and relevant documentation.

Kunz *et al.* (1994) have proposed an integrated suite of software tools to support both automation and integration of several components of a design, where a design team can propose a design, consider suggestions from multiple computer-based critiquing systems, repeatedly modify the design and consider critiques until it develops a satisfactory design, and then send the latest design version electronically to human engineering consultants for their review and suggestions.

A multimedia approach using case-based reasoning is presented by Maher and Balachandran (1994). Case-based reasoning provides a means for the reuse of previous design experience through the storage, retrieval and adaptation of specific design projects.

Arciszewski *et al.* (1994) present a methodology for applying machine learning to problems of conceptual design of wind bracing in tall buildings. Fuyama *et al.* (1994) have elaborated on their previous work (Fuyama *et al.* 1993) concerning a computer-based design support system for the conceptual design of moment resisting steel frame structures, with focus on a behaviour-based methodology for designing structural members that satisfy strength and inter-storey drift requirements under gravity, wind and equivalent static earthquake loads.

A simplified model based on a building-storey super-element that permits quick evaluation of different structural configurations at the conceptual design stage for the analysis and design of asymmetric-plan buildings is discussed by De La Lera and Chopra (1995). Chierdast and Ambo (1995) have discussed a practical approach to solving topology optimisation problems for planar structures that includes a method for the conceptual design of structural components. An adaptive topology optimisation procedure for continuum structures suitable for both the conceptual and preliminary stages of design has been presented by Maute and Ramm (1995).

A method for improving cost accounting during conceptual design in which computer-based tools allow designers to rapidly explore many options to a high level of detail, including the cost implications of their decisions is discussed by Moore and Miles (1996). Fruchter *et al.* (1996) have presented an interdisciplinary communication medium for collaborative conceptual building design. This involves intensive cross-disciplinary communication of design concepts and decisions. An application of an adaptive learning method to engineering conceptual design is presented by Imam (1996).

Hoernlein and Stettner (1997) describe typical optimisation problems at the conceptual, preliminary and detailed stages of design, and emphasize the importance of developing multi-disciplinary optimisation techniques for conceptual design. A computer-automated procedure involving a genetic algorithm used in tandem with a neural network is developed by Grierson (1997) for conceptual building design. Park and Grierson (1999) present a computer-based conceptual design procedure for generating Pareto-optimal structural layouts of buildings using a multi-criteria genetic algorithm, for the two conflicting criteria of minimizing project cost and maximizing flexibility of floor space usage. Khajehpour and Grierson (1999) use a multi-criteria

genetic algorithm and artificial neural networks in conjunction with Pareto-optimisation theory for the conceptual design of medium-rise office buildings.

There is a lot of information available in literature on conceptual design optimisation of engineering structures. The above review is just a tip of the iceberg. Recent developments in optimal structural design of multi-storey buildings (in the last five to ten years) are now reviewed.

2.4.4 Recent Advances in Optimal Structural Design of Multi-storey Buildings

As mentioned above, this section briefly reviews the *recent* developments (in the last five to ten years) in optimal structural design of multi-storey buildings.

Pullman *et al.* (2003) demonstrate the feasibility in terms of costs by using evolutionary computation in the phases of both conceptual and detailed designs of concrete tall buildings. The objective of their work is to "revolutionise" design of structural systems through the introduction of evolutionary design processes and tools.

Kim *et al.* (1998) present a stiffness-based optimal design technique for planar tall steel building frameworks subject to lateral loading. After an initial 'strength' design is performed, the lateral load resistant system is designed to control any lateral drift of the structure that still exceeds the drift criteria. The degrees of freedom at each floor level are reduced to three by accounting for the floor diaphragm effect. The design optimisation in their work is based on a mathematical programming technique that involves minimising the lateral stiffness of the lateral load resistant system while satisfying specified drift constraints. The features of the proposed method are illustrated by designing three steel frameworks.

An optimal drift design model for a multi-storey building structure under dynamic lateral forces (seismic forces) is presented by Park and Kwon (2003). Their model is formulated in a minimum weight design problem subject to constraints on stresses, the displacement at the top of the building, and inter-storey drift. It consists of three main components: an optimiser, a response spectrum analysis module and a sensitivity analysis module. The design variable considered in their work is the inertial moments of the major axis of each frame member. The exterior penalty function method together with the gradient projection method are adopted to control lateral displacements and stresses in members. Structural response is computed by performing a linear response spectrum analysis. The direct differentiation method and adjoint variable method are adopted for the calculation of sensitivity coefficients of eigen values and eigen vectors. The objective function and constraint functions are normalised to improve the

conditioning of the optimisation problem and to enhance the efficiency of the optimisation process. Three steel frame structures including a 40-storey building are tested to demonstrate the benefit of the proposed method.

Chan (2001) has presented an optimal sizing technique for the lateral stiffness design of tall steel and concrete buildings. The optimal steel and concrete element sizes are sought with the objective of minimum cost while satisfying all serviceability requirements on lateral stability by solving a rigorously derived optimality criteria (OC) method. The design variables considered in this work are the cross sectional area for each steel member, the cross-sectional width and depth for each concrete member and the thickness of structural walls, the objective function being the initial structural cost to describe the merit of a design. Critical wind drift and vibration constraints are treated as the major constraints. Cost of floor area is also included in the cost of vertical structural elements as they occupy floor space. The total cost of the structure defined in this study is the sum of individual component costs while the cost of an individual component is the volume of material in the component times a costing factor. A continuous optimal solution is obtained by applying a recursive sizing algorithm and the optimal design is rounded off to the nearest discrete section. A pseudo-discrete OC technique is adopted to achieve a smooth transition from a continuous variable design to a discrete variable design. The effectiveness and practicality of the optimisation technique is demonstrated by an actual application to the preliminary design of an 88-storey building in Hong Kong.

Later, Zou and Chan (2005) have developed an optimal resizing technique for seismic drift design of concrete buildings subjected to response spectrum and time history loadings.

Al-Khaleefi and Thomas (2002) have developed a design optimisation program called SWESA to perform design and optimisation of shear walls. In this software, wind pressures are calculated and distributed over the height of the building in accordance with specific design provisions. Storey shears and moments are determined analytically. A simple optimisation technique, based on an optimality criterion method, is utilised to obtain the optimal thickness of shear walls in order to satisfy the allowable drift requirement. The objective of the optimisation is the minimisation of structural weight and the constraints are the flexural strength and lateral deflection of the shear wall. The strength of shear walls containing uniformly distributed vertical reinforcement and subjected to combined axial load, bending moment and shear force can be calculated in the developed program. Strength of lintel beams due to the effect of openings in shear walls can also be calculated. The benefits of the proposed method are shown by applying the method on a practical apartment building.

Chan and Wang (2006) have investigated the effects of concrete cracking on the lateral stiffness of tall reinforced concrete buildings. A probability-based effective stiffness method is employed to identify cracked members and to modify their effective cracked stiffness. Nonlinear stiffness characteristics due to concrete cracking are determined by iterative procedures used in the optimisation method which is based on a rigorously derived optimality criteria approach involving minimising the cost of RC structures while satisfying the top and multiple inter-storey drift constraints along with member sizing requirements. A framework example demonstrates the applicability and efficiency of the proposed design tool.

Al-Mosawi and Saka (1999) present an algorithm for the optimum design of reinforced concrete thin-walled sections. The algorithm treats the area of reinforcement and cross-section dimensions of the thin-walled sections as design variables. Limit state theory is used in the formulation of the design problem. Constraints considered are displacement, strain limitations in concrete and the yielding constraints for rebars. A numerical procedure is presented for computations of sectional and sectorial properties. The effect of warping due to torsional deformation of the core is included using Vlaslov's theorems. The optimisation employs an optimality criteria method. A core structure with a lipped channel cross section is optimised to demonstrate the applicability of the proposed algorithm. It should be noted though that in high-rise buildings shear walls are interconnected with slabs and cannot deform freely as is assumed in the model considered in this study.

Fadaee and Grierson (1998) present an optimal design method for 3D RC structures having beams subjected to shear force and bending moment, columns subjected to biaxial moments, biaxial shears and axial loads, and shear walls subjected to pure shear. The design variables for the beam and columns are the width, depth and area of longitudinal reinforcement of member sections. The design variables for the shear walls are the thickness of the wall, the area of vertical reinforcement, horizontal distance between vertical stirrups, the area of horizontal reinforcement, vertical space between horizontal stirrups, and the area of vertical flexural reinforcement. The Optimality Criteria approach is applied to minimise the cost of the concrete, steel and formwork for the structure. ACI Code provisions (ACI 318-95) concerning the strength and ductility of beams, columns and shear walls are taken as constraints. The constraints also impose upper and lower bounds on beam and column dimensions, and on shear wall thickness, reinforcement area and the minimum and maximum vertical and horizontal spaces between the stirrups of the shear walls. Sensitivity analysis is conducted for both internal forces and the capacities of the sections of the beams, columns and shear walls. The features of the design method are illustrated by a simple example. It should be noted that this method is yet to be applied to a multi-storey building frame having shear walls. Also, the result of the

optimisation gives a uniform optimal thickness and optimum steel content for the shear wall (in addition to beam and columns) satisfying ACI code requirements. Though it is very useful and directly applicable from a practical point of view, investigations for finding the optimal thickness distribution for the shear wall along the height of the building cannot be sought using this method.

Research work has also been carried out in applying topological optimisation techniques to seek optimal bracing patterns for multi-storey buildings for various objective functions and constraints. The work of Baldock and Shea (2004, 2005) seeks to find structurally efficient configurations for the diagonal bracing elements of a steel tubular-framed tall building. Resistance to lateral loading, multiple load cases and strength constraints is the focus in this work. It involves study in material removal methods for continuum optimization and a form of pattern search applied to the design of the diagonal bracing for the steel tubular frame. Similar efforts on applying topology optimisation techniques to the bracing design of multi-storey buildings are carried out by several researchers in literature.

2.5 Comments on Current Research and Applications

It is seen that a significant amount of effort has been directed towards optimising discrete elements in multi-storey building structures (such as frame size and connection optimisation etc). However, there is little work carried out so far in employing continuum topology optimisation or size optimisation of continuum elements (such as walls and slabs) in real 3D multi-storey buildings. Moreover, there is very little work done so far in developing optimisation techniques for multi-storey buildings in which the 3D building structure is represented as a collection of objects. Several commercial building design software packages today represent structural components as objects. For e.g. SAP2000 and ETABS are two popular finite element analysis and design packages that use object-oriented (OO) representation in which each component (such as beam, slab etc) is treated as an object. They have been developed by 'Computers and Structures Inc.', based in Berkeley, California. Both ETABS and SAP2000 are widely used in many design firms around the world. ETABS is a finite element analysis program specifically tailored to multi storied buildings; while SAP2000 is a more general program which can be used to analyse details of different parts of buildings and other structures. Since the focus of the work in this research is on continuum elements, both packages were evaluated and it was observed that SAP2000 provides more control to the user in terms of meshing area objects (such as slabs and walls) compared to ETABS. The program generally does the meshing, in ETABS, internally although the user is given limited control of specifying the maximum element size value whilst meshing the area object. In SAP2000, on the other hand, the user has complete control over the fineness of the mesh he or she wishes to create and

therefore SAP2000 is chosen as the FEA engine in this research. Using SAP2000 as the FEA engine, and the concepts of the ESO method for the optimisation procedure, new algorithms are proposed in this work that perform iterative size (and topology) optimisation of continuum elements in multi-storey buildings. The continuum structural elements include slabs and structural walls. By focussing on performing structural optimisation of these continuum elements in multi-storied buildings, the benefits gained at the conceptual and preliminary design stages, for the objectives and constraints specified, are investigated. The objective in each case may be different, but it is essentially to reduce the weight and improve the response at the same time. It will be seen that the proposed algorithms are capable of dealing with large-scale 3D building structures (40-storied and multiple bays), satisfying different requirements specified in design codes. It is widely known that in spite of its tremendous advancements on the theoretical front, structural optimisation has not really been absorbed in the daily fabric of the structural designer's work due to the conflicting nature of objective functions in structural optimisation. One of the aims of this work is also to simplify the designer's task by automating the optimisation process. With this in mind, the next chapter proceeds to investigate stress-based unconstrained thickness optimisation of structural walls in multi-storey buildings.

CHAPTER 3: THICKNESS OPTIMISATION OF STRUCTURAL WALLS IN MULTI-STOREY BUILDINGS

3.1 Introduction

This chapter focuses on the application of the ESO method and the modified ESO method to size optimisation of structural walls in multi-storey buildings. The thickness of structural wall is treated as a design variable. It is shown that by effectively redistributing material in structural walls, significant design improvements in terms of weight reduction (concrete) and improvement in 'top deflection' can be attained using the proposed method. The idea of redistributing material is based on the simple ESO concept of removing material (i.e. reducing thickness) and adding material (i.e. increasing thickness) based on the stress level in elements or groups of elements. It has been shown in the past that the ESO method and its modified form (Group ESO) are well suited to discrete sizing optimisation problems and is, therefore, extended in this work for the specific application of thickness optimisation of structural walls in multi-storey buildings. The pros and cons of using the proposed approach at an element level and at a group level are investigated. A variety of examples for planar walls and structural walls in 3D building models are presented that demonstrate the benefit of using the proposed method as a conceptual design tool for the structural engineer. Implementation details and the effect of algorithmic choices on design solutions are discussed. The aim of this chapter is not to design the walls as per code specified criteria for minimum and maximum thickness and reinforcement details. Rather, it is to perform iterative size optimisation and obtain an efficient material distribution pattern that gives the designer useful information on where to add and reduce material in the walls.

3.2 Structural Wall Systems

For the purposes of this study, a structural wall element is considered to be a member that contributes to resisting lateral loads. Such wall elements may be part of a service core or a stairwell, or they may serve any other purpose such as fire barrier between tenancies. They are usually continuous down to the foundation level to which they are rigidly attached to form vertical cantilevers. Their in-plane stiffness and strength makes them well suited for bracing buildings up to 35 storeys, while simultaneously carrying gravity loading. Ideally, the wall elements are located such that they attract an amount of gravity loading, sufficient to suppress

the maximum tensile bending stresses caused by the lateral loads, resulting in minimum reinforcement requirement (Fintel 1985).

A tall building often comprises an assembly of structural walls whose length and thickness may change, or which may be discontinued, at stages up the height of the building. The walls can be planar or three-dimensional such as "L", "T", "I" or "C" shape section, as per planning requirements and to increase their flexural stiffness. Planar walls are considered to be effective only to resist horizontal loads in the plane of the walls. However, in 3D walls, such as lift core walls, they are normally designed to resist the horizontal loads in both orthogonal directions (Fintel 1985).

The wall elements may be connected by flexible slab diaphragm or alternatively by flexible beams forming a coupled wall system. In the former case, each wall element forms an individual cantilever and any applied lateral load will be resisted by individual moments in each wall element, where the magnitude of the moment is proportional to the wall flexural rigidity.

For the purposes of this study, multi-storey buildings with wall elements connected by slab diaphragms are considered. Initially, two examples of planar walls (one *parallel* to the direction of the applied lateral force, i.e. loaded in-plane and the other *perpendicular* to the direction of the applied lateral force, i.e. loaded out-of-plane) are studied and results analysed. The procedure is then applied to different building models.

3.3 Scope of the Work in This Chapter

In sizing optimisation, the geometry of structures (nodal locations and element connectivities) is fixed, i.e. elements are not removed from the structure. As mentioned previously, the objective of the work presented in this chapter is to perform iterative size optimisation of structural walls and obtain an efficient material distribution that results in reduction in weight and improvement in top deflection for the wall or structure considered. Therefore, the objective is to reduce the weight of walls for the given load case subject to a constraint on the top deflection. To reduce the weight of a structure, inefficient material is gradually removed from the structure. To improve the response of the structure, the inefficient material is systematically shifted to places where it can be more efficiently utilised. The effect of sizing elements or groups of elements on the constraint is not directly evaluated, i.e. the constraint is not formulated into the optimisation, which is effectively unconstrained. Instead, solutions obtained from the optimisation process are compared to initial designs scaled to the same weight.

3.4 Assumptions and Limitations of the Work in this Chapter

It is well known that the top deflection of a building depends on several factors, some of which are:

- Geometry of the building
- Type, location and size of lateral force resisting systems such as shear walls, bracing elements,
- column types and sizes, size of beam elements (if any), type of connections (rigid, semi-rigid or flexible connections) and type of frame (Moment resisting frames, Braced frames, Shear walls, Shear wall-frame, Tube systems such as Framed tube, Tube-in-tube, Bundled-tube, Braced tube, Outrigger-braced structures etc).
- Local winds in the area and the wind load on the building (Jayachandran 2003).

Static analysis is employed in this work. The structure is assumed to be linear elastic. Although wind and earthquake forces are transient in nature, it is accepted in practice to represent them in the majority of design situations by equivalent static force distributions. Though concrete and masonry behave in a non-linear manner, a linear elastic analysis is still the most important tool for deciding a tall building's design (Smith and Coull 1991). In this study, finite element analysis is carried out to obtain the von Mises stress in each element. The von Mises stress criterion is widely used for metal materials. However, Li *et al.* (1999) have concluded that the criterion of von Mises stress in the classical ESO method is equivalent to the criterion of stiffness maximization. The details of element stiffness matrix formulation in SAP2000 are not accessible, as it is not possible to obtain the source code of the finite element analysis software. Therefore, the von Mises stress which is a standard output of SAP2000 is used as a simpler, alternative criterion. The top deflection in the direction of the applied lateral load as calculated from the finite element analysis is recorded at each step in the iteration process. Similarly, the weight of walls in each iteration is recorded. For simplicity and clarity of understanding in interpretation of results, a single load case (parallel to the Global X direction) is employed in all the examples. However, the proposed method can be extended for multiple load cases as well.

This work does not investigate the use of High-Strength Concrete in structural walls. Uniform concrete strength of 32 MPa is used for all the examples investigated. No practical restriction or constraints are applied for wall thickness transitions. The optimisation approach for walls in this work is not intended to satisfy all detailed design criteria specified in the Australian Standard for Concrete Structures (AS3600). The objective of this work then is to develop this optimisation approach as a conceptual design tool that serves as an aid to the structural designer

in finding out the optimal material distribution pattern for the given load cases, in structural walls.

3.5 Optimisation Problem Formulation

Consider the problem of minimising the weight of concrete in a structural wall subject to top deflection constraints, where thickness of wall elements can be designed based on a given set of discrete values. Each element or each group of elements can have its own set of discrete values. The design variables in this work can only have values from given sets of discrete values. As elements cannot be removed in sizing optimisation problems, the only way to reduce the weight of the wall is to remove under-utilised material from wall elements by reducing their thickness. This can be done by simply assigning the next lower thickness available from the given set of discrete thicknesses. In order to improve the top deflection of the structure, the inefficient material is systematically shifted to places where it is more efficiently utilised (i.e. certain regions are thickened). This shifting of material in the walls is based on the stress level (von Mises) of elements or groups of elements.

3.6 Proposed Element sizing criteria

Thickness optimisation of structural walls is carried out at two levels:

- To optimise thickness of each individual finite element of the structural wall. This approach is called *element-wise optimisation*.
- To group finite elements together into a Panel and optimise thicknesses of Panels of the structural wall. This approach is called *panel-wise optimisation*.

In Morphing ESO or Morphing GESO, the set of discrete values that an element can change to are arranged in decreasing order, with the initial design generally being the thickest throughout. As the optimisation proceeds, the thickness of elements or groups is gradually reduced. In the proposed approach, the initial design is not considered the thickest. During the course of optimisation, elements or panels can be either thickened or reduced (with respect to the thickness of the initial design) based on their von Mises stress level. The thickness of the initial design therefore is chosen such that it is appropriate to the span and loading. In the proposed method, the constraint of top deflection is not formulated into the optimization, which is effectively unconstrained. The optimal solution obtained from the optimisation procedure is compared with a scaled model of the same or similar weight (having uniform thickness) and improvement in Top Deflection is compared. It is observed from almost all the examples that

there are significant improvements in top deflections of the optimised models when compared with the scaled initial models.

3.6.1 Element-wise Optimisation

The *element-wise optimisation* procedure adopted in the thickness optimisation of walls is as follows:

As mentioned previously, this work makes use of von Mises stress criterion in the thickness optimisation of walls. Four-noded rectangular elements are used. In the proposed approach, a thickness is assigned to each finite element based on the average von Mises stress in that element, i.e. the higher the stress in an element, the thicker it becomes and vice-versa. The average of the nodal von Mises stresses in each element is used. According to Li *et al.* (1999), the element von Mises stress is usually calculated from the mean of Gauss point stresses. In SAP2000, the element von Mises stress is not reported as the mean of Gauss point stresses. It is evaluated at the standard 2-by-2 Gauss integration points of the element and then extrapolated to the nodes. It is important to consider whether to use the Average or the Maximum stress in each element. We consider two options:

- **OPTION 1**

In Option 1 the *average* von Mises stress of each element is first calculated from the four nodal values for a rectangular element and then the *maximum* value among all the average von Mises stresses is found. The elements are then sorted in ascending order from *minimum to maximum* based on their *average von Mises stress*. Once sorted, there are two approaches that can be followed. These two approaches are described in Section 3.6.2.

- **OPTION 2**

In Option 2 the *maximum* von-Mises stress of each element is first calculated from the four nodal values for a rectangular element and then the *maximum* value among all the maximum von Mises stresses is found. The elements are then sorted in ascending order from *minimum to maximum* based on their maximum von Mises stress. Once sorted, either of the two approaches mentioned in Section 3.6.2 can be followed:

3.6.2 Sizing Algorithms

There are two sizing algorithms that can be followed once the element stresses are sorted based on either Option 1 or Option 2 mentioned above.

1. **Forced Zones Algorithm:** In this algorithm, the stresses are sorted from *minimum to maximum* (either Option 1 or Option 2 chosen above) and the "sort" is then split into four *zones* based on the minimum and maximum values of stress in the sort. Each zone therefore represents one of four regions which is either a lowly stressed region (0-25%), lightly stressed region (25-50%), moderately stressed region (50-75%) and highly stressed region (75-100%) of the structural wall. The thickness of each wall element is then changed into one of four discrete values (specified by the user) depending on which *zone* each wall element lies in. The following illustration explains the process and is self-explanatory.

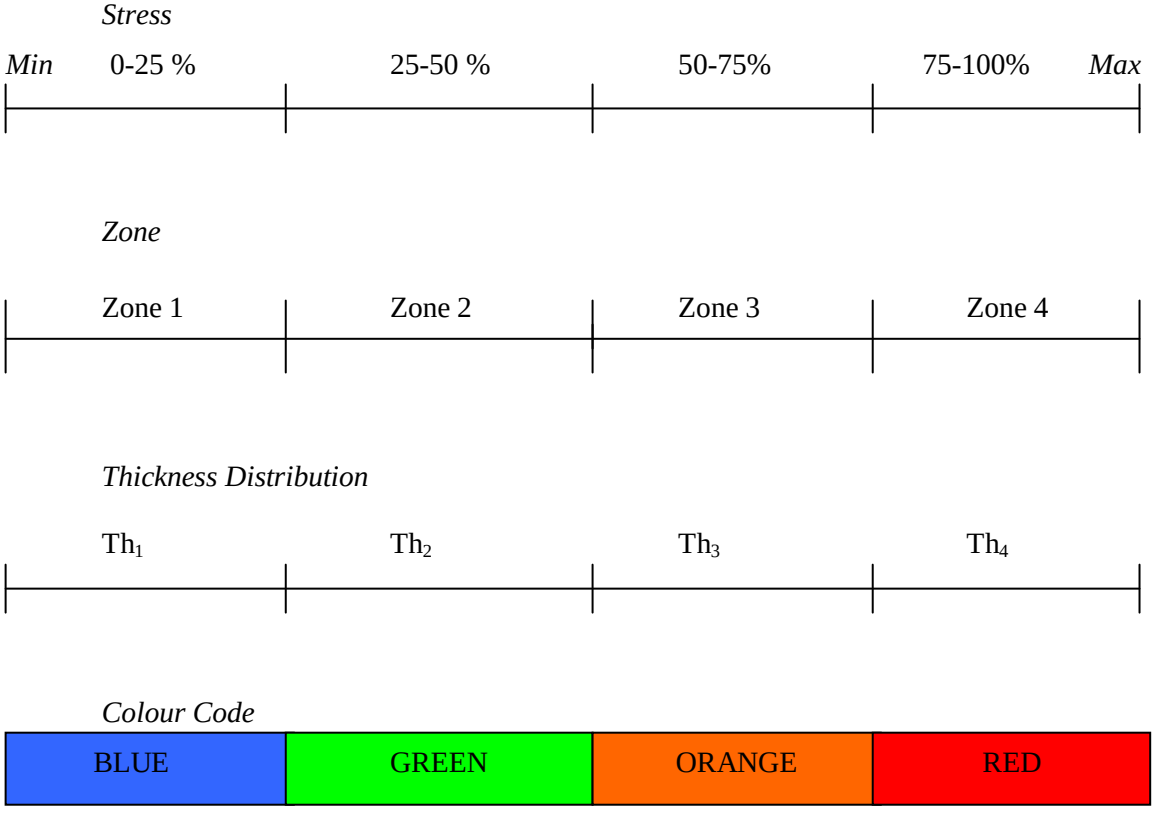

where, $Th_1 < Th_2 <$ Current or Initial Wall Thickness $< Th_3 < Th_4$

Therefore, elements lying in the first quarter of the *sort* will possess new thickness Th_1.
Elements lying in the second quarter of the *sort* will possess new thickness Th_2.
Elements lying in the third quarter of the *sort* will possess new thickness Th_3.
Elements lying in the fourth quarter of the *sort* will possess new thickness Th_4.

A comparison on the choice of the approach will be demonstrated later in the chapter.

2. Ratios Algorithm: In this algorithm, one of four discrete values for thickness is assigned to each wall element by checking the ratio of the average von Mises stress in each element to the maximum of the average von Mises stresses. Then,

- If Ratio is $\leq$ 0.25 (i.e. less than or equal to 25 % of the Maximum), assign minimum thickness Th_1.
- If Ratio is $\geq$ 0.75 (i.e. more than or equal to 75 % of the Maximum), assign maximum thickness Th_4.
- Similarly, if Ratio is > 0.25 and < 0.5 (i.e. between 25 % to 50 %), assign thickness Th_2.
- And, if Ratio is > 0.5 and < 0.75 (i.e. between 50 % to 75 %), assign thickness Th_3.

Though it appears that both the above procedures are not much different logically, there is a subtle difference when it comes to implementation, which will be demonstrated in the examples to follow and explained in Section 3.7

As can be seen from the above discussion, there is no rule-of-thumb on whether to use Option 1 above (i.e. average of the nodal values) or Option 2 above (i.e. maximum of the nodal values). Logic suggests that using the maximum of the nodal values would probably result in a more conservative design, whereas using the average of the nodal values should result in a more economical design.

The significance of using the *Forced Zones algorithm* in either of the two above options (Option 1 or Option 2) is in the fact, that whether the *average* or the *maximum* is used; the fourth quarter of the *sort* will always possess the biggest thickness. This approach can therefore be used, if the user is unsure of whether to use the *average* or the *maximum nodal value* of von Mises stress. However, it results in lesser performance in terms of weight reduction and top deflection improvement as compared to using *Ratios algorithm*. This will be clear from the comparison example demonstrated later in Section 3.7. This is because when the *Ratios algorithm* is employed (wherein the Ratio is employed to make a decision), it suggests that possibly not a quarter ($1/4^{th}$) of elements lie in the fourth quarter of the *sort*. For e.g., maybe only 10-12 elements may lie in the fourth quarter of a *sort* in a 100 element model. When using the *Forced Zones algorithm*, we would be allotting the maximum thickness to 25 elements lying in the fourth quarter of the *sort*. However, the Ratio (using *Ratios algorithm*) may suggest that not 25 actually lie in the fourth quarter and therefore may thicken only the 10-12 elements whose Ratio exceeds 0.75. This is the principal difference when using the two methods which will be clear

from the comparison example. Results in terms of weight reduction and improvement in top deflection are quite different for the two algorithms. A comparison of *Forced Zones algorithm* and *Ratios algorithm* for both *element-wise optimisation* and *panel-wise optimisation* explains these differences later in the chapter. The comparison helps us in understanding the algorithm to adopt to perform wall thickness optimisation (i.e. whether to adopt *Forced Zones* or *Ratios* algorithms' above).

3.6.3 Panel-wise Optimisation

In the *panel-wise optimisation* approach, a panel is formed by assigning a group of elements to that panel. Optimisation then proceeds by changing thicknesses of *panels* rather than individual elements. In terms of practical application, this approach is more suitable than *element-wise optimisation* as it is generally not possible and feasible to construct a wall with continuous thickness variations. Let's say, for example, that every panel comprises four elements. Using the nodal values of von Mises stresses for a rectangular element, there are the following four *options* that arise:

In each of the four options below, the rectangles represent wall panels (each wall panel comprising of four finite elements).

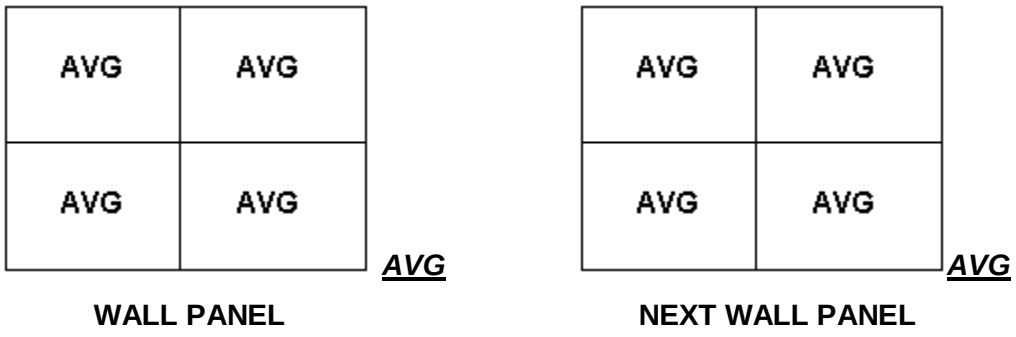

OPTION A

In Option A above, the *average* von Mises stress of *each element* is first calculated from the four nodal values for that element and this is repeated for each of the four elements in the panel. Once the *average* von Mises stress of *each element* in a panel is obtained, the *average* von Mises stress *for the panel* is then computed. This process is repeated for all designable wall panels in the structure. The *maximum* value among all *average* von Mises stresses for designable *wall panels* is then picked. The wall panels are then sorted in ascending order from minimum to maximum.

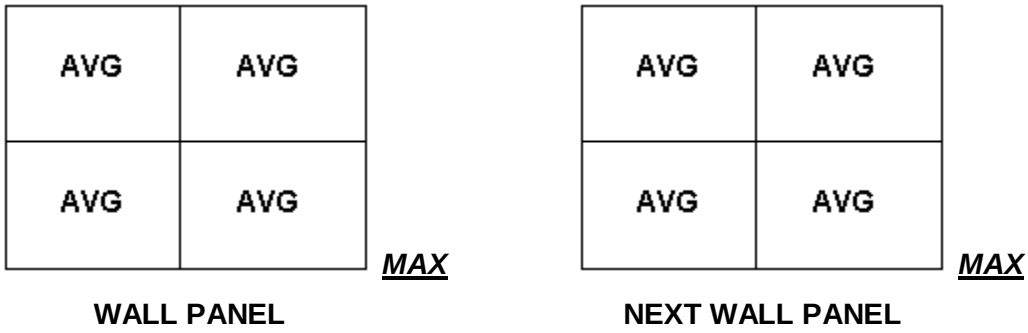

OPTION B

In Option B above, the *average* von Mises stress of *each element* is first calculated from the four nodal values for that element and this is repeated for each of the four elements in the panel. Once the *average* von Mises stress of *each element* in a panel is obtained, the *maximum* von Mises stress *for the panel* is then computed. This process is repeated for all designable wall panels in the structure. The *maximum* value among all *maximum* von Mises stresses for designable *wall panels* is then picked. The wall panels are then sorted in ascending order from minimum to maximum.

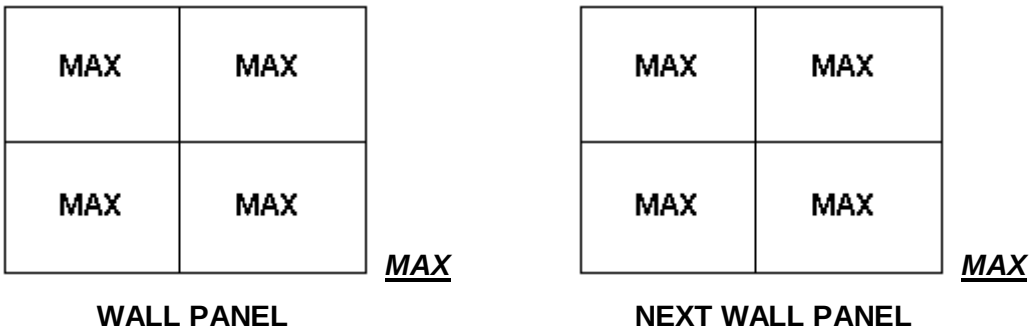

OPTION C

In Option C above, the *maximum* von Mises stress of *each element* is first obtained from the four nodal values for that element and this is repeated for each of the four elements in the panel. Once the *maximum* von Mises stress of *each element* in a panel is obtained, the *maximum* von Mises stress *for the panel* is then computed. This process is repeated for all designable wall panels in the structure. The *maximum* value among all *maximum* von Mises stresses for designable *wall panels* is then picked. The wall panels are then sorted in ascending order from minimum to maximum.

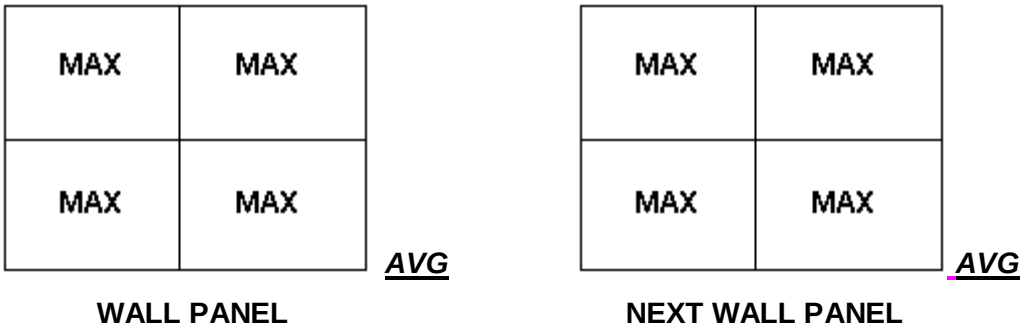

OPTION D

In Option D above, the *maximum* von Mises stress of *each element* is first obtained from the four nodal values for that element and this is repeated for each of the four elements in the panel. Once the *maximum* von Mises stress of *each element* in a panel is obtained, the *average of the max* von Mises stress *for the panel* is then computed. This process is repeated for all designable wall panels in the structure. The *maximum* value among all *average* von Mises stresses for designable *wall panels* is then picked. The wall panels are then sorted in ascending order from minimum to maximum.

It is obvious from the above discussion that the *calculated stress for each panel* will be different for each of the four options above and therefore the *maximum* value picked among all wall panels too will be different. It is here that the Forced Zones algorithm approach helps. Irrespective of the approach used, the Forced Zones algorithm creates four zones and *forces* a particular thickness on the elements (or panels) lying in each zone (after performing the *sort* from minimum to maximum). For generality, the Forced Zones algorithm can be applied to obtain a thickness pattern for the wall irrespective of the approach used.

As is mentioned previously, in SAP2000, the stresses and internal forces are evaluated at the standard 2-by-2 Gauss integration points of the element and extrapolated to the nodes. According to Li *et al.* (1999), the element von Mises stress is usually calculated from the mean of n Gauss point stresses. They have demonstrated and found that the stress criterion by the four Gauss point averaging produces a closer result to that of the stiffness criterion by the analytical integration. This suggests using either Option A or Option B above. Intuition tells us that using Option B, Option C or Option D above would result in a conservative design. Therefore, for the purposes of this study, Option A is adopted when carrying out *panel-wise optimisation* of walls, the objective being to reduce the weight of the walls by efficient redistribution of material.

For ESO 0-1 optimisation, *Li et al.* (1999) have shown the equivalence between the von Mises stress criterion and the stiffness criterion for element elimination or addition in evolutionary structural optimisation. They conclude that the criterion of von Mises stress *in the classical ESO method* is equivalent to the criterion of compliance minimization or stiffness maximization. In other words, the stiffness optimization problem can be solved by directly using the von Mises criterion and vice versa. Their results for ESO 0-1 optimisation implies that the 'strongest design' is also the 'stiffest design'. The same cannot be said of variable thickness design though.

Li *et al.* (2001) propose an Evolutionary Thickness Design with stiffness maximization and stress minimization criteria. The design objective of their work is stiffness maximization (stiffest) and stress minimization (strongest). Their work attempts to achieve both stiffness maximization and stress minimization at the same time. In their study, they derive stiffness sensitivity numbers and stress sensitivity numbers for both single and multiple load cases. They also derive an overall sensitivity number to deal with the multiple maximum stress and multiple load cases and the algorithms adopted are the *Logical AND* and *Arithmetical AND*. They have studied in their work the effect of change in element thickness on the overall strain energy of the structure and on the stress change in elements. In general, reduction in element thickness leads to decrease in the stiffness and an increase in thickness results in a corresponding increase in stiffness. Their investigations reveal that the optimized thickness distributions with the stiffness maximization criteria differ from the optimized thickness distributions with the stress minimization criteria. In other words, the 'stiffest design' may not mean the 'strongest design' and vice versa.

The work in this study does not perform stress minimization. It attempts to demonstrate the 'strongest design' and show benefits gained in weight savings as well as top deflection improvements at the same time. No access to the source code of SAP2000 means that the author does not have access to the details of element stiffness matrix formulation and hence von Mises stress is adopted as a simpler alternative evolutionary criterion.

3.6.4 Comments on the Proposed Approach for Sizing Elements/Groups

As was seen in Section 3.6.2 and Section 3.6.3, the design is performed for a set of four thicknesses. If more divisions (or thicknesses) are considered, then probably the savings attained in weight could be more. Presently, the program has only four thicknesses to choose from as shown below. For e.g., based on an initial thickness of 200 mm, the program chooses four sections as follows:

Ratio of Average von Mises Stress in Each Element/Panel to Maximum Value among All Average von Mises Stresses (of All Wall Elements/Panels)

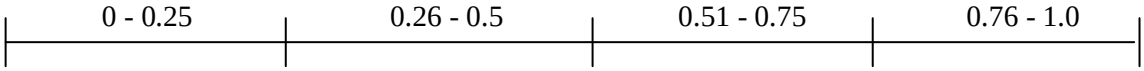

Thickness Distribution

where, $Th_1 < Th_2 <$ Current or Initial Wall Thickness $< Th_3 < Th_4$

In This Example

Th_1	= 160 mm
Th_2	= 180 mm
Current or Initial Wall Thickness	= 200 mm
Th_3	= 220 mm
Th_4	= 240 mm

That is the program decides Th_1, Th_2, Th_3 and Th_4 by incrementing or decrementing 20 mm from the Initial Wall Thickness. The user has the option to change the increment or decrement from 20 mm to a value he/she desires, say 50 mm, in which case Th_1 would be 100 mm, Th_2 would be 150 mm, Th_3 would be 250 mm and Th_4 would be 300 mm.

Though, this approach is not rigorous in a strictly mathematical sense when calculating the exact value of the new thickness, the method adopts a rational approach of variable thickness which has the advantage that no element is removed and an element which makes a small contribution (i.e. has a small thickness) at a given iteration can be reinforced at another iteration if necessary. The user is given the option to specify the increment or decrement when specifying the discrete set of thicknesses. This was done with the view of making the program more flexible and user interactive and gives more control to the structural designer in terms of entering thicknesses that closely resemble practical constraints and build ability. It should also be noted however, that the level of change in top displacement and weight depends on this step size (increment or decrement). If the step size is increased, more material is removed from

elements and the total change in top displacement will be bigger. In this work, equal step sizes are used and investigating the effect of changing the step sizes is beyond the scope of this work. It is expected that the user (an experienced structural engineer) shall specify the appropriate increment or decrement when specifying the initial thickness for the wall/s. At this stage, a reference to some of the past work carried out on thickness optimisation in general is considered necessary. Nguyen (2001) has adopted a uniform scaling technique to measure the performance of several topologies generated during the ESO optimisation process. According to his method, in each iteration, a small number of continuum elements in the design domain are gradually removed according to their strain energy density. The weight of each solution was kept constant during the optimisation process by uniformly changing the thickness of the continuum elements. He shows that the thickness of an element in the kth iteration can be calculated from the element thickness of the previous iteration by:

$$t_k = t_{k-1}\left(\frac{n_{k-1}}{n_k}\right)$$

where,

t_k = thickness of the element of the current structure in the k^{th} iteration

t_{k-1} = thickness of the element in the previous iteration (i.e. *k-1*)

n_k = total number of elements in the current structure at the k^{th} iteration

n_{k-1} = total number of elements in the structure at the previous iteration (i.e. *k-1*)

Finally, as all the topologies are uniformly scaled to be of the same weight, the optimal solution is chosen by evaluating its mean compliance value which is stored in a database each time. The optimal topology is the one, which has the same weight as all the others, but has the lowest mean compliance.

The above procedure is useful in the context of ESO 0-1 optimisation. However, being a 0-1 optimisation technique it makes use of uniform scaling in each iteration (i.e., all elements kept are assigned the same thickness). As the thickness of an element calculated by the above approach depends on the thickness of the element in the previous iteration, the total number of elements in the current structure and the total number of elements in the structure at the previous iteration, it is not applicable in the current procedure of size optimisation as no elements are removed in each iteration unlike the ESO 0-1 method. However, for comparison of top

deflection, the initial model is scaled in the current approach in such a way that the weights of the scaled model and the optimised model are the same. The top deflections are then compared to check for improvements.

It should also be noted that the method is programmed such that it requires all the walls in the initial model to be of the same thickness (for eg, say 150 mm or 200 mm etc). Walls with different initial thicknesses in a complex building model cannot be optimised with the current program at present. However, the optimisation program can easily be extended in the future for this requirement wherein the algorithm finds out the initial thicknesses of the different walls first and then begins optimising them using the proposed approach described above.

The following examples are investigated that demonstrate the benefit of using the proposed method:

- Planar wall in the direction parallel to the applied lateral force (Sections 3.8.1 & Section 3.8.3).
- Planar wall in the direction perpendicular to the applied lateral force (Sections 3.8.2 and 3.8.4).
- A ten storey 3D structure comprising slabs (as non-design region) and walls on all four sides (design domain) (Sections 3.8.6 and 3.8.7).
- Thickness optimisation of shear walls and internal core of *shear wall-slab* type structural system (Section 3.9.1).
- Thickness optimisation of core walls for a 40 storey symmetric "Tube-in-Tube" (Hull-Core) structural system (Section 3.9.2).

3.7 Comparison of Algorithms

A comparison of the *Forced Zones* algorithm and *Ratios* algorithm for both *element-wise optimisation* and *panel-wise optimisation* is first carried out for the model shown in Figure 3.1. This comparison helps us in understanding the algorithm to adopt to perform wall thickness optimisation (i.e. whether to adopt *Forced Zones* algorithm or *Ratios* algorithm).

Example 1 demonstrates the optimisation of a planar wall *parallel* to the direction of applied lateral loading i.e. *Wall A* (both *element-wise optimisation* and *panel-wise optimisation* is carried out) using *Ratios* algorithm and comparison with a scaled model is performed to show improvements in weight reduction and top deflection improvement. The scaled model is allotted a uniform thickness such that the weight of the optimised model and the weight of the scaled model are the same. The top deflection of the two models are compared when weights of both models are the same.

Example 2 demonstrates the optimisation of a planar wall *perpendicular* to the direction of applied lateral loading i.e. *Wall D* (both *element-wise optimisation* and *panel-wise optimisation* is carried out) using *Ratios* algorithm and as before, comparison with a scaled model is performed to show improvements in weight reduction and top deflection improvement.

Example 3 performs both *element-wise optimisation* and *panel-wise optimisation* of the building model shown in Figure 3.1and tabulates results for both cases.

3.7.1 Finite Element Model for Comparison Purposes

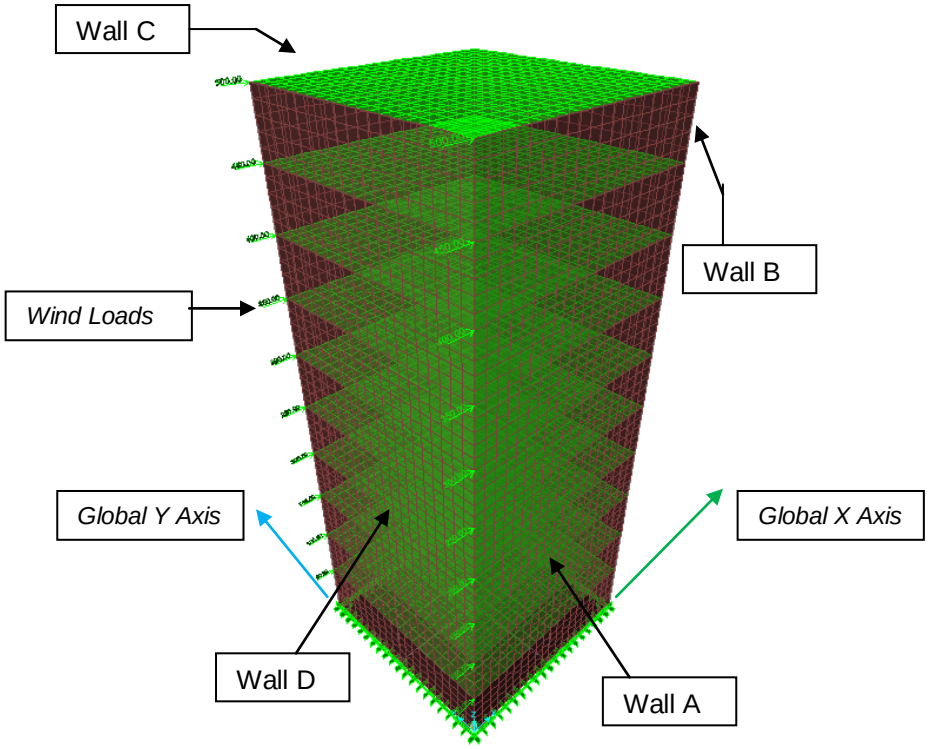

Fig. 3.1. Finite Element Model for Comparison Purposes

The above model depicts a 10 storey building with walls on all four sides. Though such a building is not encountered in real structures, the objective here is to demonstrate the effect of efficient material distribution in the walls when subjected to a lateral load (in the Global X direction in this case) with an increasing magnitude towards the top. It is expected that with efficient material distribution, the weight of the walls will be reduced and some improvement in top deflection in the Global X direction (parallel to the applied lateral load) will be observed.

As can be seen, all four walls will exhibit a cantilever action of bending with the two walls parallel to the direction of the applied lateral load exhibiting tension on the windward side and compression on the leeward side. Of the other two walls (perpendicular to the applied lateral

load), Wall D shown in Figure 3.1 will exhibit tension on both sides and Wall B at the back exhibits compression on both sides. All four walls will be optimised simultaneously using first *panel-wise optimisation* and then *element-wise optimisation*. It is important to note that optimisation of cross sections of the frame members is not carried out during this process. Obviously, the iterative frame member design process (involving iterative cross section optimisation) is available internally in SAP2000 (for various international design codes) and can be used to good effect in attempting to reduce the top deflection and inter-storey deflection of a multi storey building. Sizing optimisation of frame members such as columns and beams is beyond the scope of this work. The purpose of this research is to perform iterative size optimisation of continuum elements (in these case walls) with the aim of efficient redistribution of material.

Data for Panel-wise Optimisation Using Forced Zones Algorithm

Data for the Model

Initial Model (Initial Wall Thickness: 200 mm, Slab Thickness: 250 mm)

Symmetrical Model	**Finite Element Details**
2 BAYS in X direction and 2 BAYS in Y direction	Total No. of Elements: 8000
Each bay is 6m x 6m	Wall Elements: 4000
Floor-to-Floor Height is 3m.	Slab Elements: 4000
No of Storeys: 10	Non Design: Slab Elements
Total Building Height: 30m	Wall Panels: 160 (40 on each face)
Width at base: 12m	
Height-Width Ratio: 2.5	*Note:* There will be no Wall *Panels* for Element-wise Optimisation.

Loading:

Point loads in X-direction at each floor level with increasing magnitude towards the top.

FEA: Linear Static Analysis.

3.7.2 Panel-wise Optimisation

3.7.2.1 Panel-wise Optimisation Using Forced Zones Algorithm

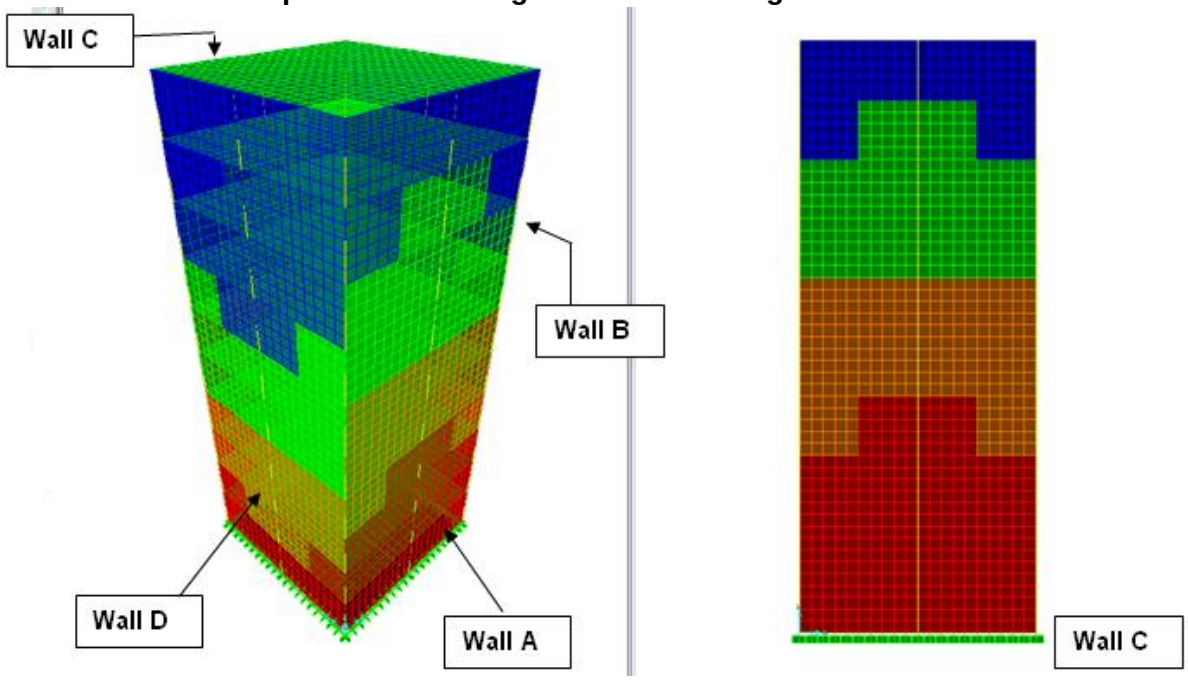

Fig. 3.2. 1st Iteration of Panel-wise Optimisation Using Forced Zones Algorithm *

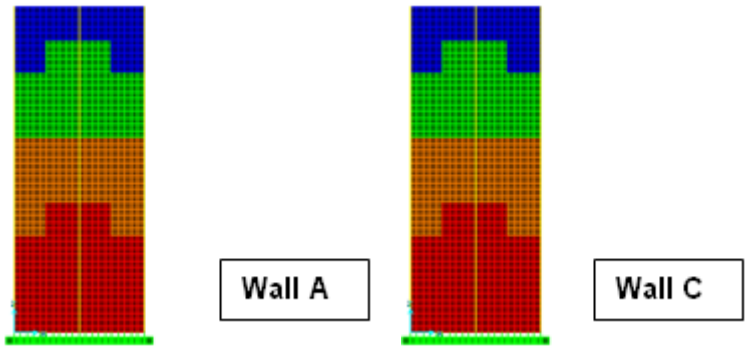

XZ @ Y=0 XZ @ Y=12

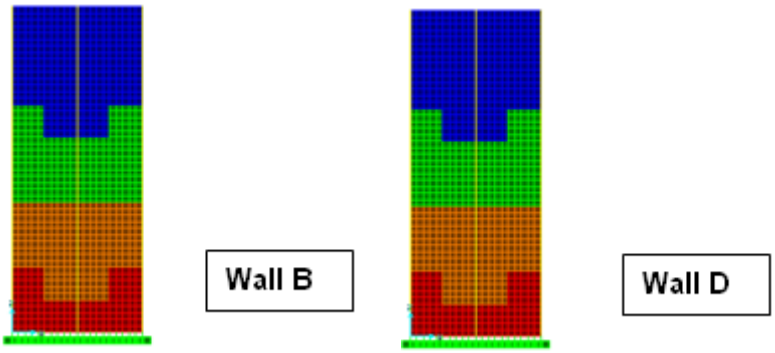

YZ @ X=12 YZ @ X=0

LEGEND:

Blue	:	160 mm
Green	:	180 mm
Orange	:	220 mm
Red	:	240 mm
Initial Thickness	:	200 mm

Fig. 3.3. Panel Thicknesses Assigned to All Four Walls after 1st Iteration

* *Note:* Wall A and Wall C are *parallel* to the direction of applied Lateral Load and Wall B and Wall D are *perpendicular* to the direction of applied Lateral Load Wall B and Wall C being at the back cannot be seen in the 3D View

3.7.2.2 Panel-wise Optimisation Using 'Ratios' Algorithm

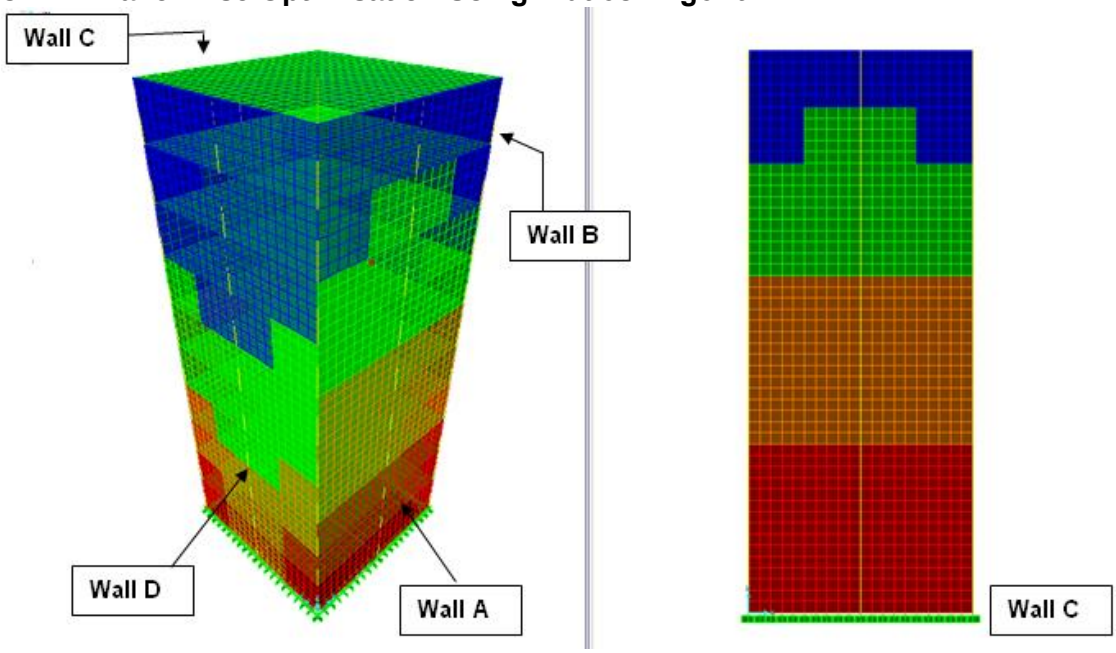

Fig. 3.4. 1st Iteration of Panel-wise Optimisation Using Ratios Algorithm *

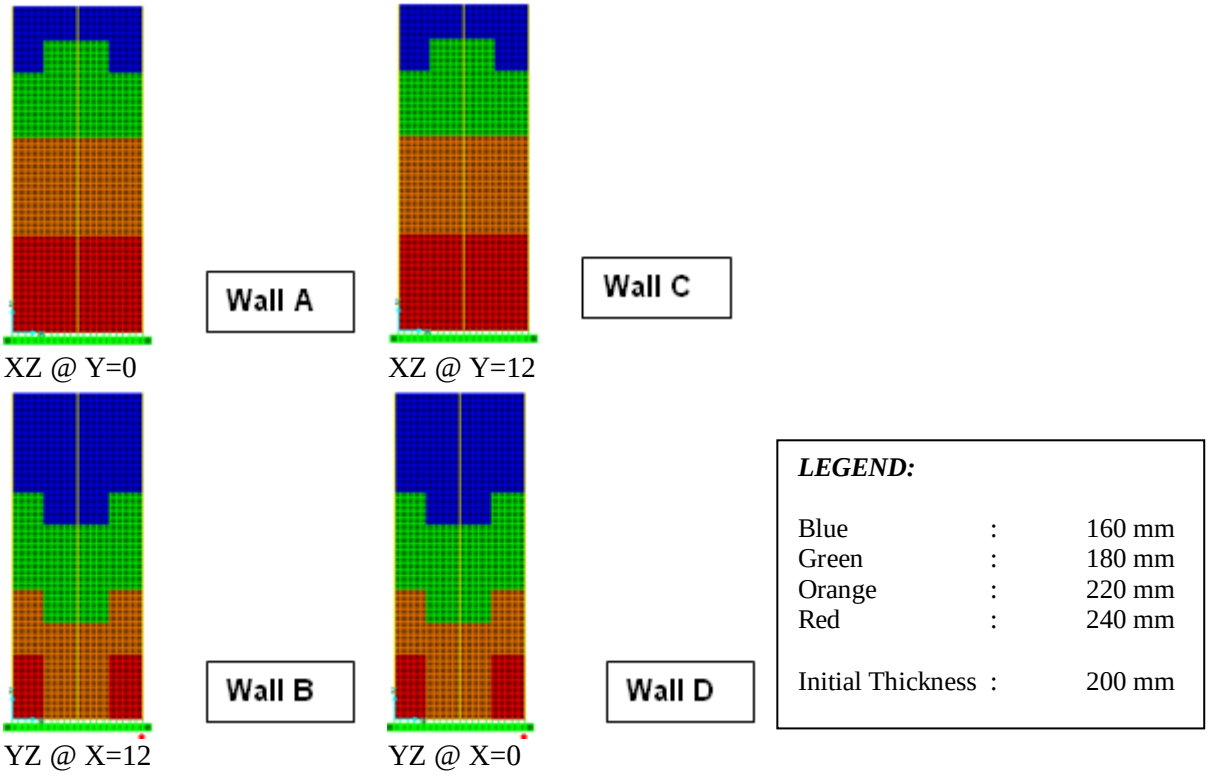

Fig. 3.5. Panel Thicknesses Assigned to All Four Walls after 1st Iteration

* Note: Wall A and Wall C are *parallel* to the direction of applied Lateral Load and Wall B and Wall D are *perpendicular* to the direction of applied Lateral Load Wall B and Wall C being at the back cannot be seen in the 3D View

3.7.2.3 Discussion of Results

Refer to Figures 3.2 and 3.4 for comparison and Figures 3.3 and 3.5 above for comparison.

On comparing Figures 3.3 and 3.5, it can be seen that for the walls parallel to the direction of loading (i.e. Wall A and Wall C), the results are almost identical except for one panel between Level 3 and Level 4. The Forced Zones algorithm (Fig. 3.3) indicates a thicker portion for the panel (shown in Red) whereas the Ratios algorithm (Fig. 3.5) indicates a lesser thick portion (shown in Orange). This reveals that this particular panel lies in Zone 4 of the *sort* (i.e., maximum thickness region) when Forced Zones algorithm is used along with other panels (i.e. the panels on Levels 1 and 2). Whereas actually the *ratio* of its average von Mises stress to the maximum (Ratios algorithm), suggests that it need not have a maximum thickness (Fig 3.5) when Ratios algorithm is employed. This therefore demonstrates that using Ratios algorithm is more logical as we are assigning the thickness to the panel based on its Ratio rather than forcing a thickness onto it based on which Zone it lies in. Moreover, it is also economical to use this algorithm.

Similar observations are seen for Wall B and Wall D for two panels at the Ground Level (Compare Figures 3.3 and 3.5 again). Forced Zones algorithm (Figure 3.3) shows thicker panels whereas actually less thick panels are sufficient (Ratios algorithm, Figure 3.5).

Similar observations are also made during *element-wise optimisation*, wherein similar differences are noticed in the same regions discussed above when using Forced Zones and Ratios algorithms. Results after one iteration are shown next for *element-wise optimisation* using both algorithms (Refer Figures 3.6, 3.7, 3.8 and 3.9).

Logically and with economic considerations use of the Ratios algorithm is more suitable rather than Forced Zones algorithm. It is therefore recommended to use Ratio's algorithm over Forced Zones algorithm. Iterative results of optimisation using Ratios algorithm for *panels* and for *elements* are shown after the next section. It should be noted that only the results after the 1st iteration are shown here as it is important to check for any difference of results using the two algorithms right at the beginning (from the first step) in order to allow the optimisation onto the right path using the correct algorithm. Otherwise it may so happen, in certain cases, that no visible differences are seen using the two algorithms at convergence. Hence, the first iteration results are critically analysed for comparison purposes and iterative results of optimisation are shown later.

3.7.3 Element-wise Optimisation

3.7.3.1 Element-wise Optimisation Using Forced Zones Algorithm

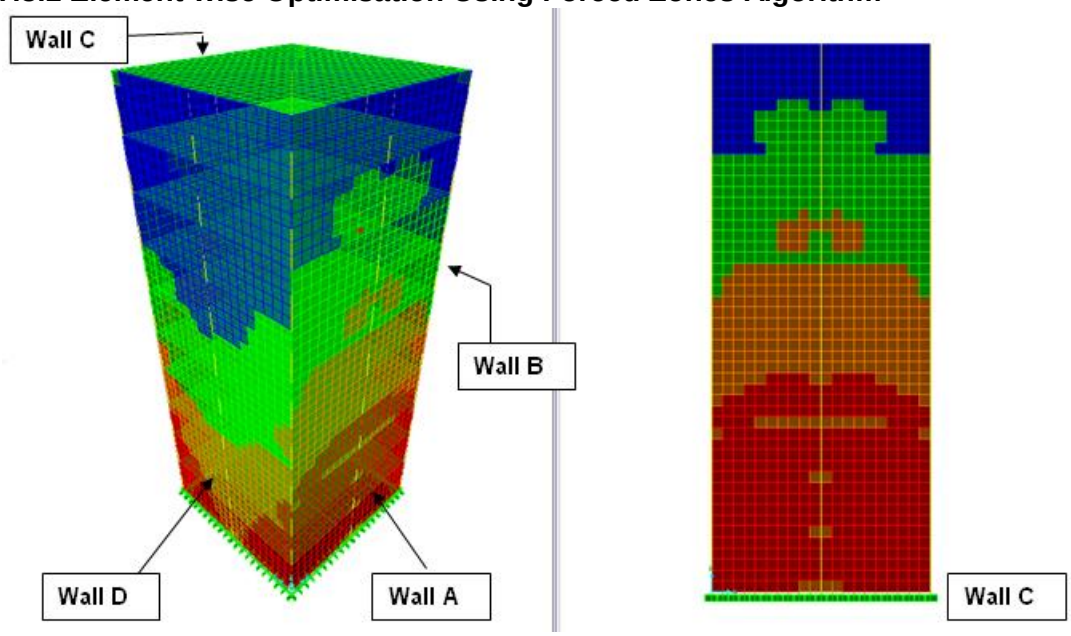

Fig. 3.6: 1st Iteration of Element-wise Optimisation Using Forced Zones Algorithm *

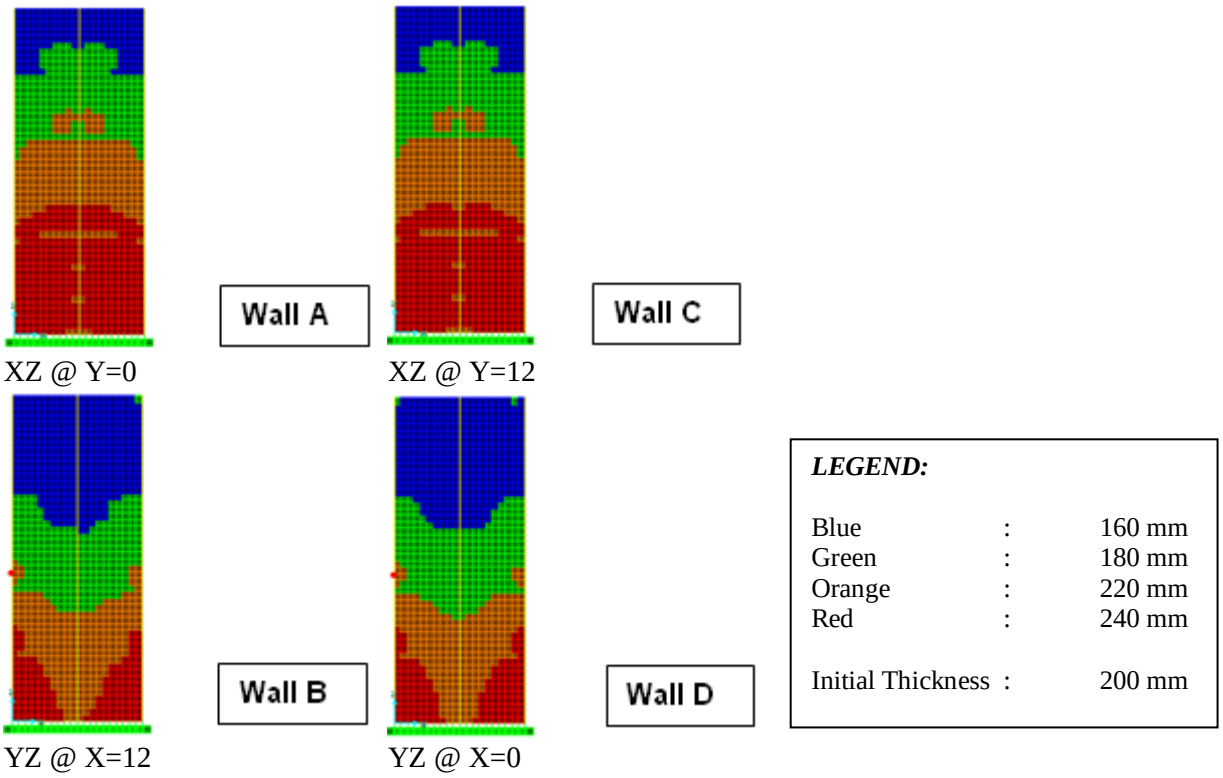

Fig. 3.7. Thicknesses Assigned to Elements on All Four Walls after 1st Iteration

* *Note:* Wall A and Wall C are *parallel* to the direction of applied Lateral Load and Wall B and Wall D are *perpendicular* to the direction of applied Lateral Load Wall B and Wall C being at the back cannot be seen in the 3D View

3.7.3.2 Element-Wise Optimisation Using 'Ratios' Algorithm

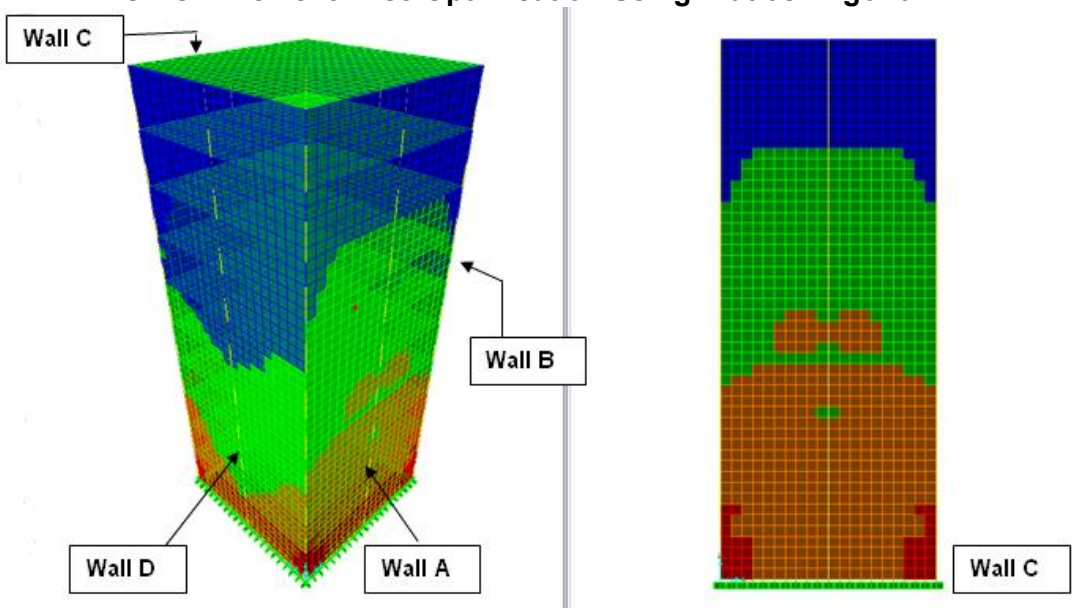

Fig. 3.8: 1st Iteration of Element-wise Optimisation Using Ratios Algorithm *

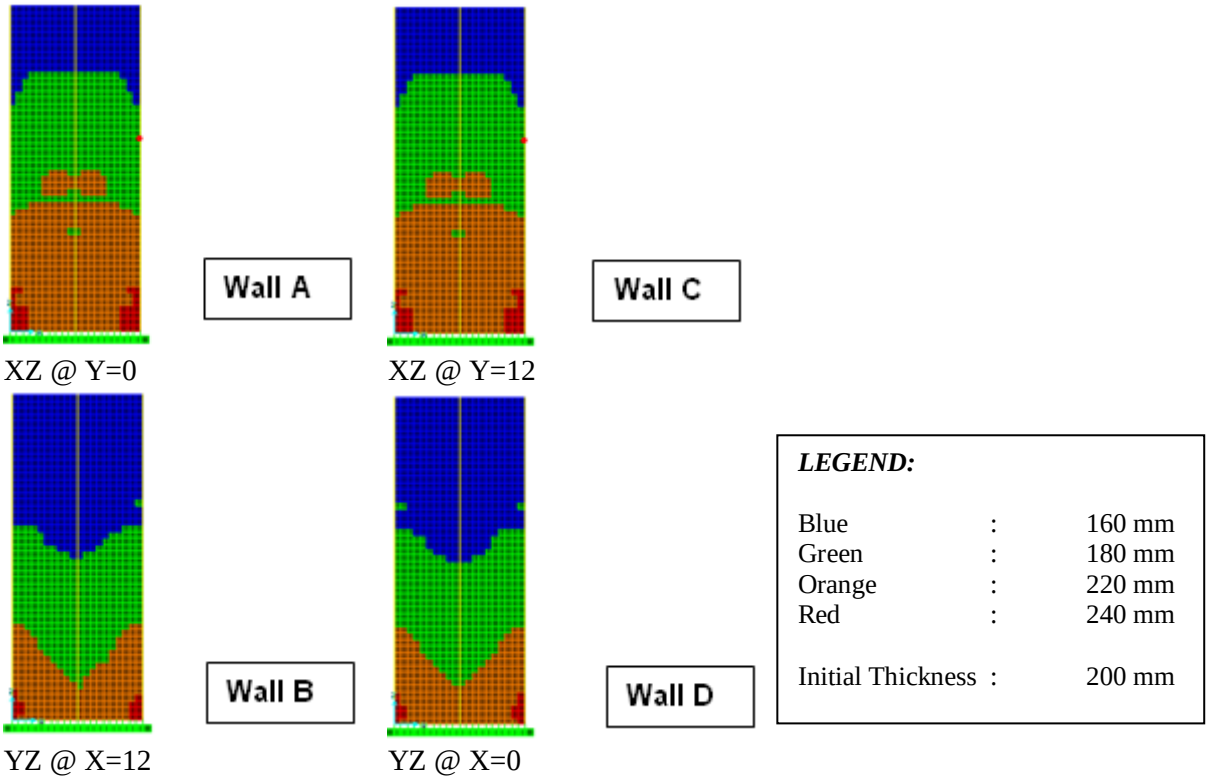

Fig. 3.9. Thicknesses Assigned to Elements on All Four Walls after 1st Iteration

* *Note:* Wall A and Wall C are *parallel* to the direction of applied Lateral Load and Wall B and Wall D are *perpendicular* to the direction of applied Lateral Load Wall B and Wall C being at the back cannot be seen in the 3D View

3.7.3.3 Discussion of Results

As mentioned previously during *panel-wise optimisation*, it is also seen here in *element-wise optimisation* that it makes more sense logically and with consideration to economy to use Ratios algorithm rather than Forced Zones algorithm. Iterative results of optimisation using Ratios algorithm for *panels* and for *elements* are shown next.

3.8 EXAMPLES

3.8.1 Example 1 - Wall A (Wall parallel to the direction of the applied lateral force – *Panel-Wise Optimisation*)

The model shown below depicts a planar wall fixed at the base and subjected to a single lateral load case in the Global X direction. The magnitude of wind load increases towards the top of the wall. The width of the wall is 12 m and total height is 30 m. The initial thickness is 200 mm throughout the height. The model is meshed into 1000 finite elements that are grouped into 40 panels.

Physical Behaviour of the "Planar Wall"

The planar wall will behave as a vertical cantilever when subjected to lateral loading. This wall will exhibit tension on the windward side and compression on the leeward side. As the loading is in the direction of the plane of the wall, its high in-plane stiffness and strength makes it suitable to resist horizontal loading in its plane.

Finite Element Model

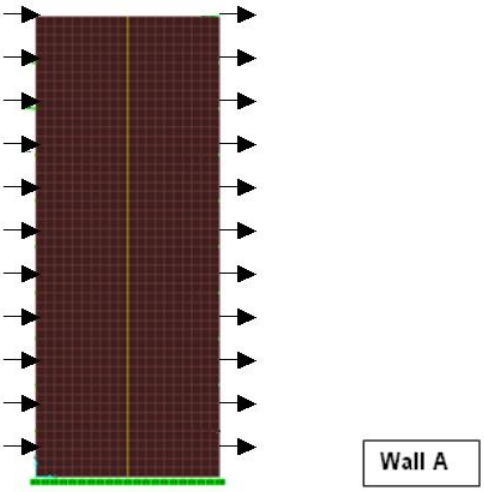

Fig. 3.10. Initial FE Model of Planar Wall Loaded In-Plane for Panel-wise Optimisation

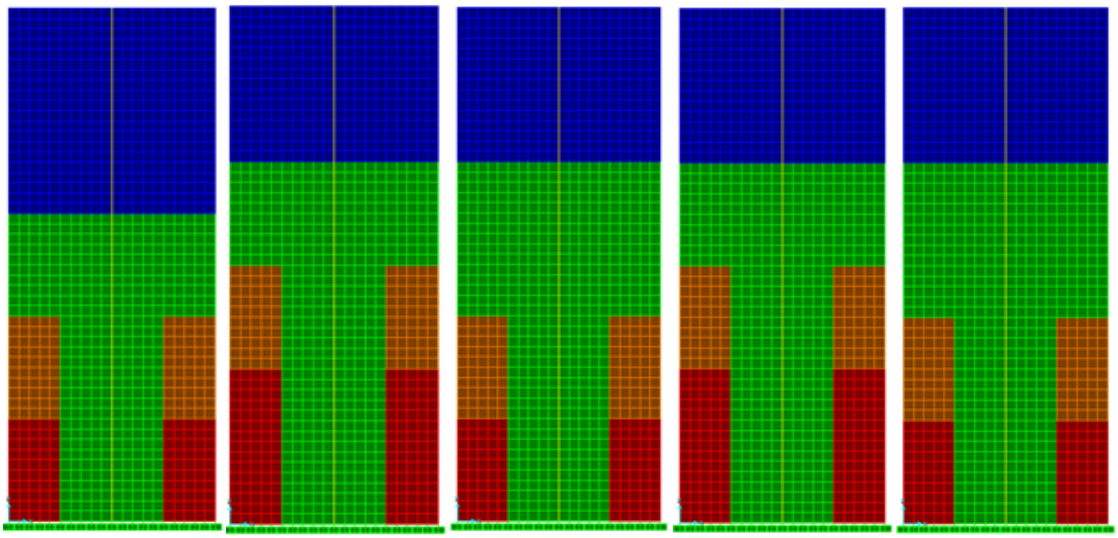

(a) 1st iteration **(b)** 2nd iteration **(c)** 3rd iteration **(d)** 4th iteration **(e)**5th iteration

Fig. 3.11. Design Solutions for Wall Loaded In-plane using Panel-wise Optimisation

Table 3.1. Results of Panel-wise Optimisation for Wall Loaded In-plane

Sr. No.	Iteration	Top Deflection (mm)	Total Weight (kN)
1	INITIAL MODEL	45.8	1696.544
2	1	43.3	1543.855
3	2	42.0	1586.269
4	3	43.1	1560.821
5	4	42.0	1586.269
6	5	43.1	1560.821
7	6	42.0	1586.269
8	7	43.1	1560.821
9	8	42.0	1586.269
10	9	43.1	1560.821
11	10	42.0	1586.269

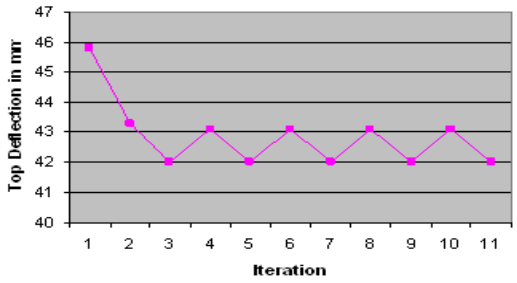

Fig. 3.12. Top Deflection History of Wall Loaded In-plane using Panel-wise Optimisation

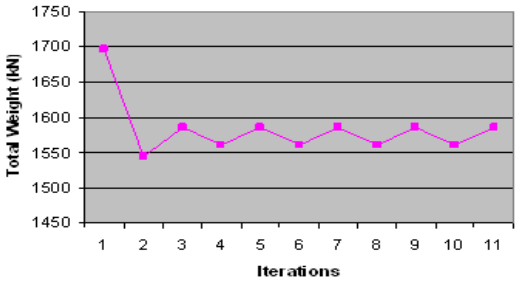

Fig. 3.13. History of Weight Reduction for Wall Loaded In-plane using Panel-wise Optimisation

Note: Iteration 1 in the above graphs represents *Initial Model*

Discussion

As is evident from the above table and graphs, the solution begins to oscillate from the 5th iteration onwards. 3rd iteration shows lesser weight between the two oscillating solutions and can be chosen as the final solution. As expected the panels subjected to the biggest bending moments (i.e. end panels at the base) are thickest and other panels allotted thicknesses based on their average von Mises stress.

Comparison with Scaled Model

Weight of Initial Model:	1696.544 kN
Weight of Optimal Solution:	1560.821 kN
Initial Wall Thickness:	200 mm

Therefore, uniform thickness of Scaled Model should be (1560.821/1696.544) x 0.2 = 0.184 m = 184 mm.

Weight of Scaled Model:	1560.821 kN
Top Deflection of Scaled Model:	49.7 mm

Weight of Optimised Model:	1560.821 kN
Top Deflection of Optimised Model:	43.1 mm

Percentage Reduction in Top Deflection: **13.28 %**

Conclusion

The results of optimisation using the proposed approach clearly show an improvement in both 'Weight' and 'Top Deflection' compared to the Initial model. Additionally, when compared with a scaled model, the optimal solution shows a reduction of 13.28 % in the Top Deflection. Moreover, the solution process does not require much iteration and converges within 10 iterations, thereby requiring less solution time. The panel wise approach thus looks to be more attractive and practical in optimising wall thicknesses.

3.8.2 Example 2 – Wall D (Wall Perpendicular to the Direction of the Applied Lateral Force) – Panel-Wise Optimisation

The model shown in Fig. 3.14 below depicts a planar wall fixed at the base and subjected to a single load case in the Global X direction. The magnitude of wind load increases towards the top of the wall. The width of the wall is 12 m and total height is 30 m. The initial thickness is 200 mm throughout the height. The model is meshed into 1000 finite elements that are grouped into 40 panels.

Physical Behaviour of the "Planar Wall"

The planar wall will behave as a vertical cantilever when subjected to lateral loading with the maximum bending moment occurring at the base. This wall will exhibit tension on both sides. Walls possess low out-of-plane stiffness and this wall too will not posses adequate out-of-plane stiffness, as the loading is perpendicular to the direction of the plane of the wall.

Finite Element Model

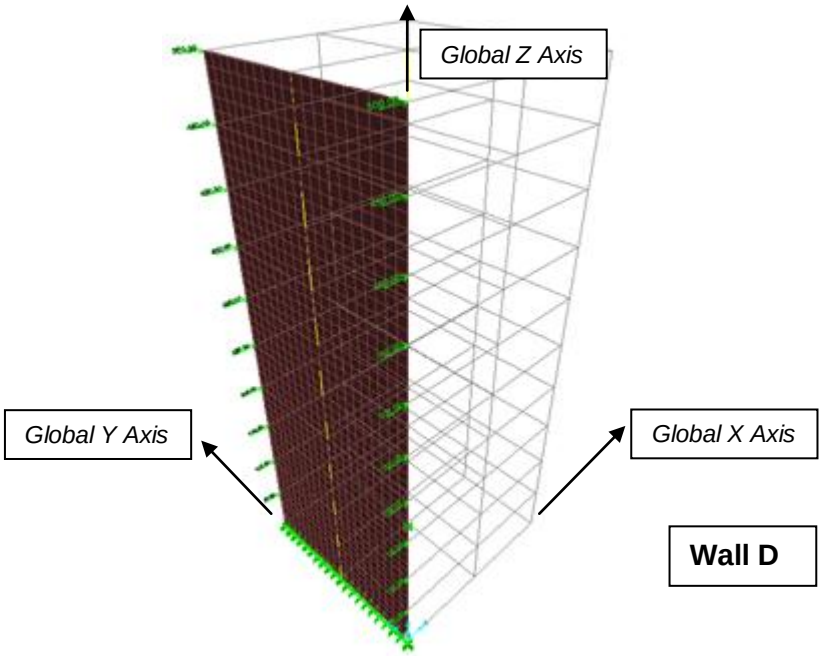

Fig. 3.14. Initial FE Model of Planar Wall Loaded Out-of-plane for Panel-wise Optimisation

Note: Moment magnification due to P-Δ effects is not considered in the model

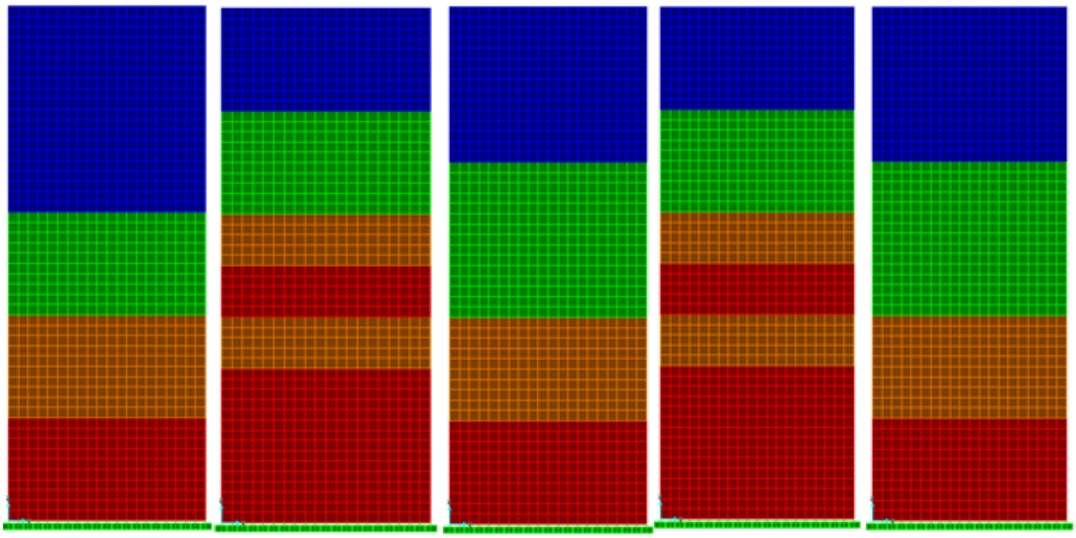

(a) 1st iteration (b) 2nd iteration (c) 3rd iteration (d) 4th iteration (e) 5th iteration

LEGEND:

Blue	:	160 mm
Green	:	180 mm
Orange	:	220 mm
Red	:	240 mm
Initial Thickness	:	200 mm

Fig. 3.15. Design Solutions for Wall Loaded Out-of-plane using Panel-wise Optimisation

Table 3.2. Results of Panel-wise Optimisation for Wall Loaded Out-of-plane

Sr. No.	Iteration	Top Deflection (mm)	Total Weight (kN)
1	INITIAL MODEL	142702.8	1696.544
2	1	110899.9	1628.682
3	2	91071.3	1764.406
4	3	108934.1	1645.648
5	4	91071.3	1764.406
6	5	108934.1	1645.648
7	6	91071.3	1764.406
8	7	108934.1	1645.648
9	8	91071.3	1764.406
10	9	108934.1	1645.648
11	10	91071.3	1764.406

Horizontal loads applied vary from 50 kN at Storey 1 to 500 kN at Storey 10. As a result, very high top deflection values are observed. Such high values never occur in practice. For code specified loading, the top deflection values observed were reasonable. The loading is exaggerated to demonstrate the applicability of the method.

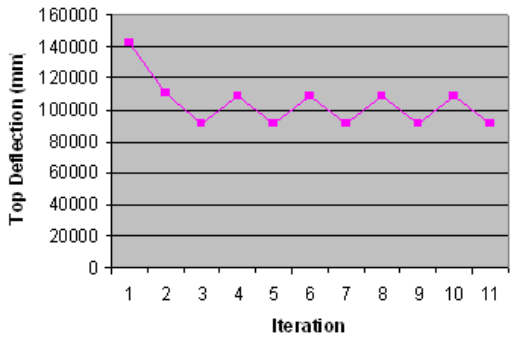

Fig. 3.16. Top Deflection History of Wall Loaded Out-of-plane using Panel-wise Optimisation

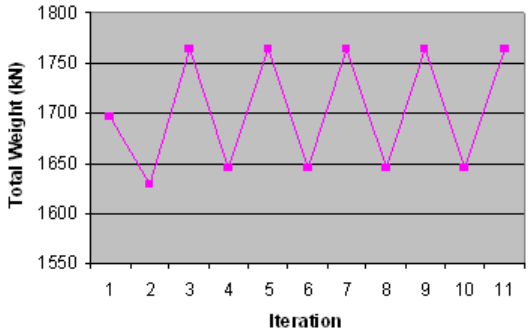

Fig. 3.17. History of Weight Reduction for Wall Loaded Out-of-plane using Panel-wise Optimisation

Note: Iteration 1 in the above graph represents *Initial Model*

Discussion

It is seen from the above graphs and table, that from the 5th iteration onwards, the solution begins to oscillate. 1st iteration shows the most weight savings and it also shows improvement in Top Deflection compared to initial model. However, the solution seems to settle on Iteration 2 or Iteration 3. Between these two, only Iteration 3 demonstrates a *saving in weight*. Top Deflections are reduced for all iterations. Iteration 3 can therefore be chosen as the optimal solution due to reduction in weight as well as Top Deflection.

Comparison with Scaled Model

Thickness of Scaled Model = (1645.648/1696.544)*0.2 = 0.194 m = 194 mm

Weight of Scaled Model: 1645.648 kN
Top Deflection of Scaled Model: 156356.7 mm

Weight of Optimised Model: 1645.648 kN
Top Deflection of Optimised Model: 108934.1 mm

Percentage Reduction in Top Deflection in the direction of lateral load: **30.33 %**

Conclusions

It is seen that the benefit of improvement in Top Deflection for Wall D (perpendicular to the direction of applied lateral loading) is much higher (30.33 % as against 13.28 % for Wall A).

Additionally, compared to the initial model, a saving in Total Weight of 3 % is attained by using the panel-wise method of optimisation.

It is evident from the results for both Wall A and Wall D above, that using *panel-wise optimisation*; the solution converges within fewer iterations. In both instances, there is an oscillating pattern observed and the solution that derives more benefits in terms of weight saving is chosen as the final solution (Top deflection in the direction of the applied lateral load is seen to decrease in every iteration).

3.8.3 Example 3 - Wall A – Element-Wise Optimisation

The model shown below is similar to Wall A used in example 3.8.1. It depicts a planar wall fixed at the base and subjected to a single lateral load case in the Global X direction. The magnitude of wind load increases towards the top. The width of the wall is 12 m and total height is 30 m. The initial thickness is 200 mm throughout the height. The model is meshed into 1000 finite elements. There are no panels in the initial model.

Physical Behaviour of the "Planar Wall"

The planar wall will behave as a vertical cantilever when subjected to lateral loading. This wall will exhibit tension on the windward side and compression on the leeward side. As the loading is in the direction of the plane of the wall, its high in-plane stiffness and strength makes it suitable to resist loading in its plane.

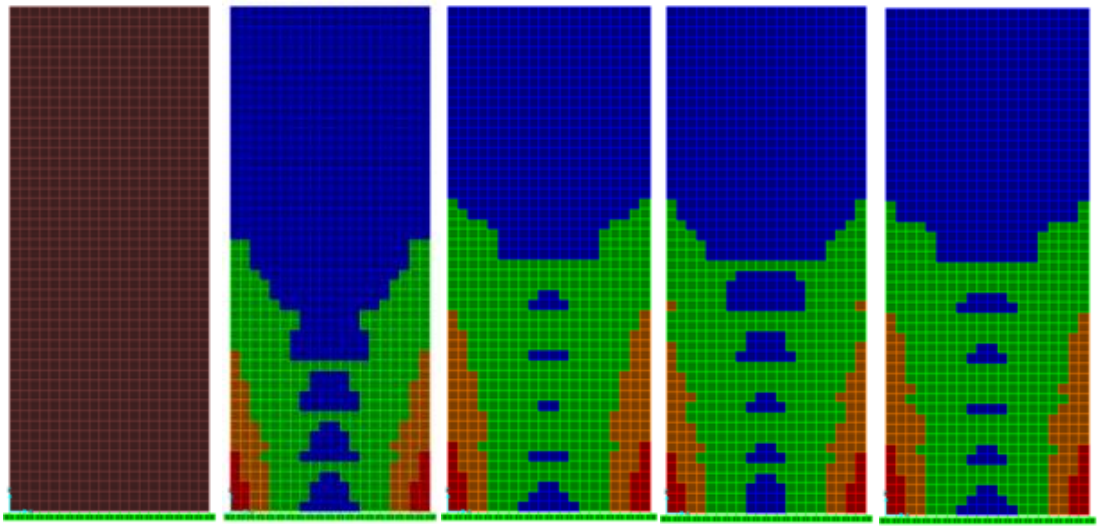

Fig. 3.18. Initial FE Model of Planar Wall Loaded In-plane for Element-wise Optimisation (a) 1st iteration (b) 2nd iteration (c) 3rd iteration (d) 4th iteration

Fig. 3.19. (a-d)

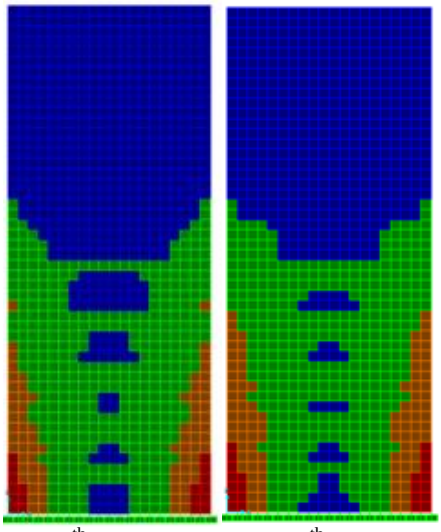

(e) 5th iteration (f) 6th iteration

Fig. 3.19. Design Solutions for Wall Loaded In-plane-plane using Element-wise Optimisation

Table 3.3. Results of Element-wise Optimisation for Wall Loaded In-plane

Sr. No.	Iteration	Top Deflection (mm)	Total Weight (kN)
1	INITIAL MODEL	45.794	1696.544
2	1	47.125	1450.545
3	2	45.673	1489.905
4	3	46.541	1470.904
5	4	45.794	1486.512
6	5	46.534	1471.582
7	6	45.797	1486.173
8	7	46.534	1471.582
9	8	45.797	1486.173
10	9	46.534	1471.582
11	10	45.797	1486.173
12	11	46.534	1471.582
13	12	45.797	1486.173
14	13	46.534	1471.582
15	14	45.797	1486.173

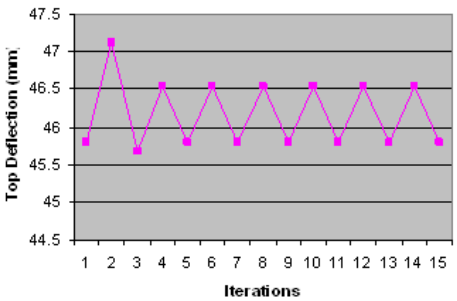

Fig. 3.20. Top Deflection History of Wall Loaded In-plane using Element-wise Optimisation

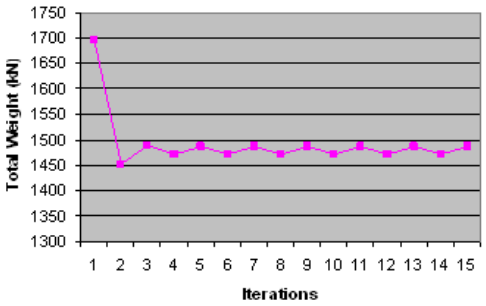

Fig. 3.21. History of Weight Reduction for Wall Loaded In-plane using Element-wise Optimisation

Discussion

As is seen from the above graphs and table, there is an oscillating pattern seen from the 5th iteration onwards. 1st iteration shows the most saving in weight, however it also shows an increase in Top Deflection compared to initial model. Reduced top deflections are not seen for all iterations. Between the 5th and 6th iterations, it is clear that the 5th iteration shows slightly more deflection than the initial model. Both of them demonstrate a saving in weight. 6th iteration can therefore be chosen as the optimal solution due to reduction in weight and almost similar deflection when compared with the Initial Model.

Comparison with Scaled Model

Thickness of Scaled Model = (1486.173/1696.544)*0.2 = 0.175 m = 175 mm

Weight of Scaled Model: 1486.173 kN
Top Deflection of Scaled Model: 52.30 mm

Weight of Optimised Model: 1486.173 kN
Top Deflection of Optimised Model: 45.794 mm

Percentage reduction in Top Deflection in the direction of lateral load: **12.43 %**

Conclusions

The comparison with a scaled model shows that the optimised model performs better (reduced Top Deflection) than the Scaled model. When compared with the panel-wise method, it is seen that the panel-wise method shows a slightly better improvement in Top Deflection (13.28 % improvement as against 12.43 % using *element-wise optimisation*). However, there is a much bigger improvement in weight savings using *element-wise optimisation* compared to *panel-wise optimisation* (12.38 % improvement compared to 3 % improvement using panel-wise method). As expected, the panel-wise method, being practical, is more conservative compared to the element-wise method.

3.8.4 Example 4 - Wall D – Element Wise Optimisation

The model shown below is similar to Wall D used in Section 3.8.2. It depicts a planar wall fixed at the base and subjected to a single lateral load case in the Global X direction. The magnitude of wind load increases towards the top of the wall. The width of the wall is 12 m and total

height is 30 m. The model is meshed into 1000 finite elements and there are no panels in the initial model.

Physical Behaviour of the "Planar Wall"

The planar wall will behave as a vertical cantilever when subjected to lateral loading with the maximum bending moment occurring at the base. This wall will exhibit tension on both sides. Walls possess low out-of-plane stiffness and this wall too will not posses adequate out-of-plane stiffness, as the loading is perpendicular to the direction of the plane of the wall.

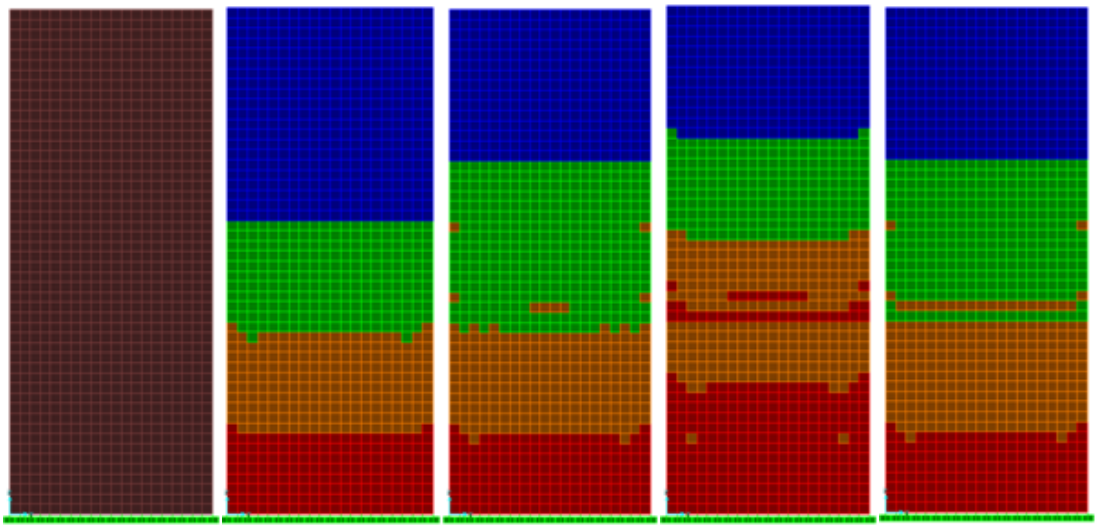

Fig. 3.22. Initial FE Model of Planar Wall (a) 1st iteration (b) 5th iteration (c) 10th iteration (d) 15th iteration

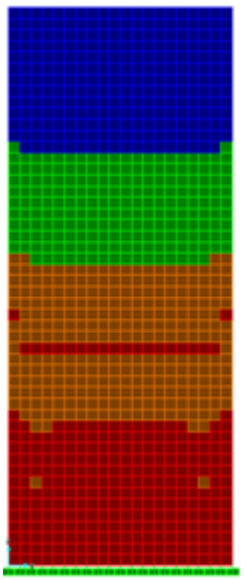

(e) 16th iteration

Fig. 3.23. Design Solutions for Wall Loaded Out-of-plane-plane using Element-wise Optimisation

Table 3.4. Results of Element-wise Optimisation for Wall Loaded Out-of-plane

Sr. No.	Iteration	Top Deflection (mm)	Total Weight (kN)
1	INITIAL MODEL	142702.846	1696.544
2	1	117069.499	1605.270
3	2	94646.091	1729.797
4	3	113855.375	1628.682
5	4	95741.235	1719.278
6	5	113321.052	1630.040
7	6	95907.306	1718.260
8	7	112639.484	1632.754
9	8	95976.528	1717.921
10	9	111922.526	1635.469
11	10	96160.628	1716.903
12	11	111624.754	1636.826
13	12	96252.534	1716.224
14	13	111006.680	1639.540
15	14	96464.114	1714.528
16	15	111006.680	1639.540
17	16	96464.114	1714.528
18	17	111006.680	1639.540
19	18	96464.114	1714.528
20	19	111006.680	1639.540

Horizontal loads applied vary from 50 kN at Storey 1 to 500 kN at Storey 10. As a result, very high top deflection values are observed. Such high values never occur in practice. For code specified loading, the top deflection values observed were reasonable. The loading is exaggerated to demonstrate the applicability of the method.

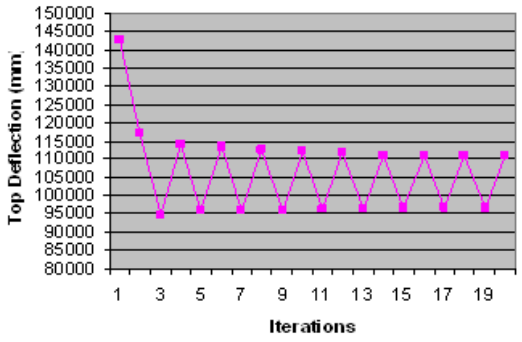

Fig. 3.24. Top Deflection History of Wall Loaded Out-of-plane using Element-wise Optimisation

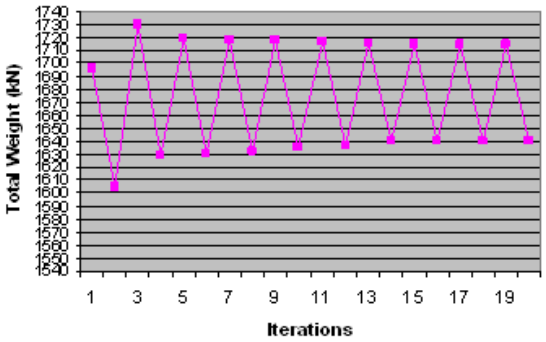

Fig. 3.25. History of Weight Reduction for Wall Loaded Out-of-plane using Element-wise Optimisation

Note: Iteration 1 in the above graph represents *Initial Model*

Discussion

It is seen from the above graphs and table, that the solution begins oscillating from the 15th iteration onwards. All the iterations show a reduced top deflection, however not all iterations show a reduced weight when compared to the Initial Model. The 15th iteration shows a weight higher than the Initial Model, whereas the weight of the 16th iteration is lesser than the Initial Model. The 16th iteration can therefore be chosen as the final solution. It exhibits less weight and lesser deflection as compared to the initial model.

Comparison with Scaled Model

Thickness of Scaled Model = (1639.54/1696.544)*0.2 = 0.193 m = 193 mm

Weight of Scaled Model: 1639.54 kN
Top Deflection of Scaled Model: 158799.63 mm

Weight of Optimised Model: 1639.54 kN
Top Deflection of Optimised Model: 111006.680 mm

Percentage reduction in Top Deflection in the direction of lateral load: **30.01 %**

Conclusions

The comparison with a scaled model shows that the optimised model performs much better (reduced Top Deflection) than the Scaled model. Using *element wise optimisation*, the benefit of improvement in Top Deflection for Wall D (parallel to the direction of applied lateral loading) is slightly less than using *panel wise optimisation* (30.01 % as against 30.33 %). However, there is a slightly increased saving in weight compared to the *panel wise optimisation* approach for Wall D (3.36 % as against 3 %). This difference is to be expected when employing the above two approaches.

3.8.5 Comparison of Results for Wall A and Wall D Using Both Methods

Table 3.5. Comparison of Top Deflection Reduction between Element-wise optimisation and Panel-wise optimisation for Wall Loaded In-plane and for Wall Loaded Out-of-plane

	Reduction in Top Deflection compared to Scaled Initial Model	
Optimisation approach	*WALL A (Loaded In-plane)*	*WALL D (Loaded Out-of-plane)*
Element wise	12.43 %	30.01 %
Panel wise	13.28 %	30.33 %

Table 3.6. Comparison of Concrete Weight Reduction between Element-wise optimisation and Panel-wise optimisation for Wall Loaded In-plane and for Wall Loaded Out-of-plane

	Reduction in Weight of the Wall	
Optimisation approach	*WALL A(Loaded In-plane)*	*WALL D(Loaded Out-of-plane)*
Element wise	12.38 %	3.36 %
Panel wise	3.00 %	3.00 %

It is seen from the above results that for both Wall A and Wall D, using a *panel wise optimisation* approach results in a slightly better performance in terms of Top Deflection improvement. This is to be expected as the *panel wise* method thickens or reduces the thickness of a group of elements together rather than individual elements. However, it is also seen that the *element wise* approach is comparably similar to the *panel wise* approach in terms of improvement in Top Deflection in the direction of the applied lateral load. On the contrary, using an *element wise optimisation* approach results in significant weight savings for Wall A (wall loaded in-plane). Even for Wall D, *element wise optimisation* shows a slightly more weight saving compared to the *panel wise* method. This too is to be expected as the *panel wise* approach, being an effort to make the design practical, is more conservative.

It is now proposed to employ these techniques on a multi-storey building having walls on all four sides.

3.8.6 Ten Storey 3D Structure (Panel-wise Optimisation using Ratios Algorithm)

The model depicts a 10-storey building with walls on all four sides. Though such a structure is not encountered in real buildings, the objective here is to demonstrate the effect of efficient material distribution in the walls when subjected to a Single Lateral Load Case (in the Global X direction in this case) with an increasing magnitude of wind load towards the top.

Data for the Model:

Initial Model (Initial Wall Thickness: 200 mm, Slab Thickness: 250 mm)

Symmetrical Model	Finite Element Details
2 bays in X direction and 2 bays in Y direction	Total No. of Elements: 8000
Each bay is 6m x 6m	WALL ELEMENTS: 4000
Floor-to-Floor Height is 3m.	SLAB ELEMENTS: 4000
No of Storeys: 10	NON DESIGN: SLAB ELEMENTS
Total Building Height: 30m	WALL PANELS: 160 (40 on each face)
Width at base: 12m	
Height-Width Ratio: 2.5	*Note:* There will be no Wall *Panels* for Element-wise Optimisation.

Loading:

Point loads in X-direction at each floor level with increasing magnitude towards the top.

Analysis:

Linear Static Analysis

Results

Panel Wise Optimisation

Physical Behaviour

All four walls will exhibit a cantilever action of bending with the two walls parallel to the direction of the applied lateral load exhibiting tension on the windward side and compression on the leeward sides. (Show figure from text). Of the other two walls (perpendicular to the applied lateral load), Wall D shown in the picture above will exhibit tension on both sides and Wall B on the back exhibits compression on both sides. All four walls will be optimised simultaneously using *panel-wise optimisation*. The resistance to lateral loading will be provided primarily by the in-plane stiffness of the walls parallel to the direction of loading. It is important to note that optimisation of cross-sections of the frame members is not carried out during this process. Obviously, the iterative frame member design process (involving iterative cross section optimisation) is available internally in SAP2000 (for various international design codes) and can be used to good effect in attempting to reduce the top deflection and inter-storey deflection of a multi storey building. Sizing optimisation of frame members such as columns and beams is beyond the scope of this work.

Finite Element Model

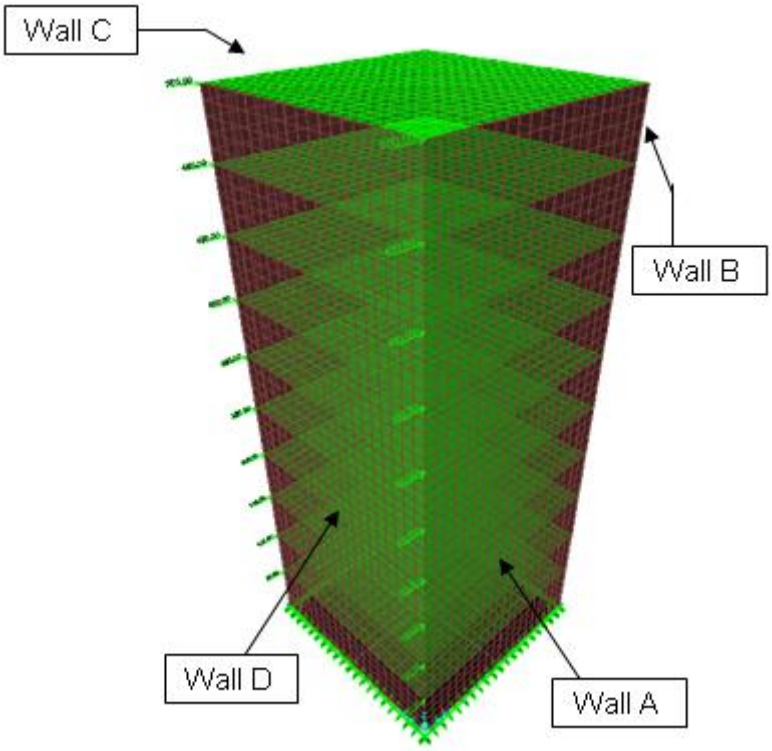

Fig. 3.26. Initial FE Model of 10-Storey 3D Structure

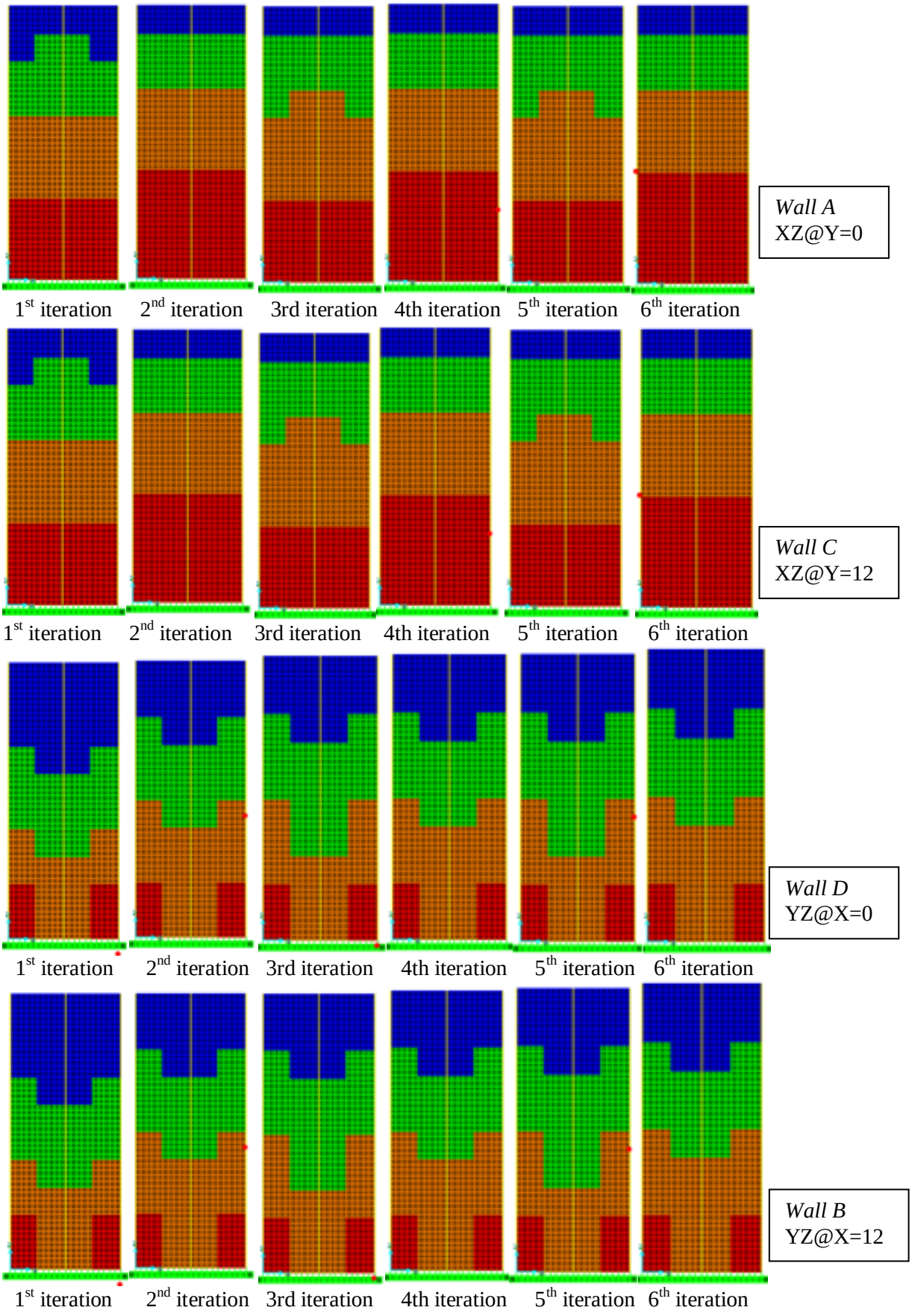

Fig. 3.27. Design Solutions for 10-Storey 3D Structure using Panel-wise Optimisation

Table 3.7. Results of Panel-wise Optimisation for 10-Storey 3D Structure

Sr. No.	*Iteration*	*Top Deflection (mm)* (Permissible Top Deflection: H/500 = 30000/500 = 60 mm)	*Total Weight (kN)*
1	Initial Model	13.92	15268.902
2	1	12.9	15201.041
3	2	12.6	15421.591
4	3	12.8	15319.799
5	4	12.6	15421.591
6	5	12.8	15319.799
7	6	12.6	15421.591
8	7	12.8	15319.799
9	8	12.6	15421.591
10	9	12.8	15319.799
11	10	12.6	15421.591
12	11	12.8	15319.799

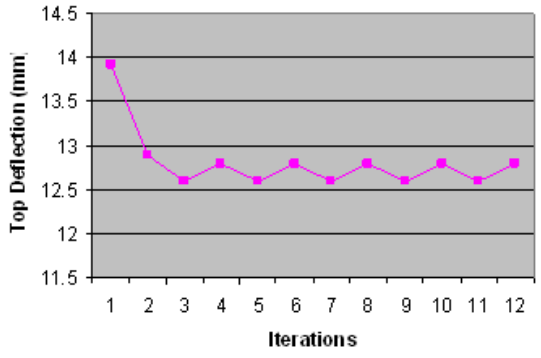

Fig. 3.28. Top Deflection History of 10-Storey 3D Structure using Panel-wise Optimisation

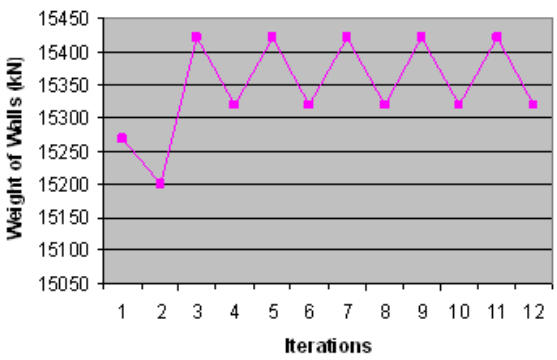

Fig. 3.29. History of Weight Reduction for 10-Storey 3D Structure using Panel-wise Optimisation

Note: Iteration 1 in the above graphs represents Initial Model

Discussion

An alternating pattern (for one panel) is seen in Wall A and Wall C from the fifth iteration onwards. The only iteration where there is a saving in Total Weight is in the first iteration. Refer the above two graphs. The solution begins to oscillate from the 5^{th} iteration onwards. Either 5^{th} iteration or 6^{th} iteration could be chosen as the optimal solutions. Compared to the initial model, the optimal solutions show an increase in weight for this 3D building model. Using the Panel based method of optimisation on individual walls (in examples 3.8.1 to 3.8.4) however does not show an increase in weight. However, it is important to note that no *panels* are allowed to remain at 200 mm (initial thickness of the wall). They are either increased or decreased. If more

divisions were created instead of four, there could have been more savings in Weight. For construction and architectural purposes, the *panel method* looks more practical.

Comparison with Scaled Model

Assuming we choose the 5^{th} iteration as the optimal solution.

Weight of Initial Model:	15268.902 kN
Weight of Optimal Solution:	15319.799 kN
Initial Wall Thickness:	200 mm

Therefore, uniform thickness of Scaled Model should be (15319.799/15268.902) x 0.2 = 0.201 m = 201 mm.

Weight of Scaled Model:	15319.799 kN
Top Deflection of Scaled Model:	13.91 mm

Weight of Optimised Model:	15319.799 kN
Top Deflection of Optimised Model:	12.80 mm

Percentage reduction in Top Deflection: **8.04 %**

Conclusions

Though there is a slight increase in weight (0.33 %) in the optimal solution, comparison with the scaled model shows that there is an improvement of 8 % in the top deflection for the marginal increase in weight. It is interesting to compare results for Wall A of this optimal solution with the optimal solution for *panel wise optimisation* of Planar Wall: Wall A (Example 1 in Section 3.8.1). Refer figures 3.30 and 3.31 on the next page. The algorithm used to assign panel thicknesses is based on Case A (Section 3.3.3: Panel wise optimisation). In Case A, the *average* von-Mises stress of *each element* is first calculated from the four nodal values for that element and this is repeated for each of the elements in the panel. Once the *average* von-Mises stress of *each element* in a panel is obtained, we then calculate the *average* von-Mises stress *for the panel*. This process is repeated for all designable wall panels in the structure. The *maximum* value among all *average* von-Mises stresses for designable *wall panels* is then found. The wall panels are then sorted in ascending order from minimum to maximum. For the same loads applied, the results show different panel thickness in the same regions for Wall A when modelled as a single planar wall and when modelled as part of a 3D building structure. This is because the maximum von Mises stress and consequently the *maximum panel stress* in Wall A

of the 3D building is *much lower* than for the planar wall, the 3D building being much stiffer. As a result, the numerical algorithm chosen assigns thickness to the panels based on the *ratios* of the *average stress in the panel* to the *maximum of the average stresses in all panels*. A brief explanation follows: Referring to Section 3.3.3 (Panel-wise Optimisation), it is clear that the maximum value of von Mises stress for all *panels* will be different for the four different cases. We have adopted Case A as the chosen approach. In the case of the building model, the *average* von Mises stress for the *middle panels at the bottom storey* is 4288.324 kN/sq.m and the *maximum* of the *average* von Mises stresses for *all panels* is 5382.815 kN/sq.m. The ratio is 0.796 > 0.75, therefore biggest thickness of 240 mm (RED) is correctly chosen. Whereas, for the planar wall (Fig 3.31 below), the ratio is 0.31 and it lies between 0.25 and 0.5, therefore a thickness of 180 mm is correctly chosen (GREEN). In the case of the planar wall, the *maximum* of the *average* von Mises stresses for all panels is *much higher* than for the building model. This is to be expected as the building model is much more stiffer than the planar wall. As a result, the numerical algorithm chosen assigns thickness to the panels based on the ratios of the *average* stress in the panel to the *maximum* of the *average* stresses in the panels. This maximum value of von Mises stress is different for the planar wall and the 3D building model. As mentioned above, it is much lower for the 3D building model than the planar wall, and this is expected as the building is much more stiffer than the planar wall. This comparison serves to illustrate this difference in results due to adopted numerical algorithms.

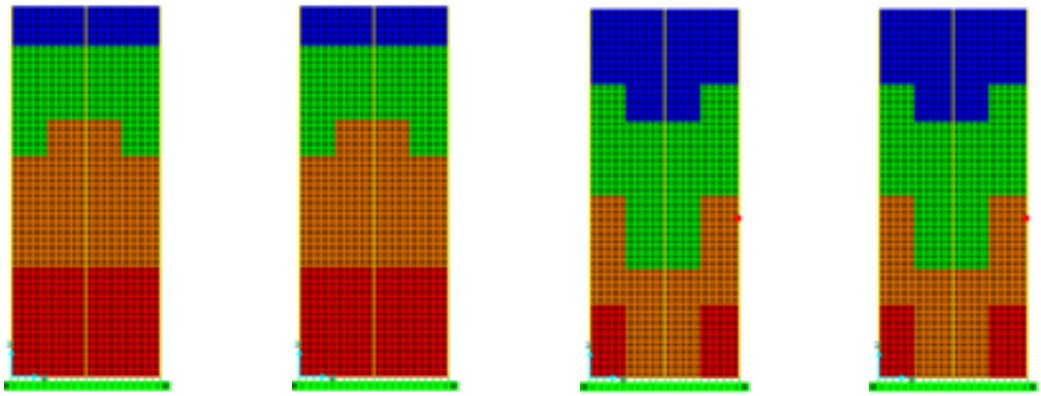

Wall A Wall C Wall B Wall D

Fig.3.30. Panel Wise Optimal Solution for *building model*

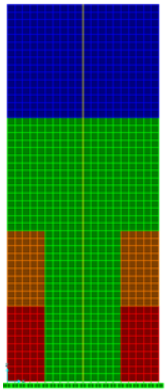

Planar Wall: Wall A

Fig. 3.31 Panel Wise Optimal solution for *Planar Wall* (Wall A)

3.8.7 Ten Storey 3D Structure (Element-wise Optimisation Using Ratios Algorithm)

This is the same model that is used in the example 3.8.6. The model this time however, is subjected to *element-wise optimisation* of its walls. It depicts a 10-storey building with walls on all four sides. Though such a building is not encountered in real structures, the objective here is to demonstrate the effect of efficient material distribution in the walls when subjected to a single lateral load case (in the Global X direction in this case) with an increasing magnitude of wind load towards the top.

Physical Behaviour

As mentioned before in example 3.8.6, all four walls will exhibit a cantilever action of bending with the two walls parallel to the direction of the applied lateral load exhibiting tension on the windward side and compression on the leeward sides. Of the other two walls (perpendicular to the applied lateral load), Wall D shown in the picture above will exhibit tension on both sides and Wall B on the back exhibits compression on both sides. All four walls will be optimised simultaneously using *Element-wise Optimisation*. The resistance to lateral loading will be provided primarily by the in-plane stiffness of the walls parallel to the direction of loading.

Finite Element Model

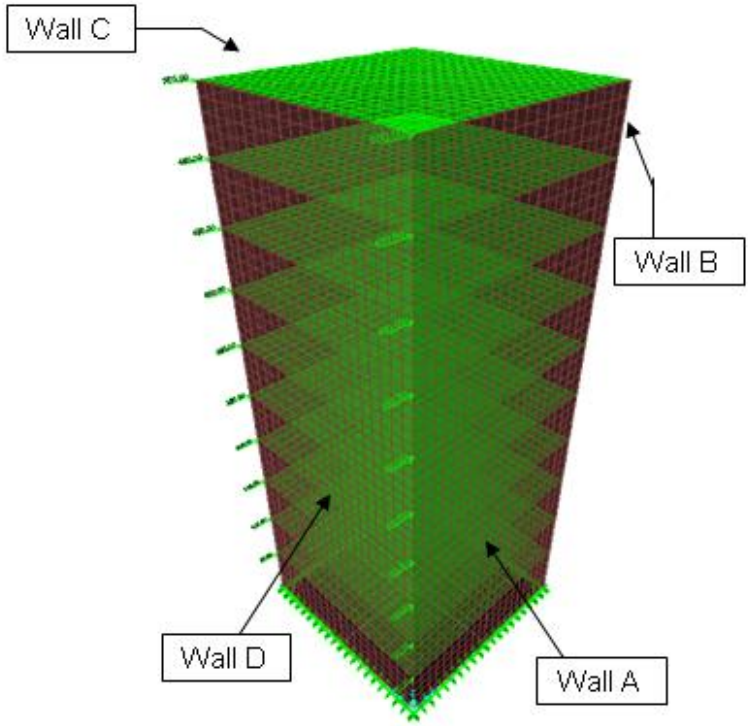

Fig. 3.32. Initial FE Model of 10-Storey 3D Structure

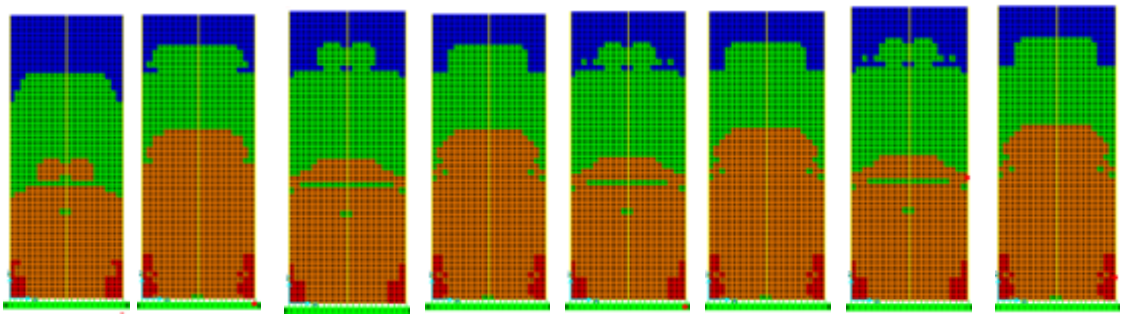

1st iteration 2nd iteration 3rd iteration 4th iteration 5th iteration 6th iteration 7th iteration 8th iteration

WALL A

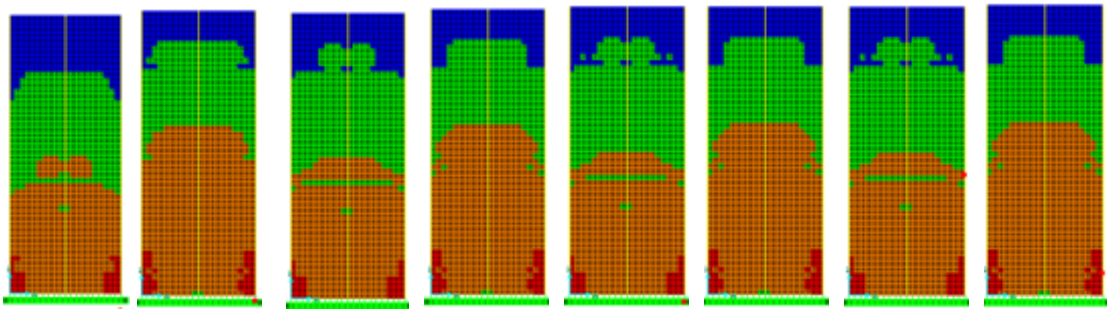

1st iteration 2nd iteration 3rd iteration 4th iteration 5th iteration 6th iteration 7th iteration 8th iteration

WALL C

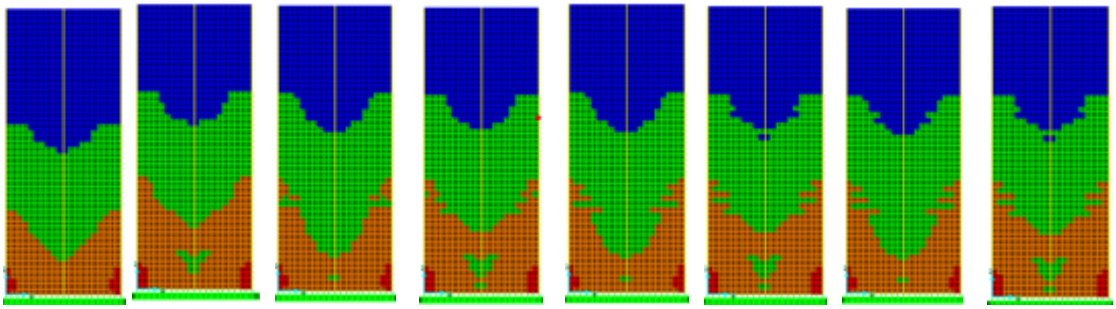

1st iteration 2nd iteration 3rd iteration 4th iteration 5th iteration 6th iteration 7th iteration 8th iteration

WALL D

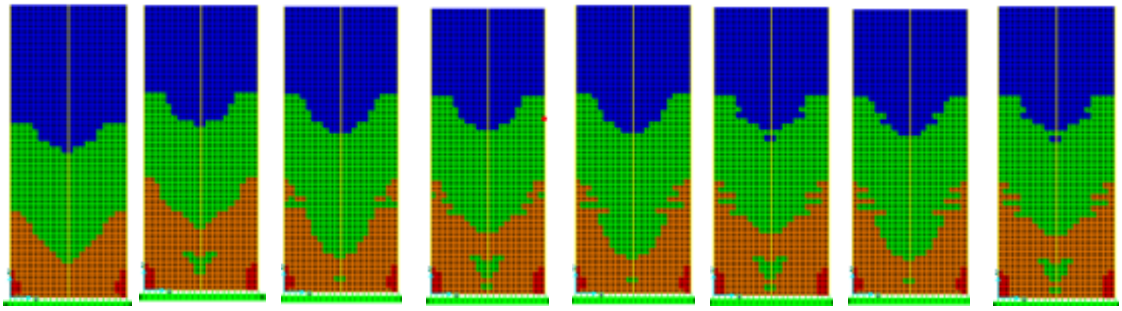

1st iteration 2nd iteration 3rd iteration 4th iteration 5th iteration 6th iteration 7th iteration 8th iteration

WALL B

Fig. 3.33. Design Solutions for 10-Storey 3D Structure using Element-wise Optimisation

Table 3.8. Results of Element-wise Optimisation for 10-Storey 3D Structure

Sr. No.	*Iteration*	*Top Deflection (mm)*	*Total Weight (kN)*
1	Initial Model	6.960	15268.902
2	1	6.892	14816.943
3	2	6.685	15037.494
4	3	6.824	14898.377
5	4	6.710	15014.421
6	5	6.818	14905.163
7	6	6.711	15013.063
8	7	6.820	14904.484
9	8	6.711	15013.063
10	9	6.820	14904.484
11	10	6.711	15013.063

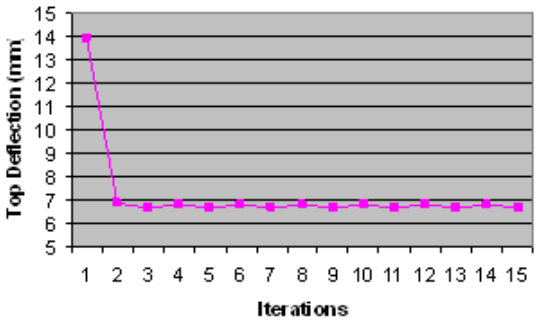

Fig. 3.34. Top Deflection History of 10-Storey 3D Structure using Element-wise Optimisation

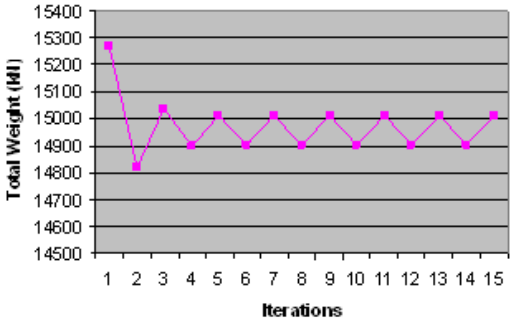

Fig. 3.35. History of Weight Reduction for 10-Storey 3D Structure using Element-wise Optimisation

Note: Iteration 1 in the above graphs represents Initial Model

Discussion

It is evident from the above table and graphs that the solution begins to oscillate from the 7th iteration onwards. Iteration 7 and Iteration 8 are the two oscillating solutions. Iteration 7 shows a lesser weight compared to Iteration 8 and can be chosen as the final solution. Though the deflection of Iteration 7 is slightly more than the deflection of Iteration 8, it is still well within the permissible limit of H/500 = 30000/500 = 60 mm. Therefore Iteration 7 is chosen as the final solution and is shown in Gray in Table 3.8 above.

Comparison with Scaled Model

Weight of Initial Model:	15268.902 kN (or 152 MN)
Weight of Optimal Solution:	14904.484 kN (or 149 MN)
Initial Wall Thickness:	200 mm

Therefore, uniform thickness of Scaled Model should be (14904.484/15268.902) x 0.2 = 0.195 m = 195 mm.

Weight of Scaled Model: 14904.484 kN (or 149 MN)
Top Deflection of Scaled Model: 7.10 mm

Weight of Optimised Model: 14904.484 kN (or 149 MN)
Top Deflection of Optimised Model: 6.82 mm

Percentage reduction in Top Deflection: **3.94 %**

Conclusion

Compared to the scaled model, the optimal model shows an improvement of almost 4 % in top deflection. When compared to the Initial Model, the optimised model shows a weight saving of 2.40 %.

It is interesting to note that weight savings and top deflection improvements are achieved in the optimal solution when *element-wise optimisation* is employed for this building model. However, when *panel-wise optimisation* is employed for this building model (refer example 3.8.6), no weight savings are achieved; though the improvement in top deflection is almost double that of *element wise optimisation* (8.04 % as against 3.94 %).

Again it is interesting to compare the results of *panel wise optimisation* and *element wise optimisation* for this 3D building model. Refer Wall A in Figure 3.36 and Figure 3.37. The difference in results for the middle panels of Wall A at the bottom storey can be explained as follows:

As explained before and in Section 3.3.3, the panels are allotted their thicknesses based on the *ratios* of the *average stress in the panel* to the *maximum of the average stresses in all panels*. The *average* von Mises stress for the *middle panels at the bottom storey* is 4288.324 kN/sq.m and the *maximum* of the *average* von Mises stresses for *all panels* is 5382.815 kN/sq.m. The ratio is 0.796 > 0.75, therefore biggest thickness of 240 mm (RED) is correctly chosen.
Whereas in *element-wise optimisation*, the thicknesses are allotted to each element based on the average von Mises stress in that element to the maximum von Mises stress in all elements. The maximum von Mises stress among all elements is 6963.581 kN/sq.m. For the single element lying in the region of the middle panel at the bottom storey (shown in Fig 3.37), the *average* von Mises stress in that element is 4285.438 kN/sq.m. The ratio is 0.615 (which is > 0.5 and less

than 0.75). Therefore, a thickness of 220 mm (ORANGE) is correctly chosen. This comparison therefore serves to explain the difference in results obtained for the same model in the same regions when using the two approaches to optimisation.

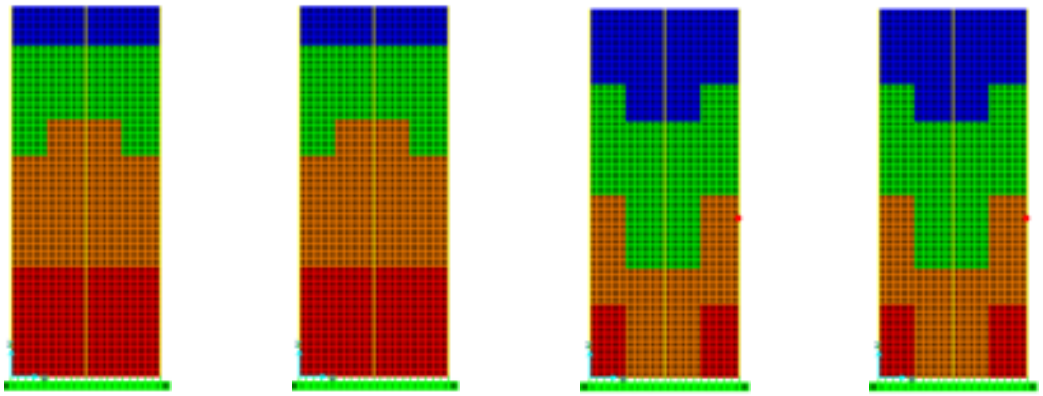

Wall A Wall C Wall B Wall D

Fig.3.36. Panel-wise Optimal Solution for *building model*

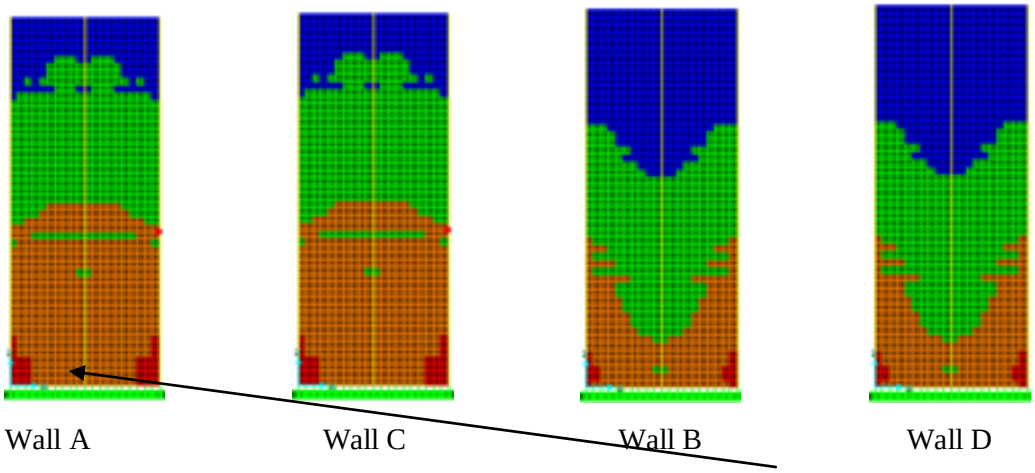

Wall A Wall C Wall B Wall D

Fig.3.37. Element-wise Optimal Solution for *building model* (Note the difference in result for region of the middle panel of Wall A at the bottom storey)

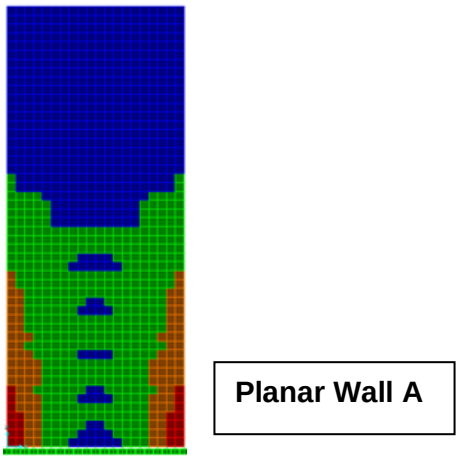

Fig 3.38. Element-wise optimal solution for *Planar Wall* A

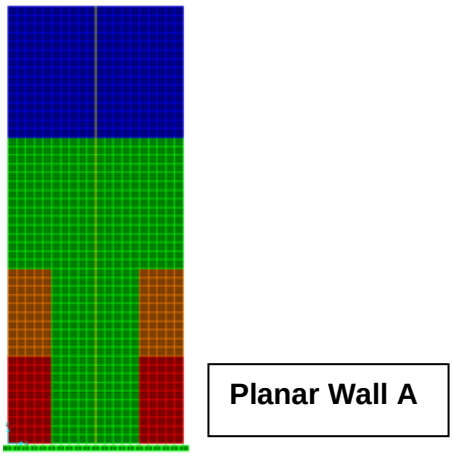

Fig 3.39. Panel-wise optimal solution for *Planar Wall* A.

Referring to Wall A in Figure 3.37 and Figure 3.38 above, the difference in results obtained in the same region of Wall A using *element-wise optimisation* for the 3D building model and the Planar Wall (Wall A) can be explained similarly to the explanation given in Section 3.5.6 of this chapter.

These comparisons therefore illustrate the differences in results obtained in the same region of a wall loaded in-plane when modelled as a planar wall and when modelled as part of a 3D multi-storey building. It also explains the differences in results obtained for the same 3D building model when using the two methods of optimisation.

From the above findings, only *element-wise optimisation* is performed in the subsequent examples using Ratios Algorithm.

The method is now applied to a shear wall – slab type structural building in the next section. External shear walls and internal core of the shear wall – slab type structural building are to be optimised.

3.9 Examples of Structural Walls in Multi-storey buildings

3.9.1 *Shear Wall – Slab* Type Structural System (Thickness optimisation of Shear Walls and Internal Core)

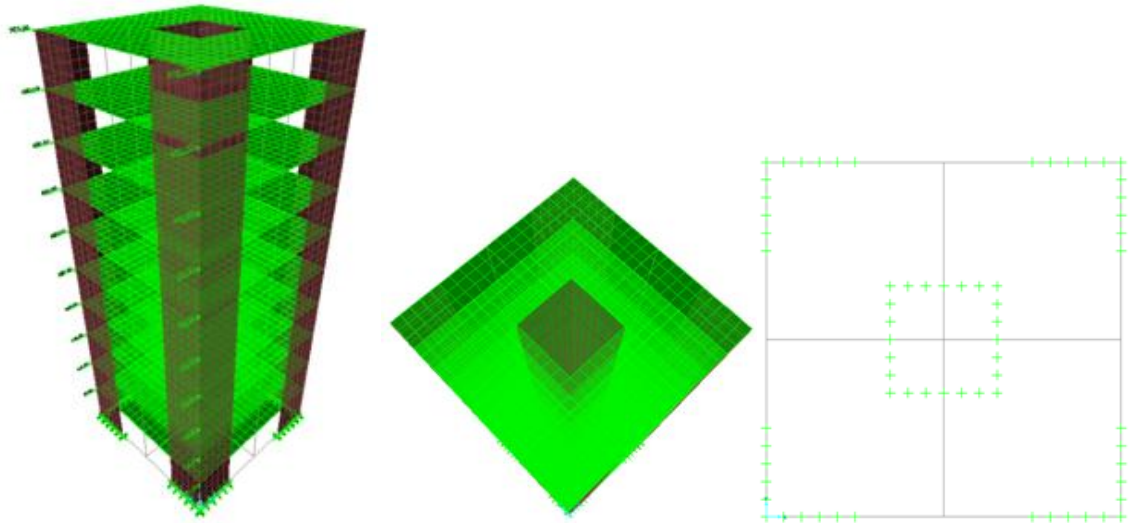

3D View | Core Wall Details | PLAN

Fig. 3.40. Initial FE Model and Plan of *Shear Wall – Slab* type structural system

The model depicts a 10-storey building with shear walls and an internal core.

Data for the Model

Initial Model (Initial Wall Thickness: 200 mm, Slab Thickness: 250 mm)

Symmetrical Model	**Finite Element Details**
2 bays in X direction and 2 bays in Y direction	Total No. of Elements: 6000
Each bay is 6m x 6m (Length of Shear Walls: 3m)	WALL ELEMENTS: 2000
Floor-to-Floor Height is 3m.	SLAB ELEMENTS: 4000
No of Storeys: 10	NON DESIGN: Slab Elements
Total Building Height: 30m	*Note:* There are no Wall *Panels* for Element wise optimisation
Width at base: 12m	Internal Core: 3m x 3m

Loading

Point loads in X-direction at each floor level with increasing magnitude towards the top.

Support Conditions

The shear walls and internal core are fixed at the base.

Analysis

Linear Static Analysis

Results

Element Based Optimisation

Physical Behaviour

In this example the resistance to horizontal loading is provided entirely by shear walls and the internal core. Their high in-plane stiffness and strength makes them well suited for bracing buildings up to about 35 stories, while simultaneously carrying gravity loading. The walls around the core can be considered as a spatial system capable of transmitting lateral loads in both directions. Additional advantage of core structures is that being spatial structures, they have the ability to resist all types of loads: vertical loads, shear forces and bending moments in two directions, as well as torsion, especially when adequate stiffness and strength are provided between flanges of open sections. The term "shear wall" is in some ways a misnomer because the walls deform predominantly in flexure. If the thickness and length of an assembly of shear walls changes over height, it generally results in a complex redistribution of the moments and shears between the walls, with associated horizontal interactive forces in the connecting girders and slabs. For simplification, it is assumed in this example that the lengths are constant over the height but the thickness of the walls are allowed to change. The total stiffness of such a system, as in the above example, exceeds the summation of the individual wall stiffnesses because; the connecting slab restrains the individual cantilever action by forcing the system to work as a composite unit (Smith and Coull 1991).

For the coupled shear walls shown in Figure 3.41, when the walls deflect under the action of the lateral loads, the slabs are forced to rotate and displace vertically, so that the slabs bend in double curvature and thus resist the free bending of the walls. The bending action induces shears in the slabs, which exert bending moments, of opposite sense to the applied external moments, on each wall. The shears also induce axial forces in the two walls, tensile in the windward wall and compressive in the leeward wall. The wind moment M at any level is then resisted by the sum of the bending moments M1 and M2 in the two walls at that level, and the moment of the axial forces N x l, where N is the axial force in each wall at that level and l is the distance between their centroidal axes.

$M = M1 + M2 + N \times l$

The last term N x l represents the reverse moment caused by the bending of the slabs which opposes the free bending of the individual walls. This term is zero in the case of linked walls, and reaches a maximum when the slabs are infinitely rigid (Smith and Coull 1991).

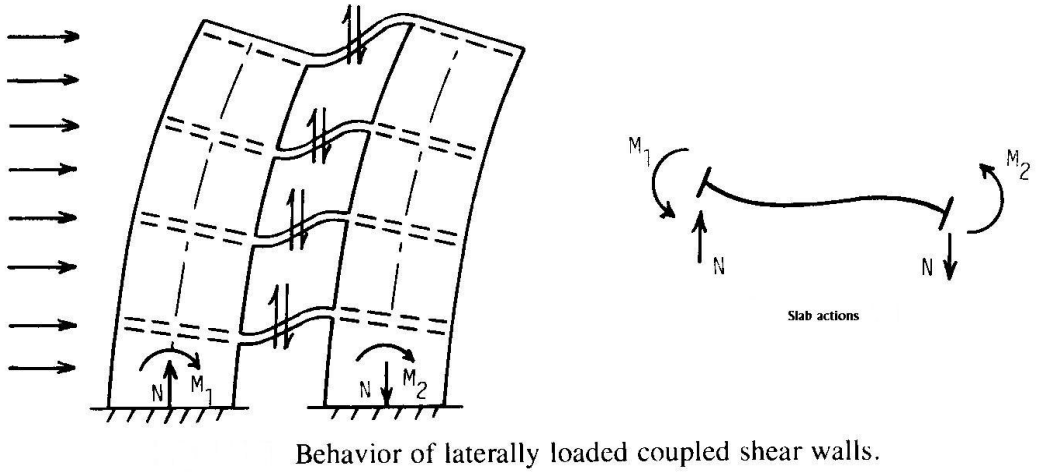

Fig. 3.41. Behaviour of laterally loaded coupled shear walls (Smith and Coull 1991)

The action of the slabs is then to reduce the magnitudes of the moments in the two walls by causing a proportion of the applied moment to be carried by axial forces. Because of the large lever arm l involved, a relatively small axial stress can give rise to a disproportionally larger moment of resistance. The maximum tensile stress in the concrete may then be greatly reduced. This makes it easier to suppress the wind load tensile stresses by gravity load compressive stresses (Smith and Coull 1991).

Optimisation Objective

The objective is to optimise the thickness of the structural shear walls and the internal core. By iteratively redistributing material, the aim is to reduce the weight of all the walls and check for improvements in Top Deflection of the optimal solution.

Optimisation History

The following illustrates the results of optimisation till convergence (six iterations in this example) for:

- Internal Core Walls parallel to the direction of applied lateral loading.
- Internal Core Walls perpendicular to the direction of applied lateral loading.
- Side Shear Walls parallel to the direction of applied lateral loading and
- Side Shear Walls perpendicular to the direction of applied lateral loading

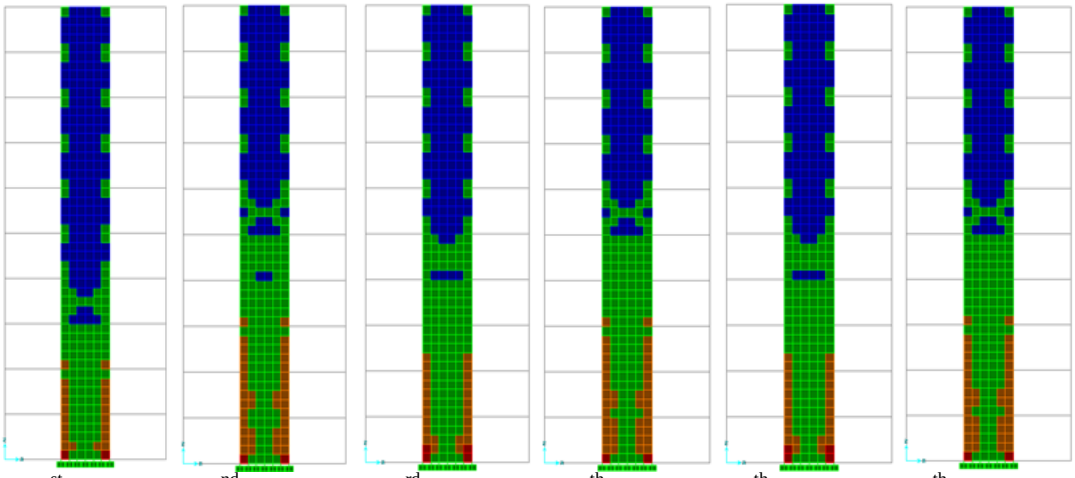

Fig. 3.42. Design Solutions for Core Wall Loaded In-plane

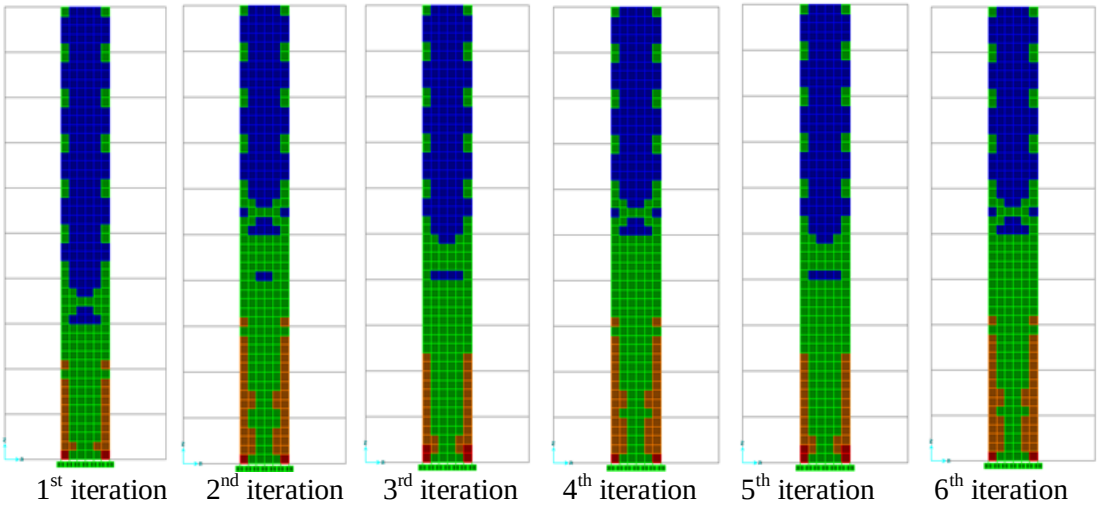

Fig. 3.43. Design Solutions for Core Wall Loaded In-plane

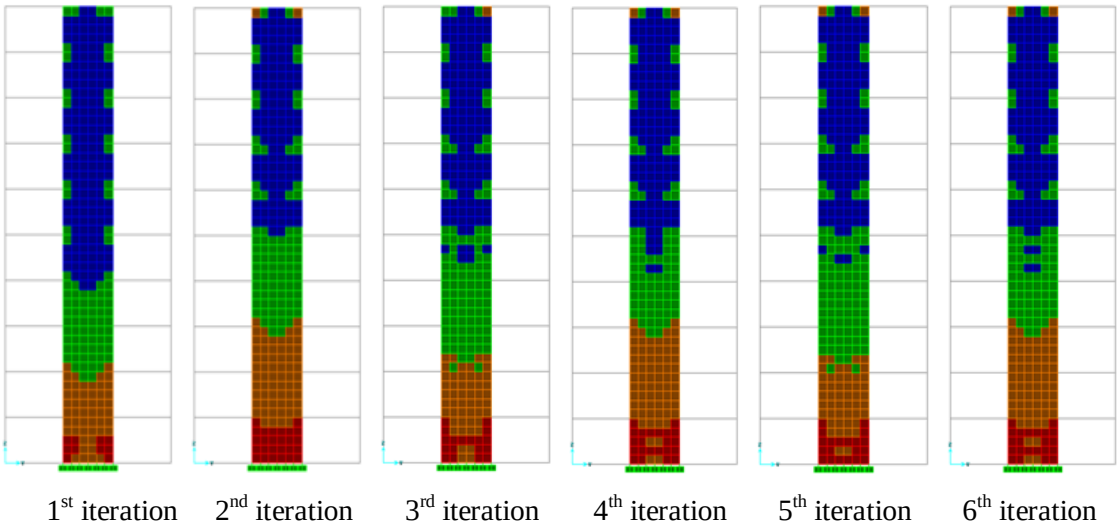

Fig. 3.44. Design Solutions for Core Wall Loaded Out-of-plane

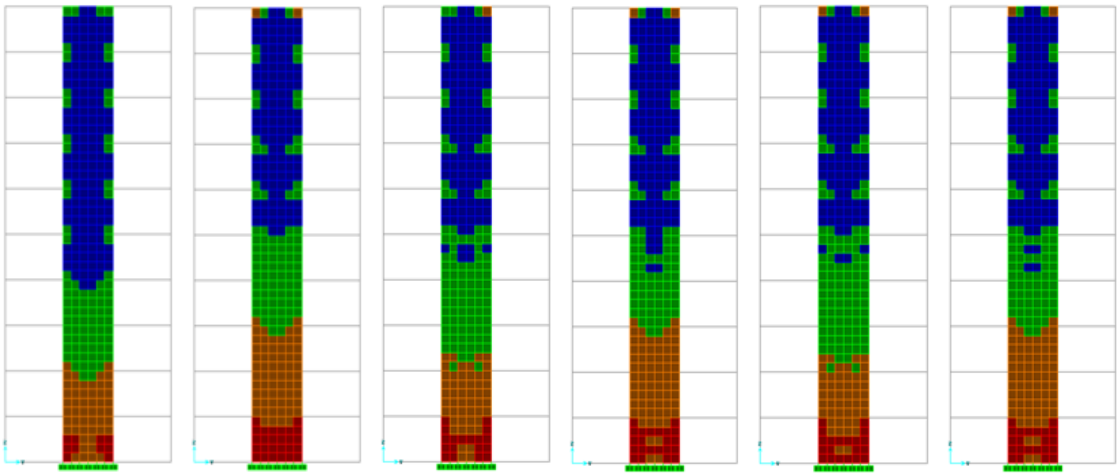

Fig. 3.45. Design Solutions for Core Wall Loaded Out-of-plane

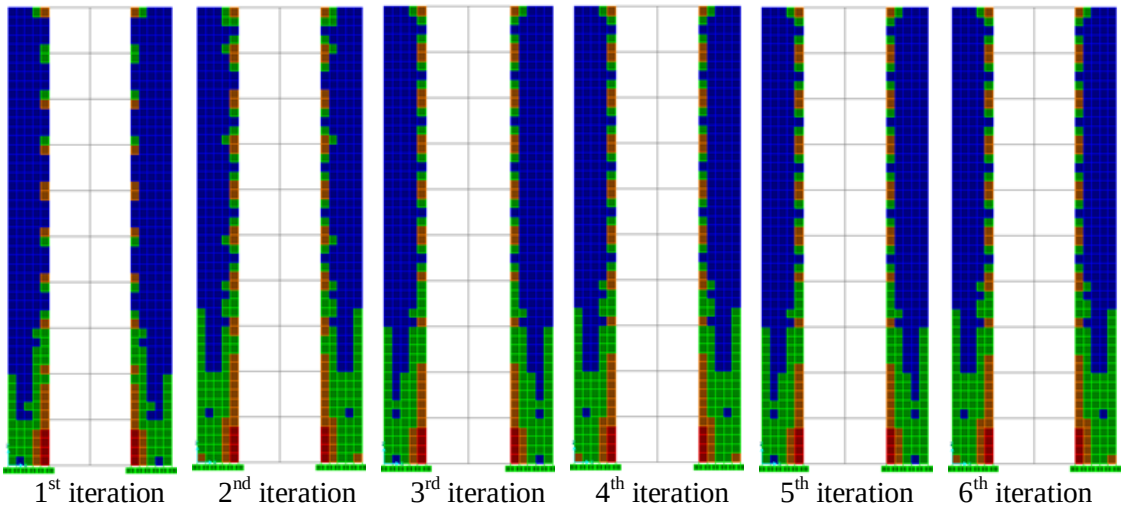

Fig. 3.46. Design Solutions for Side Shear Walls Loaded In-plane

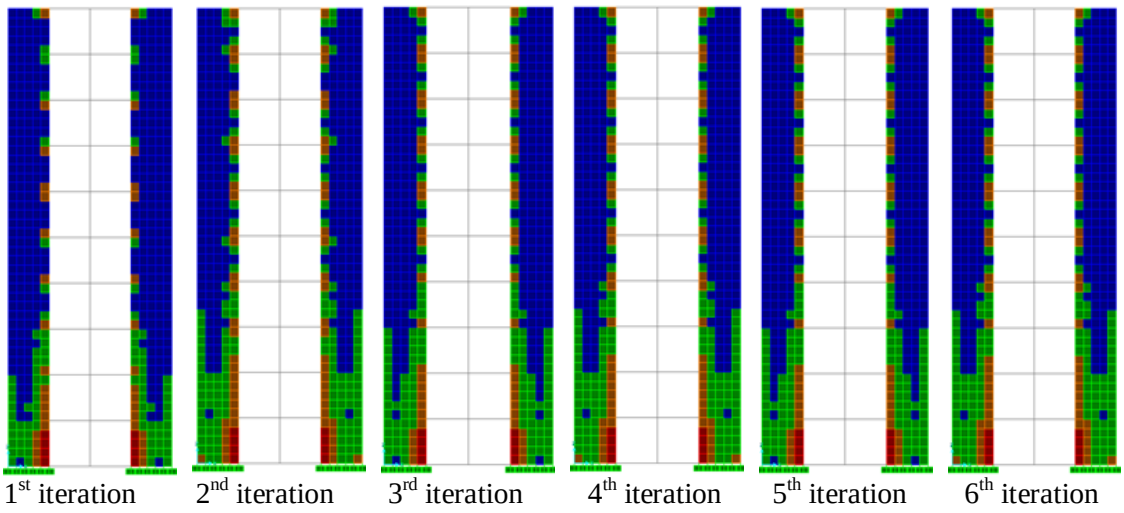

Fig. 3.47. Design Solutions for Side Shear Walls Loaded In-plane

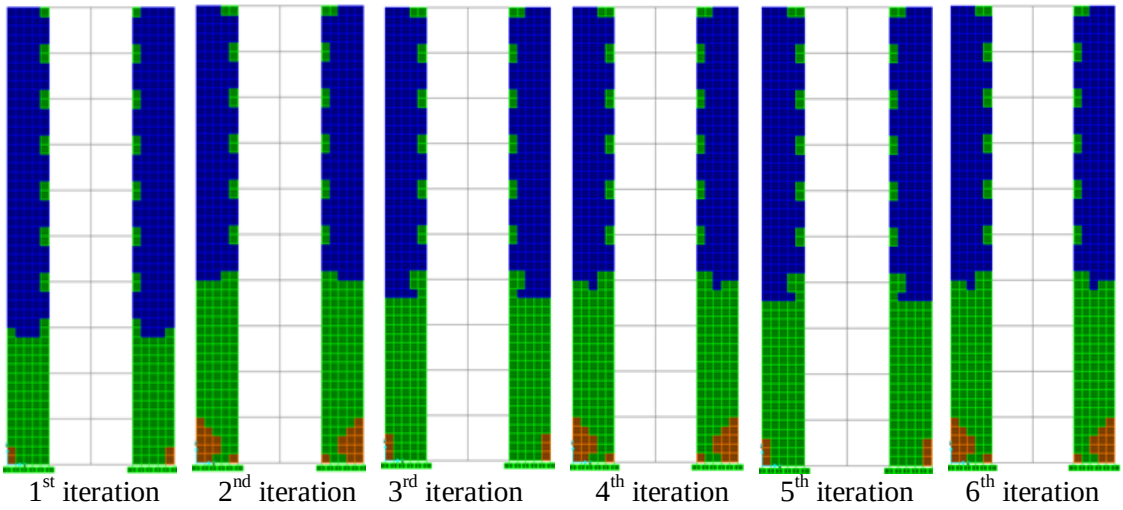

Fig. 3.48. Design Solutions for Side Shear Walls Loaded Out-of-plane

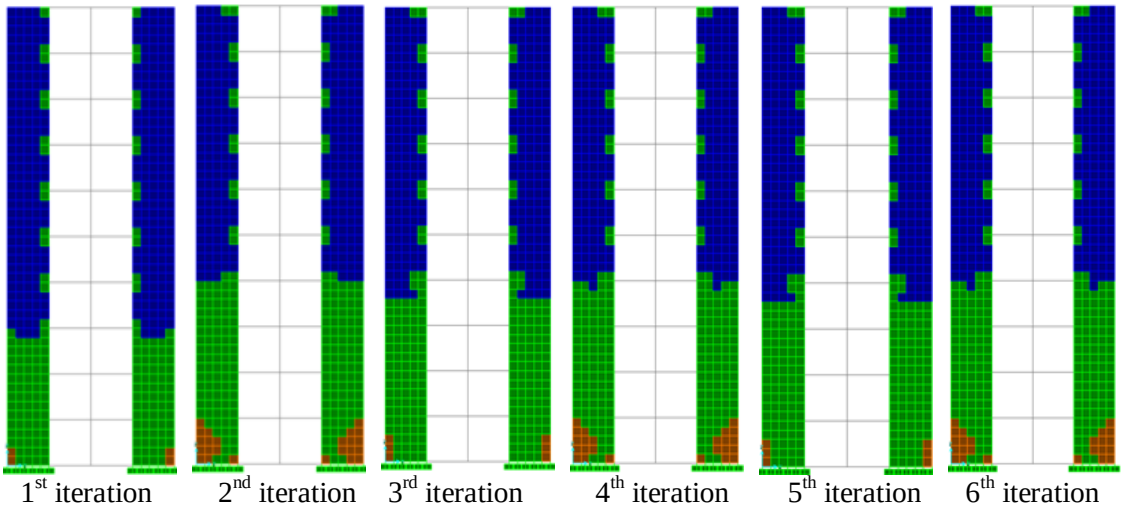

Fig. 3.49. Design Solutions for Side Shear Walls Loaded Out-of-plane

Table 3.9. Results of Element-wise Optimisation for *Shear Wall – Slab* Type Structural System

Sr. No.	*Iteration*	*Top Deflection in direction of load (mm)*	*Total Weight of all Walls (kN)*
1	Initial Model	43.90	5428.94
2	1	45.20	4634.96
3	2	43.63	4774.08
4	3	44.35	4710.29
5	4	43.63	4768.65
6	5	44.31	4712.32
7	6	43.63	4769.33
8	7	44.31	4711.64
9	8	43.63	4769.33
10	9	44.31	4711.64
11	10	43.63	4769.33

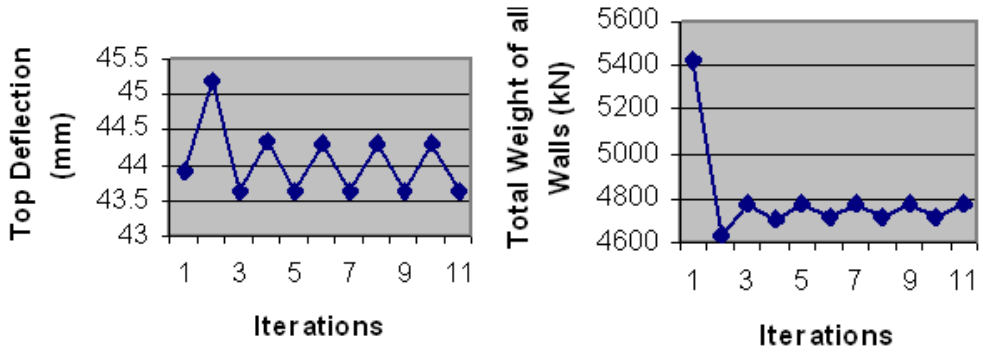

Note: Iteration 1 in the above graphs represents Initial Model

Fig. 3.50. Top Deflection History of *Shear Wall – Slab* type structure using Element-wise Optimisation

Fig. 3.51. History of Weight Reduction for *Shear Wall – Slab* type structure using Element-wise Optimisation

Discussion

The solution starts alternating in terms of weight from the 6th iteration onwards. Some walls have already settled before Iteration 6. In terms of weight savings and improvements in Top Deflection, 6th iteration is the optimum solution (as the 7th iteration shows Top Deflection more than the Initial model). From the results seen in the 'Optimisation History', it is clear that the shear walls in this example can be called as proportionate systems in which their lengths do not change throughout their height, but their changing wall thickness are the same at any level.

Comparison with Scaled Model

Thickness of Scaled Model: (4769.33/5428.94) x 0.2 = 0.175 m = 175 mm

Weight of Scaled Model:	4769.33 kN
Top Deflection of Scaled Model:	48.3 mm
Weight of Optimised Model:	4769.33 kN
Top Deflection of Optimised Model:	43.63 mm

Percentage reduction in Top Deflection: **9.73 %**

Conclusion

Comparisons with the scaled model show, that by optimising the wall thickness of all the shear walls and the internal core in the building, an improvement of almost 10 % is seen in the top deflection. Additionally, a weight saving of 13.20 % is seen in the weight of walls when compared to the initial model. It should be remembered that there are no frame elements in this building model. The lateral and gravity loads are supported by the walls and the floor slabs. The benefits of using the proposed method on a shear wall – slab type structural building is clearly seen from this example.

3.9.2 Thickness Optimisation of Core Walls for a 40 Storey Symmetric "Tube-In-Tube" (Hull-Core) Structural System

The model depicts a high-rise office building. It is a 40 storey symmetric "Tube-in-Tube" (Hull-Core) structural system. The outer framed tube consists of closely spaced columns connected by relatively deep spandrel beams. The inner tube consists of a rectangular concrete core. The following tables show the dimensions of the framing system.

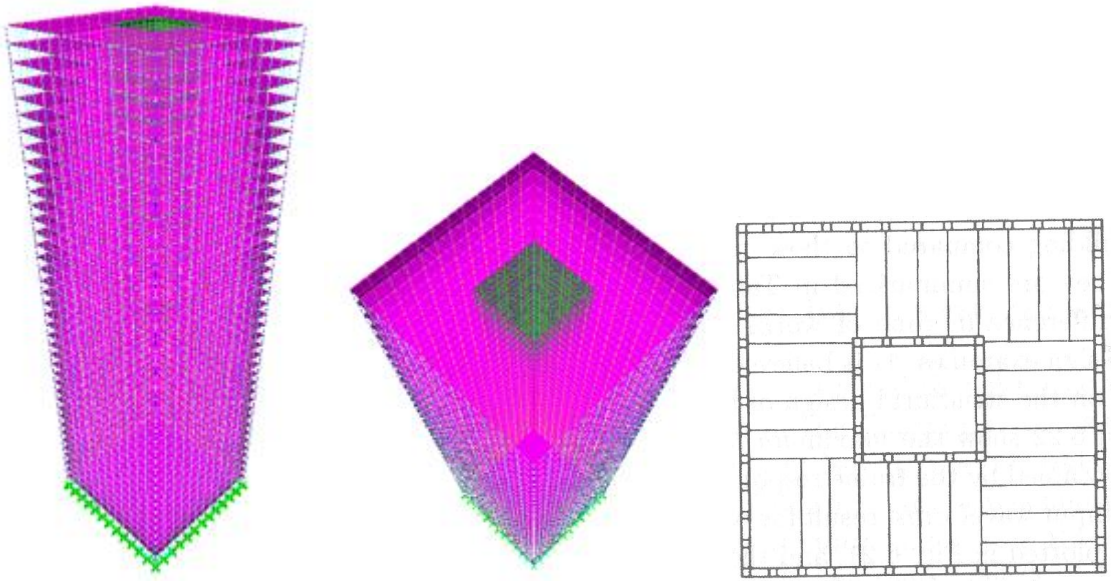

Exterior closely spaced columns and connecting Spandrel Beams forming a tube

Typical floor framing plan (Hiroyuki2001) Black lines indicate core- coupling girders

Fig. 3.52. Initial FE Model and Plan of 40-Storey Symmetric Hull-Core Structural System

Storey	*Exterior Tube*				*Material*	
	Corner Column		*Side Column*		*Concrete (MPa)*	*Steel (MPa)*
	Section	*Re-bars*	*Section*	*Re-bars*		
1-40	800 x 800	16-Y32	800 x 800	12-Y32	35	400

Storey	*GIRDERS*				*Material*	
	Exterior Tube		*Core Coupling*		*Concrete (MPa)*	*Steel (MPa)*
	Section	*Re-bars*	*Section*	*Re-bars*		
All	600 x 800	6-Y32	600 x 800	6-Y32	35	400

Initial thickness of internal core walls is 800 mm thick.

Physical Behaviour of the "Hull – Core" Structural System

The tube concept is an efficient framing system for tall slender buildings. In this system, the perimeter of the building consists of closely spaced columns connected by a relatively deep spandrel. The resulting system works as a giant vertical cantilever and is very efficient because of the large separation between the windward and leeward columns. The outer framed tube known as the "hull" or "tube" together with the internal core acts jointly in resisting both gravity and lateral loading. To some extent, the outer-framed tube and the inner core interact horizontally as the shear and flexural components of a wall-frame structure, with the benefits of increased lateral stiffness. The structural tube, however, usually adopts a highly dominant role because of its much greater structural depth. When a wall-frame structure is loaded laterally, the different free deflected forms of the walls and the frames cause them to interact horizontally through the floor slabs: consequently, the individual distributions of lateral loading on the wall and the frame may be very different from the distribution of the external loading. The horizontal interaction can be effective in contributing to lateral stiffness to the extent that wall-frames of up to 50 stories or more are economical (Taranath 1998).

We are concerned particularly, in this case, with a wall-frame structure that does not twist and, therefore, can be analyzed as equivalent planar models. These are mainly plan-symmetric structures subjected to symmetric loading.

The potential advantages of a wall-frame structure depend on the amount of horizontal interaction, which is governed by the relative stiffnesses of the walls and frames, and the height of the structure. The taller the building and, in typically proportioned structures, the stiffer the frames, the greater the interaction.

Considering the separate horizontal stiffnesses at the tops of a typical 10-storey elevator core and a typical rigid frame of the same height, the core might be 10 or more times as stiff as the frame. If the same core and frame were extended to a height of 20 stories, the core would then be only approximately three times as stiff as the frame. At 50 stories the core would have reduced to being only half as stiff as the frame. This change in the relative top stiffness with the total height occurs because the top flexibility of the core, which behaves as a flexural cantilever, is proportional to the cube of the height, whereas the flexibility of the frame, which behaves as a shear cantilever, is directly proportional to its height. Height, therefore, is a major factor in determining the influence of the frame on the lateral stiffness of the wall-frame (Taranath 1998). In this example, though the tube would play a dominant role in resisting the lateral loads, it is

expected that optimisation of the core wall thickness will result in lesser deflection at the top in the direction of the applied lateral load.

The classical mode of the interaction between a prismatic shear wall and a moment frame is shown in Figure 3.53 below.

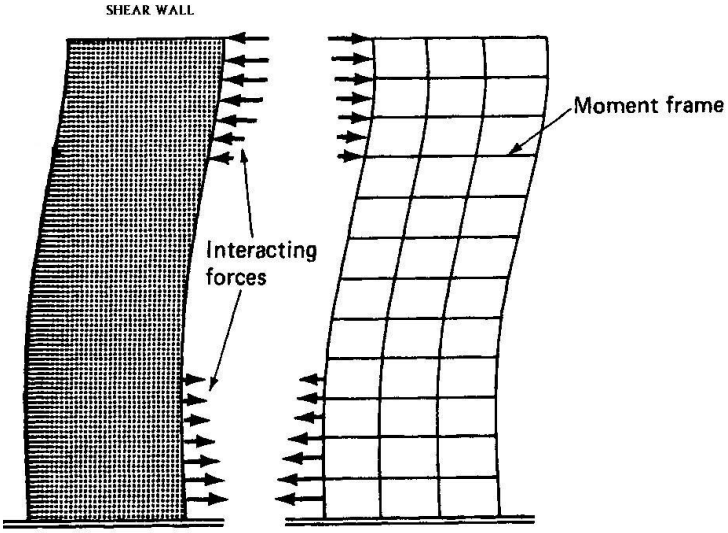

Shear wall-frame interaction.

Fig. 3.53. Shear wall – frame interaction (Taranath 1998).

The frame basically deflects in a so-called shear mode while the shear wall predominantly responds by bending as a cantilever. Compatibility of horizontal deflection produces interaction between the two. The linear sway of the moment frame, when combined with the parabolic sway of the shear wall results in an enhanced stiffness because the wall is restrained by the frame at the upper levels while at the lower levels the shear wall is restrained by the frame. However, it is not always easy to differentiate between the two modes because a frame consisting of closely spaced columns and deep beams tends to behave more like a shear wall responding predominantly in a bending mode. And similarly, a shear wall weakened by large openings may tend to act more like a frame by deflecting in a shear mode. The combined structural action, therefore, depends on the relative rigidity of the two, and their modes of deformation. Moreover, the simple interaction diagram shown above is valid only if:

- The shear wall and frame have constant stiffness throughout the height or;
- If stiffnesses vary, the relative stiffness of the wall and frame remains unchanged throughout the height. (Taranath 1998).

Optimisation Objective

The objective is to optimise the wall thickness of the internal core and check for top deflection improvements, if any. The weight of the internal core walls will be reduced during the optimisation.

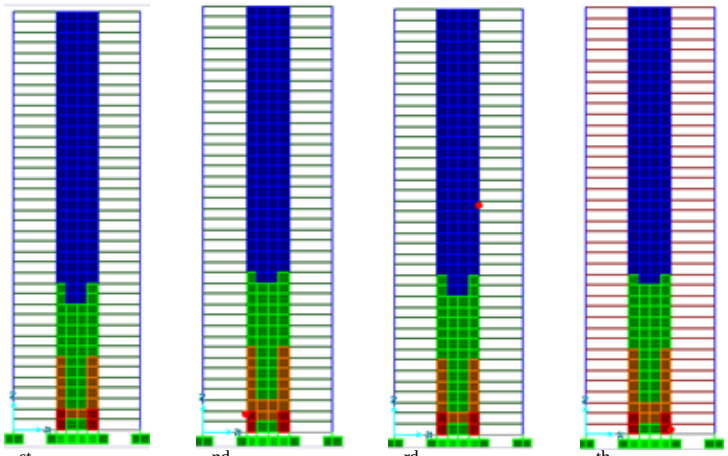

Fig. 3.54. Design Solutions for Wall Loaded In-plane

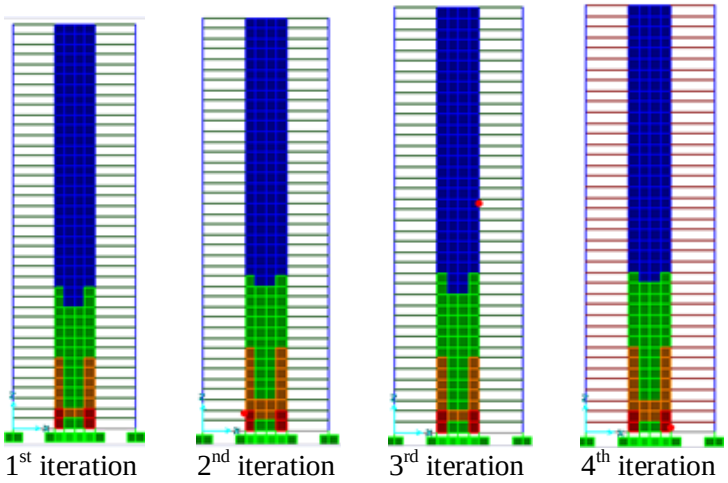

Fig. 3.55. Design Solutions for Wall Loaded In-plane

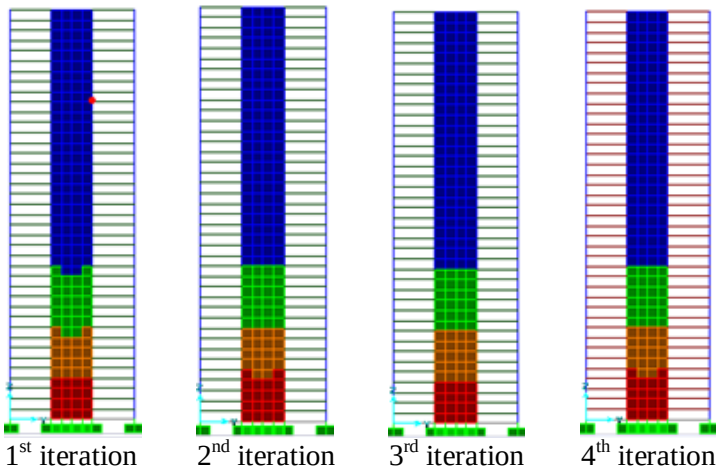

Fig. 3.56. Design Solutions for Wall Loaded Out-of-plane

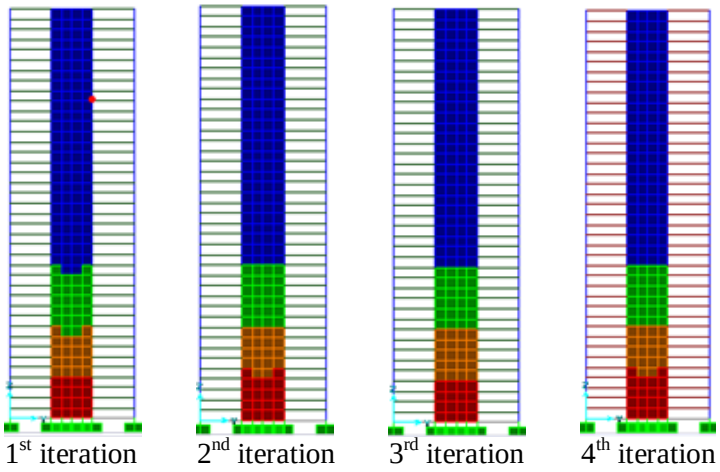

Fig. 3.57. Design Solutions for Wall Loaded Out-of-plane

Table 3.10. Results of Element-wise Optimisation for 40-Storey Symmetric Tube-In-Tube (Hull-Core) Structural System

Sr. No.	*Iteration*	*Top Deflection (mm)*	*Total Weight (kN)*
1	*Initial Model*	108.903	193029.092
2	1	108.116	186846.129
3	2	107.979	187177.897
4	3	108.061	186996.933
5	4	107.979	187177.897
6	5	108.061	186996.933
7	6	107.979	187177.897
8	7	108.061	186996.933
9	8	107.979	187177.897
10	9	108.061	186996.933
11	10	107.979	187177.897

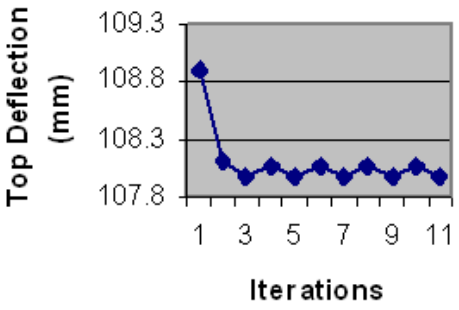

Fig. 3.58. Top Deflection History of *40-Storey Hull-Core Structural System* using Element-wise Optimisation

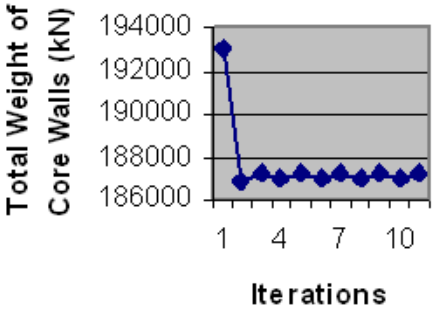

Fig. 3.59. History of Weight Reduction for *40-Storey Hull-Core Structural System* using Element-wise Optimisation

Discussion

The solution begins to alternate from the 5th iteration onwards. All the iterations show a slight improvement in top deflection. In terms of weight improvement, 3rd iteration is the optimal solution (% weight improvement: 3.13 %). In terms of deflection improvement, 4th iteration is the optimal solution. Either the third or the fourth iterations can be chosen as the optimal solutions as both demonstrate a saving in weight in addition to a marginal improvement in top deflection compared to the initial model. The iteration process converges quickly (in 4-5 iterations). Therefore, the benefits of efficient material distribution in the core wall of a 40 storey "Core-in-Tube" type building are clearly seen from the example chosen above.

Comparison with Scaled Model

Choosing iteration 3 as the optimal solution

Weight of Initial Model:	193029.092 kN (or 193 MN)
Weight of Optimal Solution:	186996.933 kN (or 187 MN)
Initial Wall Thickness:	800 mm

Therefore, uniform thickness of Scaled Model should be (186996.933/193029.092) x 0.8 = 0.775 m = 775 mm.

Weight of Scaled Model:	186996.933 kN (or 187 MN)
Top Deflection of Scaled Model:	110.195 mm

Weight of Optimised Model:	186996.933 kN (or 187 MN)
Top Deflection of Optimised Model:	108.061 mm

Percentage reduction in Top Deflection: **1.97 %**

Conclusion

Compared to the scaled model, the optimized model shows an improvement of almost 2 % in top deflection (and 3% reduction in weight). This small improvement in top deflection by optimizing the core walls thickness is to be expected as most of the resistance to lateral loads is provided by the closely spaced perimeter tube. The tube would normally assume a dominant role in resisting the lateral wind loads. This exercise demonstrates that even though the core plays a lesser role in resisting the lateral wind loads, optimizing its walls' thicknesses does result in a small improvement in top deflection.

3.10 Conclusions

- A variable thickness approach has the advantage that no element is removed and an element which makes a small contribution (i.e. has a small thickness) at a given iteration can be reinforced at a later iteration if necessary.

- When there is no further redistribution of moments and/or no further improvement in the solution, a steady state is reached. Though oscillations are observed around the solution before convergence, in all the examples the optimal solution, which has a reduced weight, performs better in terms of the top deflection compared to the scaled model. It could be said that the proposed approach does not necessarily give minimum weight designs due to the fact that no objective function is involved in the optimisation problem formulation. However, considering the benefits gained and the simplicity of the approach it is practically very useful, and it can be used as a good starting point for more rigorous design.

- For the building model, more improvement is obtained in both Top Deflection and Total Weight when using *element-wise optimisation* as compared to *panel-wise optimisation*. Though *panel-wise optimisation* is more conservative, it is more suitable for practical purposes as it is too costly to build a wall with continuous thickness variations.

- Using *panel-wise optimisation* the solution converges in less iterations. However, better improvements in terms of weight and top deflection reductions can be obtained when exploring with *element-wise optimisation* compared to *panel-wise optimisation*. Results using both approaches show good results.

- In the examples of planar walls, the results of *panel-wise optimisation* broadly follow a similar pattern to that of *element-wise optimisation*, which is to be expected.

- Generally, the thickness increases gradually towards the lower levels as anticipated, because the bending moment due to wind load is maximum at the base.

- If more thickness values are considered (i.e. more than four values are given for thickness selection), then the improvement in weight and top deflection will increase. The techniques described in this chapter can readily be extended to accommodate a large number of thickness choices.

CHAPTER 4: LAYOUT DESIGN FOR INFILL WALLS AND BRACING SYSTEMS IN MULTI-STOREY BUILDINGS

4.1 Introduction

This chapter builds on the work carried out in the previous chapter. In this chapter, the soft kill method of element removal is employed simultaneously together with thickness optimisation to obtain efficient layouts for various building models. Different problems are investigated and optimal topologies sought for each case. In this method, the thickness of each element is changed according to the procedure outlined in the previous chapter; additionally the ESO procedure of element removal is programmed in order to remove inefficient material as the design evolves. This approach is somewhat similar to Morphing ESO and the CAO/SKO method (Computer Aided Optimisation/Soft Kill Option) (Mattheck 1990). These methods remove inefficient material to improve the efficiency of the remaining material in the structure. The SKO method varies Young's modulus of the material instead of thickness. In this chapter three examples with different objectives (as the title of the chapter suggests) are presented to demonstrate the benefit and effectiveness of the proposed method. The objective is to seek the optimal topology and the thickness pattern simultaneously for the final design. The resulting solution is characterized by higher stiffness with lower consumption of material.

4.2 Assumptions and Limitations of the Work of this Chapter

The work in this chapter performs topological and size optimisation to investigate the optimal layout and thickness distribution of a structure for a given load case. The method of analysis employed is static and assumes linear elastic behaviour of the structure. A static analysis is carried out to obtain the von Mises stress in each finite element. The von Mises stress is used as a simpler, alternative criterion as the details of element stiffness matrix formulation cannot be obtained in SAP2000. The top deflection in the direction of the applied lateral load as calculated from the finite element analysis is recorded at each step in the iteration process. Similarly, the weight of the topology in each iteration is recorded during the optimisation. For simplicity and clarity of understanding in interpretation of results, a single load case (parallel to the Global X direction) is employed in all the examples. However, the proposed method can be extended for multiple load cases as well. The proposed method is not rigorous in a strictly mathematical sense, however it adopts a rational approach of variable thickness and element removal.

4.3 Optimisation Problem Formulation

Consider the problem of minimising the weight of a structure subject to a top deflection constraint in the direction of the applied lateral load. One way of achieving this objective is to derive a *sensitivity number* and perform a *sensitivity analysis* for the constraint on the specified top deflection and then apply the ESO method of structural optimisation to remove those elements that are least *sensitive*. This would reduce the weight of the structure with the least increase in top deflection in each iteration. The optimisation then proceeds until the specified amount of material is removed. A simpler approach for the objective mentioned above could be to perform unconstrained optimisation, i.e. without formulating the top deflection constraint into the optimisation and later comparing the solutions obtained from the optimisation procedure with this constraint to see if it is violated. The removal of elements in each iteration will result in a different topology each time. The thickness of the resulting topology in each iteration could be modified each time based on the element stress level so that highly stressed regions are thickened and lowly stressed ones are reduced. Although this approach is not rigorous in a strictly mathematical sense, it should achieve the dual objective of keeping the top deflection within permissible limits and reduce the weight of the structure at the same time.

For ESO 0-1 optimisation, Li *et al.* (1999) have shown the equivalence between the von Mises stress criterion and the stiffness criterion for element elimination or addition in evolutionary structural optimisation. They conclude that the criterion of von Mises stress *in the classical ESO method* is equivalent to the criterion of compliance minimization or stiffness maximization. In other words, the stiffness optimization problem can be solved by directly using the von Mises criterion and vice versa. Their results for ESO 0-1 optimisation implies that the 'strongest design' is also the 'stiffest design'.

4.4 Proposed Element Sizing and Removal Criteria

The *element-wise optimisation* procedure adopted in the previous chapter is modified in this chapter to allow for element removal as the optimisation proceeds. The removal of elements is done by implementing the ESO method (Soft Kill Option) which will be explained later in this section. As elements are removed in each iteration, the resulting design domain is assigned four different thicknesses. Depending on the ratio of the *average* von Mises stress in each element to the *maximum* of the *average* von Mises stresses, the thicknesses are assigned as follows:

- If Ratio is $\leq$ 0.25 (i.e. less than or equal to 25 % of the Maximum), assign minimum thickness Th_1.
- If Ratio is $\geq$ 0.75 (i.e. more than or equal to 75 % of the Maximum), assign maximum thickness Th_4.
- Similarly, if Ratio is > 0.25 and < 0.5 (i.e. between 25 % to 50 %), assign thickness Th_2.
- And, if Ratio is > 0.5 and < 0.75 (i.e. between 50 % to 75 %), assign thickness Th_3.

where, $Th_1 < Th_2 <$ Current or Initial Wall Thickness $< Th_3 < Th_4$

For example, if the initial thickness of a wall or design domain is 200 mm then,

Th_1	= 160 mm
Th_2	= 180 mm
Current or Initial Wall Thickness	= 200 mm
Th_3	= 220 mm
Th_4	= 240 mm

The algorithm decides Th_1, Th_2, Th_3 and Th_4 by increasing or decreasing 20 mm from the Initial Wall Thickness. The user has the option to change the increment or decrement from 20 mm to a value he/she desires, say 50 mm, in which case Th_1 would be 100 mm, Th_2 would be 150 mm, Th_3 would be 250 mm and Th_4 would be 300 mm.

It should also be noted however, that in addition to element removal, the level of change in top displacement and weight depends on this step size of increment or decrement. If the step size is increased, more material is added to or removed from elements and the total change in top displacement will be bigger. Equal step sizes are used in this study and investigating the effect of changing the step sizes is beyond the scope of this work. It is expected, that the user (an experienced structural engineer) specify the appropriate increment or decrement after specifying the initial thickness for the wall/s.

The removal of elements using the soft-kill option is performed as follows:

Using the ESO concept, if there are any elements that satisfy eq. (4.1) below, then they are assigned the least thickness (which could be $1/100^{th}$ of the minimum thickness i.e. $1/100^{th}$ of Th_1

in this algorithm). These elements (which are effectively removed) are coloured 'white' in the optimisation algorithm and will be known as 'white elements' hereafter in this chapter. The 'white elements' are present in the structure to avoid the occurrence of a singular stiffness matrix but they make negligible contribution to the load carrying behaviour of the structure. This approach is similar to the CAO/SKO method (Computer Aided Optimisation/Soft Kill Option) (Mattheck 1990), which is also used in Morphing ESO.

$$\frac{\sigma_e^{vm}}{\sigma_{\max}^{vm}} < RR_i \qquad (4.1)$$

where,

σ_e^{vm} = von Mises stress or selected criterion of element *e*.

$\sigma_{\max}^{vm}$ = Maximum von Mises stress or selected criterion of the whole structure

RR_i = Current rejection ratio.

The cycle of finite element analysis and element removal is repeated using the same value of RR_i until a steady state is reached, which means that there are no more elements being deleted at the current iteration. At this stage an evolutionary rate *(ER)* is introduced and added to the rejection ratio, i.e.

$$RR_{i+1} = RR_i + ER \qquad i = 0,1,2,3\ldots$$

With this increased rejection ratio the cycle of finite element analysis and element removal takes place again until a new steady state is reached. Such an evolutionary process continues until a desired optimum is reached, for example, when there is no material in the final structure of which the stress level is less than 25 % of the maximum (Xie and Steven 1997).

It should be noted here that in Morphing ESO, the set of discrete values that an element can change to are arranged in decreasing order, with the initial design being the thickest. As the optimisation proceeds, the thickness of elements is gradually reduced step-by-step to the next thickness specified in the list. This means that in order to 'remove' elements several iterations may initially be required in order to 'reach' the lowest specified thickness (i.e. white elements). This implies that elements will not get 'removed' until the second-last or penultimate thickness is reached by the program for some elements somewhere in the structure. Only when this penultimate thickness is reached or required for some elements in the structure, can the

morphing result in 'white elements' or element removal in the next iteration. Now, in the proposed approach, elements satisfying Equation 4.1 above are 'removed' (based on the initial value of RR specified and ER) and the resulting design domain is thickened and reduced at the same time (with respect to the thickness of the initial design). That is the solution does not have to 'reach' a particular penultimate thickness in order to 'remove' elements. Elements could therefore be 'removed' right from the first iteration, depending on the structural model, loading and evolutionary parameters. Most methods of thickness optimisation for in-plane loads are based on the SKO method and start from an initial thickest design, which is the maximum admissible thickness. Chu (1997) too adopts this approach in his work. In his work he has derived sensitivity numbers for single and multiple displacement constraints for minimum weight design, sensitivity numbers for minimum displacement design subject to weight constraint and sensitivity numbers for maximum stiffness design subject to weight constraint. The examples in his work are designed for sets of 2, 3 and 5 thicknesses. The set of discrete values are arranged in decreasing order. The thickness of elements is gradually reduced step-by-step to the next thickness specified in the list. In order to keep the change in the response quantity to a minimum, only a specified number of elements are subject to size reduction at each iteration. This number is prescribed as an integer number or as the ratio of the number of elements subjected to size changing to the total number of elements (*element changing ratio, ECR*) or as the ratio of the weight (material) to be removed in each iteration to the total weight (*material removal ratio, MRR*). The algorithm implemented in this chapter performs size optimisation (and topological optimisation) on all elements in the structure in each iteration. Size optimisation parameters such as *element changing ratio, ECR* and *material removal ratio, MRR* are not included in this approach. In this work the initial design is not the thickest. The thickness of the initial design is chosen such that it is appropriate for the span and loading. During the course of optimisation, the resulting design domain is thickened and reduced at the same time. Also, the constraint of top deflection is not formulated explicitly into the optimisation, which is effectively unconstrained. The optimal solution obtained from the optimisation procedure is then compared with a scaled model of similar weight (having uniform thickness all over) and improvement in top deflection, if any, is compared. It is generally observed, for almost all the examples, that there is an improvement in top deflection of the optimised model when compared with the scaled model.

To test the validity and effectiveness of the proposed method we now apply it on a *shear wall – slab* type structural system to investigate the need and location for infill walls.

4.5 Examples

4.5.1 Requirement for Infill Walls in a *Shear Wall – Slab* Type Structural System

In many countries infilled frames are the most usual form of construction for tall buildings up to 30 stories in height. Column and girder framing of reinforced concrete, or sometimes steel, is infilled by panels of brickwork, block work, or cast- in-place concrete. When an infilled frame is subjected to lateral loading, the infill behaves effectively as a strut along its compression diagonal to brace the frame.

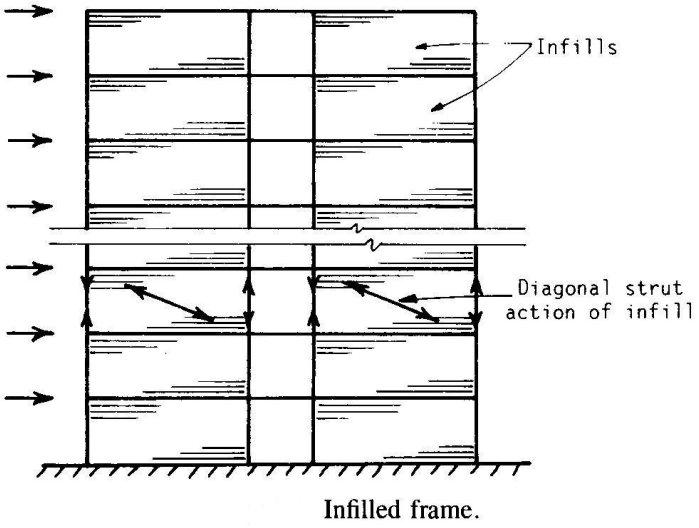

Fig. 4.1. Physical Behaviour of Infill Walls (Smith and Coull 1991)

Because the infills serve also as external walls or internal partitions, the system is an economical way of stiffening and strengthening the structure. It is difficult to predict with accuracy the stiffness and strength of an infilled frame due to the complex interactive behaviour of the infill in the frame, and the rather random quality of masonry. The finite element model of this example assumes that the infill is made up of cast-in-place concrete (RC infill). In many countries, when designing an infilled frame structure, it is common practice to design the frame for the total vertical and horizontal loading and to include the infills on the assumption that, with precautions taken to avoid load being transferred to them, the infills do not participate as part of the primary structure. However, evidence from frequently observed diagonal cracking of infill walls suggests that this approach is not always valid. The walls do sometimes attract significant bracing loads and, in so doing, modify the structure's mode of behaviour and the forces in the frame. It would have been better in such cases to design the walls for the lateral loads (Canbay *et al.* 2003).

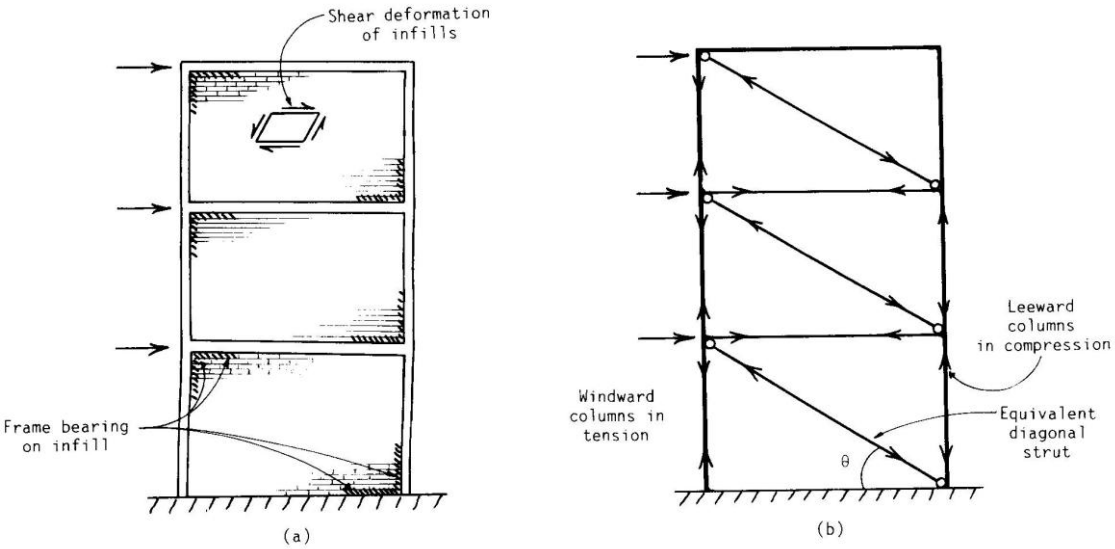

(a) Interactive behavior of frame and infills; (b) analogous braced frame.

Fig. 4.2. Interactive Behaviour of Frame and Infills (Smith and Coull 1991)

The wall braces the structure partly by its in-plane shear resistance and partly by its behaviour as a diagonal bracing strut. In a frame and masonry infilled wall structure three potential modes of failure of the wall arise and are illustrated in Figure 4.3.

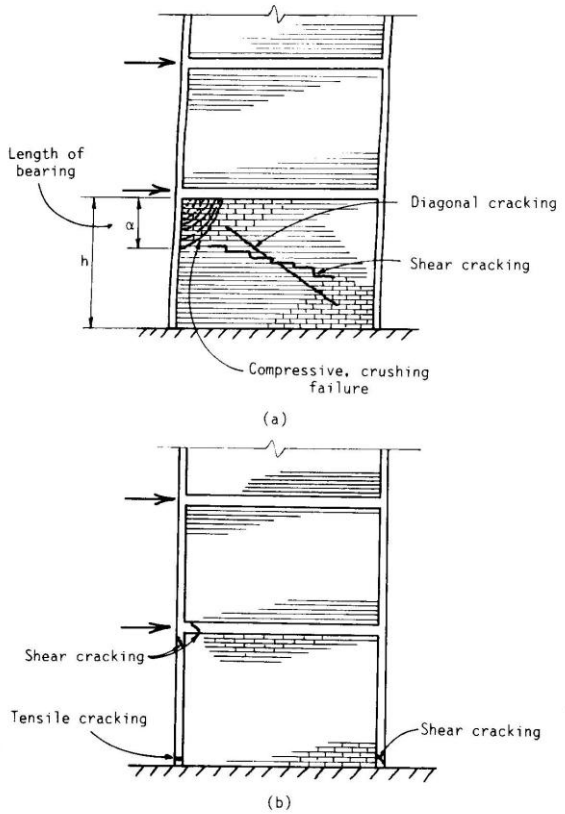

(a) Modes of infill failure; (b) modes of frame failure.

Fig. 4.3. Modes of Infill Failure and Frame Failure (Smith and Coull 1991)

The first is a shear failure stepping down through the joints of the masonry, and precipitated by the horizontal shear stresses in the bed joints. The second is a diagonal cracking of the wall through the masonry along a line, parallel to the leading diagonal, and caused by tensile stresses perpendicular to the leading diagonal. The "perpendicular" tensile stresses are caused by the divergence of the compressive stress trajectories on opposite sides of the leading diagonal as they approach the middle region of the infill. The diagonal cracking is initiated at and spreads from the middle of the infill, where the tensile stresses are a maximum, tending to stop near the compression corners, where the tension is suppressed. In the third mode of failure, a corner of the infill at one of the ends of the diagonal strut may be crushed against the frame due to the high compressive stresses in the corner. In a RC infill, the first mode of failure described above is generally not possible whereas the second and third modes of failure may occur and need to be suppressed by careful design (quantity of steel near the middle diagonal and thickness of concrete near the corners) of the infill walls (Canbay *et al.* 2003).

The model in figure 4.4 depicts an old 10-storey *shear wall – slab* type building that is supported by an internal rectangular core and four L shaped shear walls at the four corners. The thickness of these shear walls is the same as the thickness of the walls in the initial design. The shear walls and the internal core along with the slabs are treated as non-design domain to ensure that these areas remain unchanged. The walls on four sides between the shear walls represent the initial design domain for the optimisation process.

Model Data

2 bays by 2 bays 10-storied building with a rectangular core in the middle.

Span of each bay in both directions:	6 m
Length of each Shear Wall:	3 m
Floor to Floor Height:	3 m
Total Building Height:	30 m
Height-to-width ratio:	2.5
Initial Thickness of Design Domain:	200 mm
Thickness of Shear Walls and Internal Core:	200 mm
Slab thickness:	250 mm

Loads

A single lateral load case parallel to the Global X direction with magnitude of loads increasing towards the top.

Support Conditions

Fixed at the bottom of "L shaped Shear Walls" and Internal Core.

Analysis

Linear static elastic analysis.

Optimisation Objective

The objective of this optimisation is to see the need and location of infills that serve structurally to brace an old building against horizontal loading. In this example, a *shear wall-slab* type structure is chosen over a frame structure, as an ESO based optimisation for need of infill walls in a framed structure reveals a distinct bracing pattern. The purpose here instead is to check the necessity of infills *walls* in specific regions of the old building that serve structurally to brace the building against horizontal loading. It is assumed that the shear walls and the internal core in the old building require strengthening and repairing. Strengthening may be defined as rehabilitation to upgrade the strength of existing structures. Strengthening made by adding RC infills in specific locations can increase the lateral stiffness of the structure significantly. The impact of different types of connections of the infill walls to the surrounding structure (such as shear keys, dowels and chemical anchors etc) on the analysis and stiffness of the structure with the added walls is beyond the scope of this study. Similarly, this work does not take into account the different cracking histories of the old structure and the new walls, built at different times. To account for this would require experimental investigation to determine the internal force distribution.

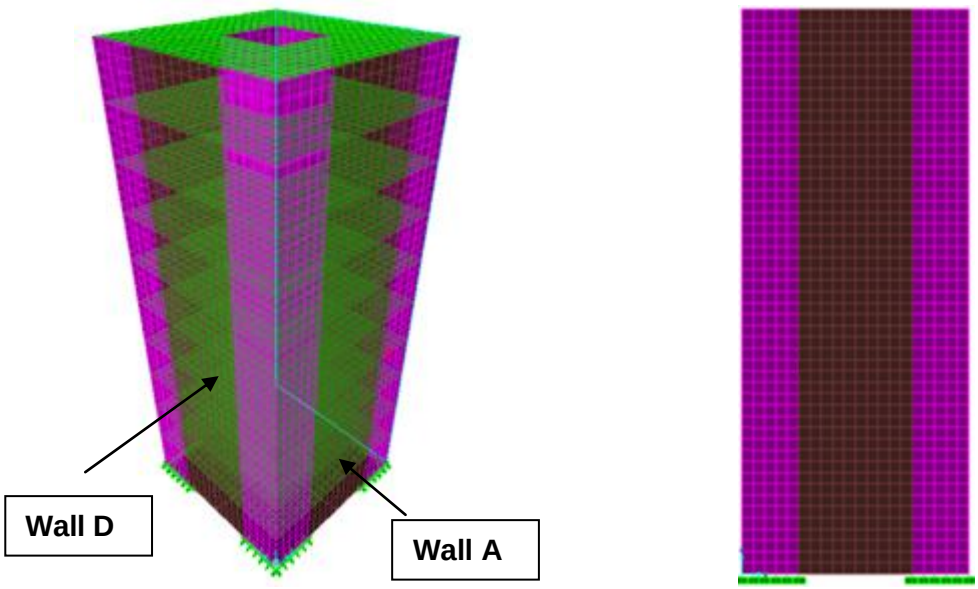

(a) 3D View **(b)** Planar View

Fig. 4.4 (a-b). Initial FE Model of Infill Walls in a *Shear Wall – Slab* Type Structural System

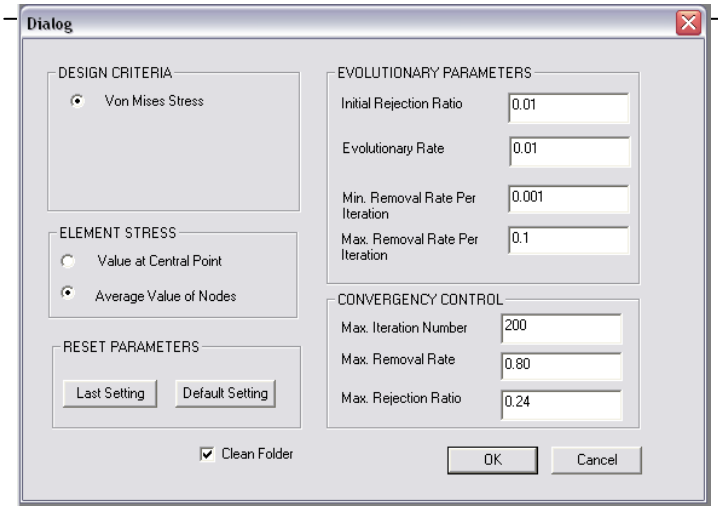

LEGEND

Blue	:	160 mm
Green	:	180 mm
Orange	:	220 mm
Red	:	240 mm
White	:	1.60 mm
Initial Thickness	:	200 mm

Fig. 4.5. ESO Optimisation Parameters for element removal

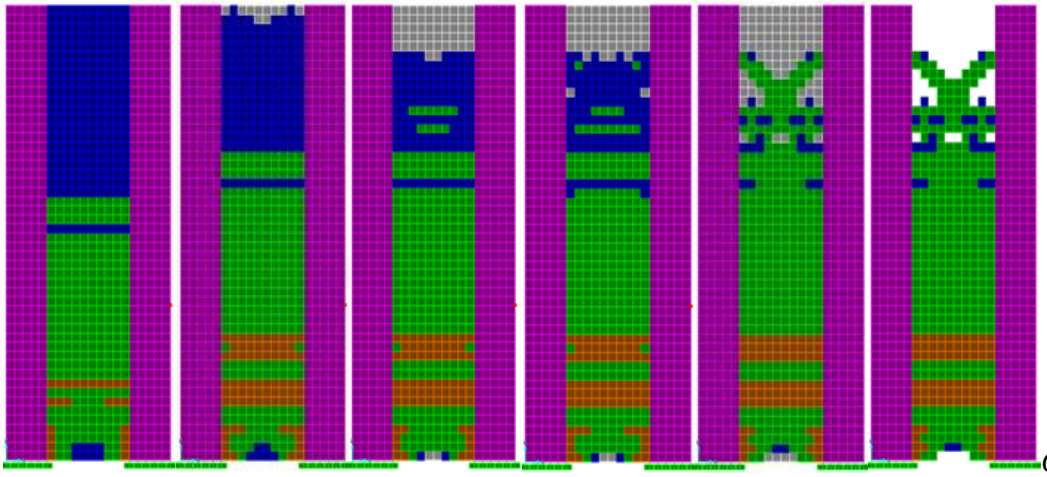

1st iteration 20th iteration 40th iteration 60th iteration 79th iteration (Max RR: 0.24 reached) *Optimal*

Fig. 4.6. Design Solutions for Infill Wall Loaded In-plane (Wall A)

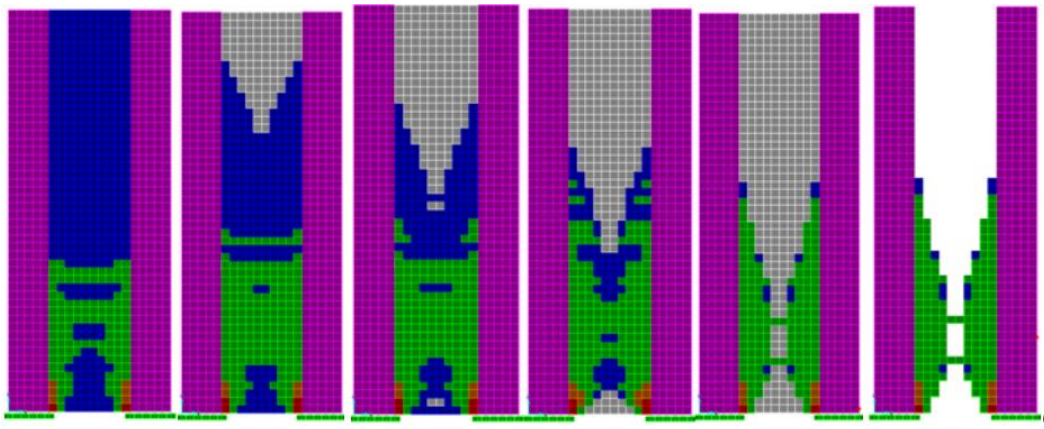

1st iteration 20th iteration 40th iteration 60th iteration 79th iteration (Max RR: 0.24 reached) *Optimal*

Fig. 4.7. Design Solutions for Infill Wall Loaded Out-of-plane (Wall D)

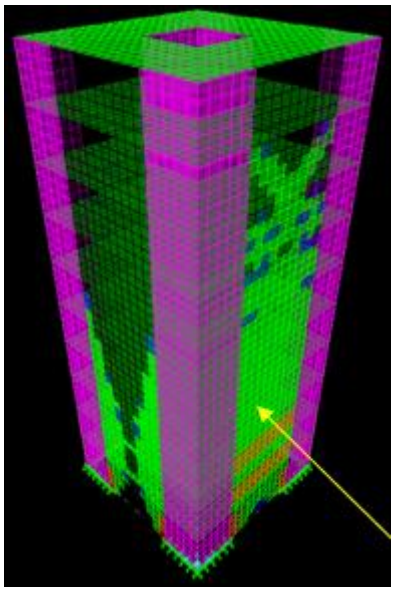

Fig. 4.8. Optimal Design Solution for Infill Wall in a Shear Wall – Slab Type Structure subjected to a Single Lateral Load Case

The side shear walls and the internal core in this old building provide the lateral load resistance. The purpose of this exercise was to find out if any additional material is required in between the shear walls with the aim of structurally improving/retrofitting the building. It is seen that, as the non-design region, which represents the old building structure, is not changed during the evolution, material of 180 mm thickness (Green colour) is generally required on Wall A to resist the lateral loading. The material distribution tries to evolve as a bracing pattern in the top two stories, with generally uniform thickness distribution in other stories except for two thicker bands of 220 mm (seen in Orange) in the lower stories. This suggests the need, up to nine stories, for infill material between the non-design shear walls to reduce lateral deflection. It is to be noted however, that the optimal solution is obtained when the Rejection Ratio of 24 % is reached. The optimisation can be continued further to a higher Rejection Ratio, however, 24 % was chosen as the algorithm allots thicknesses to the remaining elements based on whether the Ratio of the average smoothed stress in each element to the maximum von Mises stress is less than 25 % of the max, between 25 % - 50 %, 50 % - 75 % or greater than 75 %. Increasing the Rejection Ratio would result in a solution comprising lesser but thicker elements.

Comparison with Scaled Model

Weight of Initial Model: 3393.09 kN
Weight of Optimised Model: 1843.51 kN
Thickness of Scaled Model = (1843.51/ 3393.09)*0.2 = 0.108 m = 108 mm
Weight of Scaled Model: 1843.51 kN

Top Deflection of Scaled Model: 7.00 mm

Weight of Optimised Model: 1843.51 kN

Top Deflection of Optimised Model: 6.49 mm

Percentage Reduction in Top Deflection in the direction of lateral load: **7.30 %**

Conclusion

This example demonstrates effectiveness of the ESO method and the proposed procedure can be used for retrofitting an old structure by finding out the best location and distribution for infill material in certain regions for a given load case.

4.5.2 Conceptual Design of Bracing Systems

4.5.2.1 Introduction

This section demonstrates the effectiveness of the modified ESO method in determining the layout and thickness distribution of bracing pattern for a multi-storey building subjected to a single lateral load case. The method is first tested for a continuum design domain with no frame and for a single load at the top in the Global X direction as shown in Fig. 4.9 below.

4.5.2.2 Continuum Design Domain (No Frame): Single Lateral Load at the Top

The model shown in Fig. 4.9 below depicts a continuum design domain of 12.19 m x 21.95 m modelled into 1620 finite elements subjected to a single horizontal load of 40.05 kN at the top left corner. The initial thickness specified is 25.4 mm. Fixed support conditions are assumed throughout the base.

Finite Element Model and Data

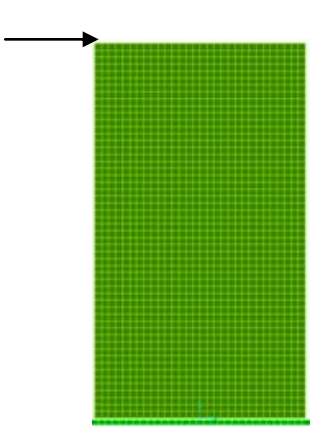

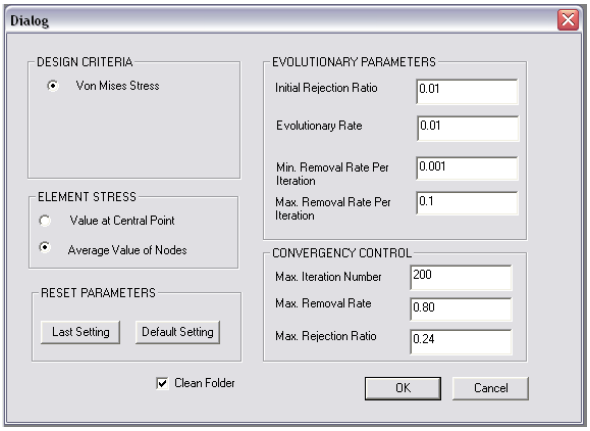

Fig. 4.9. Initial FE Model of 2D Continuum Design Domain

Fig. 4.10. ESO Optimisation Parameters

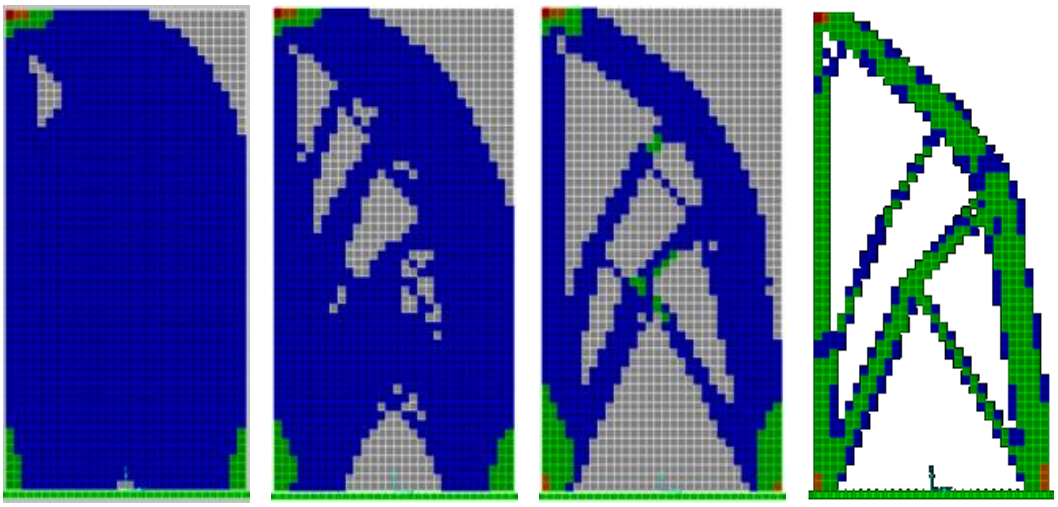

10^{th} iteration 40^{th} iteration 80^{th} iteration 119^{th} iteration (Optimal Solution, Rejection Ratio of 0.2 reached)

Fig. 4.11. Topology History of Material Layout and Thickness for a Single Horizontal Load at the Top Left Corner

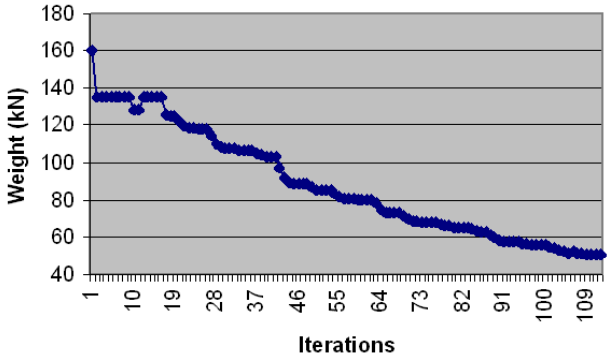

LEGEND

Blue	:	21.4 mm
Green	:	23.4 mm
Orange	:	27.4 mm
Red	:	29.4 mm
White	:	0.214 mm
Initial Thickness	:	25.4 mm

Fig. 4.12. History of Weight Reduction for the 2D Continuum example

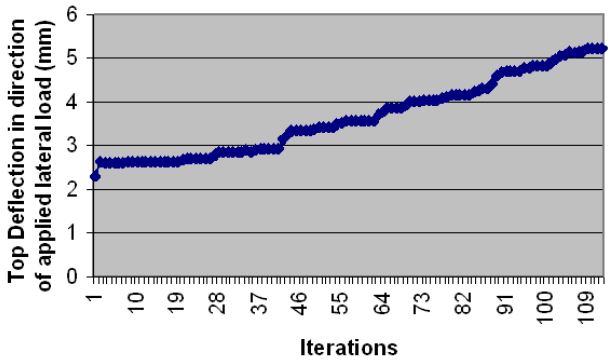

Fig. 4.13. Top Deflection History of the 2D Continuum Example

As expected if the weight reduces, the top deflection increases. The initial top deflection was 2.285 mm and the top deflection of the optimal solution is 5.22 mm. Similarly, the weight of the initial model was 160.15 kN and the weight of the optimal solution is 50.60 kN. The optimal solution needs to be compared with a scaled model such that the weights of the optimal solution and scaled model are the same; in order to compare top deflections of the two equally weighted models.

Comparison with Scaled Model

Weight of Optimal Solution: 50.60 kN
Weight of Initial Model: 160.15 kN
Thickness of Initial Model: 25.40 mm

Therefore, thickness of scaled model = (50.60 / 160.15) x 25.40 = 8.03 mm

Weight of Scaled Model: 50.60 kN
Top Deflection of Scaled Model: 7.33 mm

Weight of Optimal Solution: 50.60 kN
Top Deflection of Optimal Solution: 5.22 mm

Percentage Reduction : 28.80 %

Conclusion

Compared to the scaled model the optimised model shows an improvement in top deflection by 28.80 %. A clear and efficient bracing pattern emerges.

4.5.2.3 Optimal Bracing Pattern for a Multi-Storey Building

The model in Fig. 4.14 depicts a 10-storey *shear wall – slab* type building that is supported by an internal rectangular core and four corner columns represented by one layer of elements on each face of each side (shown in magenta colour). The thickness of this single layer of elements on each face of each side is the same as the thickness of the walls in the initial design. This single layer and the internal core along with the slabs are treated as non-design domain to ensure that these areas remain unchanged. The walls on four sides represent the initial design domain for the bracing pattern to emerge.

Model Data

2 bays by 2 bays 10-storied building with a rectangular core in the middle.

Span of each bay in both directions:	6 m
Floor to Floor Height:	3 m
Total Building Height:	30 m
Height-to-width ratio:	2.5
Initial Thickness of Design Domain:	200 mm
Thickness of Non-Design Domain:	200 mm
Slab thickness:	250 mm

Loads

A single lateral load case parallel to the Global X direction with magnitude of loads increasing towards the top.

Support Conditions

Fixed at the bottom of the "single layer of corner elements" that represents columns and at the bottom of the Internal Core.

Analysis

Linear static elastic analysis.

Physical Behaviour

The bracing that would evolve is designed to resist the lateral load case. As the core and the "single layer of corner elements" are treated as non-design, it is assumed that these carry the gravity loads, though the core will contribute to resisting the lateral loads as well.

The evolving diagonal members will provide the lateral resistance of the structure. The bracing would behave under horizontal loading as a vertical cantilever truss. The diagonal members would form the web of the vertical truss, with the "single layer of corner elements" representing columns acting as the chords. The windward chords will be subjected to tension and leeward chords will be subjected to compression. Bracing systems are highly efficient in resisting lateral loads because the horizontal shear on the building is resisted by the horizontal components of the axial tensile or compressive actions in the web members. The efficiency of bracing in being able to produce a laterally very stiff structure for a minimum of additional material makes it an economical structural form for any height of the building up to the very tallest. In this example, a 10-storied building is chosen, as adequate finite elements are needed at each level in order to obtain a clear bracing pattern. The higher the building, the higher the computational cost in terms of the finite element analysis (in SAP2000 Version 8.3.0, a 40 storied building using a relatively coarse mesh for walls and slabs still requires well over an hour for performing an FEA).

Optimisation Objective

The objective of this optimisation is to obtain a clear and efficient bracing pattern on Wall A when subjected to a single load case of a lateral load (in the Global X direction) with an increasing magnitude towards the top. It is expected that with efficient material removal and thickness redistribution, an efficient bracing pattern for the given load case will evolve on Wall A and improvement in top deflection in the Global X direction (parallel to the applied lateral load) will be observed when compared with a scaled model. The optimisation begins with an Initial Rejection Ratio of 1 % for element removal and the Maximum Rejection Ratio specified is 24 %. Changing the thickness of the remaining elements is similar to the procedure described in previous sections. The evolutionary rate is added to the Rejection Ratio only when no more elements are removed in a particular iteration. This is to obtain an accurate solution.

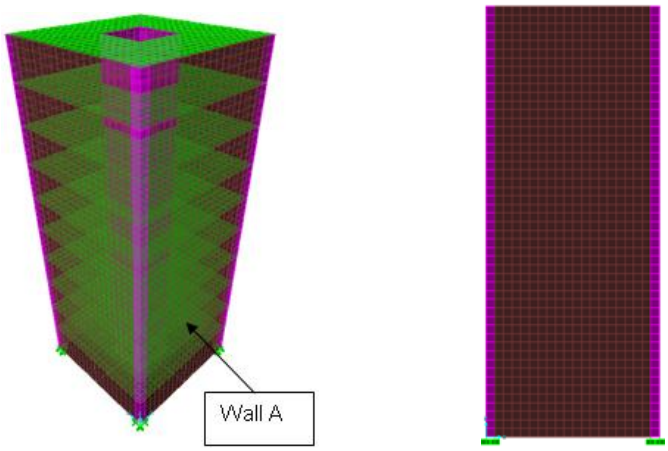

Fig. 4.14. Initial FE Model for seeking Optimal Bracing Pattern: 3D and Planar View

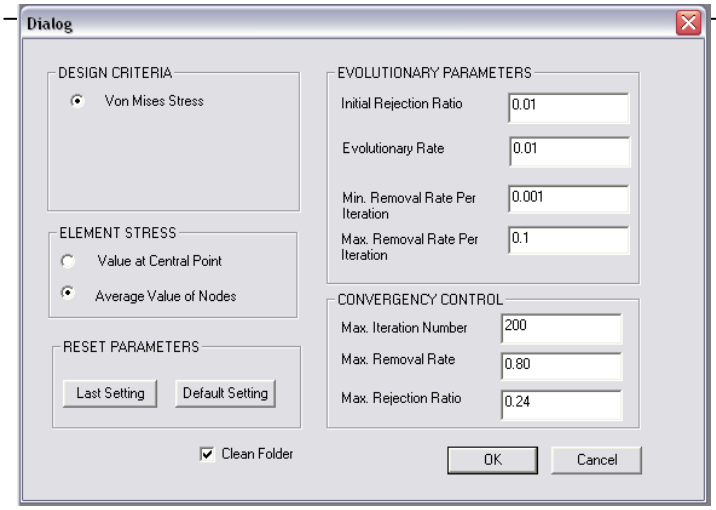

Fig. 4.15. ESO Optimisation Parameters

WALL A

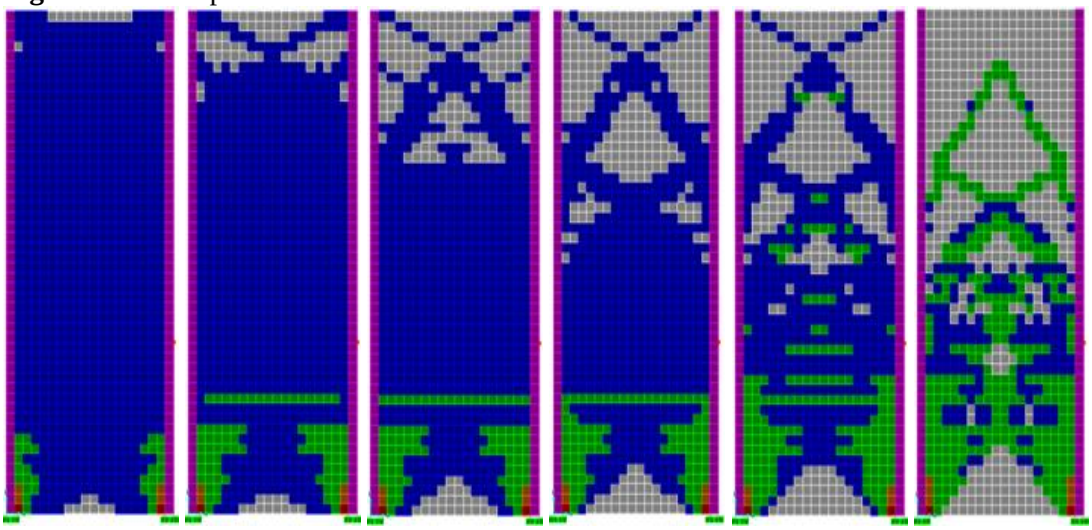

(a) 1st iteration (b) 20th (c) 40th (d) 60th (e) 80th (f) 100th iteration

Fig. 4.16 (a-e).

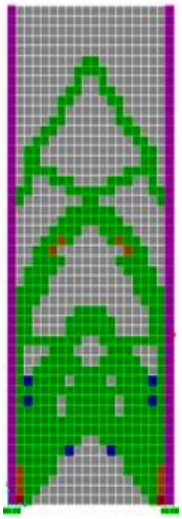

LEGEND		
White	:	1.60 mm
Blue	:	160 mm
Green	:	180 mm
Orange	:	220 mm
Red	:	240 mm
Initial Thickness	:	200 mm

(g) 113th iteration (Max RR: 0.24 reached)

Fig. 4.16 (a-g). Topology History of Evolving Bracing Pattern to resist In-plane Horizontal Loading

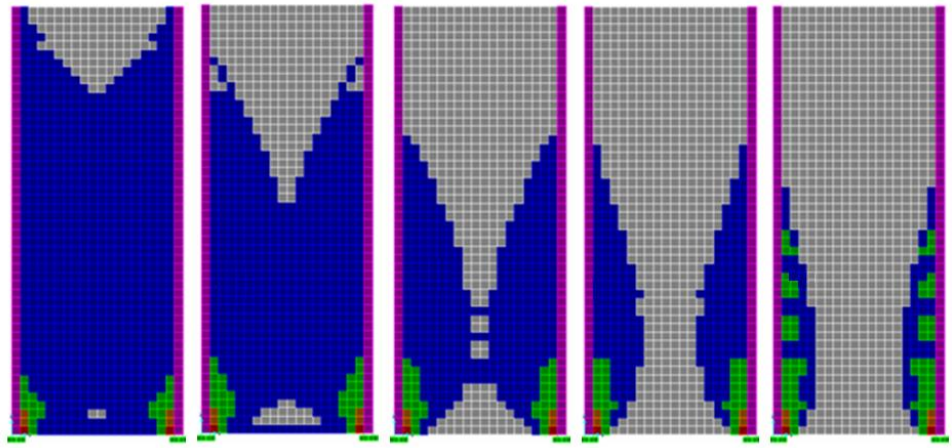

(a) 1st iteration (b) 20th iteration (c) 40th iteration (d) 60th iteration (e) 80th iteration

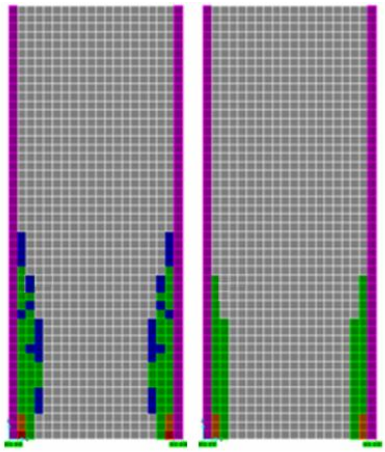

(f) 100th iteration (g) 113th iteration (Max RR: 0.24 reached)

Fig. 4.17 (a-g). Topology History of Continuum Loaded Out-of-plane

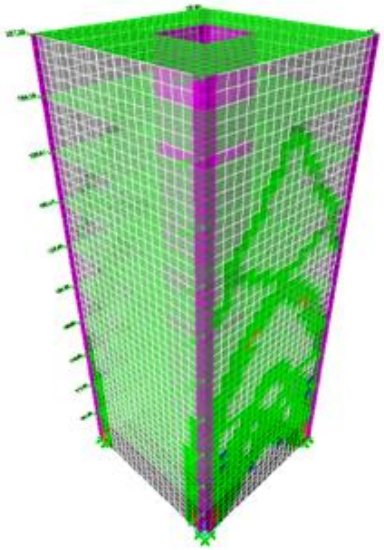

Fig. 4.18. 3D View of Optimal Topology of Bracing Pattern

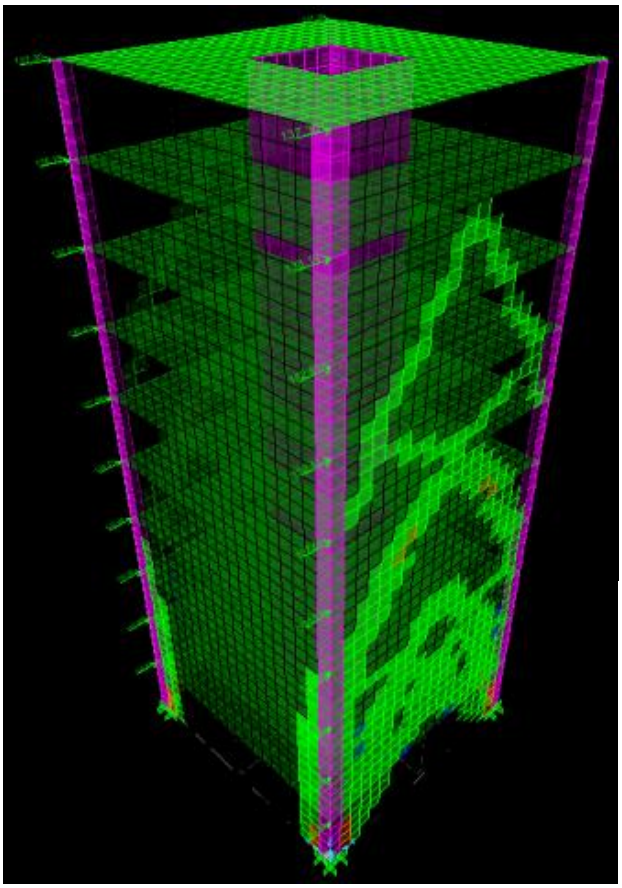

Fig. 4.19. Enlarged View of Optimal Topology of Bracing Pattern

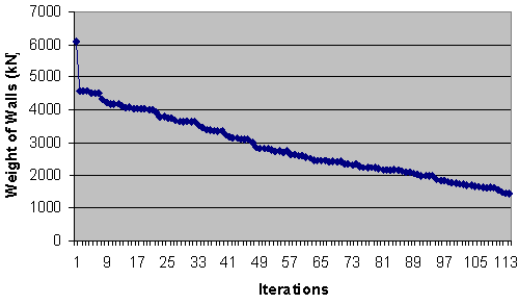

Fig. 4.20. History of Weight Reduction

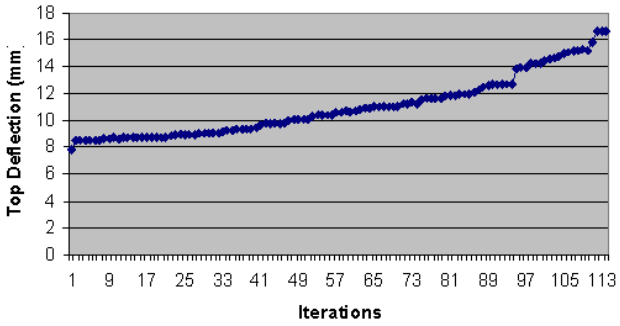

Fig. 4.21. Top Deflection History

Discussion

A clear triangulated bracing pattern similar to a K-type bracing pattern is seen to evolve. As expected, the top deflection increases as elements are gradually removed (i.e., weight is reduced). A significant advantage of the K-type bracing pattern is that the slab (or girder) moments and shears are independent of the lateral loading on the structure. Consequently, the slab design (or girder design) can be repetitive throughout the height of the structure with obvious economy in the design and construction. It is seen that the diagonals in the bracing

pattern evolved connect to the girder (slab in this case), at a significant distance from the girder ends (or slab ends). The girder, if present, can therefore be designed more economically as continuous over the connection, thus helping to offset the cost of the bracing. Another advantage of this type of bracing is that the braces, having one or both ends connected to the beam (if present), which is vertically relatively flexible; do not attract a significant load when the columns shorten under gravity loading. As before, the optimal solution is obtained when the Rejection Ratio of 24 % is reached. The optimisation can be continued further to a higher Rejection Ratio, however, 24 % was chosen as the algorithm allots thicknesses to the remaining elements based on the value of the Ratio of the average smoothed stress in each element to the Maximum von Mises stress which may be is less than 25 % of the max, between 25 % - 50 %, 50 % - 75 % or greater than 75 %. Increasing the Rejection Ratio would result in a solution comprising fewer but thicker elements.

Comparison with Scaled Model

Weight of Initial Model: 6107.561 kN

Weight of Optimised Model: 1439.864 kN

Uniform Thickness of Scaled Model = (1439.864 / 6107.561)*0.2 = 0.047 m = 47 mm

Weight of Scaled Model: 1439.864 kN
Top Deflection of Scaled Model: 17.76 mm

Weight of Optimised Model: 1439.864 kN
Top Deflection of Optimised Model: 16.64 mm

Percentage Reduction in Top Deflection in the direction of lateral load: **6.31 %**

Conclusion

The benefit of changing the thickness of the remaining elements is seen on comparing the Top Deflection in the direction of applied load with the scaled model: an improvement of 6.31 % in Top Deflection in the direction of lateral load is observed. In addition to an improvement of 6.31 % in Top Deflection, the weight is reduced by 76.42 % when compared with the weight of the Initial Model.

4.6 Discussions and Conclusion

- When material removal is employed together with thickness optimisation, initially checkerboard patterns are observed. The formation of checkerboard patterns is suppressed by employing a smoothing technique. The procedure is simple wherein, in the first step; the average von Mises stress *at each node* is calculated by averaging the von Mises stresses of remaining (non-white) elements connecting to that node. If there is a white element (i.e. Soft kill) connected to that node, then its nodal value of von-Mises stress and its "counter" is ignored in the calculation of the average. In the next step, the smoothed von Mises stress for each element is calculated by averaging the smoothed von Mises stresses of its nodes. It is seen from the examples that the optimisation procedure based on the smoothed von Mises stresses is able to suppress formation of checkerboard patterns.

- Efficient bracing patterns are obtained by employing the modified ESO method. Reductions in top deflections are observed for all examples. The benefit of changing the thickness together with element removal is seen in all the examples in which the optimal solutions generally require smaller thickness (Green colour) compared to the initial thickness (thickness of initial design), except for a few elements near the supports that are thickened, which is to be expected. This suggests that the initial thickness is an over-design for the given load case. The ability of the method to produce a topology together with the thicknesses required in different regions of the topology is a useful tool for the structural designer.

- Several examples seeking optimal bracing patterns for 2D planar frames subjected to lateral loading were also investigated by the author. Some of the solutions did not indicate a clear and distinct bracing pattern for 2D plane frames. As a result, they are not included in this work. The solutions revealed that if "top deflection" is to be used as the performance criteria, then there has to be a procedure added in the computer code that prevents removal of bracing elements in the top storey such that there is no "jump" in the lateral top deflection. Such a "jump" in the lateral top deflection is not seen for the bracing pattern obtained for the 3D building model in the last example. This is probably due to the fact that there are no frame elements in the building model and the lateral load is to be resisted by the bracing and internal core. Moreover, the building is much more stiffer than the 2D plane frame. For 2D multi-storey frames, "jumps" in top deflection values are observed for all cases when the bracing members in the top storey

are removed by the optimisation process. When this happens, the deflection at the top cannot be employed as the performance criteria to judge the topology. However, inter-storey deflections up to the penultimate storey compared well with the scaled models. It is anticipated that the frame would play a role in resisting the lateral loads as well and therefore, when the optimisation process is to be used for multi-storied framed buildings, there needs to be a procedure in the computer code that prevents removal of bracing elements in the top storey so that there is no "jump" in the lateral top deflection. Also, the top deflection constraint needs to be explicitly formulated in the optimisation problem statement.

- The present approach also led to the idea of letting the structural designer specify a range of sections to choose from, when the program makes a selection of a particular thickness (or section). Instead of the program choosing a section of say 220 mm, the program actually selects the section from a range of sections that satisfy the Australian design code (AS 3600) provisions. This way, the optimisation program designs an element or panel based on the stress in the element or panel and the stress carrying capacity of the user specified sections. The optimisation process then continues on till a steady state is reached, wherein there is no further improvement in the design. Only those designs are then chosen which satisfy specified constraints and show an improvement compared to the initial design. This approach along with a few Graphical User Interfaces (GUI's), has been developed extensively by the author to satisfy a number of code provisions in AS 3600 for the design of slabs. This is demonstrated and explained in Chapter 7.

- From this stage onwards the research moves from wall optimisation to the optimisation of slabs in building structures.

CHAPTER 5: Review of Conventional Reinforced Concrete Flat Slab Design

5.1 Introduction

In this chapter the current state-of-practice of reinforced concrete slab design is reviewed, including the Simplified Method of Design (which is based on the ACI direct design method), the Idealised Frame Method, the Yield Line Method, and the Strip Design Method. The principles of these methods along with a critical evaluation of their applicability and limitations are presented. In addition, the current state of the art of slab design based on finite element results is presented, along with various modelling techniques. Finally, AS 3600 code provisions for slab design is outlined. Much of the work in later chapters in implementing the algorithms is based on these code provisions which are therefore treated in detail in this chapter.

5.2 Flat Slab Systems

This study emphasizes particularly on reinforced concrete flat slab systems. Flat slab systems are a sub-set of the two-way slab family which deforms in two directions. Flat slab systems are reinforced concrete slabs generally of uniform thicknesses that transfer loads directly to supporting columns, and are distinguished from other two-way systems by the absence of beams. A simple representation of a flat slab system is shown in Figure 5.1 below. Flat slab systems have several advantages over other slab systems, e.g. the absence of beams allows for economical formwork and simple reinforcement layouts, leading to fast construction.

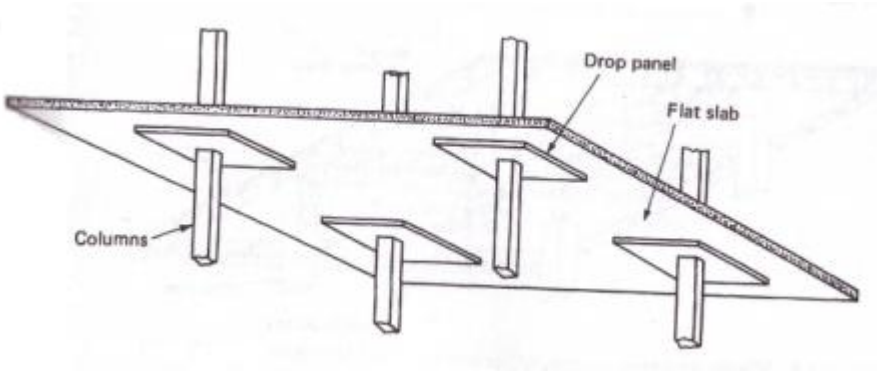

Fig. 5.1. A typical flat slab structure (Smith and Coull 1991)

Architecturally, flat slabs are advantageous as:

1. Smaller overall storey heights can be achieved due to the reduced floor structure depth required, and
2. The locations of columns and walls are not restricted by the location of beams.

In areas where height restrictions are critical, the use of flat slabs enables an additional floor for approximately every ten floors in a structure, as compared to a general two-way system with beams for the same clear storey heights (Gamble 1962). The savings in height eventually lead to financial savings in many areas such as mechanical systems, foundations, and non-structural components such as cladding. An added benefit of flat slab systems is good performance under fire conditions, due to the lack of sharp corners prone to spalling. The difficulty in shear and moment transfer at the column connections is often the limiting factor in the selection of flat slab systems as a design solution. This difficulty often requires the inclusion of drop panels or column capitals. Generally, the choice to use a flat slab system is often determined based on the span length and loading. Based on economy of construction and loading limitations, flat slab systems are well suited for use in multi-storey and high-rise reinforced concrete hotels, apartments, hospitals, and light office spaces, and are perhaps the most commonly used slab system for these types of structures today (Deaton 2005).

It is anticipated that producing optimal conceptual designs for flat slabs would aid the structural designer in generating final designs for flat slabs that result in even more savings in construction material (both concrete and steel) and is therefore the incentive for this work and the work in the following chapters.

5.2.1 Literature Review of Finite Element Application to Reinforced Concrete Slab Design

Reinforced concrete has been one of the most widely used materials in construction applications for a long time. It has several material advantages, but one of its most significant benefits is the ability to be cast into a wide variety of shapes. Actually, reinforced concrete is only geometrically limited by the complexities or cost of the construction of formwork (Deaton 2005). According to Severn and Taylor (1966), the behaviour of concrete structures easily constructed in the field often falls beyond the scope of common frame analysis programs and conventional design methods. This is certainly true for the analysis of reinforced concrete systems where slabs, shear walls, shells, tanks, deep beams, and coupling beams must be modelled. If the structural element contains holes or is subjected to concentrated or otherwise irregular loadings, the analysis is further complicated. Deaton (2005) asserts that the structural engineering community responded to this challenge with numerous approximate techniques that attempt to simplify the design of these reinforced concrete components. For flat slabs, these methods include the direct design, idealised frame, yield line, and strip design techniques, all of which approximate the results of classical plate theory. These methods have gained wide

acceptance among engineers because of their simplicity. However, these approximate techniques have significant limitations. Direct design and idealised frame methods are both limited to structures with very regular geometry. The application of yield lines or strip design may lead to overly conservative designs as well as to poor serviceability (Severn and Taylor 1966). A detailed explanation of these methods and their limitations is presented later in the chapter.

According to Deaton (2005), the unique capability of finite elements to conform to virtually any geometry that could be physically implemented has made the finite element method an obvious choice for the modelling and analysis of reinforced concrete systems for many years. For the analysis of flat slabs, the finite element method has therefore gained acceptance as an appropriate tool, especially for flat slabs having unusual or highly irregular geometries where the direct design and equivalent frame techniques are not applicable. Numerous approximations and assumptions would be invoked to accurately solve for the distribution of stress in irregular slabs if the yield line or strip design technique were applied. The finite element method on the other hand has been shown to accurately solve for the distribution of stress in such cases. Engineers, by adopting a finite element approach to slab design, would no longer need to develop multiple models to design a structure for various types of behaviour as by integrating the slab model within the three-dimensional frame, the combined effects of gravity and lateral loading conditions can be assessed together. The interaction of the slab and columns can be accurately simulated, providing favorable results to approximations of connection stiffness. These are added advantages of a finite element approach to slab design. An integrated approach to analysis and design is therefore seen to emerge (Deaton 2005).

Since the emergence of the finite element method in the nineteen fifties considerable research efforts have been spent on the application of finite elements to the analysis of reinforced concrete. Many achievements have been accomplished in research environments and a few of these achievements have also been implemented in practical applications for structural engineers in the design office. The following review details the progression from the conception of finite element based flat slab design to the current state of the art. Much of the work cited deals primarily with the modelling and analysis of flat slab systems by the finite element method, without explicitly discussing reinforcement design. “However, the primary purpose of the finite element model is the determination of design forces and moments, and once these quantities have been accurately determined, the resulting design becomes a function of the active design code” (Severn and Taylor 1966).

5.2.1.1 Design Based on Linear Finite Element Analysis

Zienkiewicz's work (Zienkiewicz and Cheung 1964) was one of the earliest published works concerning the application of the finite element method to reinforced concrete slabs. This work presented the formulation for boundary conditions typical to flat plates thus extending the general finite element method to these types of floor systems. Linear elastic isotropic analysis was extended to orthotropic slab systems with variable thickness, and the ease with which a slab can be analytically coupled to frame members or an elastic foundation was presented. Several examples show excellent agreement between finite element solutions for deflections and moments and those of available exact solutions.

Wood (1968) formulated the initial philosophy of flat plate design based on finite element results, although no clear mention of the finite element method was made in the original work. Instead, Wood describes the process of designing reinforcement in accordance with a predetermined field of bending moments provided from "analysis by the theory of elasticity.... possible with the use of computer programmes, which can print out a complete field of moments M_x, M_y and M_{xy}"(Bhatti 1979). Wood argued that design economy of such a method, whose mathematical formulation he presented, is superior to that of both the yield line and strip design techniques.

Wood's work was generalized by Armer (1968) for efficient application to both slabs with orthogonal reinforcement as well as skew reinforcement, and therefore, Wood argued that Armer's formulation should represent the general case. It was because of this collaboration that this technique of design is presently referred to as the Wood and Armer technique.

The finite element method was applied in a corner supported rectangular slab by Davies (1970) to calculate deflections and moments. A number of loading conditions with both simple supports and fixed supports were considered. The work compared analytical results with scale model tests and results showed strong correlation between the two. It also showed that actual slab to column connections were generally bounded by the simple and fixed support models evaluated.

A modelling technique based on using single elements for slab panels in the analysis of multi-storey flat plate structures subjected to lateral loading was implemented by French *et al.* (1975). They derived the stiffness of a single element panel for the implementation. Storey drifts as well as the distribution of lateral loads among columns was accurately predicted by this modelling

technique. Even though this method easily handled uneven bay spacings and nonrectangular plans, it provided no information regarding the distribution of moments throughout the floor slab.

One of the first three-dimensional applications of the finite element method in reinforced concrete was by Smith and Faulkes (1976) who applied the method to analyse a multistorey flat plate building, to analytically evaluate the flexural properties of flat plate systems. A four-node nonconforming rectangular displacement based element formulated by Zienkiewicz was used in the analyses conducted. A 6 x 6 bay floor with square column spacing was analysed, and various ratios of columns size to bay span were considered. The results of the presented analyses suggest that the flexural behaviour of a flat plate varies significantly from that of a beam, and that as a result the equivalent frame technique has limited applicability to the case where lateral loads are significant.

Other methods of reinforcement design based on a predetermined field of bending moments M_x, M_y and M_{xy} were presented by Gupta and Sen (1977). Although derived under different assumptions, the first method which was called the Principle of Minimum Resistance ultimately resulted in a formulation similar to the Wood and Armer solution. The second method applied was The Three Equivalent Moments' Method, in which the slab was reinforced according to computed equivalent normal moments in three unique specified directions based on the bending moment field of the element. The Three Equivalent Moments' Method demonstrated economy with respect to the total required design capacity, but not with regard to the actual construction cost. This work thus confirmed the general applicability of the Wood and Armer formulation.

Mohr's research (1979) on applying elastic finite element analysis to obtain approximate plastic design results for slabs (eight slabs with various boundary conditions were considered) showed strong correlation between the finite element results and other well-known plastic design techniques. The flat plate in his work was modelled as a weak core sandwich based on the assumption that the reinforcement had yielded and the concrete core was cracked. The plastic section modulus was therefore calculated and implemented instead of the elastic section modulus. This work demonstrated the successful application of elastic finite element analysis in the determination of approximate plastic design results.

An extensive review of the challenges associated with the application of linear elastic finite element analysis to reinforced concrete flat plate analysis was presented by Hrabok and Hrudey

(1982). Lack of experience, lack of knowledge of element behaviour and lack of suitable programs were cited as prime hindrances to widespread application of finite element based design techniques. They presented a detailed review of a number of common linear elastic plate bending elements, including the ACM element (Adini and Clough 1960), a hybrid stress Kirchoff element (Severn and Taylor 1966), a selectively reduced bilinear Mindlin element (Hughes and Cohen 1978), the heterosisstop dictation Mindlin element (Hughes and Cohen 1978) and a Lagrangian Kirchoff element (Hrabok 1981). Their recommendation for future application to flat plate design problems was the hybrid stress element based on its ability to account for the effects of stress singularities within the element and on the ease of determination of stiffness matrices for nonrectangular elements.

Gentry's work (1986) confirmed the application of linear elastic finite element analysis to the design of regular reinforced concrete flat plate systems. A rectangular column layout and bay spacing were considered and various methods of modelling columns and column-to-slab connections were evaluated in his work. He critically compared designs based on finite element analysis with designs based on the direct design and equivalent frame methods. Finite element designs using working stress design and ultimate strength design, based on element nodal forces as well as element stress resultants, were evaluated. His work showed that design using element forces produces results in closer correlation with the equivalent frame technique than element stress resultants, and that the ultimate strength approach is preferable to working stress with respect to performance and economy.

Using finite elements, Saleh (1987) investigated the determination of bending moment transfer at slab-column connections, shear stress along the critical column perimeter, and the effect of modelling on shear stress results for the analysis and shear design of regular reinforced concrete flat plate systems. His work showed strong correlation with the results obtained using the ACI method.

The work of Raisanen and CASE Task Group on finite element analysis (Raisanen 1987) stressed the significance of boundary conditions and modelling verification and showed the correct context of the application of a plate-bending element based on the Mindlin formulation. Their work demonstrated the successful application of linear finite element analyses to the solution of problems with closed form solutions as well as a powerhouse slab with openings.

Anderheggen (1994) presented a method of reinforcement design based on element nodal forces, in which the reinforcement and the concrete were designed based on the forces transmitted from the neighbouring elements and acting on the element as applied loads. The

design method was thus not based on stresses within the element and element stresses were therefore not computed. The principles presented were a generalization of a truss model for building an equilibrium system of forces and moments on which to base dimensioning.

Borkowski (1977) and de Figueiredo *et al.* (1999) worked hard to optimize the yield line technique using finite element analysis and obtained fruitful results in computing the associated collapse load of the flat plate by applying rigid plastic modelling techniques, coupled with linear and nonlinear optimization techniques. They assumed a finite element mesh that was adaptively modified to optimize the location of yield lines.

5.2.1.2 Design based on Non-linear Finite Element Analysis

As the finite element method was gaining acceptance, researchers were swift to begin re-evaluating the broad range of assumptions invoked when applying a linear elastic homogenous isotropic analysis to reinforced concrete (Brotchie and Russell 1964). The first published works dealing with non-linear finite element analysis of concrete systems emerged in the late nineteen sixties. These studies focused on various aspects of element formulation, including crack propagation and the bending of reinforcement (Deaton 2005).

A slab analysis model based on the effects of cracking, capable of representing the orientation of cracking with respect to the slabs coordinate system, the rigidity of the cracked region when the section has exceeded the cracking moment, and the rigidity of steel with relation to the crack direction was derived by Jofriet and McNeice (1971). The implemented program included a step-based analysis with a bilinear moment curvature relationship for each element in order to simulate progressive cracking. Post-yield behaviour of the reinforcement was neglected in their study. This approach is called a modified stiffness model (Jofriet and McNeice 1971).

A nonlayered reinforced concrete finite element model in which a non-linear variation in material properties could be represented through the depth of the slab was developed by Bashur and Darwin (1978). The non-linear aspects incorporated in their model allowed for accurate determination of the load deflection behaviour of the flat plate. Flat plates were modelled as anisotropic plates that were incrementally elastic. Steel was treated uniaxially with a bilinear stress strain curve and concrete was modelled as non-linear in compression and linearly brittle in tension. Numerical results showed that representation of cracking as a continuous process provides favourable results, and that smaller load increments provide more accurate results after cracking and/or yielding begins.

Lewinski and Wojewodzki (1991) combined the layered model approach and the modified stiffness approach to develop a non-linear slab model for accurate evaluation of in plane and out of plane effects in flat plates. This model included non-linear concrete behaviour, such as cracking, and elastic plastic steel reinforcement deformation as well as coupling between extension and flexure. The analyses were based on ten cracking patterns. They conducted a number of test analyses and comparisons with experimental test data showed that the proposed method is accurate.

Many of the common non-linear finite element reinforced concrete techniques were extended by Barzegar and Maddipudi (1994) with respect to the simulation of reinforcement in three-dimensional solid elements. They presented a model for spatially embedded reinforcement that was independent of the finite element nodal coordinates. An entire reinforcement cage is automatically mapped into a mesh of solid isoparametric concrete elements, instead of employing either a smeared or layered approach. They demonstrated that this technique was not only applicable to straight reinforcing bars, but also to prestressed systems in which the strand geometry can be approximated using a piecewise linear tendon distribution.

A general element for the design of slabs, plates and shells was presented by Lourenco and Figueiras (1995) in which reinforcement was computed locally at each integration point thereby extending non-linear finite element modelling of concrete slabs. The presented method that was validated with experimental test data took into account the biaxial behaviour of concrete and different moment arms of all internal forces, a key point that was ignored by Gupta and Sen (1977).

The extension to slabs of arbitrary shape was a topic of research in the non-linear finite element field as well. In order to calibrate the non-linear analysis of fully restrained slabs, Famiyesin and Hossain (1998) applied a three-dimensional degenerated shell reinforced concrete model to determine model parameter values. Their goal was to extend to arbitrary configurations through parametric sensitivity studies. They applied the resulting parameters to 36 previously tested slabs, with the accuracy of strength determination within a mean value of two percent of experimental data.

Of late, a new finite element for non-linear finite element analysis of reinforced concrete slab systems has been derived by Phuvoravan and Sotelino (2005). This new element is a combination of the classic four-node Kirchoff shell element with two node Euler beam elements to simulate the steel reinforcement. They have applied rigid links to couple the reinforcement to the concrete. Discrete reinforcement modelling in the past included reinforcement in a mesh of

three-dimensional solid elements. By replacing the three-dimensional mesh with a two-dimensional mesh of modified Kirchoff elements allowed for a simple and efficient, yet robust, manner of representing the system per element. Comparisons with experimental data verified that the presented element demonstrated better prediction of reinforced concrete flat plate behaviour than the general layered shell element.

5.2.1.3 Further Comments

The ASCE (American Society of Civil Engineers) Task Committee on finite element analysis of reinforced concrete structures has been instrumental in the development and implementation of finite element modelling of reinforced concrete. This committee has published several volumes of conference proceedings and has been chiefly responsible for consolidating much research and theory concerning this topic (Deaton 2005). These works contain extensive treatment of concrete cracking formulations, modelling of reinforcement and bond, constitutive relations and failure theories, thermal effects, viscoelastic effects, shear transfer, numerical optimisation, and dynamic analysis of reinforced concrete systems from a finite element perspective (Meyer and Okamura 1985, Nilson 1982, William and Tanabe 2001, Isenberg 1991). Furthermore, a good deal of research has been conducted on the general application of computers to reinforced concrete. Subjects studied include the broad development of programming tools and resources suited to analyse and design reinforced concrete structures (Malhotra 1970, Price 1987), the general optimisation of design of reinforced concrete systems using computers (Hernandez *et al.* 1999) and numerical advances in the modelling of multi-scale behaviour as well as the cyclic and seismic response of reinforced concrete structures (Bic´anic *et al.* 2003).

Numerous commercial software packages today, such as STAAD, SAFE, RAM concept (previously ADAPT floor), offer the capability to design slabs using finite elements. Finite element based slab design in STAAD is based on element stresses, using the conventional Wood and Armer approach, while finite element based slab design in SAFE, as well as RAM concept, is based on element force results (Computers and Structures, Inc. 1998, RAM International 2003). The exact algorithms and procedure that these software use to compute design moments are not revealed in the cited technical reference documentation. Another software package called DIANA is popular for finite element based reinforced concrete analysis and design. "*DIANA offers a wide range of material models for the analysis of the non-linear behaviour of concrete, which comprises cracking, crushing and shearing effects in cracks and joints, special techniques for modelling reinforcement and prestressed cables, determination and integration of creep and shrinkage and advanced solutions for the analysis of young hardening concrete" (Diana's website)*.

5.3 Limitations of Finite Element Analysis

It is to be noted that despite the volume of research associated with finite element based flat plate analysis; the finite element method is not without limitations. Though finite elements easily handle complexities that restrict simplified design methods, finite elements demonstrate several important practical constraints (Deaton 2005).

To begin with, the results of finite element analysis are usually unsuitable for direct use and can be difficult to interpret as they usually involve understanding several sign conventions and coordinate systems (Hillerborg 1996). Mistakes could easily be made, and errors in interpretation could lead to the placement of steel reinforcement on the wrong face of the member, or in the wrong direction, leading to catastrophic results (Deaton 2005).

Another limitation is the sheer volume of results produced by finite element analyses. These days it is common for a structural model to contain several thousand finite elements and a large number of loading cases. If each element contains four nodes, each node with six degrees of freedom, the volume of results computed in such an analysis would be difficult for a single engineer to reduce to a simple design. Current practices require the engineer to determine design forces along a cross section on an element-by-element basis, usually node-by-node per element. All loading conditions must be checked to determine the maximum effect and reduced to a design envelope. This procedure is inefficient and prone to mistakes on the part of the engineer (Deaton 2005).

Hrabok and Hrudey (1982) have described other limitations facing the finite element method such as "a perplexing array" of elements available to the engineer from which to choose from for the analysis. This includes elements with various shapes, nodal configurations, and nodal degrees of freedom. The engineer’s general lack of training in the finite element method complicates this further. Moreover, they pointed out that there are fewer general-purpose programs robust enough to model all aspects of flat plate systems such as:

1. The ability to model the finite size of connections between the slab and columns,
2. Techniques to evaluate the effects of stress singularities at re-entrant corners,
3. An extensive tenement library and
4. The ability to model eccentric stiffeners (Hrabok and Hrudey 1982).

It should be noted however that SAP2000 provides some of the capabilities to model the structural characteristics that they listed.

In the following sections, general AS 3600 design requirements are discussed, along with a summary of the Simplified Method of Design, the Idealised Frame Method, the Yield Line method, and the Strip Design technique. Each procedure as well as its limitations is discussed.

The following discussion is limited to flat slab systems. Prestressed concrete is not considered.

The methodologies presented in this chapter provide the background for the three design techniques developed in subsequent chapters.

5.4 General AS 3600 Requirements for Reinforced Concrete Design

The Australian Standard for Concrete Structures, AS 3600 – 2001 draws extensively on the philosophy of limit states design, in dealing with various design requirements for strength and serviceability. According to AS 3600, structures and structural members must be designed with a load capacity greater than the required strength as determined by a suitable analysis. The required strength is computed based on combinations of the loadings required in the general building code. The loads are increased by load factors, depending on the type of load and the specific loading combination. Loads which must be considered include dead loads, live loads, temperature loads, earthquake loads, and loads due to snow, rain, and wind.

The design strength at a location in the system is computed as the nominal capacity, based on mechanics and code assumptions, multiplied by the strength reduction factor, ϕ. ϕ factors are always less than one and account for inaccuracies in design equations and statistical variations in material properties. ϕ factors vary based on the specific response quantity being designed. The values of ϕ in AS 3600, for flexure, range from 0.6 to 0.8 depending on the strain condition. The basic requirement for strength designs is expressed as:

Design Strength $\geq$ Required strength

Or

$\phi \times$(Nominal Strength) $\geq$ Required strength i.e.

$$S^* \leq \phi \times R_u \tag{5.1}$$

in which R_u is the resistance of a section or region of a member (i.e. Nominal strength) and S^* is the load effect. The load effect is generally an internal action such as bending moment or

shear force. It is evaluated from structural analyses of the structure when subjected to factored load combinations. Various load combinations need to be considered, and the most severe case taken. The combinations are specified in Clause 3.3 of AS 3600.

Calculations to determine the *design resistance,* $\phi \times R_u$, are based on the *characteristic strength of concrete* and the *minimum yield strength* of reinforcing steel. The characteristic strength of concrete, $f_c^{'}$, is the 5 percent fractile, i.e. the strength value which is attained by 95 percent of the material. It is also the value applying at 28 days. The minimum yield strength of steel reinforcement, f_{sy} , too is regarded as an approximation to the 5 percent fractile value of the yield stress. Values are specified in Clause 6.2.1 of AS 3600.

5.4.1 Analysis Requirements

To determine the action effects in a structure and its component members, Section 7 of AS 3600 sets out the methods of analyses to be carried out for the purpose of complying with the requirements for stability, strength and serviceability.

Slabs and floor systems are 3D in nature and an accurate analysis is complex. However, slabs and floor systems are highly statically indeterminate and usually contain only light reinforcement. They are very ductile and can undergo considerable redistribution of internal forces. Therefore, a very accurate evaluation of moments is not needed and a certain degree of latitude is acceptable in the results. The essential requirement though is that statics must be satisfied.

Generally a linear elastic analysis is performed to provide the basis for an initial design. If inadequate reinforcement is provided in a particular location, the reinforcement will yield locally and the moment will be redistributed internally due to the redundancy of the slab system. Although such behaviour may satisfy strength requirements, it can lead to poor serviceability of the slab, evidenced by undesirable cracking. If the slab is reinforced based on the distribution of linear elastic moments, however, serviceability conditions will generally be satisfied (Cope and Clark 1984).

AS 3600 presents' two simplified linear elastic analysis techniques, which are permitted, providing the structure satisfies various requirements. These two methods are the Simplified Method and the Idealised Frame Method. Both of these methods are based on analytical studies of moment distributions using elastic theory, strength requirements from yield line theory,

experimental testing of physical models and previous experience of slabs constructed in the field.

It is seen in practice that it is acceptable to proportion reinforcement for ultimate limit states based on the results of a linear elastic structural analysis. At this limit state, the linear elastic moments do not closely predict the actual moment distribution in the slab, but are acceptable for design provided that equilibrium and compatibility are satisfied. The main benefit of distributing reinforcement for the ultimate limit state based on a linear elastic analysis is that deflection and cracking requirements are likely to be satisfied, though this is not guaranteed (Cope and Clark 1984).

The actual behaviour of the slab at the ultimate limit state is plastic, and it is permitted in AS 3600 to apply limit analysis to the design of slabs. Using such a method, the ultimate load is determined, and then the distribution of moments and shears at the ultimate level are determined. Either a lower bound method or upper bound method may be employed. A lower bound method assumes a distribution of moments at the ultimate condition such that equilibrium is satisfied at all locations in the system, the yield criterion defining the strength of the slab is not exceeded, and all boundary conditions are satisfied. Equilibrium is applied, and with the assumed distribution of moments, the ultimate load can be determined. The lower bound method converges to the correct ultimate load from below the actual value, and never over estimates the ultimate load (Gamble and Park 2000). The strip design technique is a lower bound method. An upper bound method assumes a collapse mechanism at the ultimate condition. In this collapse mechanism, the moments at the plastic hinges are assumed to be less than or equal to the ultimate moment capacity at the hinges, and the collapse mechanism must satisfy the imposed boundary conditions of the structure. The upper bound method converges to the actual ultimate load from above the actual value, and never underestimates this value. As such, it is possible to compute an ultimate load that is too high if an in incorrect collapse mechanism is assumed (Gamble and Park 2000). The yield line technique is an upper bound method.

5.4.2 Flexural Strength Requirements

The design of reinforcement to resist flexure is one of the important design limit states considered for flat slab systems. Design for flexure is the core of the implemented design techniques in this work, and as such, will be treated exclusively in this section. The general requirements for flexural design are set forth in Section 9 of AS 3600. A cross section in a flat slab system is designed using the same procedure as that in reinforced concrete beam design.

The provided ultimate strength of the member, $\phi \times M_n$, must exceed the ultimate factored moment, M_u, for all locations in a structure. During the optimisation procedure developed in this work, this condition is checked for each finite element of the slab model and only those solutions that satisfy this condition everywhere in the slab (i.e. for all finite elements in the model) are chosen as the optimal solutions.

5.4.3 Ultimate Flexural Capacity

Figure 5.2, reproduced from Warner *et al.* (1989) shows the cross section of a general reinforced concrete member reinforced for flexure. It shows the conditions of a cracked section in a simple reinforced concrete beam when the maximum moment M_u acts. This figure will be used to review the equations for the ultimate moment capacity of the section.

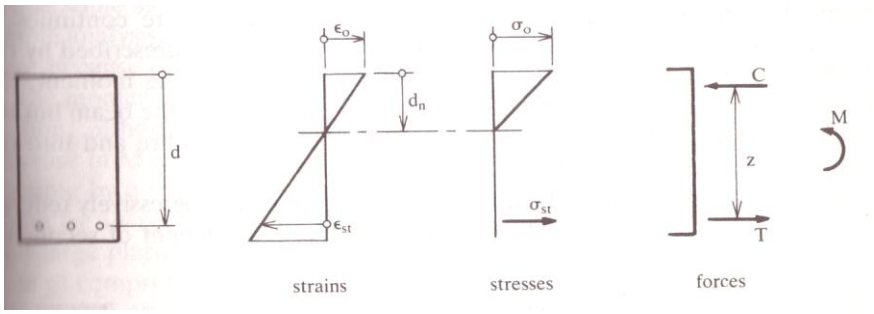

(A) *(B)* *(C)*

Fig. 5.2. Cracked Section Behaviour (Warner *et al.* 1989)

The concrete compressive strength is $f_c^{'}$. The distance d is the distance from the compression face of the member to the centroid of the layer of reinforcing steel. The width of the beam is given by b (not shown in figure 5.2 above). The area of tensile steel reinforcement is given as A_{st}, and the steel has yield strength equal to f_{sy}. When the reinforced concrete member is subjected to a loading and a moment is produced, an assumed linear distribution of strain develops through the cross section, as shown in *(A)*. In this figure, ε_o is the strain in the extreme compression fibre of the concrete, and ε_{st} is the tensile strain in the steel reinforcement at a distance d from the compression face of the member. The tensile strength of concrete is to be neglected in the calculation of required flexural reinforcement, such that the only tensile component in the system is the steel reinforcement. The neutral axis of the member is located at a distance d_n from the compression face.

For normal strength concrete up to 50 MPa, AS 3600 adopts the value of the crushing strain of the concrete ε_o as 0.003. Though experimental results show concrete can achieve compressive strains significantly higher than this value, concrete is assumed to crush when the strain reaches this lower bound for design purposes (MacGregor 1997). In flexure, there are three ways in which the section will fail.

1. First, a section is said to fail at a *balanced* strain condition when the tension reinforcement strain, ε_{st}, reaches the strain corresponding to the specified yield stress, f_{sy}, at the same time that the extreme compression fibre in the concrete reaches the assumed ultimate strain, 0.003.

2. Second, a section is said to be *compression controlled* when $f_c^{'}$ the extreme concrete fibre reaches the ultimate compressive strain prior to the tensile strain in the reinforcement reaching ε_{st}. In a compression controlled section, the concrete will crush before any significant yielding of reinforcement occurs, leading to a brittle failure mode with little or no visible warning.

3. Third, a section is said to be *tension controlled* if the tensile strain in the steel is equal to or higher than 0.0025 when the extreme compression fibre reaches its assumed strain limit of 0.003. In a tension-controlled failure, the steel will undergo large strains, and the concrete will experience significant cracking before the compression zone crushes, providing warning of impending failure. Because of this, flexural members are designed to fail in a tension-controlled manner when possible. As per AS 3600, the strength reduction factor, ϕ is to be taken from Table 2.3 of Section 2, AS 3600. The values generally range from 0.6 to 0.8. Initially in design, ϕ is assumed to equal 0.8, and after the section is designed, the strain is computed at the ultimate state and verified to be > 0.0025 in the steel.

Based on the limiting criteria for the strains in both the steel and concrete, the ultimate capacity of the cross section can be computed. Since a tension controlled failure is assumed, the strain in the steel at failure is > the yield strain. The stress in the steel, σ_{st}, is therefore set equal to the yield stress, f_{sy}, producing a tension force, T, in the section, given by *equation 5.2* below

$$T = A_{st} \times f_{sy} \tag{5.2}$$

T acts at a distance d from the compression face of the member and is shown in figure *5.2 (C)*. The tension force in the section must be resisted by an equal and opposite compression force. Although the distribution of compressive stress in the concrete is non-linear at the ultimate level, AS 3600 permits the compression zone to be represented by rectangular distribution of stress of magnitude $0.85\times f_c^{'}$. This uniform stress distribution is shown in figure 5.3 below, and extends a depth into the section from the compression face.

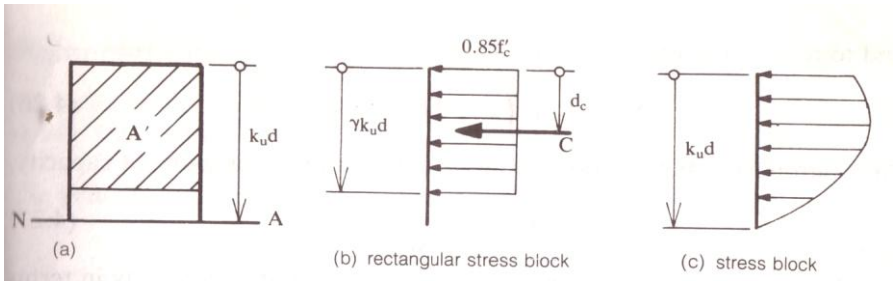

Fig 5.3. Compressive stresses at failure (Warner *et al.* 1989)

A single parameter γ is used to define both the magnitude and the location of C, the compressive force within the member. The non-linear stress distribution above the neutral axis *(Fig 5.3 C)* is replaced by a uniform stress of magnitude $0.85\times f_c^{'}$, which acts over an area $A^{'}$. $A^{'}$ is *not* the full area above the neutral axis: it is bounded by the edges of the section and a line drawn parallel to the neutral axis but located at a distance $\gamma\times d_n$ below the extreme compressive fibre, i.e. a distance $(1-\gamma)\times d_n$ above the neutral axis. The resultant compressive force thus becomes:

$$C = 0.85\times f_c^{'}\times\gamma\times b\times d_n \qquad (5.3)$$

And acts at depth $d_c = 0.5\times\gamma\times d_n$

AS 3600 specifies the values for γ for normal-strength concretes, i.e. for $f_c^{'}$ up to 50 MPa as:

$\gamma = 0.85 - 0.007(f_c^{'} - 28)$ with the limits: $0.65 \le \gamma \le 0.85$

The upper limit of 0.85 applies when $f_c^{'}$ is less than 28 MPa. The lower limit is never relevant for normal concretes because it only comes into play when the concrete strength exceeds 64 MPa.

The rectangular stress block is simple to apply in practice and is therefore often preferred in ultimate strength calculations. As per AS 3600, the stress block parameter γ is used to evaluate the moment capacity of all types of flexural members. Assuming the section is under-reinforced, the properties of the rectangular compressive stress block are used to determine the location of the force C, the internal lever arm z and hence the moment capacity.

To determine the neutral axis depth d_n, C and T, the tension and compression forces in the cross section are equated:

$$0.85 \times f_c^{'} \times \gamma \times b \times d_n = A_{st} \times f_{sy} \tag{5.11}$$

With d_n evaluated, the location of the compressive force is determined:

$$d_c = 0.5 \times \gamma \times b \times d_n \tag{5.12}$$

This in turn allows the internal lever arm $z = d - d_c$ and the moment capacity M_u *($M_u = T_z = C_z$)* to be calculated.

It is necessary to check that the tensile steel is at yield, i.e. the beam section is under-reinforced. To do this the strain distribution in the section is considered, which is known because ε_o is fixed and d_n is evaluated. The strain in the tensile reinforcing steel is obtained from similar triangles as:

$$\varepsilon_{st} = \varepsilon_o \times \frac{(d - d_n)}{d_n} \tag{5.13}$$

If ε_{st} exceeds ε_{sy}, the yield strain for the steel, then the calculation of M_u is invalid. For an assumed yield stress of 400 MPa, the corresponding ε_{sy} is 0.002 (though in practical cases the strain in the steel will normally be much larger than 0.002).

In treating simple sections with just one layer of tensile steel, it is often convenient to use the dimensionless neutral axis depth parameter K_u:

$$K_u = \frac{d_n}{d} \tag{5.14}$$

This term can be used instead of d_n to specify the neutral axis position. It is shown later that K_u is also used as an indicator of ductility of a section.

Equations for M_u are derived as follows:

First, an expression for d_n (or K_u) is obtained by equating C and T. From Eq. 5.11,

$$d_n = \frac{1}{0.85} \times \frac{f_{sy}}{f_c^{'}} \times \frac{A_{st}}{b} \tag{5.16}$$

or: $$K_u = \frac{1}{0.85} \times \frac{f_{sy}}{f_c^{'}} \times \frac{A_{st}}{bd} \tag{5.17}$$

The lever arm, z is: $z = d - d_c = d(1 - 0.5 \times \gamma \times K_u)$ (5.18)

which gives: $$M_u = f_{sy} \times A_{st} \times d \times (1 - 0.5 \times \gamma \times K_u) \tag{5.19}$$

Or, substituting for K_u: $$M_u = f_{sy} \times A_{st} \times d \times \left(1 - \frac{0.6 \times A_{st} \times f_{sy}}{b \times d \times f_c^{'}}\right) \tag{5.20}$$

Equation 5.20 above is used to calculate the Moment Capacity per metre width of each section provided by the user in the GUI for the user specified material properties. The nodal moments obtained in SAP2000 after an FEA are moments per unit width (i.e. kN-m/m). The maximum of the smoothed nodal moments in two orthogonal directions is chosen and compared with the Moment Capacities (as calculated by eq. (5.20) above) of the user defined sections in the two orthogonal directions in order to make a selection of a particular section for that finite element. This algorithm is followed in the computer program when designing for flexure and is explained later in chapter 7.

Although the case of a rectangular cross section reinforced only on the tension side is one of the more simple cases for the design of reinforced concrete beams, it provides a sound basis for the design of flat slab sections for several reasons. First of all, flat slab sections are generally rectangular, so the formulation need not be specialized for more complicated geometries. Second, although flat slabs may contain reinforcement on both faces, the width of design cross sections (large with respect to the thickness of the slab) usually produces a depth smaller than the cover between the compression side bars and the extreme compression face. Thus, compression reinforcement in flat slabs is usually located near the neutral axis and can be neglected since the strain will be very small in comparison to the strain in the tension face reinforcement (Kahn 2004).

5.4.4 Minimum Flexural Reinforcement

Clause 9.1.1 of AS 3600 dictates that a minimum area of steel is required at all sections where analysis demonstrates a need for tensile reinforcement. If the amount of reinforcement computed is very small, the computed ultimate moment strength based on a reinforced concrete cracked section analysis can be less than the computed moment strength of the same unreinforced concrete section computed based on the modulus of rupture. To prevent this, minimum flexural reinforcement must be provided in slabs and this minimum tensile reinforcement depends on the way the slab is supported. For e.g.

a) Slabs supported by columns $A_{st} > 0.0025 \times b \times d$

b) Slabs supported by beams or walls $A_{st} > 0.002 \times b \times d$

c) Slab footings $A_{st} > 0.002 \times b \times d$

where, A_{st} = Area of tensile reinforcing steel

b = width of the cross section

d = effective depth of the cross section

These requirements for Minimum Flexural Steel are programmed into the code for Techniques 1 and 3, so if the user enters a very small number of bars per m width in the GUI, the program detects this and informs the user to modify this data accordingly.

5.4.5 Shear Strength Requirements

The requirements for shear design of a reinforced concrete system are presented in chapters eight and nine of AS 3600. In general, the *shear capacity provided* must be greater than the *required shear strength computed* using the factored loading combinations of AS 3600 Section 3. The design requirement for shear is:

$$V^* \leq \phi \times V_u \tag{5.30}$$

where V^* is the factored design shear force, ϕ = 0.7 is the strength reduction factor for shear and V_u is the Ultimate Shear Strength of the section.

In eq. (5.30) above, V_u is the Ultimate Shear Strength of the section and is taken to equal the sum of $V_{uc} + V_{us}$ where V_{uc} is the shear capacity of the concrete and V_{us} is the shear strength

contributed by shear reinforcement. For flat slab systems, shear reinforcement is seldom provided so it is sufficient to set $V_u = V_{uc}$. V_{uc} is a function of the cross sectional geometry as well as the compressive strength of the concrete. AS 3600 states that the ultimate shear strength of a reinforced concrete beam without shear reinforcement, V_{uc}, and not subjected to any axial force is given by:

$$V_{uc} = \beta_1 \times b_v \times d_0 \times \left(\frac{A_{st}}{b_v d_0} f_c' \right)^{1/3} \tag{5.31}$$

where,

$$\beta_1 = \left(1.4 - \frac{d_o}{2000} \right) \geq 1.1 \tag{5.32}$$

b_v	:	Minimum effective web width in mm
d_o	:	Distance of the extreme compression fibre of concrete to the centroid of the outermost layer of tensile reinforcement in mm.
A_{st}	:	Area of fully anchored longitudinal steel provided in the tension zone.
β_1	:	Accounts for the increase in shear strength observed in shallow beams in a manner similar to the shear provisions of the CEB Model Code (1978).
f_c'	:	Characteristic Compressive Strength of concrete at 28 days

For a general cross section of a flat slab in beam action, the factored design shear force, V^* shall not exceed the value V_{uc} computed by equation 5.31 times ϕ (which is equal to 0.7). If the section fails in shear, there are several techniques to increase the shear strength of the system. One of the simplest methods is to increase the depth of the slab. Increasing the depth of the slab will increase the shear capacity. The strength of the concrete may also be increased. The column dimensions can also be increased. Finally, the section can be reinforced with either stirrups or a stud rail (Kahn 2004). Equations 5.30, 5.31 and 5.32 are programmed into the computer code to compute the ultimate shear strength of the user-defined sections in the GUI. In SAP2000, once each finite element in the general cross section of the flat slab is designed based on flexural criteria described previously, the factored ultimate shear strength of the "section

assigned", $\phi \times V_{u,}$ is then compared with the factored design shear force in each element. The design shear force, V^* in each element in SAP2000 is output as "V_{Max}". Information on V_{Max} and other output parameters of SAP2000 are explained later in Chapter 8 of this thesis. This design shear force, V^* is increased by a factor of 1.5. If the condition in Equation 5.30 is satisfied, then it means that the shear capacity of the "assigned section" is greater than the required shear strength and the "assigned section" is chosen as the final design. If however, the condition in Equation 5.30 is not satisfied, then it means that although the 'assigned section" satisfies flexural criteria, the shear capacity of the "assigned section" is less than the required shear strength and therefore another section which satisfies Equation (5.30) in addition to flexural criteria is picked. Such a section is usually thicker than the previously allotted section (since, as mentioned previously, it increases the shear capacity compared to a thinner slab).

5.4.5.1 Punching Shear with No Moment Transfer

To evaluate the shear strength of flat slab systems in regions near columns (the moment is not transferred in the beam-to-column connection), it is insufficient to assume the slab is behaving according to beam action. Thus the guidelines of the previous section are no longer valid. For punching shear, the critical section for design is a perimeter u (located around the column) and is at a distance of $\frac{d}{2}$ from the edges or corners of the column. The shear strength of the concrete slab with no moment transfer from the slab to the support is then computed from Equation 5.35.

$$V_u = V_{uo} \tag{5.35}$$

where,

$$V_{uo} = u \times d \times f_{cv} \tag{5.36}$$

where,

$$f_{cv} = 0.17 \times \left[1 + \frac{2}{\beta_h}\right] \sqrt{f_c} \leq 0.34 \times \sqrt{f_c} \tag{5.37}$$

V_u : Ultimate Shear Strength of the concrete slab near the column

V_{uo} : Ultimate Shear Strength of the slab with No Moment Transfer.

f_{cv}	:	Concrete Shear Strength
β_h	:	Ratio of the longest overall dimension of the column, *Y*, to the overall dimension, *X*, at right angles to *Y*.
f_c	:	Peak stress on the stress-strain curve of a typical specimen in compression
d	:	Effective depth of slab averaged around the critical perimeter
u	:	Total Length of the Critical Perimeter

In the proposed approach, zero moment transfer from the slab to the column support is not assumed. The region around the column is designed for moment transfer shears as explained in Section 5.4.5.2 below.

5.4.5.2 Moment Transfer Shear

In many slab-to-column connections, an unbalanced moment is transferred in addition to the shear from the slab. The result of this unbalanced moment is non-uniform shear around critical perimeter. This will generally be the case for exterior or corner columns and sometimes for interior columns depending on the geometry and loading conditions. In these cases, the shear force and unbalanced moment are transferred by a combination of bending, torsion, and shear at the faces of the critical perimeter.

The behaviour of moment transfer shear can be analysed using several techniques, including analysis based on thin plate theory, beam analogies, analysis based on a linear variation in shear stress or truss analogies. AS 3600 specifies four different formulae for four cases when determining V_u:

- If there are no closed ties in the torsion strip or spandrel beams
- If the torsion strip contains the minimum quantity of closed ties
- If there are spandrel beams perpendicular to the direction of M_v^* which contain the minimum quantity of closed ties
- If the torsion strip or spandrel beam contains more than the minimum quantity of closed ties

Case 1 above is adopted for determining V_u in the proposed approach, i.e. it is assumed that there are no closed ties in the torsion strip or spandrel beams when calculating V_u. As per AS 3600, then

$$V_u = \frac{V_{uo}}{1 + \frac{\frac{M_v^*}{a}}{\frac{8 \times V^* \times d}{u}}} \tag{5.40}$$

where,

$$V_{uo} = u \times d \times f_{cv} \tag{5.36}$$

where,

$$f_{cv} = 0.17 \times \left(1 + \frac{2}{\beta_h}\right) \times \sqrt{f_c} \leq 0.34 \times \sqrt{f_c} \tag{5.37}$$

V_u	:	Ultimate Shear Strength of the concrete slab near the column
V_{uo}	:	Ultimate Shear Strength of the slab with No Moment Transfer.
f_{cv}	:	Concrete Shear Strength
β_h	:	Ratio of the longest overall dimension of the column, *Y*, to the overall dimension, *X*, at right angles to *Y*.
f_c	:	Peak stress on the stress-strain curve of a typical specimen in compression
M_v^*	:	Difference between moments at the front and back face of column
a	:	Length of a side face of the critical perimeter
V^*	:	Design factored shear force
d	:	Effective depth of slab averaged around the critical perimeter
u	:	Total Length of the Critical Perimeter

In the computer code, Equations 5.35, 5.36, 5.37 and 5.40 are programmed to compute the ultimate shear strength of the concrete slab near the column. The implementation details are explained later in Chapter 7.

For the purpose of shear design, the bending moment transferred from the slab to the support shall be taken as the unbalanced bending moment at that support. At an exterior support, the actual moment shall be taken. At an interior support, AS 3600 requires a minimum value of M_v^*, which is the difference between moments at the front and back face of the column and this minimum value is given by Equation 5.38.

$$M_v^* \geq 0.06 \times \left[(1.25 \times g + 0.75 \times q) \times L_t \times L_o^2 - 1.25 \times g \times L_t \times \left(L_o^{'} \right)^2 \right] \quad (5.38)$$

where,

$L_o^{'}$: Smaller value of L_o for the adjoining spans

L_t : Width of the Design Strip

L_o : L minus 0.7 times the sum of the values of as at each end of the span (*Refer Fig. 5.4 below*).

g : Dead Load per unit area

q : Live Load per unit area

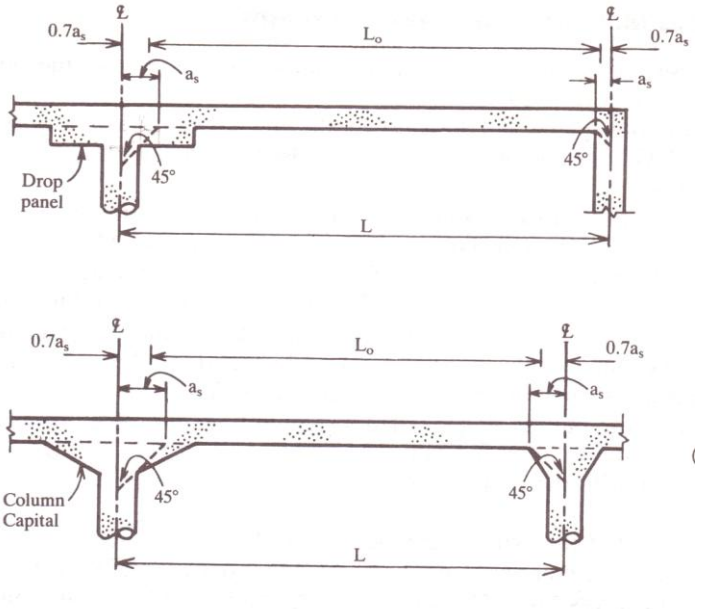

Fig. 5.4. Span Lengths (Warner *et al.* 1989)

Essentially, a flat slab has bending moments in both directions. In the conventional approach to flat slab design, the moments in the x-direction are calculated first, and for this purpose a design strip of floor bounded by centre-lines between columns is considered (*Fig 5.5 below*). In this way the 3D problem is reduced to a 2D plane frame problem. The analysis then comprises two main steps:

1. Calculation of total moments in the design strip both at support and at midspan.
2. An estimate of how these moments are distributed across the width of the design strip.

The moments in the y-direction are then determined separately in a similar manner by considering design strips running in the y-direction.

Two problems that require special attention in the design of flat slab buildings are:

- Shear combined with moment around the columns
- Deflections at the panel centres.

Both these problems are taken into consideration in the proposed approach of finite element based flat slab design.

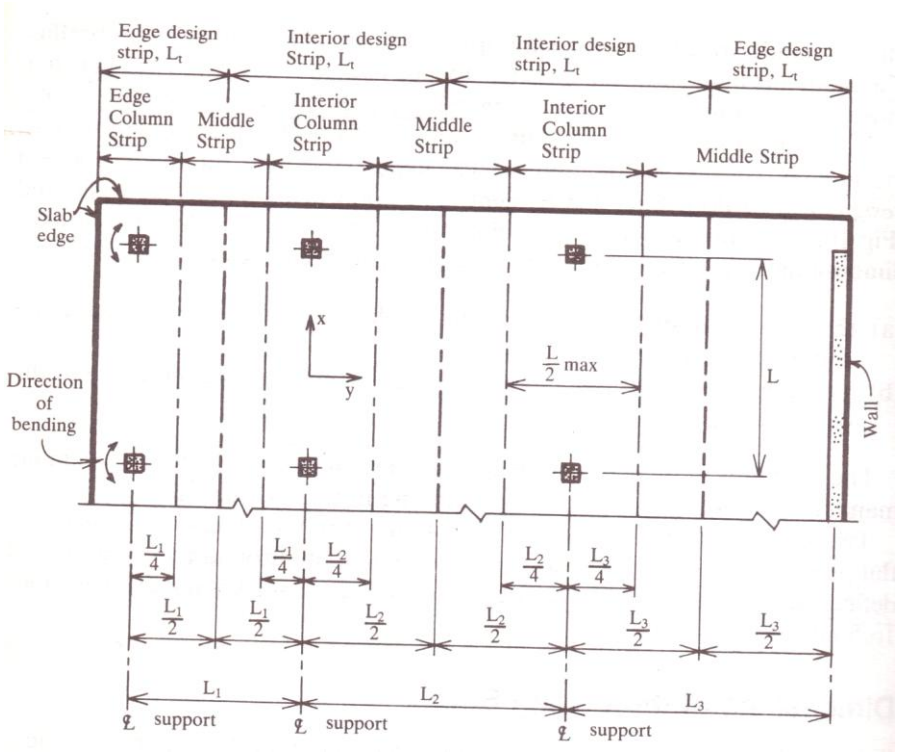

Fig. 5.5. Widths of strips for two-way slab systems (Warner *et al.* 1989)

In the proposed approach using finite element based flat slab design, strips of slab (*design strips*) are not considered for design, as is adopted in conventional design, and hence equation 5.38 is not programmed in the computer code. Moreover, difficulties in implementation restricted coding the above equation in the software. The actual moment is therefore taken for both exterior and interior supports. The values of M_v^* in the x and y directions are usually different. The values of a are also different if the column is not square. In using equation (5.40) above, the greater of the two values of $\frac{M_v^*}{a}$ is employed. This is programmed in the computer code. Description of the algorithms that calculate M_v^* for each column under the slab and the critical perimeter u for interior, exterior and corner columns is detailed later in Chapter 7.

It is usually found that the condition in Equation 5.30, $V^* \le \phi \times V_u$ is satisfied. If not, then the program chooses a section such that, in addition to satisfying flexural criteria, the section also satisfies the shear criteria of Equation 5.30. Such a section is usually thicker (in the form of a drop panel) than the previously assigned section.

5.4.7 Serviceability Requirements

The performance of a slab at service loads is an important design consideration in addition to strength requirements. Even if strength requirements are fully satisfied, excessive defections or cracking can interfere with the usefulness of the structure (Gamble and Park 2000). AS 3600 states "reinforced concrete members subjected to flexure shall be designed to have adequate stiffness to limit defections or any deformations that adversely affect strength or serviceability of a structure". Many factors influence the deflection of a slab. Some of the more important are:

- Ratio of spans
- Stiffening effect of drop panels and column capitals
- Deformations in supporting beams
- Extent of cracked regions
- Creep and shrinkage properties of concrete
- Ratio of sustained load to total load
- Construction loads

As in the case of beams, AS 3600 allows for the control of deflection of slabs either by direct calculation of deflection and comparison with allowable values, or indirectly by keeping the span/depth ratios within prescribed values. Section 9.3 of AS 3600 is to be followed in the calculation of slab deflections. Clause 9.3.4 of AS 3600 gives maximum allowable values of span/depth ratios for which deflection control can be assumed to be achieved. In the computer code, the maximum deflection of the slab is recorded after each iteration (i.e. after each FEA). This deflection that is calculated by SAP2000 is based on the assumption that the gross section (i.e. uncracked section) is resisting the applied load. However, the actual deflection of the cracked section may be more than this predicted maximum deflection. Hence, this maximum deflection is multiplied by 3 (in line with industry practice as advised by the industry-partner) to get a realistic value of the maximum deflection in the slab. It is then compared with the limiting values specified in Clause 2.4.2 of AS 3600. The justification/basis for multiplying the maximum FEA computed deflection by a factor of 3 is based on the assumption that the gross section (i.e. uncracked section) is resisting the applied load. This is explained as follows:

SAFE (slab design software by CSI) allows for an elastic (linear) analysis or a cracked deflection (nonlinear) analysis. In a cracked deflection analysis, SAFE takes into account the reduction of the gross section properties resulting from the cracking of the concrete, which results in an increase in the deflections. When performing a cracked deflection analysis, the user

has the option to assign a long-term deflection multiplier to each load case to account for behavior such as shrinkage and creep. Normally, a long-term deflection multiplier with a value greater than 1 is applied only to permanent load cases, such as the dead load case (the default value in SAFE is 3). All other temporary load cases (for example, live, wind, earthquake or snow) use a factor of 1. The long-term deflection multiplier works only with the cracked deflection analysis.

Now, as SAP2000 (and not SAFE) is being employed in this work for finite element analysis, a cracked deflection analysis for slabs is not possible in SAP2000 Version 8.3. When using the software SAFE, it was observed that if a non-linear cracked deflection analysis is performed and the computed deflections are compared with the deflections obtained from an elastic (linear) analysis (which is based on the 'gross section'), then the 'cracked' deflections are generally observed to be in range of 2.5 to 3 times that of 'gross' deflections. This was confirmed by analyzing several slab models and comparing their results for elastic and cracked deflections. Therefore, a factor of 3 is employed to the maximum deflection computed by the SAP2000 elastic (linear) finite element analysis so as to avoid performing detailed cracked deflection computations as per AS 3600 in the proposed optimization process (as this complicates the optimization process flow-control and also increases the computational cost of optimization). This factored maximum deflection is then compared with the limiting values specified in Clause 2.4.2 of AS 3600.

5.4.8 Detailing of Reinforcement

Once an area of reinforcing steel has been determined that satisfies the strength and service ability requirements, this reinforcement must be physically constructed. AS 3600 places many requirements on the actual layout and placement of reinforcing steel. Placement of reinforcing bars must satisfy geometrical constraints, and the bars or welded wire fabric must be of adequate length to fully develop their capacity. Being a preliminary design tool, specific detailing requirements are not programmed into the present computer code.

5.5 The Simplified Method of Slab Design

The simplified method of slab design is presented in section 9 of AS 3600. Bending moments are determined by means of coefficients set out in AS 3600. The values given by the Standard take advantage of the slab capacity for redistribution in order to achieve simple numerical values. A flat slab system must meet several requirements for the simplified method of design to be applicable, as per Section 7.4, AS 3600. First, there must be a minimum of two consecutive

spans, or bays, in each direction. Second, panels must be rectangular, and in each panel, the ratio of the longer to the shorter span must be less than two. Third, successive span lengths must not vary by more than 1/3 of the longer span in each direction. Fourth, columns must not be offset by a distance > ten percent of the span length in the direction of the offset between the centre lines of adjacent columns. Fifth, lateral forces are resisted by shear walls or braced frames. Finally, the structure must only be loaded with gravity loads, and applied loads must be uniformly distributed over the entire panel. The applied live load must not exceed two times the dead load.

The simplified method of slab design reduces the general slab structure to smaller panels within the slab, which are designed independently. In figure 5.6, a typical slab panel, of a slab-beam, is shown by the hatched pattern. Several key dimensions are given. The distance l_1 is the spacing between column centrelines in the direction parallel to reinforcement to be designed. The distance l_2 is the width of the slab-beam in the direction transverse to the reinforcement to be designed. The distance l_n is the clear spacing between columns in the same direction as l_1, and becomes the effective length of the slab-beam for the distribution of bending moment in the panel.

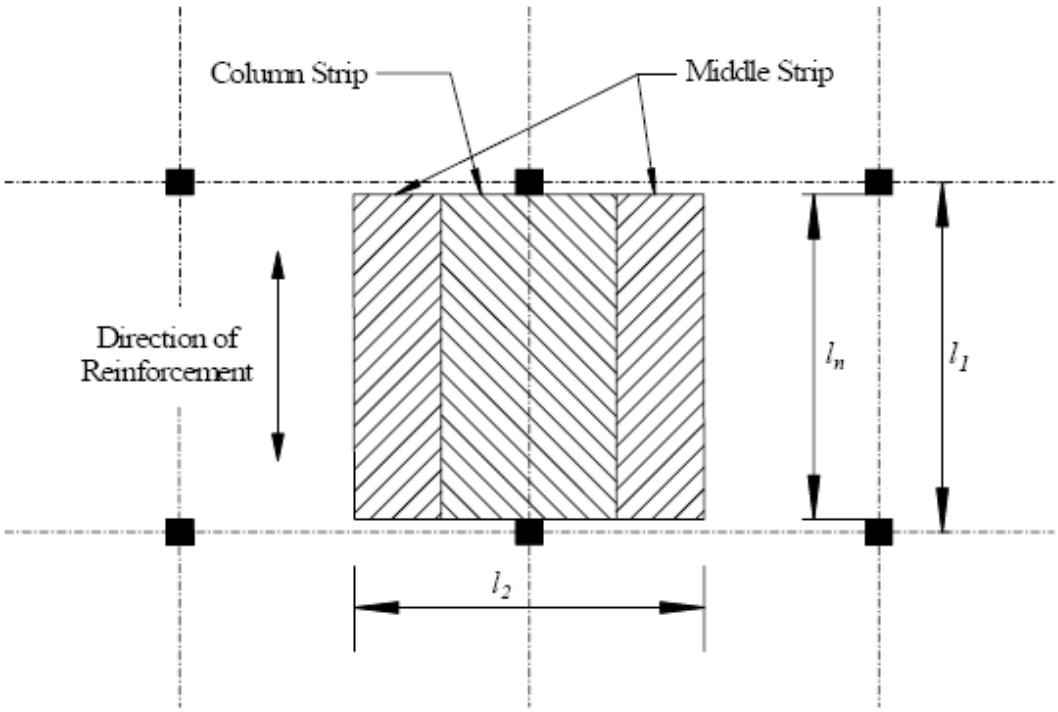

Fig. 5.6. Slab Beam Layout and Dimensions (Deaton 2005)

To compute the design moments at various sections throughout the panel, the distributed load on the panel must be computed. This load is the ultimate factored gravity load on the slab and is computed using section 3.3 of AS 3600. The fundamental calculation for a slab panel in the simplified method of slab design is the computation of the total static moment, M_o (Refer Fig. 5.7 below). For a slab-beam, the total static moment is equal to the average of the negative moments at each end of the member plus the maximum positive moment throughout the member. The formulation for M_o, as per AS 3600 is shown in Equation (5.40).

$$M_o = \left(\frac{F_d \times L_t \times L_o^2}{8} \right) \tag{5.40}$$

where,

F_d : Factored Design Load per unit area on the slab

L_t : Width of the design strip

L : Total span of design strip from centre-to-centre of supports

L_o : L minus 0.7 times the sum of the values of a_s at each end of the span (Refer Fig. 5.4 above)

a_s : Span support, which is defined for various cases as shown in Fig.5.4 above.

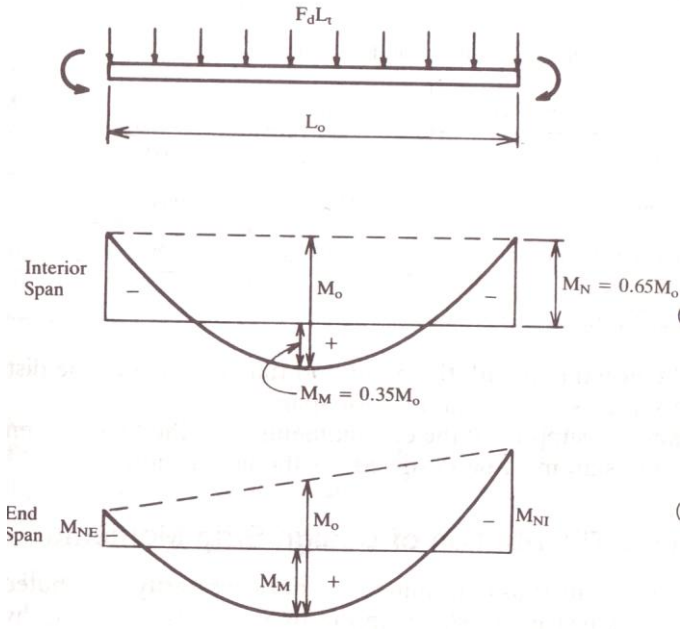

Fig. 5.7. Moment Diagrams for Flat Slabs (Warner *et al.* 1989)

The total static moment is then distributed throughout the slab panel according to the rules of AS 3600 Section 7.4.3. Depending on the location of the panel within the structure, M_o is distributed in different ways. For instance, for an internal slab-beam, 65 percent of M_o is distributed to the negative factored moment at the column faces, and 35 percent of M_o is distributed to the positive factored moment at the mid span. If the span terminates at an outside edge or at special restraints such as edge beams, the distribution of M_o changes according to the table in AS 3600 Section 7.4.3. Once the total static moment has been computed and distributed between the positive and negative moment locations of the slab-beam, these moments must be distributed between column and middle strips. For a general case, the layout of the column and middle strips is shown in Fig. 5.5 above. Definition of a column strip and middle strip is given in Section 7.1.2 of AS 3600. The percentages of the total static moment to be distributed to the column and middle strips are presented in tabular form in AS 3600 Section 7.4.3. Note that the design moment for the middle strip is divided to each side of the column strip, and subsequently added to the design moment in the middle strip from adjacent slab panels, and then the reinforcement is placed in the middle strip uniformly. The moment distribution factors are based on both experimental and analytical studies of moments in linear elastic slabs, and are intended to "ensure that steel stresses are not excessively high at service load so that crack widths and deflections remain within acceptable bounds" (Gamble and Park 2000).

5.6 The Idealised Frame Method

The idealised frame method for two-way slabs is presented in section 7.5 of AS 3600. The idealised frame method refers to two methodologies. The first is called the equivalent column method and is the focus of this section. The second is the equivalent slab method and will be discussed later in this section. The idea of the equivalent column method is that a three dimensional slab system is represented by a series of adjacent two-dimensional frames. A general plane frame model used in equivalent column design is shown in Figure 5.8 below. Applied loads act in the plane of the frame. Each frame corresponds to a column line in the structure. Idealised frames are assumed longitudinally and transversely through the building, and each frame is analysed independently.

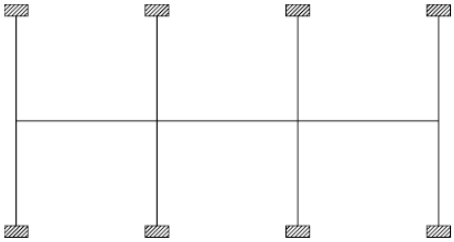

Fig 5.8. Plane frame analytical model for the equivalent column method (Deaton 2005)

In an idealised frame analysis accurate calculation of the stiffness of the slab-beams and columns is critical. A slab-beam is a horizontal member in an idealised frame and for a flat plate consists only of the slab. A slab-beam in the equivalent column method is the same as that for direct design, as shown in Figure 5.6 above. The moment of inertia of each slab-beam is computed based on the gross section area of the concrete, and variation in moment of inertia along the slab-beam must be taken into account, although there is typically none in a plate. The moment of inertia of columns from the top to bottom of the slab-beam at a connection is assumed to be infinite. The columns in the slab system will actually be modelled as equivalent columns, with geometry as shown in Figure 5.9 below. An equivalent column consists not only of the physical columns above and below the connection, but it also contains a torsional member attached at the level of the slab. For a flat plate, the torsional member consists of a portion of the slab with a width equal to that of the column in the direction of the span for which moments are being determined. Thus, the stiffness provided by the equivalent column is a combination of the stiffness of the physical columns and of the attached torsional member. The equivalent columns stiffness K_{ec} is given in equation (5.41) as a function of the column stiffness K_c and the torsional member stiffness K_t (Corley and Jirsa 1970).

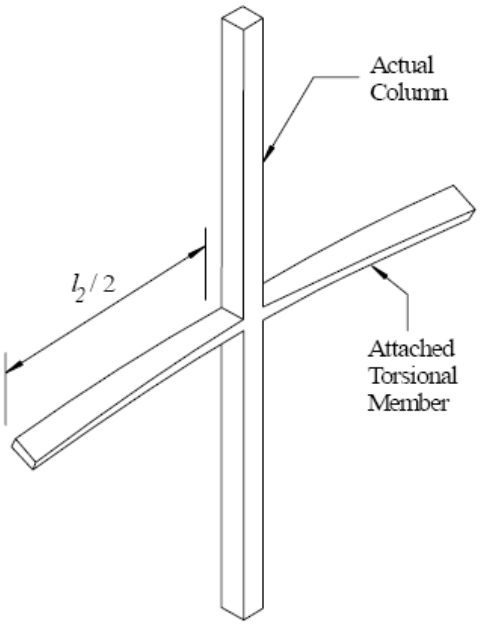

Fig. 5.9. Equivalent column with attached torsional member (Deaton 2005)

$$\frac{1}{K_{ec}} = \frac{1}{\sum K_c} + \frac{1}{K_t} \tag{5.41}$$

K_{ec}	:	Equivalent column stiffness
K_c	:	Column stiffness
K_t	:	Torsional member stiffness

The structure is analysed once the stiffness has been determined for the slab-beams and equivalent columns. Moment distribution used to be employed for the analysis when the equivalent frame technique was first introduced, although today this has been largely replaced with frame analysis programs that analyse the system using the direct stiffness procedure.

The results of the frame analysis provide the distribution of moment and shear throughout the slab-beam. The moments and shears must be determined at the face of the columns, not the centre lines, and at other sections throughout the members to find the critical effects. Once the critical design forces have been determined, the positive and negative moments are distributed between column and middle strips using the same factors as those used in the simplified design method. The reinforcement is then designed using the theory and procedures presented earlier in this chapter to resist flexure and shear, to satisfy serviceability criteria, and to provide appropriate detailing of reinforcement (Deaton 2005).

The methodology presented so far for the idealised frame technique is limited to gravity load analysis only. However, the idealised frame technique has been shown in published literature to be applicable to analyse unbraced multistorey buildings for both lateral loads as well as gravity loads using a modified technique known as the equivalent slab technique (Vanderbilt 1979). Effects of cracking must be taken into account for any analysis accounting for lateral loads and it is permissible to combine the results of lateral load analysis with the results of gravity load analysis. Literature available on the lateral load analysis of slab systems indicates that satisfactory deflections and force results can be obtained provided that the technique is limited to parallel planar frames with similar stiffnesses (Vanderbilt 1979).

5.7 Yield Line Method

The yield line method is an upper bound approach to limit analysis of reinforced concrete slab systems. Sufficient knowledge and experience is needed to apply this method in order to ensure an accurate design, as it is possible that the strength of the slab could be significantly overestimated. Yield line theory is generally applied to slabs with a uniform distribution of reinforcement, though it has also been applied to slabs with non-uniform reinforcement. In general, the yield line theory is a method to check the strength of an already reinforced slab system (Hillerborg 1996). For design, the distribution of reinforcement is assumed initially and then checked. The yield line method is particularly suitable for slab systems that cannot be analysed by either simplified design or idealised frames due to geometric limitations. It can be used to design slab systems with various shapes, boundary conditions, openings, and complicated loading conditions (Deaton 2005).

Most reinforced concrete slabs systems are under-reinforced due to the fact that they are generally designed to exhibit a tension controlled failure. As the loading on the slab increases, some of the steel begins yielding locally, and the stiffness of the system (and thus the distribution of moment) redistributes in response to this yielding. The first instance of localized yielding usually occurs at the location of maximum bending moment as determined by elastic theory (Gamble and Park 2000). Assuming sufficient ductility is present, as this redistribution occurs and subsequent progressive yielding of adjacent zones follows, large changes in curvature occur with increases in loading until a collapse mechanism is exhibited in the form of one or more plastic hinges. Yield lines are the narrow zones of localized yielding that occur as a result of this plastic behaviour (Cope and Clark 1984). According to Deaton (2005), “the fundamental idea of design based on the yield line method is that the engineer must postulate a collapse mechanism, i.e., the locations of yield lines that satisfy the boundary conditions of the

slab". For a given slab layout, he says, multiple collapse mechanisms are often possible, depending on the distribution of reinforcement, "so the engineer must examine all possible collapse mechanisms to determine the actual ultimate load" (Deaton 2005). Some examples of possible collapse mechanisms for uniformly loaded slabs with various shapes and boundary conditions are shown in Figure 5.10 below. A combination of multiple yield lines in a slab panel is called a yield pattern. "The behaviour of a yield pattern is subject to several principles that engineers may apply in the determination of the collapse mechanism. In a slab panel, the slab segments between yield lines are assumed to behave as a rigid plane and deflect as such after the plastic mechanism is formed. In addition, to act as a plastic hinge, a yield line must be straight in order to form an axis off rotation" (Deaton 2005). Plastic hinges will always develop along fixed supports. For instance, a yield line may form along a fixed edge, and plastic hinges will develop over columns. Also, a yield line must intersect at the axes of rotation of two adjacent slab segments if deflections are to be compatible (Gamble and Park 2000). Once a yield pattern has been assumed, the system must be analysed to determine the actual location of the yield lines. The two main methods employed to solve for the unknown dimensions defining the actual yield pattern are analysis using the equations of equilibrium or analysis by the principle of virtual work (Gamble and Park 2000).

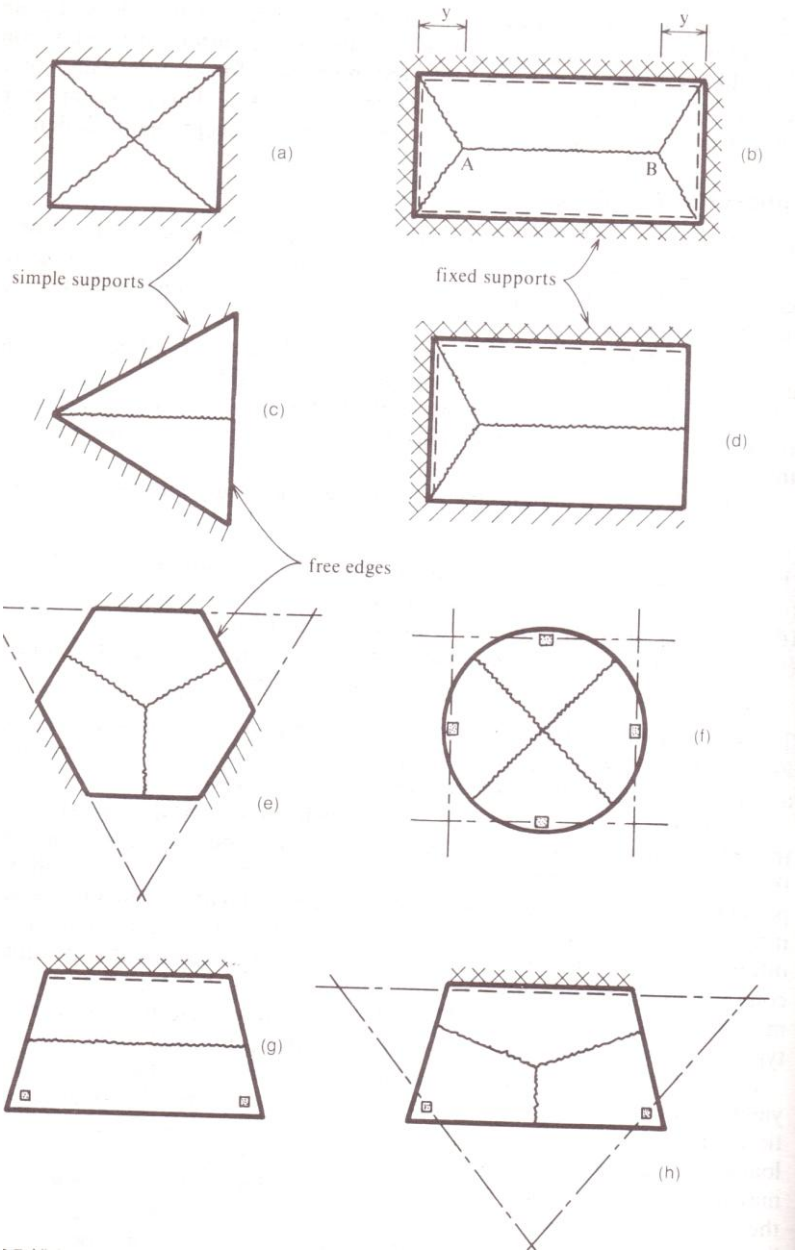

Fig. 5.10. Yield line patterns for distributed loads (Warner *et al.* 1989)

Theoretically, same yield line geometry should be computed by both solution techniques. Once the unknown yield pattern dimensions are determined, the system can be evaluated to determine the ultimate uniform load required to produce this yield pattern. After the actual collapse mechanism and ultimate load have been determined, the engineer can distribute reinforcement throughout the slab. Here, the engineer assumes the manner of yielding, and details the slab such that this assumed yield pattern occurs. The serviceability of slabs designed using the yield line method is an important concern. At services loads, the slab system must be checked to determine that deflections and crack widths are within acceptable bounds. Although uniform

distribution of steel may satisfy the ultimate states, concentrations of reinforcement may be required in some areas to provide adequate performance at service loads (Deaton 2005).

5.8 Strip Design Technique

Hillerborg (Hillerborg 1996) is credited with the development of the strip design procedure (Gamble and Park 2000). In contrast to the yield line technique, the strip design method is a lower bound approach to limit analysis of reinforced concrete slab systems. The strip design method, being a lower bound approach, will provide a value for the ultimate load for a slab that is either accurate or too low. Thus, the strip design technique is generally conservative when applied appropriately. In fact, if an unsuitable solution is computed, the strength of the slab may be so conservative as to lead to poor economy (Hillerborg 1996). Also, the strip technique is a pure method of design, not a method for checking a previously designed system (such as the yield line technique). According to Hillerborg, the stated objective of the strip design technique is to "seek a solution to the equilibrium equation [and] reinforce the slab for these moments" (Hillerborg 1996).

As stated by Hillerborg, the general idea of the strip method is that load is assumed to be carried by strips of the slab that are oriented in the directions of reinforcement (Hillerborg 1996). Strips are analogous to beams, and as such, this method is only applicable in scenarios where the strips can be suitably approximated as beams with pin or fixed supports. The slab is divided into these strips based on the assumed transfer of load to the supports. Hillerborg further stated, "the whole load within each part of the slab is assumed to be carried by strips in one reinforcement direction [where] no torsional moments act in these strips" (Hillerborg 1996). Distributing the load in this manner generally produces simple and economical designs.

The actual determination of the layout of design strips is subjective and requires a general understanding of the behaviour of the system being designed. The goal of design should be to transfer the load to supports in the most economical manner possible. Practically, this means for a rectangular slab with all edges fixed and dimensions a and b, where $a > b$, less reinforcement will be required if the load is assumed to transfer primarily to the supports on the edges of length a, between which the span is shorter but, because the moments in this direction will be less than the moments developed in the long direction, on the edges of length b. Hillerborg suggests that the portions of the slab loading to be transferred to different supports should be divided based on the location of lines of zero shear force, along which the shear force is assumed to be zero in all directions (Hillerborg 1996). Figure 5.11 shows the layout of strips commonly used for some simple slab systems.

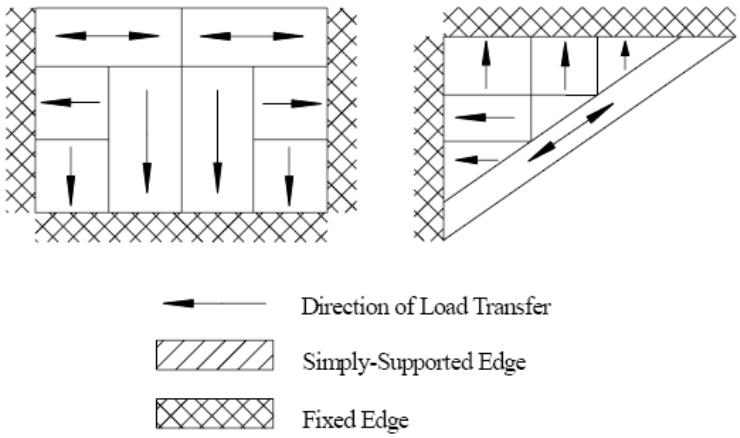

Fig. 5.11. Example strip design layout (Deaton 2005)

Once a field of strips has been determined, each strip is then analysed independently for the loading assigned to that strip. Based on the results of the simple analysis of the strip, top and bottom reinforcement is designed for each strip. Sometimes interaction of strips must be accounted for in the analysis, particularly if one strip is assumed to support others as in the case of a strong band, where a concentrated area of tensile steel may be provided. The primary drawback to the strip design technique is the possibility of poor performance with respect to serviceability. Applied incorrectly, the strip design technique can lead to wide cracking or excessive deflections at the service load level (Gamble and Park 2000). To avoid this, the distribution of moments should conform reasonably closely to that provided by elastic analysis. Also, additional models may be required beyond those used in design to appropriately evaluate the actual deflections of the slab system (Deaton 2005).

CHAPTER 6: FLAT SLAB MODELLING ISSUES

6.1 Introduction

Accurate modelling is a must if the finite element method is to be a reliable tool for the design of reinforced concrete flat slab structures. Accurate modelling involves understanding the important relationships between the physical world and the analytical simulation. As Clough (1980) states, "depending on the validity of the assumptions made in reducing the physical problem to a numerical algorithm, the computer output may provide a detailed picture of the true physical behaviour or it may not even remotely resemble it" (Clough 1980). The following sections attempt to identify possible pitfalls in numerical modelling of slab structures.

6.1.1 General Modelling Requirements

The finite element method is an approximate technique, and therefore results computed using this method must be critically evaluated before relied upon in a design application (Liepins and Bell 1992). This process of critical evaluation involves several steps for any structure being analysed (Deaton 2005). The number of elements used in a model can greatly affect the accuracy of the solution. In general, the accuracy increases as the number of elements, or the fineness of the mesh, is increased. Convergence of results to the correct numerical solution should be verified by creating a number of models with increasingly finer meshes. Convergence of results means that an increase in the number of elements should not produce a significant change in a particular response quantity such as displacement or stress. Not all response quantities will converge at the same rate, however. Displacements will generally be the most accurate response quantity computed and will converge faster than stresses (Liepins and Bell 1992). Generally, however, convergence of displacements does not guarantee convergence of stresses since stresses are computed as derivatives of the displacement field. Additionally, it may be necessary to increase the number of elements in areas of the model near either concentrated loads or supports, where the stress gradient is steeper. The quality of the results can also be affected by the type of element applied in the analysis as various finite elements are derived using different assumptions. Since flat slab systems are modelled using plate-bending elements, this discussion will be limited to several types of plate bending elements. For instance, Kirchoff plate elements are derived for application to *thin* plates and only account for flexural deformation. “Thin” generally refers to a plate with thickness much smaller than its in-plane dimensions (Logan 2002). Mindlin plate elements are derived for application to moderately thick plates and account for both flexural and shear deformations. Generally, a “thick” plate is one with a thickness greater than 1/10 the span of the plate (Logan 2002). If a

moderately thick plate is analysed using a Kirchoff element then the results could deviate significantly from the physical behaviour of the real plate, as the Kirchoff element can only represent flexural deformation while the physical structure is exhibiting considerable shear deformation - a behaviour represented by the Mindlin element. There are several other examples similar to this one that demonstrates the importance of selecting an element appropriate to the specific application of the analytical model. Generally elements with mid side nodes are more accurate than those without mid side nodes. Elements with higher order shape functions are more accurate than those with lower order shape functions. Once an engineer is confident that the numerical solution has converged and that the specific element chosen is appropriate for the current application, a number of other checks are necessary to validate the analysis. As the finite element method does not guarantee equilibrium of the structure, this important condition must be verified to be satisfactory. Hand calculations should be carried out to verify the sum of reactions of the model. The magnitude of global displacements should be checked and verified to be small with respect to the geometry of the structure otherwise; a non-linear large deformation analysis may be necessary.

After all these criteria have been satisfied, it is important to determine if the results roughly follow the expected outcome. “The engineer must determine whether or not the results make physical sense" (Clough 1980). The displaced shape of the structure and contour plots of stresses should roughly correspond to the intuitive sense of the engineer. For example, symmetric results must accompany a structure with symmetric geometry and symmetric loading. Any deviation between expected and computed results must be critically investigated.

6.1.2 Assumptions in Reinforced Concrete Flat Slab FEA

A number of important assumptions are made in the analysis of reinforced concrete flat slabs. Understanding these assumptions is essential if accurate design results are to be obtained.

To begin with, the type of analysis applied in this study is limited to a linear elastic analysis. This introduces several important factors into the analysis. Reinforced concrete is a highly nonlinear material made up of many elastic, brittle materials; the stress strain curve of concrete indicates some degree of ductility. This is due to the gradual development of micro cracking, internal to the concrete (MacGregor 1997). Concrete begins cracking at a tensile stress of approximately eight to fifteen percent of its compressive strength (McCormac 2001). This cracking could indicate a brittle mode of failure, however the reinforcing bars within the cross section may begin yielding and introduce important ductility to the failure of the component. At the ultimate level, AS 3600 states that the maximum allowable strain at the extreme concrete

compression fibre shall be assumed equal to 0.003. This limiting value of compressive strain corresponds to the lower bound of experimental test data (Lourenco and Figueiras 1995). A linear elastic analysis does not account for any of the above nonlinear failure components and instead assumes that the gross section is resisting the applied loads at all stress levels. It considers the stress strain relationship to be perfectly linear, even if the compressive strain in the concrete exceeds 0.003 or if the tensile stress at the location of the reinforcing bars exceeds the yield stress of the steel.

In finite element analysis it is assumed that the material is isotropic and homogenous. Reinforced concrete however is a composite material. Plain concrete consists of a number of materials, mainly various aggregates, bounded in a matrix of cement. Aggregates range in size from roughly graded gravel to very fine sands. It is seen from experimental tests that plain concrete can be treated as statistically homogenous. However, the introduction of reinforcing bars disrupts the isotropy of the material, reducing the actual behaviour of the material to orthotropic at best and anisotropic in some cases. As such, the actual constructed concrete component will behave preferentially in some principle direction, and the relative stiffness due to this preferential material orientation will produce a distribution of stress much different from an analysis assuming isotropic conditions (Deaton 2005).

In areas where cracking and highly nonlinear behaviour are expected the stiffness of the finite element mesh can be effectively reduced by applying one of several methods. One technique is to reduce the thickness of the elements in the areas around columns or supports. Another technique is to reduce the elastic modulus in these areas. Although these methods may produce favourable results from an analysis perspective, they would be invalid in an implemented program procedure where the thickness and elastic modulus are used internally to the program for design calculations. In other words, the section must be designed for the full thickness, not a reduced thickness; likewise for the elastic modulus.

Another important assumption is that generally both Kirchoff and Mindlin plate-bending elements are derived based on the assumptions of small displacements and rotations. The significance of this assumption is that it allows the application of a linear analysis that ignores geometric nonlinearity. The exact meaning of "small" is a matter of interpretation on the part of the engineer. However, in general the deflections are small if they are small in comparison to the thickness of the slab (Vanderbilt 1979). Even so, the requirement of small deflections will usually be satisfied as a result of AS 3600 Section 2.4 and Section 9.3.

6.1.3 Modelling of Boundary Conditions for Flat Slab Systems

The importance of accurately modelling boundary conditions should never be underestimated or neglected in the analysis of any structure, particularly reinforced concrete flat slabs. In spite of putting in great efforts to verify that a model has converged and that the specific type of element used is appropriate to the behaviour required, if the boundary conditions are modelled inaccurately then the results of such an analysis may be worthless. A number of important considerations need to be discussed regarding the suitability of various techniques of modelling boundary conditions. The two types of boundary conditions presented in this discussion pertain to *end boundary conditions* and *slab to column connection* boundary conditions.

In general, two methods are applied to simulate the boundary conditions of flat slabs. In the first method, the columns supporting the slab, as well as the columns above the slab, are modelled using either frame elements or three-dimensional solid elements. This method attempts to isolate a particular elevated floor of the structure. In the second method, the flat slab is modelled as a plane of finite elements, and the flexural and translational stiffnesses physically provided by columns are simplified to "pin" or "fixed" supports applied at the elevation of the plane of the slab. Sometimes these supports are modelled as springs with a finite elastic stiffness to improve the accuracy of the model. Gentry's work (1986) studied both these connections and investigated which among them produces the most favourable results. He found that in general, it is preferable to model boundary conditions that account for the actual flexural stiffness of the columns, such as modelling the columns with frame members or three-dimensional solids instead of approximating the columns with pin or fixed supports at the mid surface elevation of the slab. Based on Gentry's work (1986) and extensive modelling performed by the author, only frame members or three-dimensional solids will be used for column modelling in this study. It is important to remember the following considerations when applying these boundary condition techniques.

To begin with, stressing the concepts presented previously, the finite element model assumes that the material behaves in a linear elastic fashion. While this is generally untrue in a physical sense, it is especially untrue for connections in flat slabs between the slab and the column (Pfaffinger 1972). These regions are often susceptible to cracking and subsequent yielding of reinforcement, leading to highly non-linear behaviour. Even if the slab is modelled as being supported on frame members, a fully fixed connection in the model dictates that the angle between the column and the slab remain exactly 90 degrees after deformation. This idealization overestimates the stiffness of this connection. An overestimation of stiffness leads to a change

in the relative stiffness throughout the slab, thus significantly decreasing the accuracy of the representation of the physical distribution of stress in the slab (Deaton 2005).

Another important consideration involving boundary conditions is the physical size of the connection versus that incorporated in the model. When a frame member is connected to a node in the finite element plane, the connection occurs over an infinitesimally small area, even though the physical connection maintains some finite size. This is significant for several reasons. First of all, an infinitesimal connection analytically increases the clear span between adjacent columns by a distance equal to the width of the column. The moments computed across a slab section are a function of the square of the clear span. Thus, application of this technique overestimates the bending moments in the adjacent slab panels. Second, design moments at the column face will be inaccurate because the slab region between the centroid of the column and the column face is now flexible, according to the stiffness of the slab, when it should be much stiffer when this area is enclosed within the column. Third, a concentrated boundary condition, such as column connected via a single node, causes the same result that any concentrated effect in a finite element model produces: an *unrealistic stress concentration*. In fact, the analytical solution will indicate a state of infinite stress at locations such as this (shown in Fig. 6.2 (a)). Fig. 6.2 (a) shows a finely meshed symmetrical flat slab subjected to uniformly distributed dead and live loads. Columns are modelled using frame members that connect to a single node in the finite element plane. In spite of creating multiple models with increasingly finer meshes, it is seen that the value of stress (in this case bending moment in 1-1 direction, M_{11}) does not converge; on the contrary it keeps increasing further. This indicates a state of infinite stress that is known as *stress-singularity*. In the finite element method *stress singularity* occurs when the theory of elasticity equations give an infinite stress. In such cases the stresses continue to increase without convergence, as the mesh is refined. The finite element model will produce more practical results if the column-to-slab connection can *be distributed over some finite number of nodes* instead of concentrating the effect at a single node (Fig. 6.1 b & Fig. 6.2 b).

Comparing Figures 6.2 a and 6.2 b, it is seen that a converged and more realistic value of M_{11} is observed in Figure 6.2 b. The value of –147.05 kN-m/m for M_{11} seen at the column face in Fig. 6.2 b is verified to be comparably close to the value of –138 kN-m/m computed by hand calculations using the 'Simplified Method of Design'. Further, if 'plate constraints' (discussed in Section 6.3.2) are employed at the nodes of the plate elements atop the column, a closer value of -141.52 kN-m/m is observed at the column face. Therefore, in order to address the issues due to stress singularity, the first step should really be to model the finite slab-to-column connection by modelling the slab with a fine enough mesh such that multiple elements cover the cross-section of the attached column. This will usually require a mesh fine enough that the column

area is overlaid with either a 2 x 2 or 3 x 3 mesh of elements, assuming that the overall model converges with this degree of fineness. After the flat slab mesh satisfies this requirement, there are several techniques to distribute the connection over the entire area of the column. The most accurate means of accomplishing this connection is to model the columns using 3D solid elements. These elements can easily be connected to the plate bending mesh over the entire area of the column, as shown in Figure 6.1 (b). The primary drawback to this method is that the computational and modelling costs of implementing such a large number of 3D solid elements are often uneconomical. Moreover, in the case of slab design around the column for Punching Shear, the Ultimate Design Shear Force is needed in the computation. By using a frame element (i.e. line or beam element) to model the column, the Ultimate Design Shear Force is readily obtained by reading the 'axial force' in the column frame member. When modelling columns using 3D solid elements however, it is generally required to add the averaged vertical force components in each solid element. Comparison with hand calculations reveal that the value of the Ultimate Design Shear Force is predicted more accurately when using line or beam elements rather than 3D solid elements for columns. This therefore indicates a conflict of choice based on the design objective (for bending moments or shear). Chapter 7 of this thesis focuses on developing conceptual/preliminary design techniques for flexure only. Therefore, for the work in that chapter, 3D solid objects are used to model columns (Fig. 6.2 (b)) together with the use of 'Plate Constraints', which are described in Section 6.3.2.

An additional technique is to approximate the finite area of the column using joint constraints. Using this technique, the columns are modelled using 3D solids, and each member is geometrically placed according to the centroid of the column in the physical structure. Joint constraints such as the "Plate Constraint" in SAP2000 are then applied to the nodes of the slab elements (or plate bending elements) at the finite area of the column. Numerical comparisons show the effectiveness of this technique in terms of accuracy of computed bending moments. "Plate Constraints" in SAP2000 are described in Section 6.3.2.

When designing the slab region over the column for punching shear however columns modelled as line or beam elements are more suitable (compared to 3D solids), as mentioned previously. However, stress singularity effects are seen in and around the elements close to the single node where the column frame member connects to the plate-bending element (Fig. 6.2 (a)). As mentioned previously, the effect due to this stress singularity is of little use in design, since it does not represent the true physical behaviour of the slab in that region. In order to overcome this problem, it is therefore proposed to assign a 'non-design' area for all those plate elements lying immediately above the column where the effects of stress singularity are seen. This region, which is prone to stress singularity effects, is thus treated as non-design and the design of the

slab in the region over the column is based on the smoothed maximum nodal value of M_{11}, M_{22} in the designable drop panel and Punching Shear calculations. The work in Chapter 8 entitled 'Optimal Conceptual Design of Slabs for Flexure, Punching Shear and Transverse Shear' focuses on developing conceptual/preliminary design techniques for bending moment; punching shear and transverse shear (or beam shear) performance and demonstrates the effectiveness of the proposed approach. Therefore frame members are used for the work in that chapter to model columns without the use of plate constraint for the nodes atop the column frame. Using plate constraints for the nodes atop the single frame column results in inaccurate axial force (or ultimate design shear force) in the column frame and hence the use of plate constraints is avoided when performing punching shear design in which frames are used to model columns in the flat slab with the 'non-design' area taking care of problems due to stress singularity.

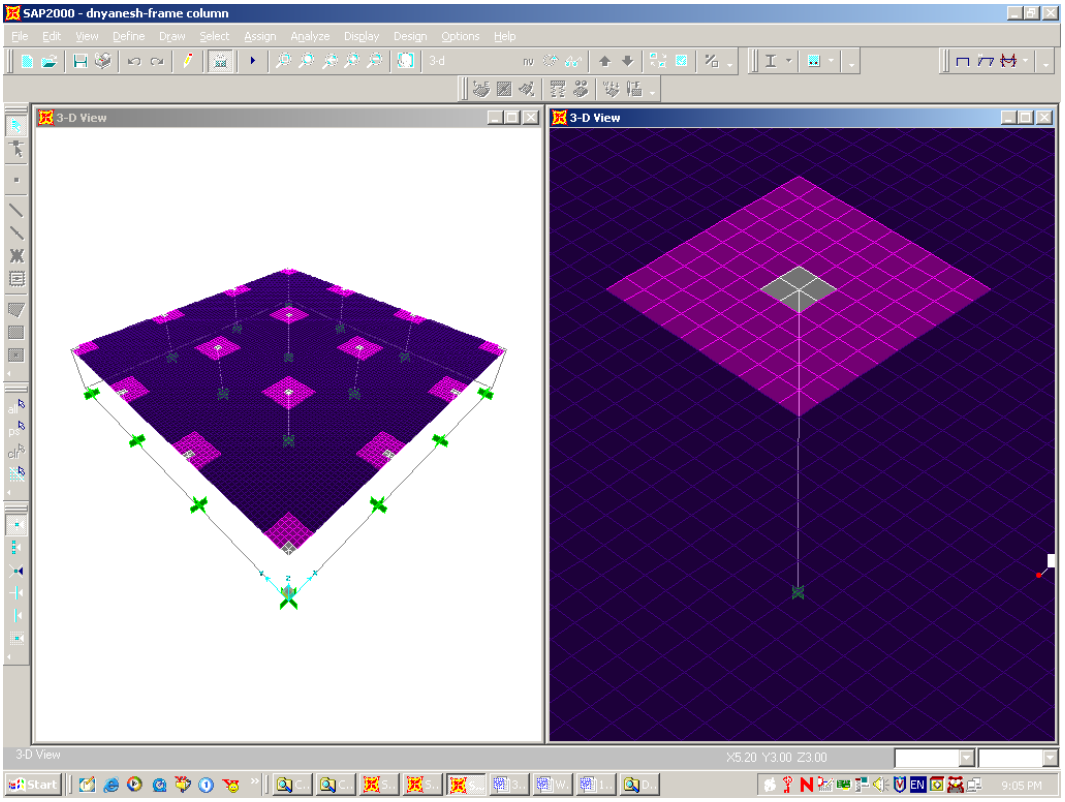

Fig. 6.1 (a). Frame element is used as a column

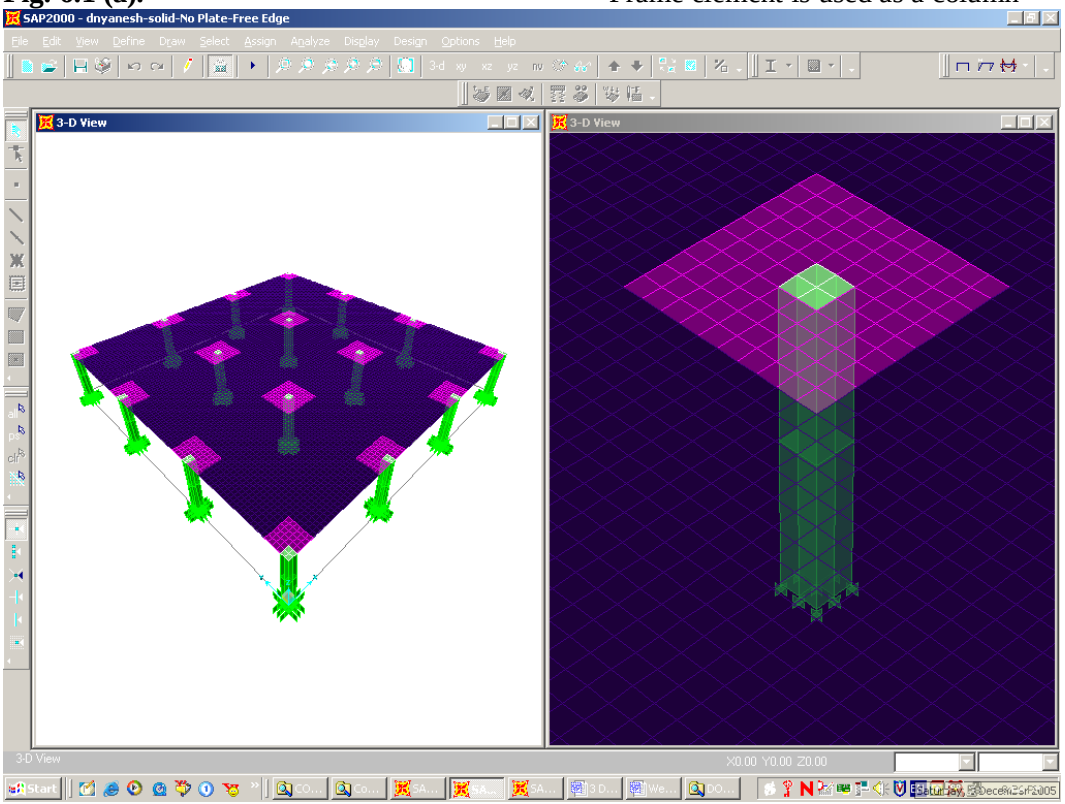

Fig. 6.1 (b). Solid Element is used as a column

Note: In Figure 6.1 (a) above, a bigger non-design area (shown in Grey) is required in order to solve problems due to stress singularity. Whereas, in Fig. 6.1 (b), stress singularity effects are not seen due to the use of 3D solid elements for the column and plate constraints for the nodes of plate-bending elements atop the column.

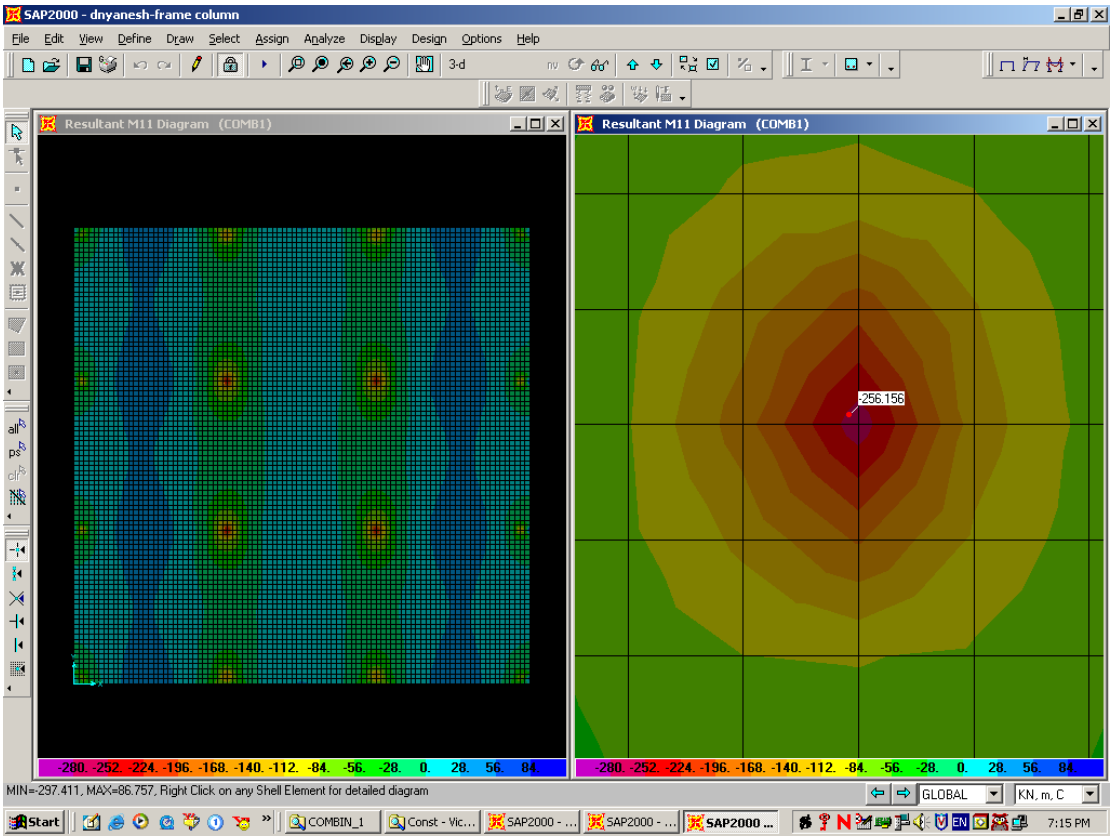

Fig. 6.2 (a). Columns modelled using Frame element – M11 distribution near central column (*No Plate Constraint*)

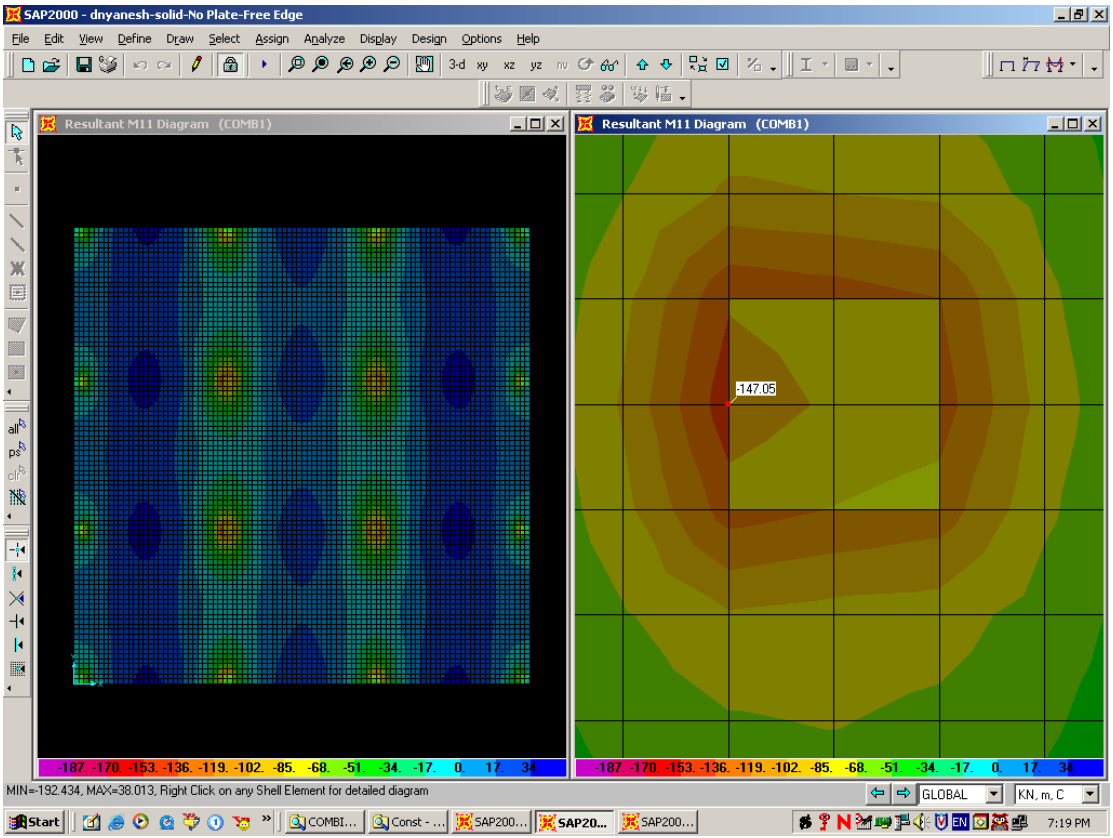

Fig. 6.2 (b). Columns modelled using Solid element - M11 distribution near central column (*No Plate Constraint*)

6.2 Conventional Techniques for Flat Slab Design Using FEA Results

There are two conventional methods for design based on FEA results, provided that sufficient care has been applied in the modelling of the flat slab system. Both these methods are presented and evaluated below. These are:

- Design using average stress resultants
- Design using element forces

6.2.1 Design Using Average Stress Resultants

6.2.1.1 Computation of Element Stress Resultants

Element stress resultants are the computed stress components per unit width located at a node of a finite element. For a plate bending analysis, the primary element stress resultants of interest are the bending moments per unit width evaluated at each node of the element, and the shear stress resultants, which are the shear forces per unit width evaluated at each node.

Element stresses can be computed in many locations throughout the element, including the centroid, Gaussian quadrature integration points, and at the nodes. Stresses computed at the integration points are generally considered to be the most accurate (Cook 2002). These results are of little use to engineers, however, because the physical locations of the Gauss points are unknown to the user. A common solution to this problem is to extrapolate the stresses to the nodes, a more useful location for the user. Element stresses can also be computed directly at the nodes by evaluating the strain-displacement relation at the nodes instead of the integration points, and then applying the material constitutive relation (Deaton 2005).

The element stress resultants (i.e. forces and moments) can be understood as the integration of the stress field over the thickness of the element, *t*. The following equations show the theoretical formulation of the element stress resultants at a typical node (Cook 2002).

Plate Bending Moments

$$M_{11} = \int_{-thb/2}^{+thb/2} t \times \sigma_{11} \times dx_3$$

$$M_{22} = \int_{-thb/2}^{+thb/2} t \times \sigma_{22} \times dx_3$$

Plate Twisting Moment

$$M_{12} = \int_{-thb/2}^{+thb/2} t \times \sigma_{12} \times dx_3$$

where, x_3 represents the thickness coordinate measured from the mid surface of the element.

The z-axis, in this case, is the direction perpendicular to the plane of the elements. The coordinate system is a common point of misinterpretation on the part of the engineer. M_{11} refers to a bending moment in the 1-1 direction. M_{22} refers to a bending moment in the orthogonal 2-2 direction. M_{12} refers to a torsional moment on both the x- and y- faces of a small volume of the element dV at a particular node, due to the shear stress at the particular node. Fig 6.3 presents a visual representation of this concept. The units of each of the bending moment resultants are force-length/length. For more information the reader is referred to the SAP2000 Analysis Reference Manual.

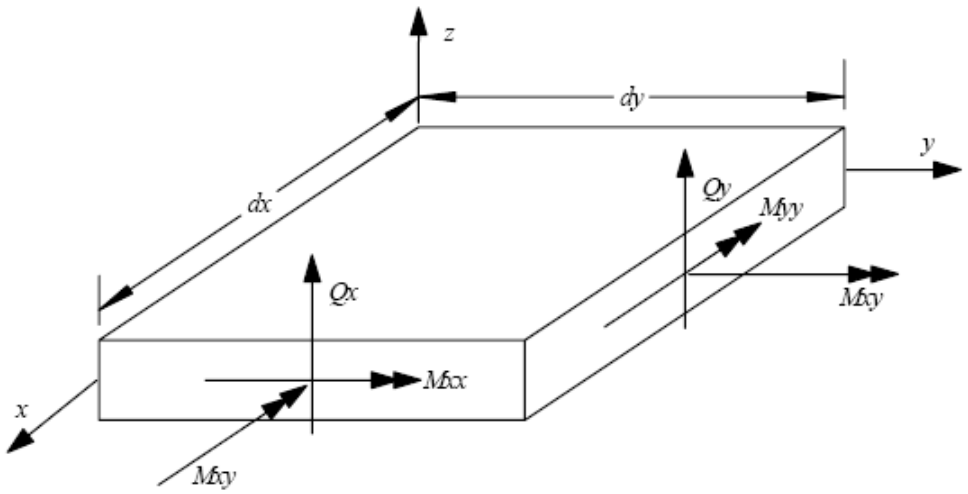

Fig. 6.3. Element stress resultants at a node (Deaton 2005)

According to Deaton (2005), once element stress resultants have been computed at each node of each element in the structure, there is no guarantee that for nodes with multiple elements connected, the element stresses computed at the node from contributing elements will be identical. This is because the finite element method only guarantees compatibility of the displacements and rotations at the nodes. Thus, if four elements are connected to a single node, it is likely that each element contributes a different state of stress at that node, i.e. four different states of stress have been computed at that node from each element. These results should

approach each other as the finite element solution converges, but even in a converged solution, there is no guarantee that these results will all lie within a small tolerance. If these results vary by more than an order of magnitude, further investigation is required as to the source of the discrepancy. (Deaton 2005). Most programs employ *smoothing algorithms* as a solution to the variation in stresses computed at a node, in which the stresses computed at a node are averaged to effectively *smooth* the solution of the stress field. An acceptable convergence criterion then is to evaluate whether the average element stresses have converged. If so, the analyst may proceed with design, understanding that stress compatibility is not satisfied i.e. each element contributes a different stress component to each node Another important consideration in the computation of element stresses is that there is no guarantee that equilibrium is satisfied. If equilibrium of a single element or the entire structure for that matter is to be considered then the stresses, being reported only at the nodes, need to be interpolated between nodes. Such an interpolation procedure will seldom predict the physical distribution of stress accurately. However this does not mean that the solution is altogether invalid, but rather that the engineer must understand that the applied technique is an approximate one, and that the resulting design should be critically evaluated, as described in the introduction of this chapter.

6.2.2 Design Procedure using Bending Moment Resultants

Different commercial slab design software available in the market today, such as SAFE from CSI, Berkeley, USA (SAFE User Manual 1998) and SLABS from Inducta Engineering, Sydney, Australia (SLABS User Manual 2005) etc, compute the *design moment* for a particular cross section of a strip, or cut which is then used to design the flexural reinforcement, using different methods. SAFE gives the user the option to compute the design moment based on either the Wood-Armer technique or the 'Nodal Integration Technique'. A brief description of these techniques follows:

6.2.2.1 Nodal Integration of Moments in "SAFE"

In SAFE, the total integrated cross-sectional moments and shears along the length of a design strip are obtained for design and display purposes. For nodal integration, the moments are integrated as follows:

- For a particular load combination or load case for each element within the design strip, SAFE calculates the nodal point reactive moments. Those moments are obtained by multiplying the slab element stiffness matrices by the element nodal displacement vectors.

- The nodal point moments for each set of slab elements with the same property type are then added to get a single positive design moment and a single negative design moment for each set of element types, one mesh line at a time. If all of the elements across the strip have the same property assignment (same thickness and material), there would be only one positive and one negative moment.
- The positive and negative moments are totaled separately.
- This process is repeated for both sides of each mesh line (SAFE User Manual 1998).

This approach is suited for use on a model where the mesh is poorly developed. However, according to CSI, the creators of the design software, the automated meshing procedure provided by SAFE makes the development of a poor mesh unlikely and therefore they recommend using the Wood-Armer integration scheme.

6.2.2.2 Wood-Armer Integration Scheme

For a particular load combination or load case for each finite element within the design strip, SAFE calculates the design moments/unit width using the internal forces.

- The nodal point design moments are then calculated by taking the above design moments per unit width of the finite element and multiplying them by one-half the associated element widths.
- The nodal point design moments for each set of slab elements with the same property type are then added to get a single bottom design moment and a single top design moment for each set of element types, one mesh line at a time.
- The bottom and top moments are totaled separately.
- This process is repeated for both sides of each mesh line (SAFE User Manual 1998).

6.2.2.3 Bending Moment Integration in "SLABS" (Inducta Engineering)

In the software "SLABS", slab bending moment results are reported at each nodal point, per unit length (1m). The design of reinforcement is based on a total value of the bending moment acting over a whole section defined by the user. When the user clicks on two points on the slab to define the length of the moment integration, the software's 'Integrate M' algorithm calculates the integrated bending moment to be used for reinforcement design. This algorithm to calculate the integrated bending moment is internal to the program and is not described in the user manual. The integration line should be perpendicular to the moment direction. A small tolerance

of up to 5 degrees is accepted. “Slabs” also has an ‘Integration’ option that summarizes the reinforcement over a certain length. In the case of flat slabs, this option is used to smear the reinforcement around the columns (SLABS User Manual 2005).

6.2.2.4 Moments Calculated In SAP2000

Stresses and internal forces such as moments are evaluated at the 2-by-2 Gauss integration points and extrapolated to the joints of the element. SAP2000 does not perform nodal integration of moments or Wood-Armer integration scheme to arrive at design moments. The maximum of the smoothed nodal moments of a single element is used as the design moment for that element in the present design approach. The maximum of the smoothed nodal moments of a group is chosen as the design moment for that group. It is shown that by designing on an element-level and group level in tandem, significant savings in concrete and steel weight and satisfactory deflection for serviceability requirements can be obtained compared to designing strips or sections of slabs.

6.2.3 Design Using Element Forces

6.2.3.1 Computation of Element Forces

Element forces are computed quite differently from element stresses. They can be computed directly from the displacement field without evaluation of the strain field. Element forces are computed as the product of the element stiffness matrix with the element displacement vector, which is extracted from the global displacements. The results of this computation are forces and moments computed at each node. For general plate bending elements, this procedure computes three components: one shear force perpendicular to the plane of the elements, and two orthogonal bending moments in the plane of the element. For a general plate element, six orthogonal force components are computed: two in-plane forces, an out-of-plane shear force, a moment perpendicular to the plane of the elements, and two bending moments in the plane of the cut (Deaton 2005). These components are shown in Fig 6.4.

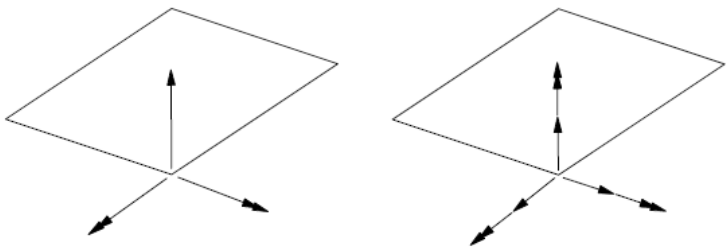

Fig. 6.4 (a) **Fig. 6.4** (b)

Fig. 6.4 Element forces at a node. (a) Plate Bending Element (b) Plate Element (Deaton 2005) (Note: Forces are shown with single arrow head. Moments are shown with double arrow head).

6.2.3.2 Computation of Resultant Design Moment using Element Forces

Once element forces have been computed at each node for the element, one way of computing the resultant design moment is to define a cut. The cut is defined by a linear list of joints. Then, the computed element forces at each node along that cut are simply summed. In-plane torsional effects are neglected in the computation. Note that for some nodes along a cut; more than one element contributes to this resultant computation. Thus, the resultant bending moment across the section, M_b, is computed as

$$M_b = \sum_{i=1}^{n} \sum_{k=1}^{m} M_{i,k}$$

where n is the number of nodes along the cut, m is the number of elements contributing force components at node n, and $M_{i,k}$ is the moment contributed at node i from element k (Deaton 2005). This concept is expressed graphically in Fig. 6.5.

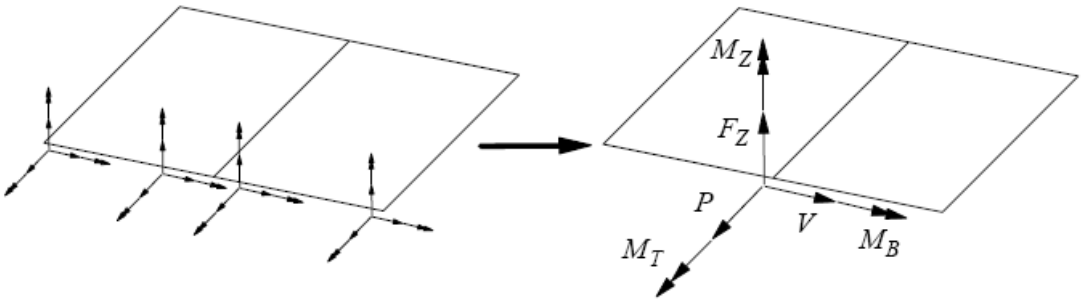

Fig.6.5. Element force resultant from nodal forces along a cut (Deaton 2005)

Once the resultant bending moment acting on the cut has been computed, flexural steel reinforcement for the cross section is designed according to the specified code such as AS 3600.

6.2.4 Approach Adopted In This Study

In this study, the maximum value of the smoothed nodal stress resultants, M_{11}, M_{22} and V_{Max} are used to design the section for each individual finite element. This method does not design "strips of slabs" or "section cuts" and therefore there is no computation involved in obtaining the "*design bending moment"* for any strip or section in a slab. Rather, each element and group is designed based on the maximum bending moment and shear in that element or group. Though such a design would not be practically possible, as mentioned previously, it serves as a useful aid to the structural designer in obtaining useful information on the strength requirements in

various regions of a slab based on a linear elastic analysis. Significant material savings (both concrete and steel) are demonstrated using the proposed approach.

6.3 Slab-to-Column Connection Issues

As mentioned in Section 6.1.3 above, accurate modelling of the slab-to-column connection in flat slabs is important if realistic design results are to be obtained in the region around the column. This section attempts to shed more light on this aspect.

6.3.1 Effects of Inaccurate Modelling of Slab-to-Column Connections

A single 3D solid element (without a 2x2 or 3x3 mesh overlay) is used to model the columns in the flat plate model shown in Fig. 6.7 below. Checking that the four nodes of the solid element and the nodes of the shell elements atop the solid element are the same ensures nodal accuracy. Nodes of adjoining elements are also checked. If the meshing produces different nodes at the same location in space it could result in serious errors. The model shown in Fig. 6.7 below depicts a 3 x 3 bay flat plate resting directly on columns. The spans in the X direction are 6.5 m each and the spans in the Y direction are 6 m each, centre-to-centre of columns. The model is meshed into 8910 elements. The size of the column modelled is 400 mm x 400 mm. The initial slab thickness assigned is 250 mm. The loads on the flat plate are self-weight plus 5 kPa LL. The load combination is 1.25 DL + 1.5 LL.

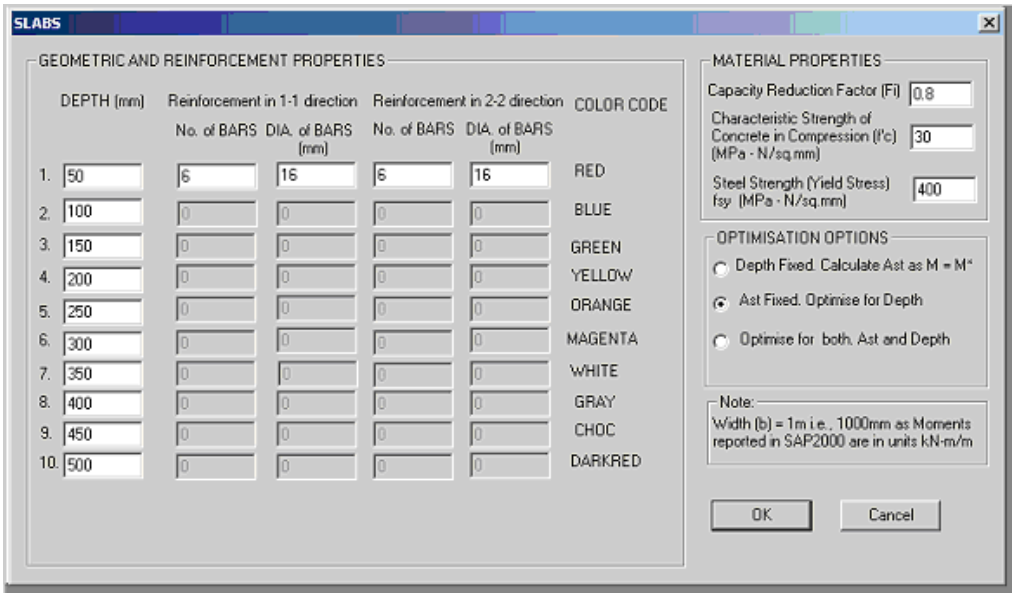

Fig. 6.6. Design Data for Technique 2.

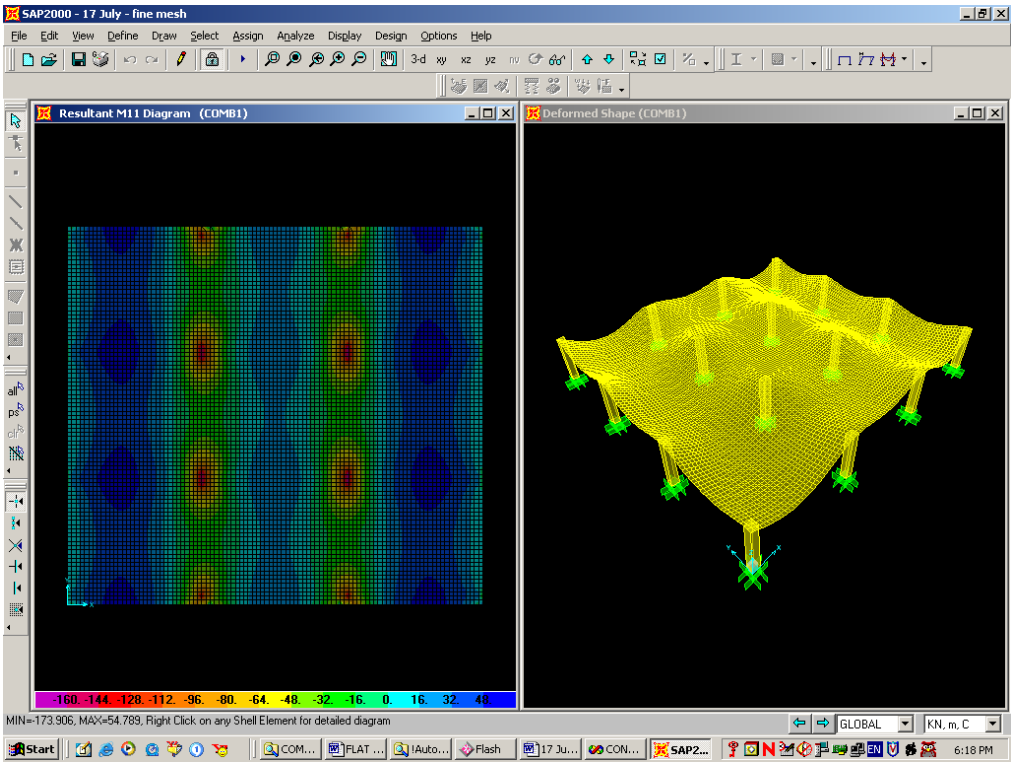

(a) M11 (Smoothed) (b) Initial Model after FEA

Fig. 6.7. FEA Results for a Symmetrical Slab

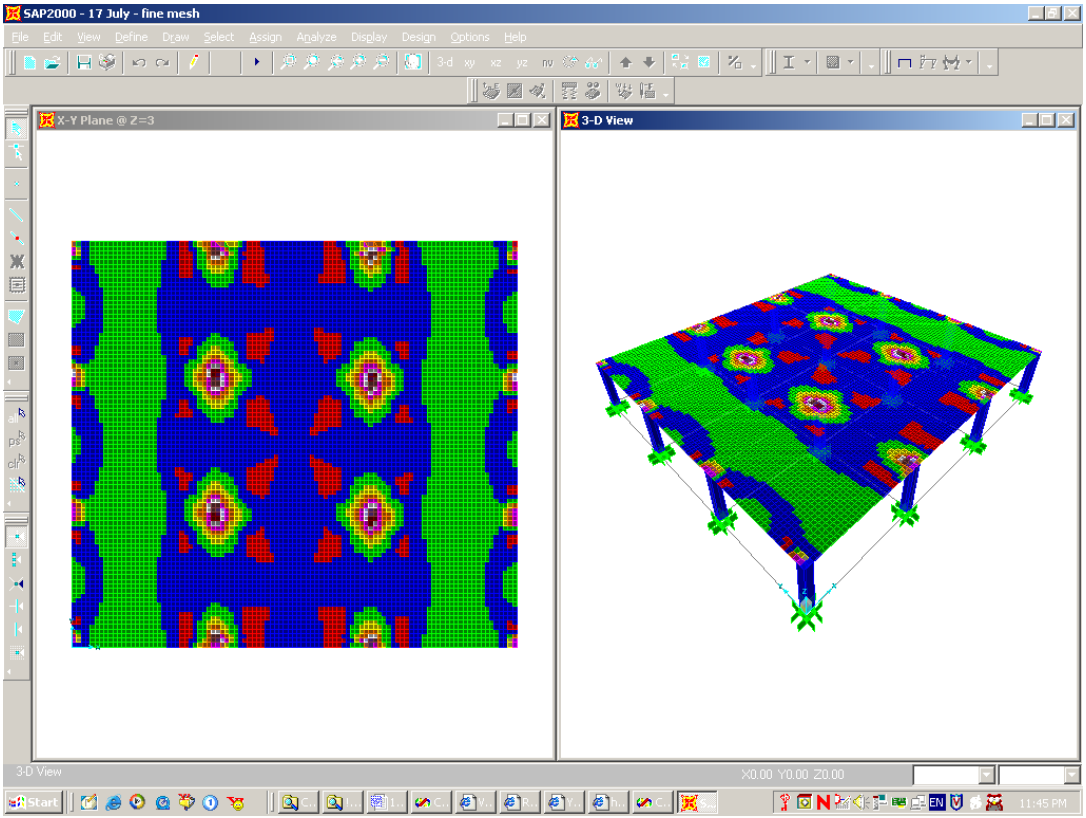

Fig. 6.8. Design Solution at first iteration (Using smoothed nodal values in the code).

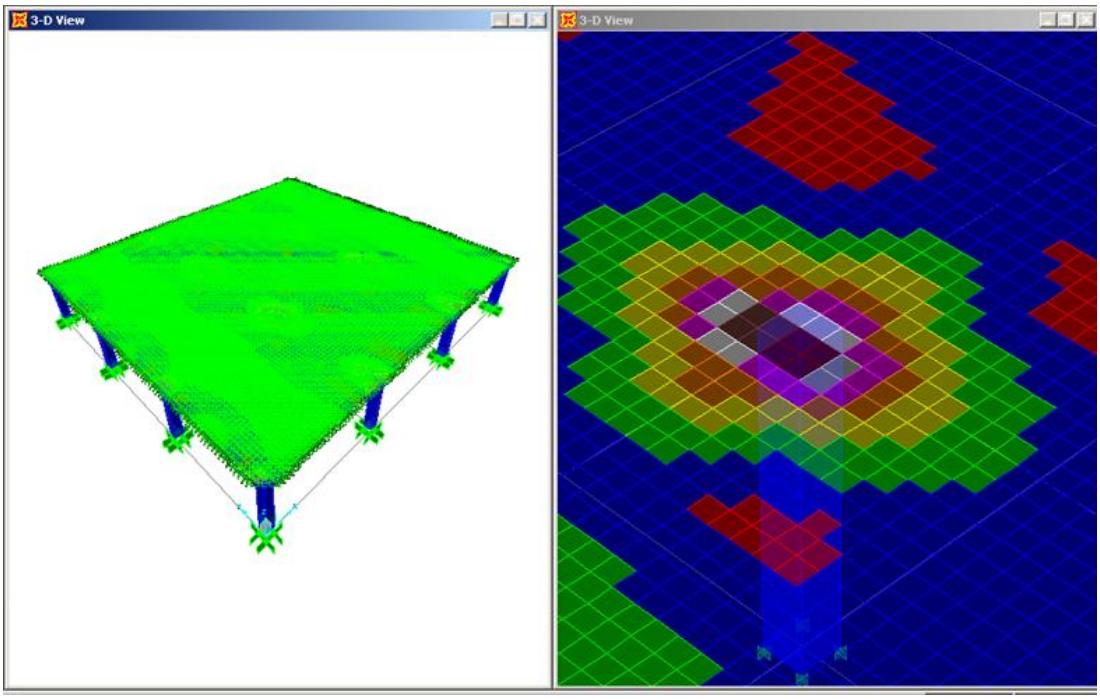

Fig. 6.9. Close-up view of depths around a central column

For explanation, only the first iteration is shown in the above example. To interpret colours, please refer to the 'Colour Code' shown in Fig. 6.6. It is evident from the results obtained above (for the design data given by the user) that thicker portions are needed in the regions around the column. This is to be expected for a flat plate since it is subjected to a combination of severe bending moments and shears in the immediate vicinity of a column. However, a closer inspection reveals that the depths chosen by the algorithm for some elements around the column are excessively high. A depth of 500 mm (dark red) is seen for some elements near the central columns when the steel specified is 6-Y16 bars. Whereas, expected depths of 300 mm (magenta) – 350 mm (white) are also seen for some elements around the column. Comparison with hand calculations using the 'Simplified Method of Design' (pg 565 of Warner *et al* 1999) indicate that for a section having 6-Y16 bars around the column, a depth of 350 mm is to be reasonably expected in spite of differences that will persist due to the difference in the two methods used for computing moments (FEA v/s Simplified Method). However, depths ranging from 250 mm (orange color) to 450 mm (choc color) are seen for elements lying around the central columns. In spite of using 3D solids to model the columns, the effects of 'stress singularity' (discussed in Section 6.1.3) are clearly seen in this region. It is clear that as the optimization proceeds these thicker elements will attract moment and keep getting thicker and thicker (this is demonstrated in Chapter 7) and the above list of depths provided by the user too would become inadequate. Continuing the optimization with such a model would therefore be incorrect. The purpose of this exercise and building this model therefore was to evaluate the depths obtained in the region around the columns (as well as various parts of the slab) of the 1st

iteration for this flat plate. It was expected that reasonable depths of around 300 mm – 400 mm would be observed around this region during the course of optimisation. However, as seen above, due to stress singularity, the algorithm picks big depths for some elements around the central columns. It should be noted that 'Plate Constraints' were not employed in this example.

In 'Numerical Studies' in Chapter 7, the 3D solid objects used to model columns are meshed into 16 objects each and the nodal accuracy checked by ensuring that the 16 nodes of the solid elements and the 16 nodes of the plate elements atop the solid elements are the same. The 4 plate elements atop the solid elements are treated as non-design and 'Plate Constraints' are employed at these nodes to constrain plate-bending behaviour. Numerical studies show that using the 'plate constraint' at these locations results in obtaining appropriate values of bending moments (both M_{11} and M_{22}) at the faces of the column supports, quite comparable with the Simplified Method of Design. The use of the 'plate constraint' and 3D solid objects thus aids in overcoming, to some extent, the problems arising at the column supports due to stress singularity. The Plate Constraint in SAP2000 is now described briefly here.

6.3.2 Plate Constraint in SAP2000

Each plate constraint in SAP2000 connects a set of two or more joints together. It causes all of its constrained joints to move together as a flat plate that is rigid against bending deformation. Effectively, all constrained joints are connected to each other by links that are rigid for out-of-plane bending, but do not affect in-plane (membrane) deformation. This constraint can be used to:

- Connect structural-type elements (Frame and Shell) to solid-type elements (Plane and Solid), as is the case in Flat Plates and Flat Slabs.
- Enforce the assumption that "plane sections remain plane" in detailed models of beam bending (SAP2000 User Manual).

6.4 Concluding Remarks

In this chapter, the significance of accurate modelling is emphasized by clearly identifying pitfalls in numerical modelling of flat slabs using the finite element method. The effects of various modelling techniques are presented and design based on element stresses is contrasted with design with design using element forces. A flat slab example using Technique 2 (which is explained in Chapter 7) shows the effects of inaccurate slab-to-column modelling on design results in this region. The work in this chapter thus provides a thorough insight into accurately modelling flat slabs, before proceeding with analysis, design and optimisation.

CHAPTER 7: Optimal Conceptual Design of Slabs for Flexure

7.1 Introduction

It has been seen in Chapter 5 that due to practical restrictions inherent in the simplified or approximate design techniques, researchers, for many years, have been working toward the successful application of finite element technology to the design of reinforced concrete slab systems. Despite promising research in this area, very few conceptual finite element based slab design tools have been implemented. The goal of study in this chapter therefore is to propose and validate such a tool. This chapter explains three new conceptual design techniques for reinforced concrete slab systems with particular emphasis on the flat-slab type of floor systems. The ESO method of structural optimisation is extended to develop these techniques using SAP2000 as the analysis engine. The reinforced concrete slabs are designed for flexure (bending moments in two orthogonal directions) and in Chapter 8 shear (transverse shear and punching shear) is treated as additional constraints besides flexure. Design variables, which are a given set of discrete values, are determined according to specified criteria of the Australian Standard, AS 3600 in order to achieve practical designs. For flexural design, it is proposed to treat each finite element as a 'designable unit', which must withstand its applied bending moments (i.e. satisfy eq. 5.2 mentioned in Chapter 5 for each designable element in the slab). The idea is therefore to seek a solution where the yield condition or the plastic moment condition requirements (i.e. eq. 5.2) is satisfied for all designable elements in the slab. The optimisation process is terminated when such a solution obtained converges. In the computer code, the program checks for five consecutive iterations and if the solution remains the same, then the process is terminated.

7.2 Scope of the Work in This Chapter

In view of the deficiencies inherent in conventional design methods, the lack of a conceptual design tool becomes more apparent as the complexity of the structural system grows from frames to wall elements, to slabs and finally to general 3D structures. At one end of the spectrum, reinforcement of frame structures is well known and is mainly governed by code specifications with little room for altering the steel distribution. For slabs, which behave as a continuum, great advantages can be gained if the design engineer is able to easily examine a large number of various steel layouts (Tabatabai 1996).

For complicated structures consisting of flat slabs and flat panels, the practice before the spread of the finite element method was to extract a panel from the system and model it with a series of line loads at the edges where the considered panel was connected to the rest of the structure. The designer would then proceed with the design and dimensioning of this panel as when a single wall or slab element was

to be reinforced. He would then take care of the reinforcement at the edges of panel connections. With the development of general-purpose finite element analysis programs, the problem of analysis of such structures has been overcome. However, the gap between analysis and design is still wide (Tabatabai 1996).

Considering all these problems for an integrated analysis, slab design and optimisation, this work was initiated for the development of a practice-oriented approach and the corresponding computer programs for the flexural and shear design of slab structures. This work tries to introduce a system that should inherit the advantages of the various existing methods while trying to alleviate some of their deficiencies. The main characteristics of such a system are:

- The finite element method is applied to make the approach general, furnish the elastic structural response and to easily handle multiple load cases.

- Optimal designs are sought by following the basic principles of Collapse Load Analysis (yield condition or plastic moment condition requirements).

- It represents a compromise between the sophistication and complexity of the model and the ease of use of the corresponding program.

7.2.1 Significance of This Research

The process of slab design essentially involves finding out the thickness of the slab and the flexural reinforcement required at different locations in the slab. Though there is a large body of knowledge available for finding out *"design bending moments"* using various methods that include linear elastic analysis or elasto-plastic non-linear analysis, it is seen that little or no effort has gone so far in applying Collapse Load Analysis to seek optimal slab designs in which the reinforcement in the slab is assumed constant throughout, and depths in various parts is changed. Similarly, optimal designs can also be sought by simultaneously changing the depths and the reinforcement required in various locations of the slab. It is anticipated, that this will result in substantial material savings compared to conventional slab design. Though the results based on treating individual finite elements as 'design units' may not truly give practical designs that can be easily constructed, the results serve the purpose of demonstrating economical conceptual designs that give the structural designer useful information on the "section requirements" needed in various parts of the slab. By critically analysing these results that satisfy code provisions, the designer may come up with a much-improved final design that can be practically constructed in the field. The final design based on this approach will be more economical when compared to conventional design.

7.2.2 Assumptions and Limitations of This work

Based on the previously mentioned requirement that a compromise should be made between the complexity of the model and the ease of practical application for the design engineer, a series of simplifying assumptions are made, and these are as follows:

No time-dependent effects:

The loads are assumed to act statically and no dynamic effects are included. Also, time dependent aspects of concrete behaviour like creep and shrinkage are not considered.

Under reinforced Structures:

Since the most important assumption for the applicability of plasticity theory is the capacity of the structure for plastic deformation and stress redistribution, the method is applicable only for those type of structures for which failure under short term loading is primarily governed by the ductile nature of mild steel and not the brittle behaviour of concrete. As a result, only under reinforced structures are dealt with here.

Ultimate Load Design:

Code provisions specify that a structure must be designed for the two requirements of serviceability and strength. The aim of the work presented here is to address solely the issue of design for strength requirements, although checks are made in the optimisation process for the serviceability requirements mentioned in the code and the "sections" are validated for minimum depth requirements in order to satisfy code provisions for serviceability.

No treatment of structural detailing:

Specific issues like detailing at supports, anchorage lengths etc. are not dealt with. These are best considered on a case-by-case basis and require the judgement of the engineer and are unsuitable for automation within a computer program.

7.3 Optimisation Problem Formulation

Consider the problem of minimising the weight of concrete and steel in a slab subject to strength constraints (bending moment and shear), where elements must be designed based on the given set of discrete values. Each element or each group of elements can have its own set of discrete values. In sizing optimisation problems elements cannot be removed. The only way to reduce the weight of the slab is to remove under-utilised material from elements by reducing the thickness and steel content. This can be done by simply assigning the next lower sections available from the given sets of discrete sections.

In the proposed method, three techniques are developed for flexure (shear is considered in the next chapter), each one of which has a specific objective function.

1. **Depth Constant, Steel Varying:**

   This technique is used to find the distribution or layout of steel required in various parts of the slab when the depth or thickness of the slab is kept constant throughout. This is similar to conventional slab design approaches and is also similar to the objective of various commercial slab design software. There is no room for optimisation in this approach as the depth is kept constant and it is not possible to specify reinforcement within each individual finite element in SAP2000. In this technique, the weight of steel is used as the objective function and the yield condition or plastic moment condition (Eq. 5.10, $\phi \times R_u > S^*$) is treated as the constraint. In other words, the objective is to seek a minimum weight of steel in the slab when its depth is constant while satisfying its yield condition or plastic moment condition requirement for all elements in the slab.

2. **Steel Constant, Depth Varying:**

   This technique is used to find the depths or thickness required in various parts of the slab when the steel in the slab is kept constant throughout. In this technique, the weight of concrete is used as the objective function and the yield condition or plastic moment condition (Eq. 5.10, $\phi \times R_u > S^*$) is treated as the constraint. In other words, the objective is to seek a minimum weight of concrete in the slab when its reinforcement is constant everywhere while satisfying its yield condition or plastic moment condition requirement for all elements in the slab.

3. **Both Depth and Steel Varying:**

   This technique is used to find the depths and steel required in various parts of the slab when both thickness and steel are treated as variables. In this technique, the weight of concrete and weight of steel is used as the objective function, and the yield condition or plastic moment condition (Eq. 5.10, $\phi \times R_u > S^*$) is treated as the constraint. In other words, the objective is to seek a minimum weight of concrete and steel in the slab while satisfying its yield condition or plastic moment condition requirement for all elements in the slab.

7.4 Element Sizing Criteria

A converged solution or stable stress field is sought in which the bending moments nowhere exceed the yield limit. This philosophy is used in the optimisation process for sizing elements. In the proposed approach, linear elastic theory is applied to uncracked and unreinforced homogeneous concrete to determine the moments at different points within the slab. This is done by using the finite element

program SAP2000. This elastic moment distribution forms the basis of design. Each finite element is designed such that it must be capable of carrying the loads applied to it. In the context of the finite element model, the resulting stresses and moments calculated at the common node of adjacent elements are discontinuous and thus not in equilibrium with one another despite the fact that they belong to the very same node. To overcome this situation, a smoothing algorithm is implemented that calculates the average values of nodal moments at each node of the finite element. Having obtained these values, the design is carried out by applying the well-known yield conditions formulated for an infinitesimal d_x-d_y element (Eq. 5.10, $\phi \times R_u > S^*$) to check whether the provided *section* can resist the bending moments in both directions. The design is based on the assumption that the reinforcement is to be fully utilized up to its tensile yield strength. The section provided for each finite element must be such that the resistance provided at a fully plastic condition is everywhere equal to or greater than the stress resultant considered (in this case bending moments). Using Technique 2 and Technique 3 mentioned above, when the depth of elements is changed and the structure analysed again, it results in a moment redistribution within the slab. This moment redistribution is fully utilised in the proposed approaches by proceeding with iterative sizing optimisation of elements until a stable stress field (or steady state) is reached wherein there is no further moment redistribution in the slab. In this study, the maximum value of the smoothed nodal stress resultants, M_{11}, M_{22} and V_{Max} are used to design the section for each individual finite element. This method does not design "strips of slabs" or "section cuts" and therefore there is no computation involved in obtaining the "*design bending moment"* for any strip or section in a slab. Rather, each element is designed based on the maximum moment and shear in that element. Though such a design would not be practically possible, as mentioned previously, it serves as a useful aid to the structural designer in obtaining useful information on the strength requirements in various regions of a slab based on a linear elastic analysis. Significant material savings (both concrete and steel) are demonstrated using the proposed approach.

7.5 Development of Conceptual Techniques and the Corresponding Computer Programs

Three techniques are developed in the course of this research. Several separate algorithms are programmed that implement each technique. As mentioned previously, the first technique is similar to conventional design and finds out the amount of reinforcement required in various parts of the slab with the slab depth constant throughout the slab. In the second technique, the amount of reinforcement throughout the slab is kept constant and optimal depths are sought in different parts of the slab. In the third technique, both slab depth and reinforcement is varied in different parts of the slab. In all three techniques, the design variables used in the optimisation process are user defined "sections" that consist of the overall slab depth and the amount of reinforcing steel per m width within that depth. The Graphical User Interfaces (GUI's) capture all required data needed for design such as the concrete

strength, steel strength, capacity reduction factor and cover to reinforcing bars etc. The following screenshots demonstrate the GUI's for each of the three techniques. The implementation details of the three techniques are explained as follows:

7.5.1 Implementation

The objective of this section is to present in detail the reinforced concrete slab design procedures implemented in SAP2000, using Compaq Visual Fortran (Version 6.5.0) and WinBatch (Version 2006A) as the programming languages. SAP2000 is a finite element analysis and design software created by CSI Inc. based in Berkeley, California. It is suited for analysis and design of civil structures. The modelling environment in SAP2000 is 3D object based and it features a powerful MS Windows integrated graphical user interface (GUI) in which creation and modification of the model, execution of the analysis and checking and optimisation of the design are all done through this single user interface. ESO optimisation, which is iterative in nature, requires performing repeated runs of the following operations such as reading the model file into SAP2000, executing the analysis and exporting the FEA results. It is not possible to execute the analysis from the command line in SAP2000 unlike some other FEA software, and hence all the abovementioned operations need to be performed from within the SAP2000 GUI. GUI event handling for SAP2000 would require extensive Windows API programming unless programmed in a scripting language such as WinBatch. WinBatch is a simple, structured scripting language that can control applications which use the Windows API (Application Programming Interface) such as SAP2000. A single line of code in WinBatch would require 10 or more lines of C, C++ or VB code to achieve the same functionality. WinBatch is therefore employed in this work to automate the windows processes such as opening and closing SAP2000 window objects, controlling mouse movements on screen, sending keystrokes to windows and applications etc. There are "timers" and "event handlers" programmed in the WinBatch code that help the program to understand when a window object is called, when it is displayed and when it is closed. These "timers" and "event handlers" are built at several locations in the program depending upon the sequence of operations needed to perform ESO optimisation. Obviously, these "timers" need to be changed each time a different model is used, as generally, a bigger building model with a fine mesh takes a much longer time to read, render, display and analyse in the SAP2000 GUI than say a simple model with a coarse mesh. This is a limitation when implementing ESO type optimisation code with SAP2000. The optimisation algorithms are written in Compaq Visual Fortran. The Visual Fortran code essentially comprises of two parts:

1. A FORTRAN console project that has the subroutines which implement the design optimisation algorithms.
2. A FORTRAN QuickWin project that contains the code for implementing the various GUI's created for enabling the user to enter design data into the program.

Details and screenshots of the GUI's developed are as follows:

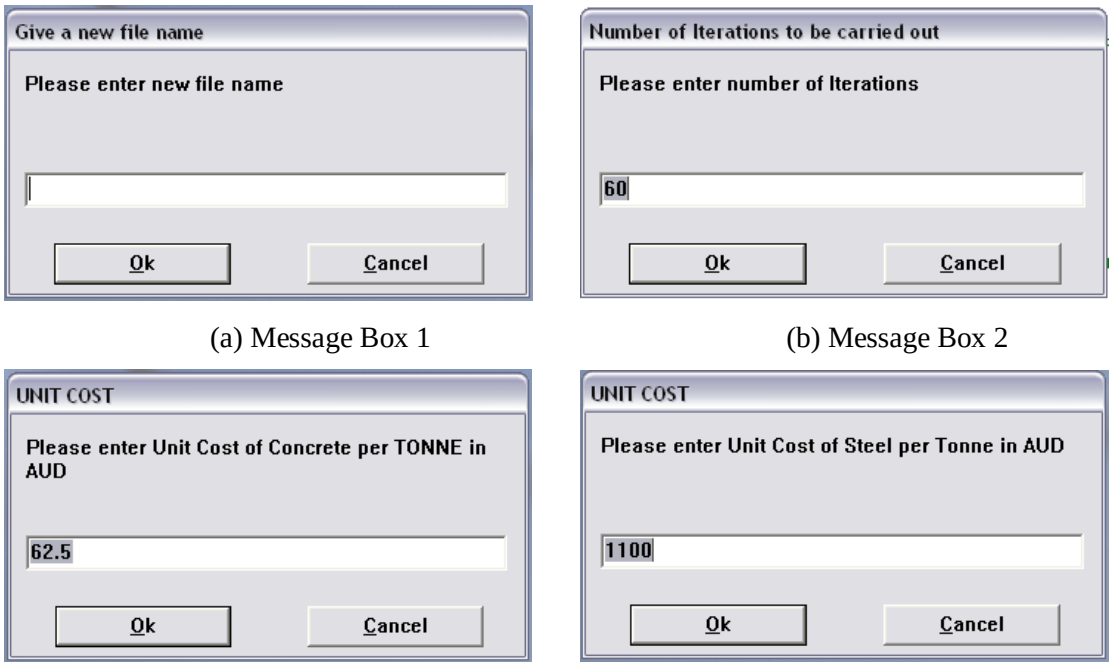

(a) Message Box 1 (b) Message Box 2

(c) Message Box 3 (d) Message Box 4

Fig. 7.1. WinBatch "Message Boxes"

The above screenshots show the four message boxes programmed in WinBatch to gather data from the user in order to commence and then drive the optimisation process by iteratively transferring control sequentially, first from the WinBatch program to the Fortran GUI's (shown in the next few pages), then to SAP2000 for FEA and then to the FORTRAN design optimisation algorithms and back again to the WinBatch program. The following flowchart explains this working. The purpose of the Message Boxes shown above is self-explanatory.

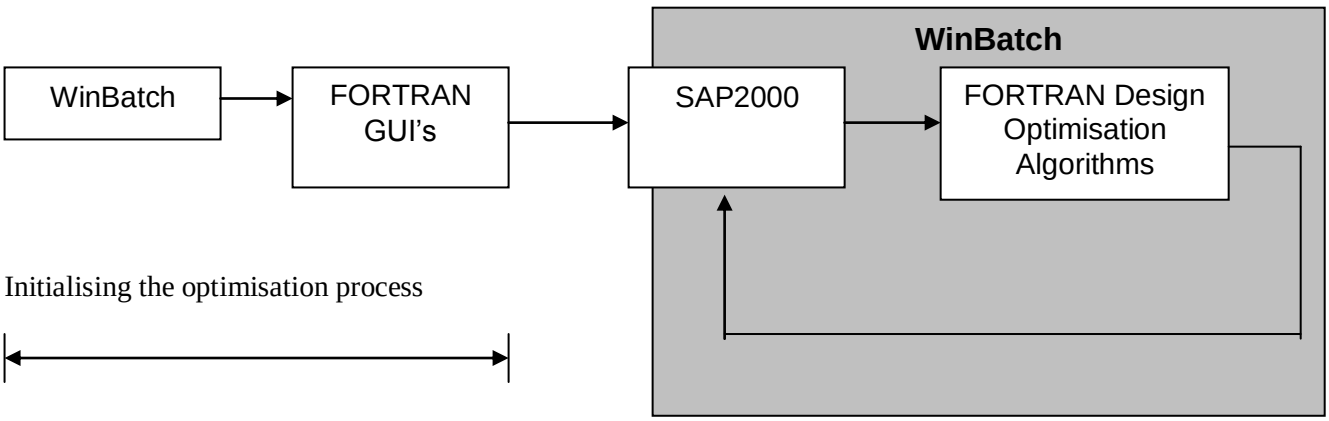

Fig. 7.2. Flowchart of Control Process during Optimisation

GUI'S developed in Compaq Visual FORTRAN

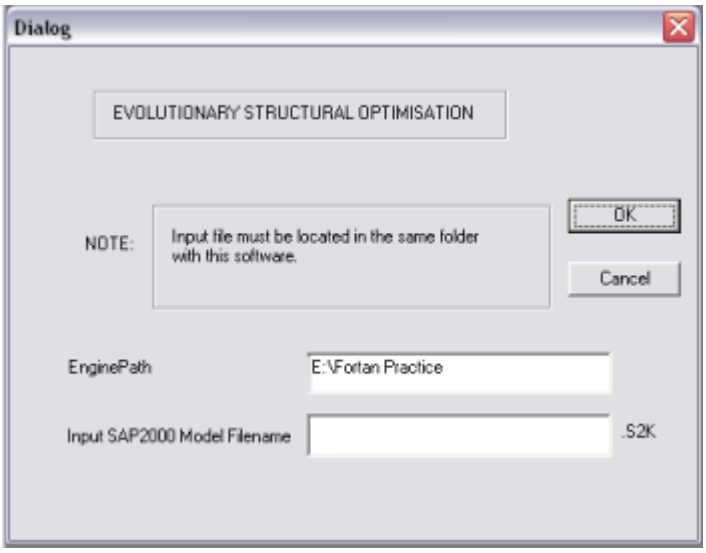

Fig. 7.3. Graphical User Interfaces (GUI) developed in Compaq Visual Fortran: (a) GUI 1

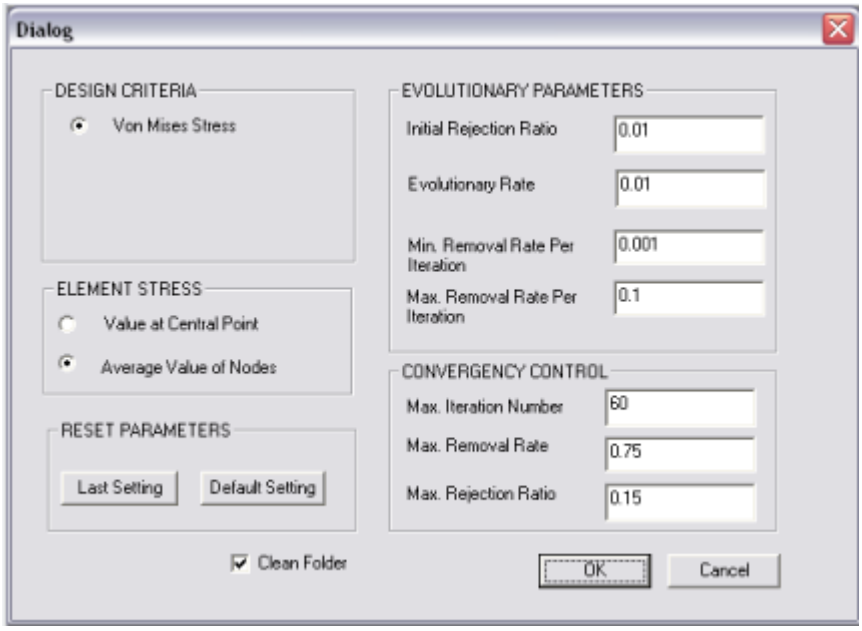

Fig. 7.3. Graphical User Interfaces (GUI) developed in Compaq Visual Fortran: (b) GUI 2

The filename for the model entered by the user in WinBatch 'Message Box 1' shown on the previous page is automatically entered by the WinBatch program into the text box named "*Input SAP2000 Model Filename*" of GUI 1 depicted above. The WinBatch program waits for the user to hit OK.

If either the "Name of the Model File" or the "Path" is incorrect, the programs displays an error message to the user. If information entered is correct then GUI 2 shows up.

GUI 2 gathers ESO optimisation parameters as depicted. These parameters are needed to drive the ESO 0-1 topological optimisation process.

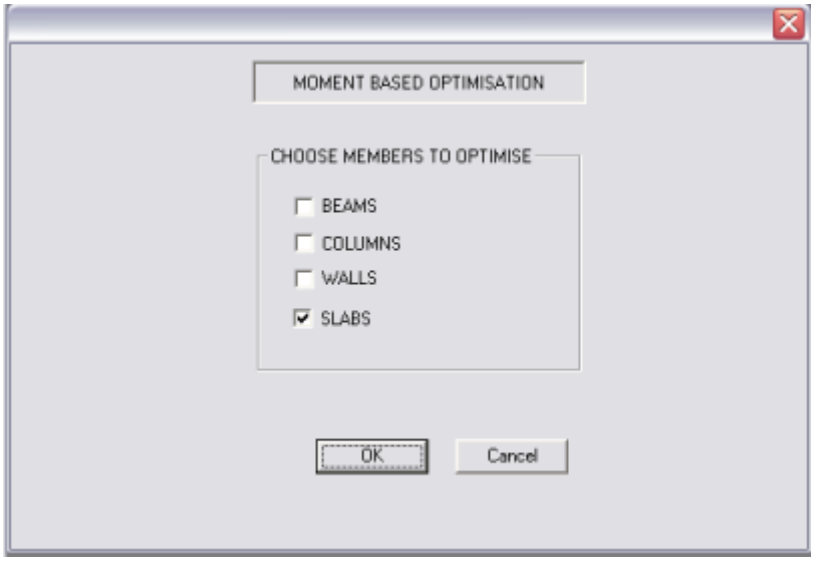

Fig. 7.3. Graphical User Interfaces (GUI) developed in Compaq Visual Fortran: (c) GUI 3

GUI 3 prompts the user whether to perform "Moment based sizing optimisation of Slabs" or "Stress based sizing optimisation of walls". If the user clicks on Walls, sizing optimisation of walls based on von Mises stress (not Moments) is performed. At present, only sizing optimisation of continuum elements like walls and slabs can be performed. However, sizing optimisation of frame elements like beams and columns, when programmed later in the optimisation algorithms, can be used as an extension in future. Each clicked button should ideally come up with its respective user interfaces. User interfaces for "slabs" are developed at present. When the user clicks on "*SLABS*", GUI 4 comes up.

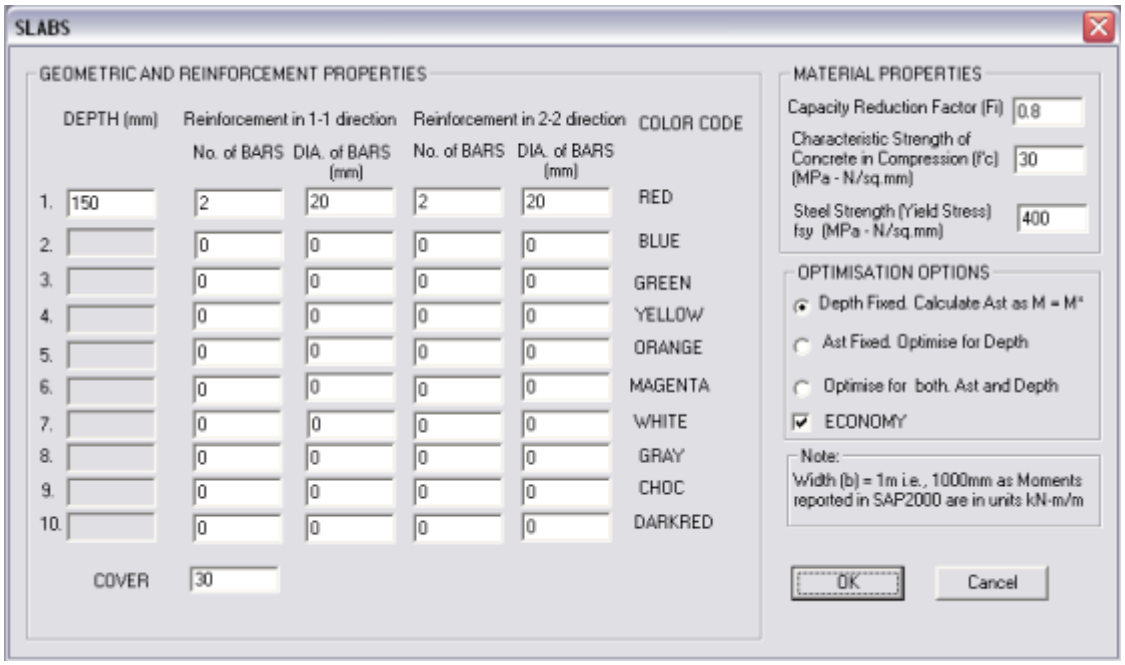

Fig. 7.3. Graphical User Interfaces (GUI) developed in Compaq Visual Fortran: (d) GUI 4

GUI 4 gathers design data for *Technique 1* (Depth Constant, Steel Varying). The user interface is broadly divided into three main parts viz., "Geometric and Reinforcement Properties", "Material Properties", "Optimisation Options" and a "Note" section. In the "Geometric and Reinforcement Properties", the user is required to enter a uniform depth for the slab and different reinforcement quantity per metre width in both directions. The user can specify ten different sections each with a *constant depth* and *varying proportion of steel* in that depth for a one-metre width of slab. *Technique 1* is as per conventional slab design where the layout of reinforcement in a slab is sought. As, "extrusion" is not available in SAP2000 Version 8.3.0, each section is assigned a specific colour as seen in the colour code in Fig. 7.3d. In the "Material Properties", the user is required to enter Material Properties such as the "Capacity Reduction Factor", the "Characteristic Strength of Concrete", and "Yield Stress of Steel". These values are read into Equation 5.20 to calculate the Moment Capacity of these ten user defined sections for the specified material properties. As is mentioned in the "Note" section above, the moment capacity of these ten sections is calculated per metre width of the slab. This is because the nodal values of moments in SAP200 are reported *per unit of in-plane length* (i.e. kN-m/m if units are set to kN, m). Therefore, when using Equation 5.10 ($\phi \times M_u > M^*$), both M_u (resistance of the section) and M^* (design moments) are compared per unit of in-plane length. The user is also required to enter the "Cover". The cover in this case is the "clear cover" measured from the bottom of the slab to the outermost surface of bottom steel. In the "Optimisation Options", the user is prompted to check one of three radio buttons, one each for *Technique 1*, *Technique 2* and *Technique 3*. By default, Technique 1 (i.e. Depth Constant, Steel Varying) is checked. The Economy button, when checked, designs the slab such that economical sections (from among the list of sections entered

by the user) are selected such that they satisfy flexural criteria. If not checked, the slab design is performed such that only flexural criteria are satisfied, with no consideration to the economy of the ten sections.

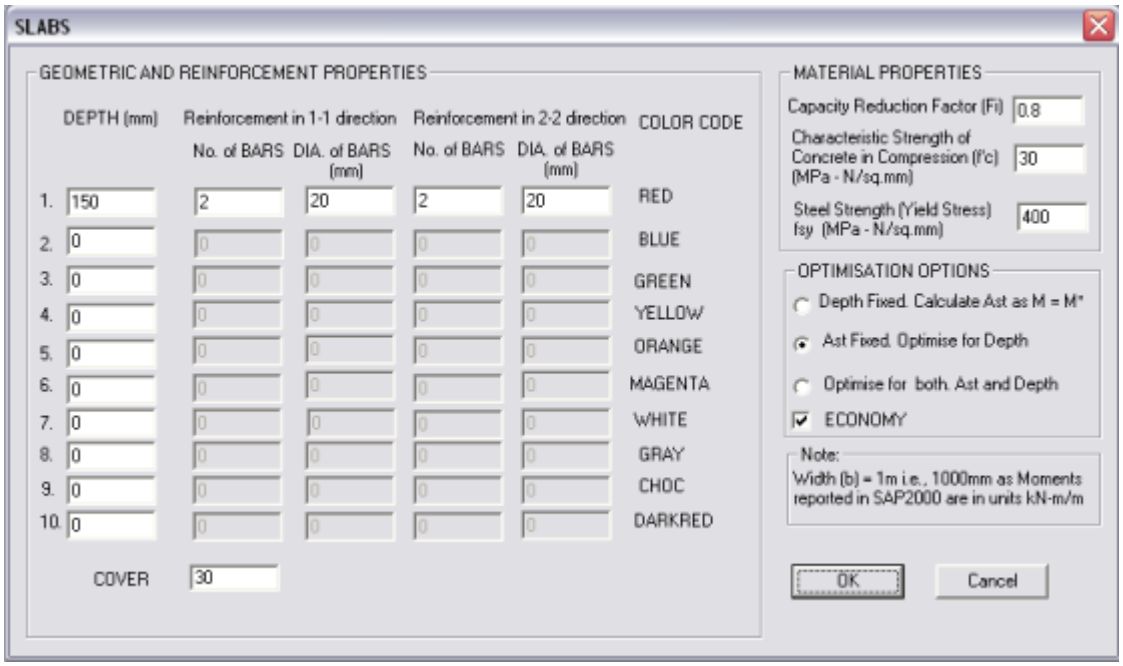

Fig. 7.3. Graphical User Interfaces (GUI) developed in Compaq Visual Fortran: (e) GUI 5

GUI 5 gathers design data for *Technique 2* (Steel Constant, Depth Varying). This user interface too is broadly divided into three main parts viz., "Geometric and Reinforcement Properties", "Material Properties", "Optimisation Options" and a "Note" section. In the "Geometric and Reinforcement Properties", the user is required to enter *uniform steel* quantity per metre width in both directions throughout the slab and *different depths*. The user can specify ten different sections each with a different depth and the same proportion of steel in that depth for a one-metre width of slab. *Technique 2* seeks to find the depths required in different regions of a slab, when the steel in the slab is kept constant throughout. Again, as "extrusion" is not available in SAP2000 Version 8.3.0, each section is assigned a specific colour as seen in the colour code above. In the "Material Properties", the user is required to enter Material Properties such as the "Capacity Reduction Factor", the "Characteristic Strength of Concrete", and "Yield Stress of Steel". These values are read into Equation 5.20 to calculate the Moment Capacity of these ten user defined sections for the specified material properties. As is mentioned in the "Note" section above, the moment capacity of these ten sections is calculated per metre width of the slab. This is because the nodal values of moments in SAP200 are reported *per unit of in-plane length* (i.e. kN-m/m if units are set to kN, m). Therefore, when using Equation 5.10 ($\phi \times M_u > M^*$), both M_u (resistance of the section) and M^* (design moments) are compared per unit of in-plane length. The user is also required to enter the "Cover". The cover in this case is the

"clear cover" measured from the depth of the slab to the outermost surface of bottom steel. In the "Optimisation Options", the user is prompted to check one of three radio buttons, one each for *Technique 1*, *Technique 2* and *Technique 3*. On checking the second radio button, viz. "A_{st} fixed. Optimise for Depth", GUI 5 above pops up. The Economy button, when checked, designs the slab such that economical sections (from among the list of sections entered by the user) are selected such that they satisfy flexural criteria. If not checked, the slab design is performed such that only flexural criteria are satisfied, with no consideration to the economy of the ten sections.

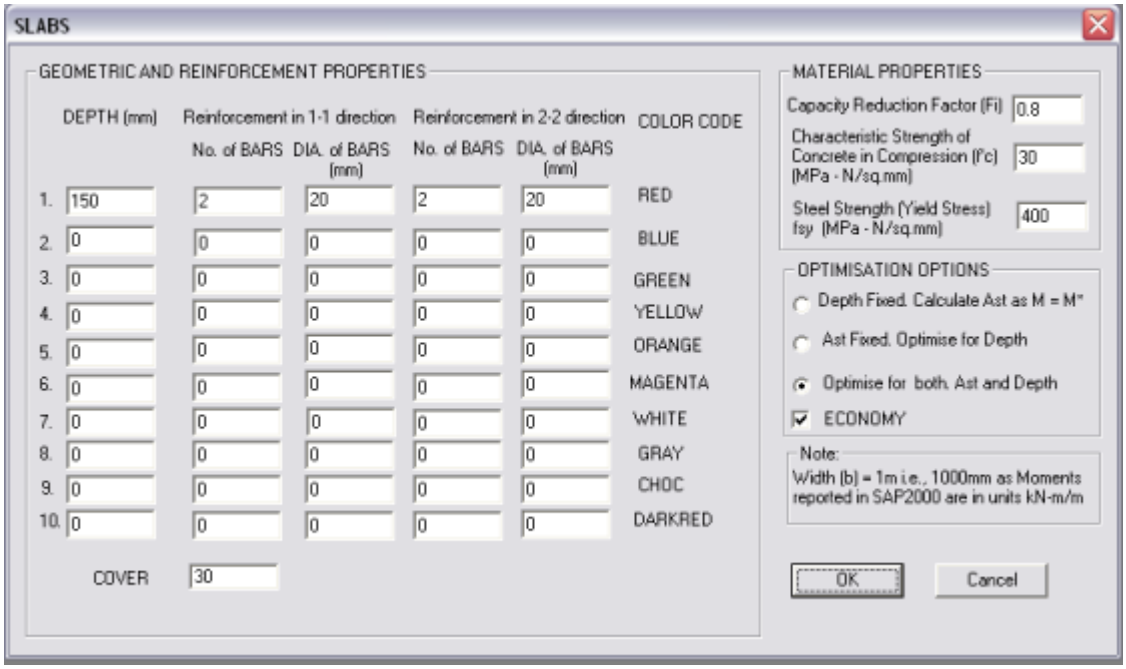

Fig. 7.3. Graphical User Interfaces (GUI) developed in Compaq Visual Fortran: (f) GUI 6

GUI 6 gathers design data for *Technique 3* (Both Steel and Depth Varying). As before, this user interface is again broadly divided into three main parts viz., "Geometric and Reinforcement Properties", "Material Properties", "Optimisation Options" and a "Note" section. In the "Geometric and Reinforcement Properties", the user is required to enter *combinations of depth and steel* in both directions throughout the slab. The user can specify ten different sections each with different depths and different steel in that depth. *Technique 3* seeks to find the optimal depths and steel quantities required in different regions of a slab. Again, as "extrusion" is not available in SAP2000 Version 8.3.0, each section is assigned a specific colour as seen in the colour code above. In the "Material Properties", the user is required to enter Material Properties such as the "Capacity Reduction Factor", the "Characteristic Strength of Concrete", and "Yield Stress of Steel". These values are read into Equation 5.20 to calculate the Moment Capacity of these ten user defined sections for the specified material properties. As is mentioned in the "Note" section above, the moment capacity of these ten sections is calculated per metre width of the slab. This is because the nodal values of moments in

SAP200 are reported *per unit of in-plane length* (i.e. kN-m/m if units are set to kN, m). Therefore, when using Equation 5.10 ($\phi \times M_u > M^*$), both M_u (resistance of the section) and M^* (design moments) are compared per unit of in-plane length. The user is also required to enter the "Cover". The cover in this case is the "clear cover" measured from the depth of the slab to the outermost surface of bottom steel. In the "Optimisation Options", the user is prompted to check one of three radio buttons, one each for *Technique 1*, *Technique 2* and *Technique 3*. On checking the third radio button, viz. "Optimise for both A_{st} and Depth", GUI 6 above pops up. The Economy button, when checked, designs the slab such that economical sections (from among the list of sections entered by the user) are selected such that they satisfy flexural criteria. If not checked, the slab design is performed such that only flexural criteria are satisfied, with no consideration to the economy of the ten sections.

The GUI's allow the user to communicate all data necessary for design. The optimisation program processes this information and generates optimal designs for the system based on the input. The design however does not provide information on which face of the slab is to be reinforced. Detailing requirements such as development length and continuity requirements are also not part of the design process. The results essentially serve as conceptual designs that inform the structural designer of the amount of reinforcement or depth required in various regions of a slab system. Several codal provisions of AS 3600 are followed in the design algorithms.

7.5.2 Algorithm

In the present optimisation approach, the plate elements of the slab are designed to resist the maximum bending moments occurring in each element. The reinforcement in a slab is usually placed in two orthogonal directions. The elements are therefore designed to resist bending in both directions i.e. direction 1-1 which is similar to the global X axis and direction 2-2 which is similar to the global Y axis. In SAP2000, plate bending moments are reported at each node as M_{11} and M_{22}. M_{11} represents the bending moment in 1-1 direction, i.e. Global X axis and M_{22} represents the bending moment in the 2-2 direction, i.e. Global Y axis. These bending moments are reported per unit of in-plane length. In the optimisation program, the moment capacities of the ten user defined sections are calculated in both directions based on the data provided by the user in the user-interface. The moment capacities are calculated by using Equation 5.20. There is no post-processing applied in the optimisation program to compute the *design moment* for a strip or section of the slab. Rather each element is designed individually and the smoothed maximum nodal moment of each element is chosen as the *design moment*. The nodal moments obtained in both directions (M_{11} and M_{22}) in SAP2000 are smoothed by employing a smoothing procedure. The procedure is simple wherein, in the first step, the average moment at *each node* (M_{11} and M_{22}) is calculated by averaging the moments (M_{11} and M_{22}) of all

elements connecting to that node. In the next step, the design moment in both directions (M_{11} and M_{22}) for each element is calculated by picking the *maximum* of the four smoothed nodal moments (M_{11} and M_{22}). The program then designs elements based on whether Technique 1, Technique 2 or Technique 3 above is chosen by the user. A brief description follows:

Technique 1

If the user chooses Technique 1 above, the program designs the steel reinforcement in both directions. The program therefore gives an indication of how much steel is required for resisting flexure when the depth of the slab is constant throughout. Two separate output files are created that contain the steel requirement in each direction. The sections (i.e. steel in this case) are allotted to each element such that Equation 5.10 ($\phi \times M_u > M^*$) is satisfied. This gives us the design of the reinforcement in the slab at an element level. No iterations are carried out as the depth in this case is constant and steel cannot be specified within the "Shell" element in SAP2000.

Technique 2

If the user chooses Technique 2 above, the program seeks the optimal thickness that satisfies bending in both directions, for each element. The program therefore gives an indication of how deep a section is required for resisting flexure in each element of the slab when the steel is kept constant throughout the slab. The program allots depth (i.e. 1 of 10 sections) to each element for resisting bending in the 1-1 direction and allots another section for resisting bending in the 2-2 direction, satisfying conditions of Equation 5.10 ($\phi \times M_u > M^*$). Both these sections allotted may be different. The program then allots the bigger of the two sections as the final section to the element. The iterative process is then continued till a steady state is reached wherein there is no further improvement in the design. Only those solutions are then chosen that satisfy Equation 5.10 for all elements in the slab. This condition is monitored in each iteration. It is seen that this condition is not necessarily satisfied in all iterations and therefore the optimal solution is that which satisfies Equation 5.10 in all elements of the slab as well as shows the most savings in weight at the same time satisfying deflection limits.

Technique 3

If the user chooses Technique 3 above, the program seeks the optimal layout of thickness and steel that satisfies bending in both directions, for each element. The program therefore gives an indication of how deep a section and how much steel is required for resisting flexure in each element of the slab when both the steel and the depth are allowed to vary throughout the slab. The program allots sections (i.e. 1 of 10 sections) to each element for resisting bending in the 1-1 direction and allots another section for resisting bending in the 2-2 direction, satisfying conditions of Equation 5.10 ($\phi \times M_u > M^*$). Both these sections allotted may be different. The program then allots the final

section, as the one having the bigger moment capacity between the two, to the element. Then, the iterative process is continued till a steady state is reached wherein there is no further improvement in the design. Only those solutions are then chosen that satisfy Equation 5.10 for all elements in the slab. This condition is monitored in each iteration. It is seen that this condition is not necessarily satisfied in all iterations and therefore the optimal solution is that which satisfies Equation 5.10 in all elements of the slab as well as shows the most savings in weight at the same time satisfying deflection limits.

If the economy button is clicked by the user, the optimization program allots a section to each element such that not only does it satisfy flexural criteria, but it selects the most economical section among the list of sections provided by the user. The cost of concrete and steel for each of the ten user-defined sections is calculated per meter width of the slab based on the unit cost of concrete and steel entered by the user in the WinBatch program. If the economy button is not clicked however, the program designs the elements based only on flexural criteria and does not take into account the economy of the sections.

Economical considerations are generally useful only when investigating with Technique 3, as it is expected with Techniques 1 and 2, that the user will provide increasing steel quantities or depths in the user interfaces (i.e. in increasing order towards the bottom). However, the program does not assume this and checks for it explicitly by calculating the cost of concrete and steel for each of the ten user-defined sections per meter width of the slab based on the unit cost of concrete and steel entered by the user in the WinBatch program. So, say for e.g. in Technique 2 above, if the user enters a higher depth for Section 3 and a lesser depth for Section 5, then the program calculates and knows that Section 5 will be economical compared to Section 3 as obviously the depth is less.

Results of investigating for Economy will therefore be shown only for Technique 3.

The design process is shown in the following flowchart.

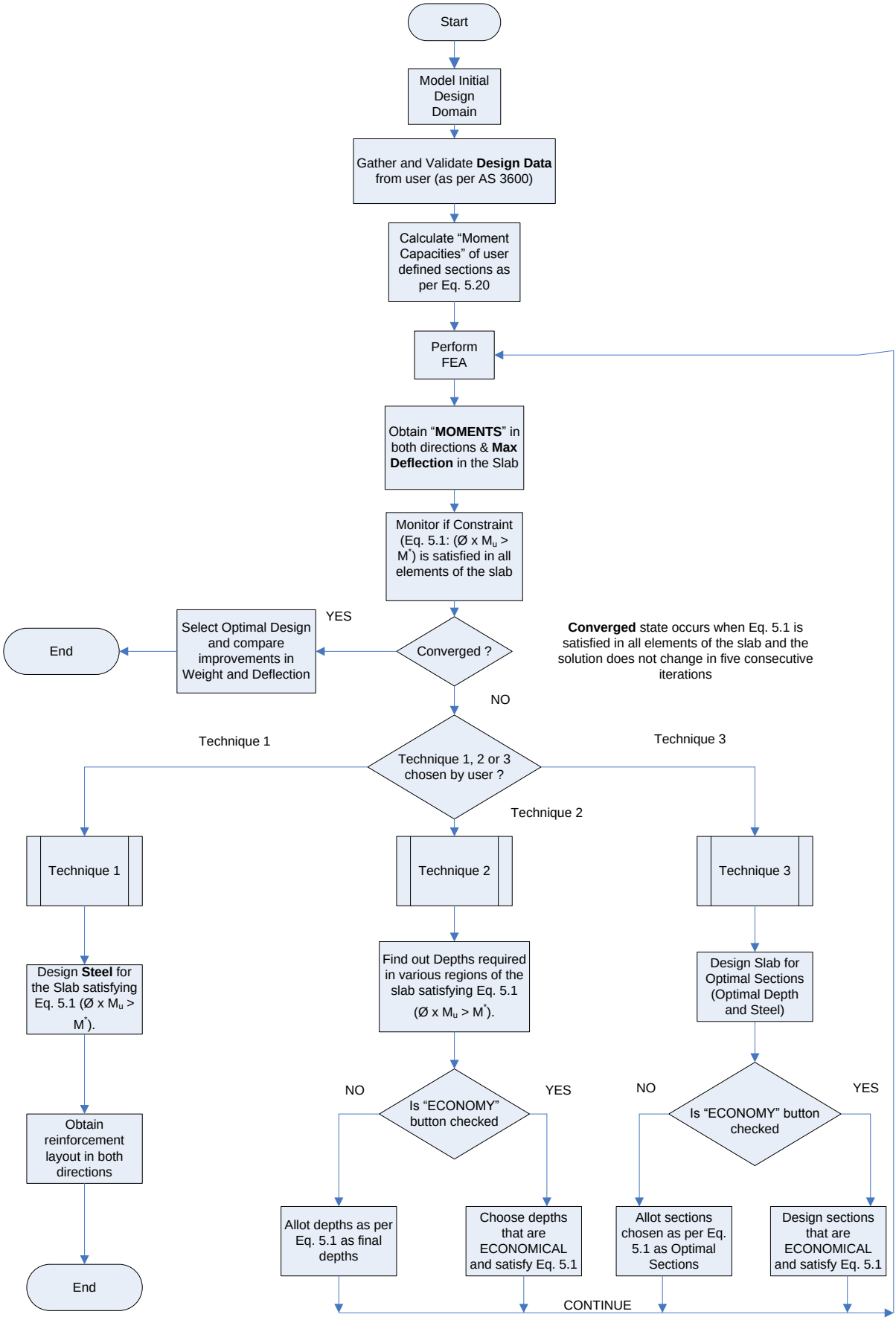

Fig. 7.4. Flowchart for Moment-based Optimisation of Slabs

7.5.3 Validation of Design Data Input by the User

The design data input by the designer in the User Interfaces (such as depths, reinforcement etc) is validated by the program for AS 3600 code requirements. This includes checking for minimum steel and ductility.

Minimum Steel

Clause 8.1.4.1 of AS 3600 specifies a lower limit on the steel content in the section, which requires that the moment capacity be at least 20% greater than the cracking moment. The intention is to prevent fracture of the steel and sudden collapse at cracking. The following limit is deemed to satisfy this requirement and is programmed in the computer code. If this requirement is not satisfied for any of the ten sections provided by the user, then the user is prompted to revise data before proceeding with optimisation. As per Cl. 8.1.4.1, AS 3600-2001 then

$$\frac{A_{st}}{b \times d} \geq 0.22\left(\frac{d}{D}\right)^2 \times \frac{f'_{cf}}{f_{sy}} \qquad (7.1)$$

where,

A_{st} = Area of tensile steel in the rectangular slab section

b = width of the section

d = effective depth of the section

D = full depth of the section

f'_{cf} = characteristic flexural tensile strength of concrete

f_{sy} = Yield strength of steel reinforcement

As per AS 3600 Cl. 6.1.1.2 the characteristic flexural tensile strength of concrete f'_{cf} is either

(a) taken as equal to $0.4\sqrt{f'_c}$ at 28 days and standard curing; or

(b) determined statistically from flexural strength tests carried out in accordance with AS 1012.10

In this work, f'_{cf} is taken as equal to $0.4\sqrt{f'_c}$

Ductility

Ductility is an important structural property because it ensures that large deformations and deflections will occur under overload conditions. In a statically determinate structure, the large deflections give warning of imminent failure. In indeterminate structures, ductility allows the structure to accommodate large imposed deformations without undue distress. It also enables a redistribution of

internal actions to occur at overload, whereby, with increases in load, the moments in overstressed regions remain constant and the moments in less highly stressed regions increase more than proportionally. Good ductility can be achieved if the quantity of reinforcement is kept well below the value which produces balanced failure condition. Although an increase in the quantity of steel in the section has a beneficial effect on moment capacity, it has an adverse effect on behaviour at high overload. An approximate measure of the ductility of a section is provided by the neutral axis parameter, k_u. For slabs, AS 3600 specifies a maximum value of 0.2 for k_u. This condition is checked for each section provided by the user in the user interface. If this condition is violated (i.e. $k_u > 0.2$) then the user is asked to revise the sections (i.e. increase depth or reduce steel) before proceeding with optimisation. Equation 7.2 below calculates the neutral axis parameter, k_u:

$$k_u = \frac{1}{0.85 \times \gamma} \times \frac{A_{st}}{b \times d} \times \frac{f_{sy}}{f_c^{'}} \tag{7.2}$$

where,

k_u = Neutral Axis Parameter

γ = Parameter used to define the magnitude and location of the compressive force C in the member (using equivalent rectangular stress block concept)

A_{st} = Area of tensile steel provided

b = width of section (1m in this case)

d = Effective depth of section

f_{sy} = Yield strength of steel reinforcement

$f_c^{'}$ = Characteristic strength of concrete in compression

Values given for γ in AS 3600 are as follows:

$$\gamma = 0.85 - 0.007\left(f_c^{'} - 28\right)$$

with the limits $0.65 < \gamma < 0.85$

The upper value of 0.85 applies when $f_c^{'}$ is less than 28 MPa, while the lower limit of 0.65 is used for high strength concretes with $f_c^{'}$ greater than 64 MPa. The value of γ is checked and validated in the computer code for the $f_c^{'}$ specified by the user in the user interface. If $\gamma < 0.65$, then 0.65 is used as the value for γ whereas if $\gamma > 0.85$, then 0.85 is used as the value for γ.

7.6 Simple Examples

For all the examples and case studies, which are presented later, please refer to the 'Colour Code' shown in the respective GUI's for the 'Colour Legend' when interpreting the results.

The proposed techniques are first tested on examples without validating user-data to AS3600 requirements. Therefore a depth of 50 mm with 2-Y16 bars (as seen in the GUI below) is permitted in this example.

7.6.1 Seeking Optimal Depths in a Single Span One-way slab

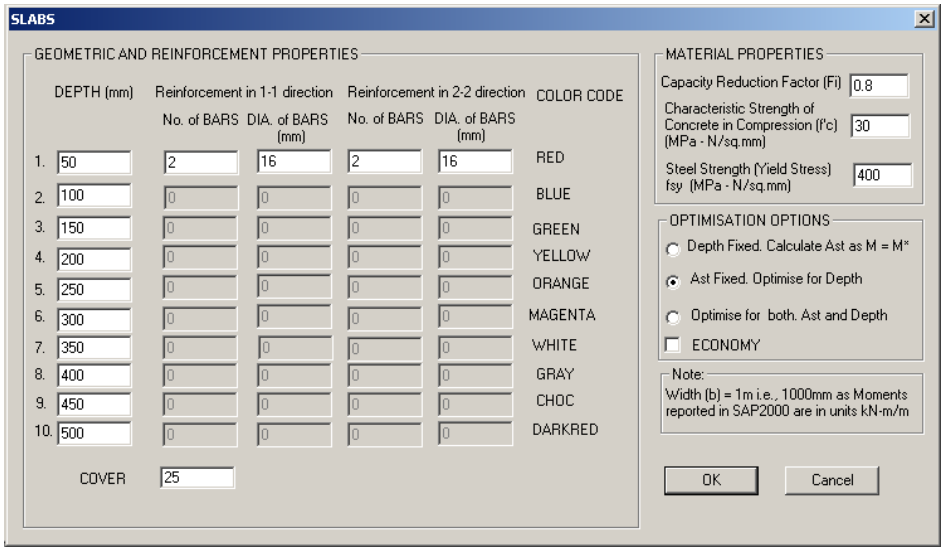

Fig. 7.5. Design Data for Technique 2.

Geometry

Span: 4m x 8.4m

Mesh of 12 x 24 elements

Initial Slab thickness: 200 mm

Loading

DL: 2 kPa, LL: 4 kPa

Load Combo: 1.25 DL + 1.5 LL

Analysis

Linear Elastic FEA

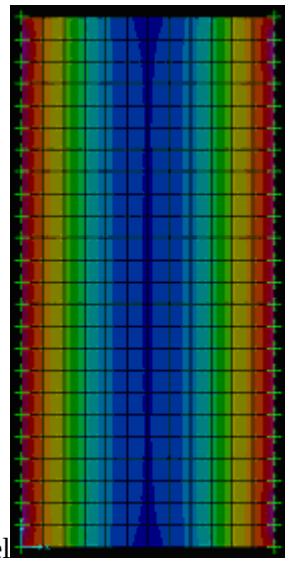

FEA of Initial Model

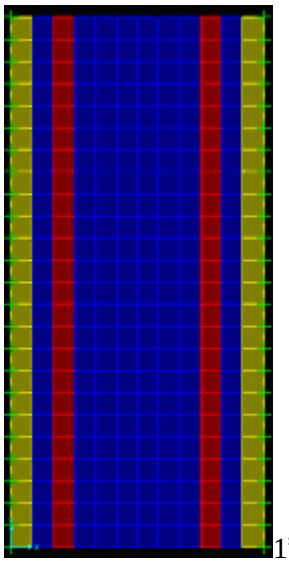

1st iteration

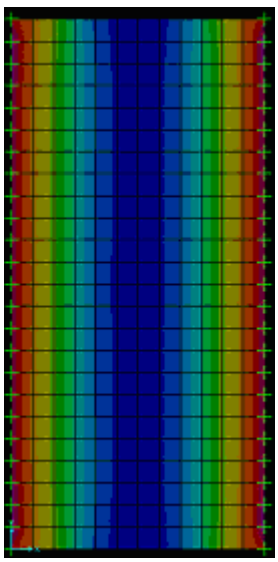

FEA of 1st iteration

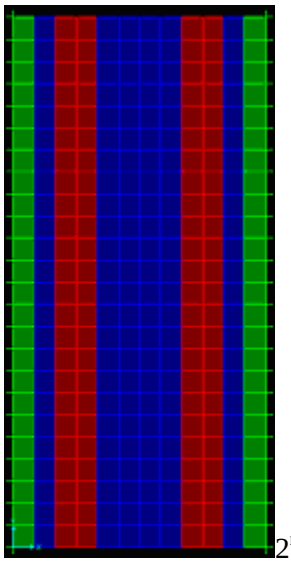

2nd iteration

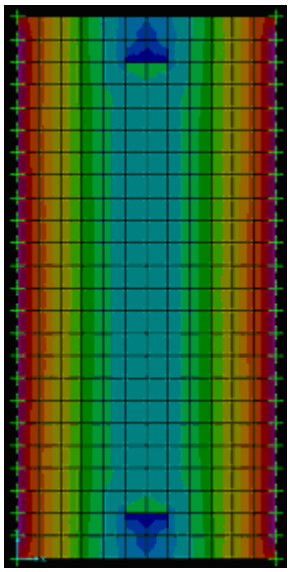

FEA of 2nd iteration

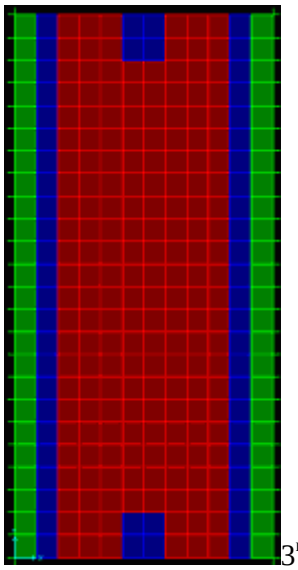

3rd – 8th iteration

Fig. 7.6. Design Solutions for One-Way Slab using Technique 2

Table 7.1. Design Optimisation Results of One-Way Slab using Technique 2

Iteration No	*Weight (kN)*	*% Saving in Weight*	*Condition Satisfied* ($\emptyset$ *x* $M_u > M^*$)
Initial Model	158.344	-	
1	85.769	45.83	YES
2	72.574	54.17	YES
3	60.478	61.81	YES
4	60.478	61.81	YES
5	60.478	61.81	YES

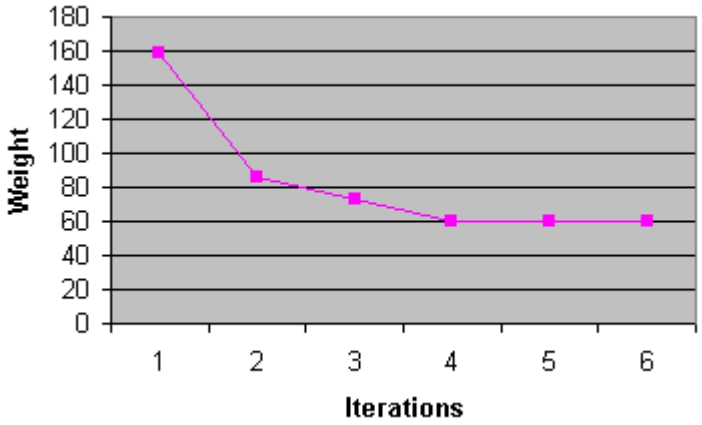

Fig. 7.7. History of Reduction in Concrete Weight for One-Way Slab using Technique 2 Optimisation

The thickness distribution follows the expected distribution of moments across the width of this one-way slab. As we know, the bending moment diagram for a beam fixed on both sides has two points of contraflexure. It is clear that the thickness should be zero (or least in this case) at the points of contra flexure and should gradually increase with increasing moment. This is observed in all iterations and the results satisfy expected outcome of thickness distribution. The constraint of providing adequate moment capacity ($\phi \times M_u > M^*$) in all elements of the slab is also satisfied in all iterations. A saving in weight of almost 62 % compared to the initial model is observed. The solution settles very quickly in 3 iterations and the 3rd iteration shows the maximum benefit in weight savings compared to the initial model. It is seen that using the proposed method, significant savings in weight are obtained.

7.6.2 Effect of Load on Convergence

In Section 7.6.1, it was observed that the solution settles quickly within three iterations and achieves the objective function (significant weight savings) while satisfying the constraint ($\phi \times M_u > M^*$). In this example, the Live Load is increased from 4 kPa to 6 kPa and results obtained are investigated for the same design data.

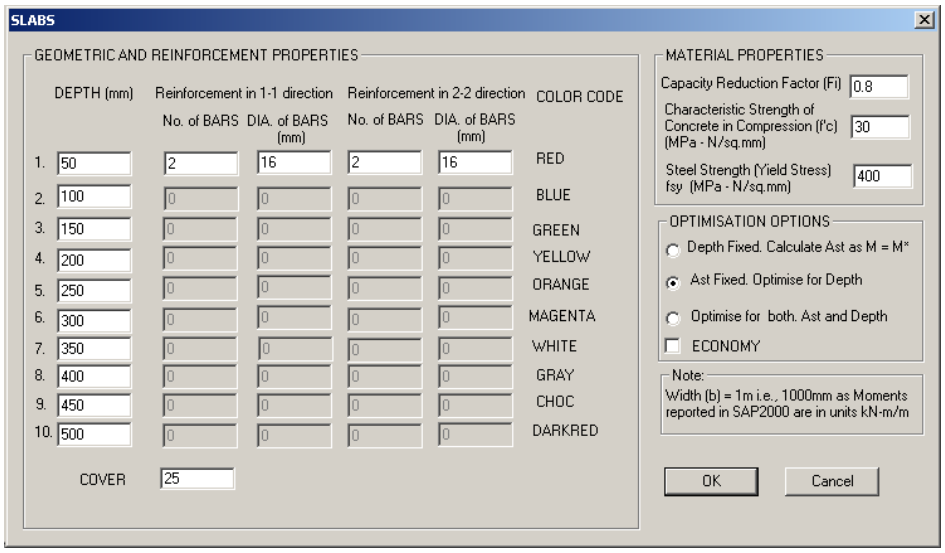

Fig. 7.8. Design Data for Technique 2 (same as in Fig. 7.5)

1st iteration 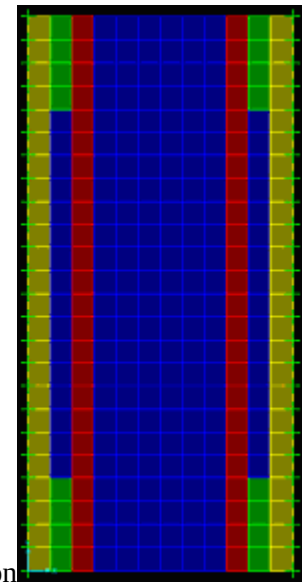 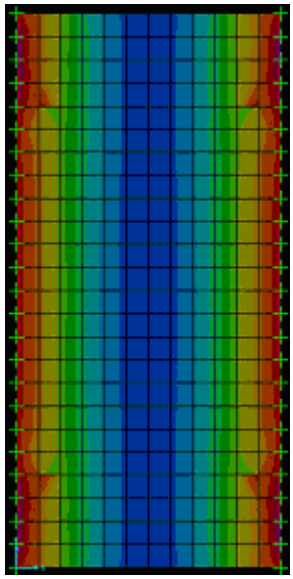 FEA of 1st iteration

(a).

2nd iteration 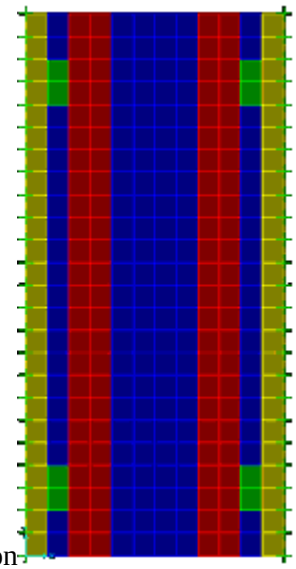 (b) 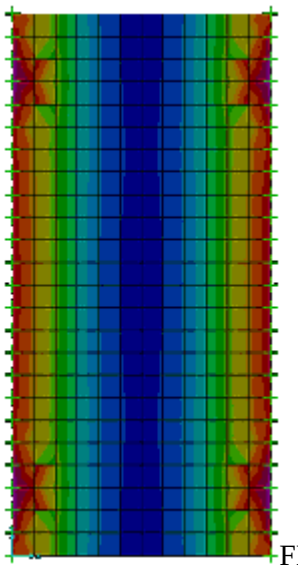 FEA of 2nd iteration

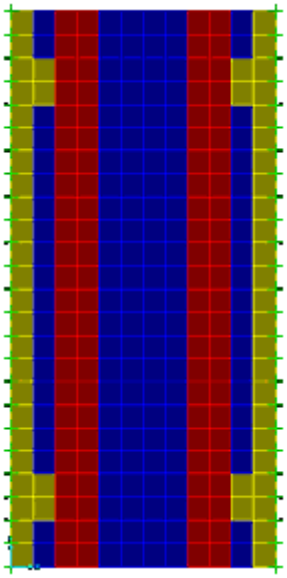

3rd iteration

(c)

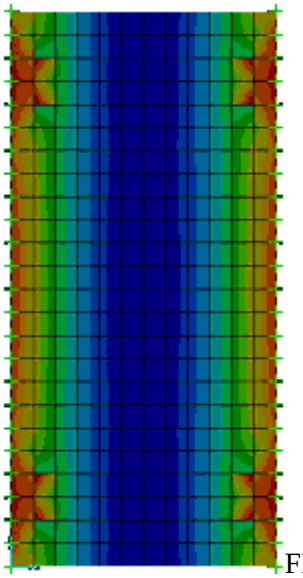

FEA of 3rd iteration

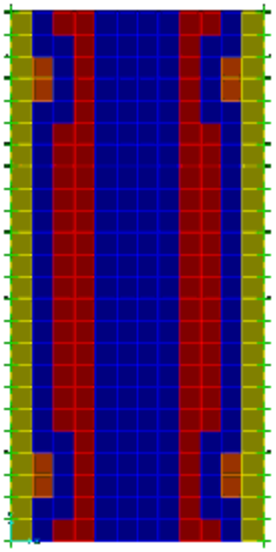

4th iteration

(d)

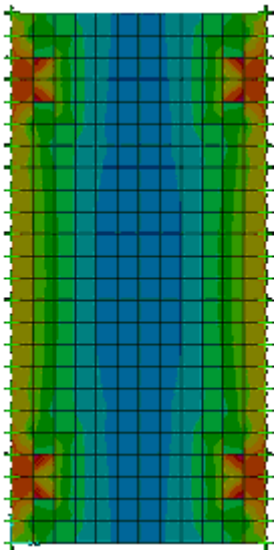

FEA of 4th iteration

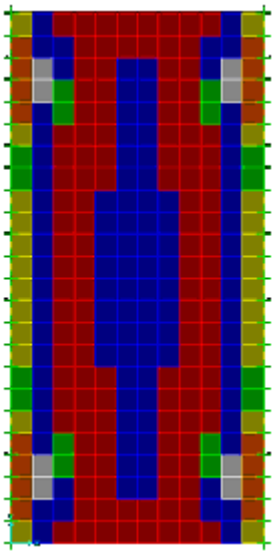

5th iteration

(e)

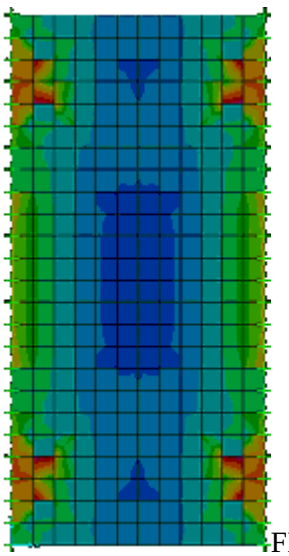

FEA of 5th iteration

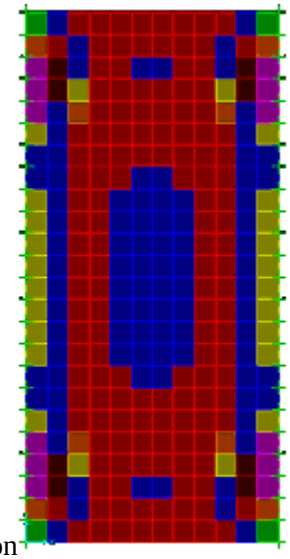

6th iteration (f)

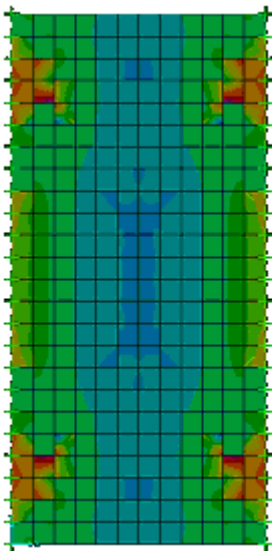

FEA of 6th iteration

Fig. 7.9. Technique 2 Design Solutions for One-Way Slab Subjected to Increased Loading

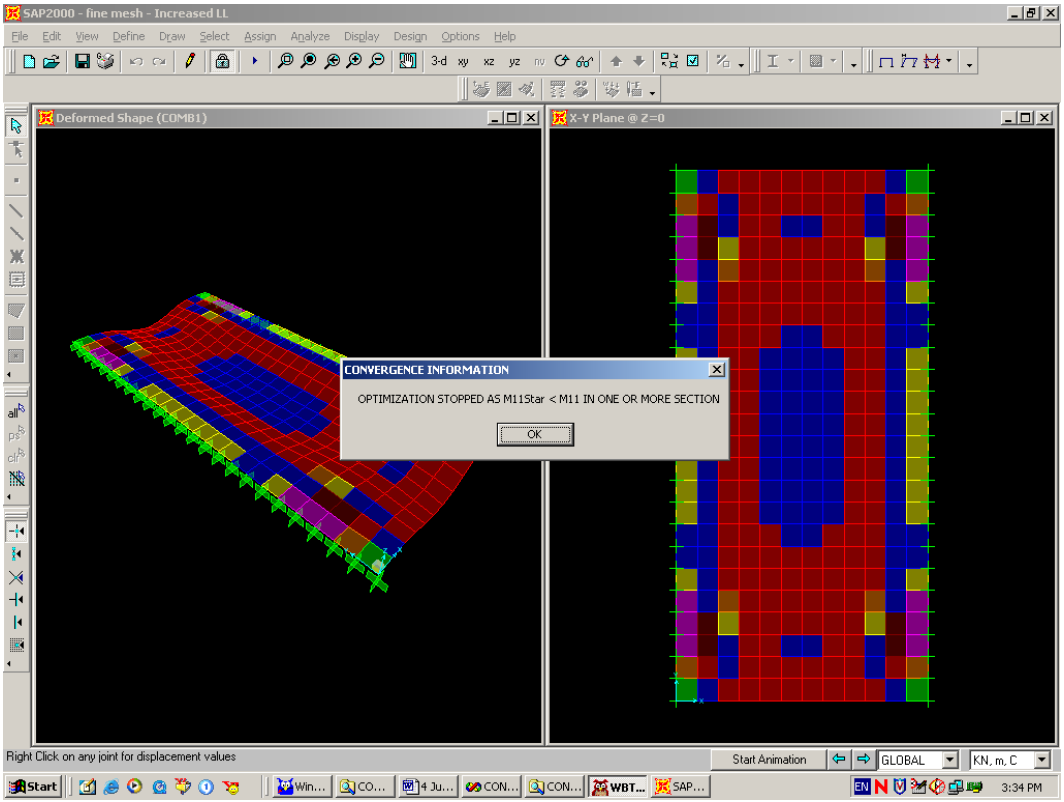

Fig. 7.10. Convergence Information

Table 7.2. Design Optimisation Results using Technique 2 for One-Way Slab Subjected To Increased Loading

Iteration	*Weight (kN)*	*Condition Satisfied (Ø x M_u > M^*)*
Initial Model	158.344	-
1	87.968	YES
2	80.271	NO
3	81.371	NO
4	84.670	NO
5	83.570	NO
6	85.769	NO

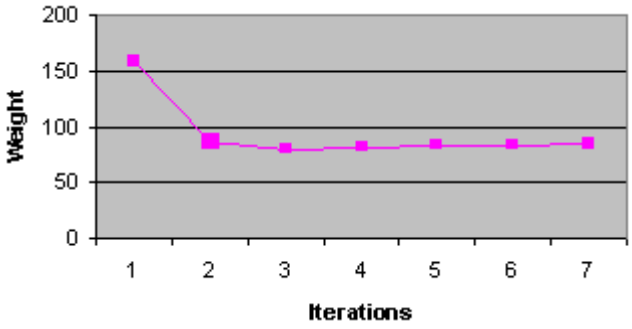

Fig. 7.11. History of Reduction in Concrete Weight for One-Way Slab Subjected to Increased Loading using Technique 2 Optimisation

It is seen from the above results, that for the same design data given by the user in the user interface, when the load is increased, the solutions do not satisfy the constraint in any iteration except the first iteration. This happens because:

A very nominal amount of steel is provided by the user (2-Y16 both ways, it is actually less than the minimum prescribed by AS 3600). Therefore, the moment capacities of these ten sections (which are the same as in the previous example) are now inadequate when compared with the increased moments from the FEA (due to the increased LL). As a result, the algorithm picks higher depths to satisfy condition $\phi \times M_u > M^*$ in each element of the slab. When a higher depth is chosen, this in turn results in higher moments in the region around the thicker depth and this process goes on till even the thickest depth is inadequate. The constraint $\phi \times M_u > M^*$ is therefore obviously not satisfied in regions around the thicker and thicker depths (Refer last figure of Optimisation History). The program stops and issues the message "Optimisation stopped as M11Star < M11 in one or more section". This message means that the program has tried all available sections provided by the user and still cannot satisfy the condition for either one or more elements in the model. Hence, the program stops. This indicates that the user needs to either revise the data provided in the user interface (i.e. steel or depths, or material properties) or revise the loads applied to the model.

This simple example demonstrates the effect of design data on results obtained for the same slab model when the load is increased. None of the iterations, except the first, satisfy the constraint. This is

the optimal solution for this particular case with this design data. % saving in weight of the optimal solution compared to initial model is 44.45 %. In the following two examples, a bigger amount of steel is employed and results are investigated for Live Loads of 8 kPa and 10 kPa respectively to see if the above pattern of results persists even with a higher amount of steel when the load is increased further.

7.6.3 Effect of Steel Quantity on Results

Geometry

Span: 4m x 8.4m

Mesh of 12 x 24 elements

Initial Slab thickness: 200 mm

Loading

DL: 2 kPa, LL: **8 kPa**

Load Combo: 1.25 DL + 1.5 LL

Analysis

Linear Elastic FEA

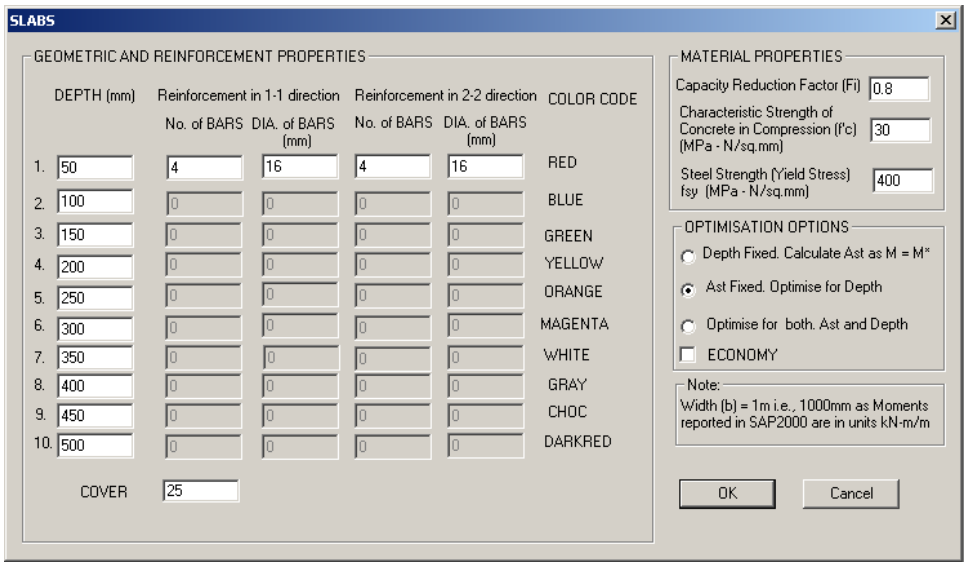

Fig. 7.12. Design Data for Technique 2

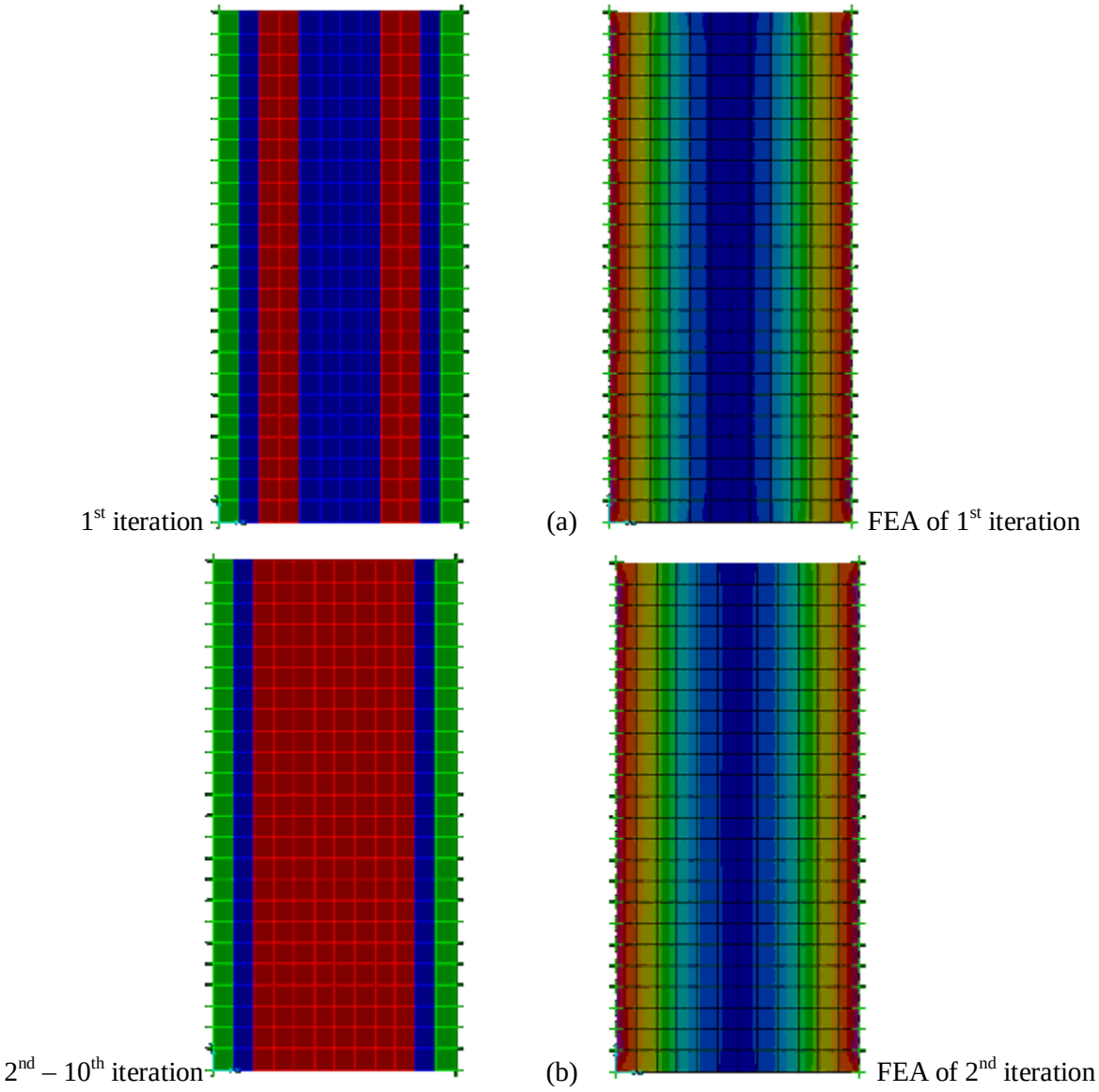

Fig. 7.13. Technique 2 Design Solutions for One-Way Slab with More Steel

Table 7.3. Design Optimisation Results using Technique 2 for One-Way Slab with More Steel

Iteration	*Weight (kN)*	*Condition Satisfied* ($Ø \times M_u > M^*$)
Initial Model	158.344	-
1	72.574	YES
2	59.379	YES
3	59.379	YES
4	59.379	YES
5	59.379	YES
6	59.379	YES

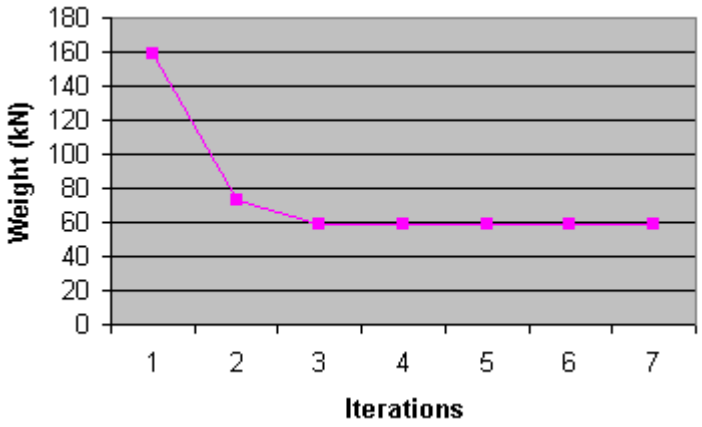

Fig. 7.14. History of Reduction in Concrete Weight for One-Way Slab with More Steel using Technique 2 Optimisation

It is seen from the above results that solution settles from the 2nd iteration. Both iterations satisfy the criterion $\phi \times M_u > M^*$, and the optimal solution shows a saving of 62.50 % saving in weight of concrete compared to the initial model.

Conclusion

It is seen that on increasing the quantity of steel (for a higher load), stable and optimal solutions are obtained in very few iterations that show a significant saving in concrete weight. Using more quantity of steel for a lesser load would have resulted in the algorithm choosing the first section (red) as the depth to be allotted for all elements in the slab. A distinct thickness pattern could not have emerged. Hence the live load was increased as was the quantity of steel. When compared with the previous example in Section 7.6.2, this example demonstrates the importance of steel quantity in the section on the results obtained. A last example is tried to see the optimal thickness distribution when the load is increased further to 10 kPa.

7.6.4 Effect of a Further Increased Load on Results

Geometry

Span: 4m x 8.4m
Mesh of 12 x 24 elements
Initial Slab thickness: 200 mm

Loading

DL: 2 kPa, LL: **10 kPa**
Load Combo: 1.25 DL + 1.5 LL

Analysis

Linear Elastic FEA

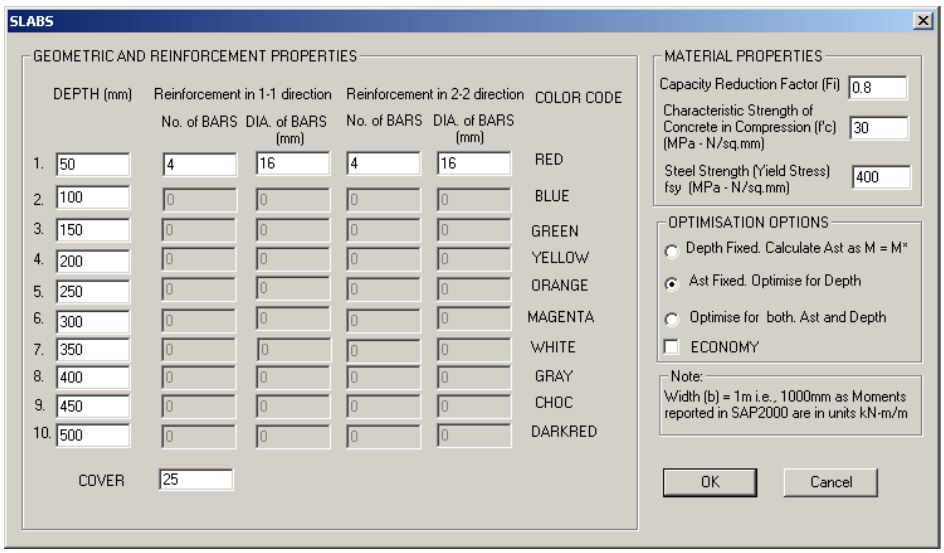

Fig. 7.15. Design Data for Technique 2

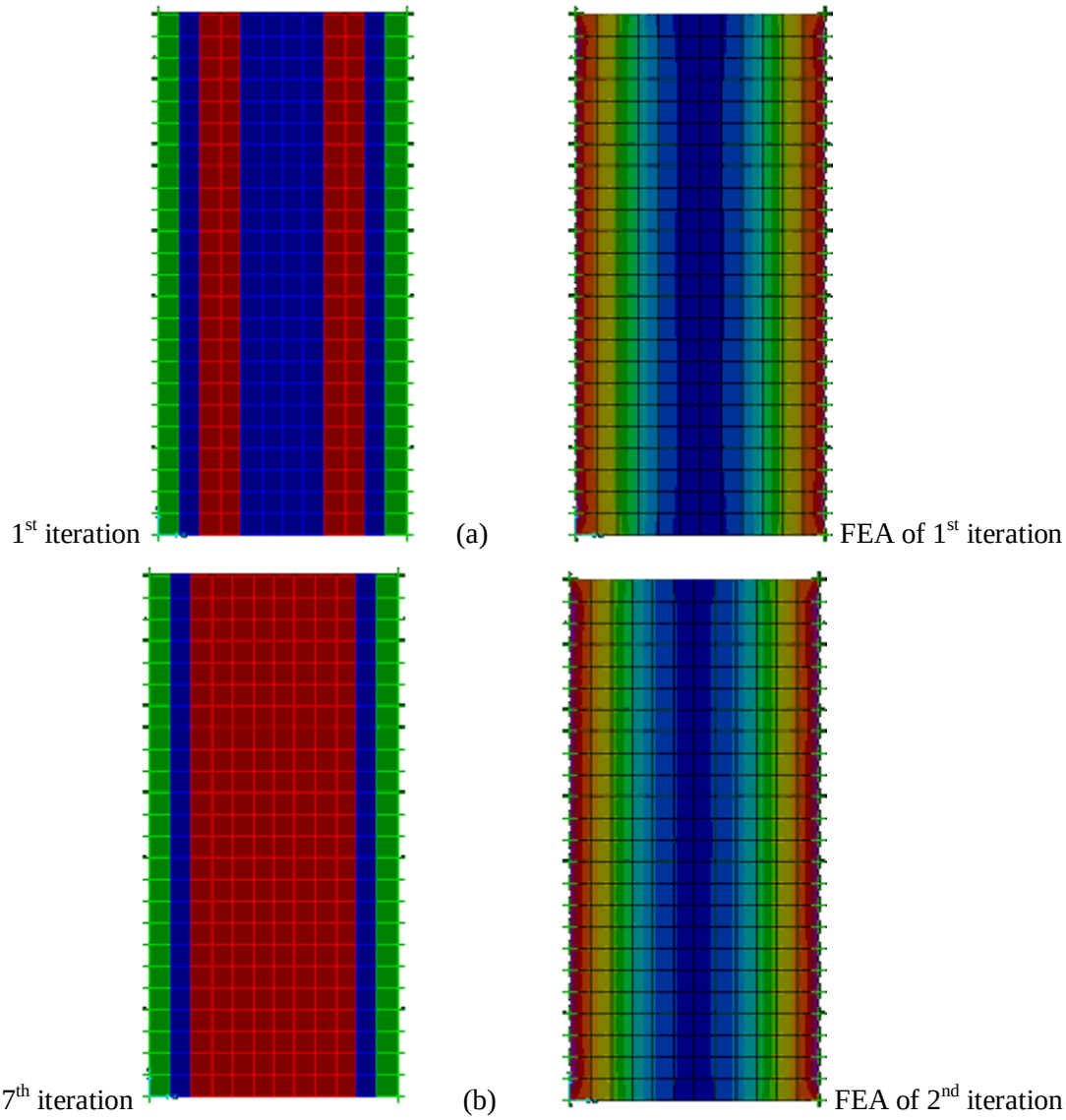

Fig. 7.16. Technique 2 Design Solutions for One-Way Slab Subjected to Further Increased Loading

Table 7.4. Design Optimisation Results using Technique 2 for One-Way Slab Subjected to Further Increased Loading

Iteration	*Weight (kN)*	*Condition Satisfied (Ø x $M_u > M^*$)*
Initial Model	158.344	-
1	72.574	YES
2	59.379	YES
3	59.379	YES
4	59.379	YES
5	59.379	YES
6	59.379	YES

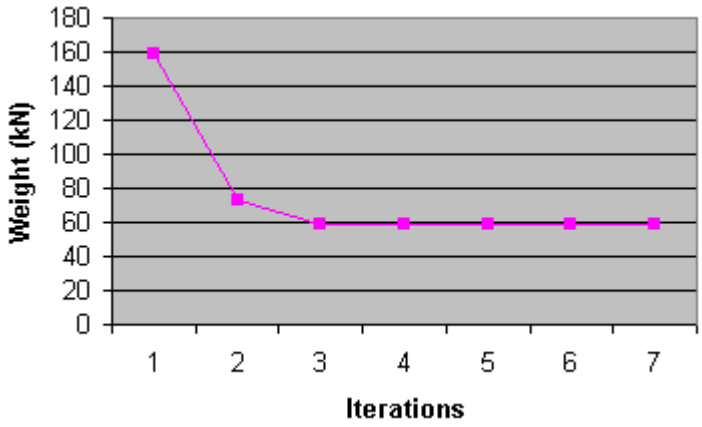

Both iterations *satisfy* the condition

Fig. 7.17. History of Reduction in Concrete Weight for One-Way Slab Subjected to Further Increased Loading using Technique 2 Optimisation

It is seen from the above results that, even with an increased LL (10 kPa as compared to 8 kPa in the previous example), the result stays the same. As in the previous example, the solution settles from the 2nd iteration onwards and a 62.50 % saving in concrete weight is obtained compared to the initial model.

This example demonstrates that for the same design data in the example of Section 7.6.3 above, the results obtained are still the same even for an increased live load of 10 kPa. However, a further example tested by the author reveals that when the load was increased to 12 kPa for the design data used in this example, again the pattern of results seen in Section 7.6.2 above emerges. This suggests that for a particular load a minimum amount of steel needs to be present in the section for the solution to settle and satisfy the constraint as otherwise the thicker regions keep getting thicker when a marginal amount of reinforcement is used in the section. A broad comparison of the four examples follows:

7.6.5 Comparison of Examples

Table 7.5. Comparison of Examples in Sections 7.6.1 to Section 7.6.4

Sr. No.	*Example*	*DL (kPa)*	*LL (kPa)*	*Steel used (both ways)*	*Solution settles*	*Satisfies constraint*	*No of iterations required for the solution to "settle"*
1.	1	2	4	2–Y16	YES	YES	3
2.	2	2	6	2–Y16	NO	Only 1st iteration	6
3.	3	2	8	4–Y16	YES	YES	2
4.	4	2	10	4–Y16	YES	YES	2
5.	5	2	12	4-Y16	NO	Only 1st iteration	

Note: All other variables such as depths, material properties and geometry are all kept constant for all examples.

These results suggest that for a particular load, when using Option 2, a minimum quantity of steel needs to be provided by the user in order to obtain an optimal result that settles and satisfies the bending moment constraint for all elements in the slab.

7.6.6 Continuous One - Way Slab - Design using Technique 1

Technique 1 is employed first, to find out the layout of steel required in the slab with constant thickness throughout.

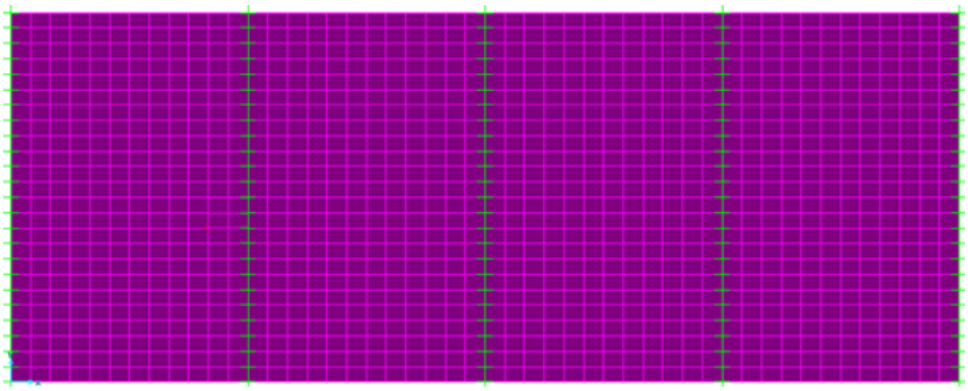

Fig. 7.18. Initial Model of Continuous One-Way Slab

Data: Span: 4.5 m c/c; Supports: Fixed; Load: Self Weight + 3 kPa LL

This initial model will be designed using all three techniques and optimal solutions in each case will be analyzed. It is to be noted that AS 3600 provisions for minimum steel, minimum slab depth, ductility etc are not followed at this stage. AS 3600 provisions are followed later in the computer code when testing the three techniques on real world case studies.

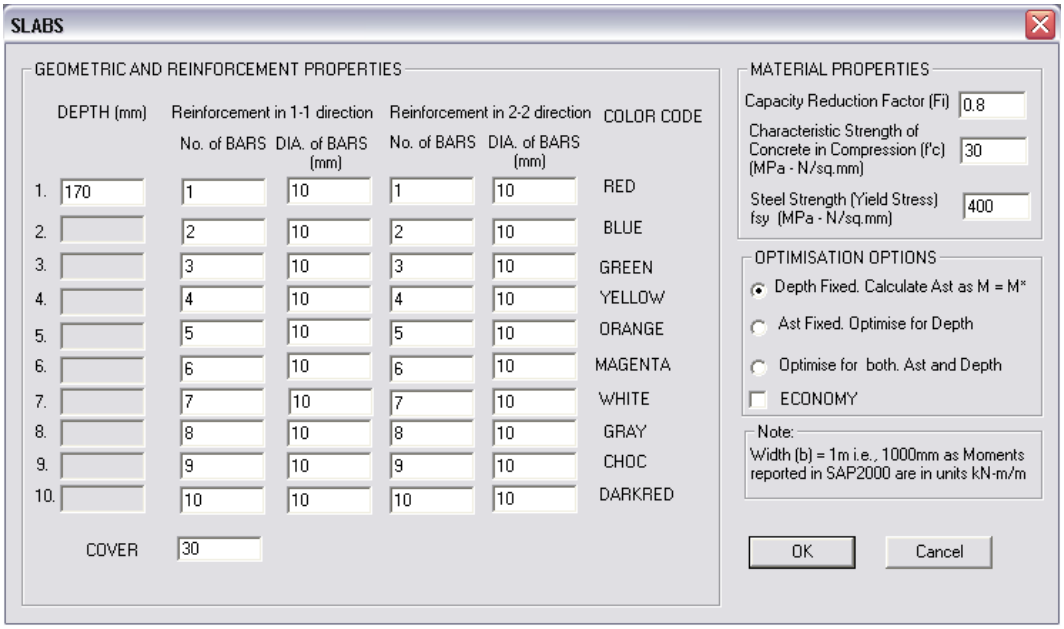

Fig. 7.19. Design Data for Technique 1

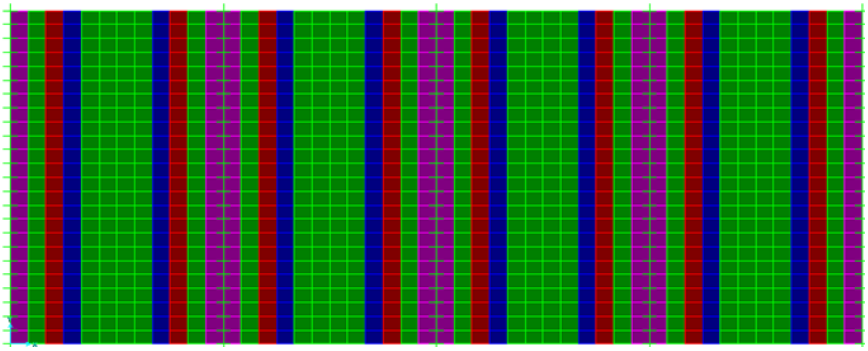

Fig. 7.20. Technique 1 Design Solution showing Main Steel Layout

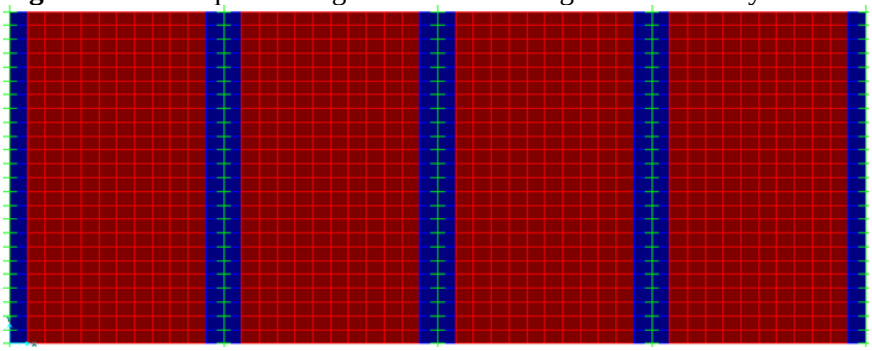

Fig. 7.21. Technique 1 Design Solution showing Transverse Steel Layout

Two files are generated, one for the main reinforcement and other for the transverse reinforcement. It is seen from the results above for Main Steel that 6 – Y10 bars are needed per meter width over the support regions (Magenta color), next to which 3 – Y10 bars (Green Color) are required. The Red colored band indicates the point of contra-flexure where the least amount of reinforcement is required (1-Y10) followed by the blue band that indicates 2-Y10 bars are needed. At the mid span of the slab, where there is positive (sagging) bending moment, 3-Y10 bars (Green color) are required. As the thickness is uniform for this slab, there is no optimisation involved and this solution indicates the requirement of steel in the slab. It is also seen from the results for Transverse Steel that only the least amount of reinforcement is required in the transverse direction (Red color indicates 1-Y10 bar). Practically, it is not possible to have 1-Y10 bar and therefore code provisions as per AS 3600 need to be programmed into the code in order to validate the design data provided by the user in the user interfaces. However, these results give a good theoretical indication of the distribution of steel required in this slab. Had the requirement of minimum steel been programmed into the code, it would not have been possible to observe the red band at the point of contra-flexure. This example provides a theoretical design for the steel requirement in the slab based on the data provided by the user in the user interface.

7.6.7 Continuous One-Way Slab – Design Using Technique 2

Different results have been obtained when the steel quantity is gradually varied in Technique 2 using examples shown in Sections 7.6.1 to 7.6.4 for the single span slab with fixed ends (which effectively acts as a fixed beam) above. A comparison is also made for that model that shows the effects of changing either the load gradually and/or the quantity of steel gradually. This example serves to reinforce that concept, however using a continuous slab in this case as compared to a single span slab. The difference in the optimal solutions obtained is analysed and improvements compared.

7.6.7.1 Case A: Less Steel

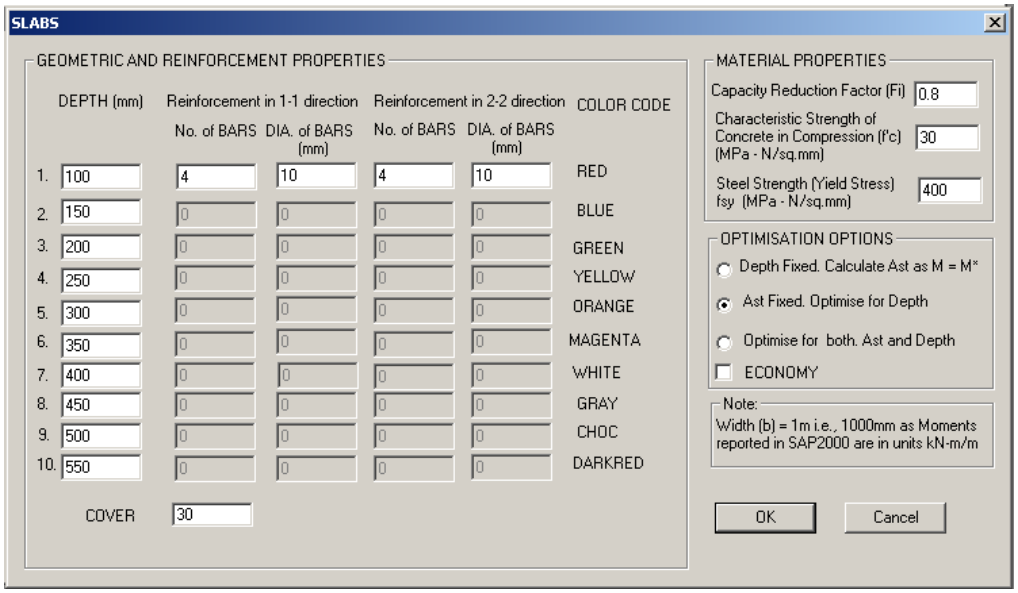

Fig. 7.22. Design Data for Technique 2

We begin first with specifying 4-Y10 bars in both directions. A range of depths is entered, material properties specified and Technique 2 chosen.

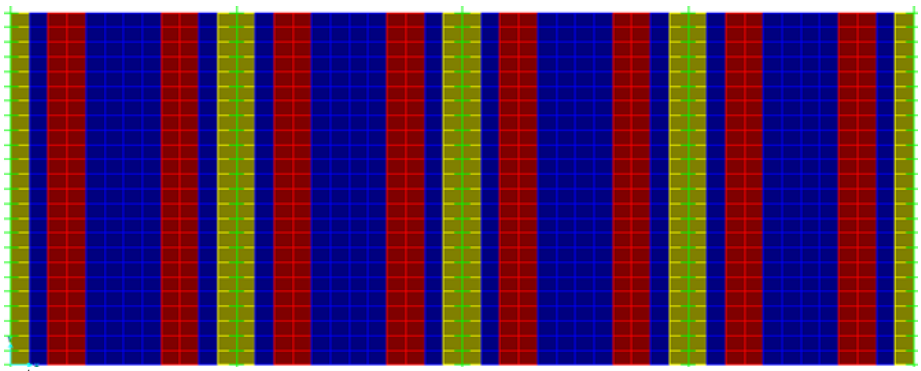

1st iteration

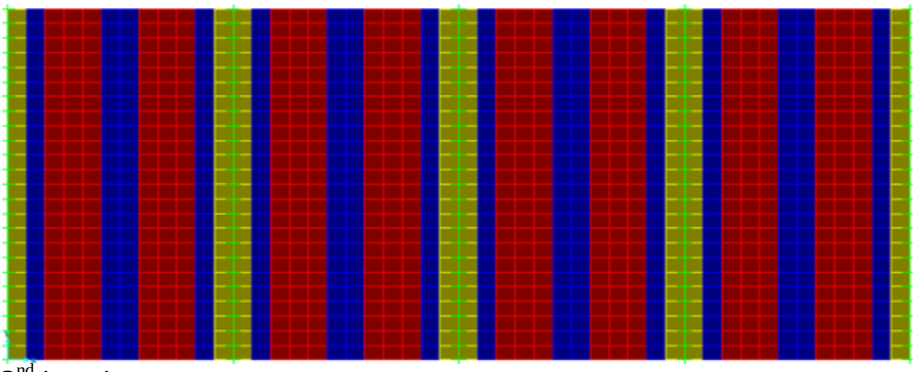

2nd iteration

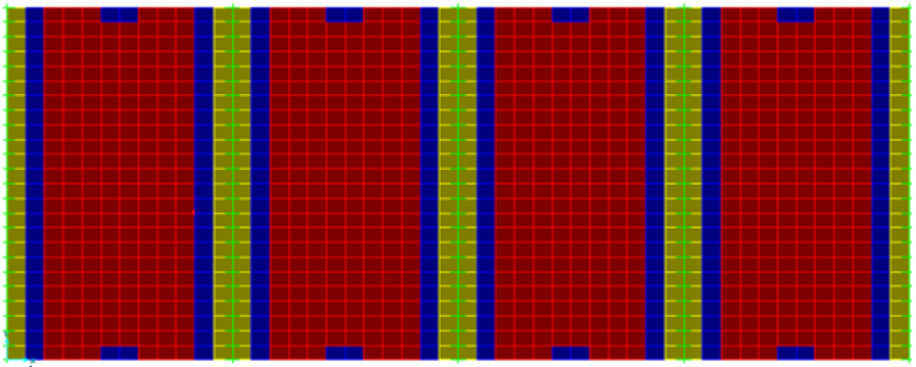

3rd iteration

Fig. 7.23. Technique 2 Design Solutions for Continuous One-Way Slab

Table 7.6. Design Optimisation Results using Technique 2 for Continuous One-Way Slab

Sr. No.	Iteration No.	Concrete Weight (TONNE)	% Saving in Concrete Weight	Weight of Steel in X direction (TONNE)	Weight of Steel in Y direction (TONNE)	TOTAL STEEL WEIGHT (TONNE)	Total Cost of Concrete (AU $)	Total Cost of Steel (AU $)	Max Deflection (mm)	Permissible Deflection (Span/250) mm	SATISFIES MOMENT CONDITION
1	Initial Model	51.465	-	0.313	0.313	0.626	3216.59	344.471 (X) + 344.471 (Y) = 688.942	1.2 x 3 = 3.60	18mm	YES
2	1	45.41	11.76 %	0.313	0.313	0.626	2838.170	344.471 (X) + 344.471 (Y) = 688.942	1.1 x 3 = 3.30	18mm	YES
3	2	42.887	16.67 %	0.313	0.313	0.626	2680.494	344.471 (X) + 344.471 (Y) = 688.942	1.3 x 3 = 3.90	18mm	YES
4	3	40.365	21.57 %	0.313	0.313	0.626	2522.818	344.471 (X) + 344.471 (Y) = 688.942	1.6 x 3 = 4.80	18mm	YES

7.6.7.2 Case B: More Steel

The steel quantity is increased nominally and the difference in results is observed as follows:

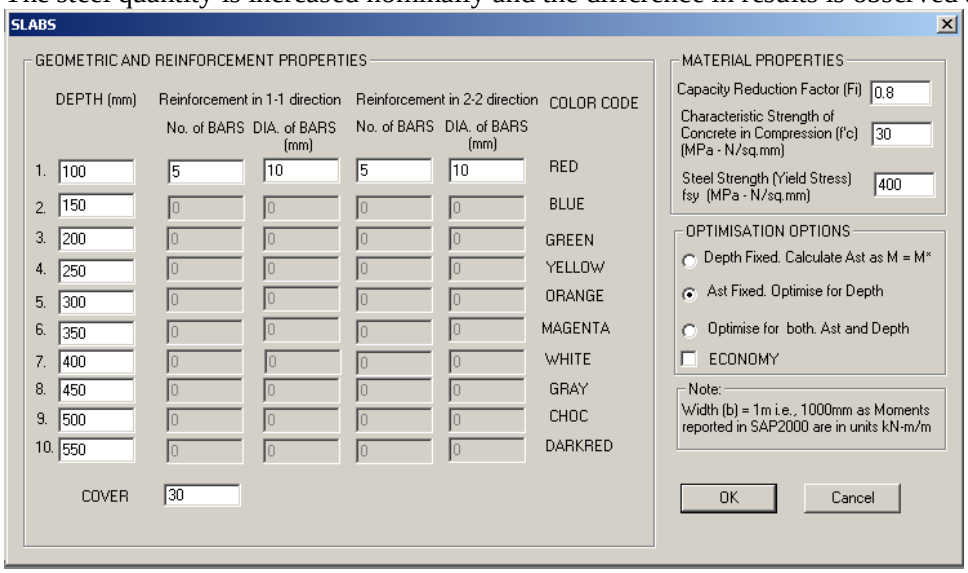

Fig. 7.24. Design Data for Technique 2

(Steel specified in this case is 5-Y16 bars in both directions and all other variables are the same as in Section 7.6.7.1).

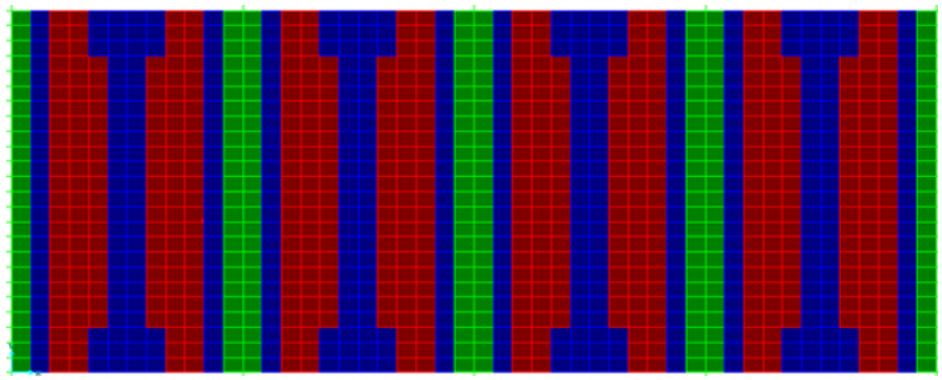

(a) 1st iteration

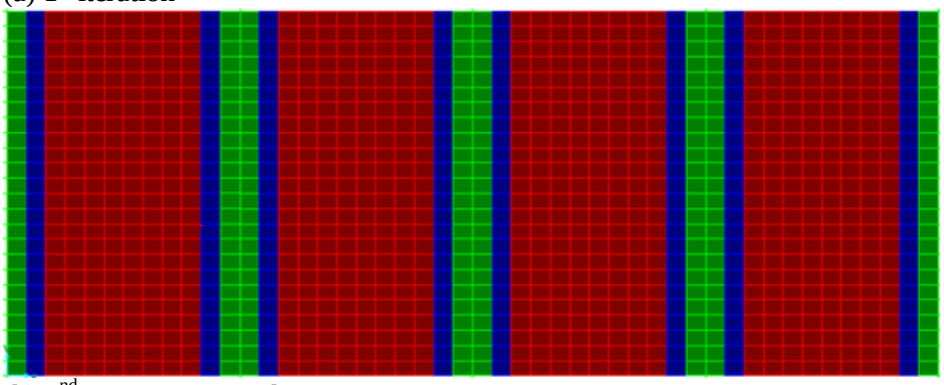

(b) 2nd iteration onwards

Fig. 7.25. Technique 2 Design Solutions for Continuous One-Way Slab Using More Steel

Table 7.7. Design Optimisation Results using Technique 2 for Continuous One-Way Slab with More Steel

Sr. No.	Iteration No.	Concrete Weight (TONNE)	% Saving in Concrete Weight	Weight of Steel in X direction (TONNE)	Weight of Steel in Y direction (TONNE)	TOTAL STEEL WEIGHT (TONNE)	Total Cost of Concrete (AU $)	Total Cost of Steel (AU $)	Max Deflection (mm)	Permissible Deflection (Span/250) mm	SATISFIES MOMENT CONDITION
1	Initial Model	51.465	-	0.391	0.391	0.782	3216.59	430.10 (X) + 430.10 (Y) = 860.20	1.2 x 3 = 3.60	18mm	YES
2	1	40.997	20.34 %	0.391	0.391	0.782	2562.312	430.10 (X) + 430.10 (Y) = 860.20	1.15 x 3 = 3.45	18mm	YES
3	2	37.842	26.47 %	0.391	0.391	0.782	2365.125	430.10 (X) + 430.10 (Y) = 860.20	1.65 x 3 = 4.95	18mm	YES

Note: Steel Weight does not change as Option 2 (Steel constant, depth varying) is chosen for optimisation.

When using 4-Y10 bars, the solution settles from the third iteration onwards whereas when 5-Y10 bars are used, the solution settles from the second iteration onwards. The solution 'settles' means that it does not change thereafter. In both cases, each iteration for either case satisfies the moment criterion. On comparing the optimal solutions for both cases above, it is noticed that when lesser steel is used (4-Y10 bars in both direction), a depth of *250 mm* (yellow color) is required over the *supports*. Also, at the centre of the free ends, a thicker portion of 150 mm (blue color) is needed. Whereas, when the quantity of steel is increased gradually from 4-Y10 bars to 5-Y10 bars in both directions, lesser depths are seen in the optimal solution. A depth of *200 mm* (green color) is required over the *supports* whereas no thicker portions are required at the centre of the free ends.

The cost savings in concrete compared to the increase in the cost of steel, when 5-Y10 bars are used, make interesting comparisons (Compare Table 7.6 and Table 7.7 above). Compared to the initial model, the optimal solution shows a concrete weight saving of *21.57 %* when 4-Y10 bars are used, whereas a concrete weight saving of *26.47 %* is attained when 5-Y10 bars are used. This is to be expected, as using more steel would generally require lesser depths when compared to using less steel. The increase in concrete weight saving is attained by increasing the quantity of steel. Therefore, when deciding between which optimal solution to choose, i.e. whether to go for 4-Y10 bars or 5-Y10 bars throughout, the cost savings in concrete weight should be judged with the increase in associated steel cost. On comparing Table 7.6 and Table 7.7 above, it is observed that the *cost of steel needed* has *gone up* by *AU $ 171.26* ($ 860.22 - $ 688.94) when 5-Y10 bars are used instead of 4-Y10 bars. However, the *cost of concrete required* has *fallen* by *AU $ 157.69* ($ 2522.818 – $ 2365.125) when 5-Y10 bars are used instead of 4-Y10 bars. The *total material cost* of steel and concrete in the optimal solution when using *4-Y10* bars is *AU $ 3211.76* whereas the *total material cost* in the optimal solution when using *5-Y10* bars is *AU $ 3225.33*. Though the difference is not much, it is clear that more premiums is to be paid for the steel and in this case, the optimal solution using 4-Y10 bars is more cost effective than the optimal solution using 5-Y10 bars. It is to be noted however, that formwork and other construction costs are not included in this estimate. Also, the cost of steel calculated is not exact meaning that, because this work is at a concept design stage, it is not possible to work out the quantity of steel based on exact detailing requirements.

Using Technique 3, therefore, a solution should be sought that optimizes both the weight of steel and concrete. The next example demonstrates the application of Technique 3 to optimize both the weight of steel and concrete at the same time.

7.6.8 Continuous One-Way Slab – Design Using Technique 3

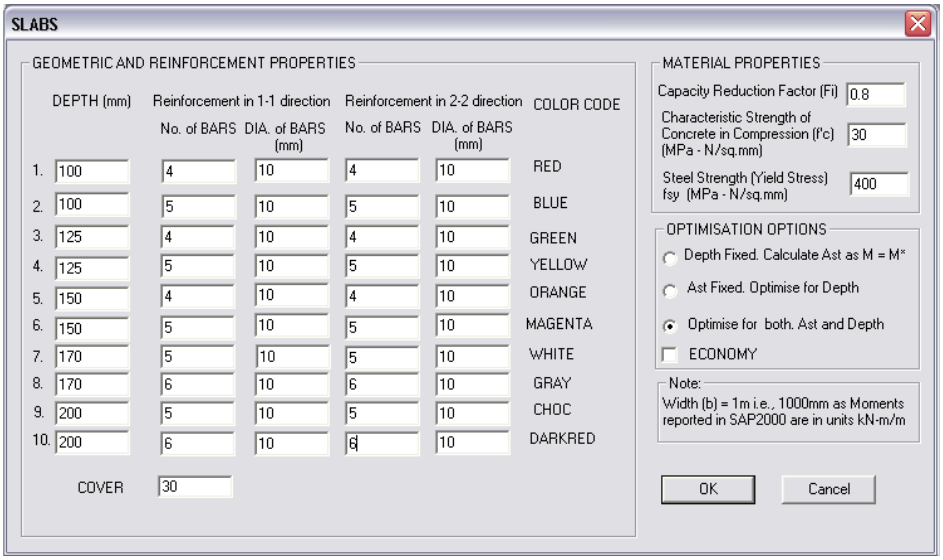

Fig. 7.26. Design Data for Technique 3

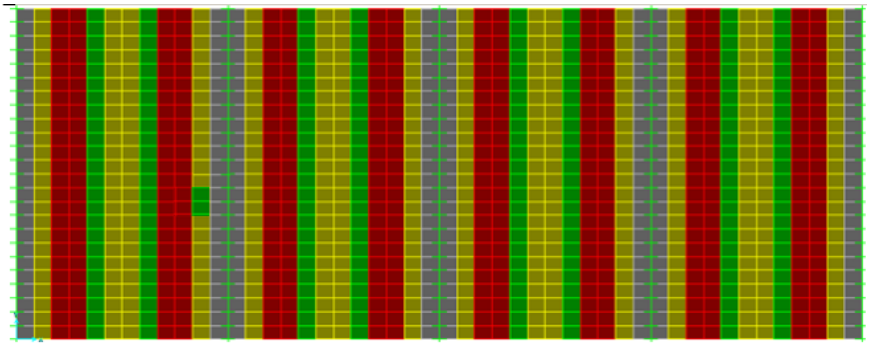

(a) 1st iteration

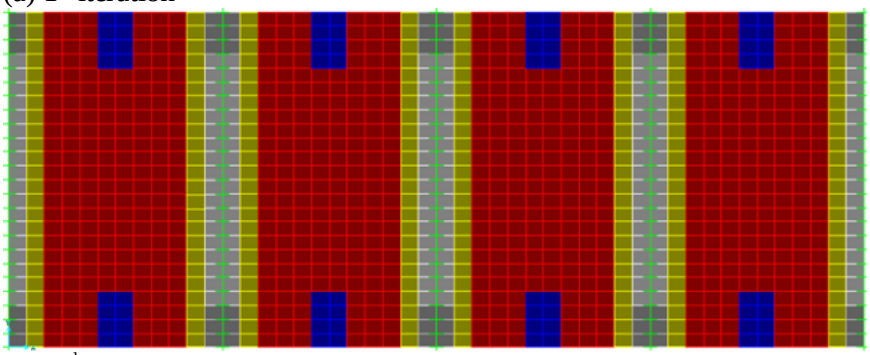

(b) 2nd iteration

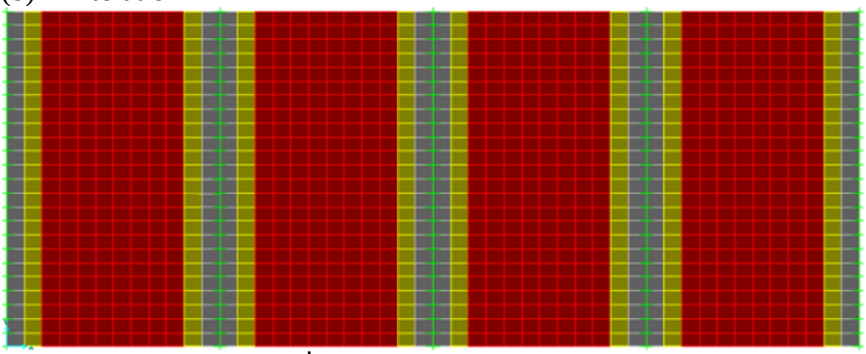

(c) 3rd iteration onwards

Fig. 7.27. Technique 3 Design Solutions for Continuous One-Way Slab

Table 7.8. Design Optimisation Results using Technique 3 for Continuous One-Way Slab

Sr. No.	Iteration No.	Concrete Weight (TONNE)	% Saving in Concrete Weight	Weight of Steel in X direction (TONNE)	% Saving in Weight for Steel (X direction)	Weight of Steel in Y direction (TONNE)	% Saving in Weight for Steel (Y direction)	TOTAL STEEL WEIGHT (TONNE)	% Saving in Total Steel Weight	Total Cost of Concrete (AU $)	Total Cost of Steel (AU $)	Max Deflection (mm)	Permissible Deflection (Span/250) mm	SATISFIES MOMENT CONDITION
1	Initial Model	51.465	-	0.605	-	0.54	-	1.15	-	3216.59	1265.00	1.20 x 3 = 3.60	18mm	YES
2	1	37.589	26.96 %	0.365	39.67 %	0.313	42.04 %	0.678	41.04 %	2349.374	401.883 (X) + 344.471 (Y) = 746.354	1.90 x 3 = 5.70	18mm	YES
3	2	35.067	31.86 %	0.346	42.81 %	0.313	42.04 %	0.659	42.70 %	2191.698	381.550 (X) + 344.471 (Y) = 726.021	2.3 x 3 = 6.9	18mm	YES
4	3	35.067	31.86 %	0.352	41.82 %	0.313	42.04 %	0.665	42.17 %	2191.698	387.530 (X) + 344.471 (Y) = 732.001	2.3 x 3 = 6.9	18mm	YES

The data for Technique 3 above is chosen based on observations of Technique 1 and Technique 2 employed for the same model above. The load in each case is the same. A depth range from 100 mm – 200 mm is specified with varying quantities of steel. The steel diameter is also kept the same for each section and 10 mm diameter bars are chosen. The number of 10 mm diameter bars per meter width of the slab is varied for each section. It is observed that the solution settles from the 3rd iteration onwards and does not improve thereafter. A section of 170 mm depth with 6-Y10 bars (Grey color) is seen over the supports. Next to the gray bands, yellow bands on either side are observed. These represent 125 mm deep sections with 5-Y10 bars. The central portions of the slab require a 100 mm deep section with 4-Y10 bars (Red color). Compared to the initial model a *31.86 %* saving in concrete weight is observed. It is to be noted that benefits observed using Technique 3 are higher in terms of concrete weight savings when compared with Technique 2 employed above. Using Technique 2, when 4-Y16 bars per meter width were specified, a saving in concrete weight of 21.16 % was observed, whereas when 5-Y16 bars per meter width were specified, the saving in concrete weight attained was 26.47 %. In comparison, Technique 3 demonstrates a concrete weight saving of 31.86 %. Additionally, a weight saving of 42.70 % (2nd iteration) in steel quantity compared to the design obtained by Technique 1 is obtained. Though the solution settles from the 3rd iteration onwards, the concrete weight savings achieved by both the 2nd and the 3rd iterations are the same, whereas the weight saving in steel is slightly more for the 2nd iteration compared to the 3rd iteration. The *total material cost* of the design using *Technique 1* is AU $ 3216.59 (cost of concrete required) + AU $ 1265.00 (cost of steel required) = *AU $ 4481.59*. This is shown in the first row of Table 7.8 above. Compared to this design, the *total material cost* of the *optimal solution* (in this case Iteration 2) using *Technique 3* is AU $ 2191.698 + AU $ 726.021 = *AU $ 2917.72*. The optimal solution therefore shows a total material cost saving of *AU $ 1563.871*. In the example above, using *Technique 2* (4-Y10 bars), the *optimal solution* showed a *total material cost saving* of *AU $ 693.77*. Technique 3 thus demonstrates an even higher cost saving compared to Technique 2. This example thus presents the advantage of using Technique 3 over the other two techniques.

7.7 FLAT SLABS

So far, simple examples like a single span slab fixed at both ends and a one-way continuous slab fixed at its supports have been studied. The work has also touched upon the problems associated at the column supports in flat slabs in Section 6.3.1 of Chapter 6. Before proceeding with designing slabs in real buildings it is important to resolve the slab-to-column connection issues in order to obtain accurate and reasonable designs for the region near supports. Therefore systematic 'Numerical Studies' are carried out in the next section and a new modelling and design approach for flat slabs is presented. The proposed approach is then tested on a few examples before applying it to real case studies. The need for integrating element level ESO optimisation together with Group ESO optimisation in order to achieve converged solutions using Technique 2 for flat slabs is presented in the next section.

7.7.1 Need for Integrating Element Level ESO Optimisation and Group ESO Optimisation

7.7.1.1 A Typical Flat Slab Model

This example illustrates the results obtained using Technique 2 for a flat slab modeled without any drop panels in the initial model and subject to optimisation on an element level. The end boundary conditions are free and the columns are modeled as 3D solid objects. Plate Constraints are employed at the nodes where the column objects frame into the plate bending elements.

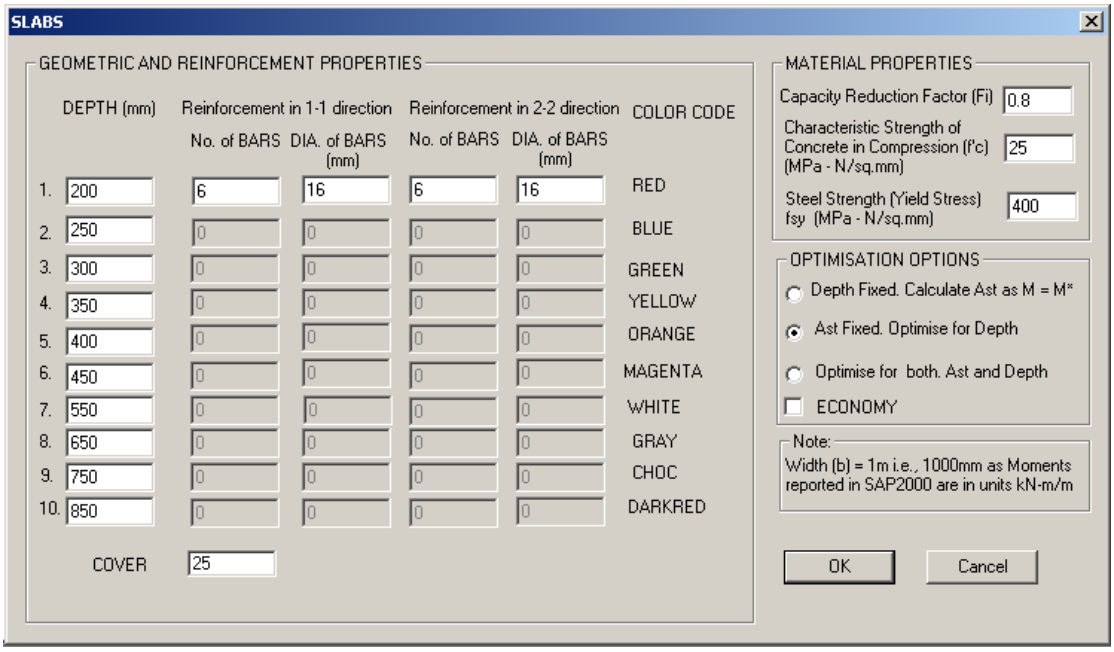

Fig. 7.28. Design Data for Technique 2

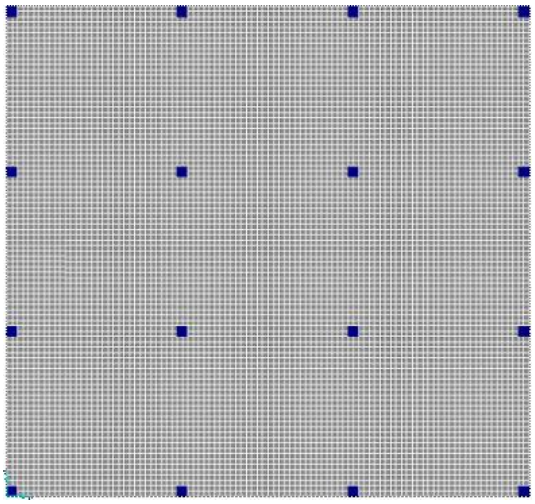

Fig. 7.29. Initial Model of Flat Slab (6.5 m x 6 m)

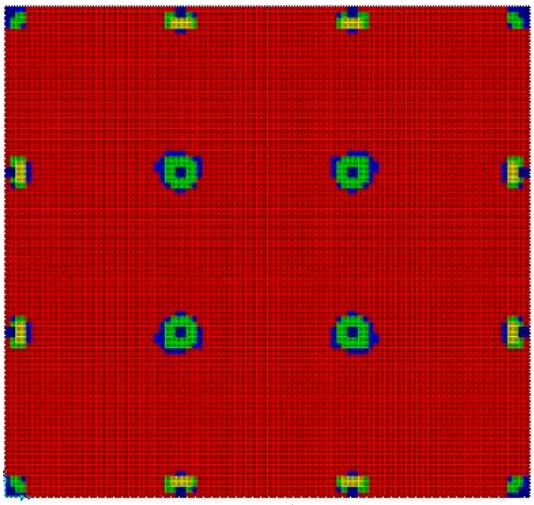

Fig. 7.30 (a) 1st Iteration

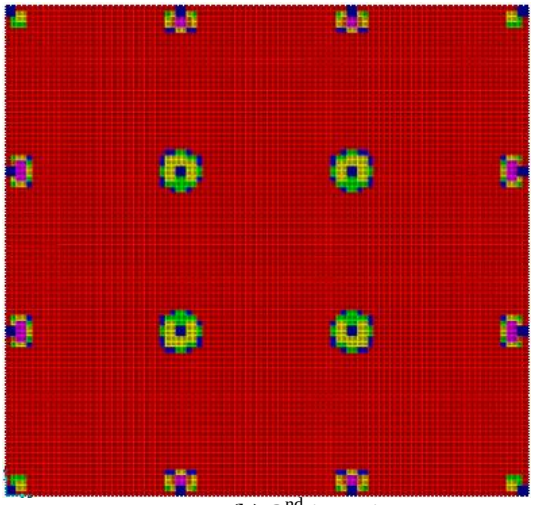

(b) 2nd iteration

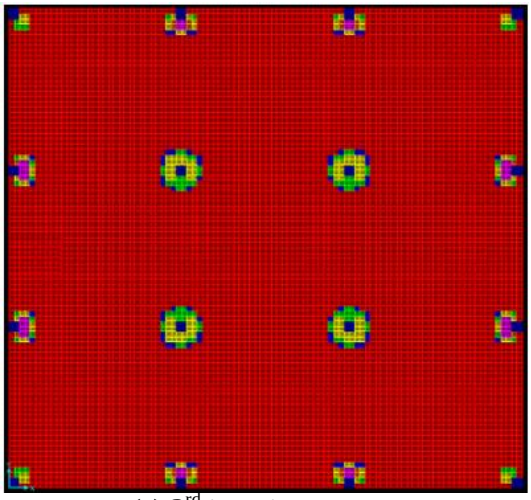

(c) 3rd iteration

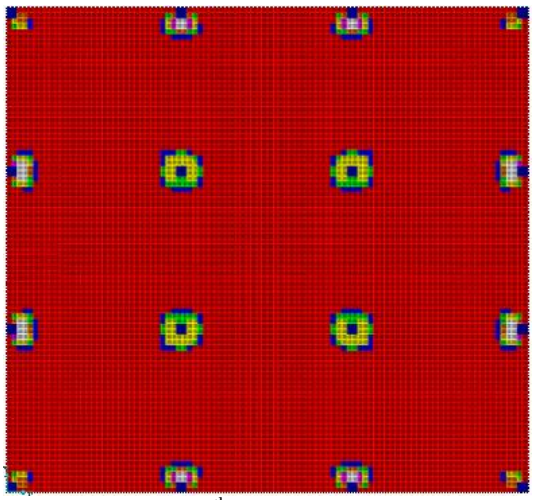

(d) 4th iteration

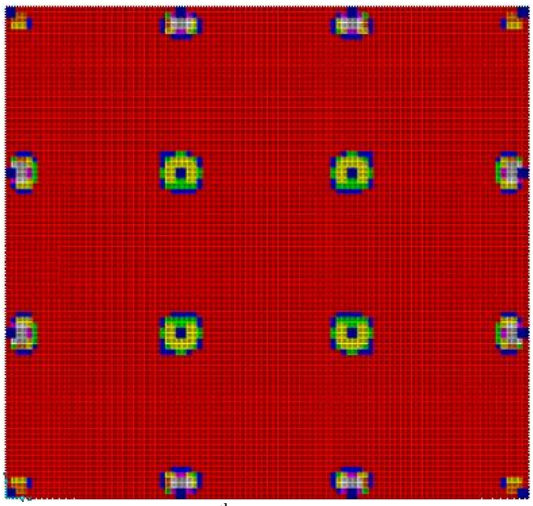

(e) 5th iteration

Fig. 7.30 (a-e).

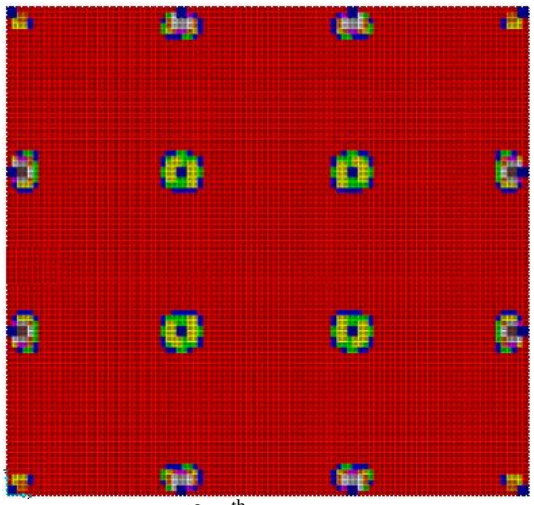

(f) 6th iteration

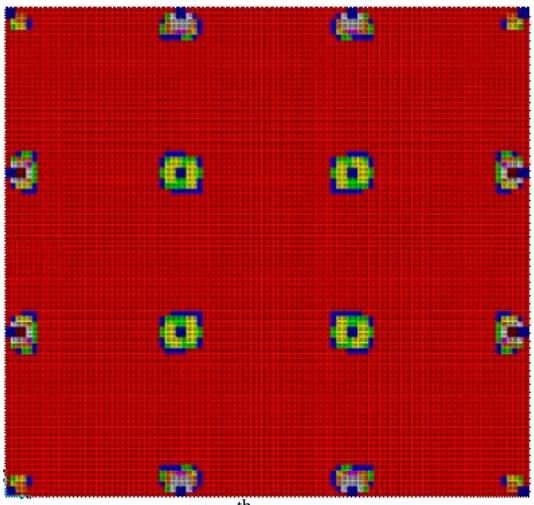

(g) 7th iteration

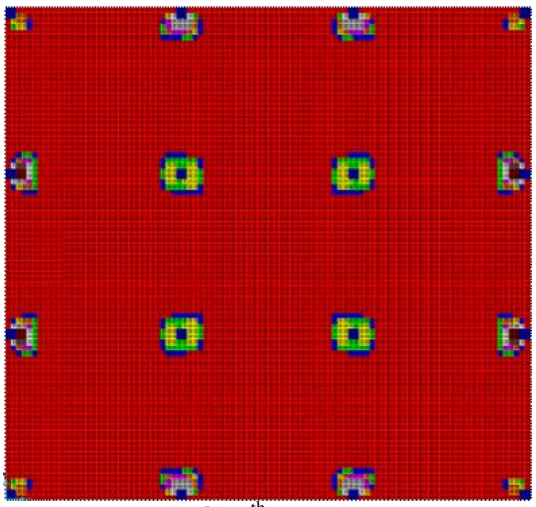

(h) 8th iteration

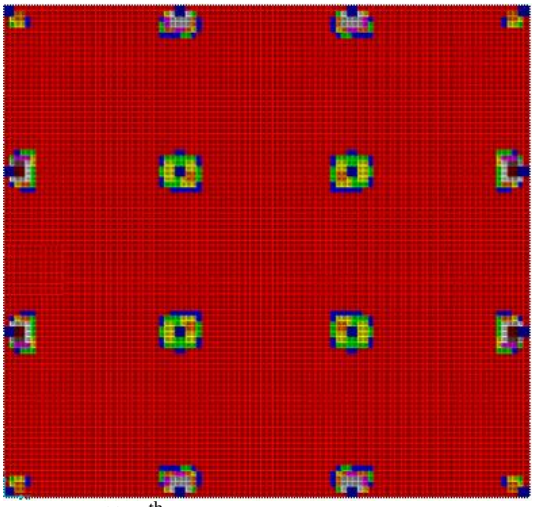

(i) 9th iteration

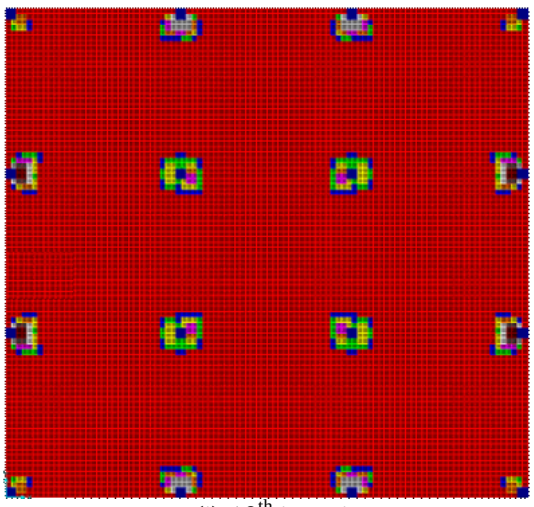

(j) 10th iteration

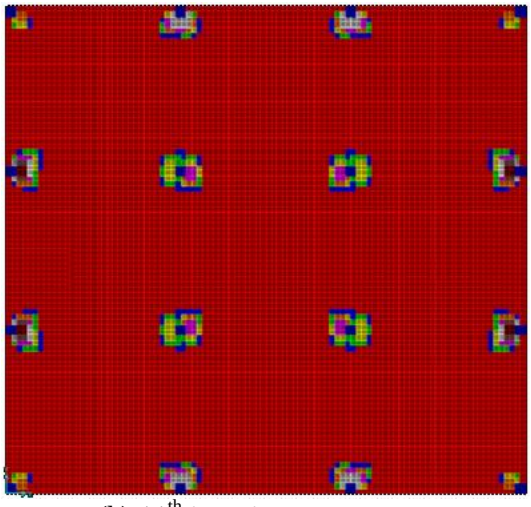

(k) 11th iteration

Fig. 7.30 (f-k).

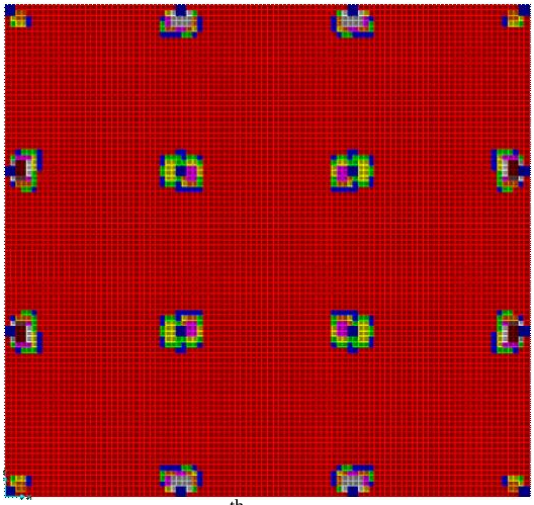

(l) 12th iteration

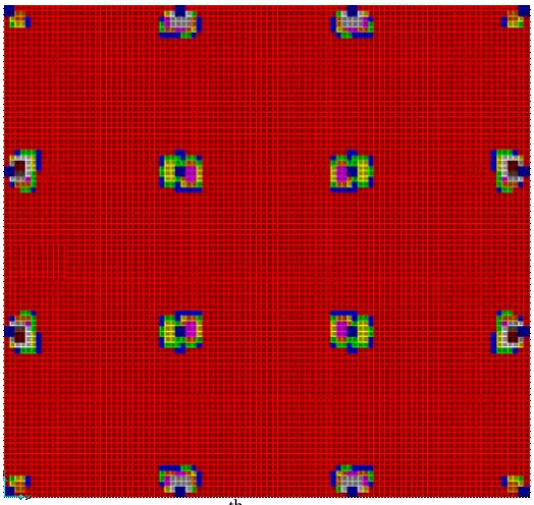

(m) 13th iteration

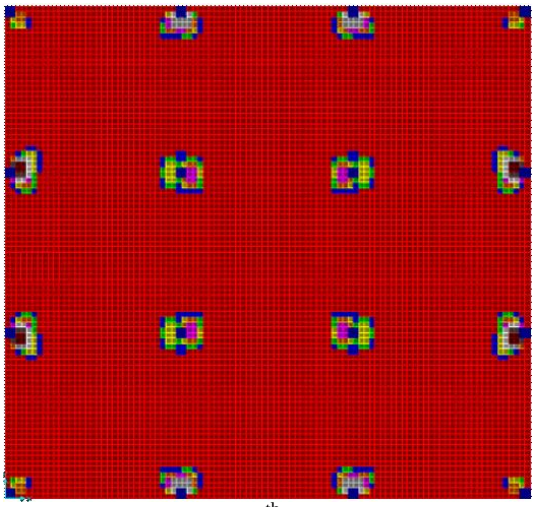

(n) 14th iteration

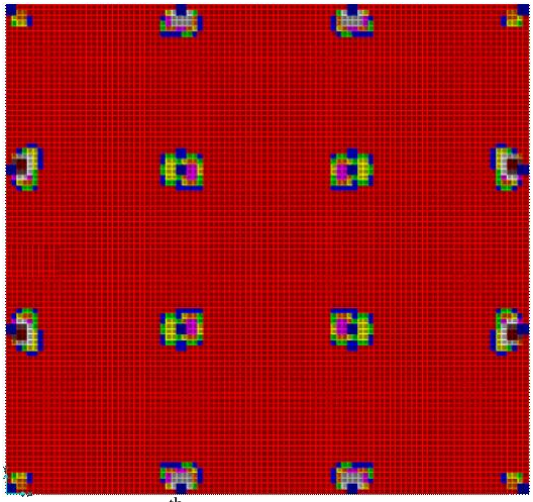

(o) 15th iteration

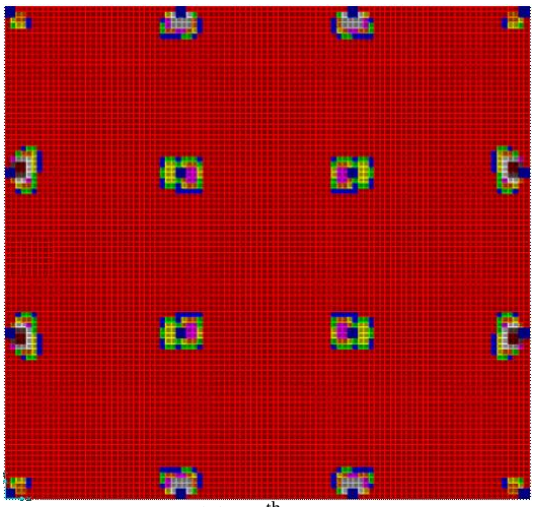

(p) 16th iteration

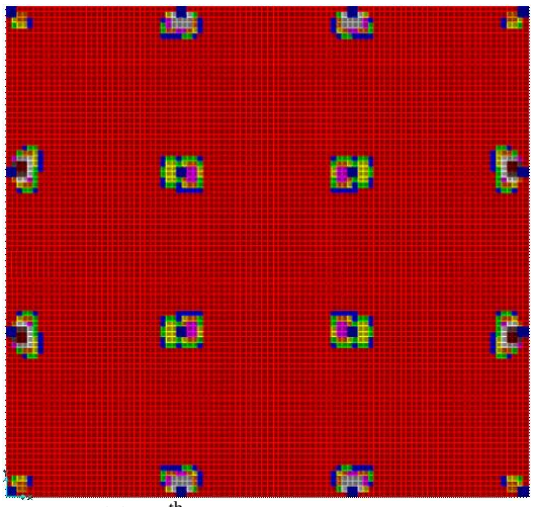

(q) 17th iteration

Fig. 7.30. Element Level Design Solutions for Flat Slab using Technique 2

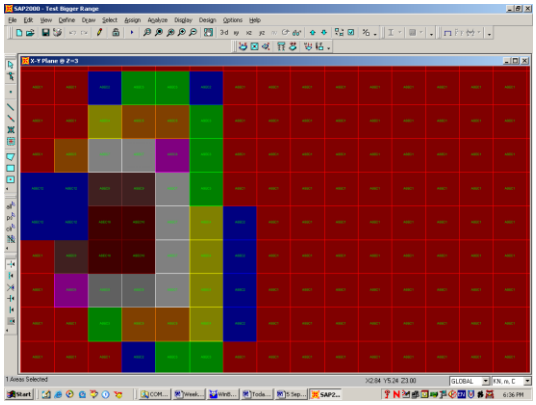

(a) Left side edge column

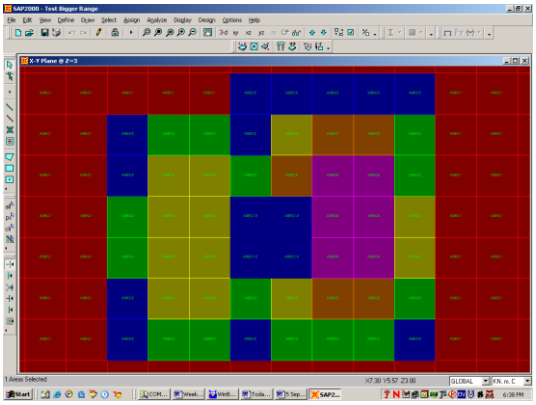

(b) Central Column

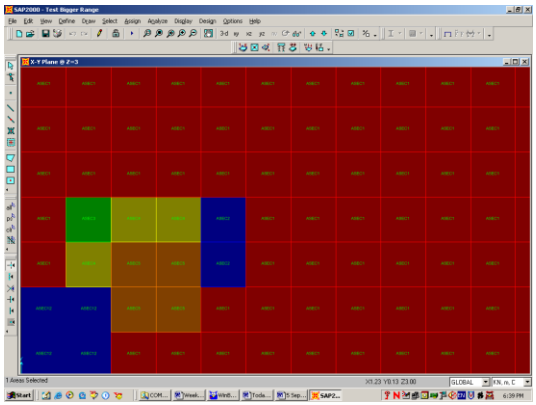

(c) Corner Column

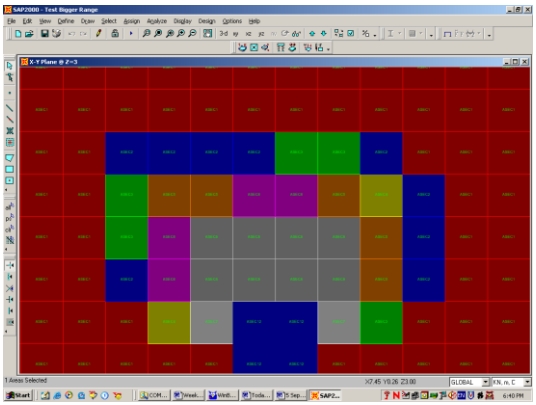

(d) Bottom Edge Column

Fig. 7.31. Enlarged Views Showing Element level Design Solution near Column Supports Using Technique 2

The results show that the constraint ($\phi \times M_u > M^*$) is satisfied in all elements of the slab from the 17th iteration onwards. Thicker elements are needed in regions around the central columns, edge columns and corner columns. However, a clear drop panel arrangement with uniform thickness for elements lying around each column is not observed. Though this example demonstrates the need for thicker regions around the column supports as expected, it does not clearly indicate the exact depth required in these regions. Excessively high depths of 850 mm (Dark Red) for some elements near the edge columns suggest that the problems due to stress singularity are clearly present and as these elements get thicker, they in turn attract more moment and this result in a further increase in thickness. Depending on the quantity of steel specified and the material strengths specified (concrete strength and yield strength of steel), the solution either converges or it does not. For example, when less steel is specified (such as 5Y16 bars in both directions), the solution does not converge and does not satisfy the constraint in any of the iterations. Furthermore, it requires a depth bigger than 850 mm, which is clearly excessive and warrants investigation. Numerous models have been prepared and

tests carried out by the author to find out the exact cause of the problem. Some of the methods used to solve this problem included changing the boundary conditions of the slab from free to fixed, using perimeter beams at the edges, with and without using the plate constraint atop the columns, using the plate constraint atop only the central columns, using symmetrical models with boundary conditions both free and fixed, and increasing the size of the column (i.e. using a coarser mesh). In several of the cases, the depths around either the central columns or the edge columns reaches to excessive heights and the optimisation stops due to convergence problems. It is to be remembered that the selection of a section for a particular element depends on many variables that are present in Equation 5.10, such as the quantity of steel, the concrete and steel strengths, and the effective depth (which is based on cover specified by the user). Altering any of these variables could lead to converged solutions, though this may not necessarily be correct or the true optimum. In the case of this example, the solution has converged as the quantity of steel (i.e. moment capacity) is increased from 5Y16 bars to 6Y16 bars both ways. Similarly, increasing both the steel and concrete strengths could have resulted in converged solutions. Both ways however, this should not have been needed in the first place and neither is the result a true picture of the design required in that region. Now, the objective here was to seek a uniform depth pattern for the elements lying around the column supports in the converged solution (for the specified material data), though this converged result may not really be the correct or optimal solution. It is seen that this is not possible by '*element-wise optimisation*' using a linear elastic analysis with 'Technique 2', as such an analysis results in high stress values at the column supports which are not representative of the true physical structural behaviour. Technique 2 was employed to obtain uniform depth patterns around the column supports. Numerical tests performed by the author reveal that the use of the plate constraint helps in obtaining values of moments close to expected values (calculated by 'Simplified Method of Design') and is therefore employed in all the flat slab models in this chapter. It is also anticipated that instead of dealing on an element level, if the elements lying near the column supports are grouped into a panel, it should result in stable thicknesses and converged solutions. This is demonstrated in the section 'Numerical Studies'.

7.7.1.2 Effect of Column Size (i.e. Mesh size) and Steel Quantity on Results using Technique 2.

Span: 6m x 6m; Column: 400 x 400 mm; Elements: 8464 (92 x 92 elements);

Support Condition: Fixed on all four sides (and at the bottom of Columns)

A. SMALLER COLUMN (FINE MESH)

4-Y16 Bars **5-Y16 Bars**

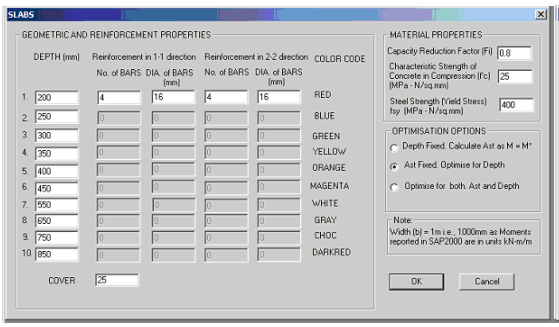

Fig. 7.32. Design Data for Technique 2 with 4-Y16 bars

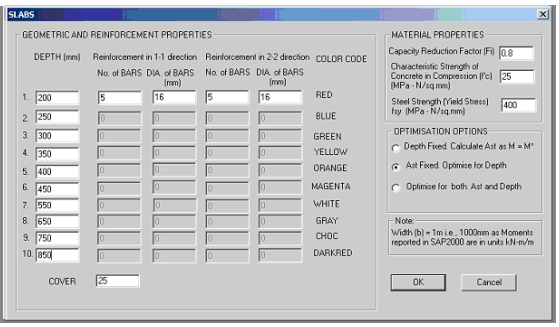

Fig. 7.33. Design Data for Technique 2 with 5-Y16 bars

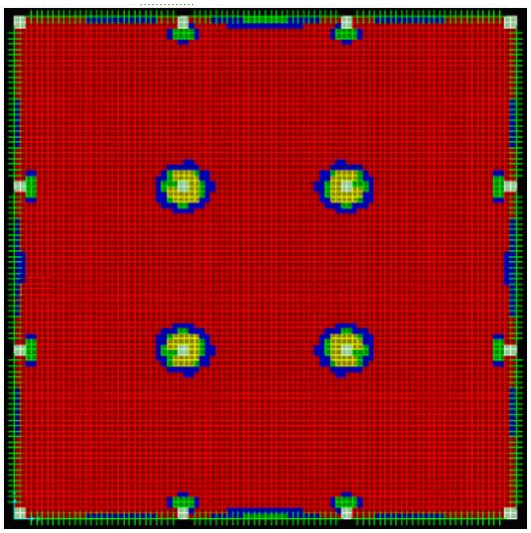

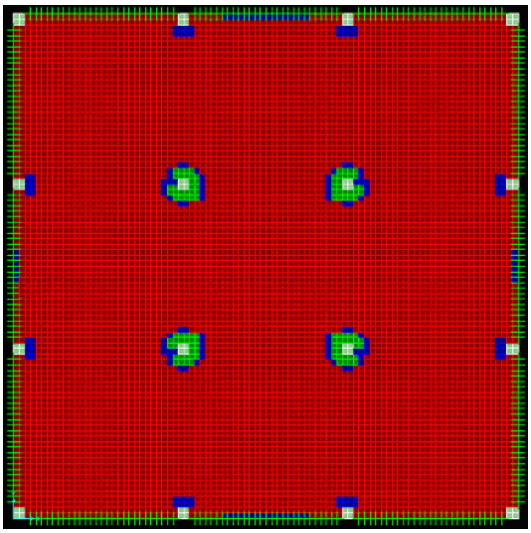

(a) 1st iteration

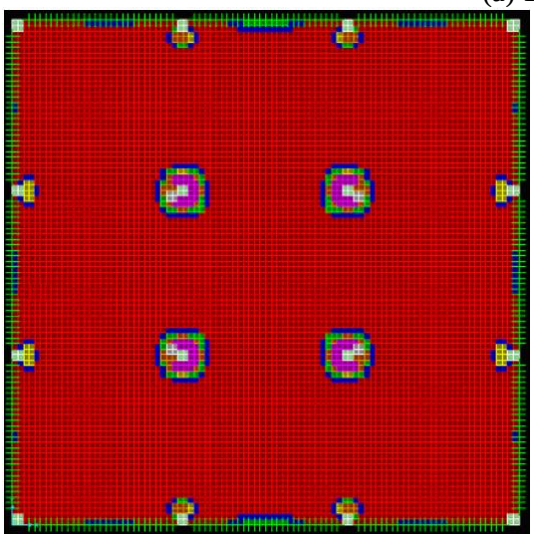

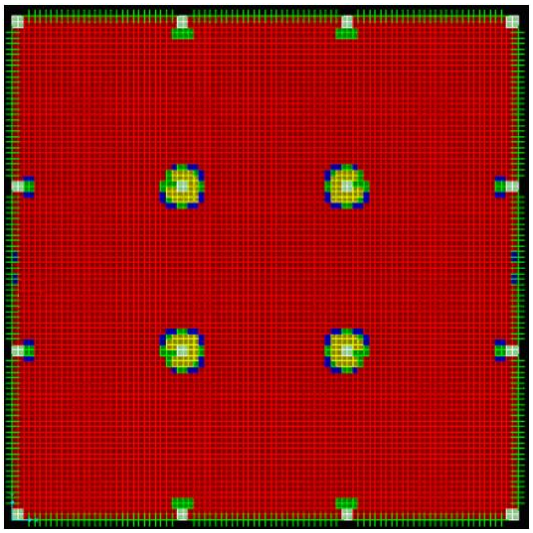

(b) 2nd iteration

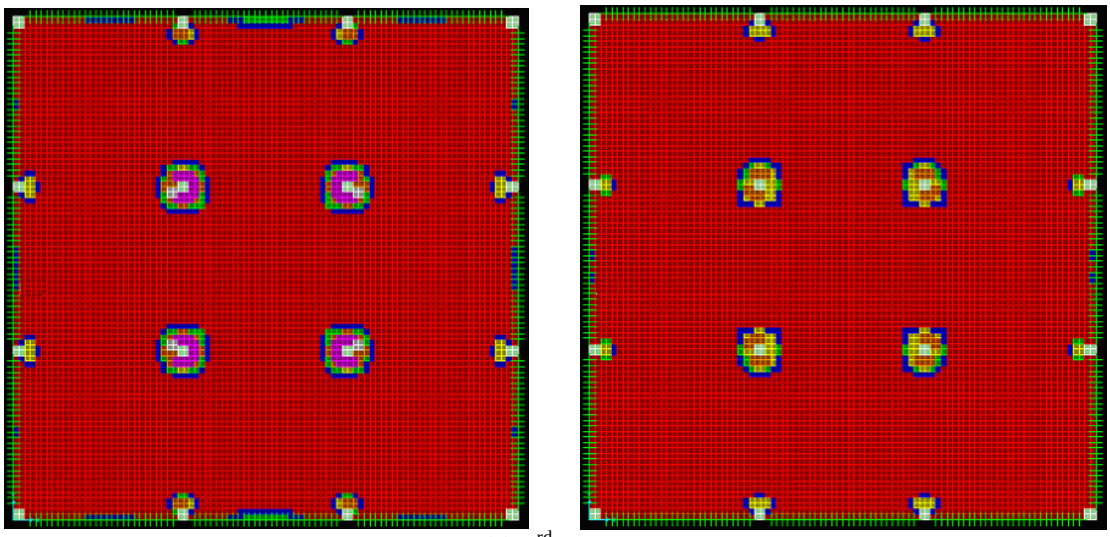

(c) 3rd iteration

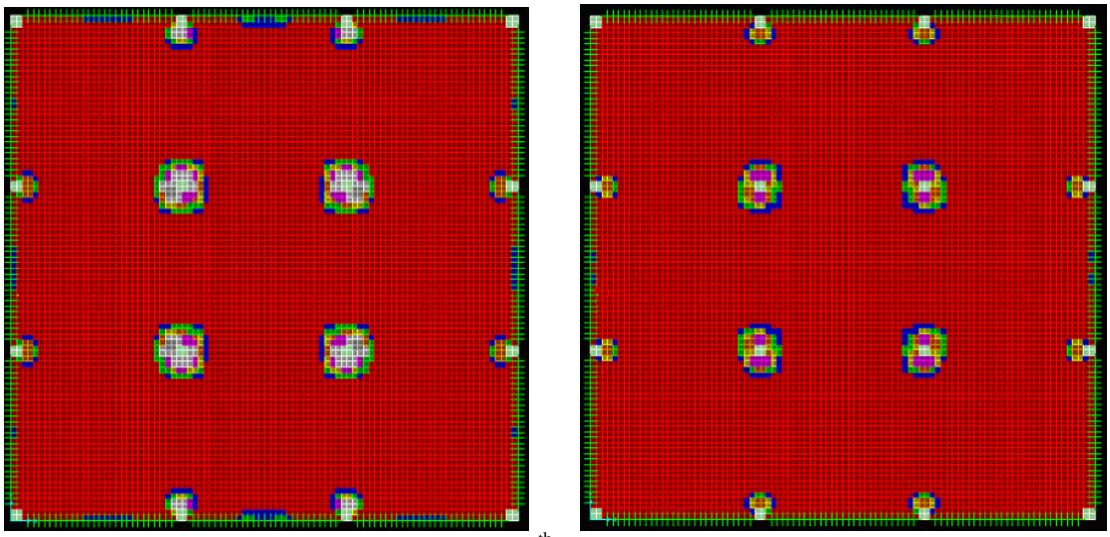

(d) 4th iteration

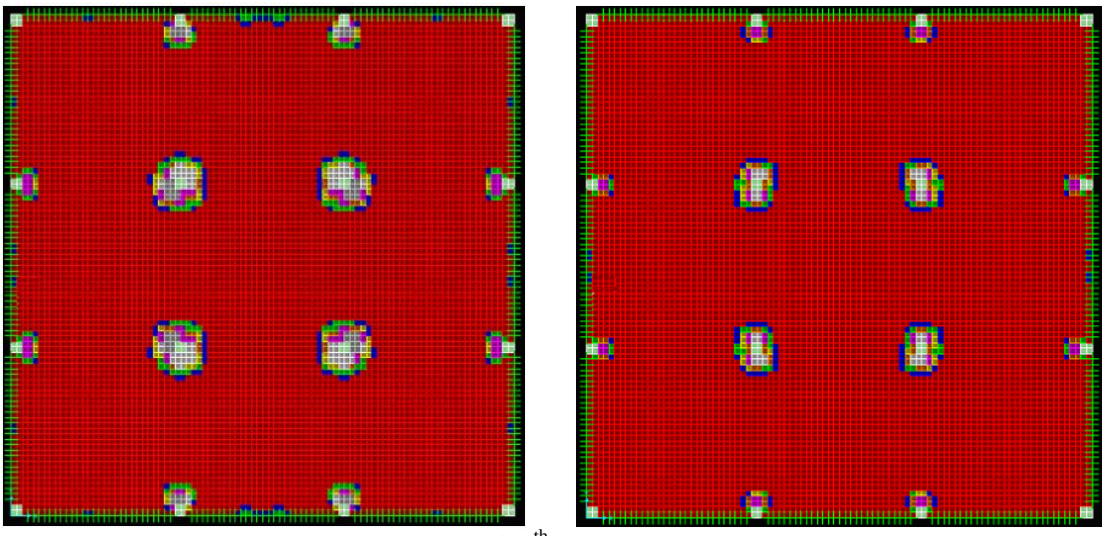

(e) 5th iteration

Fig. 7.34 (c-e).

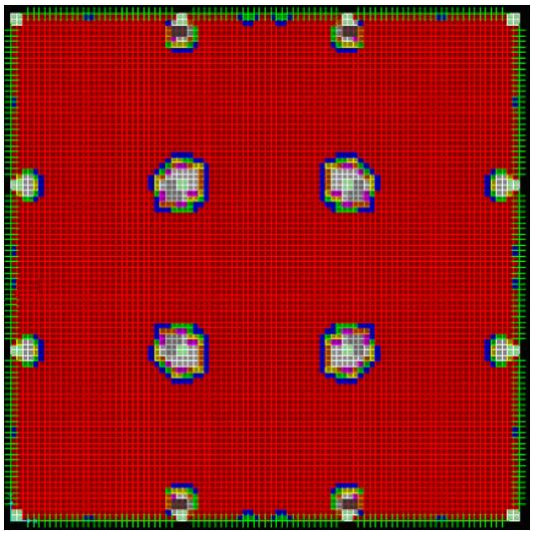
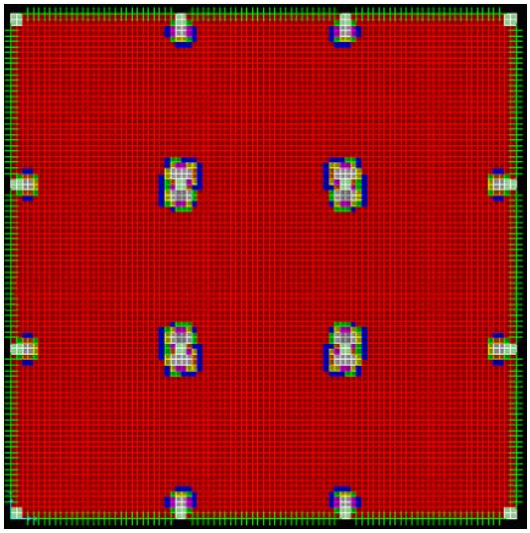

(f) 6th iteration

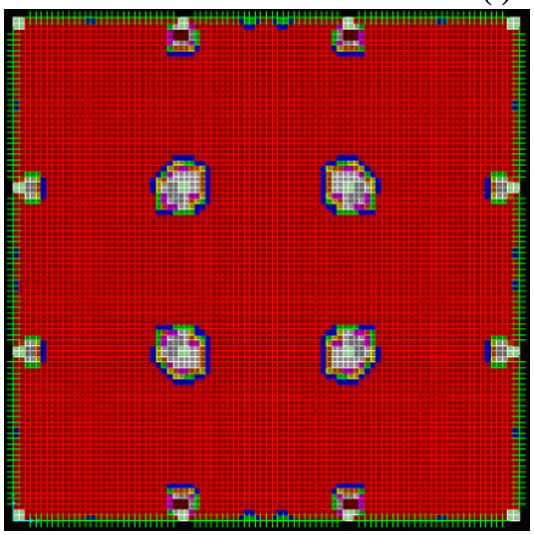
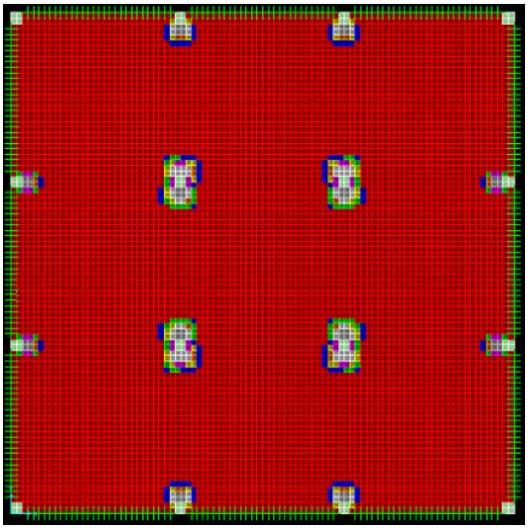

(g) 7th iteration

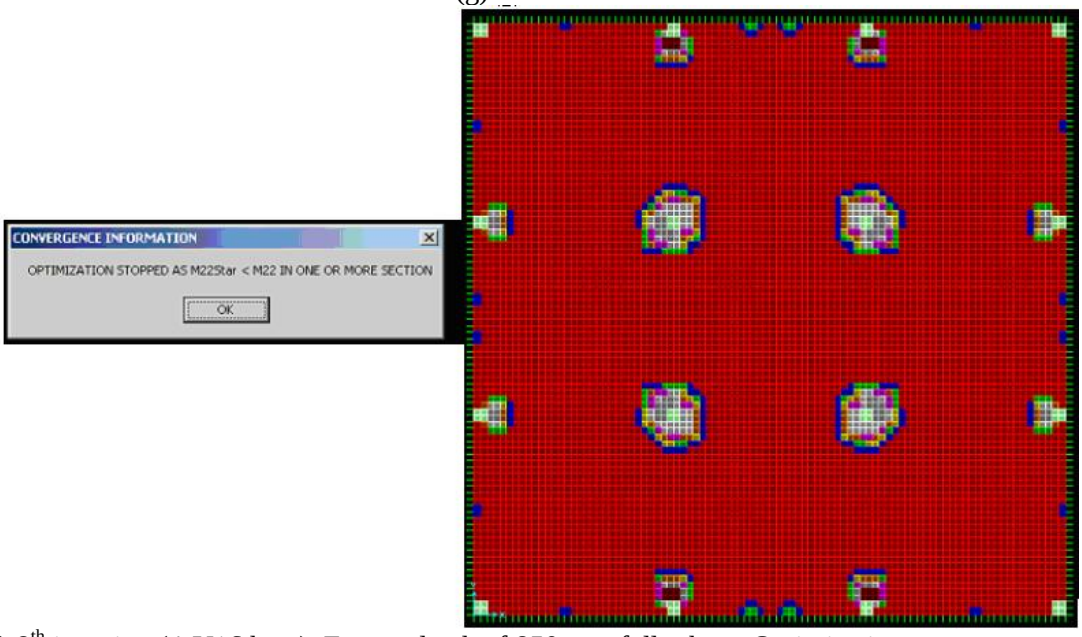

(h) 8th iteration (4-Y16 bars). Even a depth of 850 mm falls short. Optimisation stops.

Fig. 7.34 (f-h).

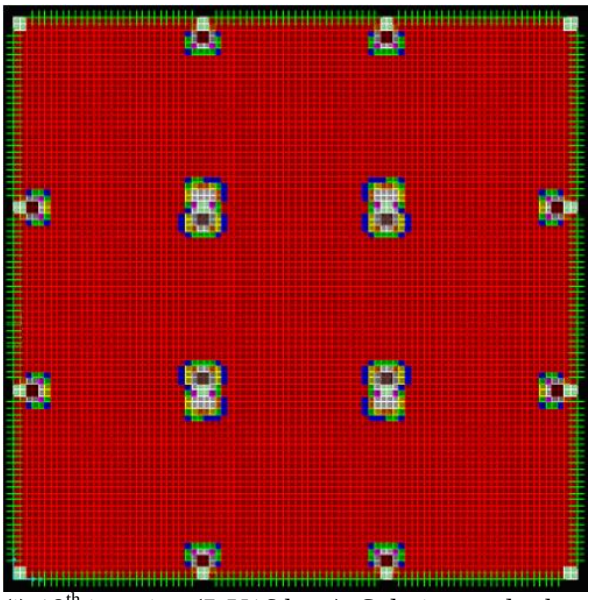

(i) 19th iteration (5-Y16 bars). Solution settles but still very high depths are seen around columns.

Fig. 7.34. Comparison between Element Level Design Solutions for a Finely Meshed Flat Slab Using Technique 2 with Different Quantities of Steel Specified

It is seen from the above results that the solution converges when more steel is used (5Y16 bars) as against when 4Y16 bars are used. However, even though the solution converges, unreasonably high depths are seen around the edge columns and central columns. It is therefore important to have a correct approach to model flat slabs and flat plates in SAP2000 to take care of the issues arising due to stress singularity.

In the next example, the effect of column size (or mesh size) on the results is investigated. The sizes of columns is increased from 400 x 400 mm to 600 x 600 mm, i.e. the mesh is made coarse from dimensions of 0.2 x 0.2 m to 0.3 x 0.3 m.

B. BIGGER COLUMN SIZE (COARSE MESH)

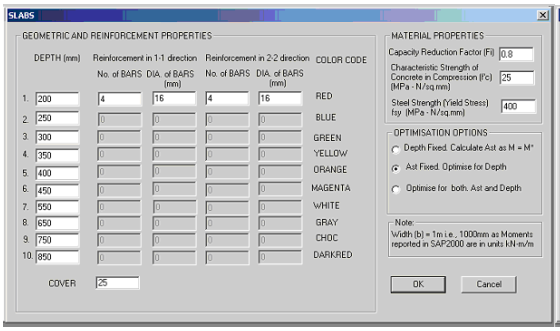

Fig. 7.35. Design Data for Technique 2 with 4-Y16 bars

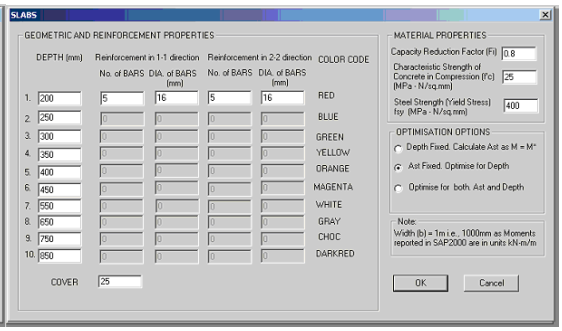

Fig. 7.36. Design Data for Technique 2 with 5-Y16 bars

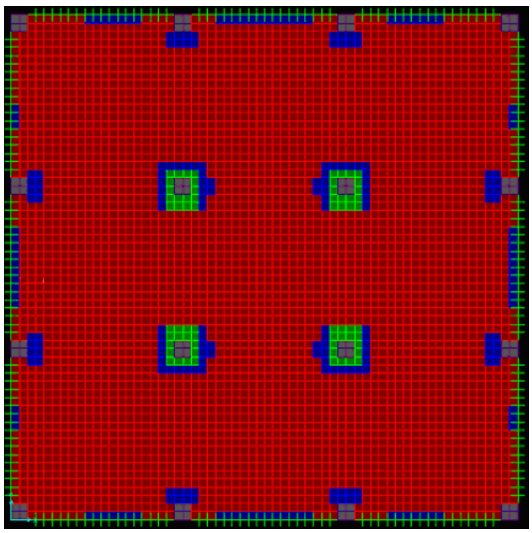

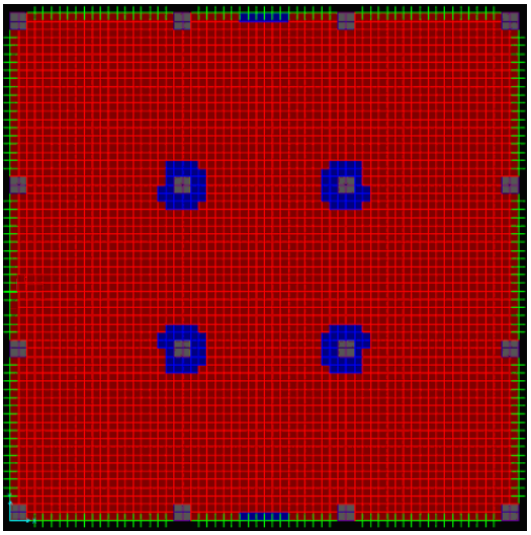

(a) 1st iteration

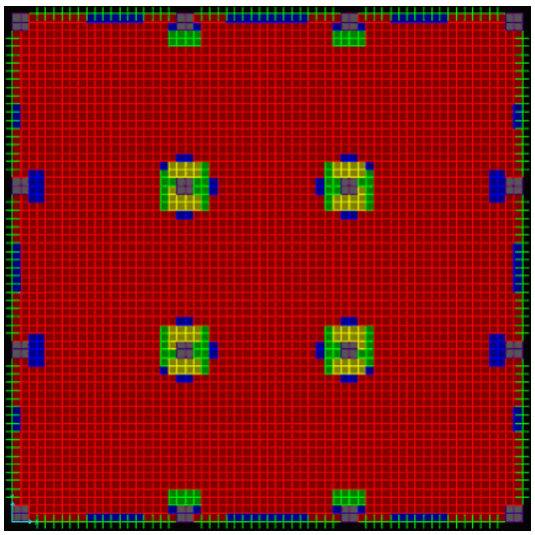

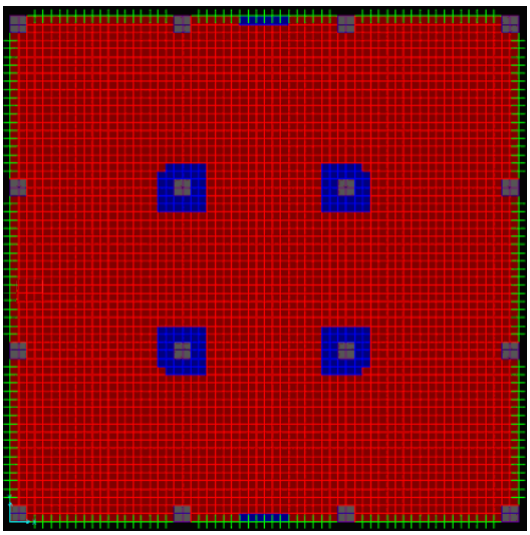

(b) 2nd iteration

Fig. 7.37 (a-b).

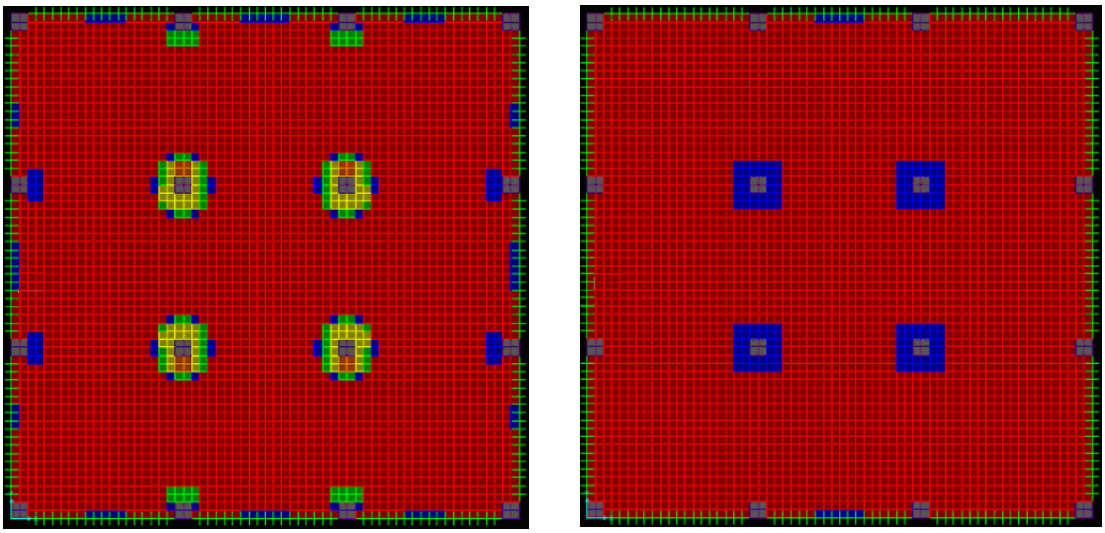

3rd iteration

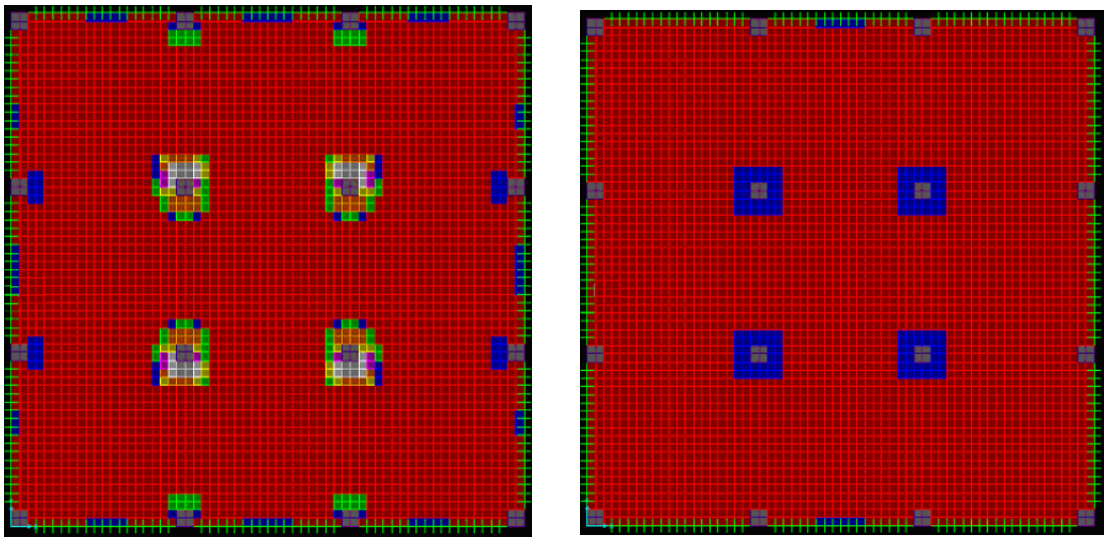

11th iteration

Fig. 7.37. Comparison between Element Level Design Solutions for a Coarsely Meshed Flat Slab Using Technique 2 with Different Quantities of Steel Specified

It is observed from the above results, that when 4Y16 bars are used, the solution settles and satisfies the constraint from the 11th iteration onwards. Due to 'different effective depths', which is explained later in Section 7.7.2.1, the edge columns settle on depths of 250 mm (Blue) and 300 mm (Green). The central columns do not still show a clear pattern and the maximum depth seen is 650 mm (Grey) with many of the elements around the central columns ranging from 250 mm (Blue) to 650 mm (Grey), i.e. Green, Yellow, Orange, Magenta and White. It is still unclear what actual depth is required around the central columns when 4Y16 bars are used.

In the case when 5Y16 bars are used, the solution settles and satisfies the constraint from the 3rd iteration onwards. A depth of 250 mm (Blue) is seen to be required for the central columns

whereas the edge columns do not require a drop panel when 5Y16 bars are used. Compared to 'hand calculations' using the Simplified Method of Design (Appendix A), this arrangement does not look satisfactory. A depth of 300 – 400 mm is to be reasonably expected around the central columns for this span and loading irrespective of the mesh size used. Though criteria for punching shear is not implemented yet, it is seen when finer mesh is used that depths bigger than 250 mm are observed in the optimal solutions around the central columns which suggests the possibility of higher depths even when 5Y16 bars are used.

It is thus seen from these examples that different results are obtained around the column supports for different quantity of steel specified in Technique 2 and for different meshes. Generally for different meshes this should not be the case. Irrespective of the mesh size used, clear and distinct thickness patterns comparable to hand calculations need to be observed around column supports. Only then can these techniques be applied to design real world flat slab situations. These examples thus suggest the need for a correct modeling approach to model flat slabs in SAP2000.

7.7.1.3 Proposed Approach to Modelling Flat Slabs in SAP2000

The results in the previous sections clearly show that the elements lying around the column supports play the major role in obtaining converged solutions (besides the influence of other variables such as steel quantity and concrete and steel strengths). In order to obtain a uniform and distinct thickness pattern around the column supports, it is proposed to group the elements lying near the column supports into one group. The maximum of the smoothed nodal moment values for all the elements lying within each group will then be used to decide the section to be allotted to the entire panel or group instead of individual elements as was seen. To achieve this, the Group ESO method of structural optimisation is the most attractive and is hence applied to model groups or panels (drop panels) at column supports. The optimisation is thus carried out at two levels simultaneously:

1. At the element level for elements lying in areas of the slab not close to the column supports.
2. At the Group or Panel level for elements lying within each group or panel.

It is hoped that by using such an approach the difficulties encountered in obtaining reasonable and converged designs around the column supports will be resolved. The ESO method of structural optimisation together with Group ESO is therefore implemented in the numerical algorithms to obtain converged and correct optimal designs. Section 7.7.2.4.4 demonstrates why the maximum of the smoothed nodal moment values for the group is chosen as the design moment as against the average of the smoothed nodal moment values for the group.

7.7.2 NUMERICAL STUDIES

7.7.2.1 Symmetrical and Asymmetrical Results: Effect of 'Avg of the two depths' and 'Different depths' on symmetrical results when calculating 'Moment Capacity'.

As mentioned before, when using Technique 2 (Steel Constant, Depth Varying), the final depth allotted to an element is based on the bigger of the two depths required for M_{11} and M_{22} (i.e. bending in the 1-1 or X direction and bending in the 2-2 or Y direction). The steel in the slab for a two-way slab system is placed in both orthogonal directions. This implies that bars in both directions do not occupy the same location (i.e. depth) in space (as is in practice). The following figure is used to visually represent the concept. Thus, if it is assumed that bars in the Y direction are placed over bars in the X direction, then the effective depth of steel is smaller in the Y direction and similarly the effective depth of steel is bigger in the X direction. Therefore, even though, the user specifies the same amount of steel in both directions for the same depth (when using Technique 2), the moment capacities calculated in each direction are usually different. Generally, based on the above assumption, the moment capacity in the Y direction is usually smaller than the moment capacity in the X direction. This can result in asymmetrical results even for a symmetrical model with uniformly distributed loading as the following example demonstrates. In later work therefore, to avoid asymmetry in results, the average of the two effective depths is used when working out the moment capacity using Eq. 5.20. Then, the moment capacities calculated in both directions are equal if the steel specified in both directions is the same. This helps to remove asymmetry from the results.

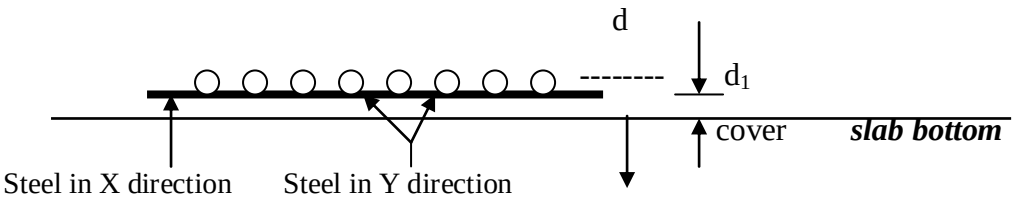

d: Effective depth of steel in Y direction from the extreme top of concrete compression fibre.
d_1: Effective depth of steel in X direction from the extreme top of concrete compression fibre.

Fig. 7.38. Effective Depths

Asymmetrical Results: Initial slab thickness of 200mm

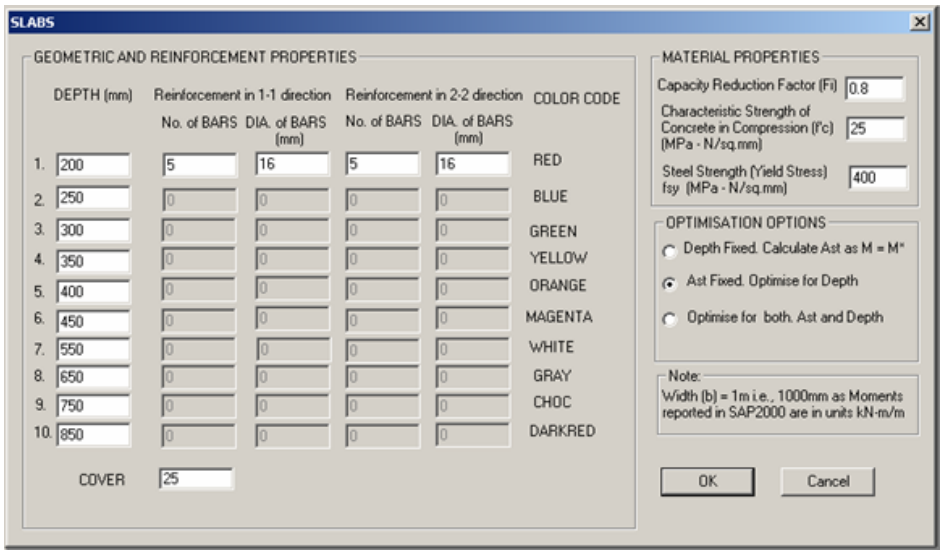

Fig. 7.39. Design Data for Technique 2

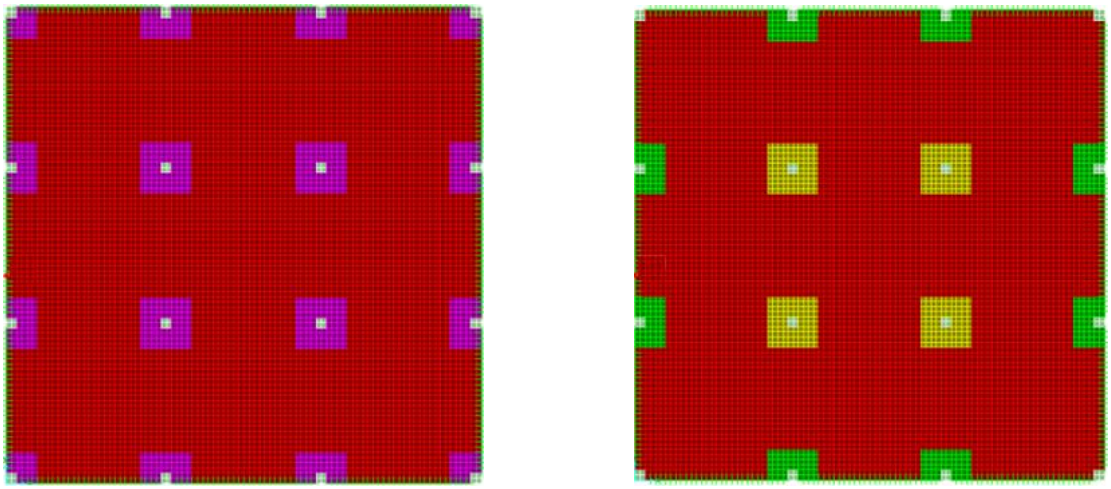

Fig. 7.40. Initial Model
(Drop Panels are grouped as Panels of elements.
Element-wise optimisation for rest of the slab.
Initial slab thickness: 200 mm

(a) 1st iteration

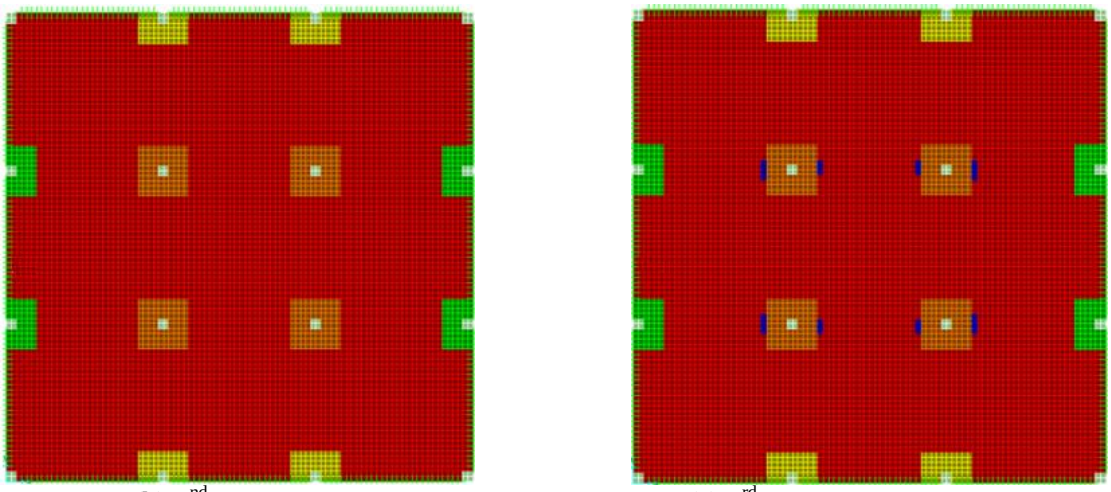

(b) 2nd iteration (c) 3rd iteration

Fig. 7.41 (a-c).

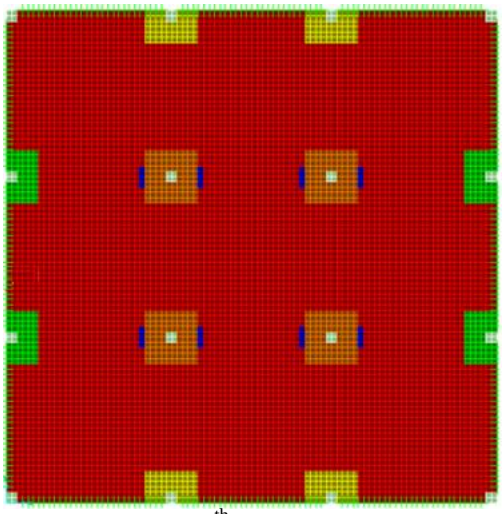

(d) 4th iteration

Fig. 7.41. Technique 2 Design Solutions using Different Effective Depths in both directions

The solution settles and stabilizes from the 4th iteration onwards. All elements (and panels) satisfy the bending moment criterion.

Asymmetrical Results: Initial slab thickness of 250 mm

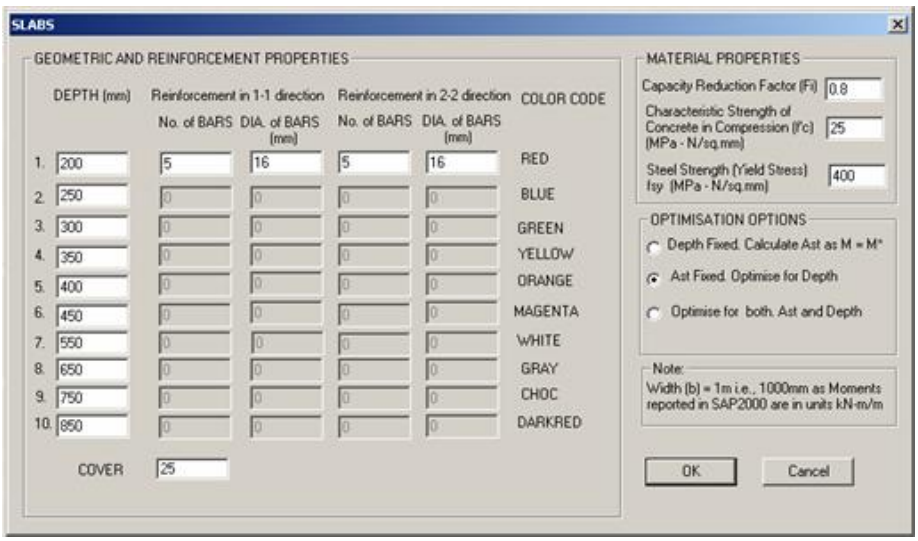

Fig. 7.42. Design Data for Technique 2

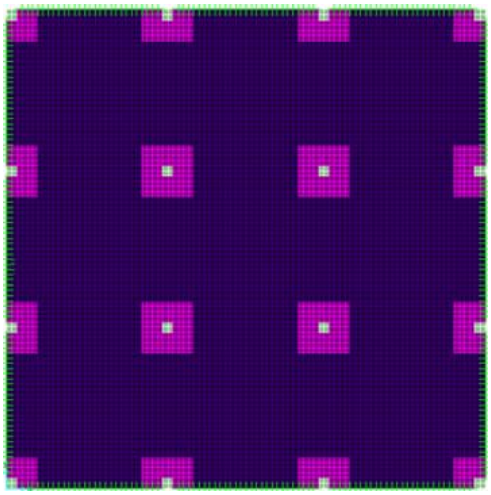

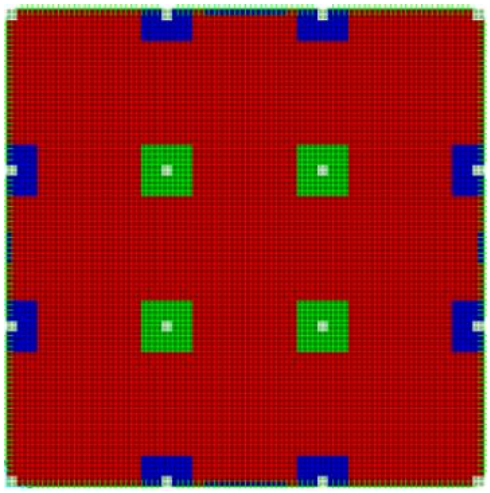

Fig. 7.43. Initial Model (Slab Thickness: 250 mm) (a) 1st iteration

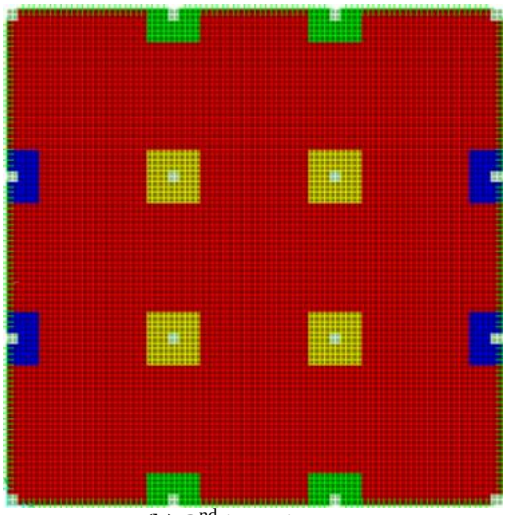

(b) 2nd iteration

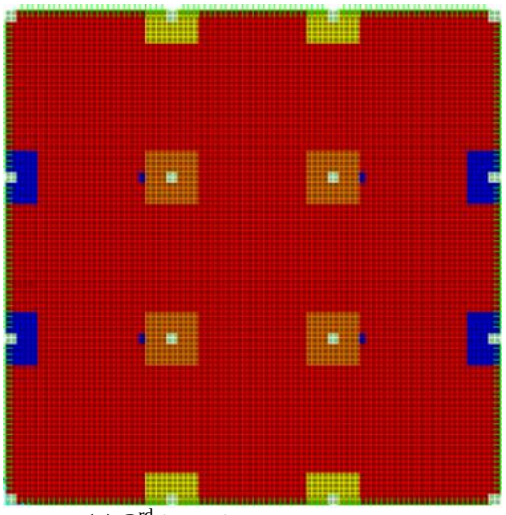

(c) 3rd iteration

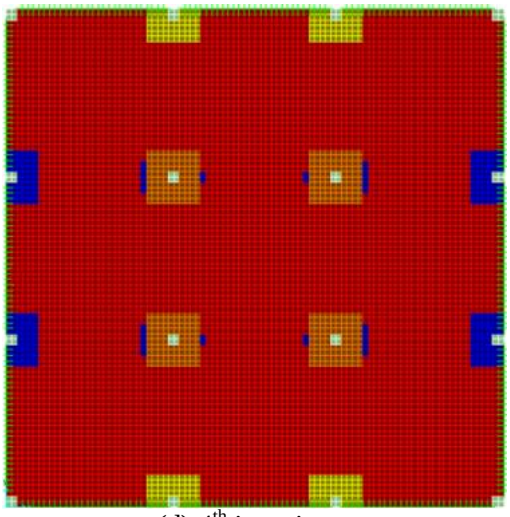

(d) 4th iteration

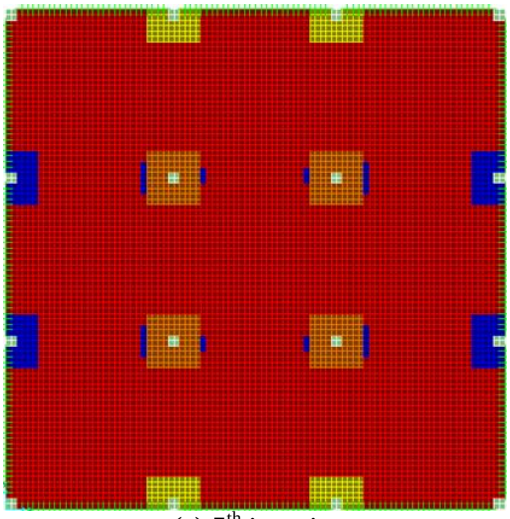

(e) 5th iteration

Fig. 7.44 (a-e).

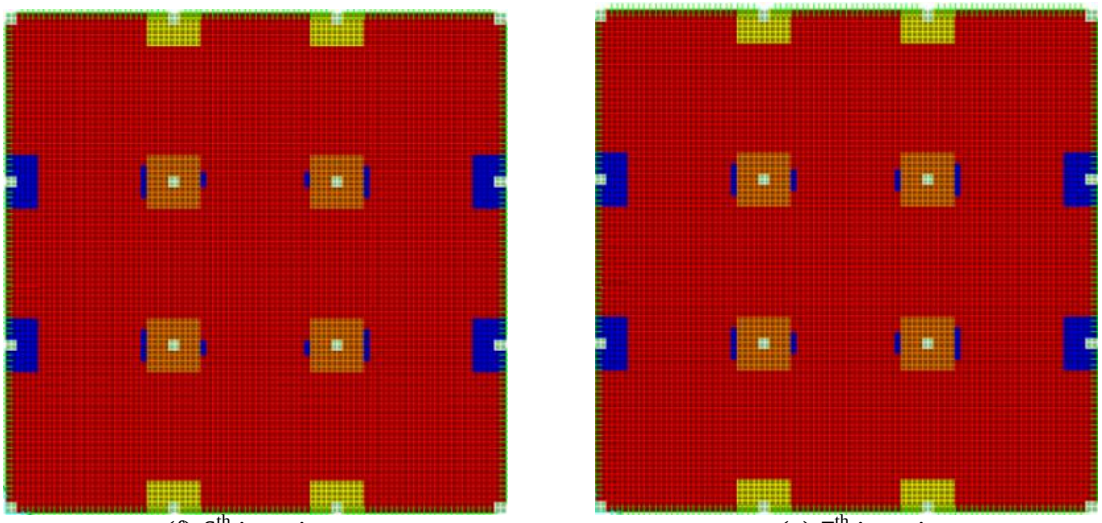

(f) 6th iteration (g) 7th iteration

Fig. 7.44. Technique 2 Design Solutions using Different Effective Depths in Both Directions

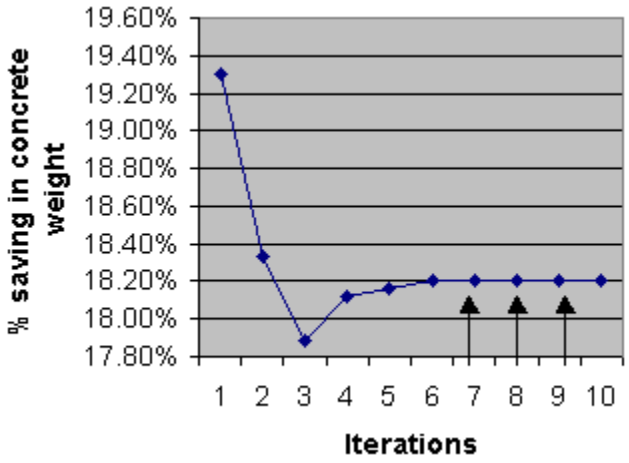

Fig. 7.45. History of Concrete Weight Reduction

1st iteration in the graph shown in Fig. 7.45 above is Initial Model. Black arrows indicate optimisation has settled on one solution and this solution *satisfies* the bending moment criterion (% saving: 19.02 %). The graph is based on the table shown on the next page.

Table 7.9. Technique 2 Design Optimisation Results using Different Effective Depths for Flat Slab

Iteration No.	Concrete Weight (Tonne)	% saving in Concrete Weight	Total Steel Weight (Tonne)	% saving in Total Steel Weight	Total Cost of Concrete (AU $)	Total Cost of Steel (AU $)	Max. Deflection (mm) * 3	Permissible Deflection (mm) (Span/250)	Satisfies Condition
Initial Model	188.79	-	2.67 X 2 = 5.34	-	11799.58	5879.43	2.968 x 3 = 8.904	24	NO
1	152.35	**19.30 %**	2.67 X 2 = 5.34	-	9521.84	5879.43	3.155 x 3 = 9.465	24	NO
2	154.19	**18.33 %**	2.67 X 2 = 5.34	-	9637.17	5879.43	2.686 x 3 = 8.058	24	NO
3	155.040	**17.88 %**	2.67 X 2 = 5.34	-	9690.02	5879.43	2.487 x 3 = 7.461	24	YES
4	154.58	**18.12 %**	2.67 X 2 = 5.34	-	9661.19	5879.43	2.474 X 3 = 7.422	24	YES
5	154.50	**18.16 %**	2.67 X 2 = 5.34	-	9656.39	5879.43	2.474 X 3 = 7.422	24	YES
6	154.425	**18.20 %**	2.67 X 2 = 5.34	-	9651.58	5879.43	2.474 X 3 = 7.422	24	YES
7	154.425	**18.20 %**	2.67 X 2 = 5.34	-	9651.58	5879.43	2.474 X 3 = 7.422	24	YES

Though the span in both directions is symmetrical and the slab is loaded with a UDL, asymmetrical results for left/right end panels compared with top/bottom end panels are observed. The top and bottom panels are seen to settle on 350 mm depths (Yellow color) and the left and right panels are seen to settle on 250 mm depths (Blue color). The central drop panels are seen to settle on 400 mm depth (Orange color). This difference in results for end panels happens because of different moment capacities calculated for the design sections in both directions, based on different effective depths, as explained in the introduction above. In this example, the solution stabilizes and settles on a solution from the 7^{th} iteration onwards. All elements (and panels) in the optimal solution satisfy the bending moment criterion. This design, which satisfies AS 3600 code provisions mentioned in Chapter 5 shows a saving of concrete weight (and cost) of 18.20 % compared to hand calculations using the 'Simplified Method of Design'. In the 'Simplified Method of Design' design, all drop panels having the same depths of 325 mm are assumed (i.e., central panels, end panels and corner panels). A uniform slab thickness of 250 mm is assumed and checked for serviceability criterion and the layout of reinforcement is sought (Appendix A). It is well known that the finite element method introduces some additional stiffness at the supports, which will result in higher negative moments at the walls and columns. This effect is local and it does not influence the results at other locations. Two approaches are used in the algorithms to rectify this problem. In the above optimisation procedure, a simple "smoothing algorithm" is employed that implements numerical smoothing i.e. averages the nodal values of moments in each direction. This helps to reduce the sharp negative moments at walls and columns. Another approach, of using the "5 % moment difference", explained later can also be used to reduce the excessive thickness of drop panels obtained at the column supports. It is anticipated that using the "5 % moment difference" in addition to numerical smoothing of the nodal moments would have resulted in the drop panels being less thick, probably around 350 mm (Yellow color). However, results obtained around the columns for the example shown above are reasonable and the design shows significant savings in concrete weight in addition to satisfying serviceability requirements.

Conclusion

This example demonstrates and explains the reasons for asymmetry in results obtained for a symmetrical model with uniformly distributed load. Though, the results for both initial thicknesses were not symmetrical, the designs showed improvements in concrete weight savings and satisfy AS 3600 codal provisions. In the above example, the difference in results obtained near the columns when the initial model is assigned a slab thickness of 200 mm and when the initial model is assigned a slab thickness of 250 mm is also clearly seen. In the next example, symmetrical results are obtained for the same model used in this example by

calculating the moment capacities based on the average of the two effective depths as explained previously.

Symmetrical Results: Initial slab thickness of 250 mm

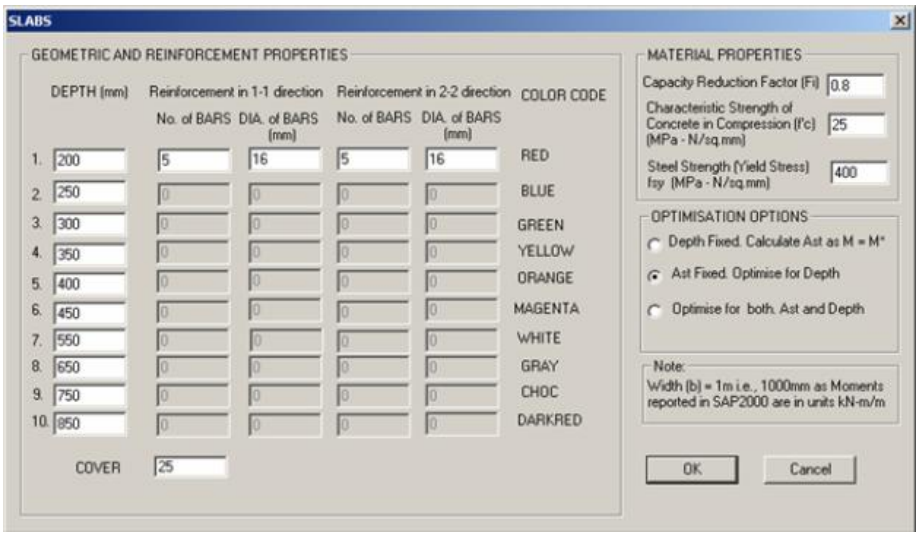

Fig. 7.46. Design Data for Technique 2

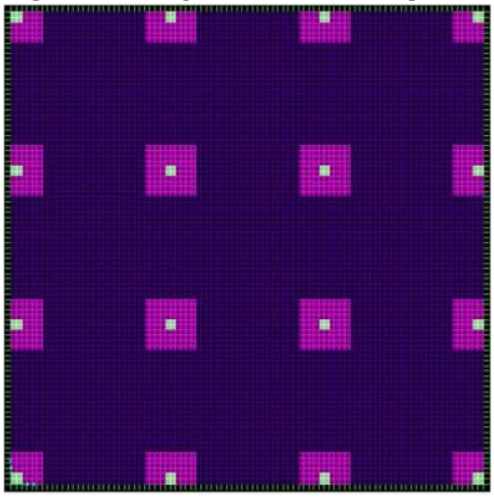

Fig. 7.47. Initial Model (Slab thickness: 250 mm)

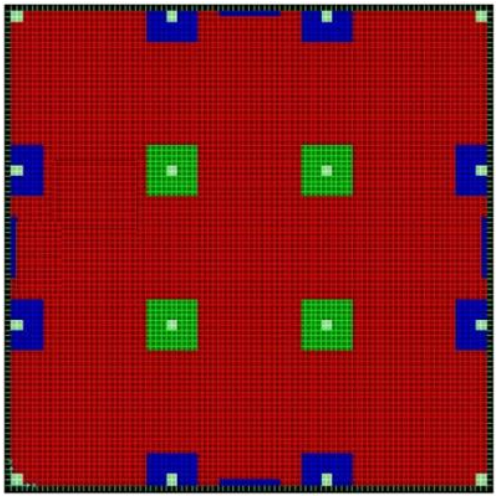

Fig. 7.48 (a). 1st iteration

.

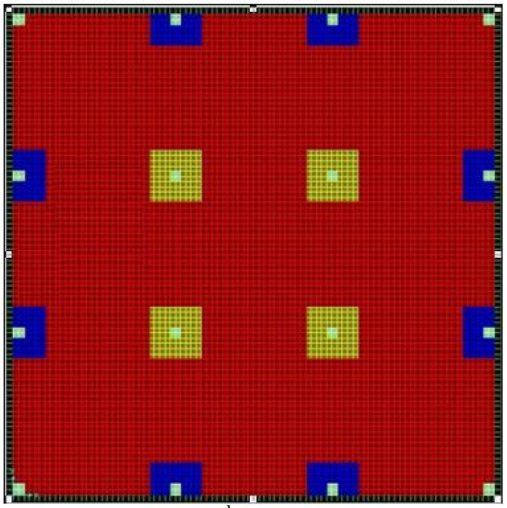

(b) 2nd iteration

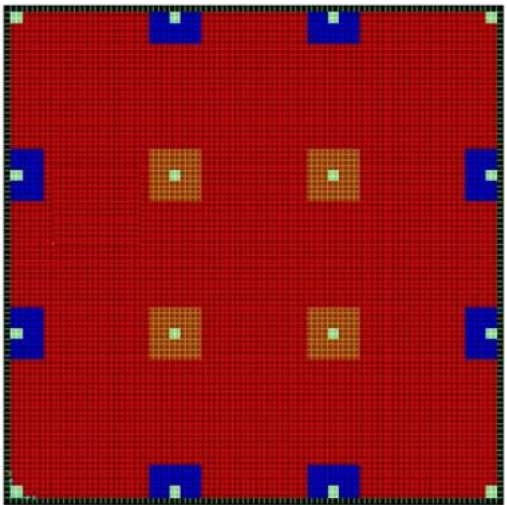

(c) 3rd iteration

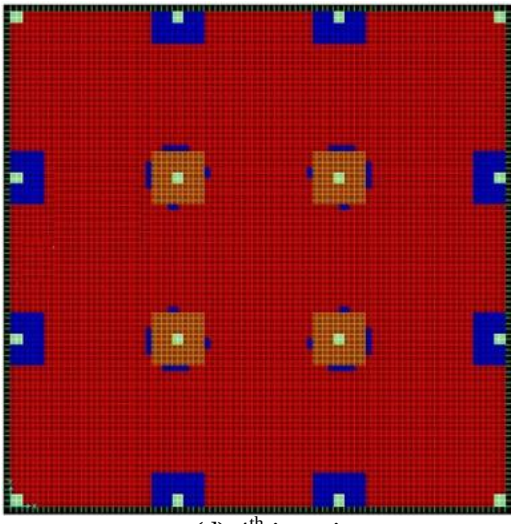

(d) 4th iteration

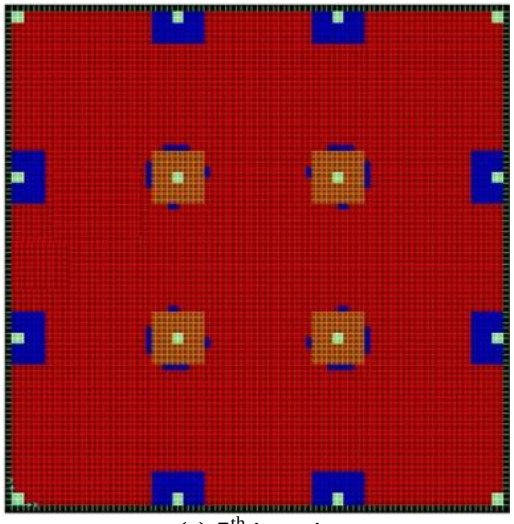

(e) 5th iteration

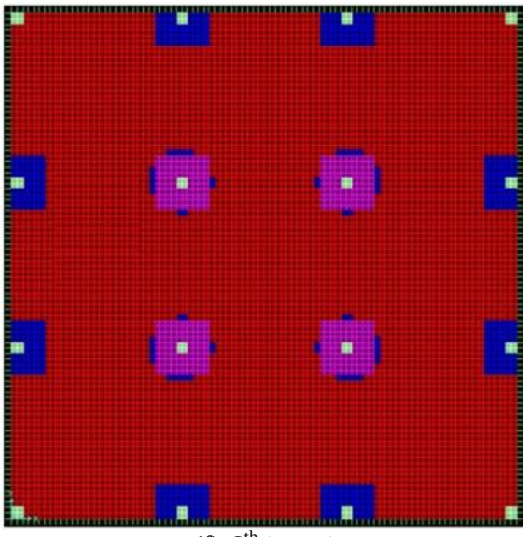

(f) 6th iteration

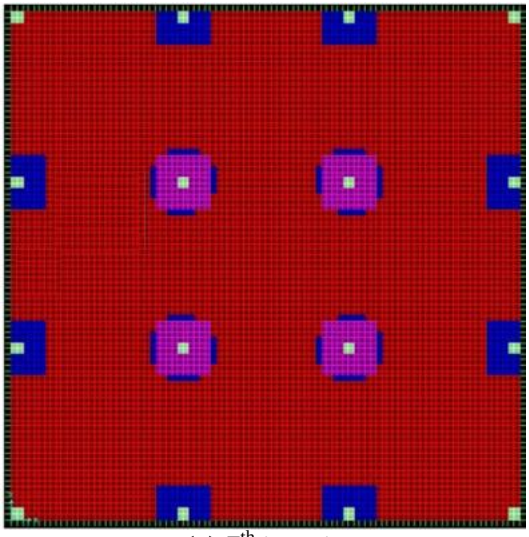

(g) 7th iteration

Fig. 7.48. Technique 2 Design Solutions using the Average Effective Depth in both directions

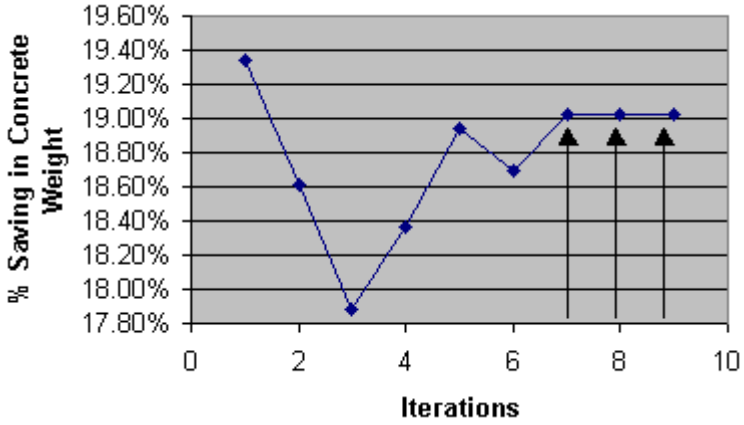

Fig. 7.49. History of Concrete Weight Reduction

Black arrows indicate optimisation has settled on one solution and this solution *satisfies* the bending moment criterion (% saving in concrete weight: 19.02 %)

Table 7.10. Technique 2 Design Optimisation Results using Different Effective Depths for Flat Slab

Iteration No.	Concrete Weight (Tonne)	% saving in Concrete Weight	Total Steel Weight (Tonne)	% saving in Total Steel Weight	Total Cost of Concrete (AU $)	Total Cost of Steel (AU $)	Max. Deflection (mm) * 3	Permissible Deflection (mm) (Span/250)	Satisfies Condition
Initial Model	188.79	-	2.67 X 2 = 5.34	-	11799.58	5879.43	2.968 x 3 = 8.904	24	-
1	152.27	**19.34 %**	2.67 X 2 = 5.34	-	9517.03	5879.43	3.155 x 3 = 9.465	24	NO
2	153.65	**18.61 %**	2.67 X 2 = 5.34	-	9603.52	5879.43	2.686 x 3 = 8.058	24	NO
3	154.11	**17.88 %**	2.67 X 2 = 5.34	-	9632.36	5879.43	2.487 x 3 = 7.461	24	NO
4	153.20	**18.37 %**	2.67 X 2 = 5.34	-	9574.69	5879.43	2.474 X 3 = 7.422	24	NO
5	153.04	**18.94 %**	2.67 X 2 = 5.34	-	9565.08	5879.43	2.470 X 3 = 7.410	24	NO
6	153.50	**18.69 %**	2.67 X 2 = 5.34	-	9593.91	5879.43	2.478 X 3 = 7.434	24	NO
7	152.88	**19.02 %**	2.67 X 2 = 5.34	-	9555.47	5879.43	2.460 X 3 = 7.38	24	YES
8	152.88	**19.02 %**	2.67 X 2 = 5.34	-	9555.47	5879.43	2.460 X 3 = 7.38	24	YES
9	152.88	**19.02 %**	2.67 X 2 = 5.34	-	9555.47	5879.43	2.460 X 3 = 7.38	24	YES

Note: Factored Max. Deflection is well within permissible limits.

The solution settles from the 7th iteration onwards and all elements satisfy the bending moment criterion from the 7th iteration onwards. It is seen that when average of the two effective depths is used in calculating the moment capacity of the sections in each orthogonal direction, symmetrical results are obtained. As explained above, this happens because the moment capacities calculated in both directions now are equal if the steel specified is the same. The thickness of the drop panels in this case is different to the thickness of the drop panels obtained when two different effective depths are used. The central drop panels seem to have settled on a depth of 450 mm (Magenta color), the end panels seem to have settled on a depth of 250 mm (Blue color) and no drop panels are observed at the corners. This is because the support conditions for the ends are fixed and also because punching shear criteria are not programmed as yet. A saving of 19.02 % is attained in concrete weight compared to the initial model (slight increase compared to the 18.20 % concrete weight saving obtained from the previous example when two different effective depths are used). It is to be noted that, due to this averaging of the depths in order to obtain symmetrical results, the effective depth is underestimated in the primary direction, which will result in slightly larger reinforcement (or depth). In the secondary direction, the effective depth is overestimated and slightly smaller values for the reinforcement (or depths) will be obtained. In both cases the error in calculations of the effective depth 'd' is equal to ½ of bar diameter. The effect of this small error is insignificant, considering that the adopted reinforcement (or depth) will always exceed the capacity required by the design. It is also to be remembered that the finite element method introduces some additional stiffness at the supports, which results in higher negative moments at the columns. This effect is local and it does not influence the results at other locations. Two approaches are used in the algorithms to rectify this problem. In the above optimisation procedure, a simple "smoothing algorithm" is employed that implements numerical smoothing i.e. averages the nodal values of bending moments in each direction. This helps to reduce the sharp negative moments at columns. Another approach of using "moment difference" can also be used to reduce the excessive thickness of drop panels obtained at the column supports. A "relaxation algorithm" can also be adopted which is explained later. Or, a non-design region over the column can be specified for all those elements over the column support in which the effects of stress singularity are observed. This method is used later when punching shear criterion is included as an additional constraint in which frame objects are used to model columns (where the effects of stress singularity are more pronounced as compared to when solid elements are used to model columns).

Conclusion

This example demonstrates and explains the symmetrical results obtained for a symmetrical model with uniformly distributed load when average of the two effective depths are used in the calculation of bending moment capacities of the user-defined sections.

The examples presented in Section 7.7.2.1 above also clearly demonstrate the reliability and stability of the proposed modelling approach (outlined in Section 7.7.1.3 above). Comparisons with hand calculations using the 'Simplified Method of Design' (Appendix A) show that reasonable and comparably similar depths are obtained for all the drop panels thereby resolving the problems encountered when performing optimisation on an element-level (observed in Section 7.7.1).

7.7.2.2 Oscillating Solutions due to Different Effective Depths When Using Technique 2

The effect 'two different depths' and 'average of the two depths' have on results was seen in Section 7.7.2.1 above. When two different effective depths are used, it results in asymmetrical results for the drop panels at the edges. However, it is to be remembered that these results also depend on other variables such as the design data provided by the designer in the user interface, the span and loading on the slab etc. In the following example, a different kind of problem was observed when 'two different depths' are used in the calculation for M_{11} and M_{22}. It was observed that the optimal solution oscillates between two sections for a few elements and it does not settle on one particular section. The cause of this occurrence was investigated and explanation follows the results presented below.

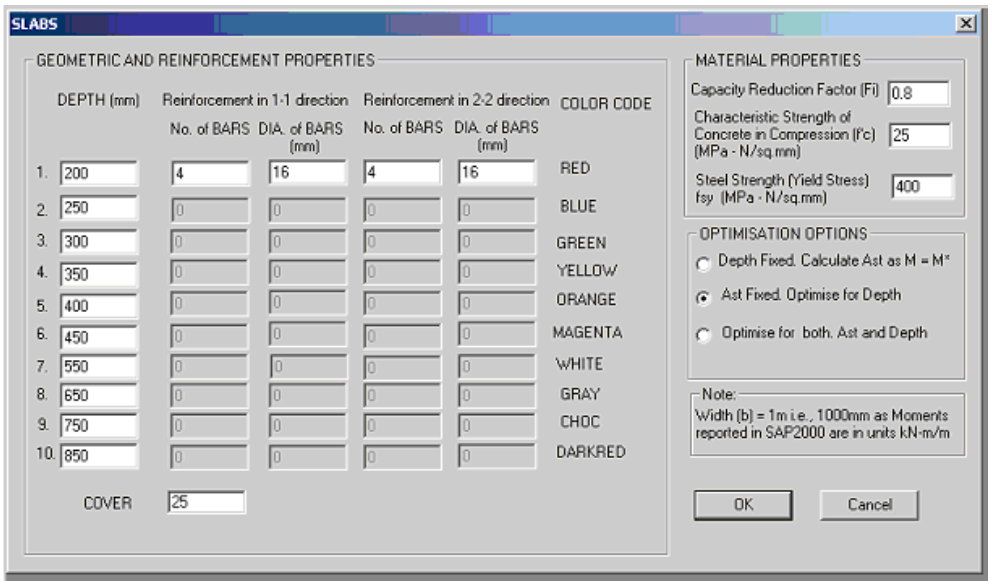

Fig. 7.50. Design Data for Technique 2

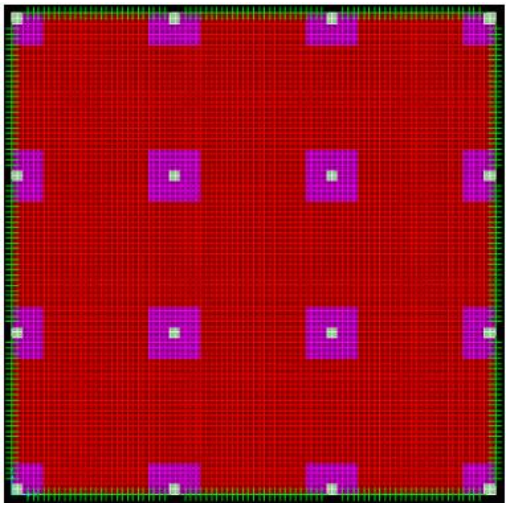

Fig. 7.51. Initial Model

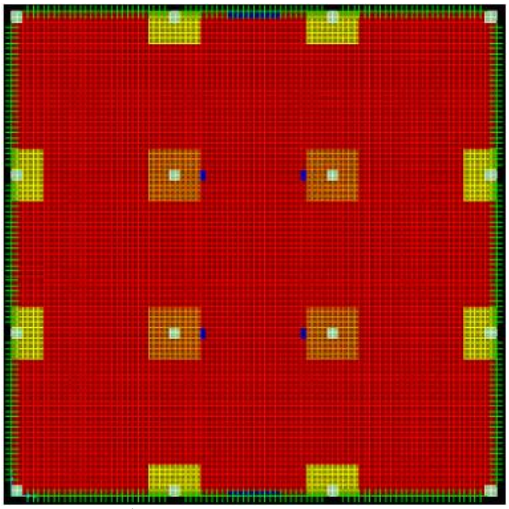

(a) 1st iteration

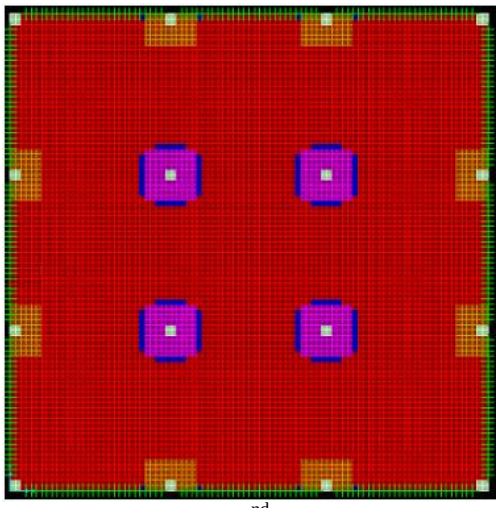

(b) 2nd iteration

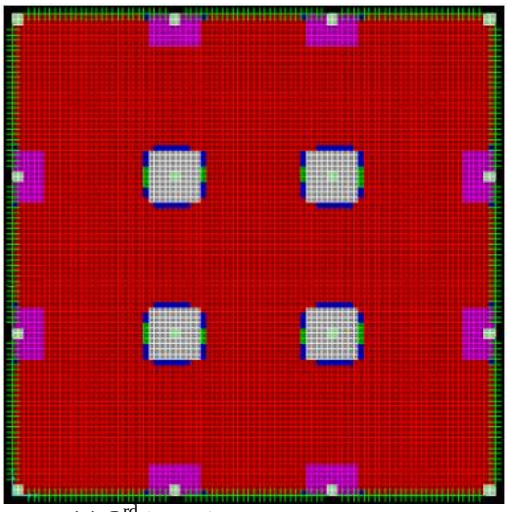

(c) 3rd iteration

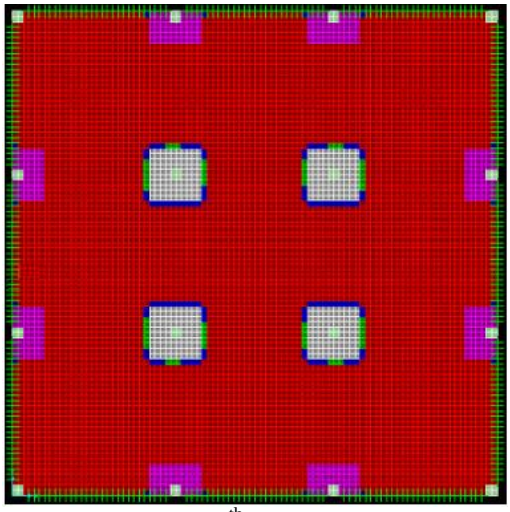

(d) 4th iteration

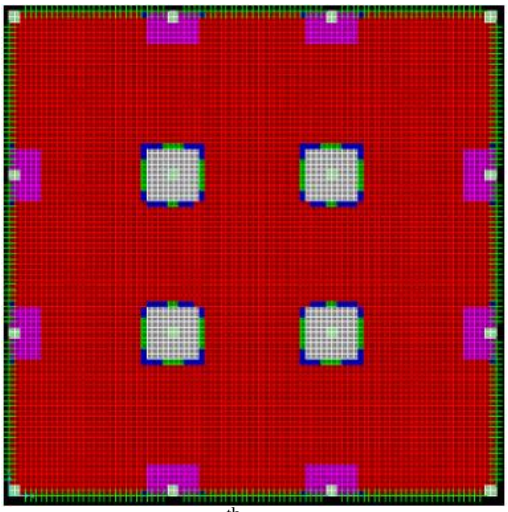

(e) 5th iteration

Fig. 7.52 (a-e).

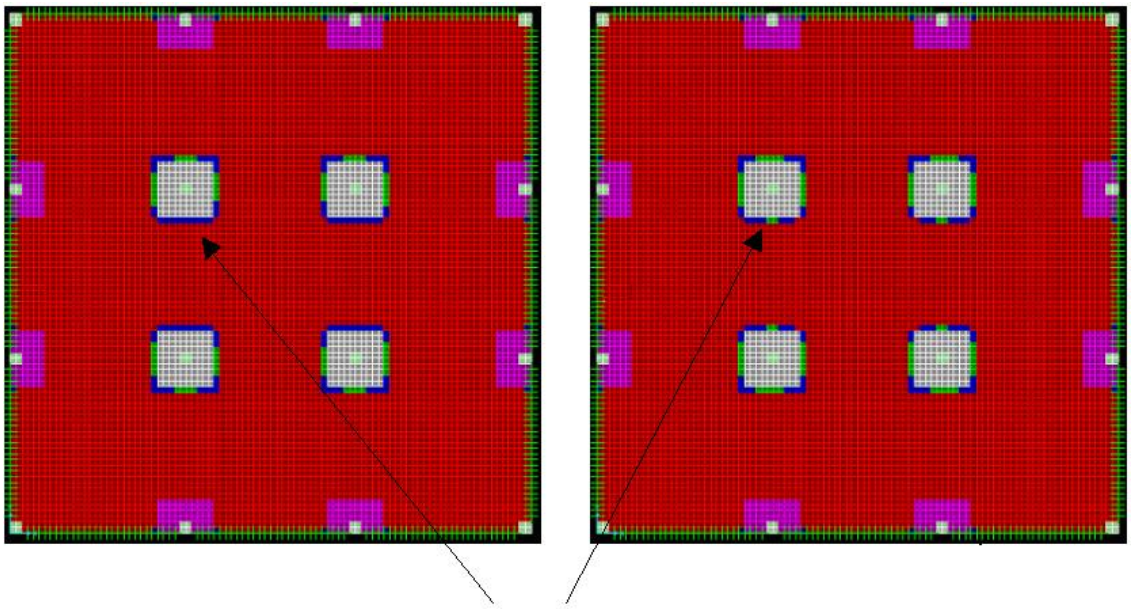

(f) 6th iteration (g) 7th iteration

Fig. 7.52. Technique 2 Design Solutions showing Oscillations due to Different Effective Depths in both directions

It is seen from the above results that both central and edge drop panels have settled on 550 mm (White) and 450mm (Magenta) depths respectively. Results from the 6th iteration onwards show that the solution keeps alternating for some elements around the central drop panels between Green (300 mm) and Blue elements (250 mm). Bending moment criterion is obviously not satisfied in these elements around the central drop panels for both 6th and 7th iteration. This oscillation continues and the reason for this is explained as follows:

Table 7.10a. Table comparing M_{11}, M_{22} with the Moment Capacities of the Two Design Sections used for the Oscillating Elements

Depth	*Color*	M^*_{11} (kN-m/m)	M^*_{22} (kN-m/m)	$ØM_{11u}$ (Moment Capacity-"Different Depths") (kN-m/m)	$ØM_{11u}$ (Moment Capacity-"Avg Depth") (kN-m/m)	$ØM_{22u}$ (Moment Capacity-"Avg Depth") (kN-m/m)
250	Blue	-93.458	-77.389	92.819	79.329	73.150
300	Green	-91.707	-83.025	112.129	98.639	92.460

Step1:

As seen in Table 7.10a, algorithm (based on "different depths") selects 250 mm depth (Blue). On performing FEA, M_{11} is –93.458 kN-m/m, which is slightly more than the moment capacity M_{11}Star for 250 mm depth (92.819 kN-m/m). Therefore, program chooses 300 mm depth (Green).

Step2:

On performing FEA with the new depth, M_{11} is found to be –91.707 kN-m/m. Therefore, algorithm chooses 250 mm depth (Blue) as M11Star of 250 mm depth is slightly more (1.2 %) than –91.707 (it is 92.819).

Here, the program should choose Green (300 mm) again instead of Blue (250 mm). That is there should be a rule which says that choose the section such that the bending moment capacity is at least say 5% more than the bending moment in the section. This way the problem of alternating solutions can be stopped.

As a result of 'different depths' and the above issue, a 5 % difference is considered in the following example.

It should be noted here that this problem disappears in some cases when optimizing with 5Y16 bars (i.e. when the quantity of steel is increased). *There is a clause in AS 3600, which specifies a minimum quantity of steel for this reason.* However, it cannot be programmed for Technique 2, as the minimum quantity of steel for each depth will be different.

It should also be noted that by using 'Average of the two effective depths' this problem is solved. However, then, the moment capacity calculated in the Y direction is slightly overestimated and the moment capacity in the X direction is slightly underestimated, but the difference can be said to be negligible.

7.7.2.3 Moment Difference Approach

It was seen in the previous example that using "two different depths" for calculating the moment capacities in each direction may result in oscillating solutions depending on the design data provided in the user interface. If an exact approach using "two different depths" is required to be adopted, then a 'Moment Difference Approach' is proposed to solve the problem of 'oscillations' observed in the previous section. In this approach, the user is prompted to specify the moment difference in percentage. Typical values can range from 2 % to 10 %. This means that if the user specifies 5 %, then when allotting the sections, the algorithm will allot sections to elements (and drop panels) such that their moment capacity is greater than 5 % of the bending moment occurring in the element. If not, the algorithm chooses sections such that the moment capacity is greater than the moment within the element, as is the general case that was seen in the previous section. It is seen that though this approach leads to slight over design (very marginal for the example in the previous section), it solves the problem of oscillating solutions seen in the previous section. Using the proposed 'Moment Difference Approach' and specifying a moment difference of 2 %, the previous example is again run and the solution obtained is observed to be the same as was in the previous example with the only difference being that the solution settles on the 7th iteration as the optimal solution and does not oscillate further. For space constraints, the optimisation history is not shown here. It is seen that this approach is thus useful in solving the problem for the example demonstrated in the previous section. It is also tested on a simple continuous beam to further reinforce the concept. The moment difference specified is 5 %.

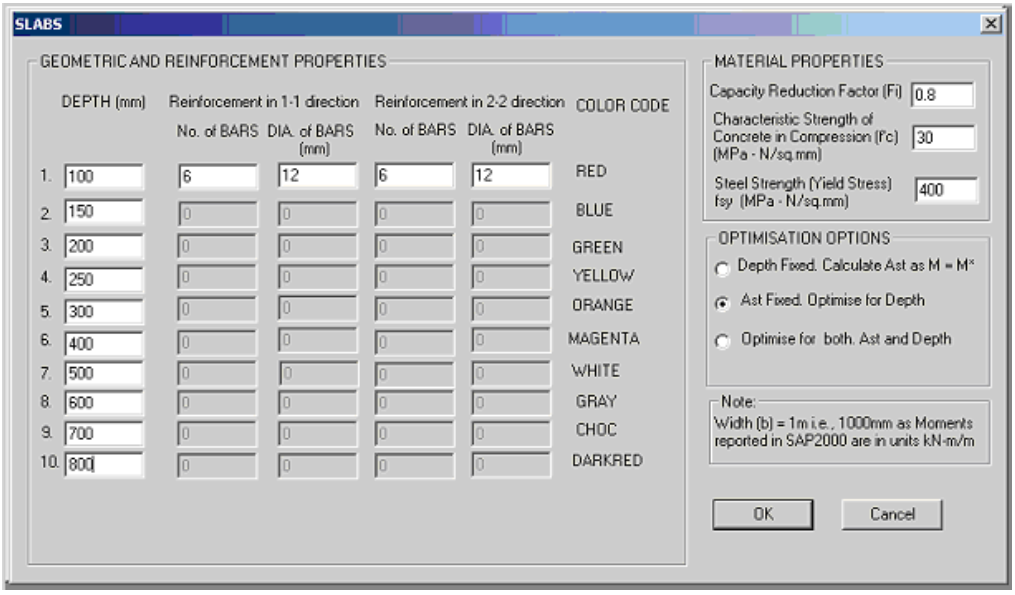

Fig. 7.53. Design Data for Technique 2 (Fixed Supports; Each Span: 4.5m; LL: 20 kPa)

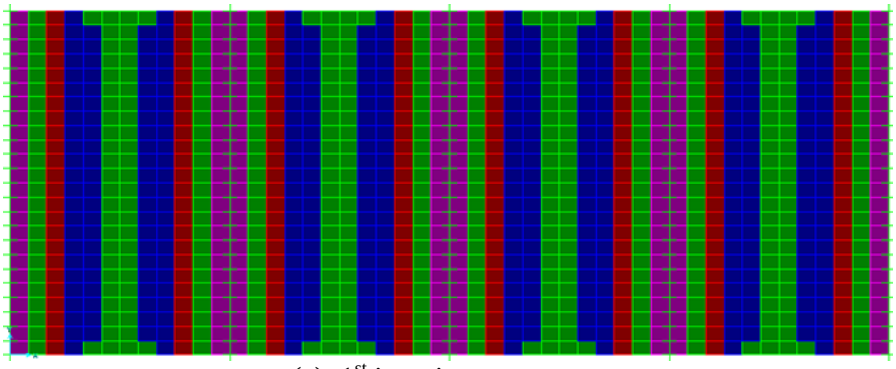

(a) 1st iteration

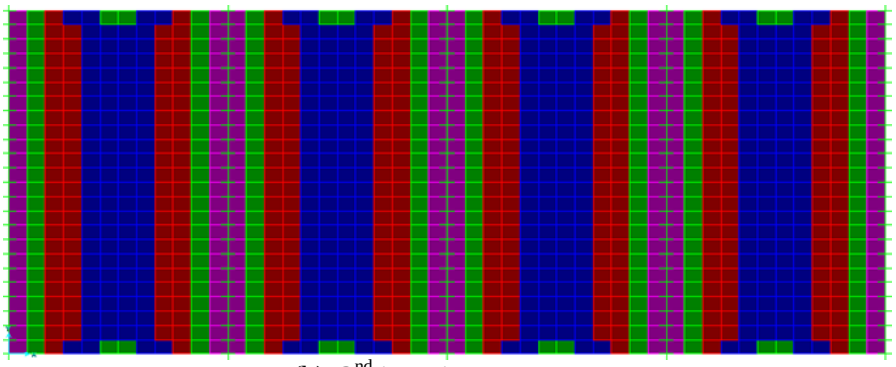

(b) 2nd iteration

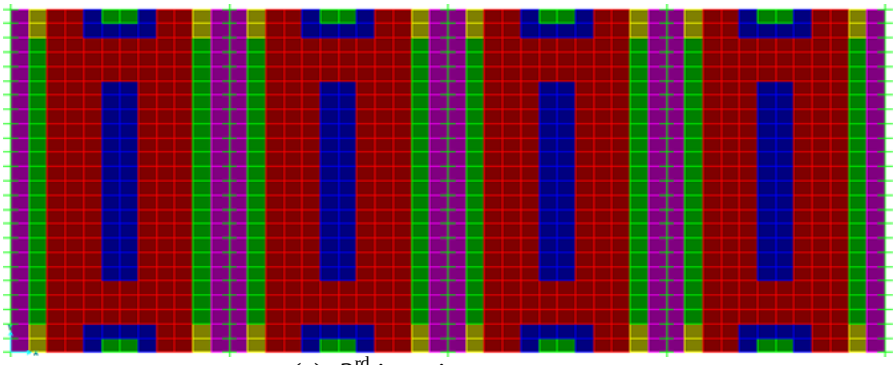

(c) 3rd iteration

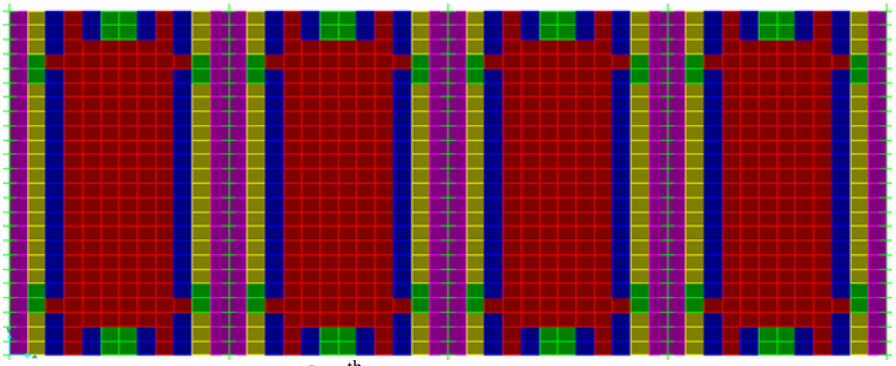

(d) 4th iteration

Fig. 7.54 (a-d).

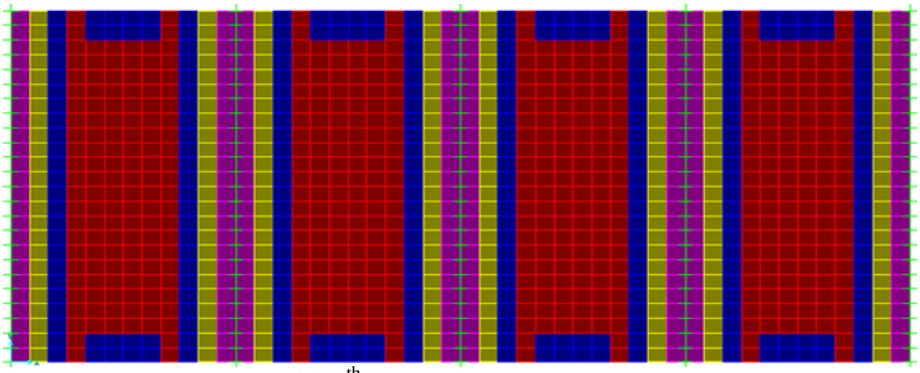

(e) 5th iteration

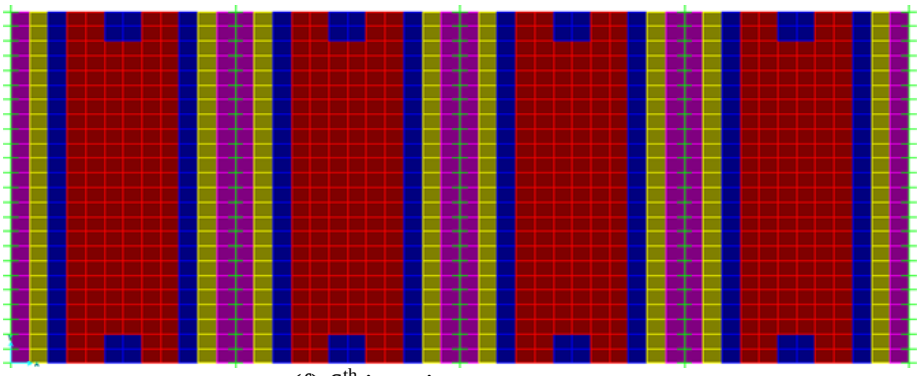

(f) 6th iteration

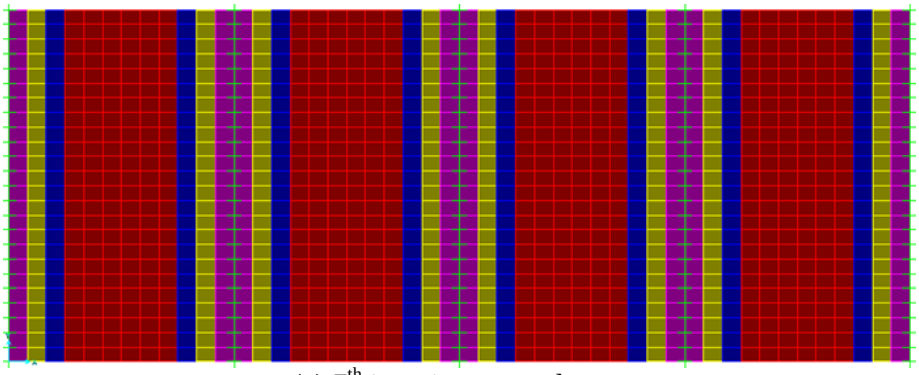

(g) 7th iteration onwards

Fig. 7.54. Technique 2 Design Solutions Using the 'Moment Difference' Approach for a Continuous One-way Slab

Table 7.11. Technique 2 Design Optimisation Results Using the 'Moment Difference' Approach for the Continuous One-way Slab

Sr. No.	*Iteration No.*	*Concrete Weight (kN)*	*% Saving in Weight*	*Max Deflection (mm)*	*Permissible Deflection (Span/250) mm*	*Satisfies Condition*
1	Initial Model	742.238	-	1.26	18mm	-
2	1	595.852	19.72	2.52	18mm	YES
3	2	548.431	26.11	2.00	18mm	YES
4	3	523.690	29.44	3.00	18mm	NO
5	4	550.493	25.83	3.12	18mm	NO
6	5	552.555	25.56	3.00	18mm	YES
7	6	548.431	26.11	3.00	18mm	YES
8	**7**	544.308	26.67	3.00	18mm	YES
9	**8**	544.308	26.67	3.00	18mm	YES
10	**9**	544.308	26.67	3.00	18mm	YES
11	**10**	544.308	26.67	3.00	18mm	YES

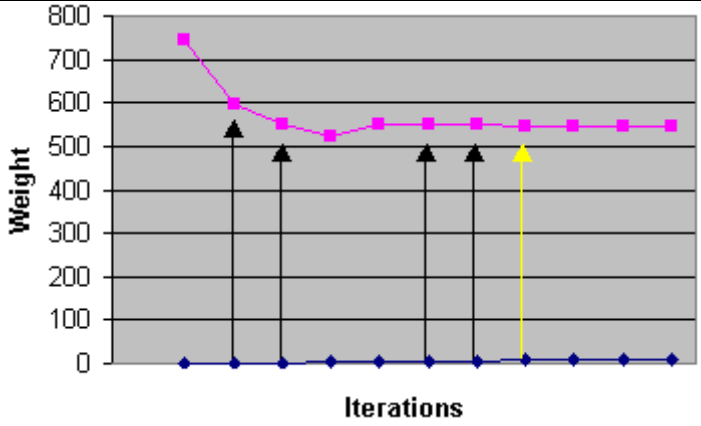

Black arrows indicate solutions that *satisfy* bending moment criteria for all elements.

Yellow arrow shows that criterion is *satisfied*, plus the solution remains the same thereafter.

Fig. 7.55. History of Concrete Weight Reduction

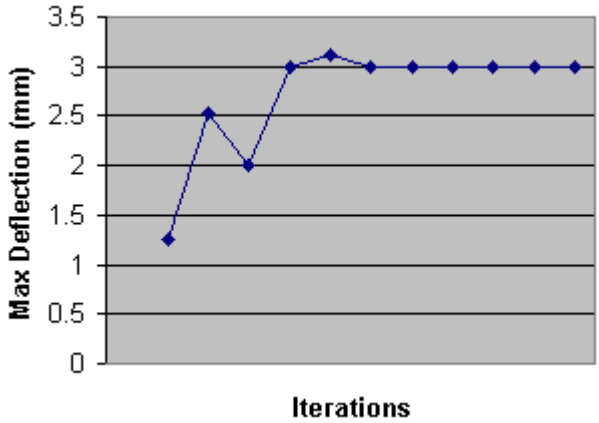

Permissible deflection (Span/250) is 4.5m/250 = 18mm

Fig. 7.56. History of Maximum Slab Deflection

It is seen from the above results that when a moment difference is employed, the solution settles from the 7th iteration onwards. Iterations 1, 2, 5, 6 and 7 onwards satisfy the 'bending moment' criterion for all elements in the model and are therefore possible solutions. The 7th iteration shows the most improvement in concrete weight saving and is therefore chosen as the optimal solution. The optimal solution shows a *26.67 %* saving in concrete weight compared to the initial model. The maximum deflection increases as expected, as more and more material is removed, and from the 7th iteration onwards remains constant at 3 mm. As the gross area is used by the FEA in the calculation of deflection (unlike a cracked section), a factor of 3 is applied to the maximum deflection in the slab and compared with the permissible limit specified by AS3600 (span/250). It is seen that even then the maximum deflection (3 x 3 = 9 mm) is well below the permissible limit of 18 mm for this particular model. To solve the problem of 'oscillations' observed in the previous section, this example demonstrates the application of the 'moment difference' approach for a simple continuous one-way slab and shows the effectiveness and stability of this approach for Technique 2. This approach is therefore particularly useful in designing flat slabs when *different depths* (Section 7.7.2.1) are to be explicitly used in the calculation of M_{11} and M_{22}.

7.7.2.4 Moment Relaxation

The problems of stress singularities at the column supports, as discussed before, need to be resolved in order to obtain a design that caters for the actual behaviour of the slab in the region around the column. Generally, stress singularities cause excessively high bending moments and shears in the region around the column. It was shown using Technique 2 that excessively high depths are observed for the drop panels around the columns as the optimisation proceeds. The optimal solution too shows a depth that is unreasonably high for the drop panels, although weight savings are observed for the entire slab. As punching shear criterion is not considered as an additional constraint in the optimisation process at this stage, the depths allotted to the drop panels are based on the maximum bending moment (in two orthogonal directions) in the regions around the columns. It is important to choose this value of the maximum bending moment correctly without picking the maximum bending moment value due to stress singularity. One of the ways to choose an appropriate value for the maximum bending moment in this region is:

1. **Moment Redistribution (Relaxation) for slabs only:** It is well known that at advanced moments the relation between bending moment and curvature becomes non-linear, i.e. the bending stiffness of the slab decreases. Due to this, at overload, the end moments required to restore continuity with adjacent spans are less than those obtained from an elastic analysis. This would mean larger mid-span moments and smaller support moments than those

obtained from the elastic analysis. As loading increases, the static moments increase proportionally, but there is a less-than-proportional increase in the support moments and the difference between negative and positive moment diminishes. Moment redistribution is said to occur. To the extent to which moment redistribution can occur depends on the ductility inherent in the structure. A designer can allow for moment redistribution at the strength limit states provided that minimum ductility requirements are met (this is taken care of by the built-in validation rules in the GUI's which check whether the user-specified thicknesses and steel meet the minimum ductility requirements of AS 3600-2001. If they do not meet, the user is prompted to revise the data). As moment redistribution often permits a more economical choice of section in the critical support region, the moment diagrams can be 'relaxed', i.e. to reduce the negative moment diagram, and to redistribute the actions to the areas with positive moments. Several levels of relaxation can be used, i.e. 5 %, 10 %, 15 %, 20 %, 25 % and 30 %. A different relaxation factor will result in different moment diagrams and different reinforcement (or depths). It is to be noted that the 'relaxation' does not apply to beam bending moments, and does not affect the deflection and the reaction results. It is done numerically. All negative bending moments at all column supports are reduced from 5 % to 30 %, as specified by the user. The moments at all other points are adjusted to accommodate the reduction of the negative moments. Since the method is based on an approximate numerical algorithm, some small inaccuracy may occur. Smooth contour lines should indicate a successful implementation of the relaxation algorithm. A careful examination of the bending moment results must be carried out, comparing the "relaxed" bending moments with the "non relaxed" results. It is worth investigating the usefulness and applicability of this approach for choosing the correct value of the design bending moment in the proposed optimisation approach using Technique 2. The next example uses a relaxation factor of 25 % over the column supports and results are investigated.

7.7.2.4.1 Technique 1 (Slab Thickness Constant, Steel Varying)

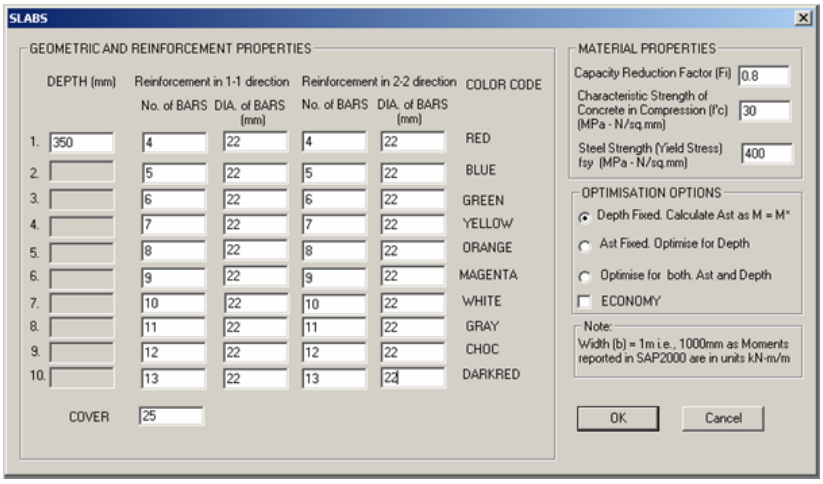

Fig. 7.57. Design Data for Technique 1

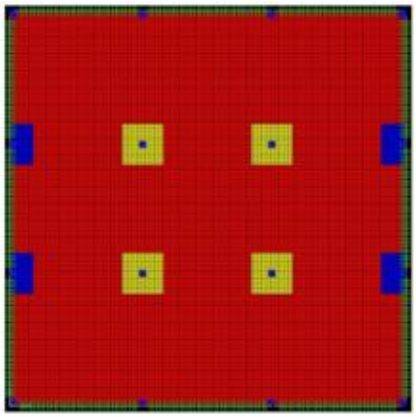

(a) Max Moment Near The Column
7Y22 bars in central drop panels (Yellow)
5 Y22 bars in end drop panels (Blue)

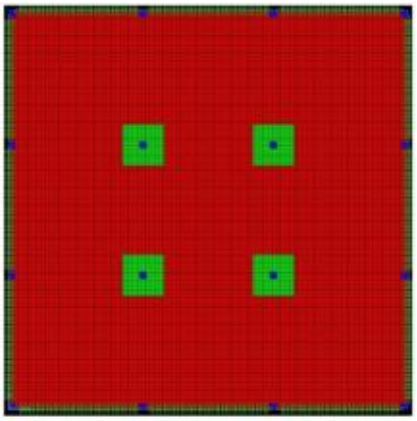

(b) "Relaxed" Moment By 25 %
6Y22 bars in central drop panels (Green)
4 Y22 bars in end drop panels (Red)

Fig. 7.58. Comparison of Technique 1 Design Solutions showing Steel in X direction

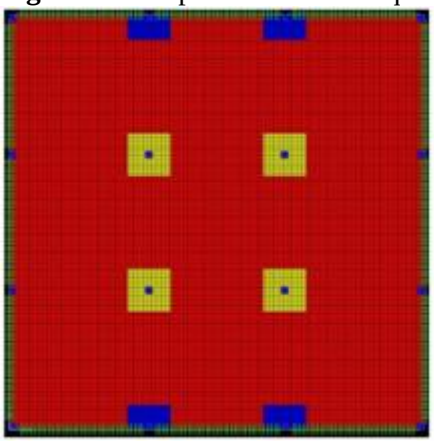

(a) Max Moment Near The Column
7Y22 bars in central drop panels (Yellow)
5 Y22 bars in end drop panels (Blue)

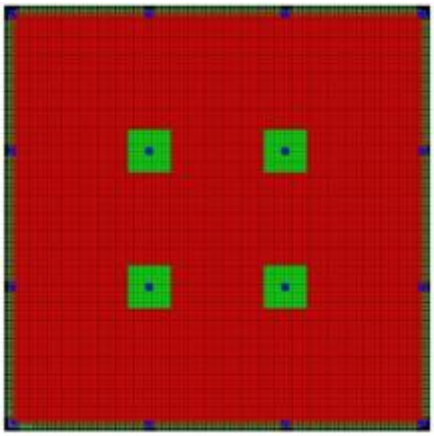

(b) "Relaxed" Moment By 25 %
6Y22 bars in central drop panels (Green)
4 Y22 bars in end drop panels (Red)

Fig. 7.59. Comparison of Technique 1 Design Solutions showing Steel in Y direction

It is observed from the above results, that when a "relaxed" value of the maximum bending moment at the column supports is chosen, lesser steel is required in both the central drop panels and the end drop panels. These results compare well with hand calculations using the Simplified Method of Design (Appendix B). To test this further, Technique 2 (Steel Constant, Depth varying) is employed and the results obtained using 'Relaxed Moments' are compared with the results obtained without using 'Relaxed Moments'.

7.7.2.4.2 Technique 2 (Steel Constant, Slab Thickness Varying)

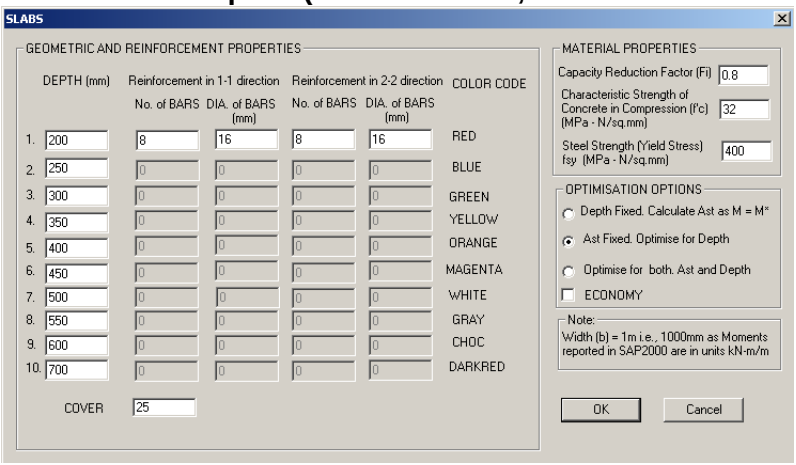

Fig. 7.60. Design Data for Technique 2

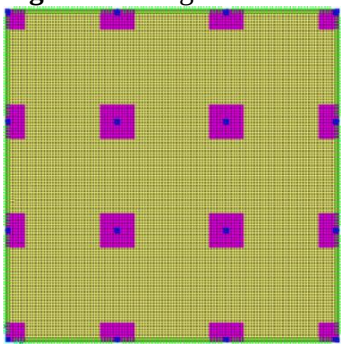

Fig. 7.61. Initial Model

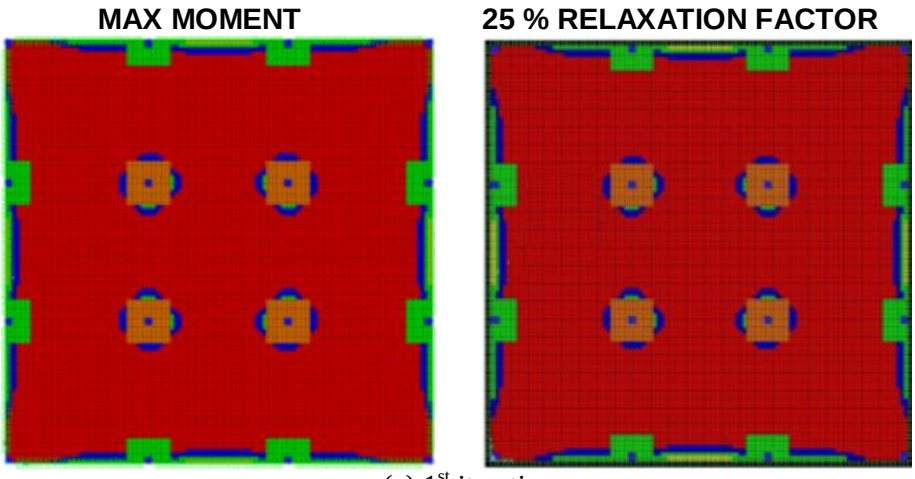

(a) 1st iteration

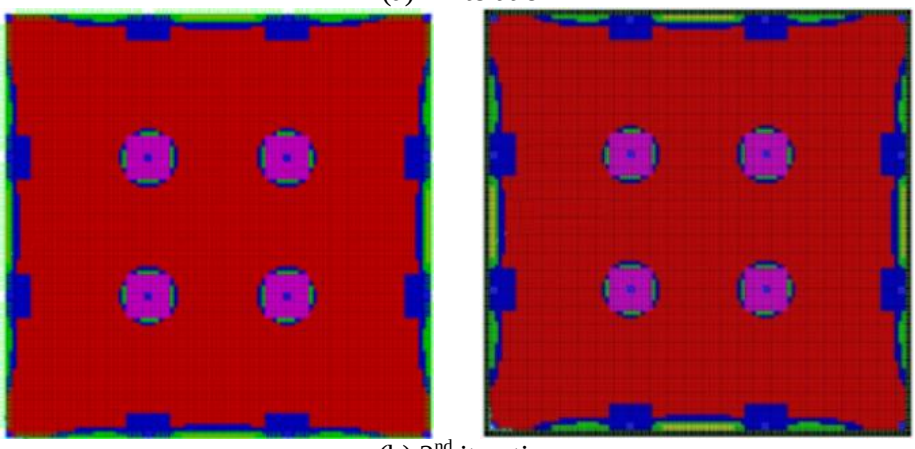

(b) 2nd iteration

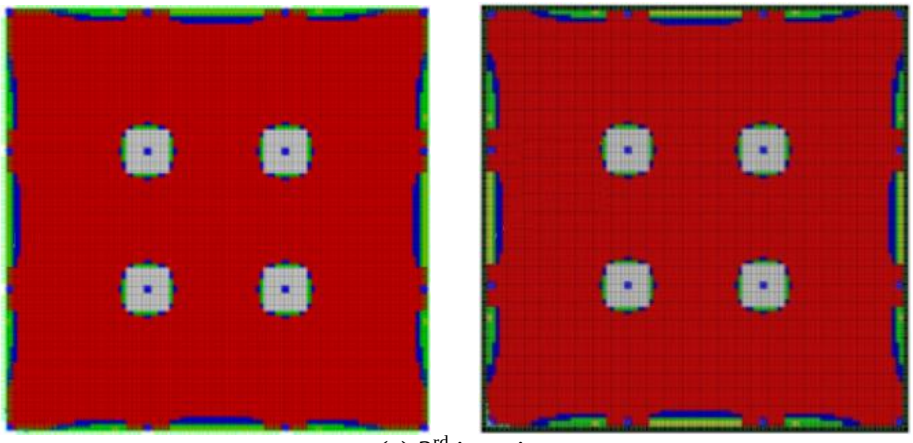

(c) 3rd iteration

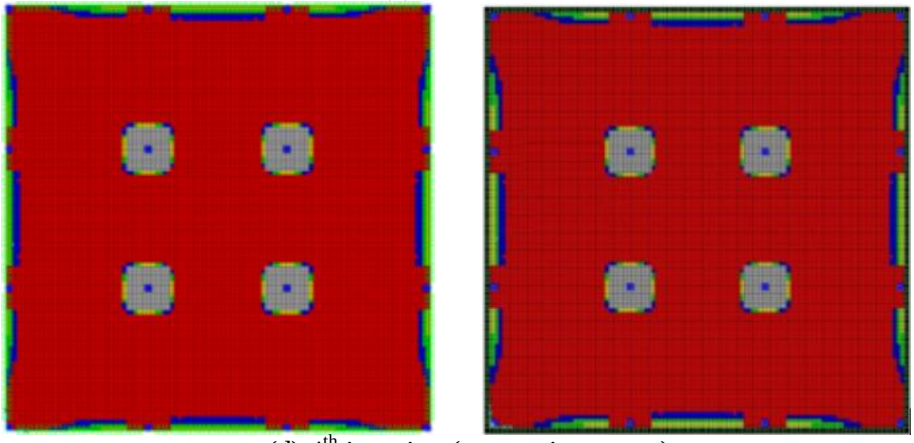

(d) 4th iteration (on previous page)

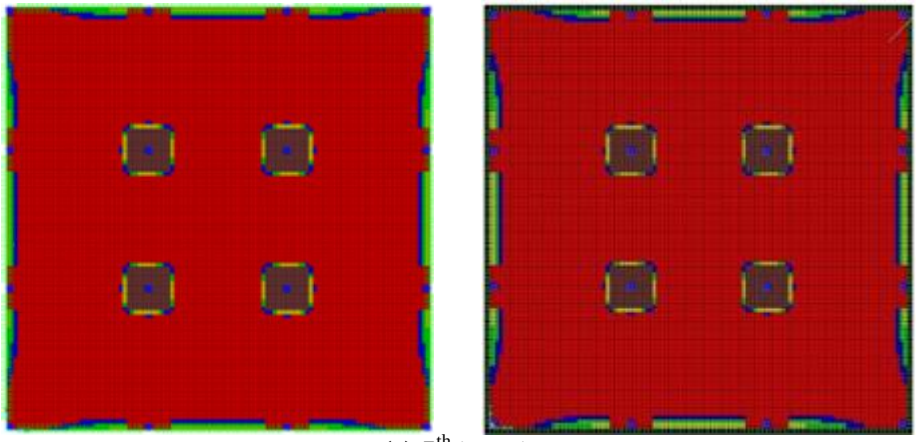

(e) 5th iteration

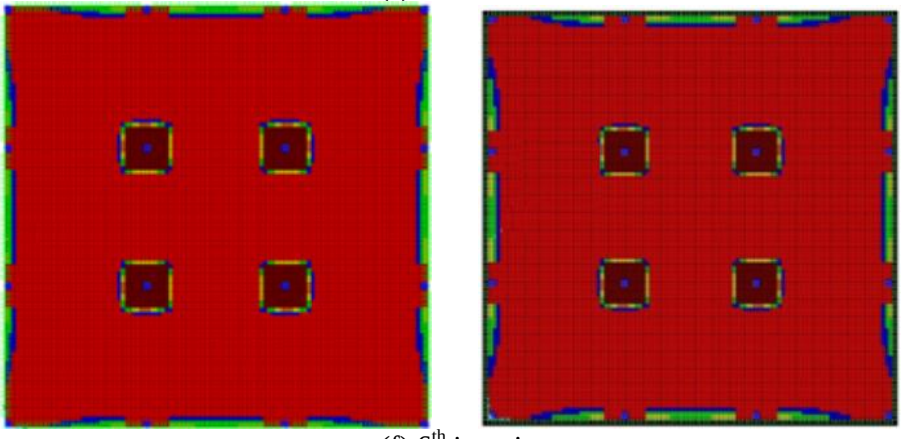

(f) 6th iteration

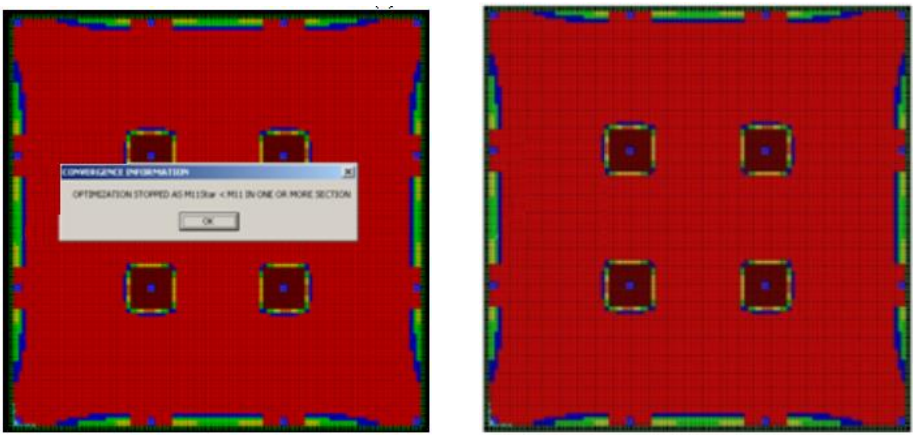

Optimisation stops. (g) Solution converges.

Max Deflection: 3.2 mm

Fig. 7.62. Comparison With and Without Moment Relaxation between Technique 2 Design Solutions

It is seen from the above comparison that when the maximum moment in the drop panels is chosen as the design moment (i.e. relaxation algorithm is not employed), the optimisation stops in the 7th iteration as the maximum moment exceeds the moment capacity of even the thickest depth provided (in this case 700 mm shown in dark red color for the central drop panels). This means that a depth bigger than 700 mm is still required. It is therefore difficult to predict the biggest thickness that should be provided in the user interface. However, when the relaxation algorithm is employed with a factor of 25 %, almost similar results are obtained in each iteration, and the solution settles on the same solution from the 7th iteration onwards and does not change thereafter. This comparison suggests that even when the maximum bending moment in the drop panel is reduced by 25 %, lesser thicknesses are not observed for the central drop panels in successive iterations. This means that this maximum bending moment, if chosen, could well be the maximum moment occurring due to the effects of stress singularity near the column. In both cases the depths of the drop panels keep on increasing. This happens because, as the depths near the column are increased, the moments in turn increase and this process goes on, i.e. thicker sections attract moment. Now, if the steel given is less than the steel needed near the column (as per Simplified Method of design), then the moment capacities of the sections provided, after a few iterations, become inadequate for the maximum moment generated near the column after about 7-8 iterations as seen above when the 'Max Moment' is used as the 'design moment'. For a flat slab modeled above, this Option (Technique 2) can only provide a converged solution when the relaxation algorithm is employed or if there is a non-design area in the drop panel for the elements exactly over and surrounding the column or if the steel provided is at least equal to or more than the steel obtained from the Simplified Method of design. The next example tries to find out if the solution converges and solves the above

problem if the steel quantity is increased. The simplest of all approaches mentioned above is to modify the initial model by assigning non-design regions even in the drop panels (i.e. all the elements over the columns where effects of stress singularity are observed should be treated as non-design). This approach is used when frame members are employed as columns while implementing punching shear criterion in addition to moment criterion. This is demonstrated in a later example. If the present approach to modeling flat slabs is used, then these results are to be expected when employing Technique 2 to seek the optimal depths in various parts of the slab. It is to be noted that employing the relaxation algorithm does not affect the results in other locations of the slab as can be seen from the comparison above. This example thus illustrates the *usefulness of using the relaxed bending moment* in the drop panel as the design moment in spite of using the 'Plate Constraint' for the nodes over the column so as *to obtain converged solutions.* However, though it helps in convergence, this approach warrants further investigation before adopting it in the proposed optimisation techniques.

In the next example, the comparison above is again investigated, however with increased steel quantity to see and compare the results obtained with more steel. These parametric studies are important in order to reach a definite conclusion on whether to use the 'Moment Relaxation Approach' for the *design bending moment* in the proposed optimisation approach using Technique 2.

All the data is kept the same as in the above example except that 10-Y16 bars are used instead of 8-Y16 bars.

7.7.2.4.3 Increasing the Quantity of Steel

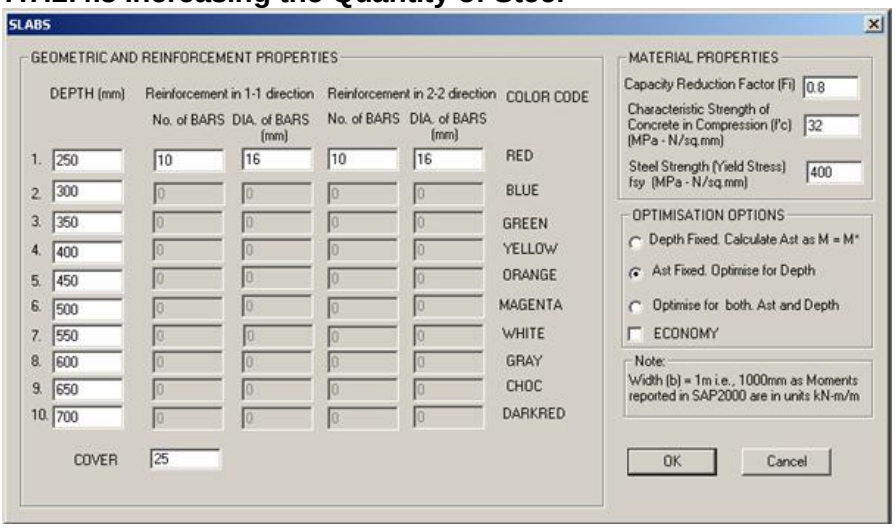

Fig. 7.63. Design Data for Technique 2

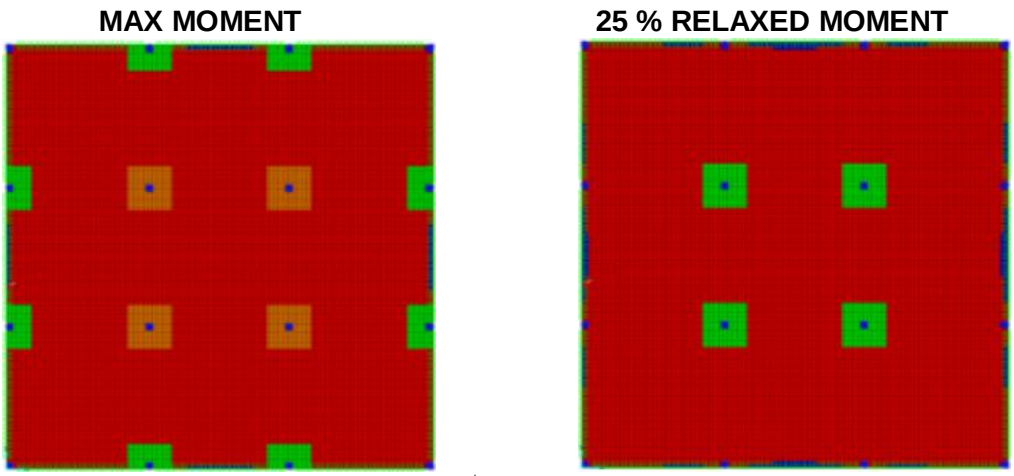

(a) 1st iteration

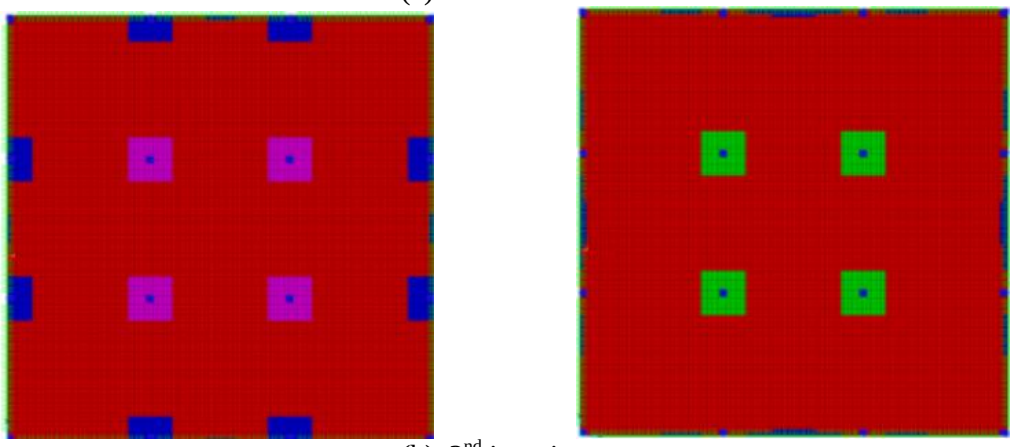

(b) 2nd iteration

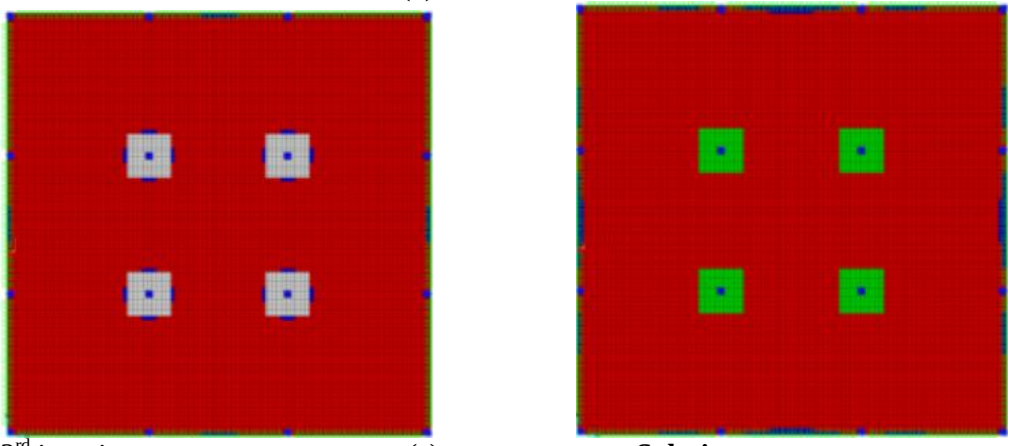

3rd iteration (c) **Solution converges**

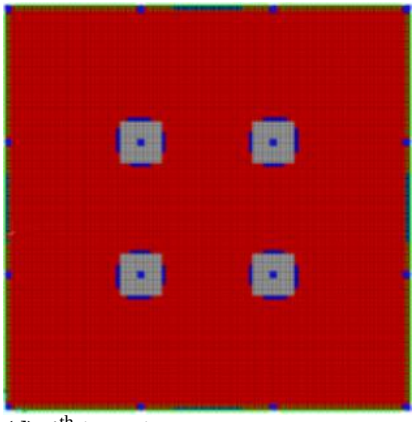

(d) 4th iteration

Fig. 7.64 (a-d).

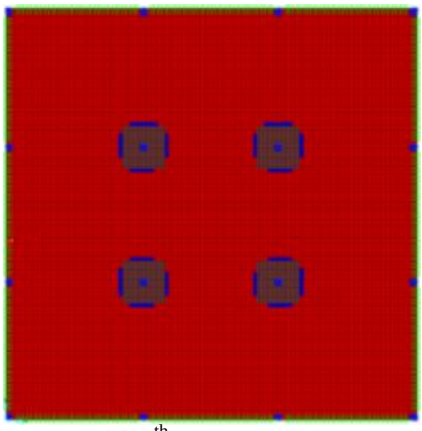

(e) 5th iteration

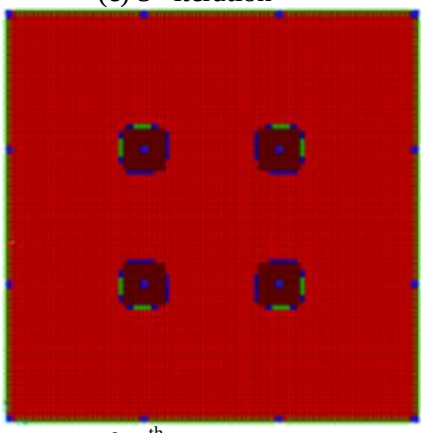

(f) 6th iteration

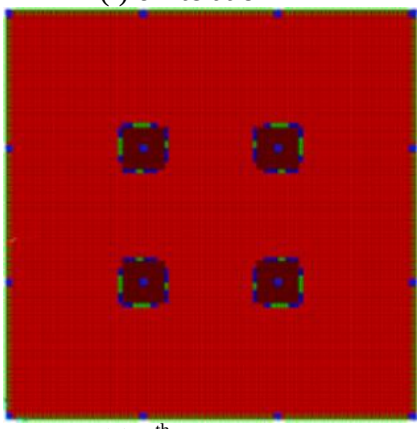

(g) 7th iteration

Fig. 7.64. Comparison With and Without Moment Relaxation between Technique 2 Design Solutions using More Steel

It is seen from the above comparison that when the steel quantity is increased, the design using the relaxed algorithm converges very quickly from the 3rd iteration onwards and settles on a depth of 350 mm (Green color) for the central drop panels. Whereas, if the 'Maximum Moment' in the drop panel is used as the 'design moment', then the solution takes longer to converge and settles on a depth of 700 mm (Dark Red color) from the 7th iteration onwards. This depth is twice that of the depth observed when the relaxation algorithm is employed.

Comparison with 'hand calculations' using the Simplified Method of Design (Appendix B) shows that a depth of 455 mm (Gray colour) with 10-Y16 bars (or 5-Y22 bars) both ways is to be reasonably expected around the central drop panels. This means that the solution obtained using the 'Relaxed Moment' as the design moment is incorrect in this case, when the steel is increased, and therefore inappropriate. Though using the 'Max Moment' as the design moment results in a depth of 700 mm with 10Y16 bars both ways, it is safer compared to the design obtained using the 'Relaxed Moment', which is 350 mm (Green color), almost half the thickness of the thickness observed with 10Y16 bars present. Based on the observations in this example, it is therefore concluded that the 'relaxation algorithm' is not always reliable in designing regions around column supports (i.e. drop panels).

It should be mentioned that through the previous example, the usefulness of the 'relaxation algorithm' in obtaining converged solutions (when lesser steel is used) is seen, however, the role steel quantity plays on convergence is more important than using a 'relaxed moment' as the design moment, which again is confirmed by this example. Therefore, it is again concluded that though the 'relaxation algorithm' helps the optimisation process to converge (in Technique 2); it still does not give a correct rational design for the drop panels. It gives converged designs using Technique 3, but the results for the drop panels could actually be incorrect. It is therefore proposed to avoid the 'relaxation algorithm' for Technique 2 and Technique 3. The 'Maximum Moment' will therefore be chosen as the design moment in all examples and case studies carried out in this work. It will be shown in Chapters 7 and 8 that designs carried out using this approach are safe and perform better (i.e. they are economical) when compared to the industry partner's final designs on his projects.

Through the next example, it is now demonstrated that using the "Average" of the maximum nodal moment values for the group (i.e. drop panel) is not the correct approach in obtaining the design bending moment. The example and data used in the previous example is reproduced for consistency.

7.7.2.4.4 "Average" of the Smoothed Maximum Nodal Moment Values

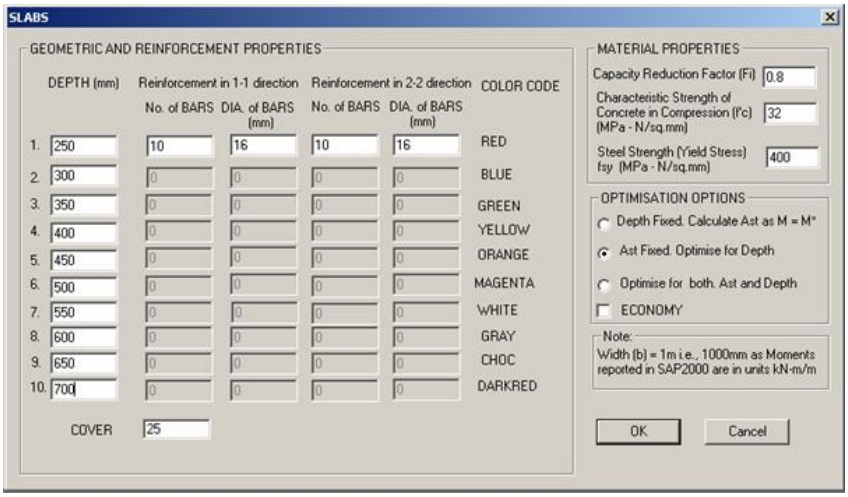

Fig. 7.65. Design Data for Technique 2

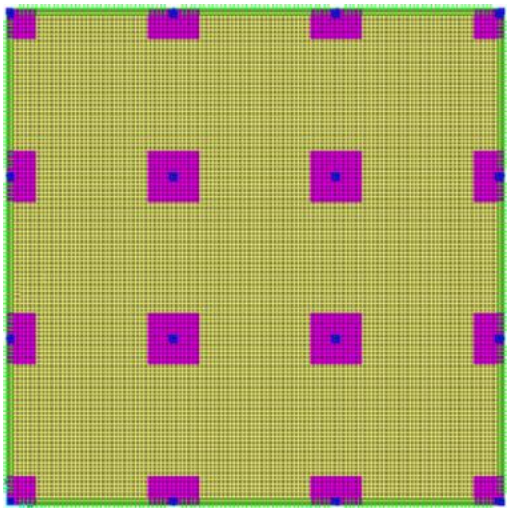

Fig. 7.66. Initial Model

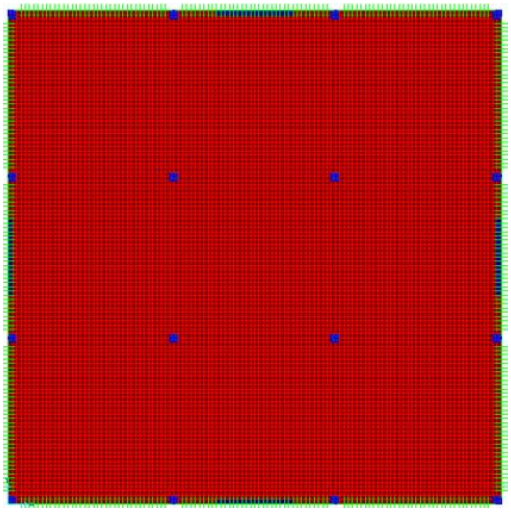

Fig. 7.67. Result when the Average of the Maximum Nodal Moment Values in the panel is chosen

It is seen from the above result, that there are no drop panels observed around the central columns and the first section (250 mm deep – 10 Y16 bars, Red Color) is found to satisfy the moment capacity requirements in all areas of the slab. When compared to the results obtained in the previous example in Section 7.7.2.4.3, it is clear that this is not the correct approach to seeking the thicknesses in various parts of the slab (drop panels will be needed in regions around central columns for 10-Y16 bars). This simple example thus demonstrates the inapplicability of using the average of the maximum nodal moment values for the group (i.e. drop panel) as the design bending moment.

In conclusion, it must be emphasized again that correct and accurate modeling of the structure is a crucial step before proceeding with analysis, design and optimisation in order to obtain realistic designs for the drop panels, as the numerical studies show.

7.7.3 Example of a Symmetrical Flat Slab with UDL Using All Three Techniques

In the following sections, simultaneous *element-wise optimisation* and *panel-wise optimisation* using the proposed approach outlined in section 7.7.1.3 is performed to render the design procedure suitable for practical application. Panels or groups of elements are created over the column supports in the initial model for reasons mentioned in section 7.7.1.3 and the rest of the slab is designed on an element level. It is clear that such an approach needs to be adopted in order to obtain efficient results that converge on a design solution and satisfy the objective function within the specified constraints if the problems associated with optimisation carried out at an element level are to be avoided. For simplification, there is no core or opening in the following flat slab example and a geometrically symmetrical flat slab with UDL is considered. All three techniques are employed. Technique 1 is first employed to find out the steel required in various parts of the slab when the thickness is kept constant throughout the slab. The results obtained using Technique 1 are critically compared with the design obtained by 'hand calculations' using the 'Simplified Method' of design (Appendix A).

7.7.3.1 Technique 1

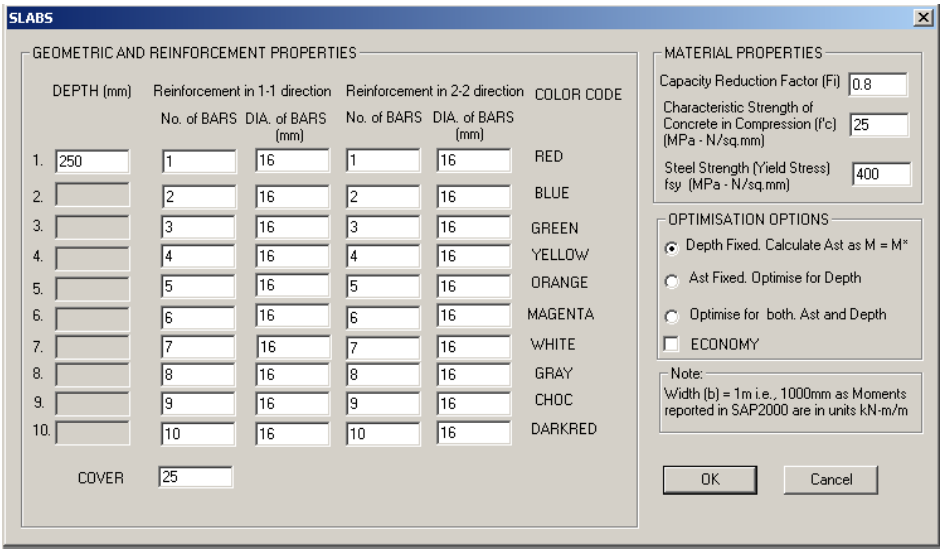

Fig. 7.68. Design Data for Technique 1 (Min-Max Steel de-activated).

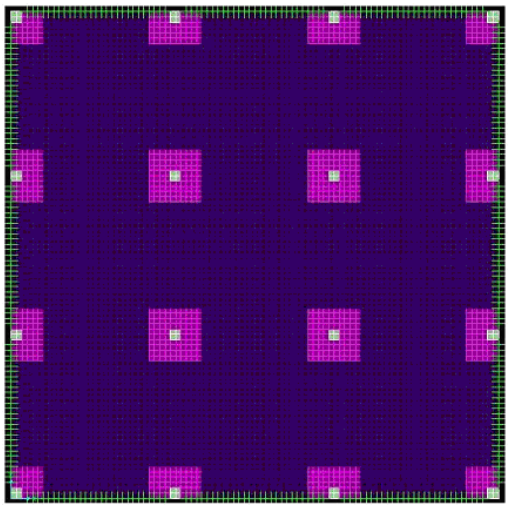

Fig. 7.69. Initial Model (250mm thick). Panels are assigned over columns

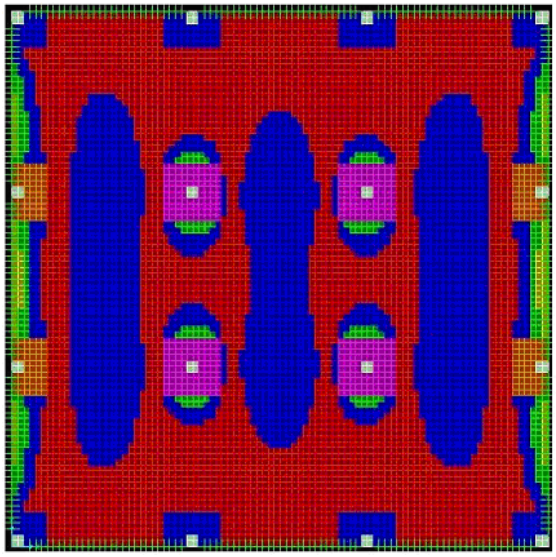

Fig. 7.70. Technique 1 Design Solution showing Steel in X direction

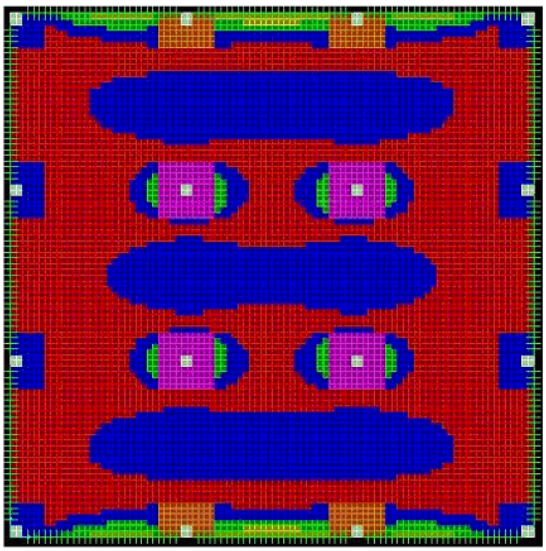

Fig. 7.71. Technique 1 Design Solution showing Steel in Y direction

It is seen that 6-Y16 bars (Magenta color) are required both ways in the drop panels over the central columns whereas 5-Y16 bars (Orange color) are required in the drop panels over the end columns for the respective 1-1 and 2-2 directions. Near the fixed end supports, 3-Y16 bars are required (Green color) followed by 2-Y16 bars (Blue color). Elsewhere in the slab, 1-Y16 bar (Red color) is found sufficient except in the mid-span regions where 2-Y16 bars (Blue color) are required. The steel requirement obtained in this design is comparable to the design obtained using the 'Simplified Method' (Appendix A), especially in regions around the column supports. In other locations of the slab, the 'Simplified Method' shows minimum steel requirement as per AS 3600. It is to be noted that the reinforcement layout obtained using Technique 1 above is not possible in practice, i.e. 1 and 2 bars etc, however this is because the data in the user interface is not validated as per minimum and maximum steel requirements of AS 3600. The intention of this example was to demonstrate a design using Technique 1 that shows the actual steel requirement at various locations in the slab and compare it with the 'Simplified Method' of design. Next, the results obtained when minimum steel requirement and minimum depth requirement for serviceability criterion as per AS 3600 are programmed into validating the data in the user interfaces are shown.

7.7.3.2 Technique 1 (Min – Max Steel)

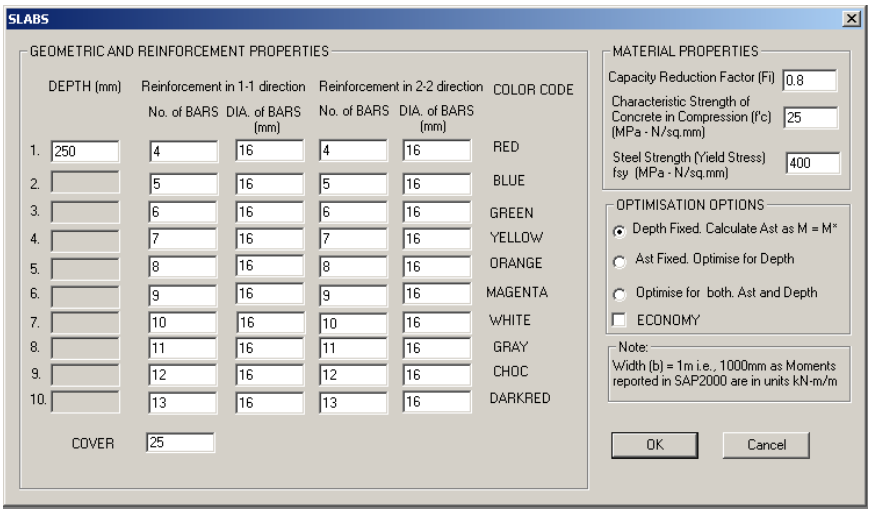

Fig. 7.72. Design Data for Technique 1 - Using Min. Steel (4-Y16)

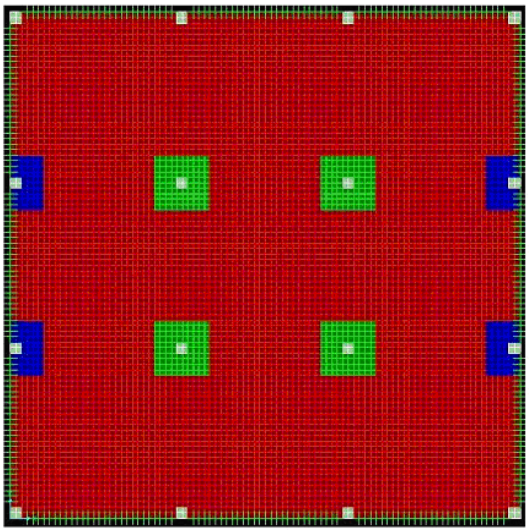

Fig. 7.73. Technique 1 Design Solution showing Steel in X direction

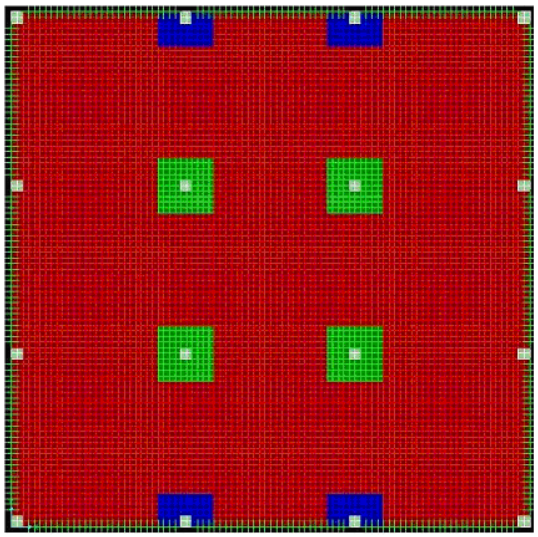

Fig. 7.74. Technique 1 Design Solution showing Steel in Y direction

It is seen from the above results that, as before, for the central drop panels, 6-Y16 bars (Green color) are needed, and for the end drop panels, 5-Y16 bars (Blue color) are needed. In the rest of the slab, minimum steel specified i.e. 4-Y16 (Red color) is required. It is to be noted that even now, sections 7, 8, 9 and 10 in the user interface (Fig. 7.72) do not meet ductility requirements as per AS 3600 (i.e. $k_u > 0.2$). This check is added later to the program to see if excess steel is not specified in the section. If it is, then the user is prompted to revise the section by changing the bar diameter and/or the number of bars. It is therefore observed in both these examples that reliable and comparable (to Simplified Method of Design; Appendix A) solutions are obtained for drop panels. Technique 2 is now employed to the same initial model used in this example.

7.7.3.3 Technique 2 (Steel Constant, Depth Varying)

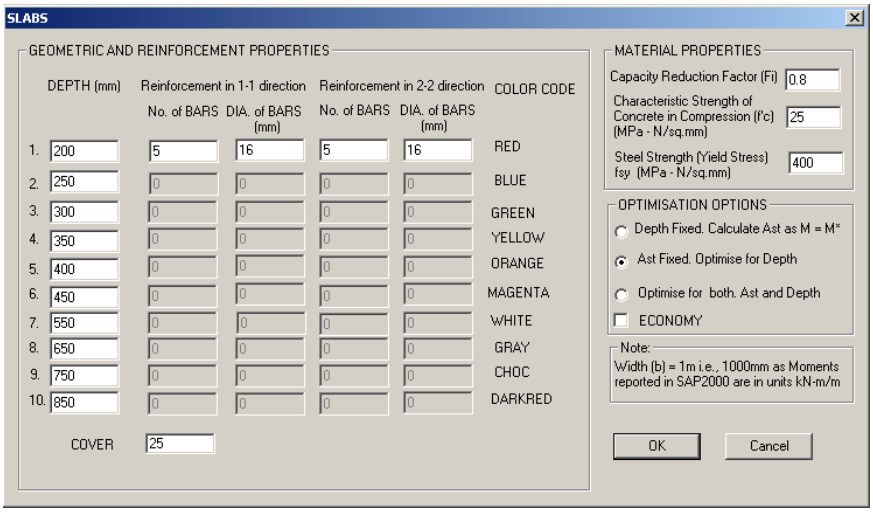

Fig. 7.75. Design Data for Technique 2

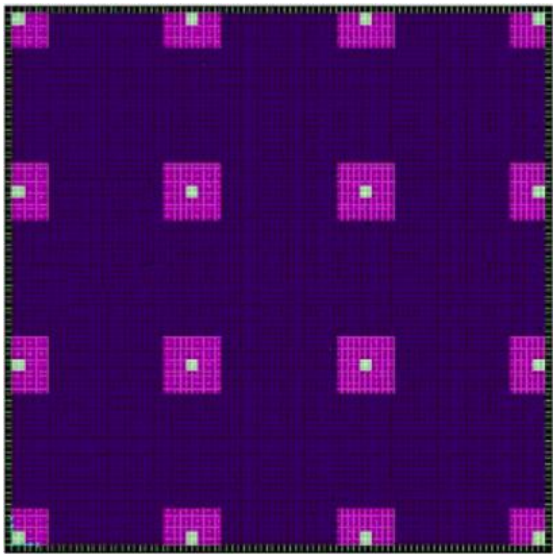

Fig. 7.76. Initial Model (Slab thickness: 250 mm)

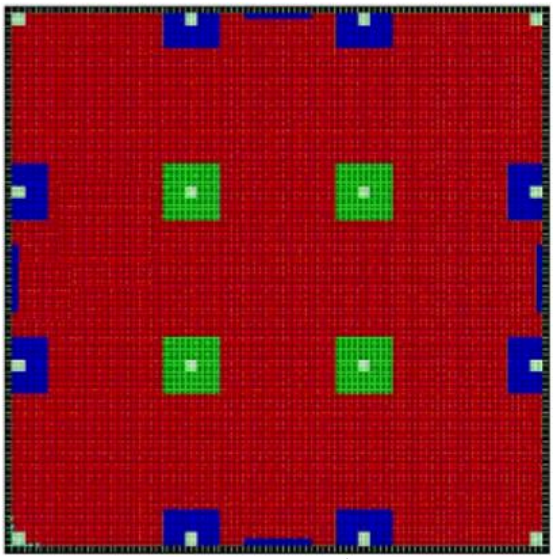

Fig. 7.77 (a) 1st iteration

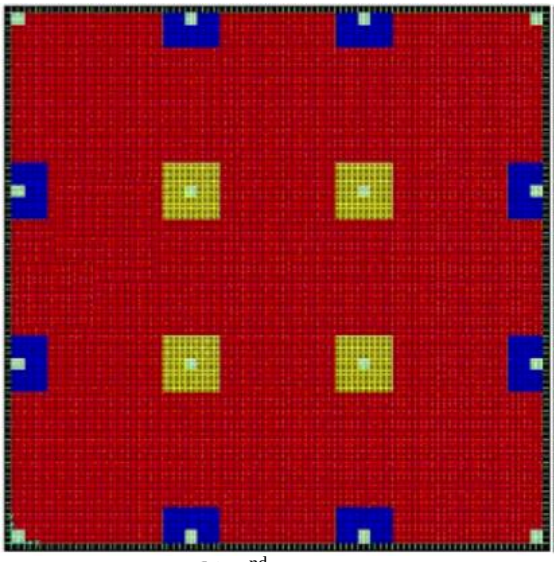

(b) 2nd iteration

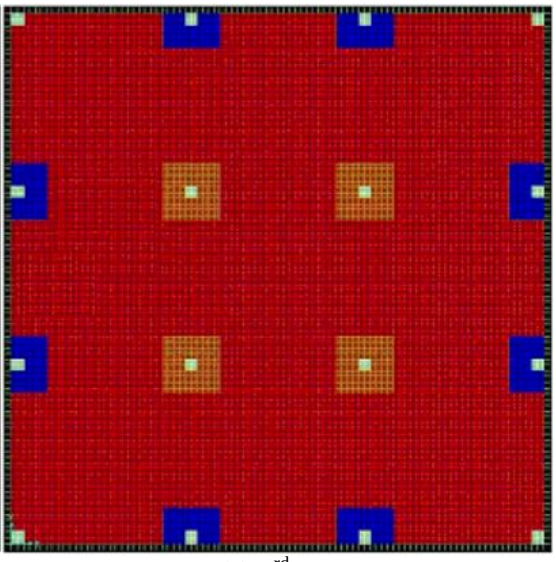

(c) 3rd iteration

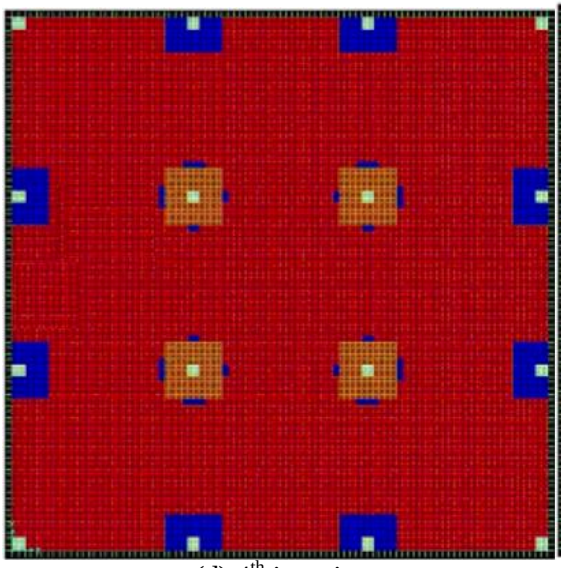

(d) 4th iteration

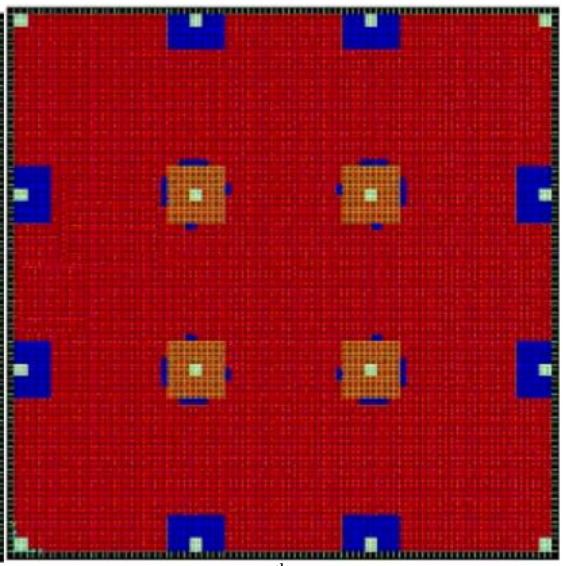

(e) 5th iteration

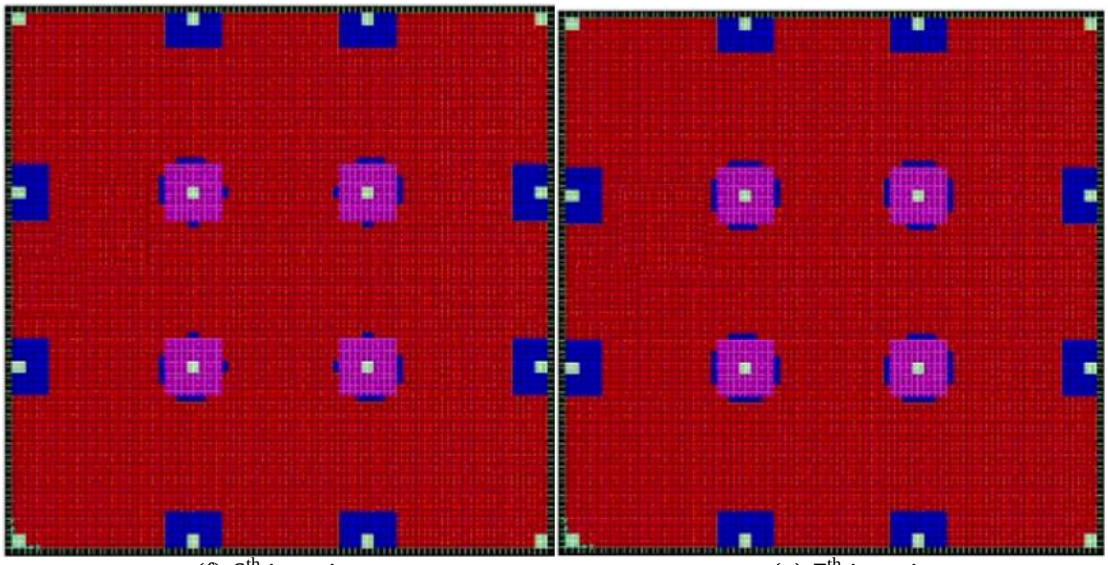

(f) 6th iteration (g) 7th iteration

Fig. 7.77 (b-g). Technique 2 Design Solutions

This graph is based on the table shown on the following page.

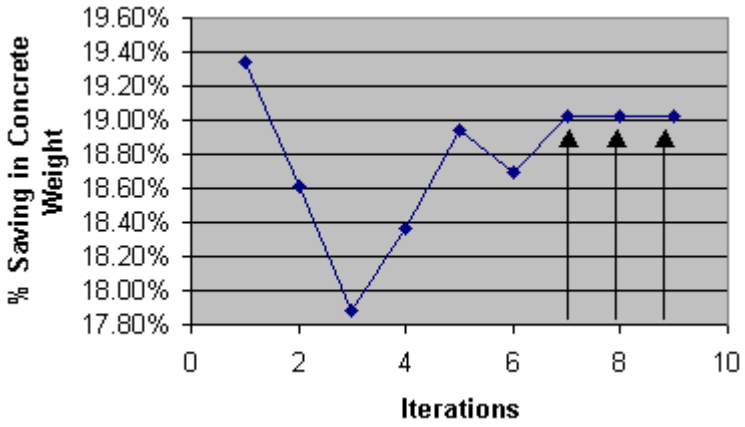

Fig. 7.78. History of Concrete Weight Reduction

Black arrows indicate optimisation has settled on one solution and this solution *satisfies* the moment criterion (% Saving in concrete weight: 19.02 %)

Table 7.12. Technique 2 Design Optimisation Results for the Symmetrical Flat Slab with UDL

Iteration No.	Concrete Weight (Tonne)	% saving in Concrete Weight	Total Steel Weight (Tonne)	% saving in Total Steel Weight	Total Cost of Concrete (AU $)	Total Cost of Steel (AU $)	Max. Deflection (mm) * 3	Permissible Deflection (mm) (Span/250)	Satisfies Condition
Initial Model	188.79	-	2.67 X 2 = 5.34	-	11799.58	5879.43	2.968 x 3 = 8.904	24	-
1	152.27	**19.34 %**	2.67 X 2 = 5.34	-	9517.03	5879.43	3.155 x 3 = 9.465	24	NO
2	153.65	**18.61 %**	2.67 X 2 = 5.34	-	9603.52	5879.43	2.686 x 3 = 8.058	24	NO
3	154.11	**17.88 %**	2.67 X 2 = 5.34	-	9632.36	5879.43	2.487 x 3 = 7.461	24	NO
4	153.20	**18.37 %**	2.67 X 2 = 5.34	-	9574.69	5879.43	2.474 X 3 = 7.422	24	NO
5	153.04	**18.94 %**	2.67 X 2 = 5.34	-	9565.08	5879.43	2.470 X 3 = 7.410	24	NO
6	153.50	**18.69 %**	2.67 X 2 = 5.34	-	9593.91	5879.43	2.478 X 3 = 7.434	24	NO
7	152.88	**19.02 %**	2.67 X 2 = 5.34	-	9555.47	5879.43	2.460 X 3 = 7.38	24	YES
8	152.88	**19.02 %**	2.67 X 2 = 5.34	-	9555.47	5879.43	2.460 X 3 = 7.38	24	YES
9	152.88	**19.02 %**	2.67 X 2 = 5.34	-	9555.47	5879.43	2.460 X 3 = 7.38	24	YES

Note: Factored Max. Deflection is well within permissible limits.

The solution settles from the 7th iteration onwards and all elements satisfy the bending moment criterion thereafter. Again it is seen that when average of the two effective depths is used in calculating the moment capacity of the sections in both orthogonal directions, symmetrical results are obtained. This follows the explanation outlined in Section 7.7.2.1. The central drop panels in this case seem to have settled on a depth of 450 mm (Magenta color), the end panels seem to have settled on a depth of 250 mm (Blue color) and no drop panels are observed at the corners, the boundary conditions being fixed. The design of drop panels looks reasonable and is comparable with the design obtained using the 'Simplified Method of Design' (Appendix A). A saving of 19.02 % is attained in concrete weight compared to the initial model (slight increase compared to the 18.20 % concrete weight saving obtained from the previous example when two different effective depths were used).

Conclusion

Confirming the work in Section 7.7.2.1, this example again demonstrates and explains the symmetrical results obtained for a symmetrical model with uniformly distributed load when average of the two effective depths are used in the calculation of moment capacities of the user-defined sections.

7.7.3.4 Technique 3 - Comparison With and Without Economy

It is now proposed to use the 'Economy' option specified in the user interface to see if a different and economical design is obtained. The 'economy' option is programmed for use with Technique 3 (i.e. both steel and depth varying). When the user ticks the 'Economy' check box, the algorithm chooses the most economical of sections from the ten sections specified by the user satisfying Equation 5.20. In each run, the most economical section is then chosen that satisfies Equation 5.20 and the optimisation continues till a steady state is reached wherein there is no further improvement in the design. If the 'Economy' check box is not ticked however, the program allots sections such that Equation 5.20 is satisfied for all elements in the slab without consideration of economy.

Data in the following comparison is specified such that it satisfies ductility, minimum steel and minimum depth requirements.

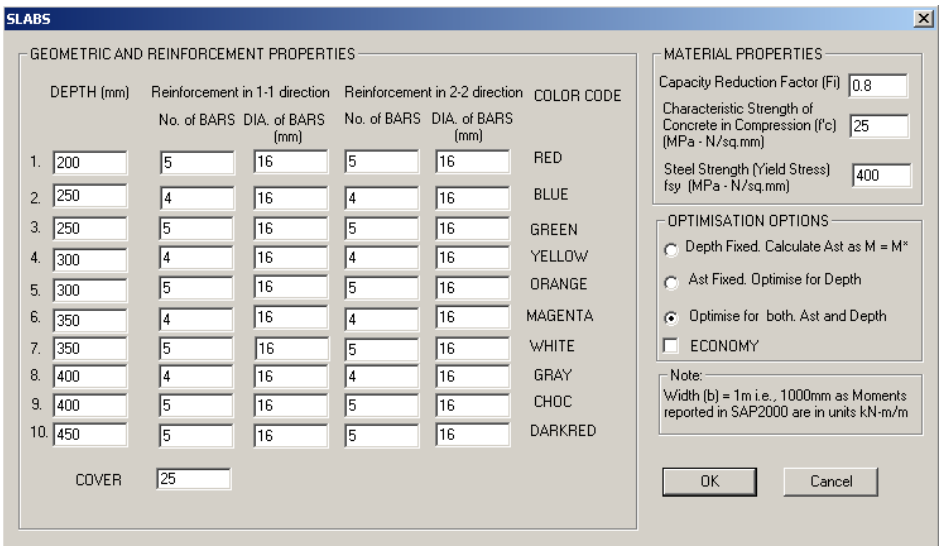

Fig. 7.79. Design Data for Technique 3 – **NO ECONOMY (Economy check box is unchecked above).** Note that bar diameter is kept same for all sections.

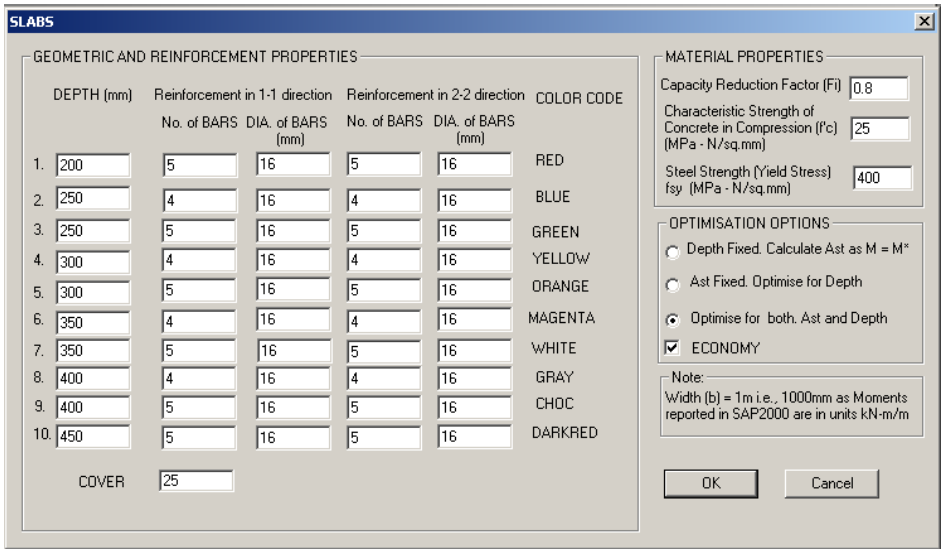

Fig. 7.80. Design Data for Technique 3 - **ECONOMY (Economy check box is checked above)**

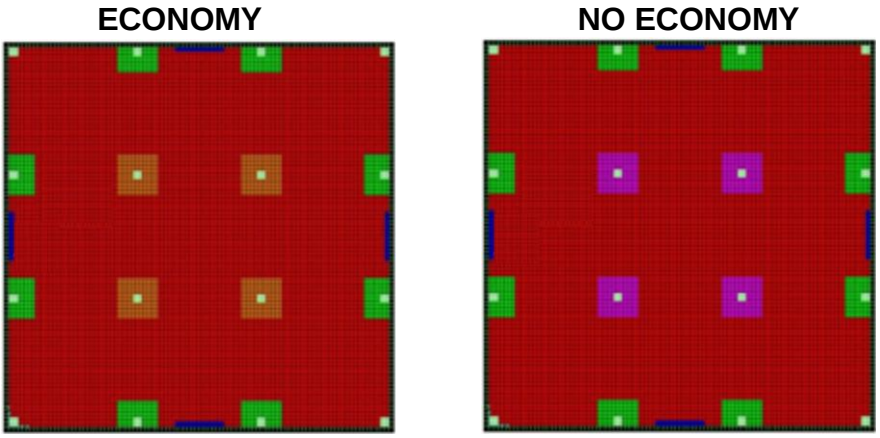

Fig. 7.81 (a) 1st iteration

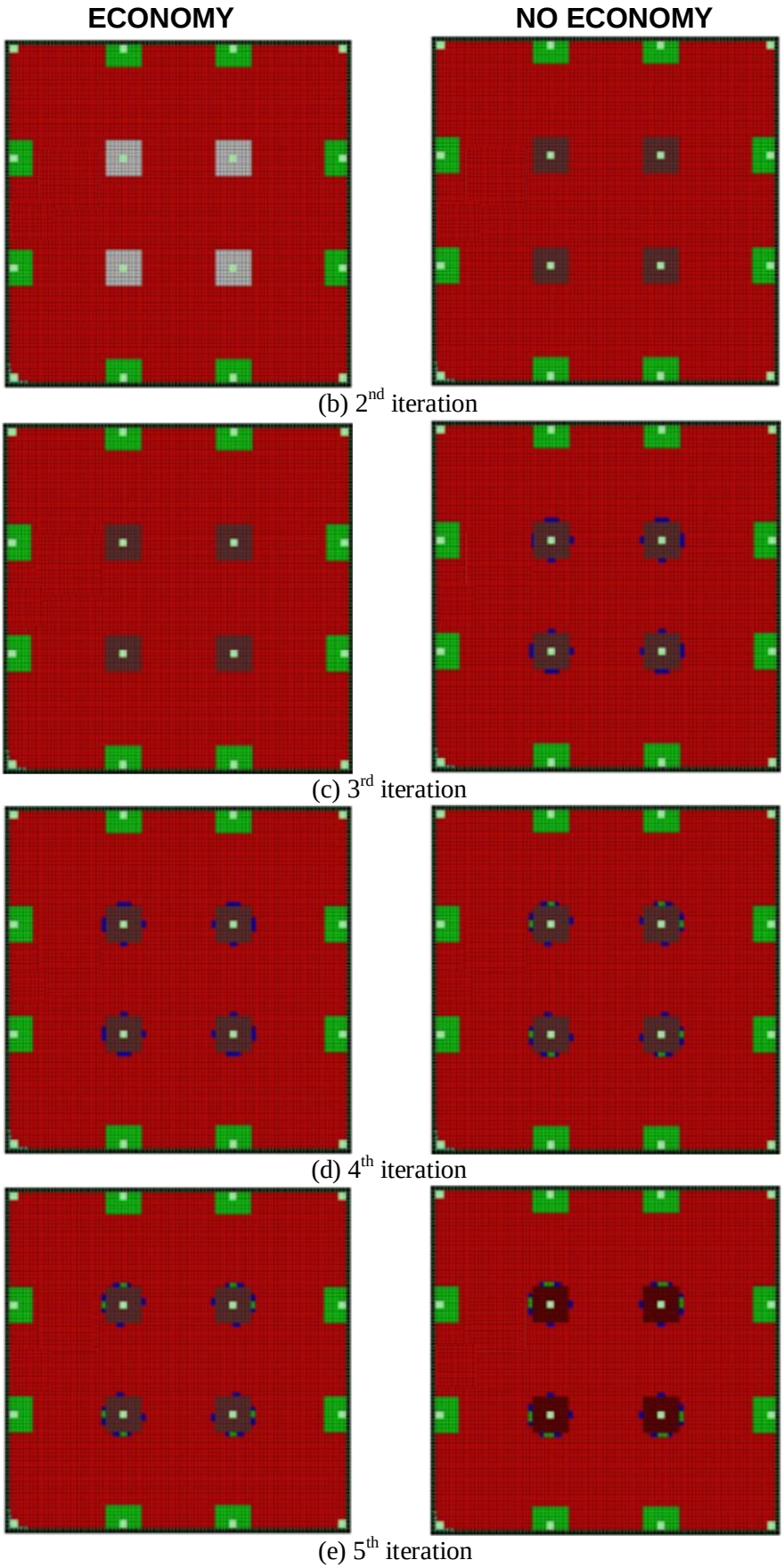

(b) 2nd iteration

(c) 3rd iteration

(d) 4th iteration

(e) 5th iteration

Fig. 7.81 (b – e)

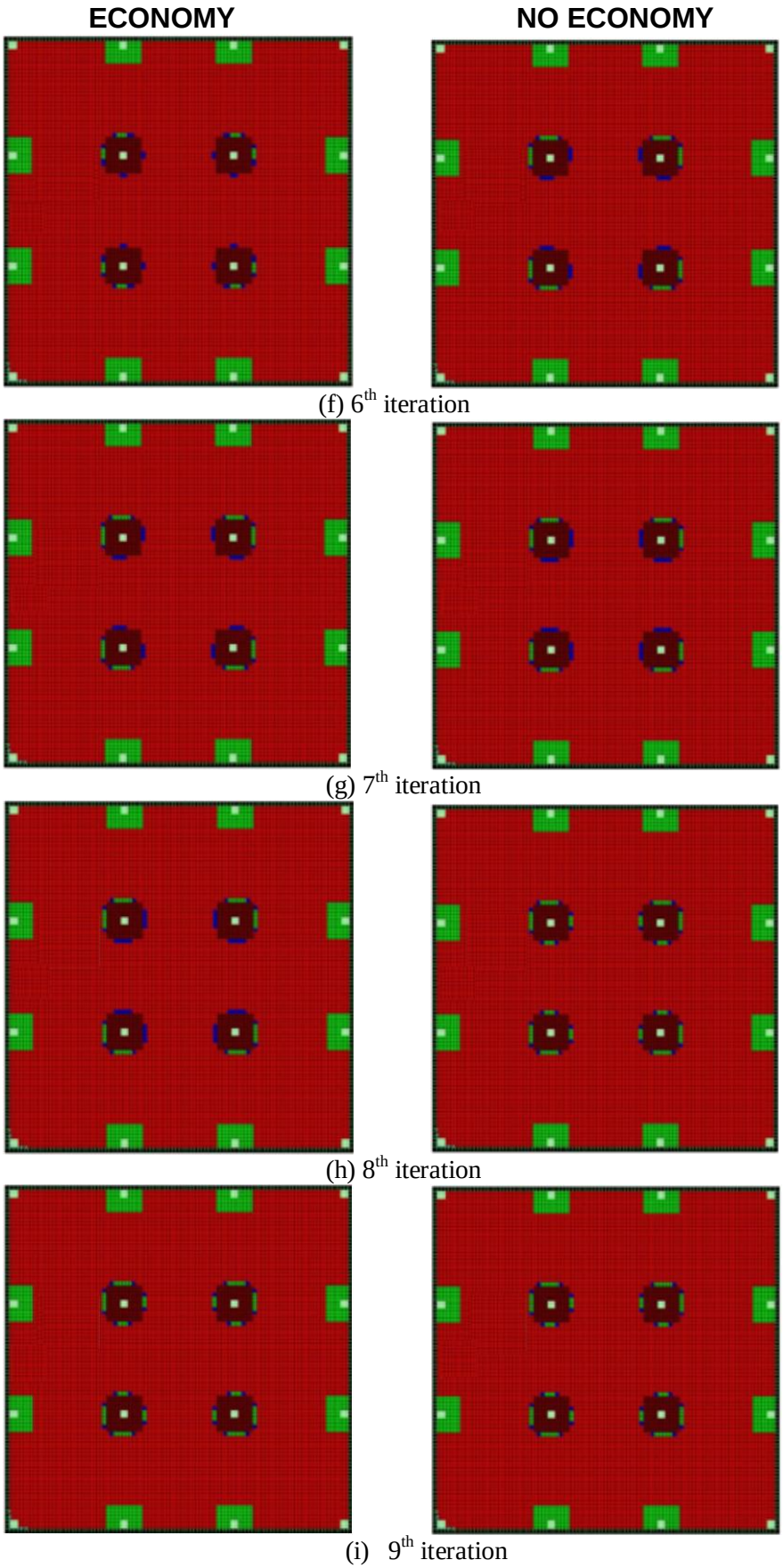

Fig. 7.81. Comparison between Economical and Uneconomical Technique 3 Designs

The solution in both cases settles from the 9th iteration onwards. It is seen from the above results and from the information in the following two tables, that the optimal solution in this case is the same when the 'Economy' button is checked and when it is not checked. However, the thickness of the central drop panels in each iteration is different for both cases. For example, in the very first iteration, the algorithm selects a section of *300 mm* depth with *5-Y16* bars both ways (*Orange Color*) for the central drop panels when the economy button is checked. Whereas, when the economy button is not checked, a section of *350 mm* depth with *4-Y16* bars both ways (*Magenta Color*) is chosen by the algorithm. It is clear that the "Orange" section is economical than the "Magenta" section. Both sections satisfy Equation 5.20, however as the "Orange" section is economical than the "Magenta" section it is chosen when the 'Economy' button is checked. The sections specified for this model are such that they satisfy ductility, minimum steel and minimum depth requirements of AS 3600; different designs are not obtained in other parts of the slab. If AS 3600 provisions are not followed, different designs for either case can be obtained that show substantial material savings when the economy button is checked and when it is not. However, these designs would not be useful from a practical perspective. It is important to note that optimal solutions for either case will depend on many factors such as:

- Type of slab: Single span one-way slab, continuous slab, flat slab etc
- Type of end support condition: free, fixed, wall, perimeter beam etc
- Loads
- Design data provided by the user in the user interfaces: To gain substantial material savings using the 'Economy' option, there should really be the facility to provide more than 10 sections in the user interface.
- Whether the design should meet AS 3600 code provisions. If yes, the above results are obtained. If not, unreasonable depths such as 50mm, 100 mm etc and lesser steel for this span and loading can be specified. It would definitely show different designs (having severe central deflections) with substantial savings in material cost. However, such a design would not be useful from a practical point of view, as it would not satisfy AS 3600 code requirements.

The economy in this case is really actually compared based on the thickness of the central drop panels. As a result, there is not much of a difference obtained, though small differences in concrete weight saving are seen in the initial few iterations when the economy button is checked.

Conclusion

This example demonstrates the potential of designing slabs based on not only the moment capacity criterion but also based on material cost considerations in the optimisation process.

Table 7.13. Technique 3 Design Optimisation Results for Economy

Iteration No.	Concrete Weight (Tonne)	% Saving in Concrete Weight compared to Initial Model	Total Steel Weight (Tonne)	% saving in Total Steel Weight compared to Initial Model	Total Cost of Concrete (AU $)	Total Cost of Steel (AU $)	TOTAL COST (AU $)	Max. Deflection (mm) * 3	Permissible Deflection (mm) (Span/250)	Satisfies Condition
Initial Model	188.79	-	5.505	-	11799.58	6055.5	17855.08	2.968 x 3 = 8.904	24	-
1	152.272	19.34 %	5.341	2.98 %	9517.00	5875.1	15392.10	3.155 x 3 = 9.465	24	NO
2	153.656	18.61 %	5.344	2.92 %	9603.50	5878.4	15481.90	2.686 x 3 = 8.058	24	NO
3	154.117	18.36 %	5.344	2.92 %	9632.31	5878.4	15510.71	2.487 x 3 = 7.461	24	NO
4	153.195	18.85 %	5.341	2.98 %	9574.68	5875.1	15449.78	2.474 X 3 = 7.422	24	NO
5	153.041	18.93 %	5.342	2.96 %	9565.06	5876.2	15441.26	2.470 X 3 = 7.410	24	NO
6	153.348	18.77 %	5.342	2.96 %	9584.25	5876.2	15460.45	2.478 X 3 = 7.434	24	NO
7	152.887	19.02 %	5.341	2.98 %	9555.43	5875.1	15430.53	2.460 X 3 = 7.38	24	NO
8	152.733	19.10 %	5.341	2.98 %	9545.81	5875.1	15420.91	2.31 X 3 = 6.93	24	NO
9	152.733	19.10 %	5.342	2.96 %	9545.81	5876.2	15422.01	2.31 X 3 = 6.93	24	YES

Table 7.14. Technique 3 Design Optimisation Results without Economical Considerations

Iteration No.	Concrete Weight (Tonne)	% saving in Concrete Weight	Total Steel Weight (Tonne)	% saving in Total Steel Weight	Total Cost of Concrete (AU $)	Total Cost of Steel (AU $)	TOTAL COST (AU $)	Max. Deflection (mm) * 3	Permissible Deflection (mm) (Span/250)	Satisfies Condition
Initial Model	188.79	-	5.505	-	11799.58			2.968 x 3 = 8.904	24	-
1	152.733	19.10 %	5.292	3.87 %	9545.86	5821.64	15367.50	3.155 x 3 = 9.465	24	NO
2	154.117	18.37 %	5.343	2.94 %	9632.36	5877.76	15510.12	2.686 x 3 = 8.058	24	NO
3	153.20	18.85 %	5.340	3.00 %	9574.70	5874.98	15449.68	2.487 x 3 = 7.461	24	NO
4	153.04	18.94 %	5.341	2.98 %	9565.08	5875.54	15440.62	2.474 X 3 = 7.422	24	NO
5	153.348	18.77 %	5.341	2.98 %	9584.306	5875.54	15459.86	2.470 X 3 = 7.410	24	NO
6	152.887	19.02 %	5.341	2.98 %	9555.47	5875.54	15431.01	2.478 X 3 = 7.434	24	NO
7	152.73	19.10 %	5.34	3.00 %	9545.86	5874.98	15420.84	2.460 X 3 = 7.38	24	NO
8	152.73	19.10 %	5.342	2.96 %	9545.86	5876.65	15422.51	2.31 X 3 = 6.93	24	YES
9	152.73	19.10 %	5.342	2.96 %	9545.86	5876.65	15422.51	2.31 X 3 = 6.93	24	YES

7.8 CASE STUDIES

7.8.1 Industry Partner's 8.4m x 8.4m model

Span: 8.4m c/c both ways; *Load: DL:* 1kPa + Self-wt; *LL:* 5kPa; *Load Combo:* 1.25DL + 1.5LL; *Column size:* 450 x 450mm; *Initial Slab Thickness:* 350mm; *Total Number of elements:* 13456

7.8.1.1 Ends Fixed – TECHNIQUE 3

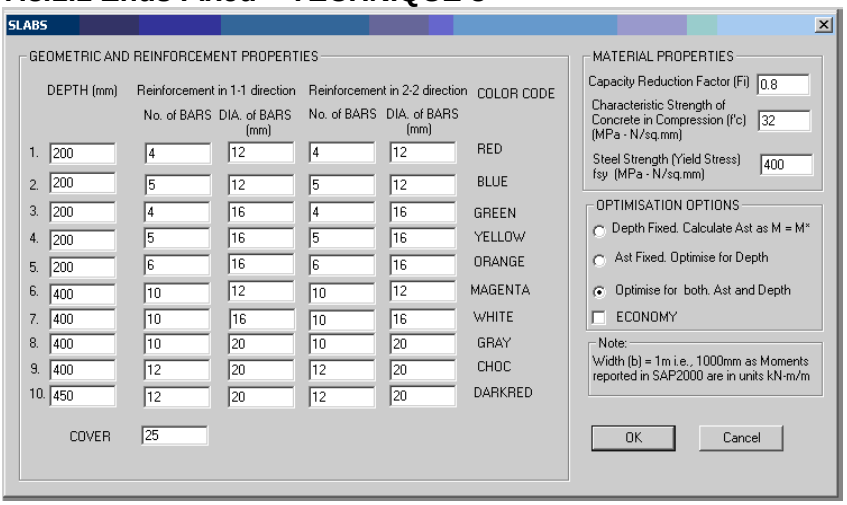

Fig. 7.82. Design Data for Technique 3

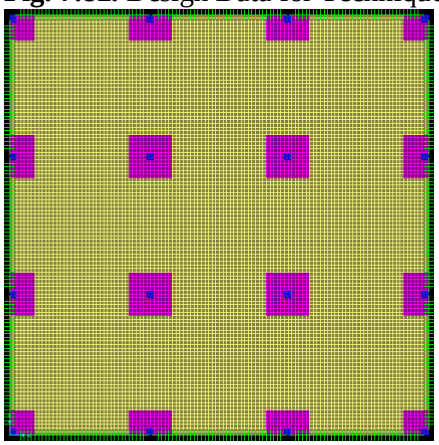

Fig. 7.83. Initial Model

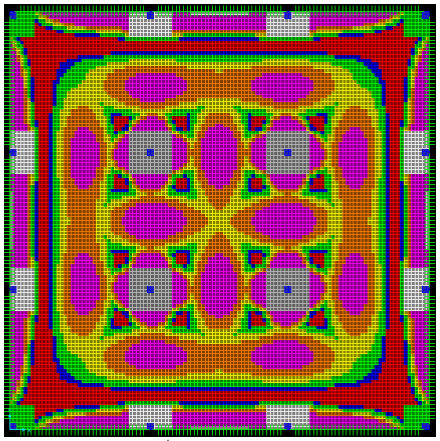

(a) 1st iteration

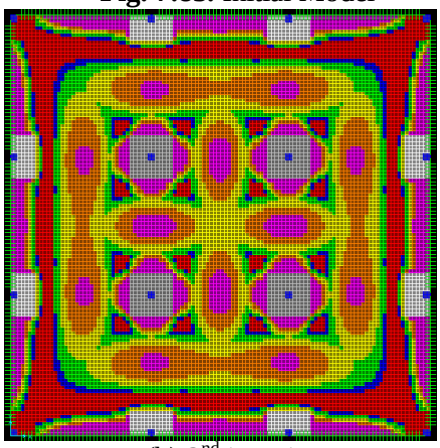

(b) 2nd iteration

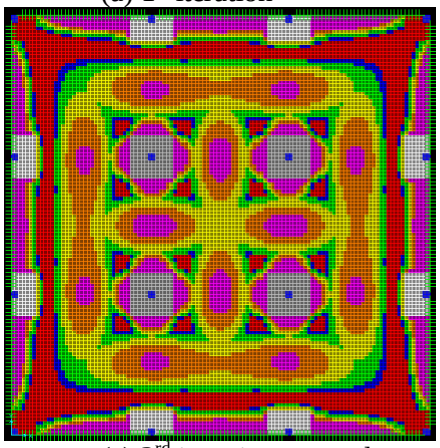

(c) 3rd iteration onwards

Fig. 7.84. Technique 3 Design Solutions

Table 7.15. Technique 3 Design Optimisation Results

Iteration No.	Concrete Weight (Tonne)	% saving in Concrete Weight	Total Steel Weight (Tonne)	% saving in Total Steel Weight	Total Cost of Concrete (AU $)	Total Cost of Steel (AU $)	TOTAL COST (AU $)	Max. Deflection (mm) * 3	Permissible Deflection (mm) (Span/250)	Satisfies Condition
Initial Model	572.86	-	9.20	-	35803.75	10120.00	45923.75	2.968 x 3 = 8.904	24	-
1	433.802	24.27 %	4.18	54.57 %	27112.63	4598.59	31711.22	3.155 x 3 = 9.465	24	NO
2	426.704	25.51 %	4.16	54.78 %	26669.00	4576.06	31245.06	2.686 x 3 = 8.058	24	YES
3	426.704	25.51 %	4.16	54.78 %	26669.00	4576.06	31245.06	2.487 x 3 = 7.461	24	YES
4	426.704	25.51 %	4.16	54.78 %	26669.00	4576.06	31245.06	2.474 X 3 = 7.422	24	YES
5	426.704	25.51 %	4.16	54.78 %	26669.00	4576.06	31245.06	2.470 X 3 = 7.410	24	YES
6	426.704	25.51 %	4.16	54.78 %	26669.00	4576.06	31245.06	2.478 X 3 = 7.434	24	YES
7	426.704	25.51 %	4.16	54.78 %	26669.00	4576.06	31245.06	2.460 X 3 = 7.38	24	YES
8	426.704	25.51 %	4.16	54.78 %	26669.00	4576.06	31245.06	2.31 X 3 = 6.93	24	YES
9	426.704	25.51 %	4.16	54.78 %	26669.00	4576.06	31245.06	2.31 X 3 = 6.93	24	YES

Note: Total Steel Weight of Initial Model is the weight of steel obtained using Technique 1. If the weight of steel obtained from the industry partner's design is compared, it should result in even more savings. This also demonstrates the effectiveness of Technique 3 over Technique 1 (or conventional design) in terms of material saving.

The solution settles and stabilizes from the 3rd iteration onwards. The optimal solution satisfies the bending moment constraint for all elements in the slab. It is seen from the above results, that a section of 400 mm depth with 10 – Y20 bars both ways (Gray color) is required for the central drop panels. Compared to hand calculations using the 'Simplified Method of Design' (Appendix B), this looks reasonable. All the end drop panels have settled on a section of 400 mm depth with 10 – Y16 bars both ways (White Color). The corner drop panels have settled on a section of 200 mm depth with 4 – Y12 bars both ways (Red color). This example especially demonstrates the usefulness of using *element-wise optimisation* and *panel-wise optimisation* in tandem. The panels are needed in order to avoid problems outlined in Section 7.7.1 and for the solution to converge. Even the *element-wise optimisation* results in other parts of the slab show a clear and distinct pattern of the sections required. A Magenta color indicates that at all the fixed ends, a section of 400 mm depth with 10 - Y12 bars is needed. The Red color indicates that minimum material is required in this region, 200 mm depth with 4 – Y12 bars. The mid-span region generally requires sections of Yellow, i.e. 200 mm depth with 5 – Y16 bars, with more material needed in the region where the sagging bending moment is the highest, Magenta color (400 – 10Y12) surrounded by Orange color (200 – 6Y16). In the region immediately surrounding the central drop panels, a section with the same depth as the drop panels but with lesser steel is seen, 400 mm depth with 10 - Y12 bars is needed (Magenta color). At the four corners of each central drop panel, symmetric triangles of minimum material are observed in the form of Red and Blue colors. A perfectly symmetric and converged solution is obtained that shows significant savings in concrete and steel weight compared to both the initial model and the industry partner's design. The results are tabulated in Table 7.15 above.

At this point it should be mentioned that in order to get the above results, it is important to give the correct data in the user interface so as to get a distinct visible pattern of different sections throughout the slab. Giving the correct data in the user interface is essentially a trial-and-error process unless the final design for the slab is obtained. In the case above, the design data given is based on studying the industry partner's final design for this slab. The design above is compared with the industry partner's final design for this slab in section 7.8.1.3.

7.8.1.2 ENDS FREE – TECHNIQUE 3

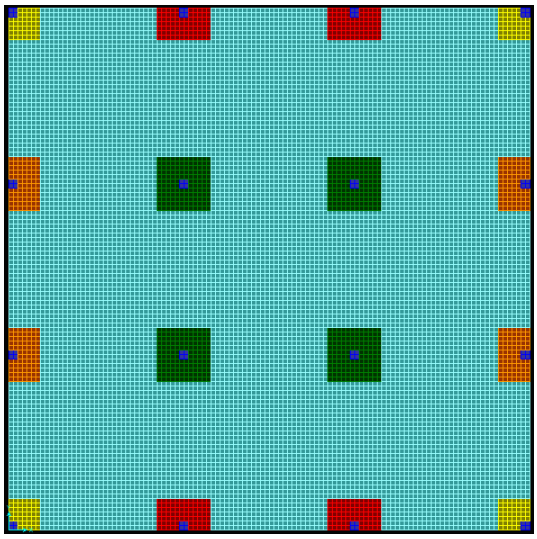

Fig. 7.85. New Initial Model

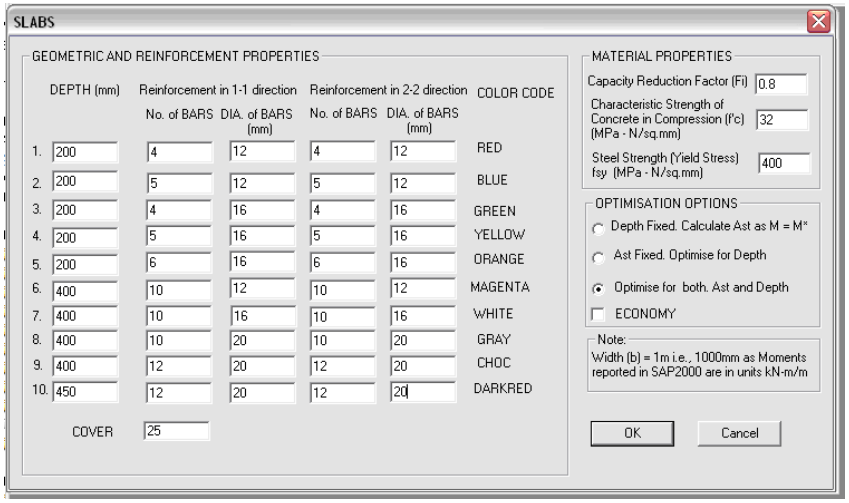

Fig. 7.86. Design Data for Technique 3

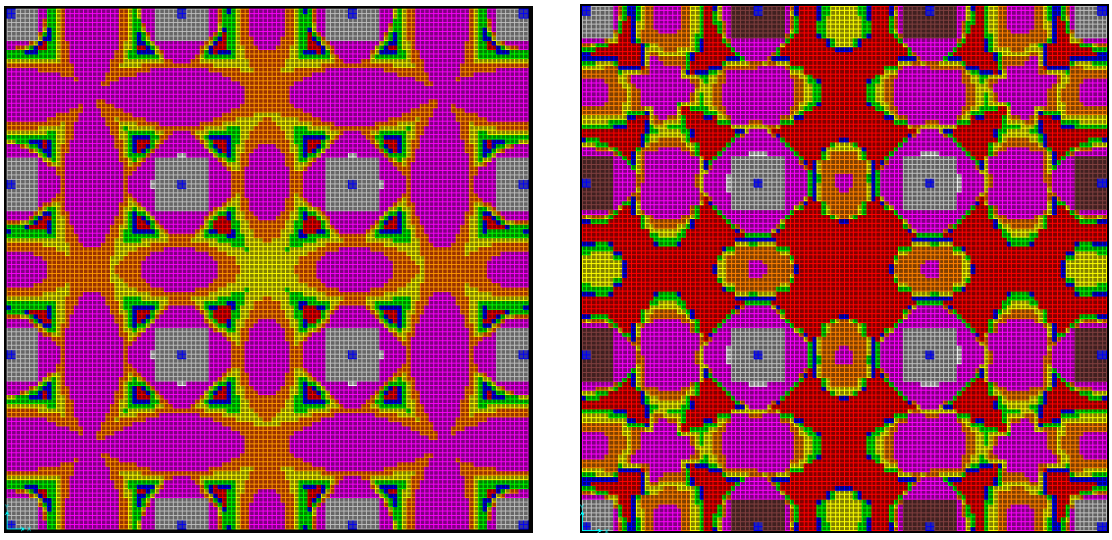

(a) 1st iteration (b) 2nd iteration

Fig. 7.87 (a-b).

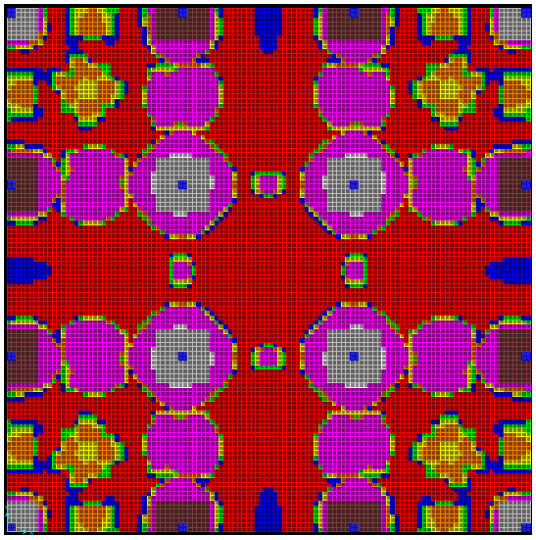

(c) 3rd iteration

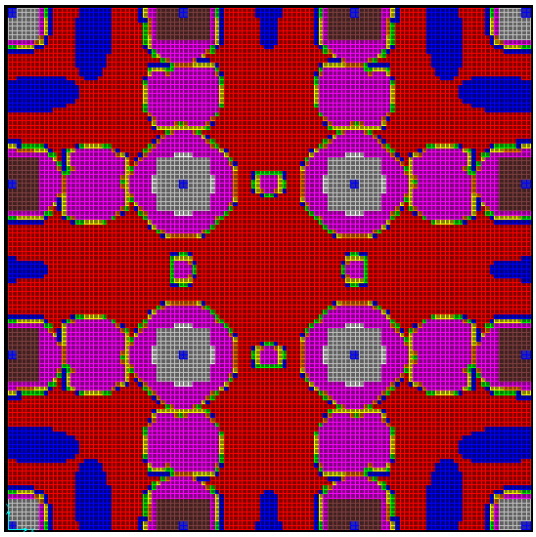

(d) 4th iteration

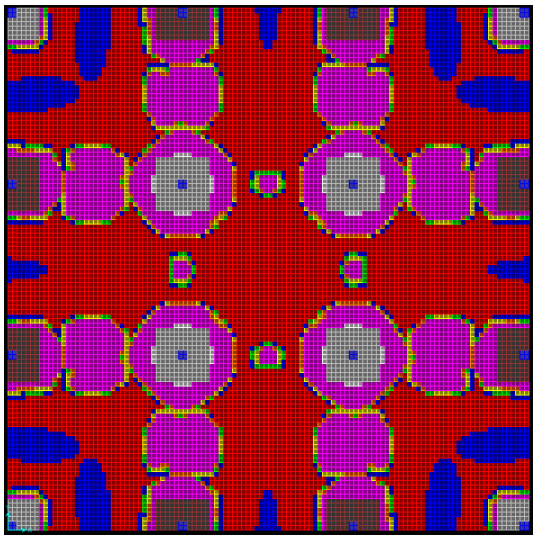

(e) 5th iteration

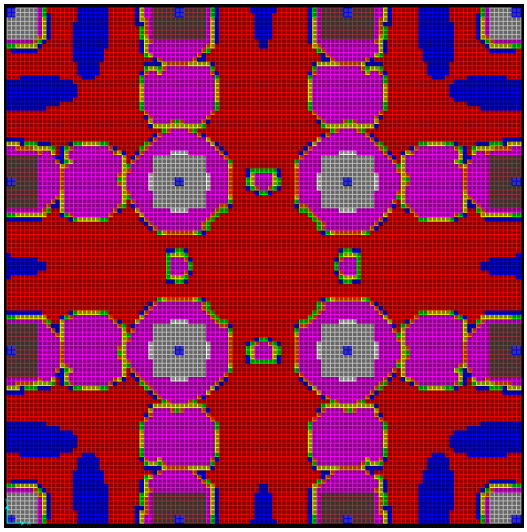

(f) 6th iteration

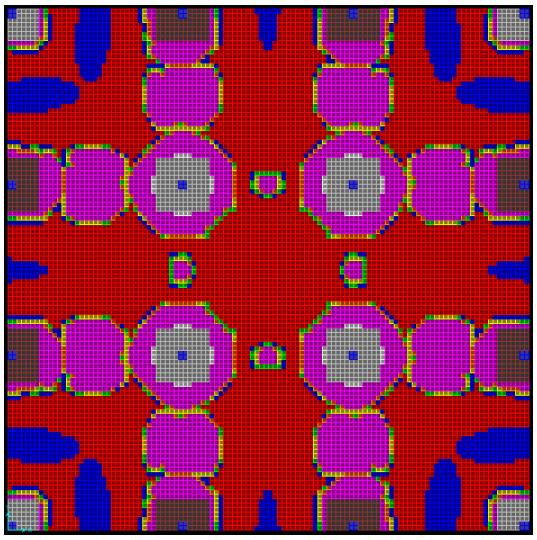

(g) 7th iteration

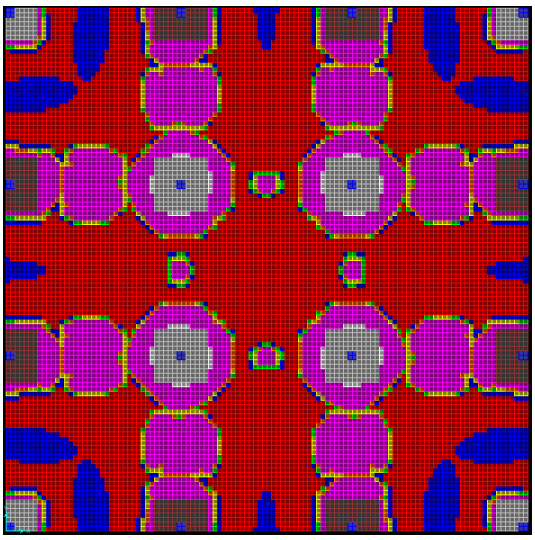

(h) 8th iteration

Fig. 7.87 (c-h).

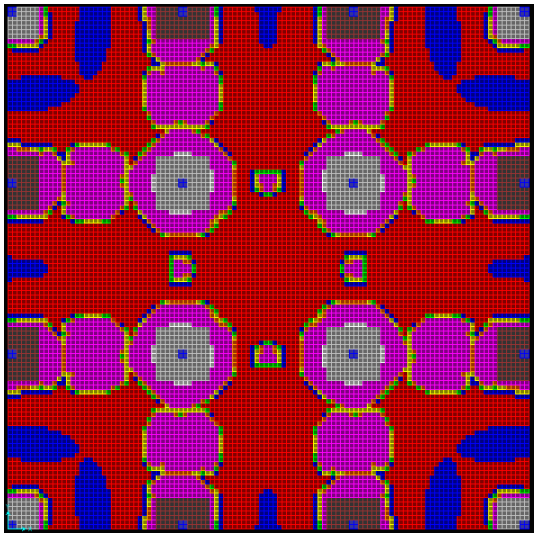

(i) 9th iteration

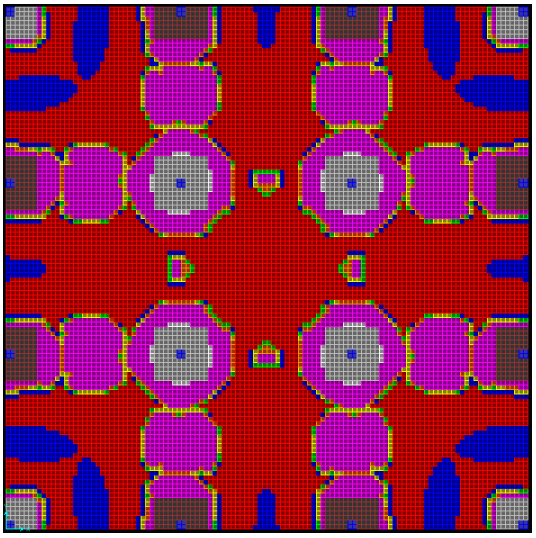

(j) 10th iteration

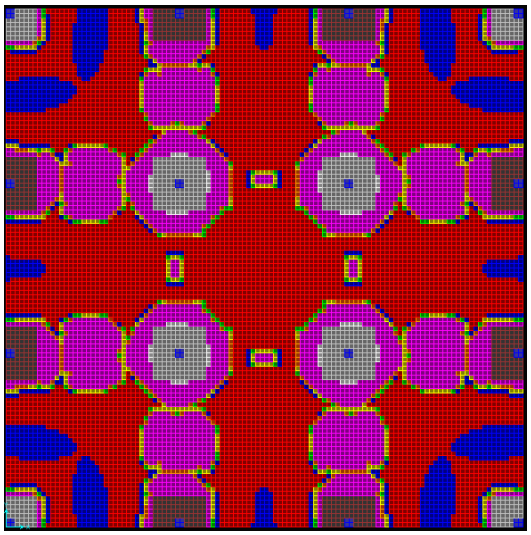

(k) 11th iteration

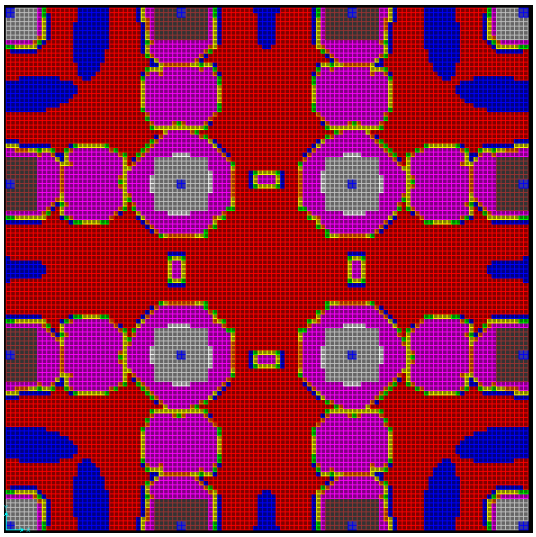

(l) 12th iteration

Fig. 7.87. Technique 3 Design Solutions

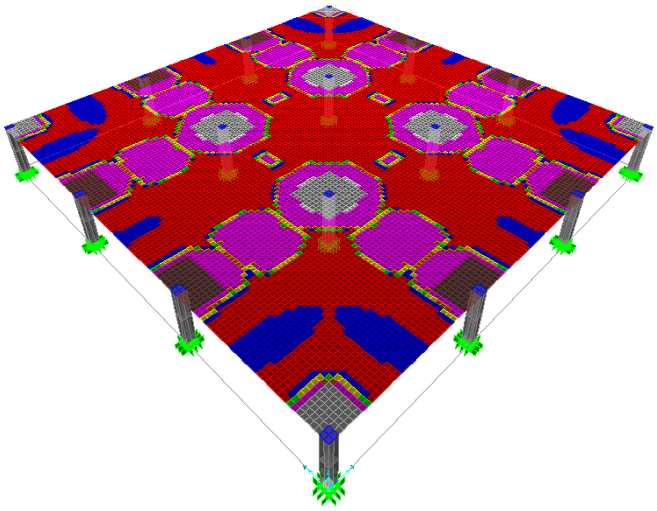

Fig. 7.88. Optimal Solution (at 12th iteration)

The solution settles and stabilizes from the 12th iteration onwards. The optimal solution satisfies the bending moment criterion for all elements in the slab. A distinctly thick pattern is seen around the interior and edge columns shown by Magenta color indicating a depth of 400 mm with 10 –Y12 bars both ways. The interior column and corner column drop panels require a section of 400 mm depth with 10-Y20 bars shown by Grey color. The edge column drop panels require a section 400 mm depth with 12-Y20 bars shown by Choc color. A thicker region is seen in the mid-span of the external spans in both directions show by Magenta color indicating a depth of 400 mm with 10 –Y12 bars both ways. For the rest of the slab the first section shown by Red indicating a depth of 200 mm with 4-Y12 bars is found sufficient with Blue (indicating 5Y12 bars) needed in some sections. It is to be remembered that the solutions are based on the design data given in the user interface and as such, a different set of data will result in a different design. The optimal solution in this case too shows significant material savings compared to the material required using Technique 1 (conventional design). The effect of boundary conditions (fixed or free) on the final solution is clearly seen from the above two examples. In both cases, different designs are obtained when the boundary conditions are changed.

Table 7.16. Technique 3 Design Optimisation Results

Iteration No.	Concrete Weight (Tonne)	% saving in Concrete Weight	Total Steel Weight (Tonne)	% saving in Total Steel Weight	Total Cost of Concrete (AU $)	Total Cost of Steel (AU $)	TOTAL COST (AU $)	Max. Deflection (mm) * 3	Permissible Deflection (mm) (Span/250)	Satisfies Condition
Initial Model	572.86	-	8.80	-	35803.75	9680.00	45483.75	7.52 x 3 = 22.56	33.60	-
1	509.70	9.07 %	6.67	24.20 %	31856.25	7336.92	39193.17	6.75 x 3 = 20.25	33.60	NO
2	449.07	21.61 %	5.80	34.09 %	28066.88	6381.30	34448.18	8.09 x 3 = 24.27	33.60	NO
3	435.06	24.05 %	5.17	41.25 %	27191.25	5687.25	32878.50	8.87 x 3 = 26.61	33.60	NO
4	437.59	23.61 %	4.94	43.86 %	27349.38	5434.13	32783.51	8.77 x 3 = 26.31	33.60	NO
5	438.57	23.44 %	4.96	43.64 %	27410.63	5457.26	32867.89	8.75 x 3 = 26.25	33.60	NO
6	438.76	23.41 %	4.96	43.64 %	27422.50	5461.32	32883.82	8.73 x 3 = 26.19	33.60	NO
7	439.54	23.27 %	4.97	43.52 %	27471.25	5465.06	32936.31	8.72 x 3 = 26.16	33.60	NO
8	439.73	23.24 %	4.97	43.52 %	27483.13	5470.88	32954.01	8.72 x 3 = 26.16	33.60	NO
9	439.34	23.31 %	4.97	43.52 %	27458.75	5468.96	32927.71	8.72 x 3 = 26.16	33.60	NO
10	438.76	23.41 %	4.97	43.52 %	27422.50	5465.56	32888.06	8.72 x 3 = 26.16	33.60	NO
11	438.95	23.38 %	4.96	43.64 %	27434.38	5455.91	32890.29	8.72 x 3 = 26.16	33.60	YES
12	438.95	23.38 %	4.96	43.64 %	27434.38	5455.91	32890.29	8.72 x 3 = 26.16	33.60	YES

7.8.1.3 Comparison with Industry Partner's Final Design Based on Conventional Approach

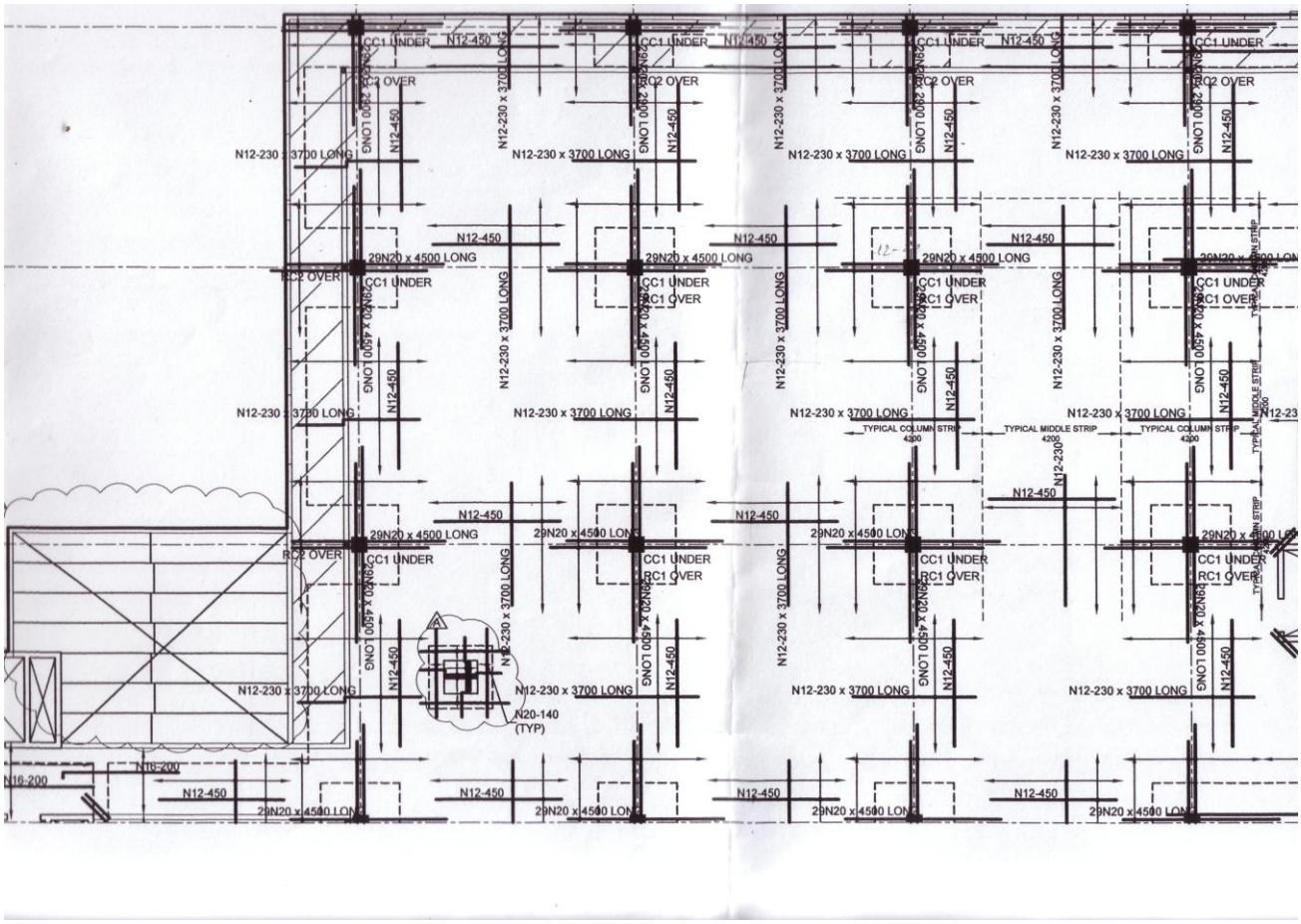

Fig. 7.89. Industry Partner's Conventional Design showing Top Steel

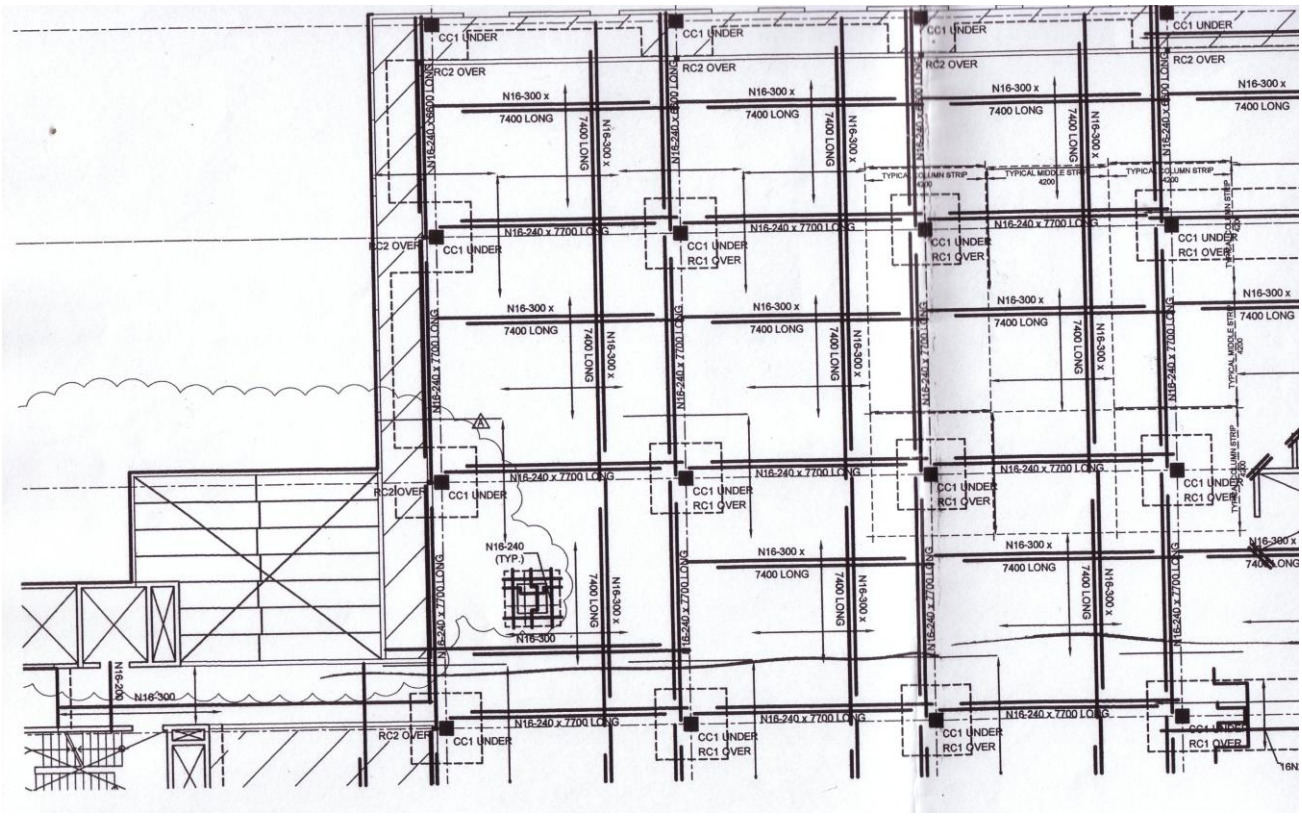

Fig. 7.90. Industry Partner's Conventional Design showing Bottom Steel

A visual comparison of the steel quantity required in the industry partner's design with the optimal solutions obtained using Technique 3 (for both fixed and free boundary conditions) demonstrates design improvements in terms of material savings at the same time satisfying code provisions for strength requirements. The optimisation program does not explicitly divide between top steel and bottom steel in the optimisation algorithms but instead indicates the total amount of steel and depth needed (i.e. section needed) at a particular location. It is obvious that top steel will generally be required over column supports and bottom steel at mid span. It is seen in the optimal solution that a drop panel of 400 mm depth is required at all the columns (similar to industry partner's design) though with less steel required in all the drop panels 10-Y20 bars per meter width i.e. 10 x 2.5 = **25** bars over a width of 2.5 m in both directions. Thus lesser steel is needed compared to the industry partner's design of **29**-Y20 bars seen at the supports. However, slightly more quantity of steel in the drop panels at the edges is observed when the boundary conditions are free. This is indicated by the Choc color in the optimal solution indicating 12-Y20 bars per meter width, i.e. 12 x 2.5 = 30 bars (as against industry partner's 29 bars). It should be noted that the industry partner's design is carried out using the slab design software 'SAFE', which uses the strip method of design. In the design therefore, the steel is obtained for the column strips and middle strips in both

directions. The optimal solution on the other hand is based on element level results. For the mid span regions in the column strip, less quantity of steel is observed in the optimal solution albeit with a bigger depth for both cases when the boundary conditions are fixed and when they are free. For the mid span regions in the middle strips, much less steel is required in both cases especially for the case when the boundary is free. This comparison thus demonstrates the effectiveness of the proposed optimisation method in obtaining efficient and economical conceptual designs for flat slabs. A tabular comparison of the design at various locations is shown below. Drop Panel size in both initial model and industry partner's design is 2.4 m x 2.4 m.

Location	**Optimal Solution**				**Industry Partner's Design**			
	Boundary fixed		Boundary free		(Free Boundary Conditions assumed)			
	Depth required at that location	Total Steel required	Depth required at that location	Total Steel required	Top Steel	Bottom Steel	Total Steel	Depth required at that location
Interior Drop Panels	400 mm	25 – Y20 bars both ways	400 mm	25 – Y20 bars both ways	29 – Y20 bars both ways	Bottom steel for positive sagging moment is extended into drop panels.	29 – Y20 bars both ways	400 mm
Edge Drop Panels	400 mm	25 – Y20 bars both ways	400 mm	30 – Y20 bars both ways	29 – Y20 bars both ways	Bottom steel for positive sagging moment is extended into drop panels.	29 – Y20 bars both ways	400 mm
Corner Drop Panels	400 mm	25 – Y20 bars both ways	400 mm	25 – Y20 bars both ways	29 – Y20 bars both ways	Bottom steel for positive	29 – Y20 bars both ways	400 mm

						sagging moment is extended into drop panels.		
Column Strips – Mid Span Region	400 mm	10Y12 (Magenta) – 1130.97 mm^2/m width	400 mm	Varies from 400-10Y12 (Magenta) near the drop panels to 200-4Y12 (Red) with 200-5Y16 (Yellow) in between. Assuming 400-10Y12 (Magenta) – 1130.97 mm^2/m width	5-Y12 bars per m width + 3-Y12 bars per m width in other direction	5-Y16 bars per m width	1910.09 mm^2/m width	200 mm
Middle Strips – Mid Span Region	200 mm	6-Y16 bars both ways (2412.743 mm^2/m width)	200 mm	4-Y12 bars both ways (904.78 mm^2/m width)	None	4-Y16 bars per m. width both ways	1608.50 mm^2/m width	200 mm

Fig. 7.91. Comparison between Optimal Solution Obtained using Technique 3 and Industry Partner's Design Obtained using Conventional Approach

7.8.2 Q2 PROJECT (WITH DROP PANELS)

Fig. 7.92. below shows the 'Q2' project being designed by the industry partner to be constructed on Queen Street in Melbourne, Australia. It is a 12 storey office building situated in the heart of Melbourne's CBD. The industry partner's design uses a band beam system (which is compared later in Sections 7.8.3 and 7.8.4). In this case study, a drop panel system is investigated for the same span and loading.

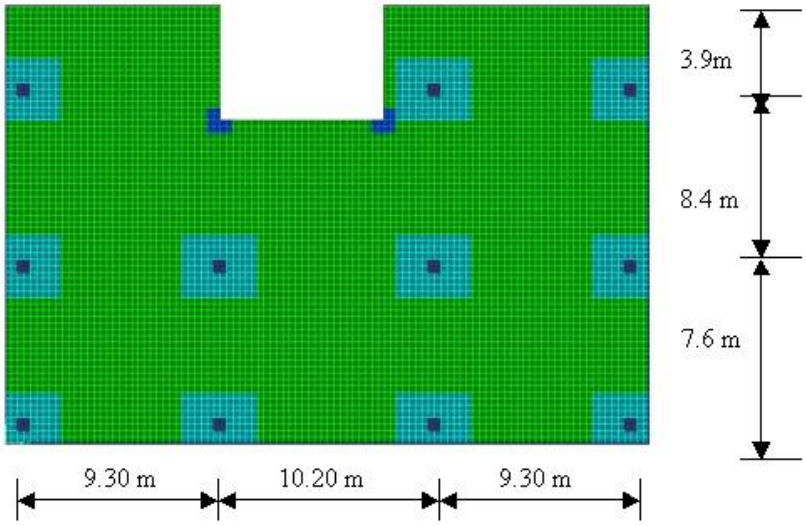

Fig. 7.92. Typical Floor Plan of Q2 Project

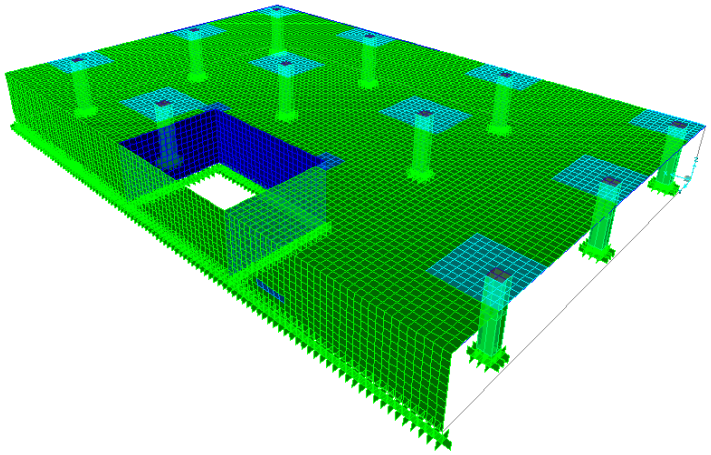

Fig. 7.93. 3D View of a Single Floor Level of Q2 Project

Data

Depth of Initial Model: 400 mm; Column sizes: 600 x 600 mm; Drop Panel: 2.4 x 2.4 m; Wall thickness (Non-Design): 150 mm; Perimeter Beam (frame element) along boundary: 1.8m wide x 450mm deep; Total No. of Elements: 8210; DL: Self Wt. + 2 kPa; LL: 3 kPa; Load Combo: 1.25 DL + 1.5 LL.

7.8.2.1 Design using Technique 1

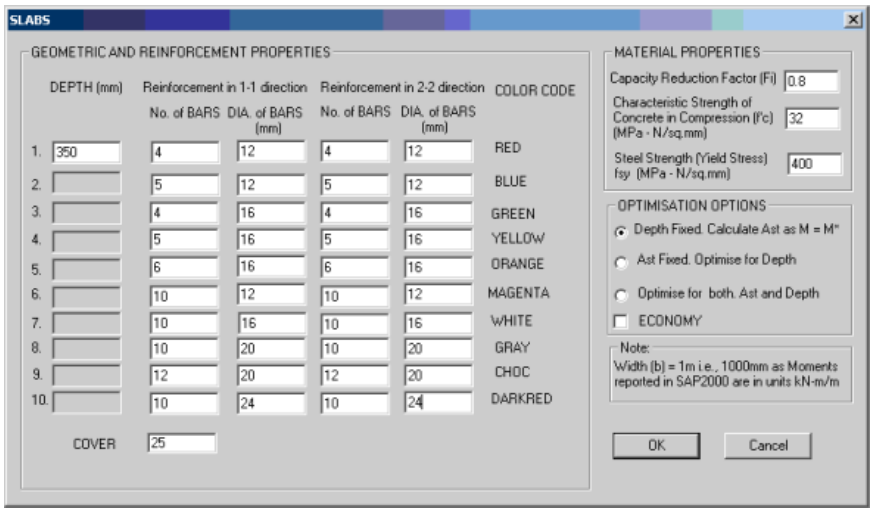

Fig. 7.94. Design Data for Technique 1

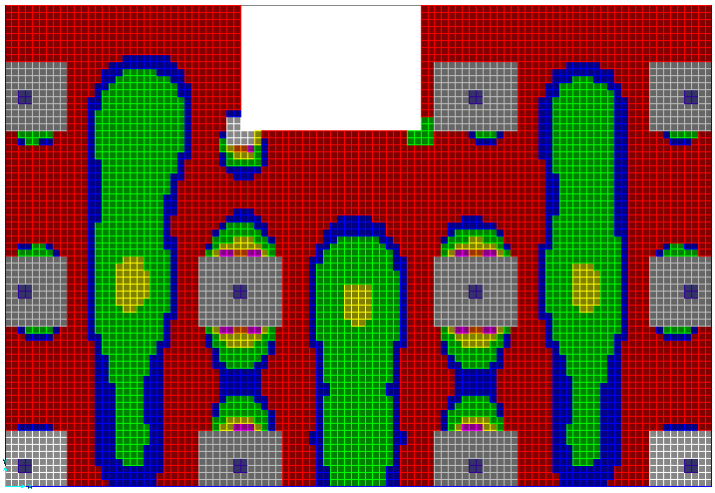

Fig. 7.95. Technique 1 Design Solution showing Steel in X direction

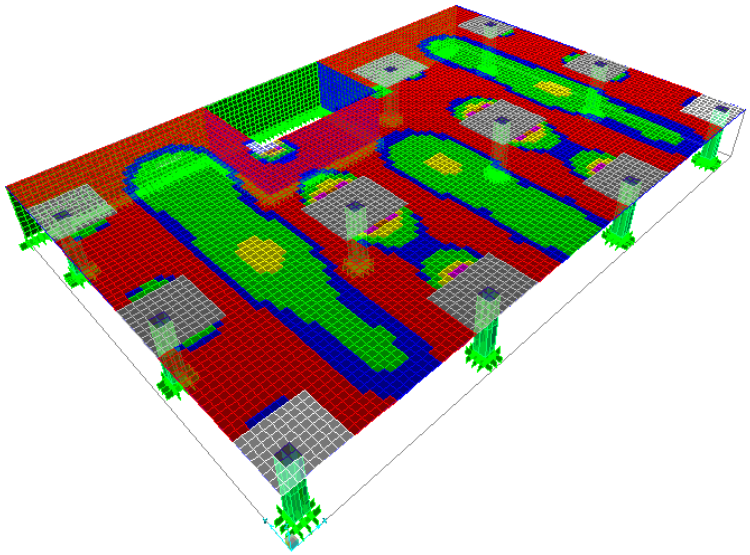

Fig. 7.96. 3D View of Technique 1 Design Solution showing Steel in X direction

(Note: For 'Colour Legend', refer to the 'Colour Code' shown in the GUI in Fig. 7.94 above).

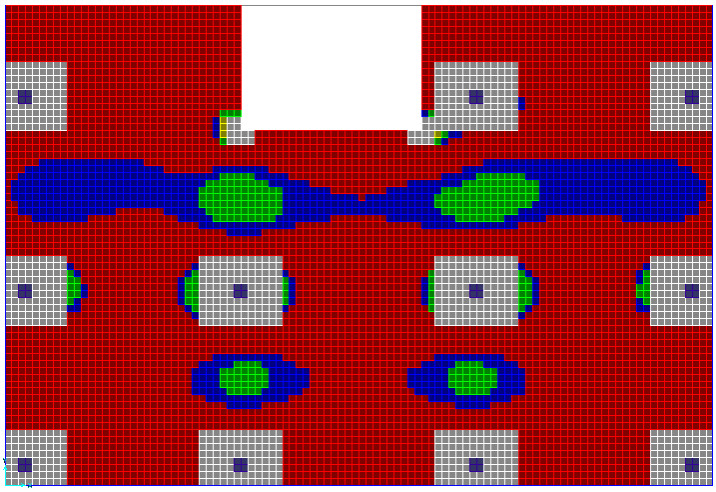

Fig. 7.97. Technique 1 Design Solution showing Steel in Y direction

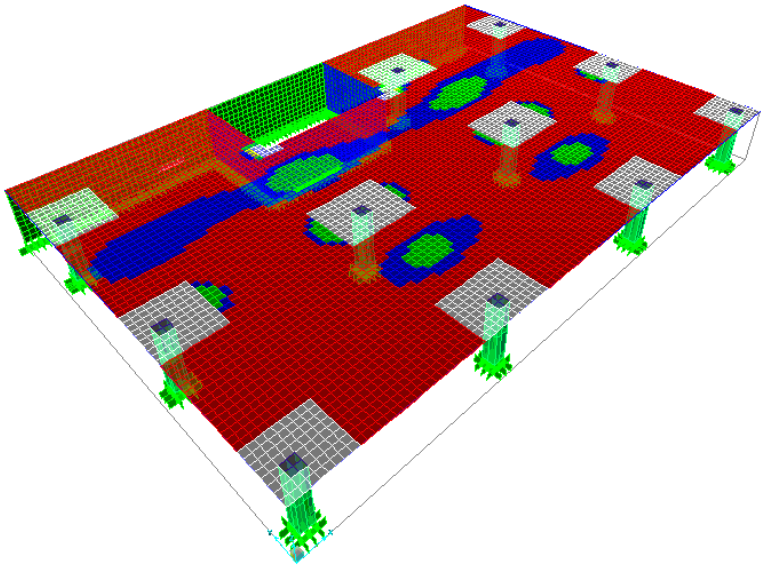

Fig. 7.98. 3D View of Technique 1 Design Solution showing Steel in Y direction

(Note: For 'Colour Legend', refer to the 'Colour Code' shown in the GUI in Fig. 7.94 above).

It is seen from the above results that for all the drop panels except the two corner drop panels at front, 10-Y20 bars (Grey) are required in the x-direction and 10-Y16 bars are required in the y-direction (White). Remember that steel required (or bars required) per metre width is being discussed. The two corner drop panels at front require 10-Y16 bars (White) in both directions. More steel is seen to be required near the interior drop panels, thereby indicating the need for drop panels of a bigger size in these regions. The panels at the corners of the lift core openings require more steel and 10-Y16 bars (White) in both directions is seen. If the slab is divided into column strips and middle strips, then in the mid span region for middle strips, 4-Y16 bars (Green) are required in the x-direction and 4-Y12 bars (Red) and 5-Y12 bars (Blue) are required in the y-direction. In the column strips, 5-Y16 (Yellow) bars are required at mid-span in x-direction for the middle line of columns and 4-Y16 bars (Green) are

required in the y-direction. The rest of the slab generally requires 4-Y12 bars (Red). Thus, even though design is being performed at an element level for most of the slab, a clear and interpretable arrangement of steel is observed for a 350 mm thick slab design. The total weight of concrete is 561.27 Tonne and the total weight of steel is 12.40 Tonne. In the next example, Technique 2 is employed to seek the depths required when the steel is constant.

7.8.2.2 Design using Technique 2

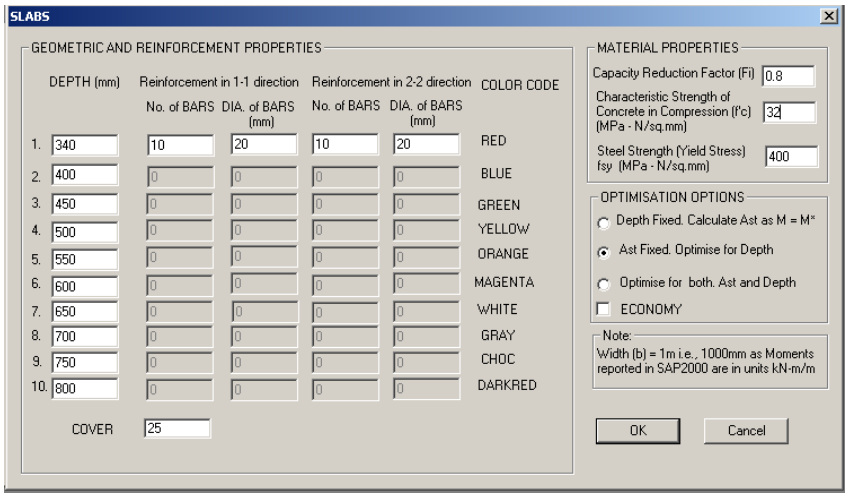

Fig. 7.99. Design Data for Technique 2

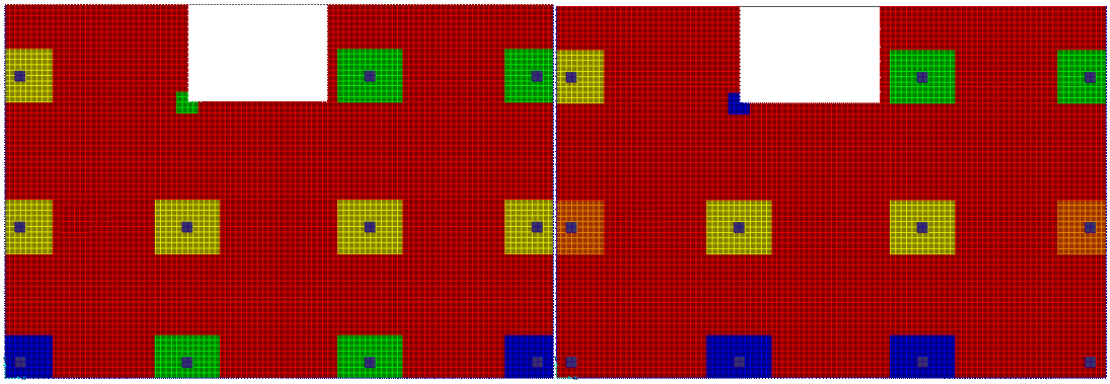

(a) 1st iteration (b) 2nd iteration

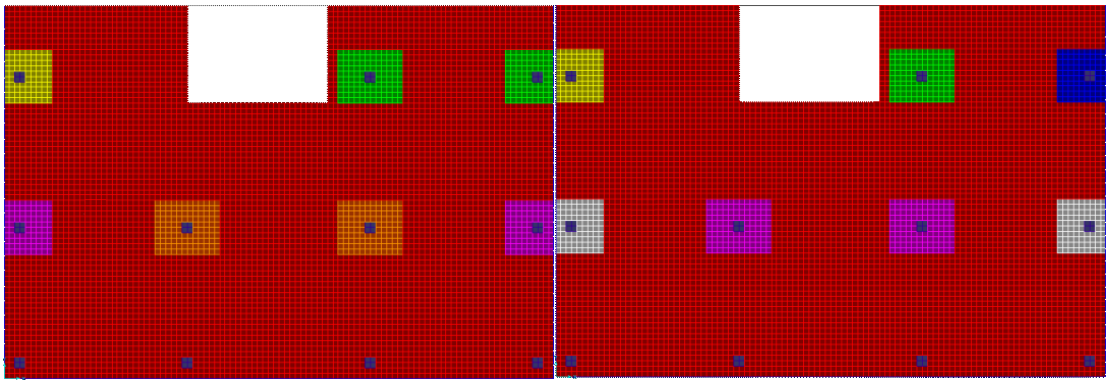

(c) 3rd iteration (d) 4th iteration

Fig. 7.100 (a-d).

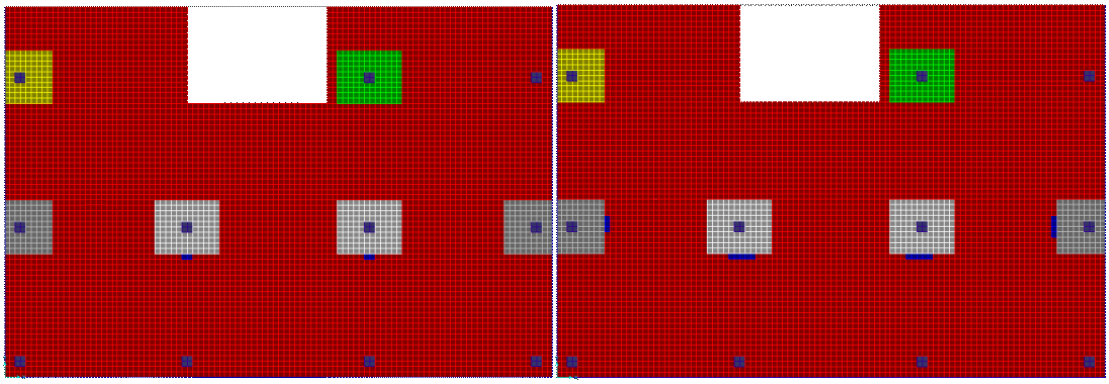

(e) 5th iteration (f) 6th iteration

Fig. 7.100. Technique 2 Design Solutions

The solution stabilises and settles from the 6th iteration onwards, satisfying moment criterion for all elements in the slab. To avoid convergence problems, the optimisation is begun with a high quantity of steel (10-Y20 bars) in order to check the maximum depths at different locations. It is clear that the entire slab including the four drop-panels in front has settled on the first section (depth of 340 mm with 10-Y20 bars both ways). Different depths are observed for the remaining drop panels. The interior columns in the middle have settled on a depth of 650 mm (White) and the two corner drop panels next to them have settled on a depth of 700 mm (Grey). The interior drop panel near the lift core opening requires a depth of 450 mm (Green) and the corner drop panel requires a depth of 500 mm (Yellow). When the thickness of the slab is increased, moment redistribution occurs, and this in turn results in a further increase in thickness in some regions. One of the reasons for obtaining different depths for the drop panels is due to asymmetry of the model in both directions. However, it needs further investigation and therefore Technique 3 is applied in the next example. A tabular comparison is shown on the next page. A 12.39 % saving in concrete weight is attained compared to the initial model. It should be noted that as the steel specified is high (10-Y20 bars) the data set too had to be started from a higher depth (340 mm) due to ductility reasons ($k_u > 0.2$). A smaller depth, say 300 mm with 10-Y20 bars results in $k_u > 0.2$ and therefore the data set is started with a depth of 340 mm (Red). The weight savings in concrete could have been more if a lesser depth (and lesser steel) was given in the data set.

Table 7.17. Technique 2 Design Optimisation Results

Iteration No.	Concrete Weight (Tonne)	% saving in Concrete Weight	Total Steel Weight (Tonne)	% saving in Total Steel Weight	Total Cost of Concrete (AU $)	Total Cost of Steel (AU $)	TOTAL COST (AU $)	Max. Deflection (mm) * 3	Permissible Deflection (mm) (Span/250)	Satisfies Condition
Initial Model	561.27	-	15.98	-	35079.38	17578	52657.38	5.86 x 3 = 17.58	37.20	-
1	482.35	14.06 %	15.98	-	23151.25	17578	40729.25	8.06 x 3 = 24.18	37.20	NO
2	480.57	14.38 %	15.98	-	23088.75	17578	40666.75	8.05 x 3 = 24.15	37.20	NO
3	482.77	13.99 %	15.98	-	23088.75	17578	40666.75	8.05 x 3 = 24.15	37.20	NO
4	486.20	13.38 %	15.98	-	23088.75	17578	40666.75	8.05 x 3 = 24.15	37.20	NO
5	491.55	12.42 %	15.98	-	23088.75	17578	40666.75	8.05 x 3 = 24.15	37.20	NO
6	491.72	12.39 %	15.98	-	23088.75	17578	40666.75	8.05 x 3 = 24.15	37.20	YES
7	491.72	12.39 %	15.98	-	23088.75	17578	40666.75	8.05 x 3 = 24.15	37.20	YES
8	491.72	12.39 %	15.98	-	23088.75	17578	40666.75	8.05 x 3 = 24.15	37.20	YES
9	491.72	12.39 %	15.98	-	23088.75	17578	40666.75	8.05 x 3 = 24.15	37.20	YES
10	491.72	12.39 %	15.98	-	23088.75	17578	40666.75	8.05 x 3 = 24.15	37.20	YES

7.8.2.3 Design using Technique 3

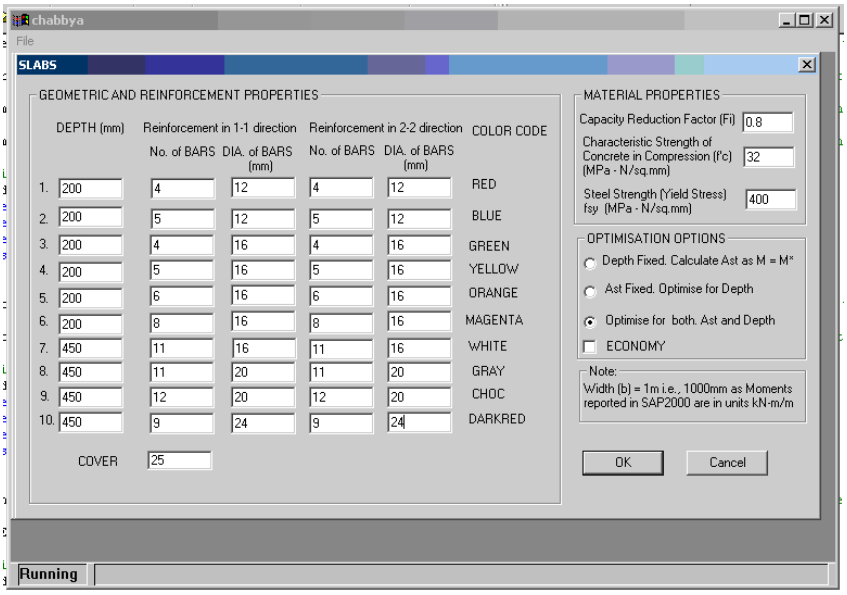

Fig. 7.101. Design Data for Technique 3

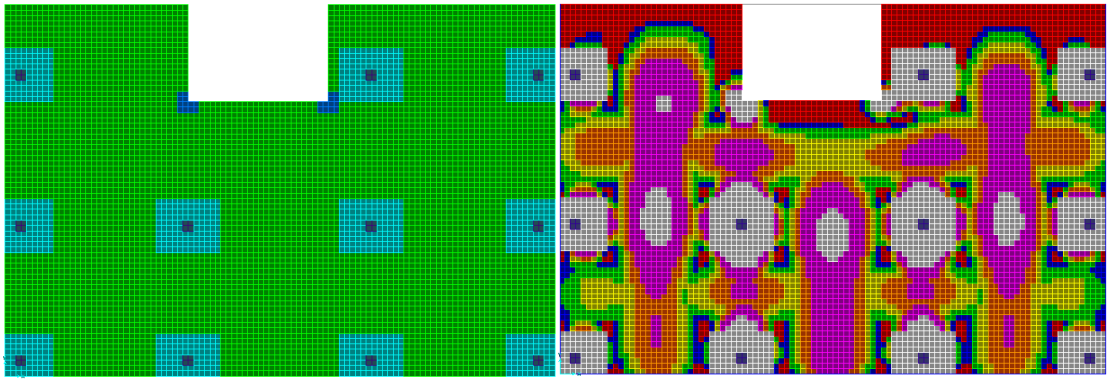

Fig. 7.102. Initial Model (a) 1st iteration

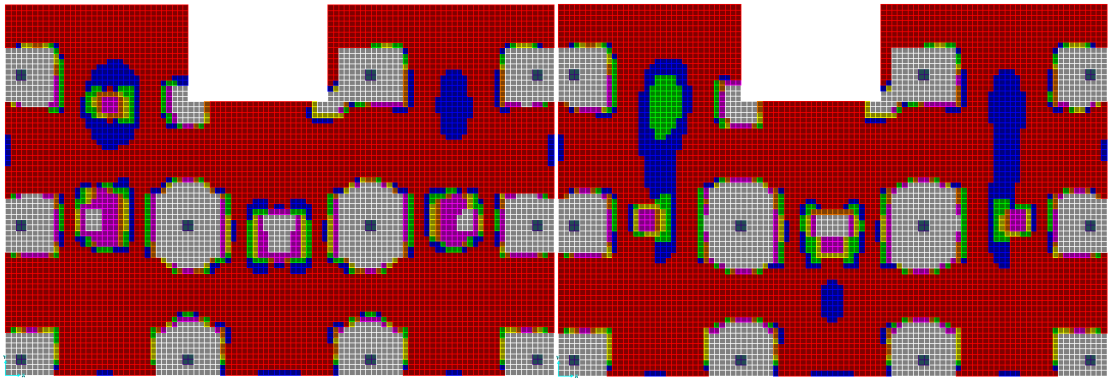

(b) 2nd iteration (c) 3rd iteration

Fig. 7.103 (a-c).

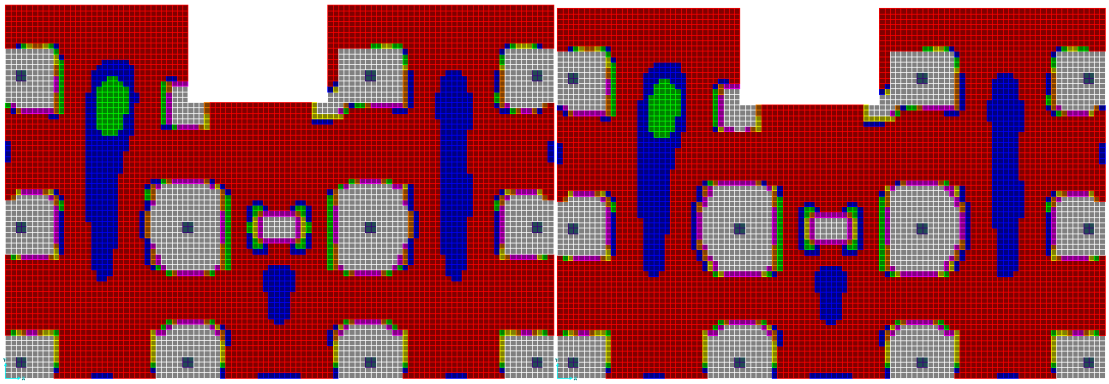

(d) 4th iteration (e) 5th iteration

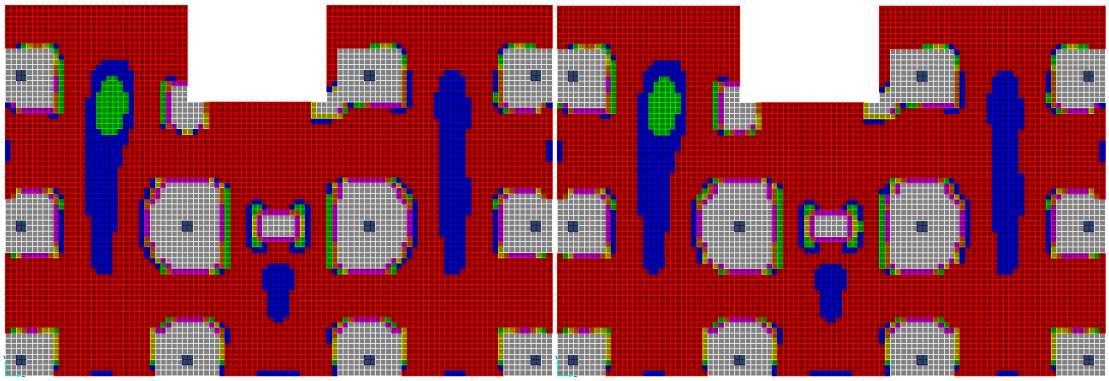

(f) 6th iteration (g) 7th iteration

Fig. 7.103. Technique 3 Design Solutions

The solution settles and stabilises from the 7th iteration onwards, satisfying moment criterion in all elements of the slab. All the drop panels have settled on a section of 450 mm depth with 11-Y16 bars both ways (White). The panels at the corners of the lift core opening and the mid span region of the interior span too require the same section. Also, this section (White) is seen to be required in elements near the interior drop panels, thereby suggesting the need for a bigger sized drop panel in these regions. The first section, 200 mm depth with 4-Y12 bars both ways (Red) is seen to suffice in most regions of the slab with 5-Y12 bars (Blue) and 4-Y16 bars (Green) required in some regions. The comparison shown on the next page shows significant weight savings (and therefore cost savings) in concrete and steel. The optimal solution demonstrates a 38.16 % weight saving of concrete compared to the design obtained using Technique 1 and a steel weight saving of 35 % compared to the design obtained using Technique 1. Compared to Technique 2 used in the previous example, this design looks much better visually, not to mention the weight savings in steel obtained and the additional weight savings in concrete.

Table 7.18. Technique 3 Design Optimisation Results

Iteration No.	Concrete Weight (Tonne)	% saving in Concrete Weight	Total Steel Weight (Tonne)	% saving in Total Steel Weight	Total Cost of Concrete (AU $)	Total Cost of Steel (AU $)	TOTAL COST (AU $)	Max. Deflection (mm) * 3	Permissible Deflection (mm) (Span/250)	Satisfies Condition
Initial Model	561.27	-	12.40	-	35079.38	13640.00	48719.38	5.16 x 3 = 15.48	37.20	-
1	348.81	37.85 %	10.13	18.31 %	21800.63	11143.00	32943.63	9.31 x 3 = 27.93	37.20	NO
2	346.06	38.34 %	8.18	34.03 %	21682.75	8998.00	30626.75	9.65 x 3 = 28.95	37.20	NO
3	346.38	38.29 %	8.07	34.92 %	21648.75	8877.00	30525.75	9.49 x 3 = 28.47	37.20	NO
4	347.35	38.11 %	8.05	35.08 %	21709.38	8855.00	30564.38	9.40 x 3 = 28.20	37.20	NO
5	347.35	38.11 %	8.07	34.92 %	21709.38	8877.00	30586.38	9.42 x 3 = 28.26	37.20	NO
6	347.19	38.14 %	8.07	34.92 %	21699.38	8877.00	30576.38	9.46 x 3 = 28.38	37.20	NO
7	347.08	38.16 %	8.06	35.00 %	21692.50	8866.00	30558.50	9.47 x 3 = 28.41	37.20	YES
8	347.08	38.16 %	8.06	35.00 %	21692.50	8866.00	30558.50	9.47 x 3 = 28.41	37.20	YES
9	347.08	38.16 %	8.06	35.00 %	21692.50	8866.00	30558.50	9.47 x 3 = 28.41	37.20	YES
10	347.08	38.16 %	8.06	35.00 %	21692.50	8866.00	30558.50	9.47 x 3 = 28.41	37.20	YES

7.8.2.4 Comparison with Industry Partner's Final Design Based on Conventional Approach

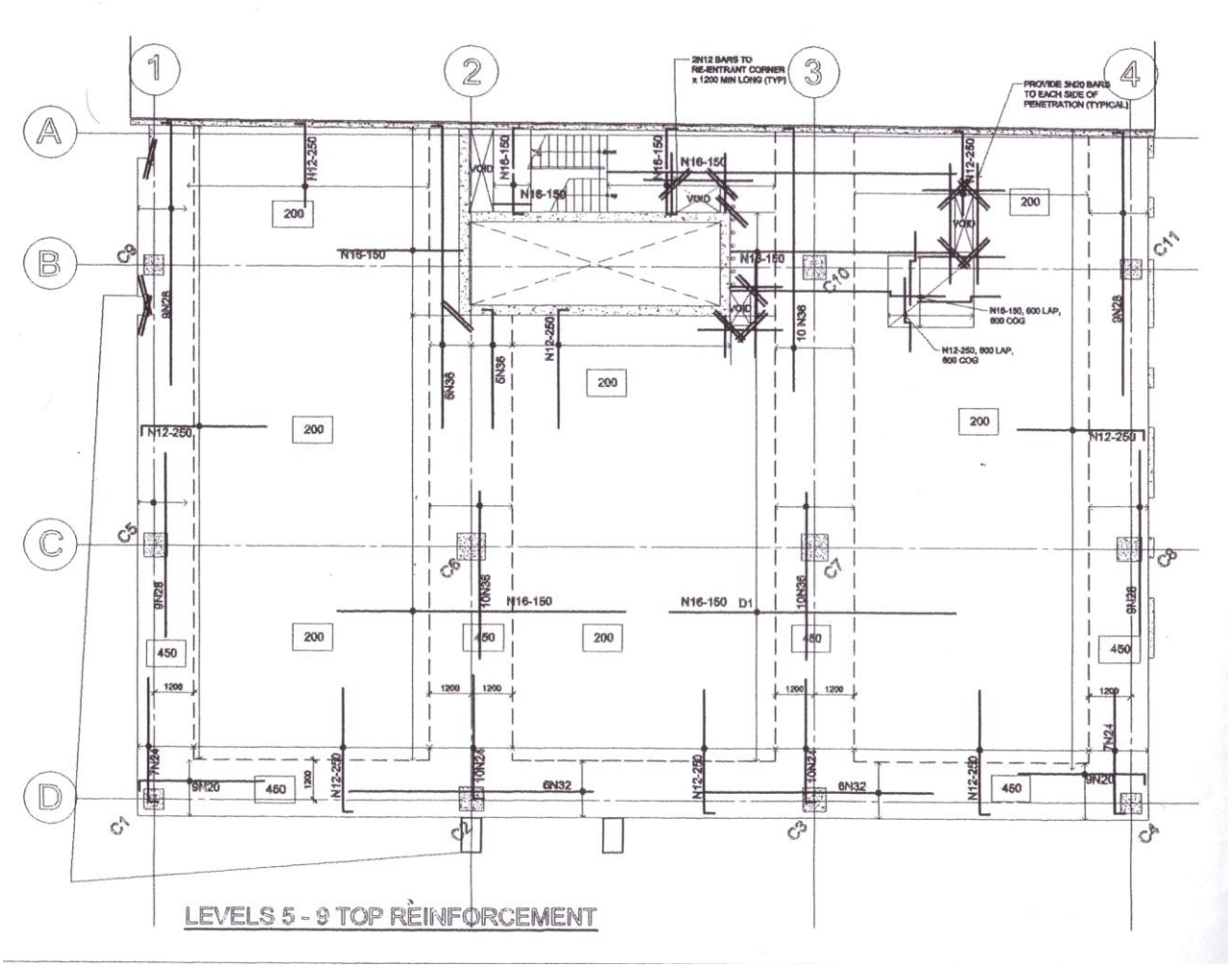

Fig. 7.104. Industry Partner's Conventional Design for Q2 Project showing Top Steel

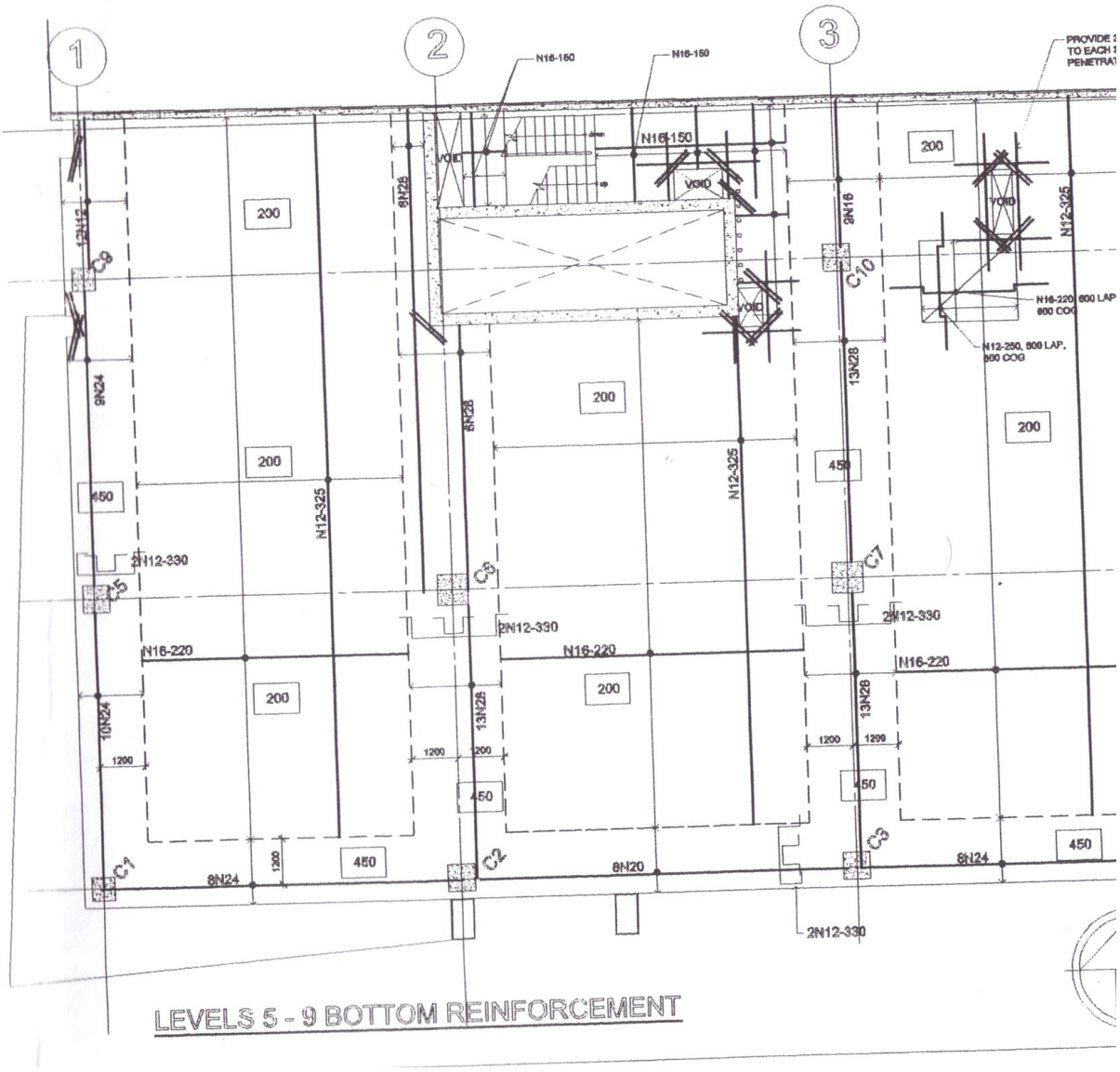

Fig. 7.105. Industry Partner's Conventional Design for Q2 Project showing Bottom Steel

In the industry partner's final design for this slab, a band beam system is used. 450 mm deep band beams are used with the rest of the slab being 200 mm thick. The steel quantities required in various locations are shown in the attached drawings (Fig. 7.104 and Fig. 7.105 above). The band beam system makes use of wide beams through a slab that support a one-way slab in the transverse direction. The flat slab system on the other hand is a two-way system that transfers load in two directions. Based on the industry partner's final design, the author decided to allot sections with only two depths of 200mm and 450mm respectively with varying quantities of steel for each depth while specifying the dataset in Technique 3 above to compare the two floor systems. The optimal design does not explicitly indicate the requirement of a band beam arrangement; rather the design is more of that obtained for a flat slab with significant savings in concrete and steel weight observed. Comparing the design of an interior drop panel (Column C6 in Fig. 7.104), the White colour indicates that a section of 450 mm depth with 11 – Y16 bars per m width is needed. As the drop panels are of dimensions 2.4m x 2.4m, total number of bars needed in this interior drop panel in both directions is: 2 x 11 x 2.4m = 54-Y16 bars (total steel area of *10857.34 mm*^{2}). The industry partner's design shows that 10-N36 bars are needed in the direction of the band beam (10178.76 mm^2) and N16 bars @150mm c/c are needed in the transverse direction (i.e. 7-N16 bars needed per metre width, over 2.4m width: 2.4 x 7 = 17-N16 bars which is a steel area of 3418.05 mm^2). The total steel requirement at the column support is therefore 10178.76 mm^2 + 3418.05 mm^2 = *14275.39 mm*^{2}. The design using Technique 3 clearly shows a weight saving in steel of *23.94 %* at this interior drop panel compared to the design obtained by the industry partner using conventional method. Similar comparisons apply at all other locations. Note that the thickness designed by Technique 3 for this interior drop panel is 450mm, which is similar to the industry partner's thickness for the band beam. On the contrary the drop panel design of Technique 3 results in a saving in concrete weight compared to the band beam system. Thus the steel and concrete quantity actually required is seen to be much less when compared to the industry partner's final design (at the drop panel locations, throughout the band beam locations and mid-span locations in both directions). The deflections recorded in each iteration are scaled by a factor of three and checked with the permissible limit specified by AS 3600 and are observed to be quite satisfactory. The above solution therefore demonstrates a much more efficient design compared to the industry partner's final design for the slab (without considering build-ability issues), thereby suggesting the choice of a flat slab arrangement over a band beam system. In the next example, the initial model for this project is modified to include band beams of the dimensions given on the plans and check for design similarities. The different design methods (strip method of design v/s design using element stress resultants) and design approaches for the choice of system (flat slab v/s band beam arrangement) result in different designs and should be appreciated in this comparison.

7.8.3 Q2 PROJECT WITH BAND BEAMS

7.8.3.1 Design using Technique 3

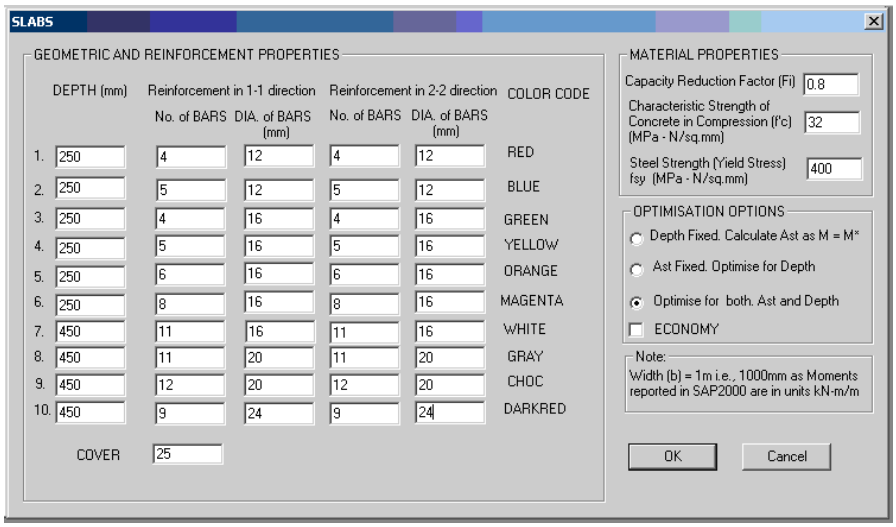

Fig. 7.106. Design Data for Technique 3

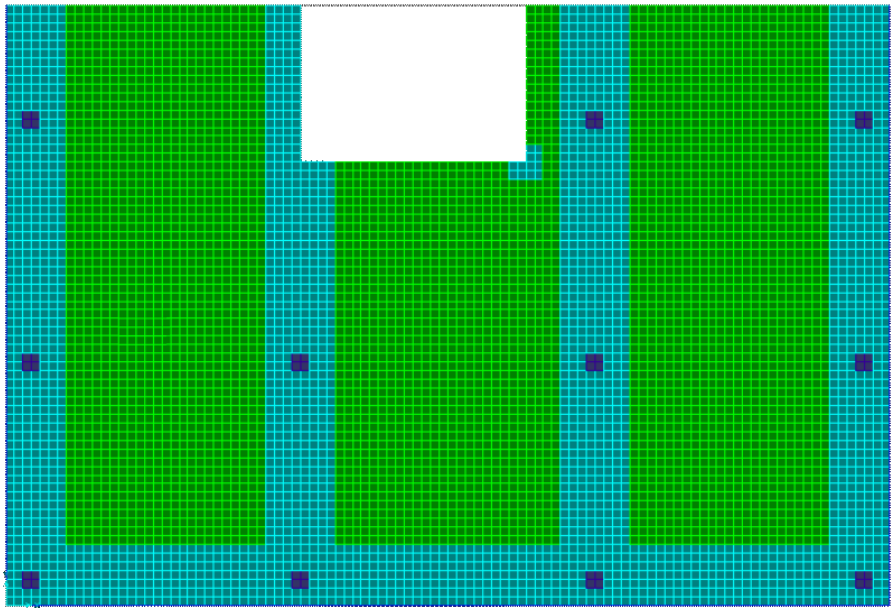

Fig. 7.107. Initial Model of Q2 Project with Band Beams

Spans

X direction: 9.3m, 10.2m and 9.3m

Y direction: 7.5m, 8.4m and 3.9m

Loading: Self Weight, Dead Load: 2 kPa, LL: 3 kPa.

Load Combo: 1.25 DL + 1.5 LL

Initial SlabThickness: 400 mm thick everywhere

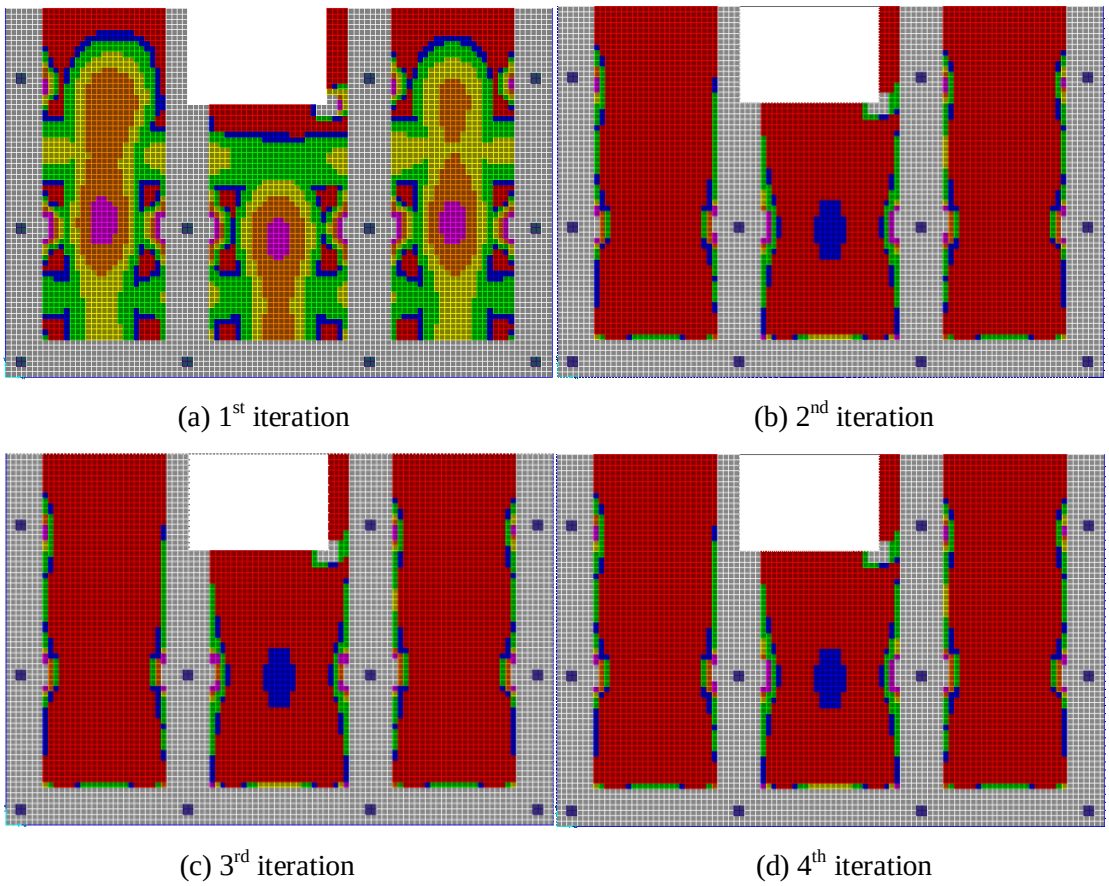

(a) 1st iteration (b) 2nd iteration

(c) 3rd iteration (d) 4th iteration

Fig. 7.108. Technique 3 Design Solutions for Q2 Project with Band Beams

7.8.3.2 Comparison with Industry Partner's Final Design

The solution settles and stabilises from the 4th iteration onwards, satisfying bending moment criterion in all elements of the slab. The band beams require a section of 450 mm depth with 11-Y16 bars (White). Similar to the discussion in Section 7.8.2.4, significant weight saving in steel is attained for this example as well. Slightly more steel compared to mid span steel is seen to be required along the inside edges of the band beams (Blue, Green, Yellow) near column supports. This suggests the need for some extra negative reinforcement in this area. It is known that in band beam systems, one of the concerns is the transfer of force from beam to column. This problem arises because the beam is typically much wider than the column. The problem involves two aspects: moments across planes parallel to the beam, and transfer of shear to the column. Such force transfer is analogous to the situation in a two-way flat slab where minimum specific consideration is given to the moment transfer. If consideration is given to a possible failure model, the moment transfer problem can be simplified. A flexural failure could be considered along a face parallel to the beam, say adjacent to the face of the column at the critical section for negative moment. From yield line concepts a mechanism is

needed for failure to occur. The mechanism could include a yield line along the entire length of the beam. The one-way span design of the slab would provide for this failure pattern. Even so, under service loads the moment distribution would not be uniform and larger negative moments would be expected near the columns. Such moments near the columns could cause cracking at service loads, and, to avoid cracking, it is generally appropriate to concentrate some of the negative (one-way slab) reinforcement into the 'column strip'. That is, some extra reinforcement could be provided in this area. The need for some extra negative reinforcement in this area is seen in the solution above and caters to this need and it should be pointed out that moment transfer and shear is not included in the algorithm at this stage. Even then, the solution specifically indicates the requirement of more negative steel in this area. For the rest of the slab, the first section, 250 mm depth with 4-Y12 bars (Red) with some portion in the interior span requiring 5-Y12 bars (Blue) is seen to suffice. Compared to the industry partner's design, which shows the main steel bottom reinforcement as 5-N16 bars per m width (N16-220 mm c/c, refer Fig. 7.105 above), Technique 3 design above in Fig. 7.108 shows a significant weight saving for bottom steel (36 %). The steel quantity actually required is also seen to be much less when compared to the industry partner's final design at the column supports, band beam locations and mid-span locations in both directions. The table on the next page shows that the weight savings obtained in concrete weight and steel weight are less compared to the solution obtained using drop panels in the previous example. This is to be expected as the band beams occupy more area and require more steel as is seen from the above optimal solutions for a band beam and flat slab arrangement.

Table 7.19. Technique 3 Design Optimisation Results for Q2 Project with Band Beams

Iteration No.	Concrete Weight (Tonne)	% saving in Concrete Weight	Total Steel Weight (Tonne)	% saving in Total Steel Weight	Total Cost of Concrete (AU $)	Total Cost of Steel (AU $)	TOTAL COST (AU $)	Max. Deflection (mm) * 3	Permissible Deflection (mm) (Span/250)	Satisfies Condition
Initial Model	561.27	-	12.40	-	35079.38	13640.00	48719.38	5.16 x 3 = 15.48	37.20	-
1	379.41	32.40 %	10.92	11.94 %	23713.13	12012.00	35725.13	8.57 x 3 = 25.71	37.20	NO
2	379.47	32.39 %	9.63	22.34 %	23716.88	10593.00	34309.88	8.57 x 3 = 25.71	37.20	NO
3	379.47	32.39 %	9.63	22.34 %	23716.88	10593.00	34309.88	8.57 x 3 = 25.71	37.20	NO
4	379.52	32.38 %	9.63	22.34 %	23716.88	10593.00	34309.88	8.57 x 3 = 25.71	37.20	YES
5	379.52	32.38 %	9.63	22.34 %	23716.88	10593.00	34309.88	8.57 x 3 = 25.71	37.20	YES
6	379.52	32.38 %	9.63	22.34 %	23716.88	10593.00	34309.88	8.57 x 3 = 25.71	37.20	YES
7	379.52	32.38 %	9.63	22.34 %	23716.88	10593.00	34309.88	8.57 x 3 = 25.71	37.20	YES
8	379.52	32.38 %	9.63	22.34 %	23716.88	10593.00	34309.88	8.57 x 3 = 25.71	37.20	YES
9	379.52	32.38 %	9.63	22.34 %	23716.88	10593.00	34309.88	8.57 x 3 = 25.71	37.20	YES
10	379.52	32.38 %	9.63	22.34 %	23716.88	10593.00	34309.88	8.57 x 3 = 25.71	37.20	YES

7.8.4 Q2 PROJECT WITH BAND BEAMS – DIFFERENT INITIAL MODEL

7.8.4.1 Design using Technique 3

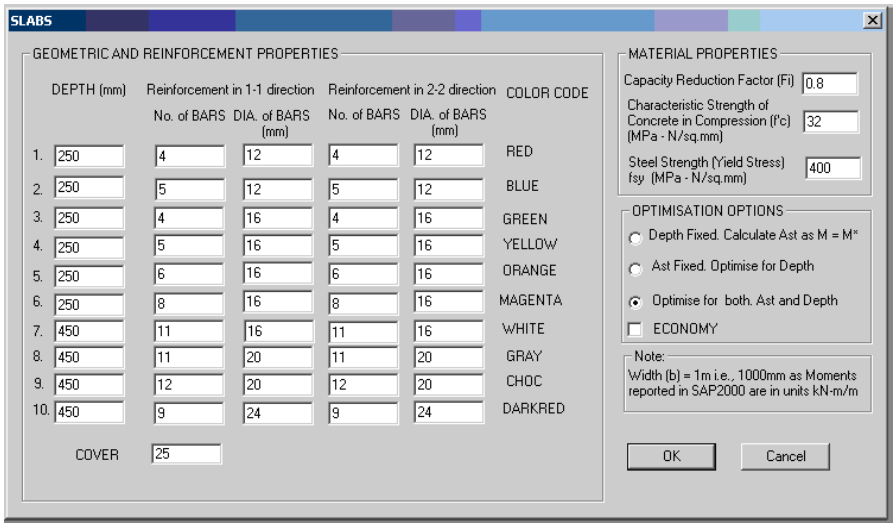

Fig. 7.109. Design Data for Technique 3

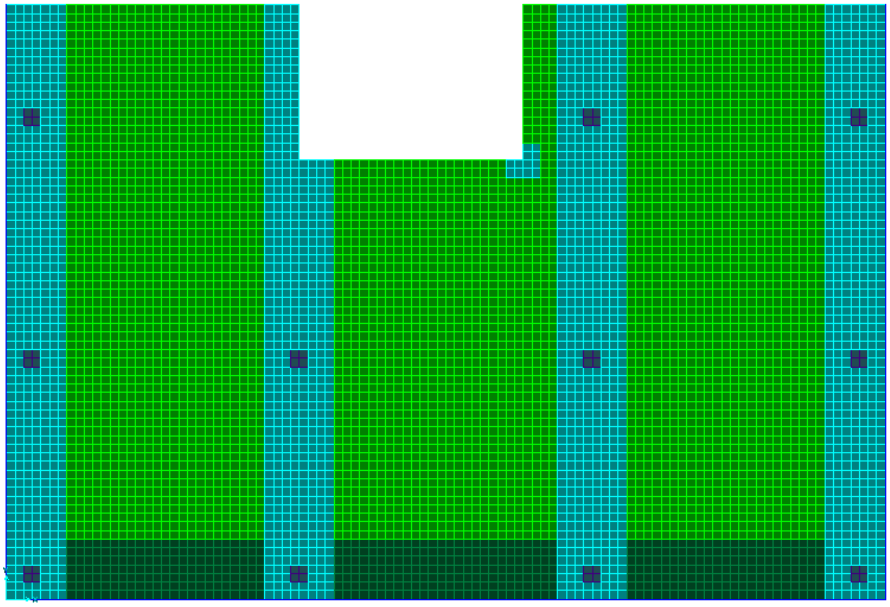

Fig. 7.110. Different Initial Model of Q2 Project with Band Beams

Spans

X direction: 9.3m, 10.2m and 9.3m

Y direction: 7.5m, 8.4m and 3.9m

Loading: Self Weight, Dead Load: 2 kPa, LL: 3 kPa.

Load Combo: 1.25 DL + 1.5 LL

Initial SlabThickness: 400 mm thick everywhere

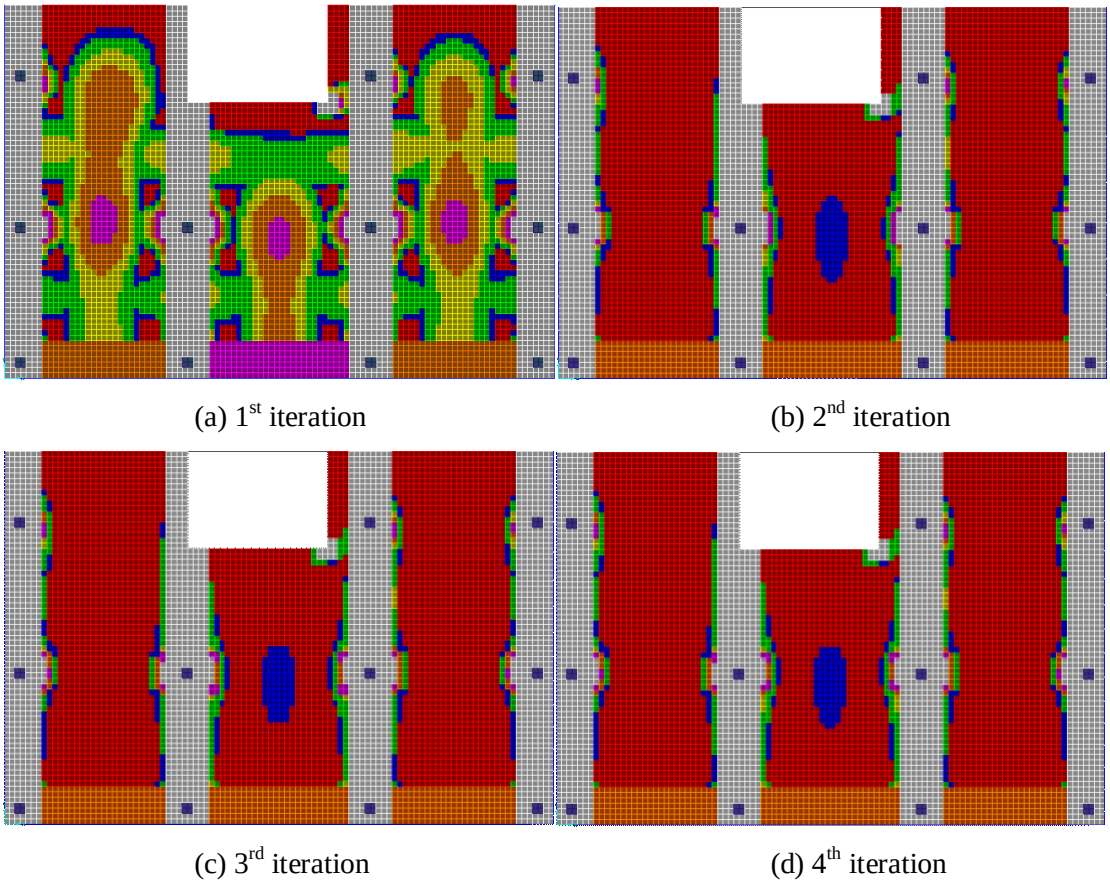

(a) 1st iteration (b) 2nd iteration

(c) 3rd iteration (d) 4th iteration

Fig. 7.111. Technique 3 Design Solutions for Q2 Project with Different Band Beams

The program settles and stabilizes from the 4th iteration onwards, satisfying bending moment criterion in all elements of the slab. The only difference observed compared to the previous example is that a lesser section (250 mm depth – 6Y16 bars, Orange) is required for the three separate band beams in the x-direction. This means, that the White section is not actually required for the entire band beam arrangement as was seen in the previous example. If the band beams are further subdivided in the initial model, then a different design is obtained for the band beams. As seen from the above results, the thickest section (White) is really actually required only in the y-direction and not for the band beams in the x-direction. The design for the one-way slabs in both examples is quite similar. This example again demonstrates the effectiveness of employing ESO and Group ESO optimisation approaches together in tandem when designing band beams.

Table 7.20. Technique 3 Design Optimisation Results for Q2 Project with Different Band Beams

Iteration No.	Concrete Weight (Tonne)	% saving in Concrete Weight	Total Steel Weight (Tonne)	% saving in Total Steel Weight	Total Cost of Concrete (AU $)	Total Cost of Steel (AU $)	TOTAL COST (AU $)	Max. Deflection (mm) * 3	Permissible Deflection (mm) (Span/250)	Satisfies Condition
Initial Model	561.27	-	12.40	-	35079.38	13640	48719.38	5.16 x 3 = 15.48	37.20	-
1	353.24	37.06 %	9.52	23.23 %	22077.50	10472	32549.50	8.96 x 3 = 26.88	37.20	NO
2	353.61	37.00 %	8.46	31.77 %	22100.63	9306	31406.63	8.83 x 3 = 26.49	37.20	NO
3	353.51	32.99 %	8.46	31.77 %	22094.38	9306	31400.38	8.92 x 3 = 26.76	37.20	NO
4	353.51	37.02 %	8.46	31.77 %	22094.38	9306	31400.38	8.92 x 3 = 26.76	37.20	YES
5	353.51	37.02 %	8.46	31.77 %	22094.38	9306	31400.38	8.92 x 3 = 26.76	37.20	YES
6	353.51	37.02 %	8.46	31.77 %	22094.38	9306	31400.38	8.92 x 3 = 26.76	37.20	YES
7	353.51	37.02 %	8.46	31.77 %	22094.38	9306	31400.38	8.92 x 3 = 26.76	37.20	YES
8	353.51	37.02 %	8.46	31.77 %	22094.38	9306	31400.38	8.92 x 3 = 26.76	37.20	YES
9	353.51	37.02 %	8.46	31.77 %	22094.38	9306	31400.38	8.92 x 3 = 26.76	37.20	YES
10	353.51	37.02 %	8.46	31.77 %	35079.38	9306	31400.38	8.92 x 3 = 26.76	37.20	YES

Permissible deflection taken is 9.3 m / 250

7.8.5 Q2 PROJECT WITH ATRIUM

7.8.5.1 Design using Technique 1

The model used in Section 7.7.2 is reproduced here, but this time with an atrium or opening in the middle. The span, loading and all other parameters are the same.

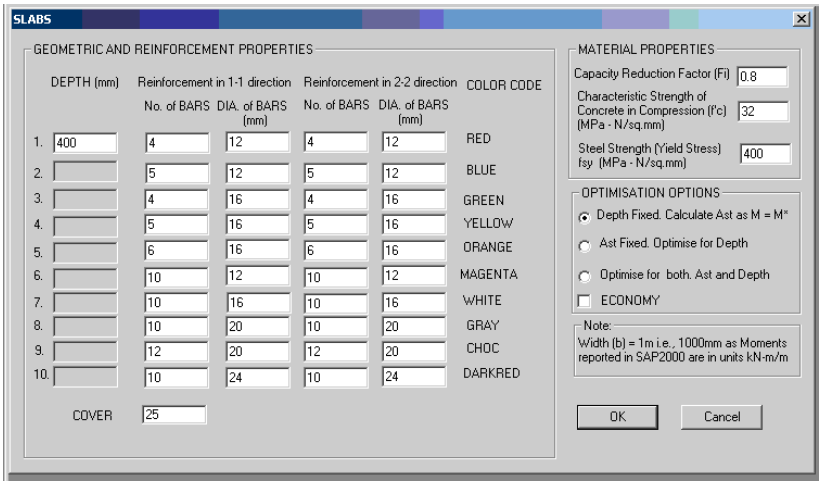

Fig. 7.112. Design Data for Technique 1

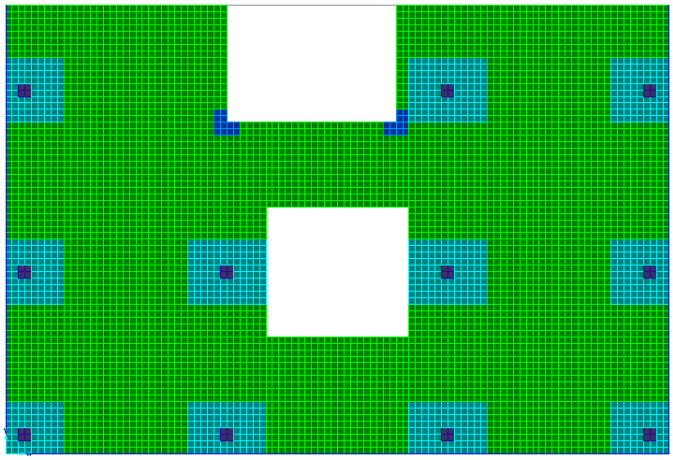

Fig. 7.113. Initial Model of Q2 Project with Atrium

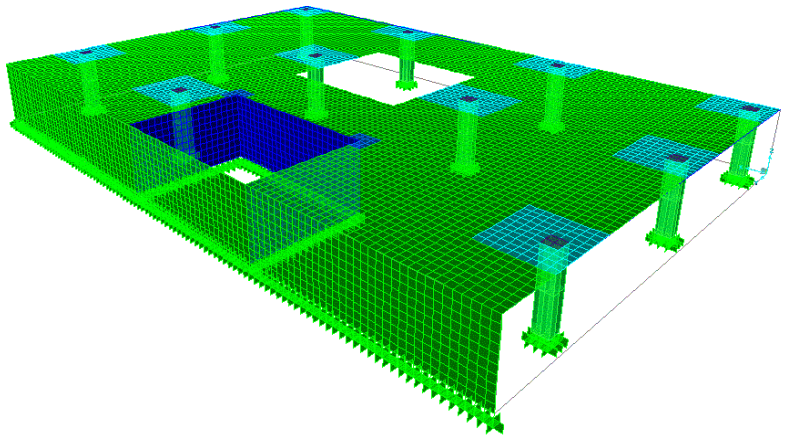

Fig. 7.114. 3D View of Initial Model of Q2 Project with Atrium

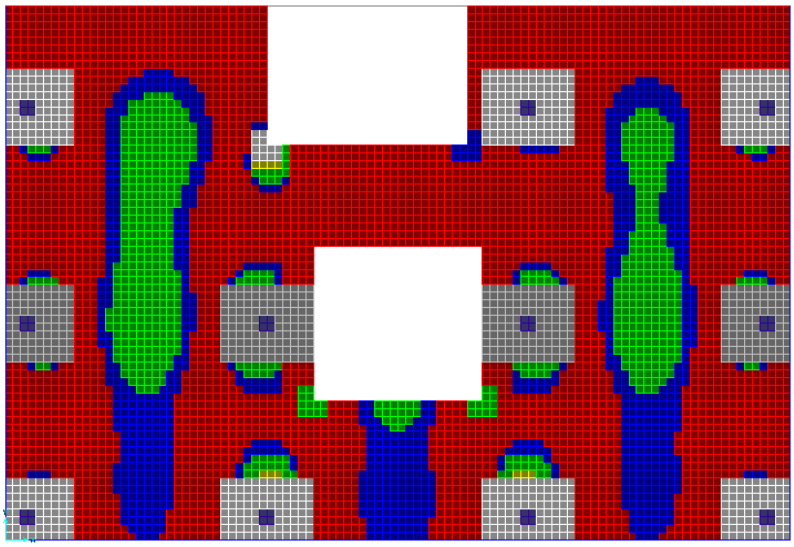

Fig. 7.115. Technique 1 Design Solution showing Steel in X direction

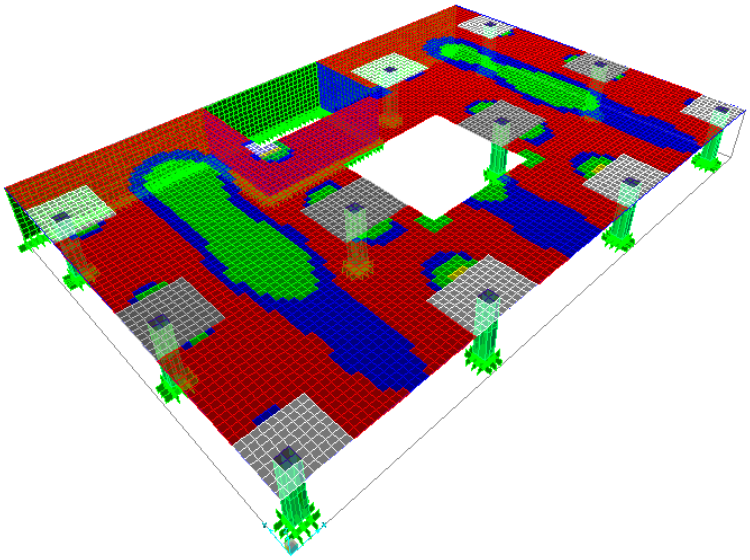

Fig. 7.116. 3D View of Technique 1 Design Solution showing Steel in X direction

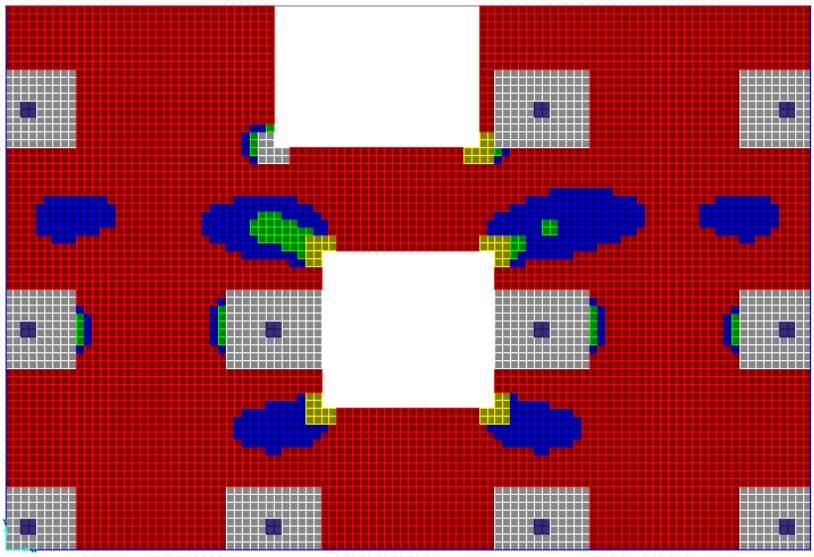

Fig. 7.117. Technique 1 Design Solution showing Steel in Y direction

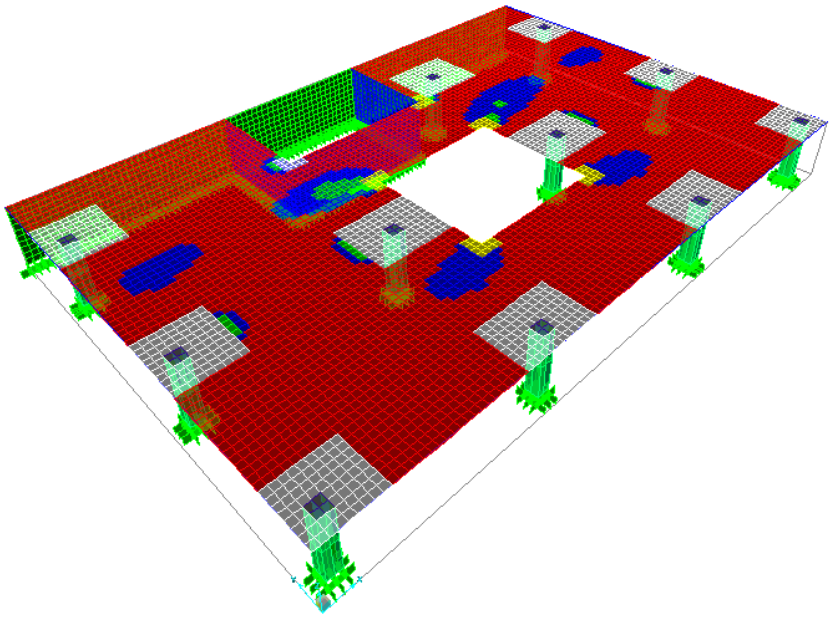

Fig. 7.118. 3D View of Technique 1 Design Solution showing Steel in Y direction

It is seen that for a 400 mm depth slab throughout, 10-Y20 bars (Grey) are required in the x-direction for the interior drop panels, with 10-Y16 bars (White) needed in the x-direction for all other drop panels. The steel required in the y-direction in all drop panels is 10-Y16 bars (White). Remember the steel requirement per metre width is being discussed. 5-Y12 bars (Blue) and 4-Y16 bars (Green) are needed in the x-direction for the mid span regions of the exterior spans. In all other regions, 4-Y12 bars (Red) is seen to suffice in both directions. Near the atrium more steel is needed in the x-direction in the interior span and at corners (5-Y12 bars, Blue and 4-Y16 bars, Green) and in the y-direction more steel is seen at the four corners of the atrium (5-Y12 bars, Blue and 4-Y16 bars, Green). More steel in both directions is also observed for the corner panels near the lift core openings. Thus a clear and interpretable reinforcement design is obtained. The weight of concrete is 522.78 Tonnes and weight of steel obtained is 9.38 Tonnes. Technique 2 is now employed in the next example to investigate depths for this model.

7.8.5.2 Design using Technique 2

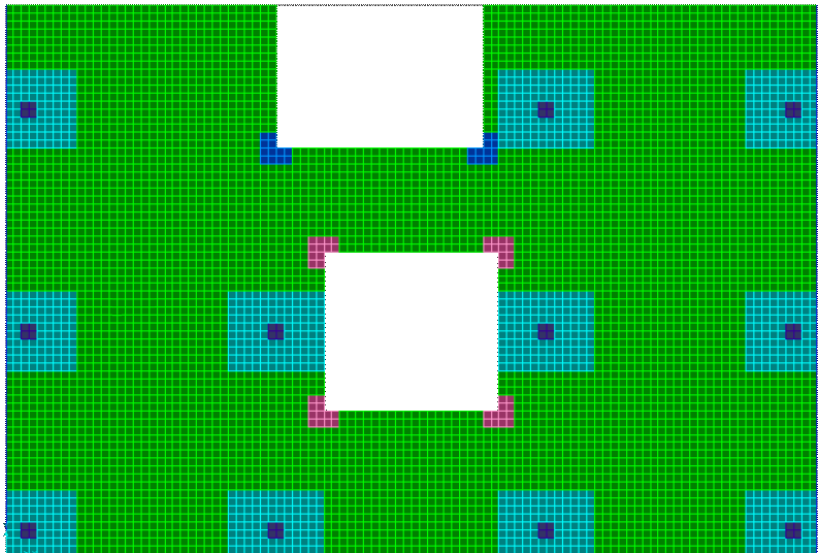

Fig. 7.119. Initial Model of Q2 Project with Atrium

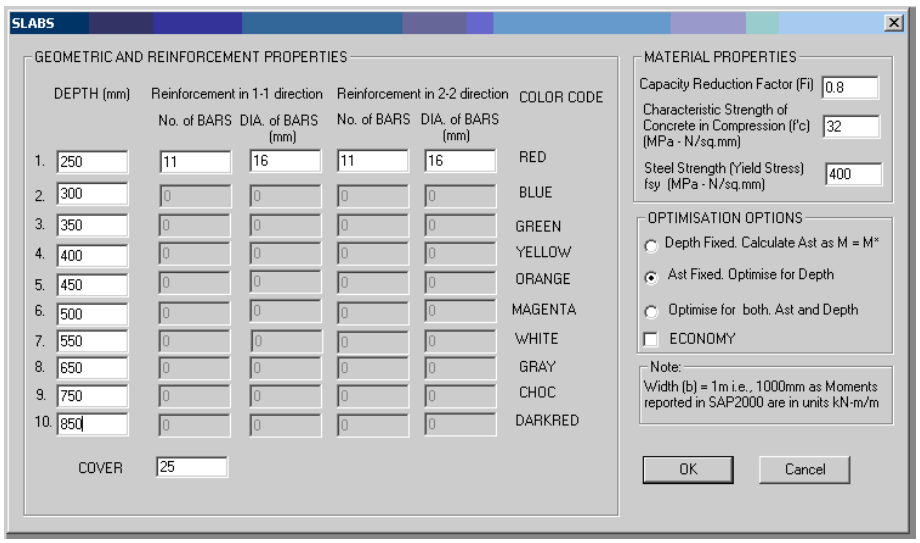

Fig. 7.120. Design Data for Technique 2

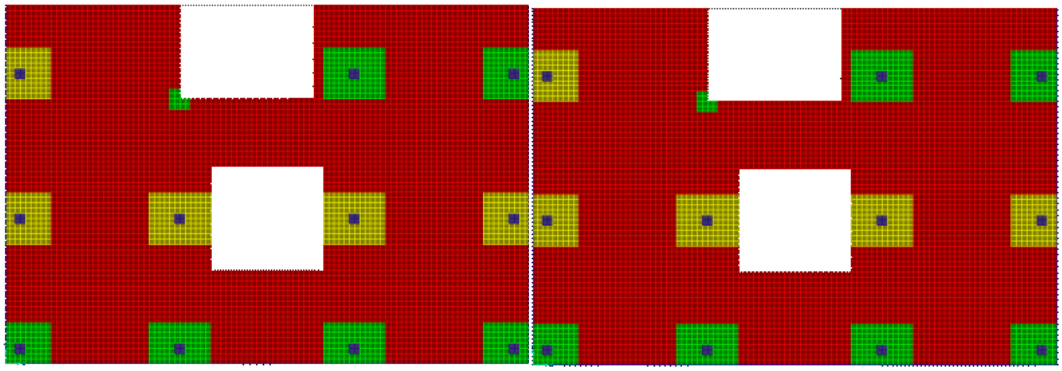

(a) 1st iteration (b) 2nd iteration

Fig. 7.121 (a-b).

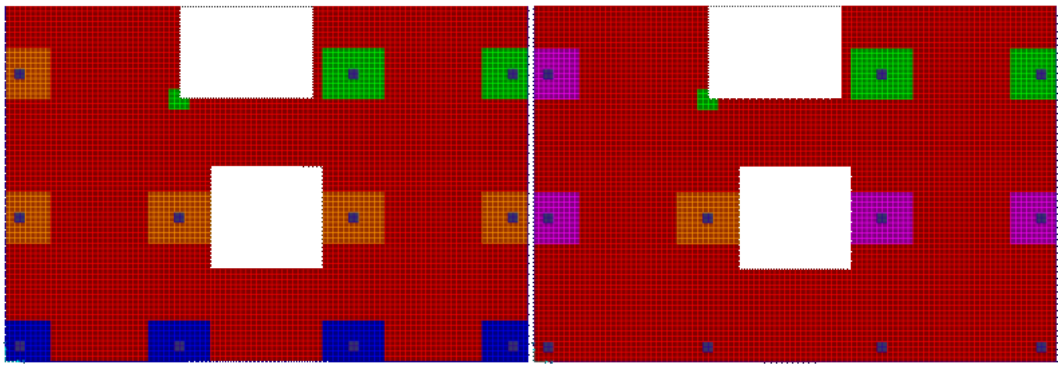

(c) 3rd iteration (d) 4th iteration

Fig. 7.121. Technique 2 Design Solutions for Q2 Project with Atrium

The solution settles and stabilizes from the 4th iteration onwards, satisfying bending moment criterion in all elements of the slab. Most of the slab has settled for a depth of 250 mm with 11-Y16 bars. For 11-Y16 bars specified throughout the slab, different depths are observed for the drop panels. No drop panels are needed in front for the four drop panels in the initial model. The drop panels near the atrium have settled on 450 mm (Orange) and 500 mm (Magenta) depths respectively. Three exterior drop panels too seem to have settled on 500 mm depths (Magenta). The drop panels near the lift core opening and the exterior drop panel next to it have settled on a depth of 350 mm (Green) respectively. Due to asymmetry of the model, and due to moment redistribution when the thickness is changed, all drop panels have settled on different depths. It is important to use Technique 3 to find out the optimal requirement of depth and steel in all regions. This is investigated in the next example.

Table 7.21. Technique 2 Design Optimisation Results for Q2 Project with Atrium

Iteration No.	Concrete Weight (Tonne)	% saving in Concrete Weight	Total Steel Weight (Tonne)	% saving in Total Steel Weight	Total Cost of Concrete (AU $)	Total Cost of Steel (AU $)	TOTAL COST (AU $)	Max. Deflection (mm) * 3	Permissible Deflection (mm) (Span/250)	Satisfies Condition
Initial Model	522.78	-	15.61	-	32673.75	17171	49844.75	5.23 x 3 = 15.69	37.20	-
1	352.81	32.51 %	15.61	-	22050.63	17171	39221.63	9.40 x 3 = 28.20	37.20	NO
2	353.72	32.34 %	15.61	-	22107.50	17171	39278.50	9.72 x 3 = 29.16	37.20	NO
3	353.38	32.40 %	15.61	-	22086.25	17171	39257.25	10.26 x 3 = 30.78	37.20	NO
4	353.38	32.40 %	15.61	-	22086.25	17171	39257.25	10.26 x 3 = 30.78	37.20	YES
5	353.38	32.40 %	15.61	-	22086.25	17171	39257.25	10.26 x 3 = 30.78	37.20	YES
6	353.38	32.40 %	15.61	-	22086.25	17171	39257.25	10.26 x 3 = 30.78	37.20	YES
7	353.38	32.40 %	15.61	-	22086.25	17171	39257.25	10.26 x 3 = 30.78	37.20	YES
8	353.38	32.40 %	15.61	-	22086.25	17171	39257.25	10.26 x 3 = 30.78	37.20	YES
9	353.38	32.40 %	15.61	-	22086.25	17171	39257.25	10.26 x 3 = 30.78	37.20	YES
10	353.38	32.40 %	15.61	-	32673.75	17171	49844.75	10.26 x 3 = 30.78	37.20	YES

7.8.5.3 Design using Technique 3

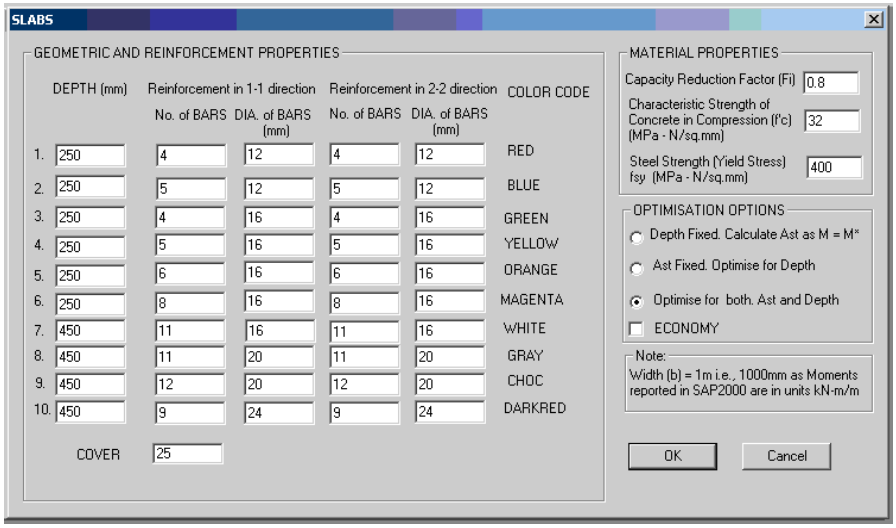

Fig. 7.122. Design Data for Technique 3

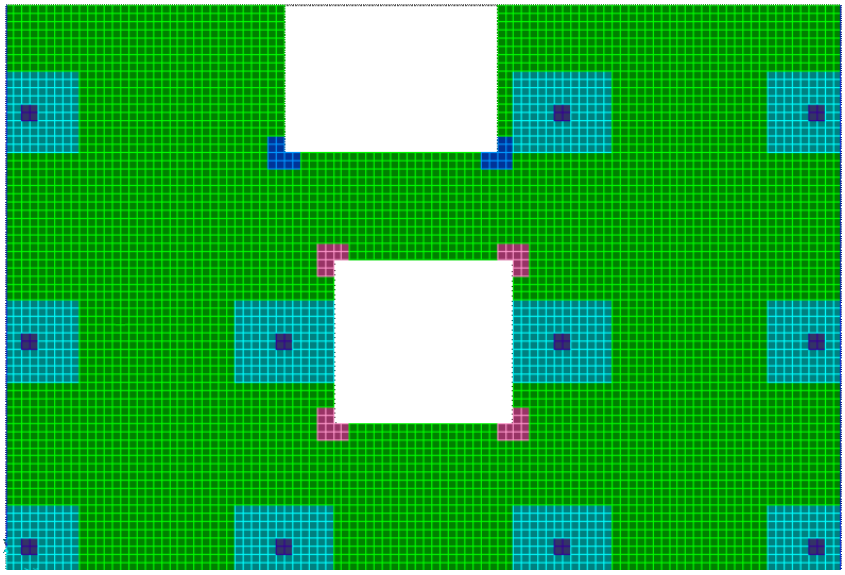

Fig. 7.123. Initial Model of Q2 Project with Atrium

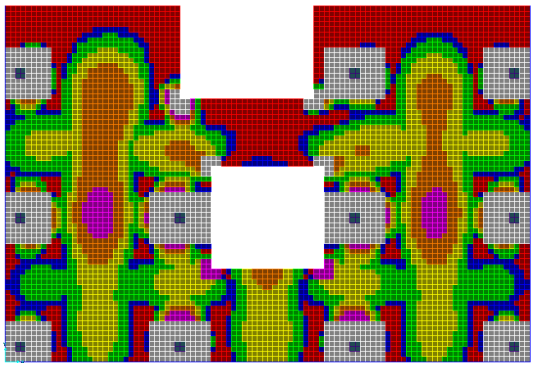

(a) 1st iteration

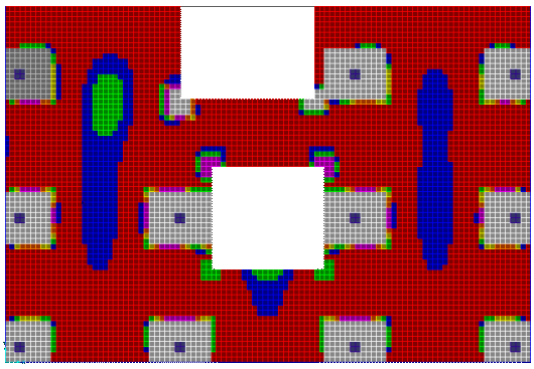

(b) 2nd iteration

Fig. 7.124 (a-b).

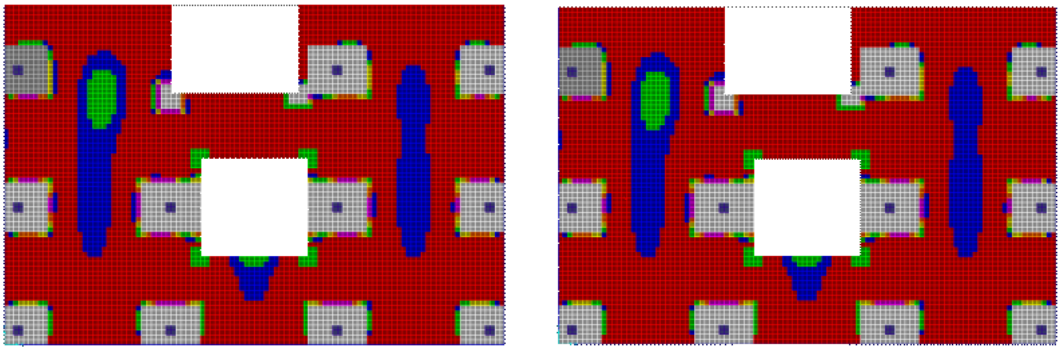

(c) 3rd iteration (d) 4th iteration

Fig. 7.124. Technique 3 Design Solutions for Q2 Project with Atrium

The solution settles and stabilizes from the 4th iteration onwards, satisfying the bending moment criterion in all elements of the slab. All the drop panels have settled on White sections (450 mm depth – 11Y16 bars) with one edge drop panel requiring Grey (450 mm depth – 11Y20 bars). White sections are also seen for the corner panels near the lift core opening. The corner panels near the atrium require a section of 250 mm depth – 4Y16 bars (Green). Most of the slab has settled on the first section of 250 mm depth with 4-Y12 bars (Red) with more steel seen in the mid span regions of the exterior spans (5-Y12 bars, Blue and 4-Y16 bars, Green). This design is very similar to the design obtained in Section 7.8.2.3 for the same model without the atrium opening using Technique 3. The tabular comparison on the next page shows the weight savings obtained for concrete and steel compared to the design using Technique 1.

Table 7.22. Technique 3 Design Optimisation Results for Q2 Project with Atrium

Iteration No.	Concrete Weight (Tonne)	% saving in Concrete Weight	Total Steel Weight (Tonne)	% saving in Total Steel Weight	Total Cost of Concrete (AU $)	Total Cost of Steel (AU $)	TOTAL COST (AU $)	Max. Deflection (mm) * 3	Permissible Deflection (mm) (Span/250)	Satisfies Condition
Initial Model	522.78	-	9.38	-	32673.75	10318	42991.75	5.23 x 3 = 15.69	37.20	-
1	370.42	29.14 %	7.79	20.40 %	23151.25	8569	31720.25	8.06 x 3 = 24.18	37.20	NO
2	369.42	29.34 %	6.88	26.65 %	23088.75	7568	30656.75	8.05 x 3 = 24.15	37.20	NO
3	369.42	29.34 %	6.86	26.65 %	23088.75	7546	30634.75	8.05 x 3 = 24.15	37.20	NO
4	369.42	29.34 %	6.86	26.65 %	23088.75	7546	30634.75	8.05 x 3 = 24.15	37.20	YES
5	369.42	29.34 %	6.86	26.65 %	23088.75	7546	30634.75	8.05 x 3 = 24.15	37.20	YES
6	369.42	29.34 %	6.86	26.65 %	23088.75	7546	30634.75	8.05 x 3 = 24.15	37.20	YES
7	369.42	29.34 %	6.86	26.65 %	23088.75	7546	30634.75	8.05 x 3 = 24.15	37.20	YES
8	369.42	29.34 %	6.86	26.65 %	23088.75	7546	30634.75	8.05 x 3 = 24.15	37.20	YES
9	369.42	29.34 %	6.86	26.65 %	23088.75	7546	30634.75	8.05 x 3 = 24.15	37.20	YES
10	369.42	29.34 %	6.86	26.65 %	32673.75	10318	30634.75	8.05 x 3 = 24.15	37.20	YES

7.8.6 "SAFE" Example

The following model is used in the software 'SAFE' as a tutorial problem. It is built in SAP2000 for the specified spans, loading and other design parameters and Technique 3 is applied to investigate the results obtained. A comparison with the design obtained using the software 'SAFE' is performed at the end to investigate design improvements using the proposed optimisation approach to slab design. The project is an irregularly shaped suspended concrete slab with overall dimensions of 35.0 m x 36.60 m. A large opening exists in the interior for stair access. The 250 mm thick slab is supported by 300 mm thick walls, 400 mm thick drop panels in the SAFE model (our aim is to find out the design of the drop panels as well, therefore thickness of drop panels in the initial model in SAP2000 is kept the same as the slab thickness that is 250 mm), 300 x 600 mm beams on two perimeter sides. Columns are typically 460 mm square, and the story height below the slab is 3.60 m. The model will be analysed for a uniform dead load of 30 pounds per square foot (i.e. 1.44 kPa) plus the self-weight of the structure and a live load of 50 pounds per square foot (i.e. 2.4 kPa). The loads are mentioned in foot-pound units, as that is how they have been specified in the SAFE model. The total number of elements in the initial model is 5688 elements. The dimensions and screenshots are shown below.

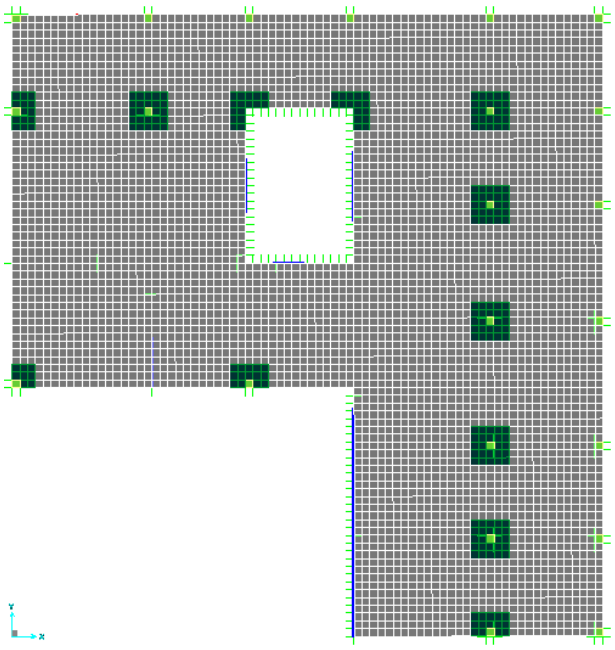

Fig. 7.125. Plan View of Initial Model of SAFE Example

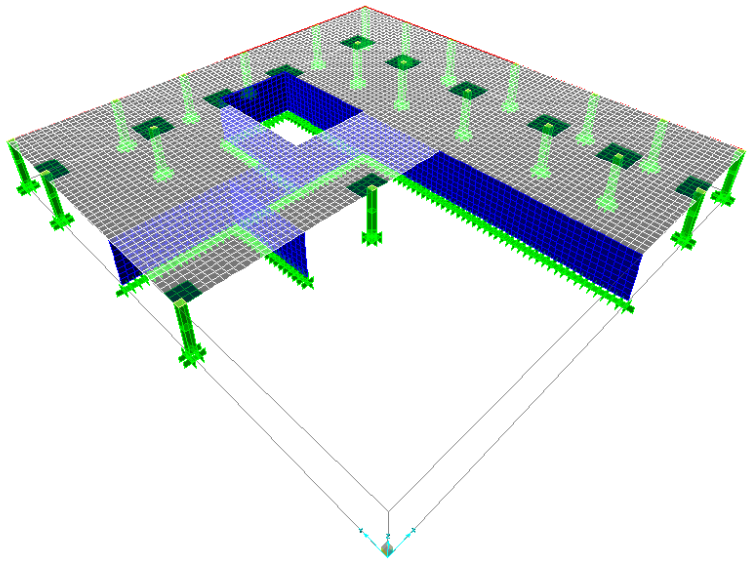

Fig. 7.126. Frontal 3D View of Initial Model of SAFE Example

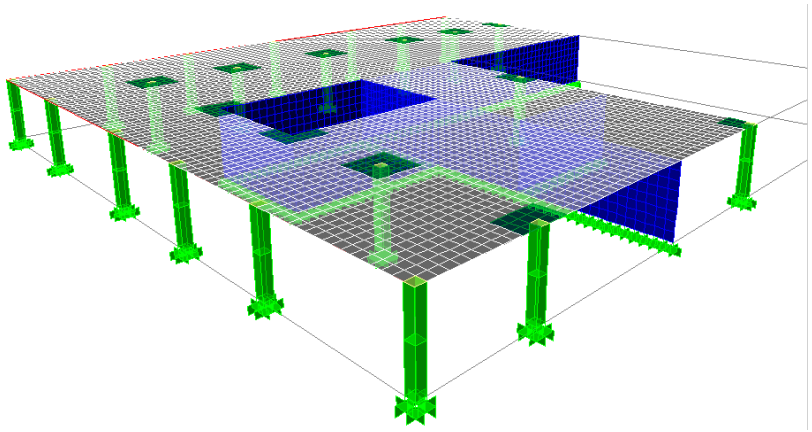

Fig. 7.127. Backside 3D View of Initial Model of SAFE Example

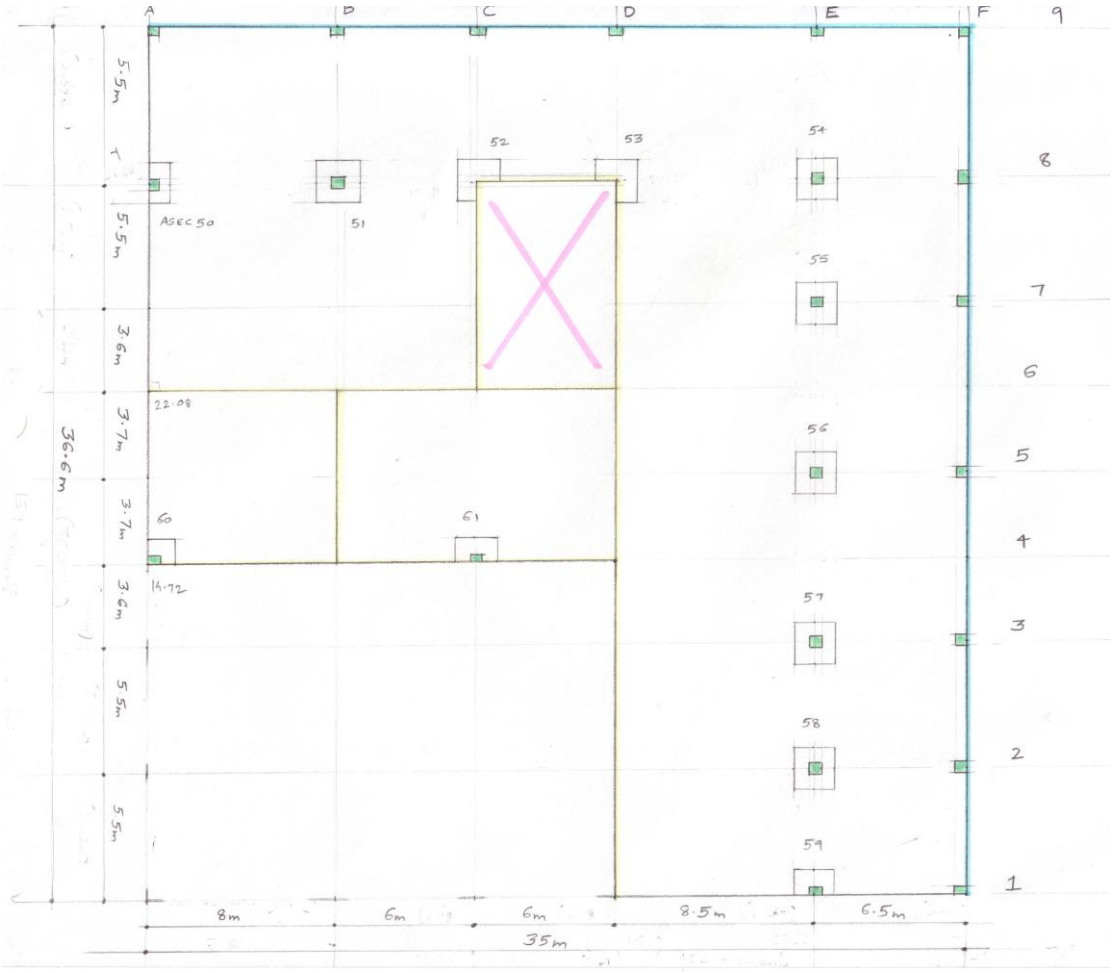

Fig. 7.128. Plan Dimensions of Initial Model of SAFE Example

7.8.6.1 Design using Technique 3

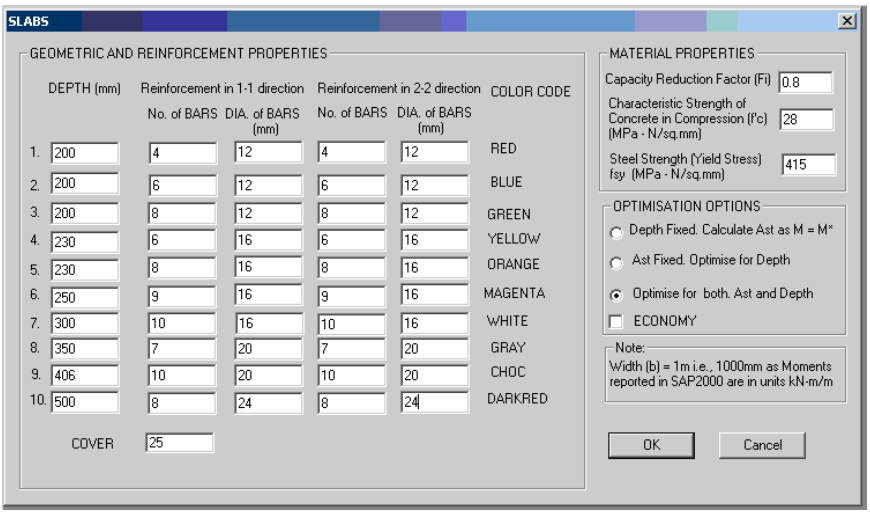

Fig. 7.129. Design Data for Technique 3

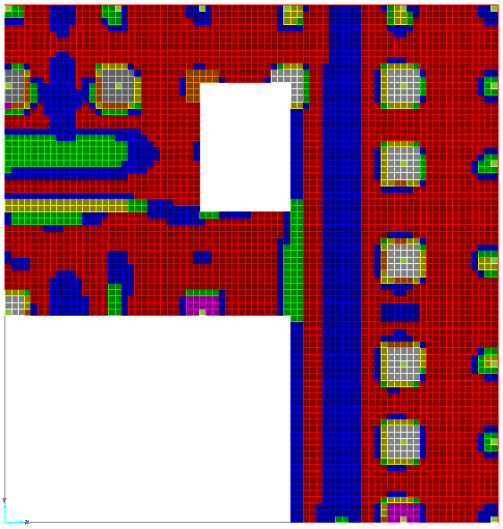

(a) 1st iteration

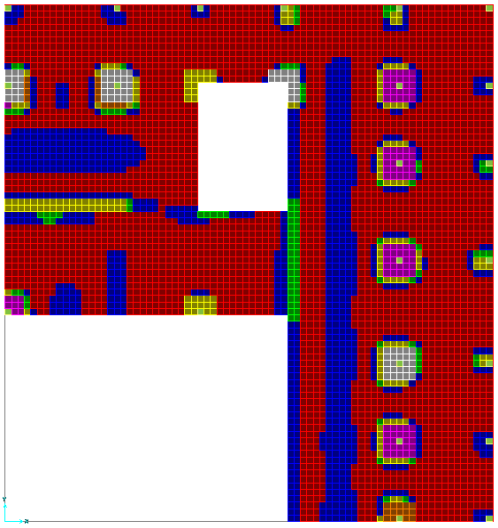

(b) 2nd iteration

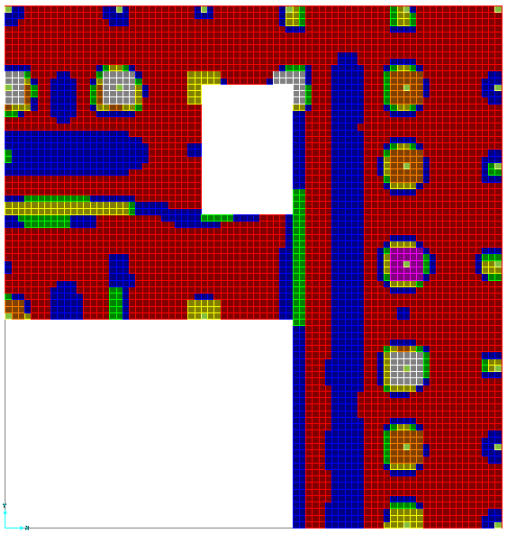

(c) 3rd iteration

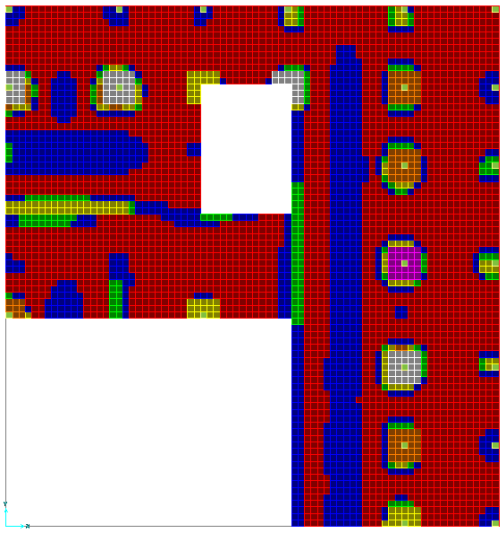

(d) 4th iteration

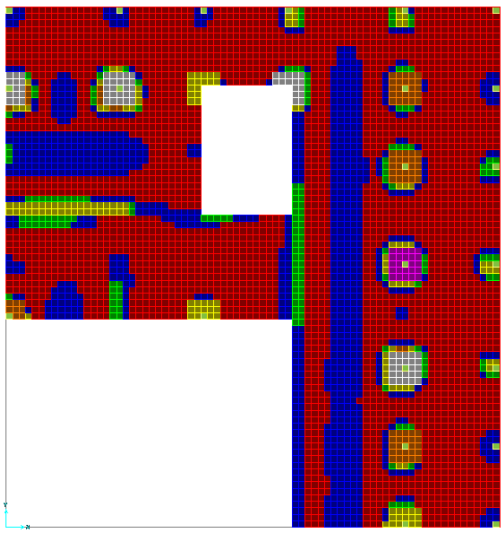

(e) 5th iteration

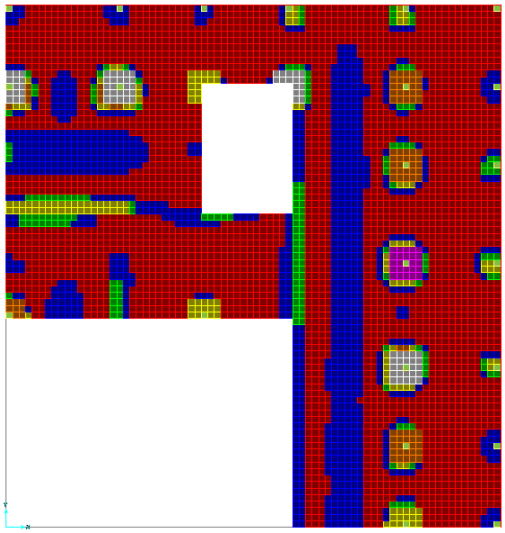

(f) 6th iteration

Fig. 7.130. Technique 3 Design Solutions for SAFE Example

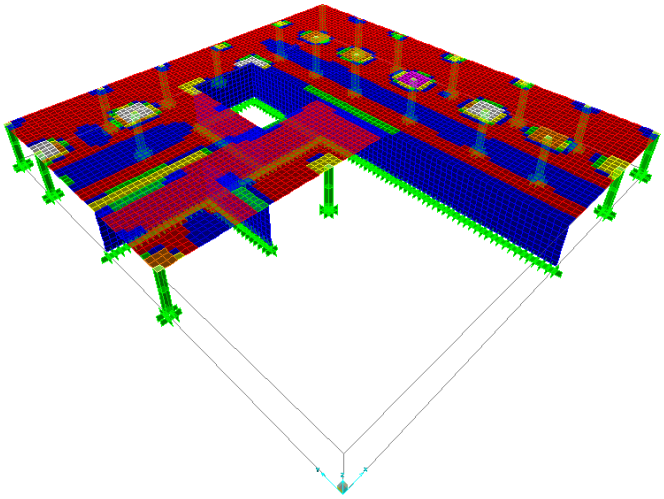

Fig. 7.131. Optimal Design Solution using Technique 3 for SAFE Example

The solution settles and stabilizes from the 6th iteration onwards, satisfying bending moment criterion for all elements in the slab. The first section is seen to suffice in most regions of the slab (200 mm depth – 4Y12 bars, Red) with more steel required in the areas where the wall meets the slab. A vertical blue band indicating 200 mm depth with 6-Y12 bars is seen at the mid span of the slab next to the opening. Most of the interior drop panels require different sections as is seen in the optimal solution above. The sections required for the drop panels vary probably due to asymmetry of the model. It is also seen that more steel is required at the edge column supports compared to the design in the surrounding areas, though thicker drop panels are not required. The table on the next page shows the savings in weight attained for concrete and steel compared to the design obtained using Technique 1. The optimal solution shows a concrete weight saving of 22.09 % and a steel weight saving of 32.16 % compared to the design obtained using Technique 1. Comparison with 'SAFE' design is carried out in the next section.

Table 7.23. Technique 3 Design Optimisation Results for SAFE Example

Iteration No.	Concrete Weight (Tonne)	% saving in Concrete Weight	Total Steel Weight (Tonne)	% saving in Total Steel Weight	Total Cost of Concrete (AU $)	Total Cost of Steel (AU $)	TOTAL COST (AU $)	Max. Deflection (mm) * 3	Permissible Deflection (mm) (Span/250)	Satisfies Condition
Initial Model	581.78	-	7.40	-	36361.25	8140	44501.25	6.80 x 3 = 20.40	34	-
1	458.71	21.15 %	5.28	28.65 %	28669.38	5808	34477.38	10.33 x 3 =30.99	34	NO
2	454.78	21.83 %	5.07	31.49 %	28423.75	5577	34000.75	11.29 x 3 =33.87	34	NO
3	453.48	22.05 %	5.04	31.89 %	28342.50	5544	33886.50	11.30 x 3 =33.90	34	NO
4	453.30	22.08 %	5.03	32.03 %	28331.25	5533	33864.25	11.30 x 3 =33.90	34	NO
5	453.27	22.09 %	5.03	32.03 %	28329.38	5533	33862.38	11.30 x 3 =33.90	34	NO
6	453.27	22.09 %	5.02	32.16 %	28329.38	5522	33851.38	11.30 x 3 =33.90	34	YES
7	453.27	22.09 %	5.02	32.16 %	28329.38	5522	33851.38	11.30 x 3 =33.90	34	YES
8	453.27	22.09 %	5.02	32.16 %	28329.38	5522	33851.38	11.30 x 3 =33.90	34	YES
9	453.27	22.09 %	5.02	32.16 %	28329.38	5522	33851.38	11.30 x 3 =33.90	34	YES
10	453.27	22.09 %	5.02	32.16 %	28329.38	8140	33851.38	11.30 x 3 =33.90	34	YES

Note: Permissible deflection is taken as the ratio of the maximum span (8.5 m) by 250, which is 34 mm.

7.8.6.2 Comparison with SAFE Design

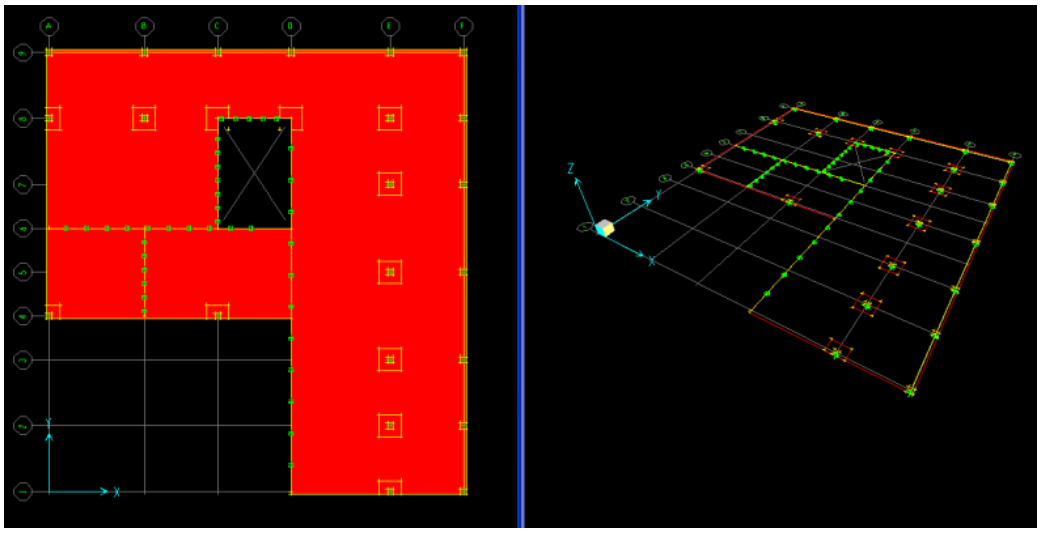

(a) Planar View (b) 3D View

Fig. 7.132. Initial Model created in SAFE

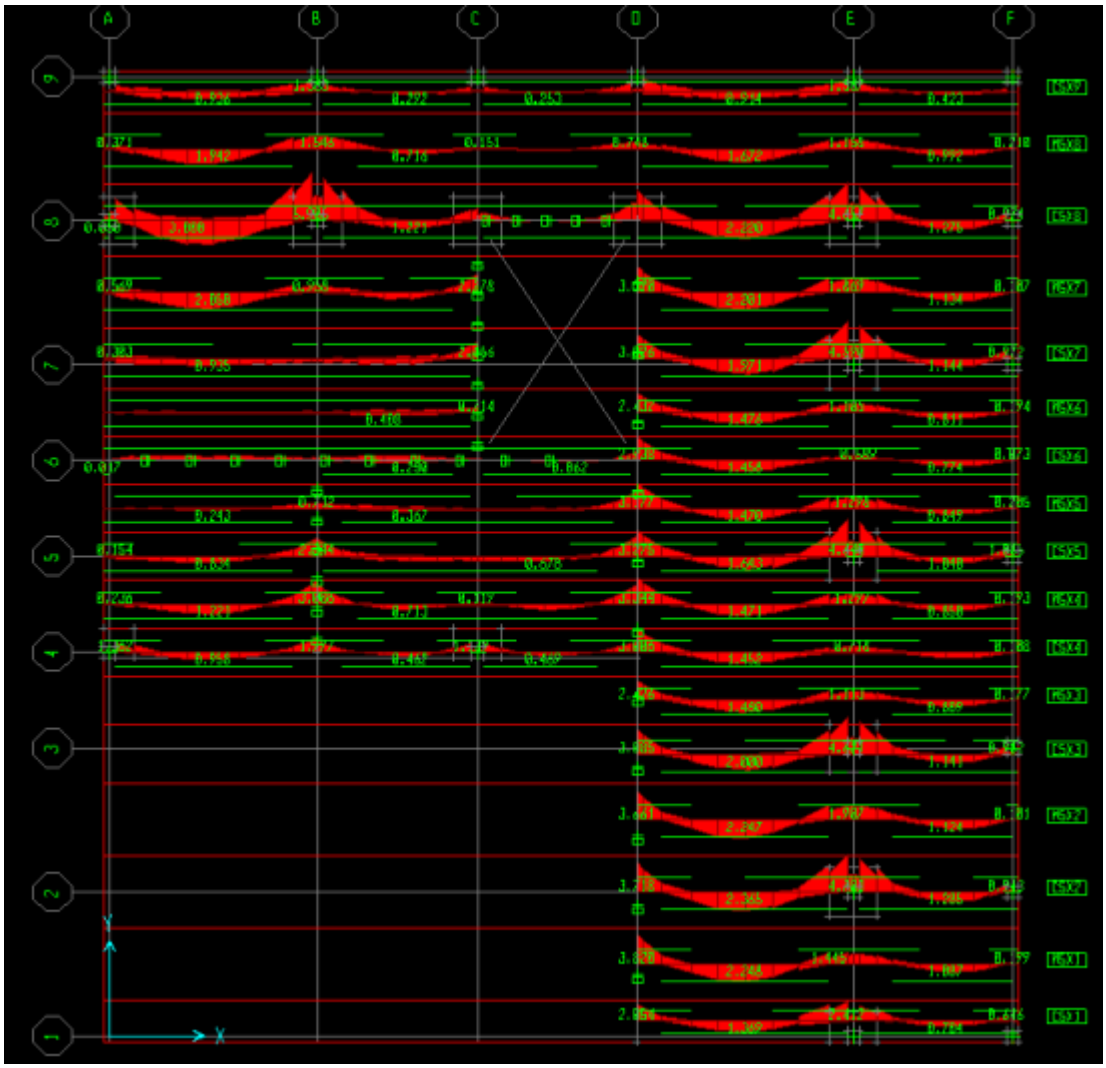

Fig. 7.133. Reinforcement required in X-strip direction (Shows rebar area required in *inches*^{2})
(Design obtained using software 'SAFE' based on the Conventional Strip Design Method)

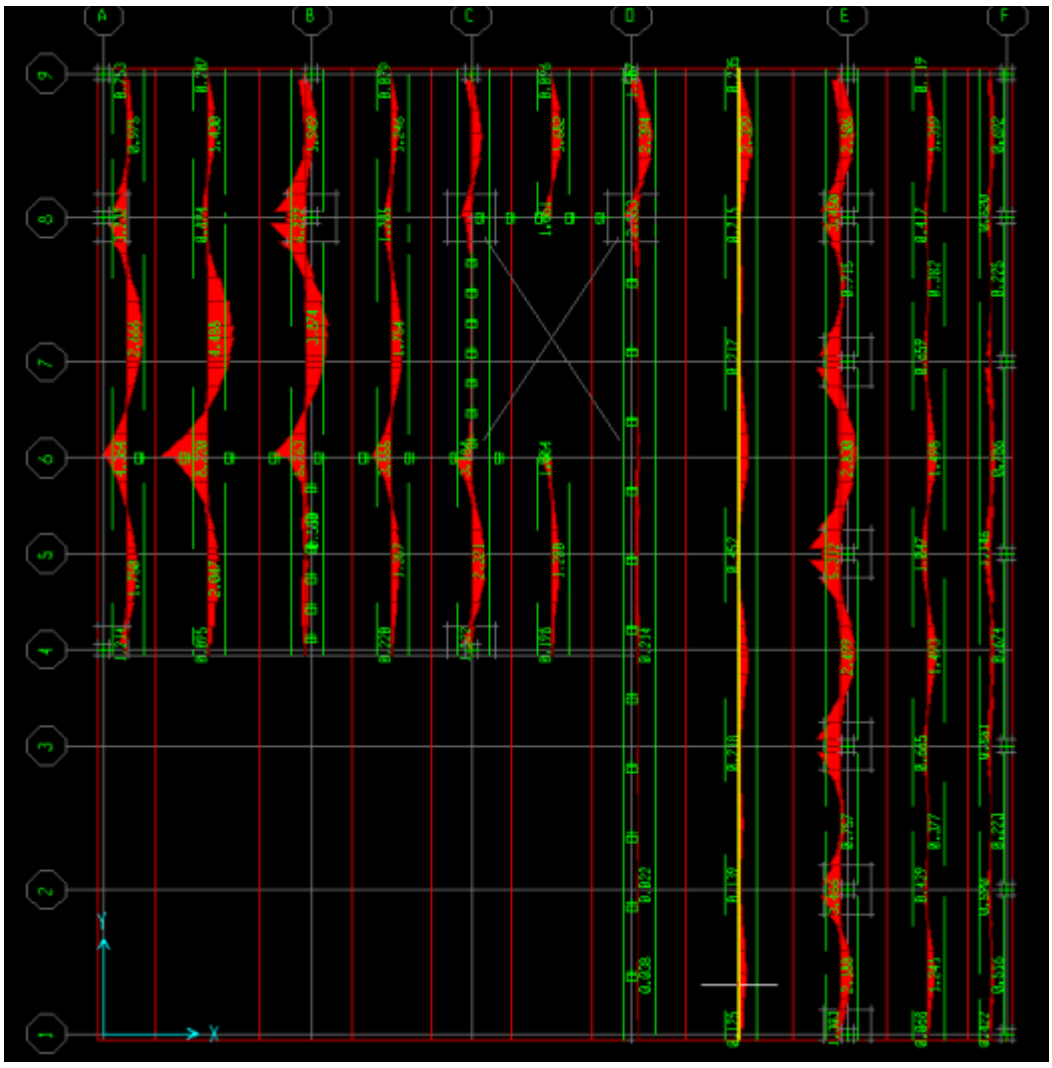

Fig. 7.134. Reinforcement required in Y-strip direction (Shows rebar area required in *inches*^{2})
(Design obtained using software 'SAFE' based on the Conventional Strip Design Method)

The design obtained using Technique 3 (Fig. 7.130-f above) in Section 7.8.6.1 is based on AS 3600 code provisions whereas the design obtained using the software *SAFE* (shown above in Fig. 7.133 and Fig. 7.134) is based on ACI 318-02 code provisions (as AS 3600 design code provisions are not available in *SAFE*). Although differences may exist in the designs, it is worthwhile to study the comparison. Let's briefly compare the designs at the following two locations:

1. For bottom steel in both directions at mid-span (consider the region between grid lines AB and 7-8 for middle strips in both directions)
2. Top steel in a drop panel at one of the column supports (drop panel design at column location E2).

1. Bottom steel at mid-span:

X-direction:

SAFE DESIGN (Refer Fig. 7.133 above):

2.068 $inches^2$ $\times$645.16 (to convert into mm^2) = 1334.19 mm^2

Let's consider Y-12 bars (area of one bar is 113.08 mm^2), then 1334.19/113.08 = 11.8 i.e. 12 bars of Y12 diameter. This quantity of steel is needed in a region of 2.75 m width (width of middle strip in X-direction). Therefore, steel quantity needed per metre width = 12/2.75 = 4.36 i.e. *5-Y12 bars per metre width*.

TECHNIQUE 3 DESIGN (Refer Fig. 7.130-f above):

X-direction: *6-Y12 bars per metre width* as shown by the Blue colour in Fig. 7.130-f above.

COMMENT:

Though an additional bar of 12 mm diameter is needed per metre width in the middle strip in the x-direction at this location using Technique 3, it should be noted that in the dataset given in Fig. 7.129 above, 5-Y12 bars are not specified (either 4 or 6 Y-12 bars are given, Red and Blue sections). The algorithm could probably have chosen it if it had been specified. Moreover, Technique 3 design in this region indicates a slab depth of 200 mm (Blue indicates a section requirement of 200mm depth with 6-Y12 bars both ways). Whereas, in the *SAFE* design, the slab depth everywhere is 250mm as is specified in the initial model.

Y-direction:

SAFE DESIGN:

4.488 $inches^2$ $\times$645.16 (to convert into mm^2) = 2895.48 mm^2

Let's consider Y-12 bars (area of one bar is 113.08 mm^2), then 2895.48 /113.08 = 25.61 i.e. 26 bars of Y12 diameter. This quantity of steel is needed in a region of 4 m width (width of middle strip in Y-direction). Therefore, steel quantity needed per metre width = 26/24 = 6.5 i.e. *7-Y12 bars per metre width*.

TECHNIQUE 3 DESIGN:

Y-direction: *6-Y12 bars per metre width* as shown by the Blue colour

in Fig. 7.130-f above.

COMMENT:

A saving of 1-Y12 bar per metre width is seen in the Y-direction in addition to the concrete weight saving (200 mm depth designed in this region as against 250 mm depth in *SAFE*).

2. Drop Panel Design for Top Steel at Column Location E2:

X-direction:

SAFE DESIGN:

4.703 $inches^2$ $\times$645.16 (to convert into mm^2) = 3034.19 mm^2

Let's consider Y-16 bars (area of one bar is 201.06 mm^2), then 3034.19/201.06 = 15.09 i.e. 16 bars of Y16 diameter. This quantity of steel is needed in a region of 2.75 m width (width of column strip in X-direction). Therefore, steel quantity needed per metre width = 16/2.75 = 5.81 i.e. *6-Y16 bars per metre width*.

TECHNIQUE 3 DESIGN:

X-direction: *8-Y16 bars per metre width* as shown by the Orange colour in Fig. 7.130-f above.

COMMENT:

Though two additional bars of 16 mm diameter are needed per metre width at the drop panel of column location E2 in the x-direction using Technique 3, it should be noted that the thickness designed for bending by Technique 3 is of 230mm (as against 400mm considered in the *SAFE* model). Punching shear as an additional constraint is not included at this stage; otherwise the design obtained would have been thicker. This reduced depth explains the need for more steel.

Y-direction:

SAFE DESIGN:

3.466 $inches^2$ $\times$645.16 (to convert into mm^2) = 2236.12 mm^2

Let's consider Y-16 bars (area of one bar is 201.06 mm^2), then 2236.12 /201.06 = 11.12 i.e. 12 bars of Y16 diameter. This quantity of steel is needed in a region of 3.75 m width (width of column strip

in Y-direction). Therefore, steel quantity needed per metre width = 12/3.75 = 3.2 i.e. *4-Y16 bars per metre width*.

TECHNIQUE 3 DESIGN:

X-direction: *8-Y16 bars per metre width* as shown by the Orange colour in Fig. 7.130-f above.

COMMENT:

It should be remembered that in the dataset given in Fig. 7.129 above, equal amount of reinforcement is specified in both directions. If less quantity of steel had been specified for steel quantity in the Y-direction, then probably the algorithm would have chosen this. However, for a complex model such as the one in this example, it is not easy to anticipate the correct quantity of steel to be specified in both directions. This requires the judgement and experience of the engineer as well as several trials of various datasets before optimising.

Conclusion

Although the Technique 3 design for this drop panel (at column location E2) shows that slightly more steel is required in both directions, it should be noted that the thickness of the drop panel obtained for bending moment criterion is 230mm in the optimal solution, which is much smaller than the 400 mm depth specified in the *SAFE* model (Note that is *specified* in SAFE by the designer, not *determined* by SAFE). Punching shear as an additional constraint is not included at this stage in the optimisation algorithms; otherwise the design obtained would have been thicker with probably less steel. SAFE too does not design drop panels for punching shear. It only reports the 'Punching Shear Stress Ratios" that indicate whether the provided drop panels satisfy punching shear requirements or no. The design of the slab in SAFE is thus based only on bending moments. This flexural design comparison is therefore logical and useful. Moreover, savings in weight for bottom steel in both directions are also attained at other locations in the slab. Concrete weight savings are clearly demonstrated by Technique 3, which indicates that a slab depth of 200mm is generally needed throughout the slab (with satisfactory deflections) as against the 250 mm depth considered in the *SAFE* model. Remember AS 3600 design is being compared with an ACI-318-02 design. It should also be noted that in this model, there is only a single shell element atop the column supports, which are modelled as 3D solids. In Chapter 6 it was recommended to construct a mesh such that there is an overlay of at least 2x2 or 3x3 elements atop the column. This

would have resulted in more accurate solutions as observed in the Case Studies from Sections 7.8.1 to 7.8.5. However, for the model in this particular example, such an overlay results in a very fine mesh comprising 22752 elements. The FEA of such a finely meshed model requires well over 45 minutes for the SAP2000 solver. As a result, only a single element was considered atop the column in order to reduce the computational cost.

7.9 Concluding Remarks

Three new techniques for slab design based on finite element results have been developed in this chapter to obtain optimal conceptual designs. The emphasis of the proposed techniques is based on design, not on a precise stress analysis. The algorithms and implementation details of the techniques proposed have been discussed. To test the proposed methods, all three techniques are applied to a wide variety of examples with different geometries beginning with a simple single-span one-way slab system, to a continuous one-way slab, symmetrical and asymmetrical flat slabs and case studies involving openings and complicated geometries.

Parameter studies investigating the effect of load and steel quantity on results are first carried out for the simple example of a single span one-way slab. Economical considerations (cost of concrete, cost of steel and total material cost) in the choice of design solutions obtained using all three techniques is discussed in the example of the continuous one-way slab system and the advantage of Technique 3 over the other two design techniques is clearly demonstrated (Section 7.6.6 to Section 7.6.8).

Moving onto the flat slab system of floor slabs, the problems associated at the column supports are first investigated. Effects of column size (i.e. mesh size) and steel quantity on results are studied. Design optimisation solutions reveal the necessity of a new modelling and design approach for flat slabs especially for regions near the column supports. A new modelling and design approach that integrates the ESO method together with the Group ESO method is therefore presented before applying the techniques to slabs in real buildings. The benefits of using this new modelling approach are clearly demonstrated first by exhaustive examples and then by case studies.

'Numerical studies' investigating the cause of asymmetrical design solutions and oscillating results for doubly symmetrical flat slabs are carried out. The suitability of a couple of design approaches such as the *Moment Difference Approach* and the *Moment Relaxation Approach* is investigated. Section 7.7.2.4.4 in 'Numerical studies' clearly demonstrates the need for adopting the maximum value (and not the average value) of the maximum smoothed nodal

values among the group as the design bending moment. Technique 2 is mostly applied in the numerical studies rather than Techniques 1 or 3, the simple reason being it is easier to critically analyse and investigate the design solutions for drop panels by comparing the *'thickness design'* with hand calculations using the 'Simplified Method of Design'.

The design solutions of a symmetrical flat slab using all three techniques are critically investigated (Section 7.7.3) before proceeding with applying these techniques to slabs in real buildings (case studies). The advantage of using the 'Economy' option with Technique 3 clearly demonstrates the potential for designing slabs based on not only the bending moment capacity criterion but also based on material cost considerations in the optimisation process. Each of the three techniques gives a different concept design for the structural engineer to consider and significant material savings are seen in all the examples. To make the work in this chapter suitable for practical application, side constraints are imposed on all the design variables (as per most requirements of the Australian Standard, AS 3600). Multiple models are created for the case studies and different concept designs are produced in each case using the three proposed techniques. Comparisons with the industry partner's design, which uses conventional method, show significant saving in material (both concrete and steel).

The optimal solution in each case does not take long to converge and is generally obtained within ten iterations.

It should be remembered that the design solutions obtained using the proposed techniques are based on a linear elastic finite element analysis, ease of practical application for the design engineer being one of the objectives. However, although it would have increased the computational cost, a non-linear finite element analysis would have predicted more accurately the physical behaviour of the slab near the column supports. Though the proposed modelling and design techniques give rational, safe and economical design solutions for the drop panels and are adequate from a practical point of view, future work could look into extending the proposed techniques from a non-linear perspective.

CHAPTER 8: Optimal Conceptual Design of Slabs for Flexure, Punching Shear and Transverse Shear

8.1 Introduction

Conceptual design for flexure using the ESO method for sizing optimisation problems of slabs has been treated in Chapter 7. In this chapter, the procedure is extended to include punching shear and transverse shear as additional constraints in the optimisation process. The goal of the optimisation then is to seek an optimal solution that satisfies bending requirements in both directions, punching shear requirements at column supports and transverse shear requirements. To reduce the weight of a slab for given strength design constraints, inefficient material is gradually removed from the slab. The weight is reduced by sizing the element from the discrete set of values (sections provided by the user in the interface) for the objective constraints (bending moment and shear). The problem therefore may be modelled with an initial uniform thickness that lies between the minimum and maximum thickness of the sections provided by the user in the interface in order to achieve the desired objective of minimum steel and concrete consumption. Such an initial uniform thickness is chosen such that it satisfies serviceability requirements for the given geometry and loading. Three techniques, each with a specific objective, are formulated. It should be noted here that a rigorous sensitivity analysis is not performed to determine the effect of size change (whether increase or decrease in thickness) on the objective displacement or stiffness. Rather, the elements are designed for strength in bending and strength in shear and the process of finite element analysis and design optimisation is repeated until a steady state is reached wherein there is no further moment redistribution in the slab. It should also be noted that the discrete set of thicknesses (or sections) too have constraints imposed on them as per AS 3600 code provisions for minimum thickness, minimum steel, maximum steel and ductility. As these constraints are treated in a special way, they are not directly included into the constraint set in the problem formulation. Examples are presented at the end of the chapter that demonstrate the need to include shear requirements in addition to flexure. The criteria for punching shear and transverse shear are programmed for the requirements in AS 3600 and follow the procedures described in Section 5.4 of Chapter 5. The optimisation formulation is described in Section 8.3 and element-sizing criteria are covered in Section 8.4. Section 8.5 presents the optimisation procedure and algorithm followed by the examples.

8.2 Scope of the Work in This Chapter

As mentioned in Section 8.1, the scope of work in this chapter is to extend the system developed in Chapter 7 to include shear as an additional constraint in addition to flexure. To obtain practical designs of real slabs it is necessary to follow code specifications, such as AS3600 provisions relating to flexural and shear design of slabs. The work in this chapter is therefore to investigate the differences in results obtained when the punching shear and transverse shear criteria are added. New algorithms are programmed for all three techniques (Technique 1, Technique 2 and Technique 3) to include the above mentioned shear constraints. The idea is therefore to seek a solution where in addition to satisfying the yield condition or the plastic moment condition requirements (i.e. eq. 5.20) in all designable elements in the slab, the punching shear and transverse shear requirements (eq. 5.30) are also satisfied for all designable elements in the slab. This would mean that the slab designed is safe for flexure as well as for shear for the load specified.

The punching shear strength requirements included in this approach can only be used to design drop panels that do not have an opening near them. If there is an opening near an internal column, then the calculation for the critical perimeter will change and this is not accounted for in this study. This work can therefore be tested on regular flat slabs without any openings. It is to be remembered that this work is conducted with the specific intention of designing flat slabs and therefore beam-and-slab models will not be considered in this work. Beam and slab models can however be designed using the techniques developed in Chapter 7.

8.3 Optimisation Problem Formulation

In the extended method, the three techniques developed, each one of which has a specific objective function is modified to include additional shear constraints.

1. Depth Constant, Steel Varying:

This technique is used to find the distribution or layout of steel required in various parts of the slab when the depth or thickness of the slab is kept constant throughout. This is similar to conventional slab design approaches and is also similar to the objective of various commercial slab design software. There is no room for optimisation in this approach as the depth is kept constant and it is not possible to specify reinforcement within each individual finite element in SAP2000. In this technique, the weight of steel is used as the objective function and the

constraints are the yield condition or plastic moment condition (Eq. 5.10, $\phi \times R_u > S^*$) and shear strength requirements (Eq. 5.30, $V^* \leq \phi \times V_u$). In other words, the objective is to seek a minimum weight of steel in the slab when its depth is constant while satisfying its yield condition or plastic moment condition requirement and shear strength requirement for all elements in the slab.

2. Steel Constant, Depth Varying:

This technique is used to find the depths or thickness required in various parts of the slab when the steel in the slab is kept constant throughout. In this technique, the weight of concrete is used as the objective function and the yield condition or plastic moment condition (Eq. 5.10, $\phi \times R_u > S^*$) and shear strength requirements (Eq. 5.30, $V^* \leq \phi \times V_u$) are treated as the constraints. In other words, the objective is to seek a minimum weight of concrete in the slab when its reinforcement is constant everywhere while satisfying its yield condition or plastic moment condition requirement and shear strength requirement for all elements in the slab.

3. Both Depth and Steel Varying:

This technique is used to find the depths and steel required in various parts of the slab when both thickness and reinforcement are treated as variables. In this technique, the weight of concrete and weight of steel is used as the objective function, and the yield condition or plastic moment condition (Eq. 5.10, $\phi \times R_u > S^*$) and shear strength requirements (Eq. 5.30, $V^* \leq \phi \times V_u$) are treated as the constraints. In other words, the objective is to seek a minimum weight of concrete and steel in the slab while satisfying its yield condition or plastic moment condition requirement and shear strength requirement for all elements in the slab.

It should be noted here, that V_u is calculated differently for Punching Shear and Beam Shear. This is explained in Section 8.5.

8.4 Element Sizing Criteria

The philosophy used in the optimisation process for sizing elements mentioned in Section 7.4 of Chapter 7 is adopted in this work as well. Additionally, shear criteria are taken into consideration. A converged solution or stable stress field is sought in which the bending moments and shear nowhere exceed the yield limit. As mentioned previously, linear elastic

theory is applied to uncracked and unreinforced homogeneous concrete to determine the moments and shears at different points within the slab. This is done by using the finite element program SAP2000. This elastic moment distribution forms the basis of design. Each finite element is designed such that it must be capable of carrying the loads applied to it. In the context of the finite element model, the resulting stresses, moments and shears calculated at the common node of adjacent elements are discontinuous and thus not in equilibrium with one another despite the fact that they belong to the very same node. To overcome this situation, a smoothing algorithm is implemented that calculates the average values of nodal moments and shears at each node of the finite element. Having obtained these values, the design is carried out by applying the well-known yield conditions formulated for an infinitesimal d_x-d_y element (Eq. 5.10, $\phi \times R_u > S^*$) to check whether the provided *section* can resist the bending moments in both directions. The design is based on the assumption that the reinforcement is to be fully utilized up to its tensile yield strength. The section provided for each finite element must be such that the resistance provided at a fully plastic condition is everywhere equal to or greater than the stress resultant considered (in this case bending moments, punching shear and normal beam shear). Using Technique 2 and Technique 3 mentioned above, when the depth of elements is changed and the structure analysed again, it results in a moment redistribution within the slab. This moment redistribution is fully utilised in the proposed approaches by proceeding with iterative sizing optimisation of elements until a stable stress field (or steady state) is reached wherein there is no further moment redistribution in the slab. In this study, the maximum value of the smoothed nodal stress resultants, M_{11}, M_{22} and V_{Max} are used to design the section for each individual finite element. This method does not design "strips of slabs" or "section cuts" and therefore there is no computation involved in obtaining the "*design bending moment"* for any strip or section in a slab. Rather, each element and group is designed based on the maximum moment and shear in that element or group. Elements near the column supports are grouped into a 'Panel' and the capacity of each 'Panel' to resist punching shear is checked. If Eq. 5.30, $V^* \le \phi \times V_u$ is not satisfied, the slab thickness is increased uniformly for the drop panel. In all other regions of the slab, normal beam shear or transverse shear is also checked for the sections provided. If Eq. 5.30, $V^* \le \phi \times V_u$ is not satisfied for any element, then depending on the technique employed (Technique 1, Technique 2 or Technique 3), a new section is chosen such that it satisfies Eq. 5.30 in addition to Eq. 5.10. This is explained in detail in Section 8.5. It should be noted that V_u is calculated differently for Punching Shear and Beam Shear. This is also explained in Section 8.5

8.5 Optimisation Procedure

8.5.1 Algorithm

In the present optimisation approach, the plate elements of the slab are designed to resist the maximum bending moments and shear occurring in each element. The reinforcement in a slab is usually placed in two orthogonal directions. The elements are therefore designed to resist bending in both directions i.e. direction 1-1 which is similar to the global X-axis and direction 2-2 which is similar to the global Y-axis. In SAP2000, plate bending moments are reported at each node as M_{11} and M_{22} and plate transverse shear forces are reported at each node as V_{13} and V_{23}. M_{11} represents the bending moment in 1-1 direction, i.e. Global X axis and M_{22} represents the bending moment in the 2-2 direction, i.e. Global Y axis. The transverse shear forces are computed from moments using the equilibrium equations:

$$V_{13} = \frac{-dM_{11}}{dx_1} - \frac{dM_{12}}{dx_2}$$

$$V_{23} = \frac{-dM_{12}}{dx_1} - \frac{dM_{22}}{dx_2}$$

where x_1 and x_2 are in-plane coordinates parallel to the local 1 and 2 axes (SAP2000 Manual).

These bending moments and shears are reported per unit of in-plane length. In the optimisation program, the moment capacities in both directions and shear capacities of the ten user-defined sections are calculated based on the data provided by the user in the user-interface. The moment capacities are calculated by using Equation 5.20. The normal beam shear or transverse shear capacities are calculated by using Equation 5.31. The punching shear capacities of 'panels' over column supports are calculated by using Equation 5.40. As mentioned in Chapter 7, for flexural design, there is no post-processing applied in the optimisation program to compute the *design moment* for a strip or section of the slab. Each element is designed individually and the smoothed maximum nodal moment of each element is chosen as the *design moment*. The nodal moments obtained in both directions (M_{11} and M_{22}) and shears (V_{13}, V_{23} and V_{Max}) in SAP2000 are smoothed by employing a smoothing procedure. The procedure is simple wherein, in the first step, the average moment at *each node* (M_{11} and M_{22}) is calculated by averaging the moments (M_{11} and M_{22}) of all elements connecting to that node. In the next step, the design

moment in both directions (M_{11} and M_{22}) for each element is calculated by picking the *maximum* of the four smoothed nodal moments (M_{11} and M_{22}). This procedure is also used to smooth the shear stress resultants, V_{13}, V_{23} and V_{Max}. The program then designs elements and 'panels' based on whether Technique 1, Technique 2 or Technique 3 is chosen by the user.

Technique 1

If the user chooses Technique 1 above, the program designs the steel reinforcement in both directions. The program gives an indication of how much steel is required for resisting flexure and shear when the depth of the slab is constant throughout. Two separate output files are created that contain the steel requirement in each direction. The sections (i.e. steel in this case) are allotted such that Equation 5.10 ($\phi \times M_u > M^*$) and Equation 5.30 ($V^* \le \phi \times V_u$) are satisfied. This gives us the design of the reinforcement in the slab. No iterations are carried out as the depth in this case is constant and steel cannot be specified within the "Shell" element in SAP2000.

Technique 2

If the user chooses Technique 2 above, the program seeks the optimal thickness that satisfies bending in both directions and shear. The program gives an indication of how deep a section is required for resisting flexure and shear when the steel is kept constant throughout the slab. The program allots depth (i.e. 1 of 10 sections) to each element for resisting bending in the 1-1 direction and allots another section for resisting bending in the 2-2 direction, satisfying conditions of Equation 5.10 above ($\phi \times M_u > M^*$). Both these sections allotted may be different. The program then allots the bigger of the two sections as the final section to the element. The algorithm then checks if this provided section satisfies shear strength requirements (punching shear and normal beam shear) as per Equation 5.30 according to the procedure mentioned above. If Equation 5.30 is not satisfied, a deeper section is generally chosen. The iterative process is then continued till a steady state is reached wherein there is no further improvement in the design. Only those solutions are then chosen that satisfy Equation 5.10 and Equation 5.30 for all elements in the slab. This condition is monitored in each iteration. It is seen that this condition is not necessarily satisfied in all iterations. Therefore the optimal solution is that which satisfies Equation 5.10 and Equation 5.30 in all elements of the slab as well as shows the most savings in weight at the same time satisfying deflection limits prescribed in the code.

Technique 3

If the user chooses Technique 3 above, the program seeks the optimal layout of thickness and steel that satisfies bending in both directions and shear strength requirements. The program gives an indication of how deep a section and how much steel is required for resisting flexure and shear when both the steel and the depth are allowed to vary throughout the slab. The program allots sections (i.e. 1 of 10 sections) to each element for resisting bending in the 1-1 direction and allots another section for resisting bending in the 2-2 direction, satisfying conditions of Equation 5.10 above ($\phi \times M_u > M^*$). Both these sections allotted may be different. The program then allots the final section, as the one having the bigger moment capacity between the two, to the element.

The algorithm checks if this allotted section satisfies shear strength requirements as per Equation 5.30. If it does not satisfy Equation 5.30, then a deeper section is chosen such that it has a moment capacity equal to or higher than the allotted moment capacity of the section for flexure. Thus, this section then satisfies flexural strength requirements and shear strength requirements. In the code, it is important to choose a deeper section and not just a section having a higher moment capacity, as it may otherwise not satisfy shear strength requirements as per Equation 5.30. The iterative process is then continued till a steady state is reached wherein there is no further improvement in the design. Only those solutions are then chosen that satisfy Equation 5.10 and Equation 5.30 for all elements in the slab. This condition is monitored in each iteration. It is seen that this condition is not necessarily satisfied in all iterations and therefore the optimal solution is that which satisfies Equation 5.10 and Equation 5.30 in all elements of the slab as well as shows the most savings in weight at the same time satisfying deflection limits.

8.5.2 Punching Shear Design

In order to design the 'panels' over column supports for punching shear, it is necessary to calculate the ultimate shear strength of the concrete slab near the column, which is denoted by V_u. This ultimate shear strength is calculated by using Equation 5.40, which is reproduced here from Chapter 5.

$$V_u = \frac{V_{uo}}{1 + \dfrac{\dfrac{M_v^*}{a}}{\dfrac{8 \times V^* \times d}{u}}} \qquad (5.40)$$

where,

$$V_{uo} = u \times d \times f_{cv} \tag{5.36}$$

where,

$$f_{cv} = 0.17 \times \left(1 + \frac{2}{\beta_h}\right) \times \sqrt{f_c} \le 0.34 \times \sqrt{f_c} \tag{5.37}$$

V_u	:	Ultimate Shear Strength of the concrete slab near the column
V_{uo}	:	Ultimate Shear Strength of the slab with No Moment Transfer.
f_{cv}	:	Concrete Shear Strength
β_h	:	Ratio of the longest overall dimension of the column, Y, to the overall dimension, X, at right angles to Y.
f_c	:	Peak stress on the stress-strain curve of a typical specimen in compression
M_v^*	:	Difference between moments at the front and back face of column
a	:	Length of a side face of the critical perimeter
V^*	:	Design factored shear force
d	:	Effective depth of slab averaged around the critical perimeter
u	:	Total Length of the Critical Perimeter

In the computer code, Equations 5.35, 5.36, 5.37 and 5.40 are programmed to compute the ultimate shear strength of the concrete slab near the column.

The values of M_v^* in the x and y directions are usually different. The values of a are also different if the column is not square. In using equation 5.40 above, the greater of the two values of $\frac{M_v^*}{a}$ is employed. This is programmed in the computer code.

It is usually found that the condition in Equation 5.30, $V^* \le \phi \times V_u$ is satisfied. If not, then the program chooses a thicker or deeper section such that, in addition to satisfying flexural criteria, the section also satisfies the shear criteria of Equation 5.30.

It follows that in order to correctly calculate the various terms in Equation 5.40 above (especially M_v^*, a and u); a correct labelling approach for the columns and drop panels has to

be followed in the initial model. Figure 8.1 below depicts such a labelling scheme for a flat slab, the details of which are shown on the next page:

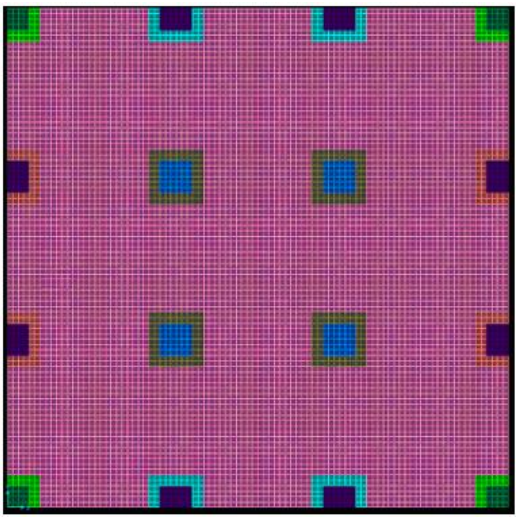

Fig. 8.1. Labelling Scheme for Drop Panels

8.5.2.1 Labelling Schema

Type	*Labelling ID for Area Elements*	*Description*
Design and Non-Design	ASEC1 – ASEC10	DESIGN SECTIONS
	ASEC11	Initial Thickness (Initial Design)
	ASEC12 – ASEC50	Non Design
	ASEC51 onwards	Design Domain
Non-design element ID's over COLUMNS		
	ASEC12 – ASEC20	CORNER COLUMNS
	ASEC21 – ASEC35	EDGE COLUMNS
	ASEC36 – ASEC46	INTERNAL COLUMNS
	ASEC47 – ASEC50	WALLS
Designable element ID's for PANELS		
	ASEC51 – ASEC60	CORNER COLUMN PANELS
	ASEC61 – ASEC80	EDGE COLUMN PANELS
	ASEC61 – ASEC70	Top and bottom Edge Panel (i.e. horizontal rectangle)
	ASEC71 – ASEC80	Left and right Edge Panel (i.e. vertical rectangle)
	ASEC81 – ASEC99	INTERIOR COLUMN PANELS
	ASEC100 onwards	Panels required near corners of openings or any other panels as required (for e.g., for Beam Shear)

Columns are modeled as frame elements with their labeling scheme as follows (required for obtaining Punching Shear Force, V^*, needed in punching shear design calculations).

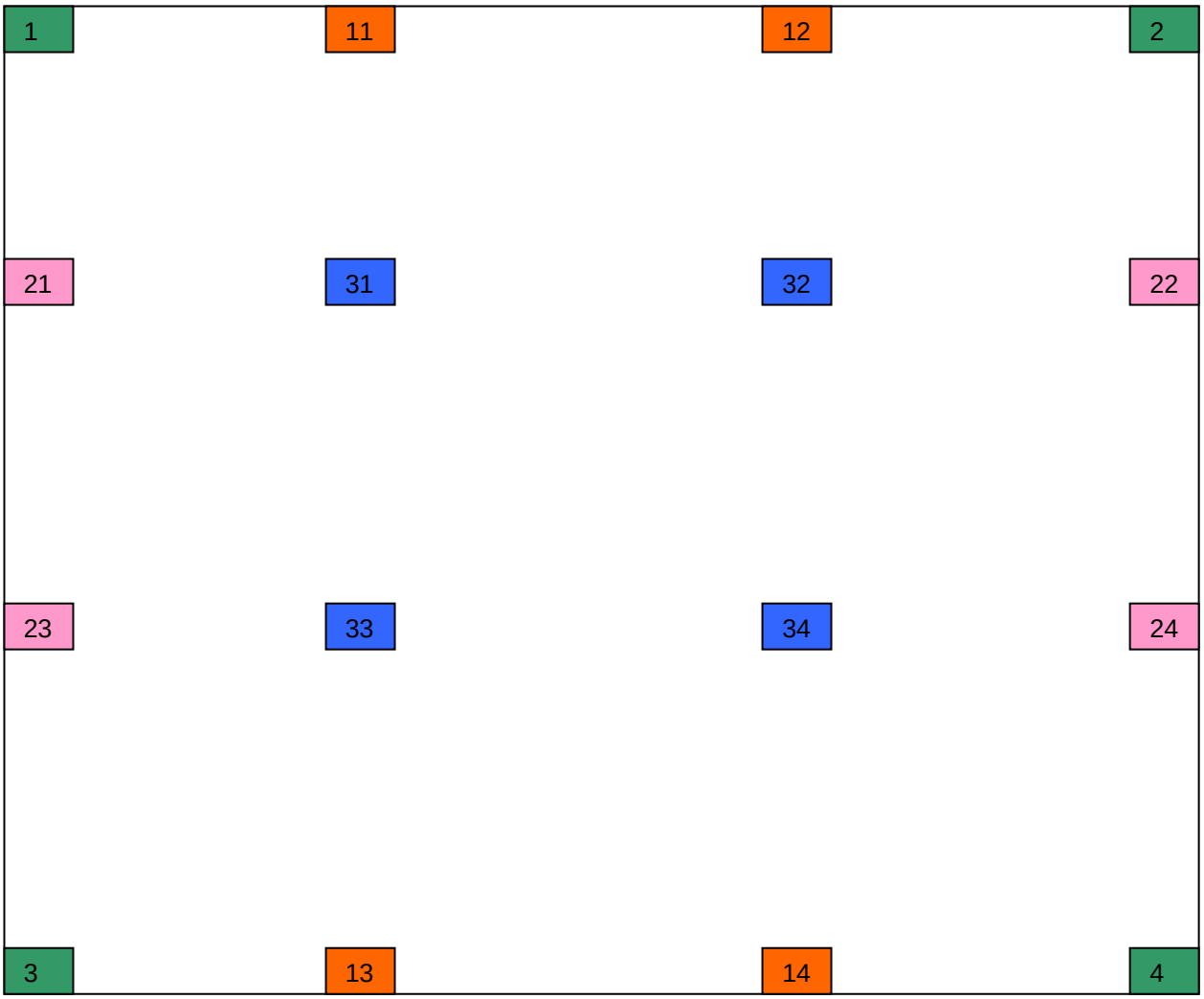

Fig. 8.2. Labelling schema for frames modeled as columns (Planar View)

Frame ID	Column Designation
1 – 10	CORNER COLUMNS
11 – 20	EDGE COLUMNS (Top and Bottom)
21 - 30	EDGE COLUMNS (Left and Right)
31 – 50	INTERNAL COLUMNS

The Punching Shear Force, V^*, needed in punching shear design calculations is obtained by reading the value of the vertical axial force in each of these columns.

8.5.3 Normal Beam Shear/Transverse Shear

Normal beam shear capacity of a section is calculated using Equation 5.31, which is reproduced from Chapter 5 as follows:

$$V_{uc} = \beta_1 \times b_v \times d_0 \times \frac{A_{st}}{b_v d_0} f_c' \qquad (5.31)$$

where,

$$\beta_1 = \left(1.4 - \frac{d_o}{2000}\right) \geq 1.1 \qquad (5.32)$$

b_v	:	Minimum effective web width in mm
d_o	:	Distance of the extreme compression fibre of concrete to the centroid of the outermost layer of tensile reinforcement in mm.
A_{st}	:	Area of fully anchored longitudinal steel provided in the tension zone.
β_1	:	Accounts for the increase in shear strength observed in shallow beams in a manner similar to the shear provisions of the CEB Model Code (1978).
f_c'	:	Characteristic Compressive Strength of concrete at 28 days

For a general cross section of a flat slab in beam action, the factored design shear force, V^* shall not exceed the value V_{uc} computed by equation 5.31 times ϕ (which is equal to 0.7). If the section fails in shear, there are several techniques to increase the shear strength of the system. One of the simplest methods is to increase the depth of the slab, which is adopted in the present algorithm. Increasing the depth of the slab will increase the shear capacity. The strength of the concrete may also be increased. The column dimensions can also be increased. Finally, the section can be reinforced with either stirrups or a stud rail (Kahn 2004). Equations 5.30, 5.31 and 5.32 are programmed into the computer code to compute the ultimate shear strength of the user-defined sections in the GUI. In SAP2000, once each finite element in the general cross section of the flat slab is designed based on flexural criteria described previously, the factored

ultimate shear strength of the "section allotted", $\phi \times V_u$, is then compared with the factored design shear force in each element. The design shear force, V^* in each element in SAP2000 is output as "V_{Max}". This design shear force, V^*, is increased by a factor of 1.5. If the condition in Equation 5.30 is satisfied, then it means that the shear capacity of the "allotted section" is greater than the required shear strength and the "allotted section" is chosen as the final design. If however, the condition in Equation 5.30 is not satisfied, then it means that though the 'allotted section" satisfies flexural criteria, the shear capacity of the "allotted section" is less than the required shear strength and therefore another section which satisfies Equation 5.30 (i.e. whose factored normal beam shear capacity is greater than the design shear force), in addition to flexural criteria is picked.

8.5.4 Shell Element in SAP2000

The "Shell" element in SAP2000 is a three or four node formulation that combines separate membrane and plate bending behavior. The plate bending behavior includes two-way, out-of-plane, plate rotational stiffness components and a translational stiffness component in the direction normal to the plane of the element. Plate structures, such as floor slabs in SAP2000 are modeled using this "Shell" element. Full shell behavior, i.e. a combination of membrane and plate behavior (all forces and moments can be supported) is recommended to model floor slabs in SAP2000 and is used in this study. Two thickness formulations are available in SAP2000, which determine whether or not transverse shearing deformations are included in the plate-bending behavior of a shell element:

- The thick-plate (Mindlin/Reissner) formulation, which includes the effects of transverse shear deformation
- The thin-plate (Kirchoff) formulation, which neglects transverse shearing deformation.

Shearing deformations tend to be more important when the thickness is greater than about one-tenth to one-fifth of the span. They can also be quite significant in the vicinity of bending-stress concentrations, such as near sudden changes in thickness or support conditions, and near holes or re-entrant corners. It is generally recommended by CSI (makers of SAP2000) to use the thick-plate formulation unless one is sure that shearing deformations will be small. Therefore the thick-plate formulation is employed in this study. The thickness formulation has no effect upon membrane behavior, only upon plate bending behavior.

The shell element internal forces, like stresses, act throughout the element. They are present at every point on the midsurface of the shell element. SAP reports values for the shell internal

forces at the element nodes. It is important to note that the internal forces are reported as forces and moments per unit of in-plane length.

The basic shell element forces and moments are identified as F_{11}, F_{22}, F_{12}, M_{11}, M_{22}, M_{12}, V_{13} and V_{23}. F_{21} and M_{21} are not reported as F_{21} is always equal to F_{12} and M_{21} is always equal to M_{12}. Figure 8.3 shows internal F_{11} forces acting on the midsurface of a shell element. In figure 8.3, the force distribution labelled (a) represents an actual F_{11} force distribution. The force distribution labelled (b) in figure 8.3 shows how SAP2000 calculates only the internal forces at the corner points of the shell element. Note that these stresses could be calculated at any location on the shell element. They are calculated only at the corner points because that is a convenient location and it keeps the amount of output to a reasonable volume.

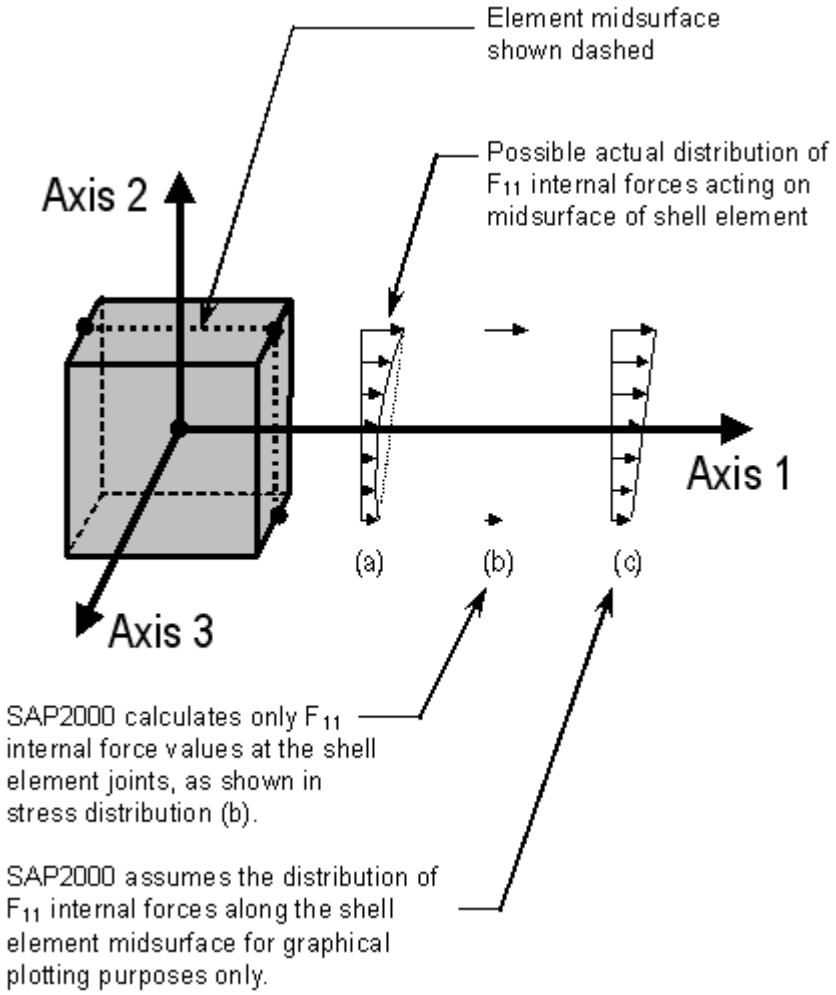

Fig. 8.3. Calculation of Internal Force F_{11} in SAP2000 (SAP2000 Manual).

The force distribution labelled (c) in figure 8.3 shows how SAP2000 assumes that the F_{11} forces vary linearly along the length of the shell element between the calculated F_{11} force values at the element nodes for graphical plotting purposes only.

Figure 8.4 illustrates the positive directions for shell element internal forces F_{11}, F_{22}, F_{12}, V_{13} and V_{23}. *Note that these shell element internal forces are forces per unit length acting on the midsurface of the shell element. SAP2000 reports only the value of these forces at the shell element corner points.*

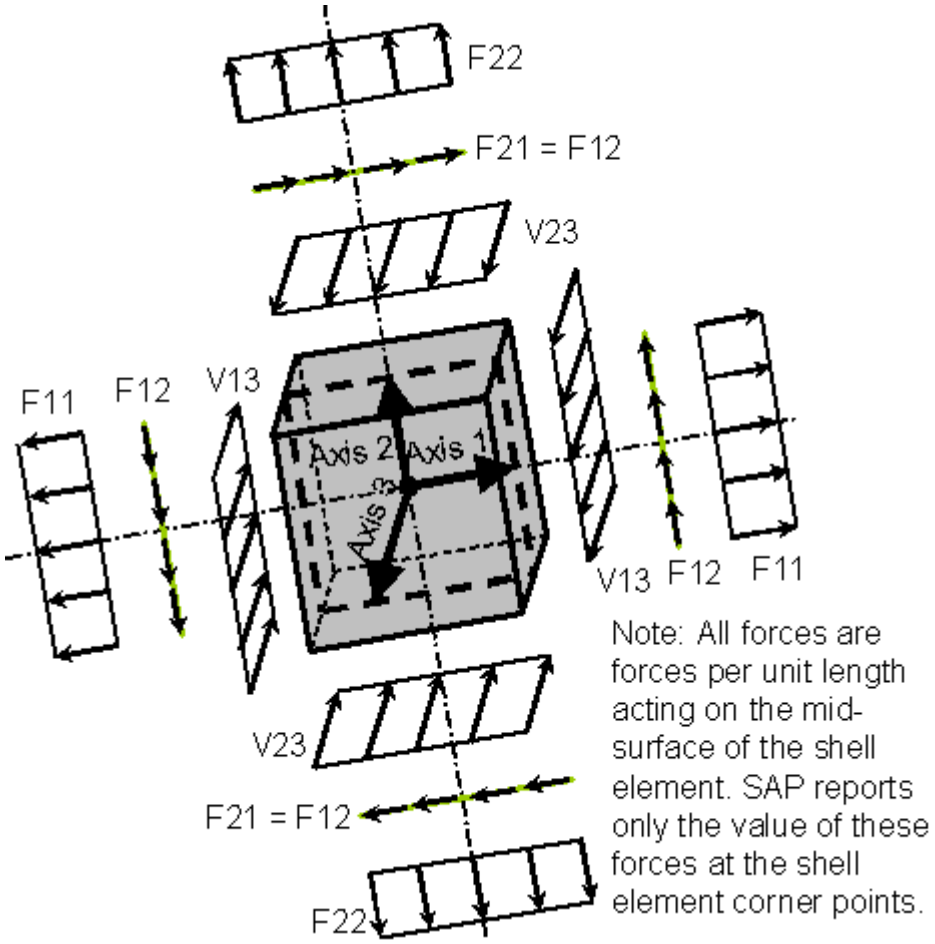

Fig. 8.4. Positive Direction for Shell Element Internal Forces in SAP2000 (SAP2000 Manual)

Figure 8.5 illustrates the positive direction for shell element principal forces, F_{max} and F_{min}. It also illustrates the positive direction for the shell element maximum transverse shear force, V_{max}.

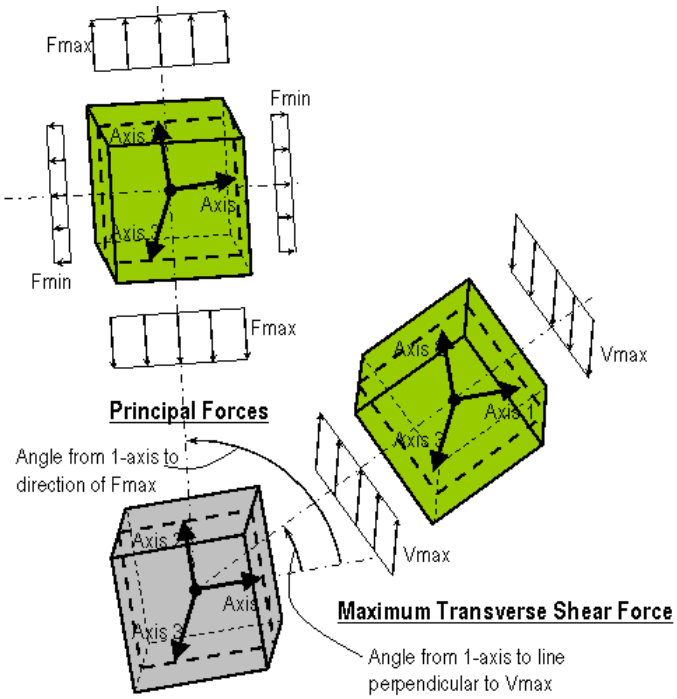

For values of V13 and V23 at any angle, the maximum transverse shear stress, V-Max, can be calculated as:

$$V - Max = \sqrt{V_{13}^2 + V_{23}^2}$$

Fig. 8.5. Positive Direction for Shell Element Principal Forces in SAP2000 (SAP2000 Manual)

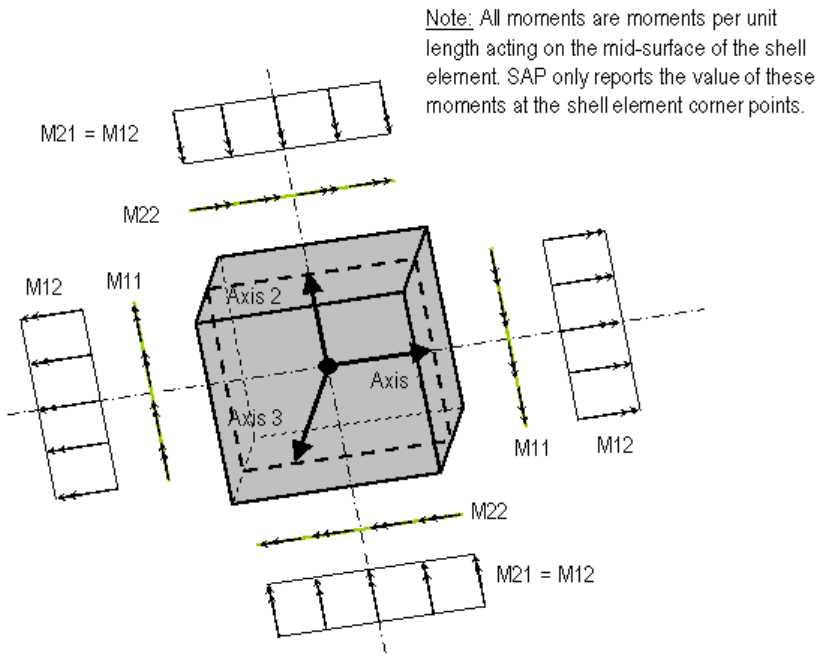

Use the right-hand rule to determine the sense of the moments shown in the figure above.

The figure below illustrates the positive direction for shell element principal moments, Mmax and Mmin.

Fig. 8.6. Shell Element Stress Resultants - Moments in SAP2000 (SAP2000 Manual)

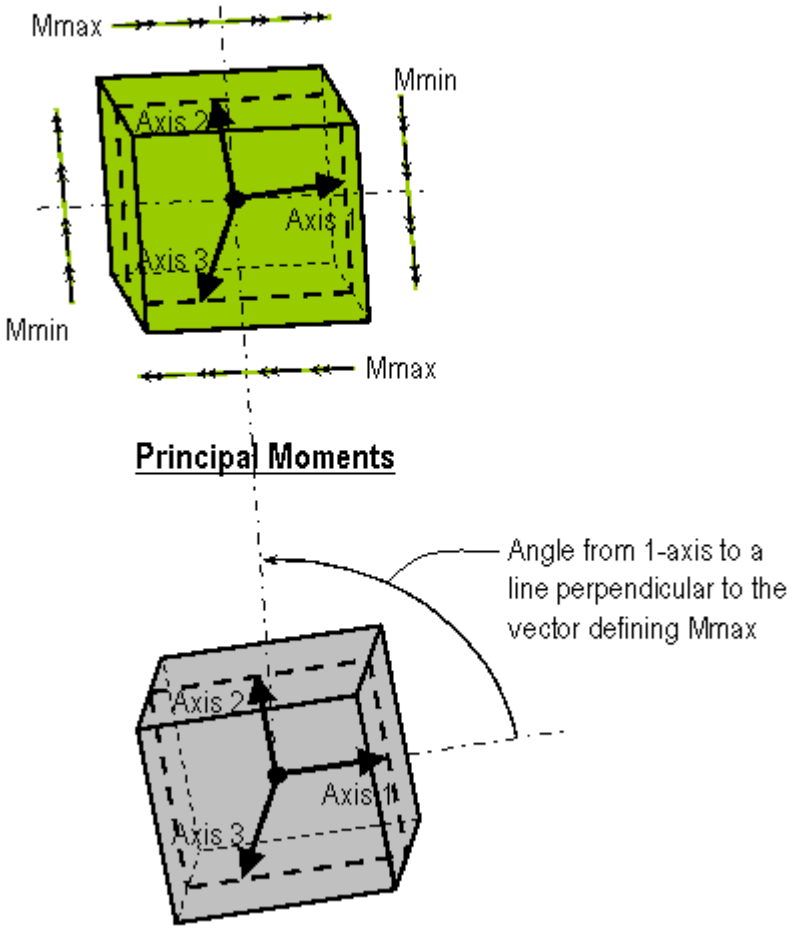

Fig. 8.7. Positive Direction for Shell Element Principal Moments in SAP2000

The content of this section was reproduced from the SAP2000 Analysis Reference Manual.

8.5.5 Flowchart for Flexural and Shear Design Optimisation of Slabs

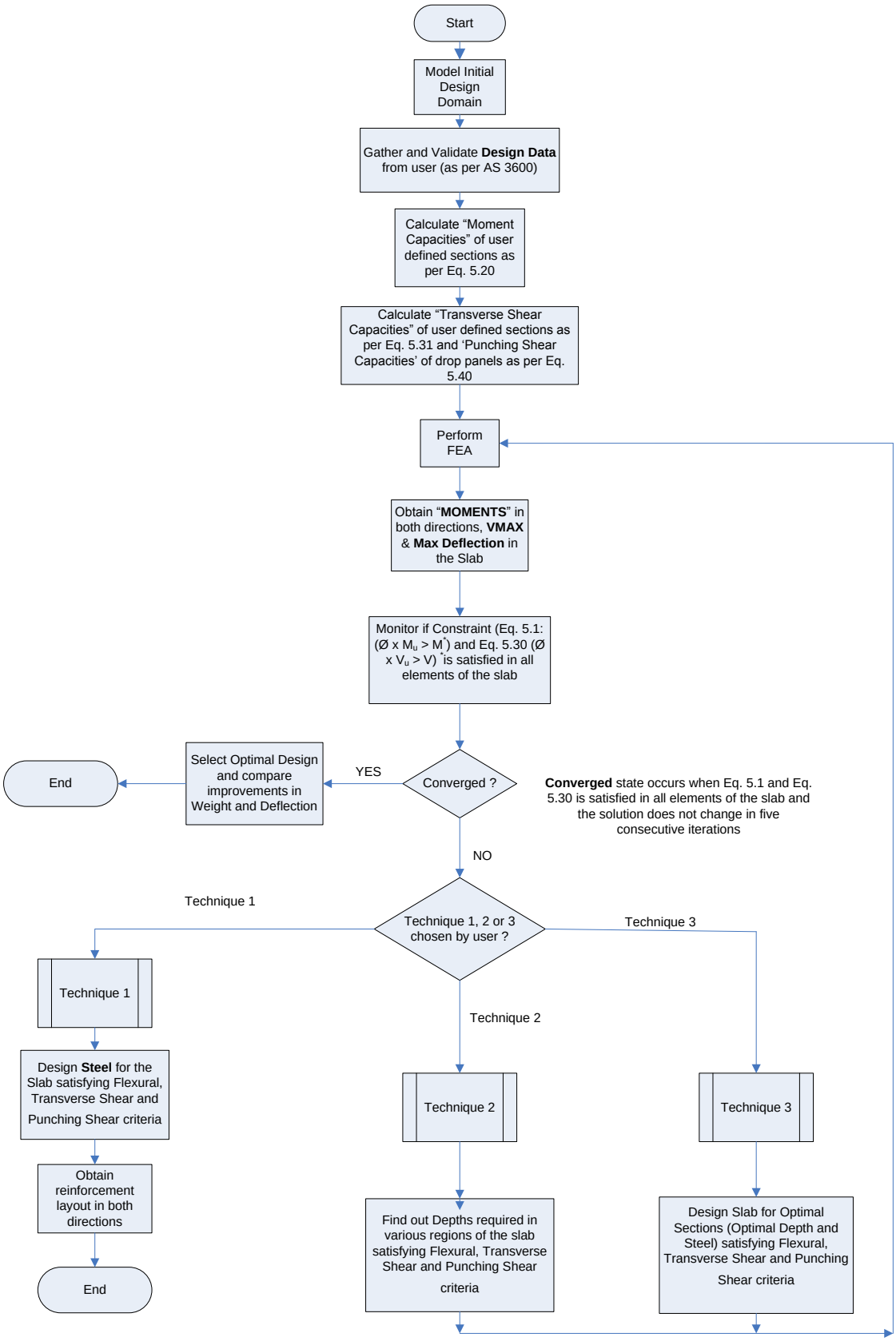

Fig. 8.8. Flowchart for Flexural and Shear Design Optimisation of Slabs

8.6 Examples

8.6.1 Comparison between Bending Moment and Shear Plus Bending Moment as Constraints

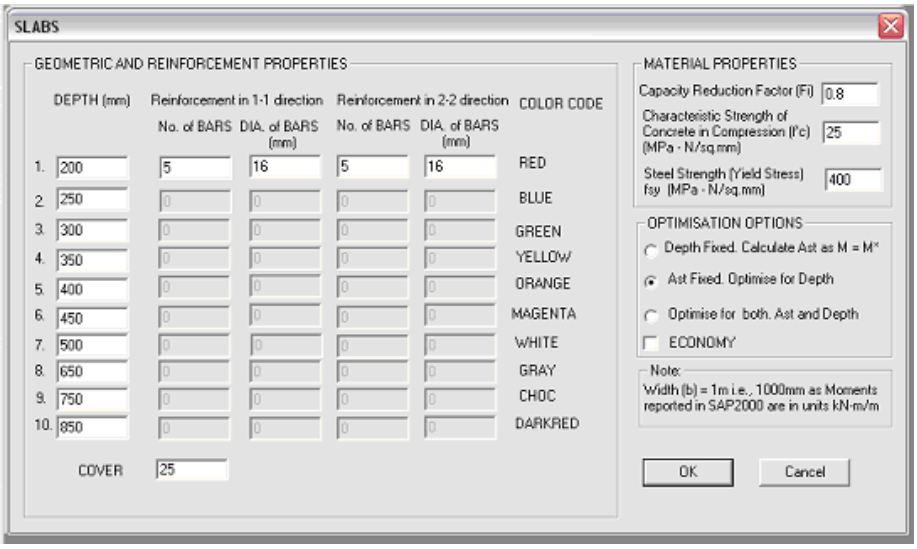

Fig. 8.9. Design Data for Technique 2

MOMENT & PUNCHING SHEAR **ONLY MOMENT**

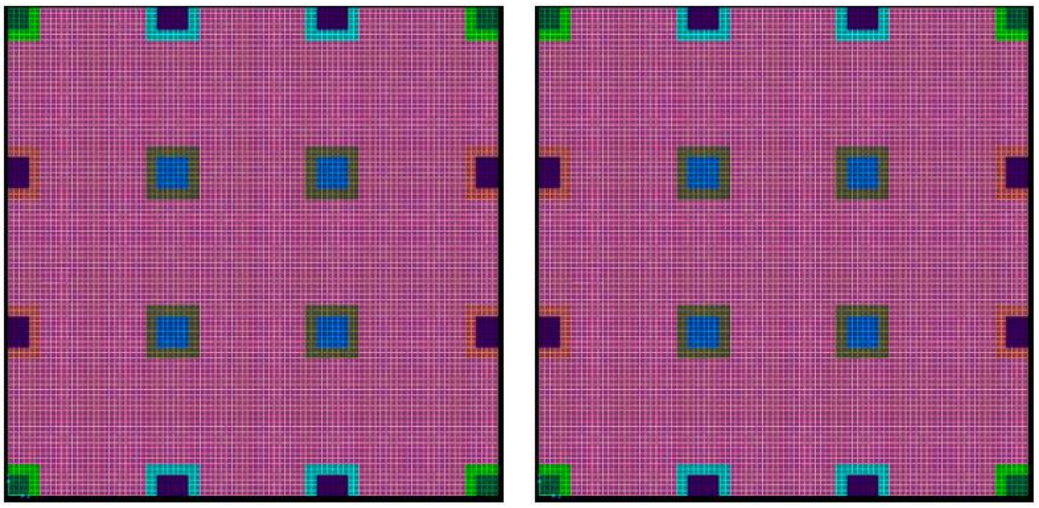

Fig. 8.10. Initial Model of Symmetrical Flat Slab

Model Data

Span: 6m x 6m

Total No of Elements: 8464

Total No of Designable Elements: 8268

Loading: Self Weight + 5kPa Live Load; *Load Combination:* 1.25 DL + 1.5 LL

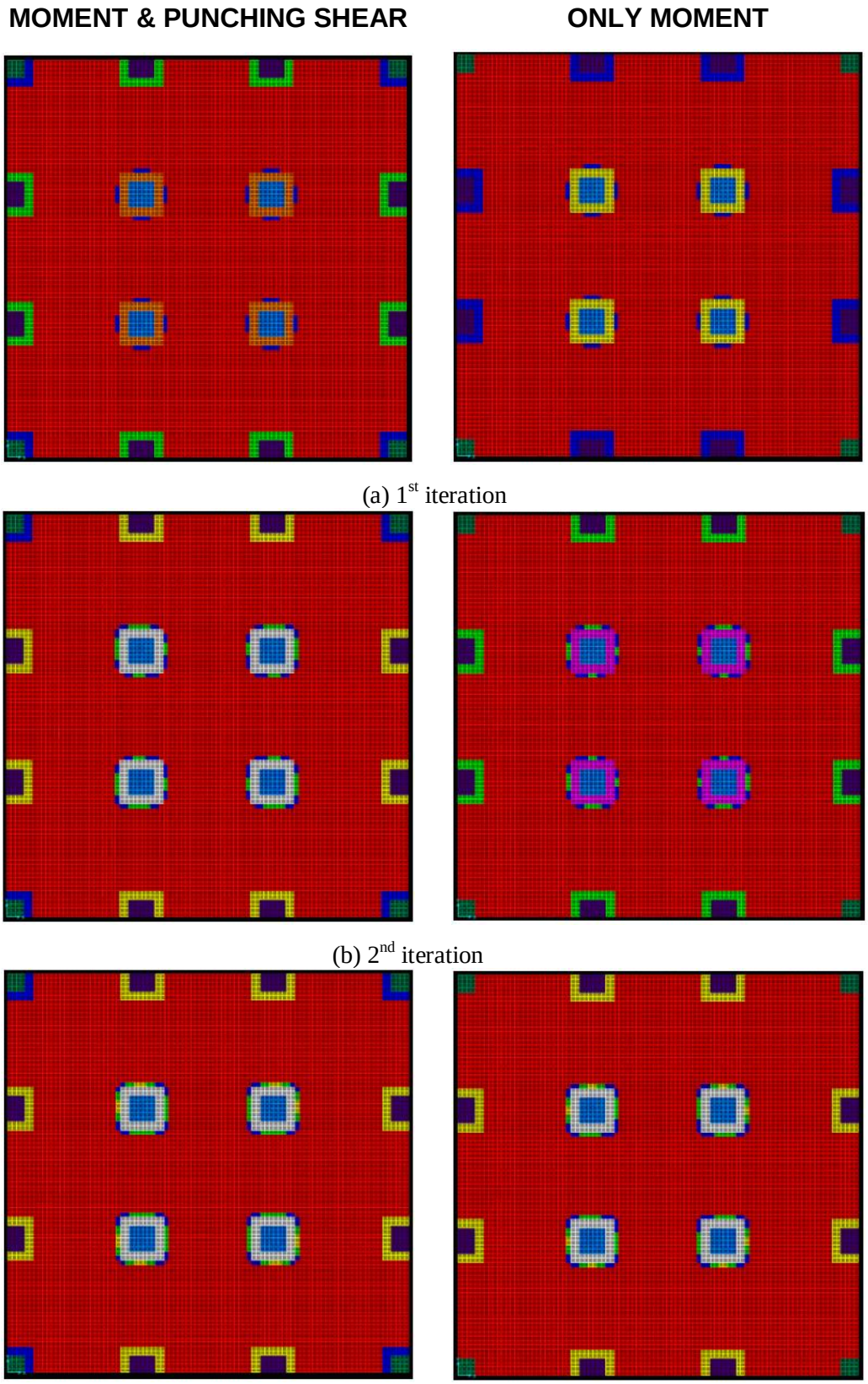

(a) 1st iteration

(b) 2nd iteration

(c) 3rd iteration

Fig. 8.11 (a-c).

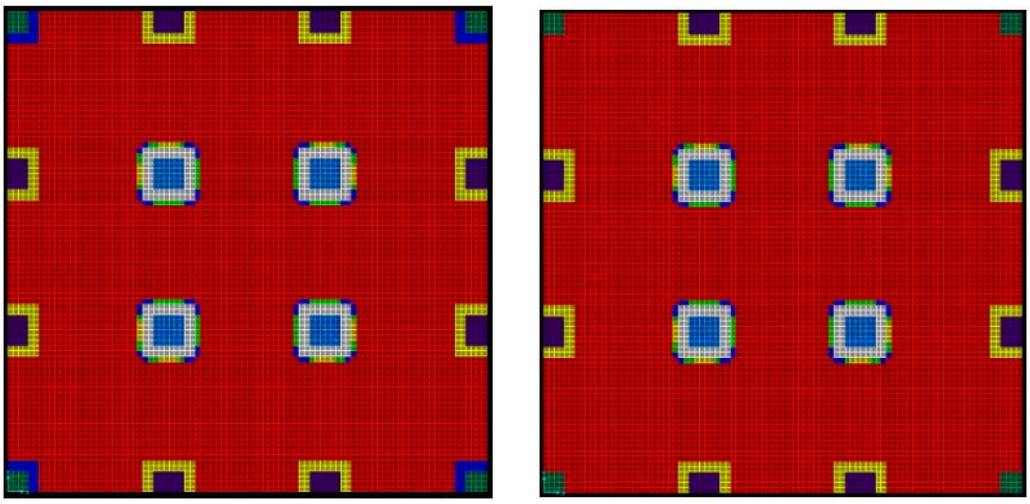

(d) 4th iteration onwards

Fig. 8.11. Comparison between Only Bending Moment and Bending Moment with Shear as Design Constraints

The differences obtained using the Punching Shear Criterion (in addition to the bending moment criterion) for the drop panels over the column supports is clearly seen from the results shown in Fig. 8.11 (a-d). In both cases, the solution settles and satisfies their respective criteria from the 4th iteration onwards (Fig. 8.11 d). It is seen from the optimisation history that right from the first iteration (Fig. 8.11 a), thicker drop panels are needed when the punching shear criterion is implemented as an additional constraint compared to when only the bending moment criterion is used as the constraint. Drop panels are also observed around corner columns when the punching shear constraint is used. From the 4th iteration onwards (Fig. 8.11 d), the solutions in both cases stay the same with the only difference being the presence of drop panels for the corner columns. This example clearly illustrates the importance of implementing punching shear criterion as an additional constraint with the bending moment criterion for the design of flat slabs.

8.6.2 Calculation of Moment Difference between Column Faces for Punching Shear

In Equation 5.40, M_v^* is the difference between moments at the front and back face of column. The column in this case (frame member) meets the slab elements at a single node. When a single frame member is connected to a single node in the finite element plane, the connection occurs over an infinitesimal area, even though the physical connection maintains some finite size. Design moments at the column face will be inaccurate because the distance between the centroid of the column and the column face is now flexible, according to the stiffness of the

slab, when it should be much stiffer when this area is enclosed within the column. Also, a concentrated boundary condition, such as column connected via a single node, causes an *unrealistic stress concentration known as stress singularity*. To overcome these problems, non-design areas are therefore employed over column frames to ignore the results due to stress singularity. The front and back faces of the columns in the prepared initial model are therefore the front and back faces of the non-design areas over the column frames which are used to compute the difference between moments, M_v^*. To calculate M_v^* correctly, it is important to consider whether to use the *maximum* moment among the finite number of nodes on each face or to use the *average* moment among the finite number of nodes on each face. Both approaches give different values for M_v^*. Looking at Equation 5.40 above, it is intuitively clear that the bigger of the two 'differences' needs to be used in order to obtain a safe design. In the following work, both approaches are tested using all three techniques and the results compared visually.

8.6.2.1 Design using Technique 1

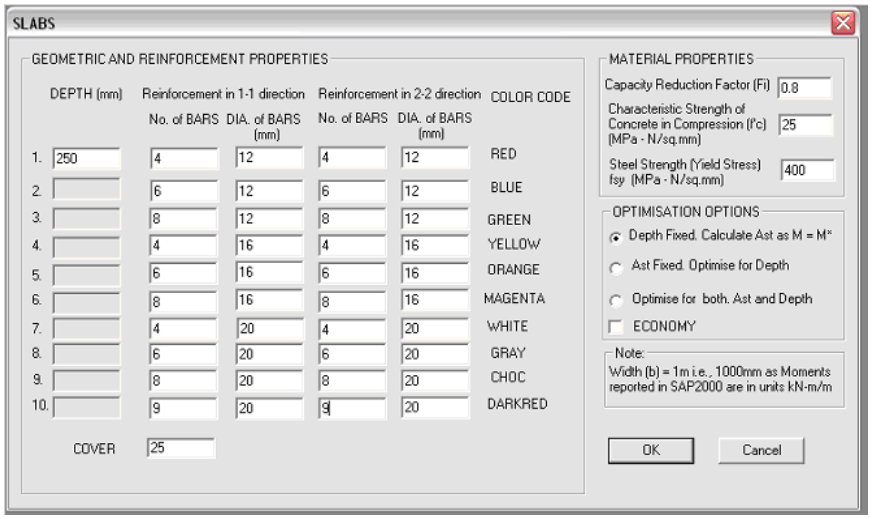

Fig. 8.12. Design Data for Technique 1

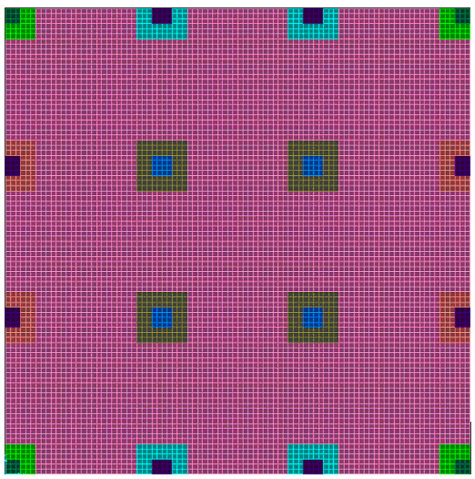

Fig. 8.13. Initial Model of Symmetrical Flat Slab

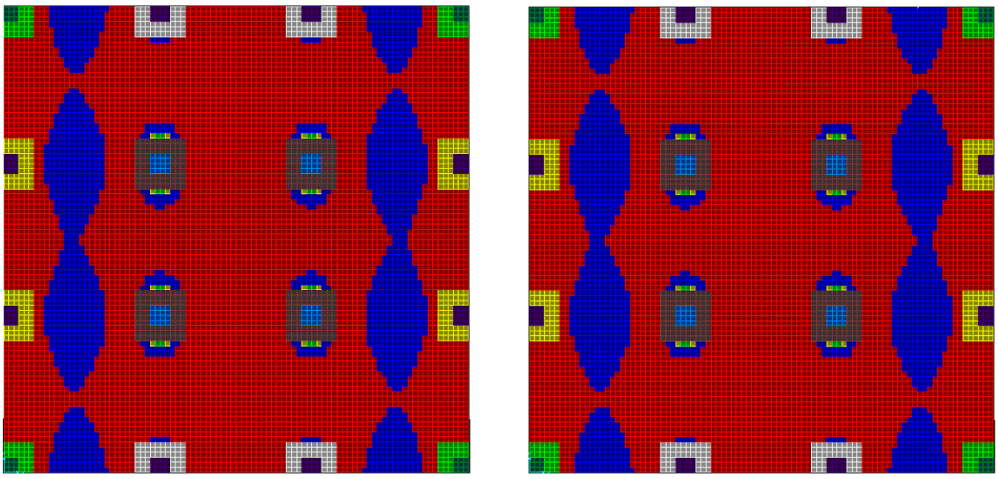

(a) **AVERAGE** (b) **MAXIMUM**

Fig. 8.14. Technique 1 Design Solutions showing Steel Required in Global X direction

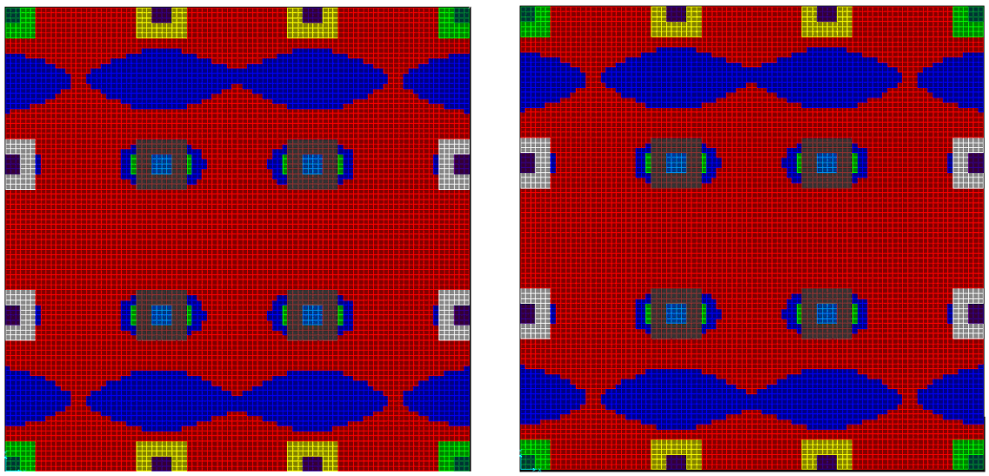

(a) **AVERAGE** (b) **MAXIMUM**

Fig. 8.15. Technique 1 Design Solutions showing Steel Required in Global Y direction

8.6.2.2 Design using Technique 2

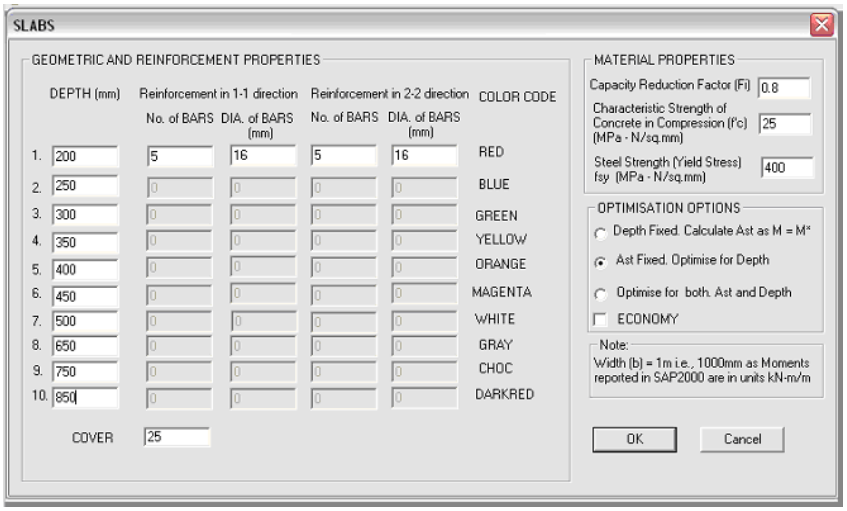

Fig. 8.16. Design Data for Technique 2

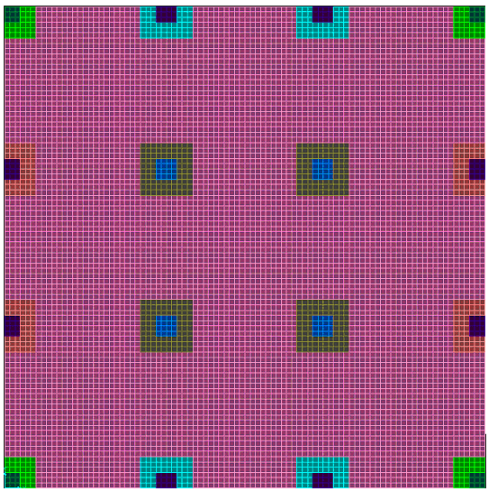

Fig. 8.17. Initial Model of Flat Slab

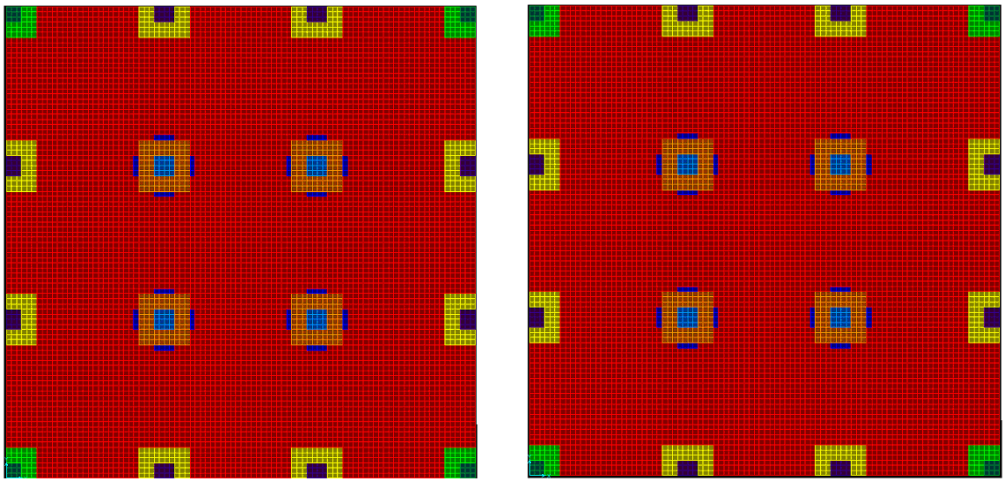

(a) AVERAGE **(b) MAXIMUM**

Fig. 8.18. Technique 2 Design Solutions at 1st Iteration

8.6.2.3 Design using Technique 3

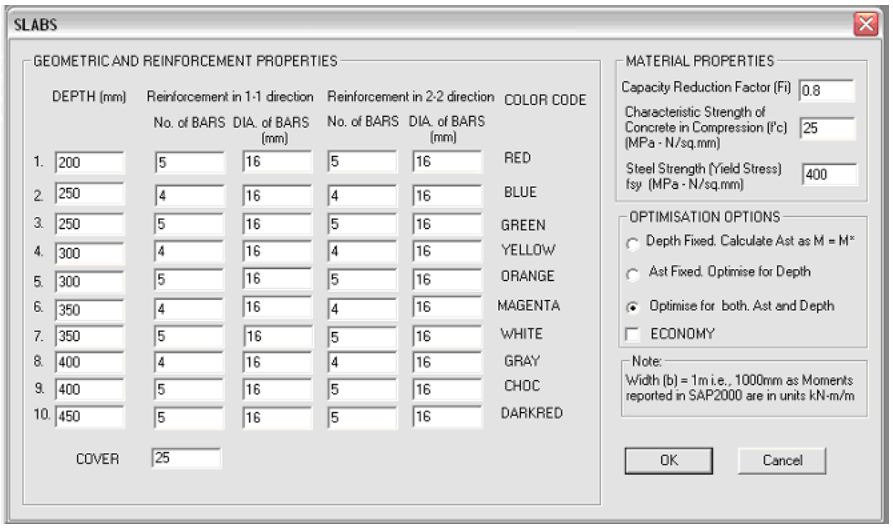

Fig. 8.19. Design Data for Technique 3

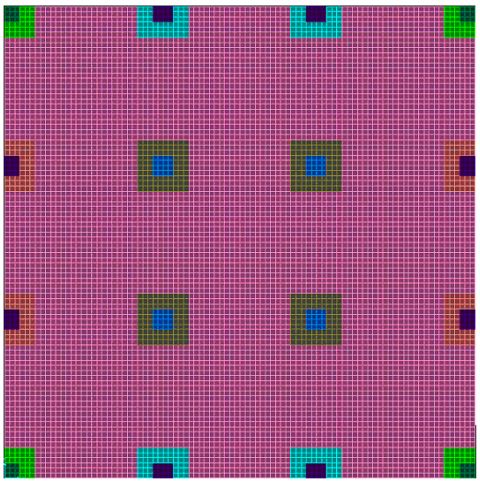

Fig. 8.20. Initial Model of Flat Slab

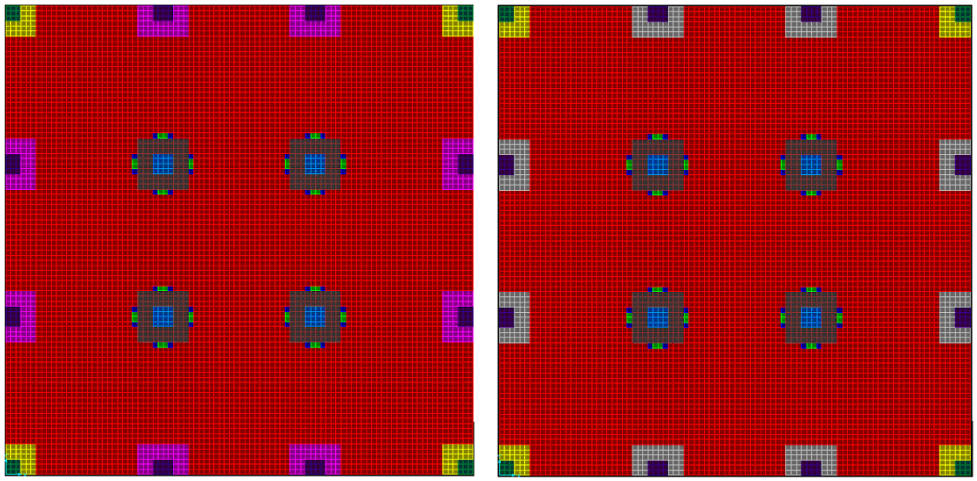

(a) AVERAGE **(b) MAXIMUM**

Fig. 8.21. Technique 3 Design Solutions at 1st Iteration

8.6.2.4 Recommendation

Using all three techniques it is seen that no difference in results was observed in Techniques 1 and 2 when either the *average* of the smoothed nodal moment on the column faces is chosen or when the *maximum* of the smoothed nodal moment on the column faces is chosen. However, different designs for the edge panels are seen using Technique 3. It is seen that a 350 mm deep section with 5Y16 bars both ways (White) is needed when the *maximum* of the smoothed nodal moments on the column faces is chosen in the calculation of M_v^*. Whereas when the *average* of the smoothed nodal moments on the column faces is chosen, a 350 mm deep section with 4Y16 bars is needed (Magenta). Thus, slightly more steel is seen to be required when the *maximum* of the smoothed nodal moments on the column faces is chosen to compute M_v^*. To be on the safer side, it is therefore recommended to use the *maximum* of the smoothed nodal moments on the

column faces when computing M_v^* which is to be used in the calculation for the 'Ultimate Shear Strength' of the concrete slab near the column. This approach is hence adopted for all examples and case studies designed in this chapter including the examples in the previous section, Section 8.6.1.

8.6.3 Transverse Shear Performance

8.6.3.1 Comparison with and without transverse shear constraint

This section attempts to demonstrate the importance of using the Transverse Shear criterion or normal beam shear criterion as an additional constraint to the bending moment constraint. A comparison of the results obtained using only the bending moment constraint and the results obtained using the bending moment and transverse shear constraint is carried out. Technique 3 is employed in this study. The model chosen for this exercise is a 3x3 bay symmetrical model, each span being 6m c/c in both directions with a central elevator core in the middle. The blue panels over the columns (frame members) are non-design regions where the effects of stress singularity are seen. On all four edges of the slab and at the four edges of the opening, red and yellow coloured panels are assigned, each with a separate panel ID. Elements lying in these panels are subjected to a load of 175 kN. The entire slab is loaded with its own self-weight and a live load of 5 kN/m^2. It is anticipated that thicker sections (with more steel) will be observed for the Red coloured panels which are subject to high beam shear/transverse shear compared to the Yellow coloured panels.

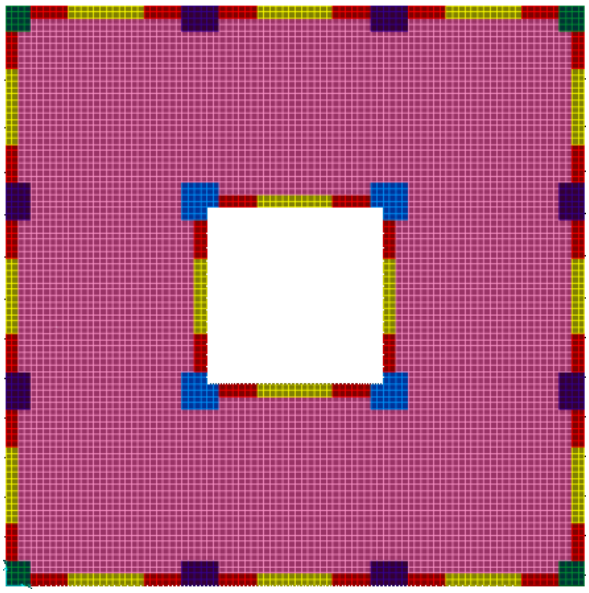

Fig. 8.22. Initial Model for Comparison With and without Transverse Shear Constraint

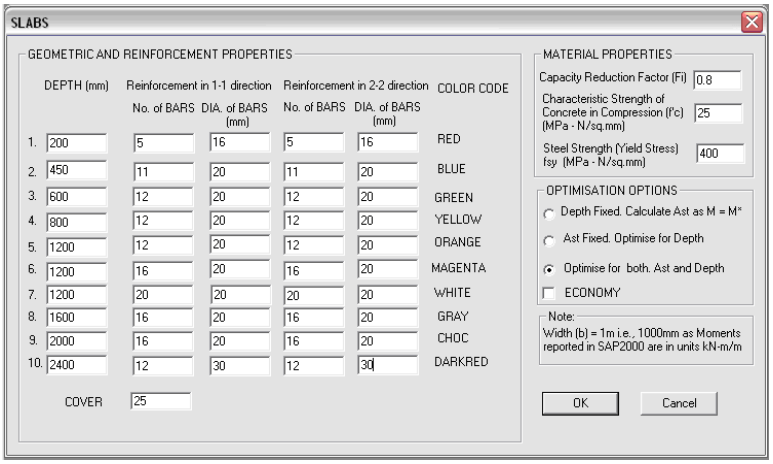

Fig. 8.23. Design Data for Technique 3

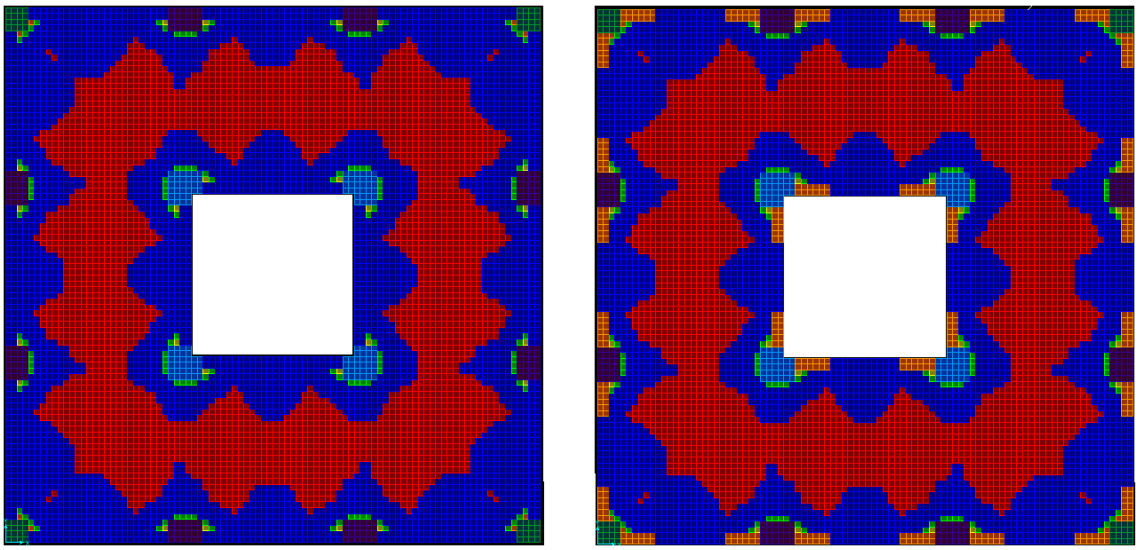

(a) Design obtained for Bending Moment

(b) Design obtained for Bending Moment and Transverse Shear

Fig. 8.24. Comparison Between Design Solutions Obtained for only Bending Moment Constraints and Bending Moment with Shear Constraints

Fig. 8.24 (a) on the left shows the design obtained for bending moment and fig. 8.24 (b) on the right shows the design obtained for bending moment and transverse shear. The difference in results obtained using only the bending moment criterion as the constraint and using moment criterion with transverse shear criterion as the constraint is seen from the above results. It is seen that the panels marked Red in the initial model (which are subject to the maximum beam shear/transverse shear) are allotted bigger sections with more steel (Orange) when the transverse shear criterion is implemented in conjunction with bending moment criterion. The image on the left shows that a lesser section is sufficient (Blue) for these same panels (marked Red in the

initial model) when only the bending moment criterion is used (i.e. when designed only for bending moments). Rest of the slab is not generally affected and is observed to be the same as the loading is quite small compared to the loading applied on the Red and Yellow Transverse Shear panels. As a result, bending moment is seen to govern the design over transverse shear in these areas, whereas for the Transverse Shear Panels (Red and Yellow), transverse shear is seen to govern the design over bending moment. These results are to be expected for the loading applied and this comparison therefore serves to illustrate the importance of applying the Transverse Shear criterion in addition to the Bending Moment criterion.

8.6.3.2 Design using Technique 3

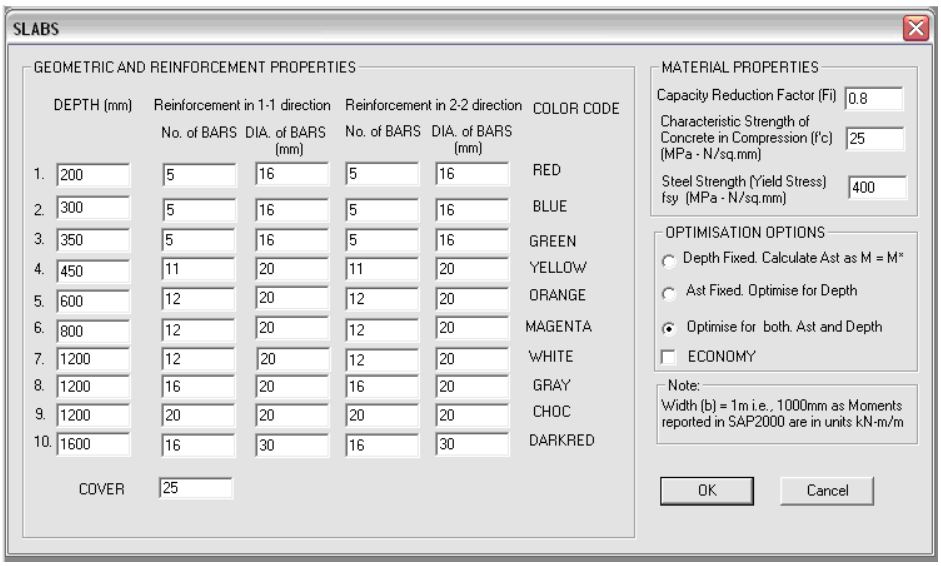

Fig. 8.25. Design Data for Technique 3

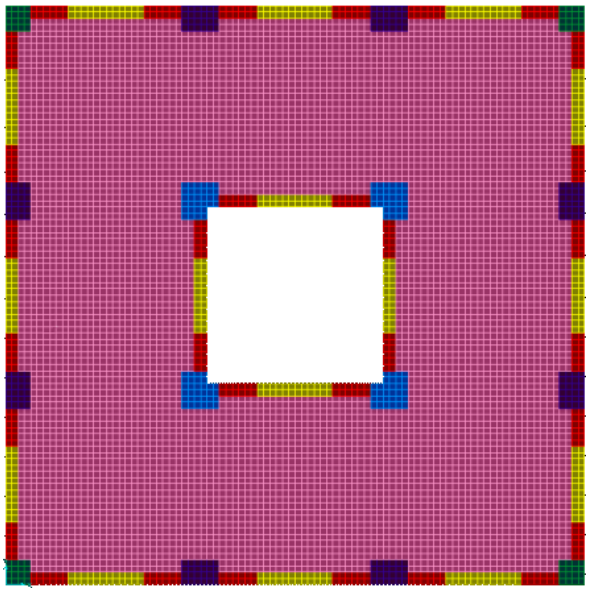

Fig. 8.26. Initial Model for Bending Moment and Transverse Shear Design

A design using Technique 3 for the example used in Section 8.6.3.1 is performed with another set of data. The geometry and loading are as before.

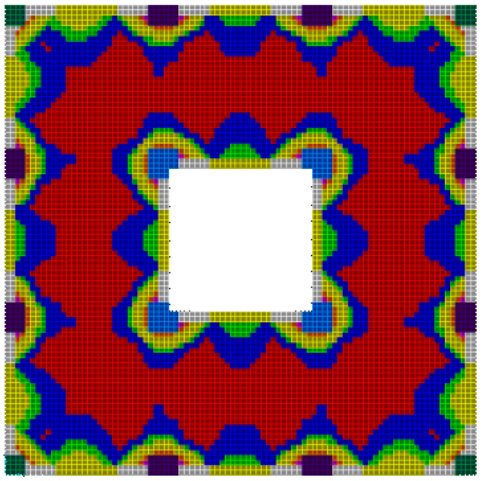

(a) 1st iteration

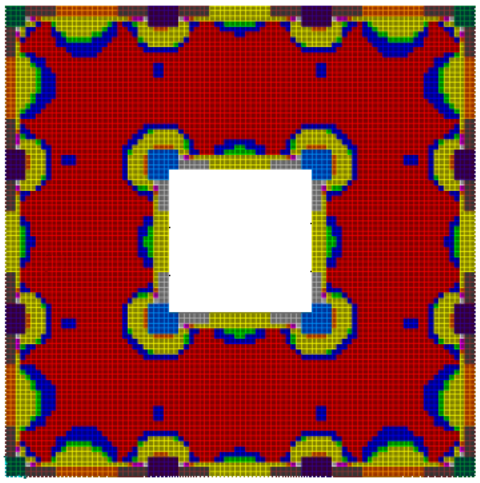

(b) 2nd iteration

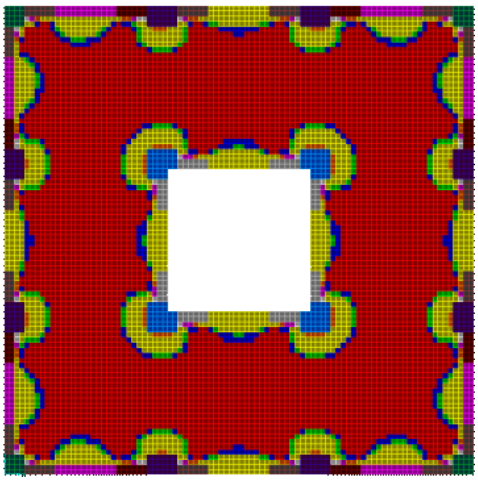

(c) 3rd iteration

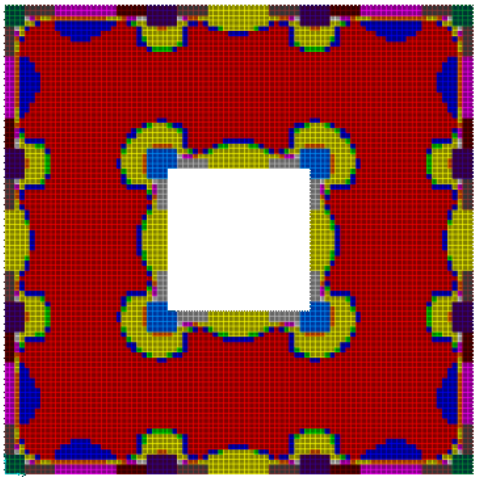

(d) 4th iteration

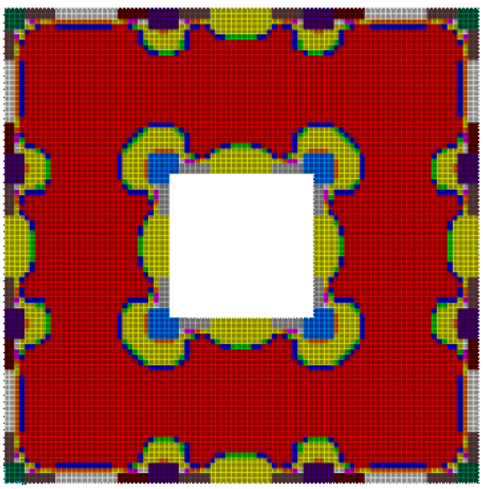

(e) 5th iteration

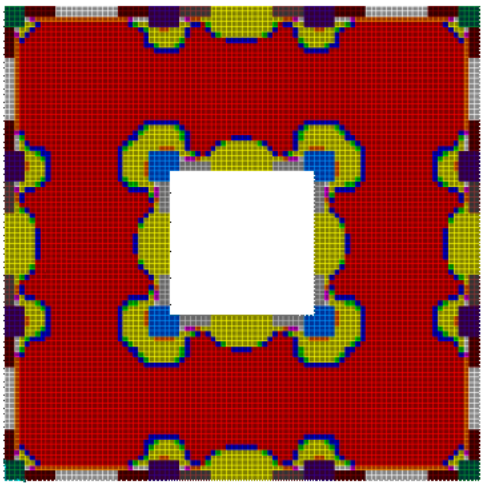

(f) 6th iteration

Fig. 8.27 (a-f).

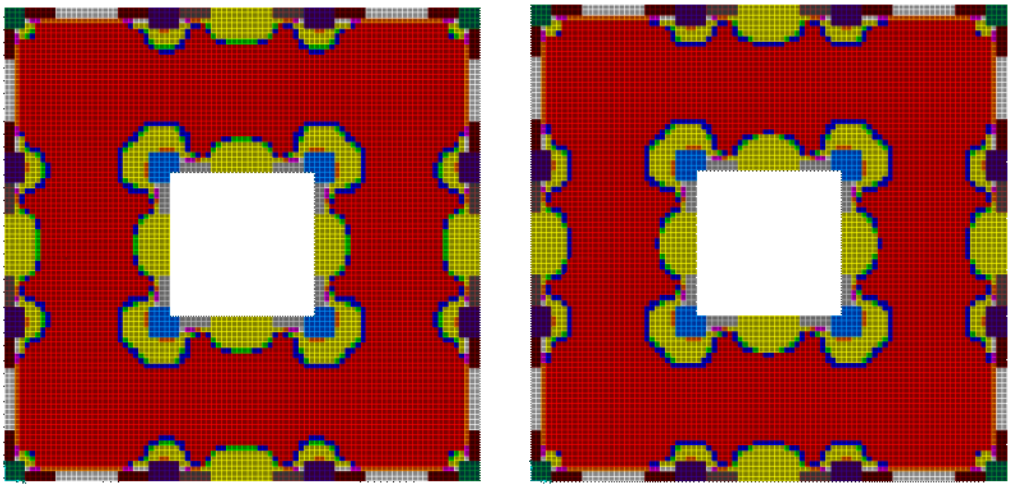

(g) 7th iteration (h) 8th iteration

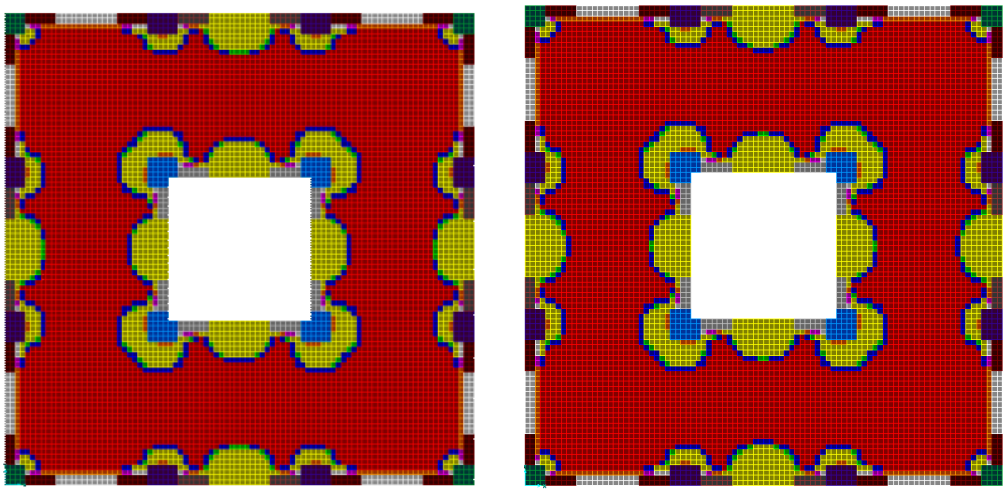

(i) 9th iteration (j) 10th iteration

Fig. 8.27. Technique 3 Design Solutions for Bending Moment and Transverse Shear Constraints

The solution settles from the 10th iteration onwards satisfying both flexure and shear constraints. As expected, for the given loading, thickest sections with more steel are observed for the panels subjected to highest transverse shear i.e. Red panels on the boundary – 1600 mm deep sections with 10-Y30 bars shown by Dark Red (last section). The interior span Red panels along the boundary show that a 1200mm deep section with 20-Y20 bars shown by Choc colour is required. The Yellow panels for the exterior spans along the boundary require less material and have settled on a section of 1200 mm depth with 12-Y20 bars shown by White colour. The Yellow panels for the interior spans along the boundary have settled on a section of 450mm depth with 11-Y20 bars shown by yellow colour. Along the boundaries of the opening, Red panels are seen to settle on a section of 1200 mm depth with 16-Y20 bars shown by Grey colour. The Yellow panels have settled on a section of 450mm depth with 11-Y20 bars shown

by yellow colour. As expected, for the given load, due to high beam shear along the boundaries of the opening and at the corners of the opening, bigger sections show by yellow colour (450mm depth with 11-Y20 bars) are required whereas for the rest of the slab the first section, 200 mm depth with 5-Y16 bars shown by red colour is generally found sufficient.

8.6.4 Industry Partner's Project (8.4m x 8.4m model) - Design using Technique 3

In this section the design obtained for flexure in Section 7.7.1 of Chapter 7 is compared with the design obtained in this section for Flexure, Punching Shear and Transverse Shear.

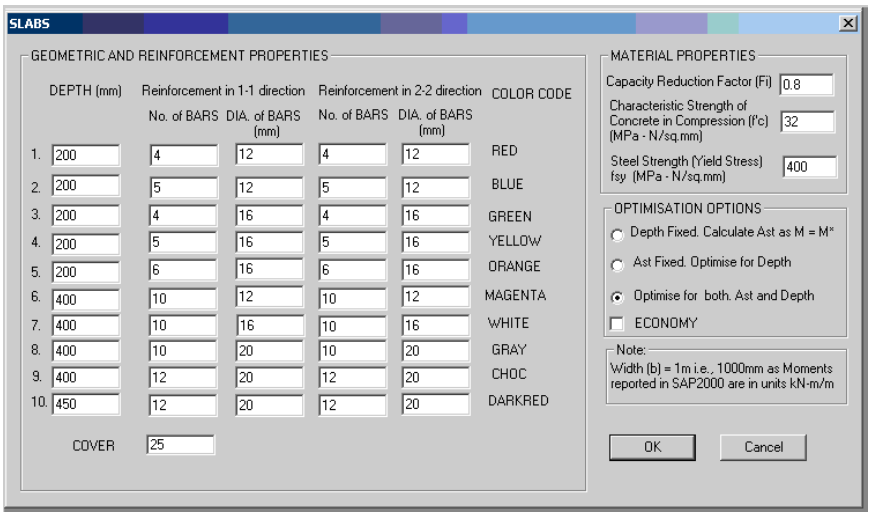

Fig. 8.28. Design Data for Technique 3

FLEXURE ONLY

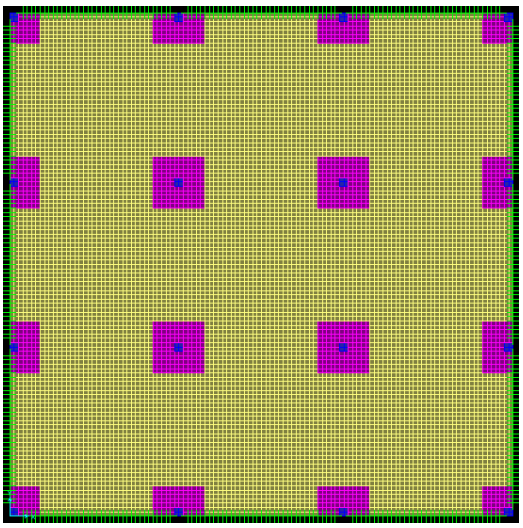

Fig. 8.29. Initial Model using 3D solids to Model Columns

FLEXURE, PUNCHING & TRANSVERSE SHEAR

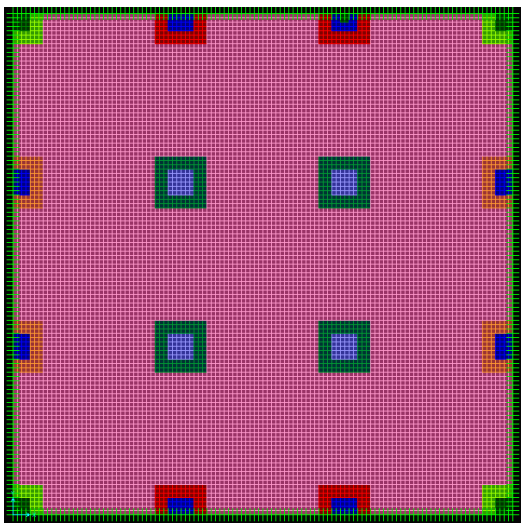

Fig. 8.30. Initial Model using Single Frame Members to Model Columns

FLEXURE ONLY **FLEXURE, PUNCHING & TRANSVERSE SHEAR**

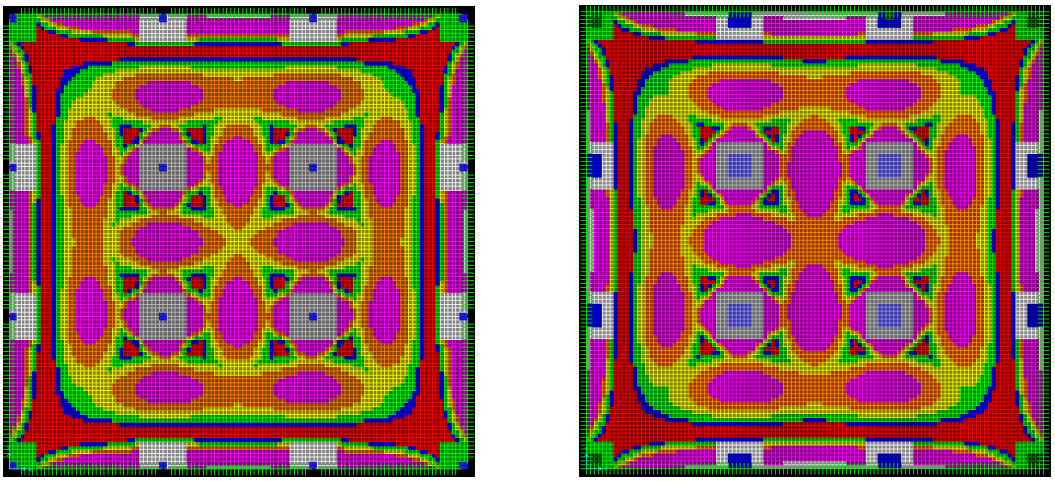

(a) 1st iteration

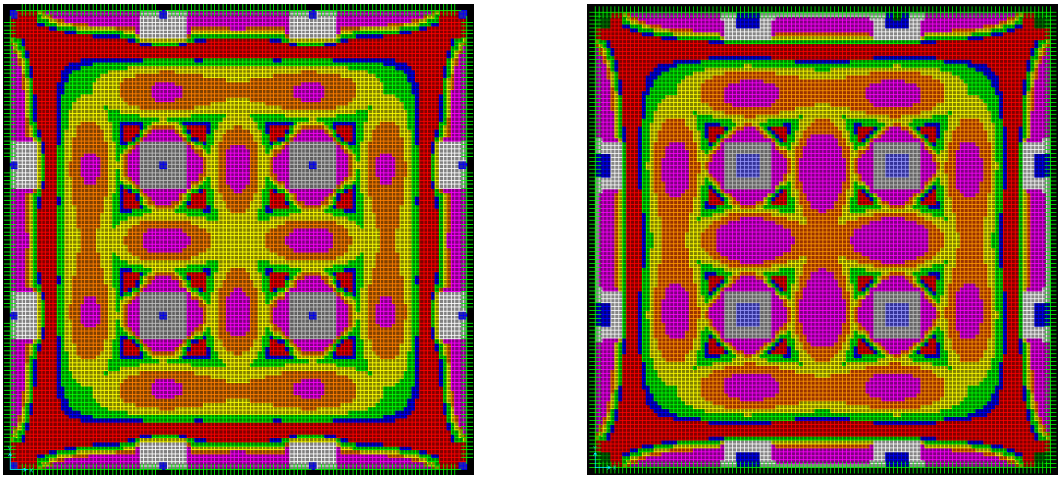

(b) 2nd iteration

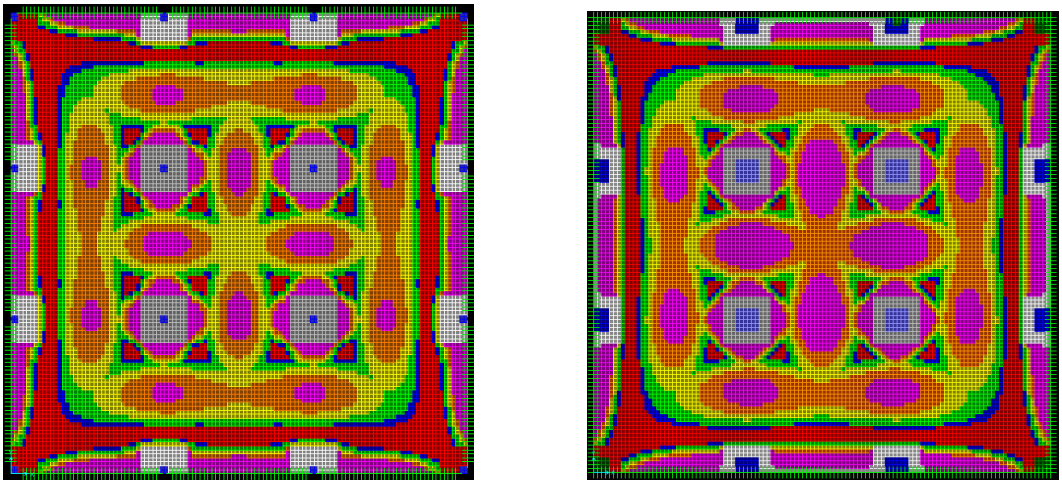

(c) 3rd iteration onwards

Fig. 8.31. Comparison between Technique 3 Design Solutions for only Bending Moment and Bending Moment with Punching Shear and Transverse Shear Constraints.

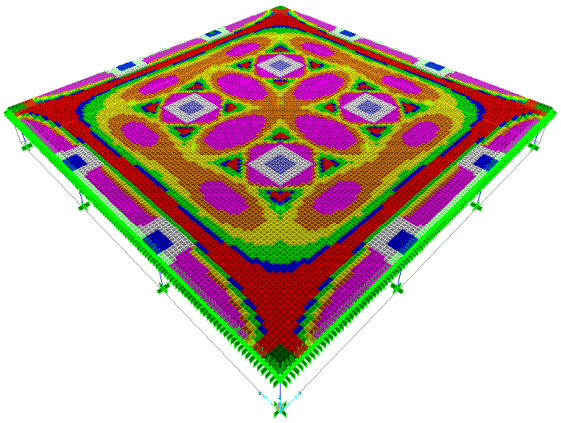

Fig. 8.32. 3D-View of Optimal Solution

It is seen from the results above, that almost similar designs are obtained for the given loading when designed using only flexural criteria and when designed using both flexural and shear criteria. This example also shows that even when Punching shear criteria are not implemented, in some instances, a design by Technique 3 using only Bending Moments too results in safe design for the drop panels over the columns.

8.7 Concluding Remarks

It has been shown that the proposed method can easily and directly deal with discrete design variables in sizing problems for strength design that includes flexure and shear. The importance of using shear as an additional constraint in the optimisation process is clearly demonstrated in this chapter. Punching shear criteria for designing the regions of slab over column supports and normal beam shear criteria are implemented to make the design results practically useful for the structural engineer. It is shown that by giving appropriate data in the user interface the proposed techniques can attain significant weight savings and numerous conceptual designs can be investigated before the structural design engineer finalises on a particular design for his slab. The criteria for punching shear developed in this work, at the present stage, cannot be applied for accurately estimating the punching shear strength of a slab region close to an opening (i.e. if there are openings close to columns). However, it is not difficult to extend the current work to include this aspect into the algorithms as well. At present, the shear criteria are programmed for all three techniques, viz., Technique 1, Technique 2 and Technique 3. It is seen that an optimal solution is generally obtained in very few iterations (usually between 2 and 10 iterations); therefore there is no issue of excessive computational cost involved as such. A future enhancement to the current process can be to let the user supply more than ten design sections to the optimisation process. This should then result in even more economical, attractive and efficient design solutions.

CHAPTER 9: CONCLUSIONS AND (RECOMMENDATIONS FOR) FURTHER WORK

9.1 Conclusions

This study has explored possible benefits from, and developed algorithms for, incorporating size and topological optimisation techniques in the conceptual and preliminary design of continuum elements in multi-storey building structures. The continuum elements investigated for design improvements are structural walls and floor slabs of multi-storey buildings.

Stress-based optimisation of the thickness of structural walls has been investigated in Chapter 3. A simple procedure based on the ESO concept of removing material (i.e. reducing thickness) and adding material (i.e. increasing thickness) based on the stress level (von Mises) in elements or groups of elements has been developed. The benefits and limitations of using the proposed approach at an element level and at a group level are investigated. It could be argued that the proposed method is not rigorous in a strictly mathematical sense when calculating the exact value of the new thickness; however it is still a rational and easy-to-implement and easy-to-understand conceptual/preliminary design tool for the structural engineer. Also, another argument could be that being a fully stressed design procedure, it does not necessarily give minimum weight designs due to the fact that no objective is strictly specified. In spite of these arguments and the inherent limitations, the benefits of employing the proposed method in a variety of real building models and situations are clearly demonstrated in Chapter 3 keeping in mind the need for developing practice-oriented tools. In Chapter 4, the method has been extended to allow for removing elements using the Soft-Kill option of element removal. Three examples with different objectives have been investigated and benefits observed. The location and thickness of infill walls required in a shear wall – slab type building (3D model) has been investigated. The benefit of employing the proposed method in obtaining the thickness in various regions of the resulting optimal topology is clearly seen in all the examples in which a lesser overall thickness has been seen to be generally required compared to the initial thickness of the model. It should be noted that this initial thickness was not necessarily very thick in the initial model but was given according to the span and loading on the model. Thus, weight savings by element removal and variable thickness are clearly seen when seeking the optimal topology. The proposed method is then tested on a 3D multi-storey building to obtain the bracing pattern on two parallel in-plane loaded faces of the building. The applicability and benefits of the proposed method is clearly shown in Chapters 3 and 4.

From Chapter 5 onwards, the focus has been on conceptual/preliminary design optimisation of floor slabs in multi-storey buildings. A single level of the floor slab is extracted to reduce the computational time. Three new design techniques have been developed in the course of the work and most of the practical requirements specified by AS3600 for the design of concrete floor slabs are included as constraints in the optimisation process. The need for making the work practically applicable is thus taken care of and results are critically compared with the conventional designs of the slabs designed by the industry partner to check for improvements and benefits. It should be noted that very little similar work on floor slab design optimisation with AS3600 practical requirements has been carried out in the past. Original optimum solutions in each case are obtained that show material savings for both concrete and steel. The focus has largely been on the flat-slab type of floor system, and modelling and numerical issues are thoroughly investigated in Chapters 6 and 7 respectively. Accurate modelling is emphasized before proceeding with analysis, design and optimisation. A new modelling and design approach that employs the ESO method in tandem with the Group ESO method is presented before applying the techniques to slabs in real buildings. The benefits of using this new modelling approach are clearly demonstrated by the wide variety of examples and case studies designed. It should be noted that using Technique 2, in which the steel is kept constant throughout the slab but the slab depth or thickness is allowed to change in different locations, convergence issues are observed for the solutions near the slab-to-column connections. Also, the effects of stress singularity on rational design solutions for drop panels are examined by critically evaluating various approaches by way of example problems. The reasons for choosing the appropriate value of the design bending moment are then outlined before proceeding with optimising real slabs. Technique 2 has mostly been the focus of the numerical studies as it is easier to critically analyse and evaluate the design solutions for drop panels by comparing the *'thickness design'* with hand calculations using the 'Simplified Method of Design'. The potential for designing slabs based on not only the bending moment criterion but also based on material cost considerations in the optimisation process is clearly demonstrated by using the 'Economy' option with Technique 3. In Chapter 8 the importance of using *shear* as an additional constraint has been presented. It should however be noted that, even without using *shear* as an additional constraint, reasonable designs for drop panels are observed in Chapter 7 that have been verified by the author using hand calculations for shear requirements. This proves the abilities of Techniques 2 and 3 to find correct design solutions for drop panels in spite of lack of punching shear criteria. Comparisons were also made in Chapter 8 between flexural design and flexure-shear design which reinforce this suggestion. Though it increases the complexity of the algorithms substantially, the use of *shear* as additional constraints in the optimisation makes the process robust and complete from a practical point of view.

The optimal designs in this work are for a single load case (generally the worst load case is employed); however the proposed methods can easily be extended to multiple load cases.

The benefits of employing material cost considerations for both concrete and steel using Technique 3 in the optimisation process are also clearly shown in Chapter 7. Significant cost savings are demonstrated using the proposed techniques.

The objective throughout this work has been to make this work suitable for practical application and use. The techniques developed in this work on floor slabs are subject to a combination of different constraints such as flexure and shear stress constraints with checks on serviceability requirements. They can be directly applied in the structural designer's office to real projects (as has been demonstrated by the case studies). Also, the methods developed have been studied and applied on three-dimensional building models, not just simple 2D plane stress and plate bending examples. It should also be remembered that in this work optimisation is carried out on building models, in which the components are represented as 'objects' (*object-oriented representation*). Very little past work has focussed on modifying (in this case optimising) 'objects' in building models. A systematic computer program has been developed in the course of this work to be used with the FEA package SAP2000. Considerable effort has been spent on programming the necessary numerical algorithms and user-friendly graphical interfaces (GUI's). The program should help the structural designer in two different ways:

1. Inexperienced designers, in particular, can take advantage of the possibilities in easily investigating different section layouts corresponding to the linear elastic solution. Since the program is conceived to directly address the problem of conceptual/preliminary design, the engineer can immediately see the consequences of his/her choice of design sections. Without having to handle a large amount of stress data, he/she is therefore able to conveniently examine different scenarios and subsequently choose the most suitable option.

2. An experienced designer, on the other hand, knows in advance by examining the linear elastic solution furnished by the program, how he/she would like to define their design sections. The ease in examining design section configurations corresponding to the linear elastic solution is, as a result, not as vital to him/her as the inexperienced designer. The optimisation stage however can be promising to him/her since his/her engineering judgement together with the computational capabilities of the program can lead to favourable design solutions. He/she can therefore show the program the way to go as well as control how far to proceed.

It should be mentioned that the proposed techniques and the developed computer program based on it is not intended to be a push-button piece of computer software to accomplish the task of design. It is conceived to be a powerful *tool* and not a substitute for the design engineer. Also, the programming of specific AS3600 provisions for reinforcement *dimensioning* was not of importance in this research work (as it is not meant to be a detailed design tool) and should therefore be taken into account by the design engineer separately.

9.2 Further Work

Through the thesis, we have explicitly pointed out the assumptions and limitations of the work in each chapter. Certainly this work can be enhanced in many aspects.

Recommendations for further work are summarised as follows:

1. The methods developed in this work could be based on a more rigorous mathematical basis, however, keeping in mind the need for developing a practical design tool that can be used in routine design office work.
2. The methods developed could be extended for multiple load cases.
3. The methods developed could be extended to dynamic problems like floor vibrations.
4. A technique could be developed to eliminate the effect of finite element meshes on the optimal solutions.
5. Incorporate formwork costs and maybe construction time costs in the optimisation process.
6. If "top deflection" is to be used as the performance criteria in seeking optimal bracing patterns, then a procedure can be added in the computer code that prevents removal of bracing elements in the top storey such that there is no "jump" in the lateral top deflection. Inter-storey drifts could also be considered.
7. In thickness optimisation of walls, reinforcement design optimisation could be developed (similar to the three techniques developed for slabs).
8. The labelling process for panels in flat slabs and walls is cumbersome and time-consuming at present. Though it has to be done only once at the beginning when creating the initial model, the process could be automated.
9. At present, the estimates of concrete quantity and steel quantity (and costs) are calculated for regular meshes. The estimation algorithms would not accurately calculate the quantities

if a model has a coarse mesh with a region inside it having a fine mesh. This could be addressed in future work.

10. The design solutions for slabs obtained using the proposed techniques are based on a linear elastic finite element analysis, thus avoiding non-linear analysis with complex material models. This makes the techniques easier to understand for a typical engineer and attractive for his everyday design. A non-linear finite element analysis however would have predicted more accurately the physical behaviour of the slab near the column supports, although it would have increased the computational cost. It is seen that the proposed modelling and design techniques demonstrate rational, safe and economical design solutions for the drop panels and are adequate from a practical point of view. However, future work could look into extending the proposed techniques from a non-linear perspective.

11. The element stress resultants computed (bending moments and shears) from the finite element analysis could have been more accurate if it would have been possible to specify the reinforcement within the plate-bending element. However, this is not possible in SAP2000 Version 8.3, but it could be looked at in future work when CSI (creators of SAP2000) implement this in later versions of SAP2000.

12. As it is not possible to obtain the stiffness matrix in SAP2000, the design of slabs is based on element stress resultants and not element forces, although it is well known that equilibrium is preserved when element force results are employed since forces are computed directly from element stiffnesses. However, the benefits of using the ESO method in obtaining a stable stress field or converged solution is clearly seen wherein repeated finite element analysis and element sizing are performed till all the constraints are satisfied and/or no further improvement can be achieved. The design is carried out till convergence meaning that although the resulting stresses and moments calculated at the common node of adjacent elements are discontinuous and thus not in equilibrium with one another, a smoothing algorithm together with the ESO method seeks a stable solution such that the design converges (or settles) and stays the same thereafter. The bending moments in the converged optimal design nowhere exceed the yield limit, which is important for strength design.

13. Though large-scaled 2D structures can clearly be treated with both topology and sizing optimisation methods, the computational costs for obtaining optimal solutions for real 3D structures (such as the 40-storey Hull-Core structural system in Chapter 3) is still high. Improvement in the numerical algorithms could be considered.

14. It is important to investigate methods that may be useful in finding a practically admissible design. In practice, many variables should be linked and variables that can really be changed should be carefully selected. We have seen this being employed in the proposed optimisation procedures for flexural and shear design of slabs developed in Chapters 7 and

8 (Techniques 1, 2 and 3). It is clear that the 'bending moment capacity' calculated for a discrete 'section' specified by the user depends on several linked discrete variables (including requirements on ductility etc). This means that once a 'section' is specified by the designer in the user interface, each of its linked variables required for the computation of the flexural and shear capacity of that section for a one-metre width of slab are calculated and validated to AS 3600 code provisions. If any of the linked discrete variables is found to not satisfy the code requirement, then the upper or lower bound as per AS 3600 (based on the calculation) is chosen. As mentioned in Chapter 2, certain values for a particular variable (e.g. minimum reinforcement quantity) can only be used when appropriate values for other variables (e.g. slab thickness and material properties for steel and concrete) are also assigned. It is seen that in the three techniques developed, the objective used in the optimisation in each case is different. Similar work could also be done for walls and bracing systems.

15. Isotropic behaviour is usually assumed for concrete and steel, although this is not always the case. A slab is said to be isotropically reinforced if it is reinforced identically in orthogonal directions and its ultimate resisting moment is the same in these two directions as it is along any line regardless of its direction. Identical reinforcement is generally provided for each design section in the GUI's (design data) for almost all the examples. However, it is possible to specify different quantities of steel in both orthogonal directions in the GUI's. In either case, the algorithm calculates the moment capacities in both orthogonal directions and designs a section based on which Technique is chosen by the user. If the quantities of steel specified are different in both directions, then different moment capacities are computed in either direction. This would mean that the slab is orthotropically reinforced as its ultimate strength would be different in two perpendicular directions. However, it is not possible to specify two different thicknesses in both the X and Y directions for the slab in SAP2000 Version 8.3 to account for orthotropic effects in the finite element analysis. As a result, the design algorithms developed in this work design sections based on the bigger of the two moment capacities in either directions. Moreover, we have seen a number of issues in 'Numerical Studies' in Chapter 7 such as for e.g. the effect 'two different depths in two orthogonal directions' have on symmetrical results (Section 7.7.2.1), oscillating solutions (Section 7.7.2.2) and a few design approaches (Section 7.7.2.3 and Section 7.7.2.4) to solve those issues. If, in later versions of SAP2000, it is possible to specify two different thicknesses in both the X and Y directions for the slab to account for orthotropic effects in the finite element analysis, then the present work could be extended to take this into account.

16. An integrated process for optimising slabs and walls simultaneously in a 3D building model could be investigated.

17. The software system developed in the course of this research work can be used with SAP2000 Version 8.3. For each newer version of SAP2000, significant changes need to be made to the design optimisation algorithms due to the changing nature of the SAP2000 data file. A robust and scalable software system needs to be developed that handles version changes of SAP2000 with relative ease.

18. For 3D object based finite element engines (such as SAP2000) that use a single graphical user interface for all operations based on the Windows API (Application Programming Interface), it is difficult to implement ESO type optimisation code. ESO optimisation, which is iterative in nature, requires performing repeated runs of operations such as reading the model file into SAP2000, executing the analysis and exporting the FEA results. These operations need to be performed from within the SAP2000 GUI. Use of a scripting language such as WinBatch is an absolute necessity in order to perform ESO type optimisation in SAP2000. Even then, the WinBatch code needs to be changed each time a different model is used (re-set timers i.e. event-handlers for different operations), as generally, a bigger building model with a fine mesh takes a much longer time to read, render, display and analyse in the SAP2000 GUI than say a simple model with a coarse mesh. Work could be carried out in this regard to ease the process of performing ESO type optimisation in SAP2000 with minimal delays.

APPENDIX A

The purpose of Appendix A is to show hand calculations using the Simplified Method of Design for the flat slab example in Section 7.7.2.1 on page 7-66 and Section 7.7.3.3 on page 7-91. The geometry and loading in both examples is the same. Refer to Warner *et al* (1999) for design formulae and tables.

Data:

Effective span in both directions: 6 m x 6 m (Total: 18 m x 18 m)

Initial Thickness: 250 mm (Computations below show why an initial thickness of 250 mm was chosen).

Thickness of Drop Panels: 325 mm

f'_c: 25 MPa

f_{sy}: 400 MPa

Clear cover: 25 mm

Column sizes: 400 mm x 400 mm

DL: Self Weight

LL: 5 kPa

Load Combination: 1.25 DL + 1.5 LL

DESIGN COMPUTATIONS

(1) THICKNESS OF SLAB:

The adequacy of 250 mm thickness will be checked by Eq. 19.4 (pg 553 of Warner *et al* 1999)

Self Wt = 0.25 x 24 = 6 kPa

Short term live load factor = 0.6

Service Load = 6 + (0.6 x 5) = 9 kPa

For this slab, $L_n = L'_n = 6 - 0.4 = 5.6$ m & $k_1 = 1.6$ (as edge panel controls)

Eq. 19.4

$$\frac{L_n}{D_s} \leq 65 \times \left[\left(\frac{L_n}{L'_n} \right) \times \frac{1}{w \times K_1} \right]^{1/3}$$

Where,

L_n = Longer clear span of slab = 5.6 m

L'_n = Shorter clear span of slab = 5.6 m

D_s = total thickness of slab = 250 mm

K_1 = 1 for interior panels

= 1.3 for exterior panels with edge beams

= 1.6 for exterior panels with no edge beam

w = service load (kPa) including self weight = 9 kPa

$$\frac{5600}{D_s} \leq 65 \times \left[\left(\frac{5600}{5600} \right) \times \frac{1}{9 \times 1.6} \right]^{1/3}$$

Or $D_s \geq 210mm$ ……..Therefore, a thickness of 250 mm chosen is OK

Because, this is a retail floor store, it may be necessary to limit the incremental part of the total deflection in order to avoid damage to non-structural elements. Therefore, increase the above thickness by 10%. Hence, minimum thickness = 1.1 x 210 = 231 mm. Stick to D_s = 250 mm.

Projection of the drop panel below the slab is taken as $0.3D_s$ i.e. 0.3 x 250 = 75 mm

Total thickness of slab in the vicinity of the column is 250 + 75 = 325 mm

(2) MOMENTS IN X-DIRECTION – INTERIOR DESIGN STRIP

Design Load, F_d = (1.25 x 6) + (1.5 x 5) = 15 kPa

From Fig. 18.9 (a) (page 537 of Warner *et al* 1999), a_s = 275 mm for this case

Total Static Moment for a span = Eq. 18.14 (page 536 of Warner *et al* 1999) which is given as follows:

$$M_o = \frac{F_d \times L_t \times L_o^2}{8}$$

F_d = (1.25 x 6) + (1.5 x 5) = 15 kPa

L_t = 6 m

L_o = 6000 – 2(0.7 x 275) = 5615 mm

Eq. 18.14:

$$M_0 = \frac{15 \times 6 \times 5.615^2}{8} = 354.70 \text{ kN-m, say } 355 \text{ kN-m}$$

INTERIOR SPAN

Total Negative Moment (each end) = 0.65 x 355 = 231 kN-m

Total Positive Moment (mid-span) = 0.35 x 355 = 125 kN-m

From Table 18.3 (page 538), the negative moment is distributed 0.75 to the interior column strip (width = 3 m) and 0.25 to two half-middle strips (width = 1.5 m each).

Negative moment in column strip = 0.75 x 231 = 174 kN-m

Negative moment in two half-middle strips = 0.25 x 231 = 58 kN-m

The positive moment is distributed uniformly across the design strip, i.e. 0.5 to the column strip and 0.5 to the two half-middle strips.

Positive moment in each strip = 0.5 x 125 = 62.5 kN-m

END SPAN

As before, $M_0 = \frac{15 \times 6 \times 5.615^2}{8}$ = 354.70 kN-m, say 355 kN-m

This moment is apportioned between the exterior end, mid-span and interior end according to the coefficients in Table 18.2 (page 536).

Total Negative Moment (Exterior End), M_{NE} = 0.25 x 355 = 89 kN-m

Total Positive Moment, M_M = 0.5 x 355 = 178 kN-m

Total Negative Moment (Interior End), M_{NI} = 0.75 x 355 = 267 kN-m

At the exterior end, the moment M_{NE} is all assigned to the column strip (width = 3m, because there is no edge beam)

At mid-span, M_M is distributed uniformly across the design strip.

Positive moment in each strip = 0.5 x 178 = 89 kN-m

At the interior end, M_{NI} is distributed 0.75 to the column strip and 0.25 to the two half-middle strips:

Negative moment (Interior) in Column strip = 0.75 x 267 = 201 kN-m

Negative moment (Interior) in middle strips = 0.25 x 267 = 67 kN-m

(3) MOMENTS IN X-DIRECTION – EDGE DESIGN STRIP

L_t = 3 m ; L = 6 m

As before, A_s = 280 mm; L_o = 6000 – 2(0.7 x 280) = 5608 mm & F_d = 15 kPa

Eq. 18.14:

$$M_0 = \frac{15 \times 3 \times 5.615^2}{8} = 177 \text{ kN-m}$$

This moment is first apportioned between positive and negative moments and then further distributed to the column and middle strips.

INTERIOR SPAN:

Total Negative Moment (each end) = 0.65 x 177 = 116 kN-m

Total Positive Moment (mid-span) = 0.35 x 177 = 62 kN-m

From table 18.3, negative moment is distributed 0.75 to the interior column strip (width = 1.5 m) and 0.25 to the half middle strip (width = 1.5 m).

Negative moment in column strip = 0.75 x 116 = 87 kN-m

Negative moment in half-middle strip = 0.25 x 116 = 29 kN-m

The positive moment is distributed uniformly across the design strip, i.e. 0.5 to the column strip and 0.5 to the half middle strip.

Positive moment in each strip = 0.5 x 62 = 31 kN-m

END SPAN:

As before, $M_0 = \frac{15 \times 3 \times 5.615^2}{8}$ = 177 kN-m

Total negative moment (exterior end), M_{NE} = 0.25 x 177 = 45 kN-m

Total positive moment, M_M = 0. 5 x 177 = 89 kN-m

Total negative moment (interior end), M_{NI} = 0.75 x 177 = 133 kN-m

At the exterior end, M_{NE} is all assigned to the column strip (width = 1.5 m)

At mid-span, M_M is distributed uniformly across the design strip

Positive moment in each strip = 0.5 x 89 = 45 kN-m

At interior end, M_{NI}, is distributed 0.75 to the column strip and 0.25 to the half middle strips

Column strip = 0.75 x 133 = 100 kN-m

Half Middle Strips = 0.25 x 133 = 34 kN-m

(4) MOMENTS IN Y-DIRECTION

As spans are the same in both directions, moments in Y-direction will be the same as moments in x-direction; for both Interior Design Strip and Edge Design Strip

(5) DESIGN OF REINFORCEMENT

At each location, the various strips of the slab are designed as rectangular shallow beams and the areas of tensile reinforcement required are calculated by Eqns. 19.5 and 19.6 (Warner *et al 1999*).

As spans are same and the slab is subjected to a UDL, moments in both directions will be same. We assume that bars in x-direction will be placed closer to the slab surface. We use Y16 bars. With a clear cover of 25 mm, the effective depth of x-bars for negative moment in the column strips is then 325 – 25 – 8 = 292 mm.

For y-bars, effective depth is 292 – 16 = 276 mm.

For negative moments in middle strips, as well as mid-span moments in both column and middle strips, the effective depth of x-bars is 250 – 25 – 8 = 217 mm

For y-bars, effective depth is 217 – 16 = 201 mm

At the first interior columns, the reinforcement is designed for the greater of the moments shown, i.e. those in the end-span.

Each middle strip is designed to resist the sum of the moments assigned to its two adjoining halves.

Note that minimum area of reinforcement in each strip is as follows: Eq. 19.10 (Warner *et al* 1999)

$P_{min} = 1/f_{sy} = 1/400 = 0.0025$

Negative moment steel in column strips in x-direction:

0.0025 x 1000 x 292 = 730 mm^2/m, i.e. Y16 bars at 270 mm spacing (4 bars per m width)

Negative moment steel in column strips in y-direction:

0.0025 x 1000 x 276 = 690 mm^2/m, i.e. Y16 bars at 290 mm spacing (4 bars per m width)

Negative moment steel in middle strips and Positive moment steel in both column and middle strips in x-direction:

0.0025 x 1000 x 217 = 543 mm^2/m, i.e. Y16 bars at 365 mm spacing (3 bars per m width)

Negative moment steel in middle strips and Positive moment steel in both column and middle strips in y-direction:

0.0025 x 1000 x 201 = 503 mm^2/m, i.e. Y16 bars at 395 mm spacing (3 bars per m width)

The spacing of bars should not exceed 500 mm (lesser of 2.5 D_s or 500 mm) which is satisfied.

A quarter model of the reinforcement layout is shown on the next page.

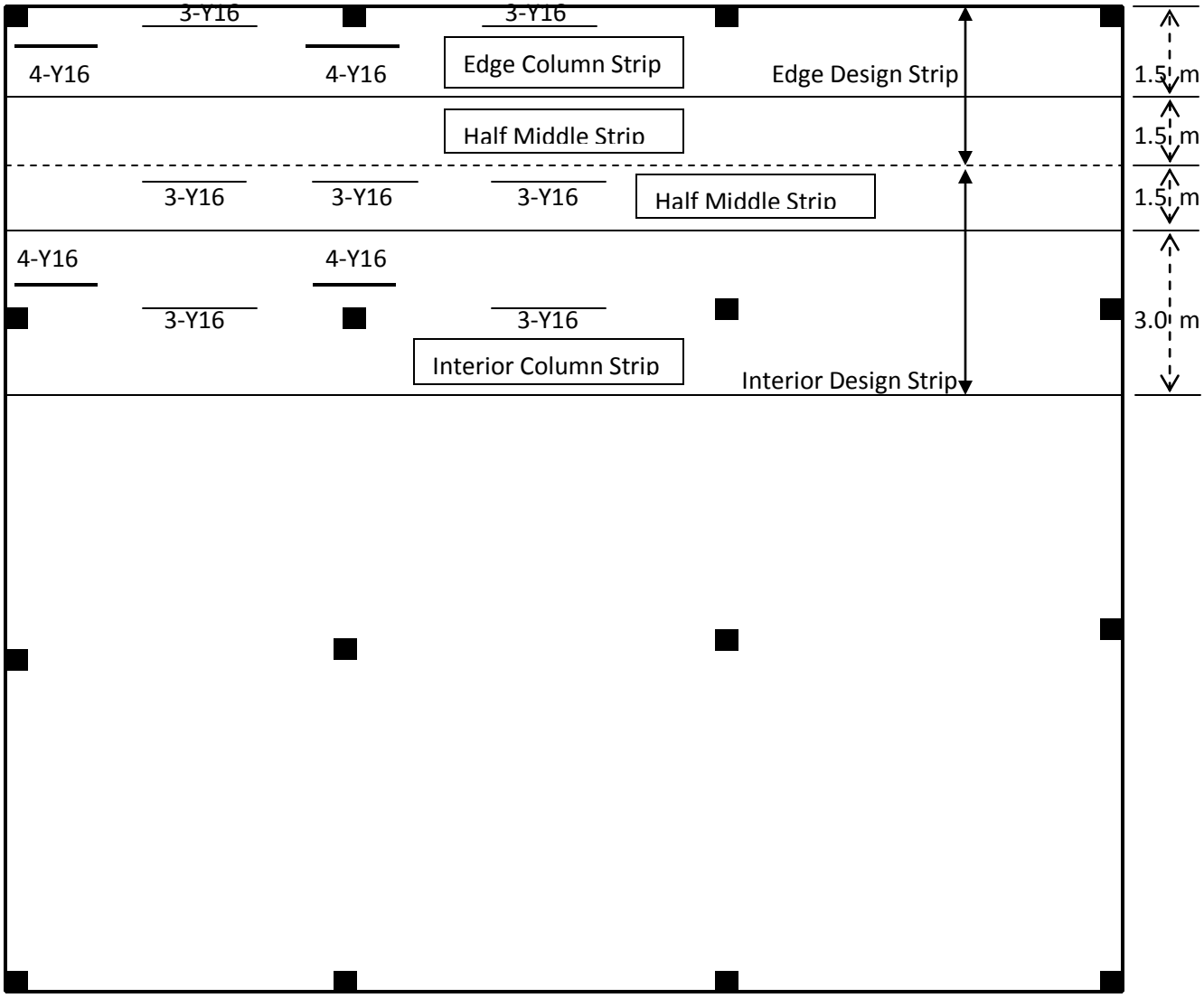

Note: Steel quantity shown is number of bars required per metre width. Reinforcement shown is for strips in x-direction. The same amount of steel is seen to be required in y-direction (as spans are same in both directions). Therefore, steel shown above may be considered "BOTH WAYS" i.e. 4-Y16 in the figure above means 4-Y16 bars both ways (4-Y16 bars needed in x-direction and 4-Y16 bars needed in y-direction). For simplicity, only a quarter of the model is populated.

The reinforcement may be arranged as illustrated in Fig. 9.1.3.4 of AS 3600-2001.

It can be seen that in most regions of the slab the steel is controlled by the minimum reinforcement requirements.

APPENDIX B

The purpose of Appendix B is to show hand calculations using the Simplified Method of Design for the flat slab example in Section 7.7.2.4.1 on page 7-78. Refer to Warner *et al* (1999) for design formulae and tables.

Data:

Effective span in both directions: 8.4 m x 8.4 m (Total: 25.2 m x 25.2 m)

Initial Thickness: 350 mm (Computations below show why an initial thickness of 350 mm was chosen).

Thickness of Drop Panel: 455 mm

f'_c: 30 MPa

f_{sy}: 400 MPa

Clear cover: 25 mm

Column sizes: 450 mm x 450 mm

DL: Self Weight + 1 kPa

LL: 5 kPa

Load Combination: 1.25 DL + 1.5 LL

DESIGN COMPUTATIONS

(1) THICKNESS OF SLAB:

The adequacy of 350 mm thickness will be checked by Eq. 19.4 (pg 553 of Warner *et al* 1999)

Self Wt = 0.35 x 24 = 8.4 kPa

Short term live load factor = 0.6

Service Load = 8.4 + 1 + (0.6 x 5) = 12.4 kPa

For this slab, $L_n = L'_n = 8.4 - 0.45 = 7.95$ m & $k_1 = 1.6$ (as edge panel controls)

Eq. 19.4

$$\frac{L_n}{D_s} \leq 65 \times \left[\left(\frac{L_n}{L'_n} \right) \times \frac{1}{w \times K_1} \right]^{1/3}$$

Where,

L_n = Longer clear span of slab = 7.95 m

L'_n = Shorter clear span of slab = 7.95 m

D_s = total thickness of slab = 350 mm

K_1 = 1 for interior panels

= 1.3 for exterior panels with edge beams

= 1.6 for exterior panels with no edge beam

w = service load (kPa) including self weight = 12.4 kPa

$$\frac{7950}{D_s} \leq 65 \times \left[\left(\frac{7950}{7950} \right) \times \frac{1}{12.4 \times 1.6} \right]^{1/3}$$

Or $D_s \geq 331.11$ mm ……..Therefore, a thickness of 350 mm chosen is OK

Projection of the Drop Panel below the slab = 0.3 D_s = 0.3 x 350 = 105 mm.

Total thickness of slab in the vicinity of columns = 350 + 105 = 455 mm.

(2) MOMENTS IN X-DIRECTION – INTERIOR DESIGN STRIP

Design Load, Fd = (1.25 x 9.4) + (1.5 x 5) = 19.25 kPa

From Fig. 18.9 (a) (page 537 of Warner *et al* 1999), a_s = 200 mm for this case

Total Static Moment for a span = Eq. 18.14 (page 536 of Warner *et al* 1999) which is given as follows:

$$M_o = \frac{F_d \times L_t \times L_o^2}{8}$$

F_d = (1.25 x 9.4) + (1.5 x 5) = 19.25 kPa

L_t = 8.4 m

L_o = 8400 – 2(0.7 x 200) = 8120 mm

Eq. 18.14:

$$M_0 = \frac{19.25 \times 8.4 \times 8.12^2}{8} = 1332.70 \text{ kN-m, say } 1333 \text{ kN-m}$$

INTERIOR SPAN

Total Negative Moment (each end) = 0.65 x 1333 = 867 kN-m

Total Positive Moment (mid-span) = 0.35 x 1333 = 467 kN-m

From Table 18.3 (page 538 of Warner *et al* 1999), the negative moment is distributed 0.75 to the interior column strip (width = 4.2 m) and 0.25 to two half-middle strips (width = 2.1 m each).

Negative moment in column strip = 0.75 x 867 = 651 kN-m

Negative moment in two half-middle strips = 0.25 x 867 = 217 kN-m

The positive moment is distributed uniformly across the design strip, i.e. 0.5 to the column strip and 0.5 to the two half-middle strips.

Positive moment in each strip = 0.5 x 467 = 234 kN-m

END SPAN

As before, $M_0 = \frac{19.25 \times 8.4 \times 8.12^2}{8}$ = 1332.70 kN-m, say 1333 kN-m

This moment is apportioned between the exterior end, mid-span and interior end according to the coefficients in Table 18.2 (page 536 of Warner *et al* 1999). Since the outer end is fully restrained, we have:

Total Negative Moment (Exterior End), M_{NE} = 0.65 x 1333 = 867 kN-m

Total Positive Moment, M_M = 0.35 x 1333 = 467 kN-m

Total Negative Moment (Interior End), M_{NI} = 0.65 x 1333 = 867 kN-m

At the exterior end, the moment M_{NE} assigned to the column strip is 0.75 x 867 = 651 kN-m (as the ends are fully restrained)

At mid-span, M_M is distributed uniformly across the design strip.

Positive moment in each strip = 0.5 x 467 = 234 kN-m

At the interior end, M_{NI} is distributed 0.75 to the column strip and 0.25 to the two half-middle strips:

Negative moment (Interior) in Column strip = 0.75 x 867 = 651 kN-m

Negative moment (Interior) in middle strips = 0.25 x 867 = 217 kN-m

(3) MOMENTS IN X-DIRECTION – EDGE DESIGN STRIP

L_t = 8.4 m ; L = 8.4 m

As before, A_s = 200 mm; L_o = 8400 – 2(0.7 x 200) = 8120 mm & F_d = 19.25 kPa

Eq. 18.14:

$$M_o = \frac{19.25 \times 4.2 \times 8.12^2}{8} = 667 \text{ kN-m}$$

This moment is first apportioned between positive and negative moments and then further distributed to the column and middle strips.

INTERIOR SPAN:

Total Negative Moment (each end) = 0.65 x 667 = 434 kN-m

Total Positive Moment (mid-span) = 0.35 x 667 = 234 kN-m

From table 18.3, negative moment is distributed 0.75 to the interior column strip (width = 2.1 m) and 0.25 to the half middle strip (width = 2.1m).

Negative moment in column strip = 0.75 x 434 = 326 kN-m

Negative moment in half-middle strip = 0.25 x 434 = 109 kN-m

The positive moment is distributed uniformly across the design strip, i.e. 0.5 to the column strip and 0.5 to the half middle strip.

Positive moment in each strip = 0.5 x 234 = 117 kN-m

END SPAN:

As before, $M_0 = \frac{19.25 \times 4.2 \times 8.12^2}{8}$ = 667 kN-m

Total negative moment (exterior end), M_{NE} = 0.65 x 667 = 434 kN-m

Total positive moment, M_M = 0.35 x 667 = 234 kN-m

Total negative moment (interior end), M_{NI} = 0.65 x 667 = 434 kN-m

At the exterior end, M_{NE} is assigned 0.75 x 434 = 326 kN-m to the column strip (width = 2.1 m) as ends are fully restrained

At mid-span, M_M is distributed uniformly across the design strip

Positive moment in each strip = 0.5 x 234 = 117 kN-m

At interior end, M_{NI}, is distributed 0.75 to the column strip and 0.25 to the half middle strips

Column strip = 0.75 x 434 = 326 kN-m

Half Middle Strips = 0.25 x 434 = 109 kN-m

(4) DESIGN OF REINFORCEMENT

Reinforcement design computations are similar to the computations performed in Appendix A and are not repeated here. The only difference is Y22 bars are chosen in this example, therefore effective depth of x-bars is "*350 mm – 25 – 11 = 314 mm*" and effective depth of y-bars is "*314 – 22 = 292 mm*" (assuming x-bars are placed closer to the slab surface). The reinforcement design in x-direction for a quarter of the slab (as spans are same in both directions) is shown in the following figure. Not that as spans are same in both directions steel required in Y-direction is found to be the same as that required in x-direction in the various regions even though effective depths are different. Hence, to save space, reinforcement drawing in y-direction is not shown.

Also, spacing of bars should not exceed 500 mm (i.e. lesser of $2.5D_s$ or 500 mm) which is satisfied in this case.

The reinforcement may be arranged as illustrated in Fig. 9.1.3.4 of AS 3600-2001.

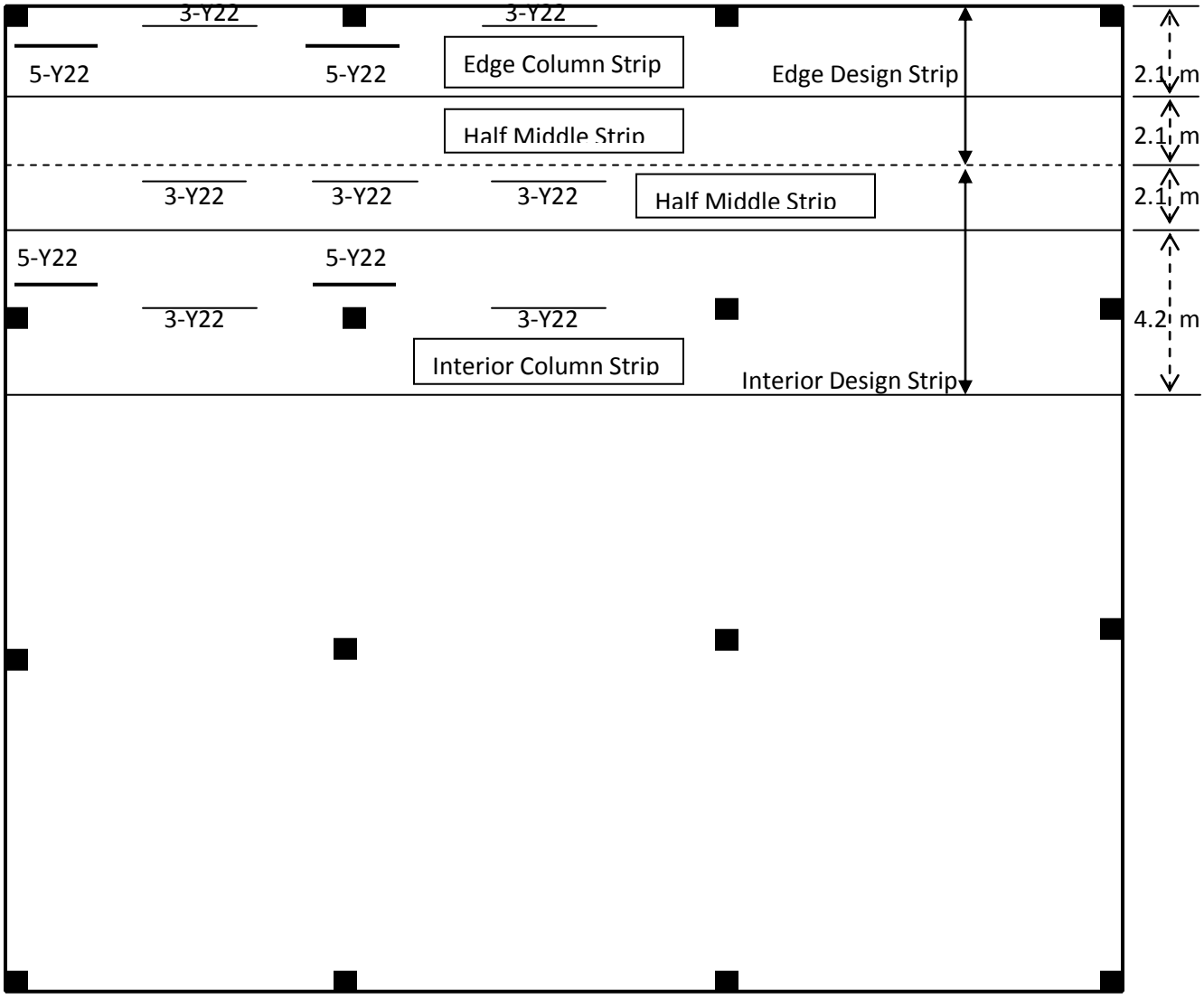

Note: Steel quantity shown is number of bars required per metre width. Reinforcement shown is for strips in x-direction. The same amount of steel is seen to be required in y-direction (as spans are same in both directions). Therefore, steel shown above may be considered "BOTH WAYS" i.e. 5-Y22 in the figure above means 5-Y22 bars both ways (5-Y22 bars needed in x-direction and 5-Y22 bars needed in y-direction). For simplicity, only a quarter of the model is populated.

REFERENCES

- Adini, A. and Clough, R. W. (1960) *Analysis of Plate Bending By the Finite Element Method*. G7337 Report to the National Science Foundation
- Al-Khaleefi, A.M., Jan Thomas, C.C. (2002). SWESA – Optimisation in the design of shear walls. *Journal of Scientific Engineering*, 29(2).
- Al-Mosawi, S.S. and Saka, M.P. (1999). Optimum design of single core shear walls. *Computers and Structures*, **71**, 143-162.
- Almussallam, T.H. (1995). Effect of connection flexibility on the optimum design of steel frames, *Developments in Computational techniques for Civil Engineering*, 129-135.
- Al-Saadoun, S.S. and Arora, J.S. (1989). Interactive design optimisation of framed structures, *Journal of Computing in Civil Engineering*, ASCE, **3**(1), 60-74.
- Ambrose, J.E. (1997). *Simplified design of concrete structures.* 7th ed. New York : Wiley.
- American Concrete Institute (1995) Building Code Requirement for Structural Concrete (ACI 318-95) and Commentary (ACI 318R-95)
- American Concrete Institute (2002) Building Code Requirement for Structural Concrete (ACI 318-02)
- Anderheggen, E., e. a., (June 1994). Reinforced-Concrete Dimensioning Based on Element Nodal Forces, *ASCE Journal of the Structural Division*, **102**, 1718–1731.
- Aoyama H., (2001). *Design of Modern High-rise Reinforced Concrete Structures*, Imperial College Press.
- Arciszewski, Tomasz; Bloedorn, Eric; Michalski, Ryszard S; Mustafa, Mohamad; Wnek, Janusz, (1994). Machine learning of design rules: methodology and case study, *ASCE Journal of Computing in Civil Engineering*, **8**(3), Jul, 286-308.
- Arora, J.S. (1989). *Introduction to Optimal Design*, McGraw-Hill Book Co., New York
- Arora, J.S. (1997). *Guide to Structural Optimisation*, ASCE Manuals and Reports on Engineering Practice, No. 90, American Society of Civil Engineering, 1801 Alexander Bell Drive, Reston, VA 20191.
- Arora, J.S., Huang, M.W. and Hsieh, C.C. (1994). Methods for optimisation of Nonlinear problems with Discrete Variables: A Review. *Structural Optimisation*, **8**(2/3), 69-85
- Australian Standard for Concrete Structures AS 3600 – 2001 (Incorporating Amendment 1 and Amendment 2) (2001). Standards Australia.
- Baker W, Novak L, Sinn R, Viise J, *Structural optimisation of 2000' Tall 7 South Dearborn building*, ASCE Library.
- Baker, Nelson. C.; Fenves, Steven J., (1989). Towards a grammar for structural design. *Sixth conference on Computing in Civil Engineering*, Sep 11-13, Atlanta, GA, USA, 178-185.

- Baldock, R. and Shea, K. (2004). Structural systems optimization techniques for the building industry. In: Next Generation - Intelligent Systems in Engineering, *the 11th International Workshop of the European Group for Intelligent Computing in Engineering (EG-ICE)*, Weimar, Germany, 199(4), 11-15
- Baldock, R. and Shea, K. (2005). Combining continuum topology optimization and structural design guidelines for bracing system design in multistory steel building frames. In: Soft Computing in Engineering, *the 12th International Workshop of the European Group for Intelligent Computing in Engineering (EG-ICE)*, Radziejowice, Poland.
- Baldock, R., Shea, K. and Eley, D. (2005). Evolving optimized braced steel frameworks for tall buildings using modified pattern search. In: *International Conference on Computing in Civil Engineering*, ASCE 2005, Cancun, Mexico
- Balling, R.J. (1991). Optimal Steel Frame Design by Simulated Annealing, *Journal of Structural Engineering*, **117**(6), 1780-1795
- Balling, R.J. and Fonseca, F. (1989). Discrete optimisation of 3D steel frames, *Computer Utilization in Structural Engineering*, ASCE, New York, N.Y., 458-467.
- Barzegar, F. and Maddipudi, S., (1994).Generating Reinforcement in FE Modelling of Concrete Structures, *ASCE Journal of the Structural Division*, **120**, 1656–1662, May 1994.
- Bashur, F. K. and Darwin, D., (1978). Nonlinear Model for Reinforced Concrete Slabs, *ASCE Journal of the Structural Division*, **104**, 157–170, January 1978.
- Bhatti, M.A. (1979). *Optimal design of localised nonlinear systems with dual performance criteria under earthquake excitations*. UCB/EERC-79/15, University of California, Berkeley, CA.
- Bhatti, M.A. and Pister, K.S. (1981). A dual criteria approach for optimal design of earthquake-resistant structural systems. *Earthquake engineering and structural dynamics*, John Wiley and Sons, Ltd., **9**, 557-572.
- Bic´anic, N., de Borst, R., Mang, H., and Meschke, G., eds., (2003). *Computational Modelling of Concrete Structures*. Lisse, The Netherlands: A.A. Balkema Publishers.
- Bong, B.C. (1998). *Optimal Applications of High-Strength Concrete in Structural Walls of Tall Buildings*. Master's Thesis, Victoria University of Technology, Melbourne, Australia.
- Borkowski, A., (1977). Optimization of Slab Reinforcement by Linear Programming, *Computer Methods in Applied Mechanics and Engineering*, **12**, 1–17, September 1977.
- Brokowski, A.; Fleischmann, N.; Bletzinger, K.U., (1991). Supporting conceptual decisions in structural design, *Second International Conference on the Application of Artificial Intelligence to Civil and Structural Engineering*, Sep 3-5, Edinburgh UK, 87-96.
- Brotchie, J. F. and Russell, J. J., (1964). Flat Plate Structures: Elastic-Plastic Analysis, *Journal of the American Concrete Institute*, **61**, 959–996, August 1964.
- Bungale, T.S. (1988). *Structural Analysis and design of tall buildings*. McGraw-Hill, New York.
- Bungale, T.S. (1998). *Steel, Concrete and Composite Design of Tall Buildings*. McGraw-Hill, New York.

- Burns, S.A. (2002). *Recent advances in optimal structural design*. ASCE, Structural Engineering Institute.
- Cagan, Jonathan; Mitchell, William, J., (1993). Shape annealing approach to creative design of structures, *5th International Conference on Computing in Civil and Building Engineering*, Jun 7-9, New York, NY, USA, 1642-1646.
- Cameron, G.E., Xu, L., and Grierson, D.E. (1991), Discrete optimal design of 3D frameworks. In: *Electronic Computation, Proceedings of the tenth conference, O. Ural and T-L. Wang, Eds.*, American Society of Civil Engineers, 1801 Alexander Bell Dr., Reston, VA, 181-188.
- Canbay E., Ersoy U., Ozcebe G., (2003). Contribution of reinforced concrete infills to seismic behaviour of structural systems, *ACI Structural Journal*, **100**(5), Sep-Oct 2003
- Chan, C.M. (1992). An Optimality Criteria Algorithm for Tall Steel Building Design using Commercial Standard Sections, *Structural Optimisation*, **5**, 26-29.
- Chan, C.M. (2001). Optimal lateral stiffness design of tall buildings of mixed steel and concrete construction. *The Structural Design of Tall Buildings*, **10**, pp 155-177
- Chan, C.M. and Wang, Q. (2006). Nonlinear stiffness design optimisation of tall reinforced concrete buildings under service loads. *Journal of Structural Engineering*, **132**, Jun 1 2006, 978-990.
- Chan, C.M., Grierson, D.E. and Sherbourne, A.N. (1995). Automatic Optimal Design of Tall Steel Building Frameworks, *Journal of Structural Engineering*, ASCE, **121**(5), 838-847.
- Charney, F.A. (2000). Needs in the development of a comprehensive performance based optimisation process. *Advanced Technology in Structural Engineering – Structures Congress 2000, Elgaaly, M., Ed*., ASCE, May 8-10.
- Cheng, F.Y. and Botkin, M.E. (1976). Nonlinear optimum design of dynamic damped frames. *Journal of the Structural Division*, ASCE, **102** (ST3), 609-627.
- Cheng, F.Y., and Li, D. (1997). Multi-objective optimisation design with Pareto genetic algorithm. *Journal of Structural Engineering*, ASCE, **123** (9), 1252-1261.
- Cheng, F.Y., Ang, A.H.S., Lee, J.H. and Li, D. (1999). Genetic algorithm for multi-objective optimisation and life-cycle cost. *Structural engineering in the 21st century, Avent, R.R. and Alawady, M., Ed.*, ASCE-Structural engineering institute, April 18-21, 484-489.
- Cheung, Y. K., King, I. P., and Zienkiewicz, O. C., (1968). Slab Bridges with Arbitrary Shape and Support Conditions: A General Method of Analysis Based on Finite Elements, *Institution of Civil Engineers – Proceedings*, **40**, 9–36, May 1968.
- Chierdast, M.; Ambo, S.D., (1995). Topology optimisation of planar cross-sections. *Structural Optimisation*, **9**(3-4), Jul, 266-268.
- Cho, H.N. and Park, J.B., (1992). Optimum design of beam-to-column connections in steel frameworks. *Proc. of Korea-Japan Joint Seminar of Structural Optimisation*, Seoul, Korea, 18-20.
- Chu, D.N., Xie Y.M., Steven G.P., (1998). An evolutionary structural optimisation method for sizing problems with discrete design variables, Computers and Structures **68**, 419 – 431.

- Chu, D.N. (1997). *Evolutionary Structural Optimisation method for systems with stiffness and displacement constraints*. Ph.D. Thesis, Victoria University of Technology, Australia.
- Clough, R., (1980). The Finite Element Method after Twenty-Five Years. *Computers and Structures*, **12**, pp. 361–370.
- Collins, K.R., Wen, Y.K.W. and Foutch, D.A. (1996). Dual-level seismic design: A reliability based methodology. *Earthquake Engineering and Structural Dynamics*, John Wiley and Sons, Inc., **25**, 1433-1467.
- Computers and Structures, Inc., (July 2002) *SAP2000 Analysis Reference Manual*, Version 8.0.
- Computers and Structures, Incorporated, Berkeley, California, (1998). *SAFE - Integrated Analysis and Design of Slabs by The Finite Element Method - User's Manual*, Version 6.0.
- Cook, R. D. e. a., (2002). *Concepts and Applications of Finite Element Analysis*. New York: John Wiley & Sons, Inc., fourth edition.
- Cope, R. and Clark, L., (1984). *CONCRETE SLABS: Analysis and Design*. London: Elsevier Applied Science Publishers.
- Corley, W. G. and Jirsa, J. O., (1970). Equivalent Frame Analysis for Slab Design. *Journal of the American Concrete Institute*, **67**, 875–884, November 1970.
- Cusens, A. R. and Besser, I. I., (1980). Elastic Stress Parameters in Simply Supported Skew Plates in Flexure. *Journal of Strain Analysis*, **15**(2), 103–111, 1980.
- Davies, J. D., (1970). Analysis of Corner Supported Rectangular Slabs. *The Structural Engineer*, **48**, 75–82, February 1970.
- Davies, J. D., Ma, S. P. K., and Cheung, Y. K., (1968). Analysis of Corner Supported Skew Slabs. *Building Science*, **3**, 81–92, November 1968.
- de Figueiredo, A. J. M., da Fonseca, A. M. A., and Azevedo, A. F. M., (1999).Analysis and Optimization of Reinforced Concrete Slabs. In: *Computer Aided Optimum Design of Structures VI (Hernandez, S., Kassab, A. J., and Brebbia, C. A., eds.), (Southhampton, Boston, Massachusetts)*, WIT Press.
- De La Lera, Juan C.; Chopra, Anil K., (1995). Simplified model for analysis and design of asymmetric-plan buildings, *Earthquake Engineering and Structural Dynamics*, **24**(4), Apr, 573-594.
- Deaton, J.B. (2005). *Finite Element Approach to Reinforced Concrete Slab Design*. Masters Thesis, Georgia Institute of Technology, USA.
- 'Diana' retrieved May 2007 from http://www.tnodiana.com/index-vervolg.php?scherm=3&pagina_id=43
- Domeshek, Eric A., Zimring, Craig M.; Kolodner, Janet L., (1994). Scaling up is hard to do: Experiences in preparing a case-based design aid prototype for field trial. *1st ASCE Conference on Computing in Civil Engineering*, Jun 20-22, (1) Washington, DC, USA, 430-437.
- Donaldson B., (1991). *Exterior Wall Systems: Glass and Concrete Technology: Design and Construction*, ASTM.

- Douglas, M. R. and Lunniss, R. C., (1970). An Application of the Finite Element Technique in Bridge Design, *Concrete*, **4**, 197–200, May 1970.
- Drucker, D.C. (1961). On Structural concrete and the theorems of limit analysis. *IABSE*, **21**, 49-60.
- Drucker, D.C., Greenberg, H.J., Prager, W. (1951). The safety factor of an elastic-plastic body in plane-stress, *Journal of Applied Mechanics*, **18**, 371-378.
- Ellingwood, B. (2000). Performance-Based Design: Structural Reliability Considerations. *Advanced technology in structural engineering: Proceedings of the 2000 Structures Congress, Elgaaly, M., Ed.*, ASCE, May 8-10.
- El-Sayed, Mohammed E.M,; Ridgely, Bobbie Jo; Sandgren, E., (1989). Non-linear structural optimisation using goal programming, *Computers and Structures*, **32**(1), 69-73.
- Elwakeil, O. and Arora, J.S. (1995). Methods for finding feasible points in constrained optimisation, *AIAA Journal*, **33**(9), 1715-1719.
- Eschenauer H.A., Olhoff N., (2001). Topology Optimisation of Continuum Structures: A review, *Applied Mechanics Reviews*, **54**, 331 – 390.
- Fadaee, M. J. and Grierson, D. E. (1998). Design optimisation of 3D RC structures having shear walls. *Engineering with Computers*, **14**, 139-145.
- Famiyesin, O. O. R. and Hossain, K. M. A., (1998). Optimized Design Charts for Fully Restrained Slabs by FE Predictions, *ASCE Journal of the Structural Division*, **124**, 560–569, May 1998.
- Fintel M., (1985). *Handbook of Concrete Engineering*, Van Nostrand Reinhold Company, NY.
- Fleury, C. (1980), Structural weight optimisation by dual method of convex programming, *International Journal for Numerical Methods in Engineering*, **14**, 1761-1783
- Foley, C.M. and Schinler, D. (2001). Optimised design of steel frames using distributed plasticity. *Structures Congress 2001, Chang, P., Ed.*, ASCE, May 8-10.
- Frangopol, D.M. (1997). How to incorporate reliability in structural optimisation, *Guide to Structural Optimisation*, ASCE, Structural Engineering Institute, Technical Committee on Optimal Structural Design, Reston, VA.
- Fraser, D.J. (1981). *Conceptual designs and preliminary analysis of structures*. Marshfield, Mass: Pitman Pub
- French, S., Kabaila, A. P., and Pulmano, V. A., (1975). Single Element Panel for Flat Plate Structures, *ASCE Journal of the Structural Division*, **101**, 1801–1812, September 1975.
- Fruchter, Renate, (1993). Deriving alternative structural modifications based on qualitative interpretation at the conceptual design stage, *5th International Conference on Computing in Civil and Building Engineering*, Jun 7-9, New York, NY, USA, 1243-1250.
- Fruchter, Renate; Clayton, Mark; Krawinkler, Helmut; Kunz, John; Teicholz, Paul, (1996). Interdisciplinary communication medium for collaborative conceptual building design, *Advances in Engineering Software*, **25**(2-3), Mar-Apr, Elsevier Science Ltd., Oxford, England, 89-101.

- Fuyama, Hiroyuki; Law, Kincho H, Krawinkler, Helmut, (1993). Interactive computer assisted system for conceptual.structural design of steel buildings, *5th International Conference on Civil and Structural Engineering Computing*, CIVIL-COMP, Aug 17-19, Heriot-Watt Univ., UK, 647-662.
- Fuyama, Hiroyuki; Law, Kincho H, Krawinkler, Helmut, (1994). Computer-based design support system for steel frame structures, *Structural Design of Tall Buildings*, **3**(3), Sept, 183-200.
- Fuyama, Hiroyuki; Law, Kincho H, Krawinkler, Helmut, (1994). Drift control in moment resisting steel frame structures, *Structural Design of Tall Buildings*, **3**(3), Sept, 163-181.
- Fuyama, Hiroyuki; Law, Kincho H,; Krawinkler, Helmut, (1993). Computer assisted conceptual structural design of steel buildings, *5th International Conference on Computing in Civil and Building Engineering*, Jun 7-9, New York, NY, USA, 969-976.
- Gamble, W. L. and Park, R., (2000). *Reinforced Concrete Slabs*. New York: John Wiley & Sons, Inc., second ed.
- Gamble, W. L., (1962). *Measured and Theoretical Bending Moments in Reinforced Concrete Floor Slabs*. PhD thesis, University of Illinois, Urbana, Illinois, June 1962.
- Ganzerli, S., Pantelides, C.P. and Reaveley, L.D. (2000). Performance based design using structural optimisation. *Earthquake Engineering and Structural Dynamics*, John Wiley and Sons, Inc., **29**, 1677-1690.
- Gentry, T. R., (1986). *The Use of Elastic Finite Elements in the Design of Reinforced Concrete Flat Plates*, Master's thesis, Georgia Institute of Technology.
- Grierson, D.E. and Cameron, G.E. (1989). Microcomputer based optimisation of steel structures in Professional Practice, *Microcomputers in Civil Engineering*, **4**, 289-296.
- Grierson, D.E. and Lee, W.H. (1984). Optimal synthesis of Frameworks under elastic and plastic performance constraints using discrete sections, *Journal of Structural Mechanics*, **14**(4), 401-420.
- Grierson, D.E. and Lee, W.H. (1984). Optimal synthesis of Frameworks using standard sections, *Journal of Structural Mechanics*, **12**(3), 335-370.
- Grierson, D.E. and Pak, W.H. (1993). Optimal sizing, geometrical and topological design using a genetic algorithm. *Structural Optimisation*, **6**, 151-159.
- Grierson, Donald E., (1994). Conceptual design using evolutive-cognitive computing techniques, *1st ASCE Congress on Computing in Civil Engineering*, Jun 20-22, (2), Washington, DC, USA, 2183-2190.
- Grierson, Donald E., (1997). Conceptual design using a genetic algorithm, *Proceedings of the 15th Structures Congress, Building to Last*, Part 2 (of 2), Apr 13-16, **2**, Portland, OR, USA, Sponsored by: ASCE, New York, NY, USA, 798-802.
- Gupta A., Moss P., *Guidelines for Design of low- rise buildings subjected to lateral forces*, CRC Press.
- Gupta, A. K. and Sen, S., (1977). Design of Flexural Reinforcement in Concrete Slabs, *ASCE Journal of the Structural Division*, **103**, 793–804, April 1977.

- Haber, David; Karshenas, Saeed, (1990). CONCEPTUAL. An expert system for conceptual structural design, *Microcomputers in civil engineering*, **5**(2), Jun, 119-127.
- Hager, K. and Balling, R.J. (1988), New approach for discrete structural optimisation, *Journal of Structural Engineering*, ASCE, **114**(5), 1120-1134.
- Hajela, P, Fu, B.; Berke, L, (1991). ART Networks in automated conceptual design of structural systems, *Second International Conference on the Application of Artificial Intelligence to Civil and Structural Engineering*, Sep 3-5, Edinburgh UK, 263-271.
- Haririan, M., Cardoso, J.B. an Arora, J.S. (1987). Use of ADINA for design optimisation of Nonlinear structures. *Computers and Structures*, Pergamon Journals, Ltd., **26** (1/2), 123-133.
- Hernandez, S., Kassab, A. J., and Brebbia, C. A., eds., (1999). *Computer Aided Optimum Design Of Structures VI*. Southhampton, Boston, Massachusetts: WIT Press.
- Hill, R., (1951). On the state of stress in a plastic-rigid body at the yield point, Phil. Mag. **42**, 868-875
- Hillerborg, A., (1996). *Strip Design Method Handbook*. London, Great Britain: E & FN Spon.
- Hoernlein, H.E.R.M.; Stettner, M., (1997). Structural design process: projects-programs-prospects, *Proceedings of the Conference on Optimisation in Industry*, Mar 23-27, Palm Coast, FL, USA, ASME, Fairfield, NJ, USA, 89-101.
- Hrabok, M. M. and Hrudey, T. M., (1982). Finite Element Analysis in Design of Floor Systems, *ASCE Journal of the Structural Division*, **109**, 909–929, April 1982.
- Hrabok, M. M., (1981). *Stiffened Plate Analysis by the Hybrid Stress Finite Element Method*. PhD thesis, University of Alberta, Edmonton, Alberta, Canada.
- Huang, M.W. (1995). *Algorithms for mixed continuous-discrete variable problems in structural optimisation*, Ph.D. Thesis, Civil and Environmental Engineering, The University of Iowa, Iowa City, IA, U.S.A.
- Huang, M.W. and Arora, J.S. (1997b). Optimal Design of Steel Structures using Standard Sections, *Structural Optimisation*, **14**, 24-35.
- Huang, Y. H. and Wang, S. T., (1973). Finite-Element Analysis of Concrete Slabs and its Implications for Rigid Pavement Design. *Highway Research Record*, **466**, 55–69
- Hudson, W. R. and Stelzer, C. F., (1968). A Direct Computer Solution for Slabs on Foundation, *Journal of the American Concrete Institute*, **65**, 188–201, March 1968.
- Hughes, T. J. R. and Cohen, M., (1978). The Heterosis Finite Element for Plate Bending, *Computers and Structures*, **9**, 445–450.
- Hughes, T. J. R., Taylor, R. L., and Kanoknukulchai, W., (1977). A Simple and Efficient Finite Element for Plate Bending, *International Journal for Numerical Methods in Engineering*, **11**, 1529–1543.
- Imam, I. F., (1996). Learning flexible concepts for the wind-bracing problem, *Computing in Civil Engineering* (New York), 859-866.
- Inducta Engineering, (Mar 2005). *SLABS 3.5 User's Manual*. Version 3.5.

- Isenberg, J., ed., (1991). *Finite Element Analysis of Reinforced Concrete Structures II*, (New York, New York), Committee on Finite Element Analysis of Reinforced Concrete Structures, American Society of Civil Engineers, June 1991.
- Jayachandran P., (2003). Design of Tall buildings: Preliminary design and optimisation, *International Conference on Tall Buildings and Industrial Structures*, Coimbatore, India, Jan 2003, Keynote Lecture.
- Jirsa, J. O., Sozen, M. A., and Siess, C. P., (1969). Pattern Loadings on Reinforced Concrete Floor Slabs, *ASCE Journal of the Structural Division*, **95**, 1117–1137, June 1969.
- Jofriet, J. C. and McNeice, G. M., (1971). Finite Element Analysis of Reinforced Concrete Slabs, *ASCE Journal of the Structural Division*, **97**, 785–806, March 1971.
- Juang, D.S. (1989), Effects of semi-rigid connections and P-delta forces on the optimum design of seismic steel frames, *Proc. of Structures Congress '89*, ASCE, 586-595.
- Kahn, L., (2004). *Reinforced Concrete Slab Systems*. New York: John Wiley & Sons, Inc., second edition.
- Kameshki, E.S. and Saka, M.P. (2001). Optimum design of nonlinear steel frames with semi-rigid connections using a genetic algorithm. *Computers and Structures*, **79**(17), 1593-1604.
- Khajehpour, S.; Grierson, D.E., (1999). Multi-criteria conceptual design using adaptive computing, *Proceedings of the Structures Congress 'Structural Engineering in the 21st century*, Apr 18-21, New Orleans, LA, USA, Sponsored by: ASCE, Reston, VA, USA, 586-589.
- Kicinger, R. and Arciszewski, T. (2004). Multi-objective evolutionary design of steel structures in tall buildings. *Proceedings of the AIAA 1st Intelligent Systems Technical Conference*, Chicago, IL, Sep 20-23, 2004, American Institute of Aeronautics and Astronautics Press, Reston, VA, AIAA 2004-6438.
- Kim, C.K., Kim, H.S., Hwang, J.S., Hong, S.M., (1998). Stiffness-based optimal design of tall steel frameworks subject to lateral loading. *Structural Optimisation*, **15**, 180-186.
- Kirsch, U. (1989b). Optimal topologies of truss structures. *Appl. Mech. Rev.*, **42**, 223-239.
- Kohno, M. and Collins, K.R. (2000a). *Merging life-cycle cost analysis and performance-based design of Steel buildings*. Research Report UMCEE 00-06, University of Michigan, Ann Arbor, MI.
- Kohno, M. and Collins, K.R. (2000b). Merging life-cycle cost analysis and performance-based design. *8th ASCE Specialty conference on Probabilistic Mechanics and Structural Reliability*, Kareem, et. al., Ed., ASCE, Jul 24-26, Paper No. PMC2000-149, 6 pages.
- Kozak, J. (1991). *Steel-concrete structures for multi storey buildings*. Amsterdam; New York: New York, NY: Elsevier; Elsevier Science Pub. Co.
- Kroll, E. (2001). *Innovative conceptual design: theory and application of parameter analysis*. Cambridge University Press.
- Kunz, John; Clayton, Mark, Fischer, Martin, (1994). Circle Integration, *1st ASCE Conference on Computing in Civil Engineering*, Jun 20-22, Washington, DC, USA, 55-62.

- Larsen, O.P. (2003). *Conceptual structural design: bridging the gap between architects and engineers*. London: Thomas Telford.
- Law, F. M., (1971). Design of Irregular Shaped Two-Way Slabs, *Journal of the American Concrete Institute*, **68**, 844–847, November 1971.
- Lencus A, Querin O.M., Steven G.P., Xie Y.M., (2002). Aircraft wing design automation with ESO and GESO, *International Journal of Vehicle Design*, **28**(4).
- Lencus, A., Querin O.M., Steven, G.P. and Xie, Y.M. (1999). Group ESO with Morphing, *1st ASMO UK/ISSMO Conference on Engineering Design Optimisation*, July 8-9, Ilkley, West Yorkshire.
- Lencus, A., Querin O.M., Steven, G.P. and Xie, Y.M. (1999). *Modifications to the Evolutionary Structural Optimisation (ESO) Method to support configurational optimisation*. 06-EVM1-5.
- Lewi´nski, P. M. and Wojew´odzki, W., (1991). Integrated Finite Element Model for Reinforced Concrete Slabs, *ASCE Journal of the Structural Division*, **117**, 1017–1038, April 1991.
- Li Q., Steven G.P., Xie Y.M., (1999). On equivalence between stress criterion and stiffness criterion in evolutionary structural optimisation, *Structural Optimisation* **18**, 67-73, Springer-Verlag.
- Li Q., Steven G.P., Xie Y.M., (2001). Evolutionary thickness design with stiffness maximization and stress minimization criteria, *International Journal for Numerical Methods in Engineering*, **52**, 979-995.
- Li, T.Q., Nethercot, D.A. and Tizani, W.M.K., (1997). Integrated design system for semi-rigidly connected steel frames. *Journal of Advances in Structural Engineering*, **1**(1), 47-61.
- Liang, Q. Q. (2001). *Performance-based Optimisation Method for Structural Topology and Shape Design*. Ph.D. Thesis, Victoria University of Technology, Australia.
- Liebman, J.S., Khachaturian, N. and Chanaratna, V. (1981). Discrete Structural Optimisation, *Journal of Structural Engineering*, ASCE, **107**(ST11), 2177-2197.
- Liepins, A. A. and Bell, G. R., (1992). *How to Avoid Common Pitfalls in Structural Analysis by Computer*. ASCE International Convention Exposition.
- Liew R., Balendra T., Chen W.F., (1999). *Multistorey Frame Structures*, Structural Engineering Handbook, CRC Press LLC.
- Logan, D. L., (2002). *A First Course In The Finite Element Method*. Pacific Grove, CA: Brooks/Cole, third ed.
- Lourenc¸o, P. B. and Figueiras, J. A., (1995). Solution for the Design of Reinforced Concrete Plates and Shells, *ASCE Journal of the Structural Division*, **121**, 815–823, May 1995.
- MacGregor, J. G., (1997). *Reinforced Concrete: Mechanics and Design*. Upper Saddle River, New Jersey: Prentice Hall, third ed.
- Machaly, E.S.B., (1986) Optimum Weight Analysis of Steel Frames with Semi-Rigid Connections, *Computers and Structures*, **23**(4), 565-574.

- Maher, Mary Lou; Balachandran, Bala, (1994). Multi-media approach to case-based structural design, *ASCE Journal of Computing in Civil Engineering*, **8**(3), Jul, 359-376.
- Mainstone, R. (2001). *Developments in structural form*. 2nd ed. Oxford: Architectural Press.
- Malhotra, V. M., ed., (1970). *Impact of Computers on the Practice of Structural Engineering in Concrete*. Detroit, Michigan: American Concrete Institute, SP-33.
- Manickrajah, D. (1998). *Optimum Design of Structures with Stability Constraints using the Evolutionary Optimisation Method*. Ph.D. Thesis, Victoria University of Technology, Australia.
- Marckmann G., Bettess P., Peseux B., Self designing structures: a new evolutionary rule for thickness distribution in 2D problems, *Communications in Numerical Methods in Engineering*, **18**(10), 743-755.
- Maute, K; Ramm, E., (1995). Adaptive Topology Optimisation, *Structural Optimisation*, **10**(2), Oct, Springer Verlag GmbH & Company KG, Berlin, Germany, 100-112.
- May, S.A. and Balling, R.J. (1991), Strategies which permit multiple discrete section properties per member in 3D Frameworks. In: *Electronic Computation, Proceedings of the tenth conference, O. Ural and T-L. Wang, Eds.*, American Society of Civil Engineers, 1801 Alexander Bell Dr., Reston, VA, 189-196
- May, S.A. and Balling, R.J. (1992). A filtered simulated annealing strategy for discrete optimisation of 3D steel frameworks, *Structural Optimisation*, **4**, 142-148.
- McCormac, J. C., (2001). *Design of Reinforced Concrete*. New York: John Wiley & Sons, Inc., fifth ed.,
- Melosh, R. J., (1963). Basis of Derivation of Matrices for the Direct Stiffness Method, *Journal of the American Institute of Aeronautics and Astronautics*, **1**, 1631–1637.
- Meyer, C. and Okamura, H., eds., (1985). *Finite Element Analysis of Reinforced Concrete Structures*, (New York), Committee on Finite Element Analysis of Reinforced Concrete Structures, American Society of Civil Engineers, May 1985.
- Mijar A. R., Swan C.C., Arora J.S., Kosaka I., (1998). Continuum Topology Optimisation for Concept Design of Frame Bracing Systems, *Journal of Structural Engineering* – May 1998, 541 – 550.
- Mohr, G. A., (1979). Elastic and Plastic Predictions of Slab Reinforcement Requirements, *Institute of Engineers, Australia, Civil Engineering Transactions*, **CE 21**(1), 16–20.
- Moore, C.J; Miles, J.C., (1996). Improving the consideration of cost during conceptual design, *Proceedings of the IEEE Colloquium on Manufacturing "Progress in Design"*, Jun 3, (121), London, UK, IEE, Stevenage, England, 3/1-3/4.
- Nguyen, D.Q. (2001). *Extended Evolutionary Structural Optimisation Method for Multi-storey Buildings*. Master's Thesis, Victoria University of Technology, Australia.
- Nilson, A. H., ed., (1982). *Finite Element Analysis of Reinforced Concrete*. New York, New York: American Society of Civil Engineers,. Committee on Finite Element Analysis of Reinforced Concrete Structures.

- Ohmori, H., Futai, H., Iijima, T., Muto, A., Hasegawa, Y. (2005). Application of computational morphogenesis to structural design. *Proceeding of Computational Science Symposium, Information Processing Society of Japan*, Oct 11-13, 2005, (11).
- Park, H.S. and Kwon, J.H. (2003). Optimal drift design model for multi-storey buildings subjected to dynamic lateral forces. *The structural design of tall and special buildings*, **12**, 317-333.
- Park, Kwang-Wook; Grierson, D.E.; (1999). Pareto-Optimal conceptual design of the structural layouts of buildings using a multi-criteria genetic algorithm, *Computer-Aided Civil and Infrastructure Engineering*, **14**(3), May, Blackwell Publ. Inc, 163-170.
- Pfaffinger, D. D., (1972). Column-Plate Interaction in Flat Slab Structures, *ASCE Journal of the Structural Division*, **98**, 307–326, January.
- Phuvoravan, K. and Sotelino, E. D., (2005). Nonlinear Finite Element Analysis for Reinforced Concrete Slabs, *ASCE Journal of the Structural Division*, **131**, 643–649, April 2005.
Portland Cement Association, Shokie, Illinois, (2000). *Concrete Structural Floor Systems and More...*,. CD-ROM Version 1.
- Price, W. A., ed., (1987). *Computer Applications in Concrete Technology*, (Farmington Hills, Michigan), ACI Committee 118 - Use of Computers, American Concrete Institute, SP-98.
- Pullman, T., Skolicki, Z., Freischlad, M., Arciszewski, T., Jong, K.D., Schnellenbach-Held, M. (2003). Structural Design of Reinforced Concrete Tall Buildings: Evolutionary Computation Approach using Fuzzy Sets. *Journal of Engineering with Computers*, **16**, 275-286.
- Querin, O.M. (1997). *Evolutionary Structural Optimisation: Stress based formulation and Implementation*, PhD Thesis, Department of Aeronautical Engineering, University of Sydney, Australia.
- Raisanen, David, e. a., (1987). *A CASE Project Study of Finite Element Analysis of Concrete Flat Slabs*, U.S. Army Engineer Waterways Experiment Station - Technical Report ITL-87-2.
- RAM International, (2003). Carlsbad, CA, *RAM Concept*, Version 1.0.
- Rangan, B.V., Warner R.F. (1996). *Large Concrete Buildings*. Harlow: Longman.
- Reddy, R. Ramesh; Gupta, Ashok; Singh, R.P., (1993). Expert system for optimum design of concrete structures, *Journal of computing in civil engineering*, **7**(2), Apr, 146-161.
- Reese, R.C., MacGregor, J.G., Lyse, Inge. (1978). *Structural design of tall concrete and masonry buildings*. Council on Tall Buildings and Urban Habitat. New York : American Society of Civil Engineers.
- Rivard, H. and Fenves, S.J. (2000). A representation for conceptual design of buildings. *Journal of Computing in civil engineering*, ASCE, **1**4(3), 151-159.
- Rosenbluth, E. (1976). Towards Optimum Design through Building Codes. *Journal of the Structural Division*, ASCE, **102** (ST3), 591-607.
- Ryu, Y.S., Haririan, M., Wu, C.C. and Arora, J.S. (1985). Structural design sensitivity analysis of nonlinear response.*Computers and Structures*, Pergamon Press, Ltd., **21**(1/2), 245-255.
- Saleh, L. R. R., (1987). *Finite Element Analysis of Shear in Reinforced Concrete Flat Plates*,

Master's thesis, Georgia Institute of Technology.

- Sause, R., Martini, K. and Powell, G.H. (1992). Object-oriented approaches for integrated engineering design systems. *Journal of Computing in Civil Engineering*, ASCE, **6**(3), 248-265.
- Sawko, F. and Cope, R. J., (1969). The Analysis of Skew Bridge Decks - a New Finite Element Approach, *The Structural Engineer*, **47**, 215–224, June 1969.
- Schinler, D. (2001). *Design of partially and fully-restrained steel frames using an object-oriented evolutionary algorithm*, MS Thesis, Marquette University, Milwaukee, WI.
- Severn, R. T. and Taylor, P. R., (1966). The Finite Element Method for Flexure of Slabs when Stress Distributions are Assumed, *Proceedings of the Institution of Civil Engineers*, **34**, 153–170.
- Simoes, L.M.C. (1996) Optimisation of frames with semi-rigid connections, *Computers and Structures*, **60**(4), 531-539.
- Smith B., Coull A., (1991). *Tall Building Structures: Analysis and Design*, John Wiley & Sons, Inc.
- Smith, E. T. and Faulkes, K. A., (1976). Flexural Properties of Flat Plate Floors, *Institute of Engineers, Australia, Civil Engineering Transactions*, **CE 18**(2), 140–145.
- Steven, G.P. and Xie, Y.M. (1993). A Simple evolutionary procedure for structural optimisation, *Computers and Structures*, **49**(5), 885-896.
- Tabatabai, S.M.R. (1996). *Finite Element Based Elasto-Plastic Optimum Reinforcement Dimensioning of Spatial Concrete Panel Structures*. Ph.D. Thesis, Institute of Structural Engineering, Swiss Federal Institute of Technology, Zurich, Switzerland.
- Taranath B., (1998). *Steel, Concrete and Composite Design Of Tall Buildings*, McGraw Hill.
- Timoshenko, S. and Woinowsky-Krieger, S., (1959). *Theory of Plates And Shells*. New York: McGraw –Hill Book Company, second ed..
- Topping, B.H.V. (1992). Mathematical programming techniques for shape optimisation of skeletal structures. In: *Shape and Layout Optimisation of Structural Systems and Optimality Criteria methods*, Rozvany, G.I.N. (Ed.), 349-375, Springer.
- van de Lindt, J.W. and Niedzwecki, J.M. (2000). A time variant approach to performance-based engineering. *Advanced Technology in Structural Engineering – Structures Congress 2000*, Elgaaly, M., Ed., ASCE, May 8-10.
- Vanderbilt, D. M., (1979). Equivalent Frame Analysis for Lateral Loads, *ASCE Journal of the Structural Division*, **105**, 1981–1998, October 1979.
- Vanderplaats, G.N. (1981). *Structural optimisation: past, present and future*. AIAA Paper No. 81-0897, AIAA 1981 Annual Meeting and Technical Display "Frontiers of Achievement", California, USA.
- Warner R., Rangan B., Hall A., (1989). *Reinforced Concrete*. 3rd Edition, Longman Cheshire.
- Warner R., Rangan B., Hall A., Faulkes K., (1999). *Concrete Structures*, Longman.
- Warner, R. (1989). *Reinforced Concrete*. 3rd Edition, Melbourne : Longman Cheshire.

- Wen, Y.K. and Kang, Y.J. (2001a). Minimum building life-cycle cost design criteria. I: Methodology. *Journal of Structural Engineering*, ASCE, **127**(3), 330-337.
- Wen, Y.K. and Kang, Y.J. (2001a). Minimum building life-cycle cost design criteria. II: Applications. *Journal of Structural Engineering*, ASCE, **127**(3), 337-346.
- Willam, K. and Tanabe, T., eds., (2001). *Finite Element Analysis of Reinforced Concrete Structures*. Farmington Hills, Michigan: American Concrete Institute, SP-205.
- Wood, R. H., (1968). The Reinforcement of Slabs in Accordance with a Pre-Determined Field of Moments, *Concrete*, **2**, 69–76, February 1968.
- Xie, Y.M. and Steven, G.P. (1996). *Evolutionary Structural Optimisation*. Springer-Verlag, Berlin.
- Xu, L., Sherbourne, A.N. and Grierson, D.E. (1995). Optimal cost design of semi-rigid, low-rise industrial frames. *Engineering Journal*, (Third Quarter), 87-97.
- Yang, X. (2002). *Evolutionary Methods for Topology Optimisation of Continuum Structures: Static and Dynamic Problems*. Ph.D. Thesis, Victoria University of Technology, Australia.
- Yau, N.J.; Melin, J.W.; Garret, J.H.; Kim, S., (1991). Integrating the process of design, scheduling and cost estimating within an object-oriented environment, *ASCE, Construction Div; American Institute of Mining Engineers; American Arbitration Assoc, Preparing for construction in the 21str century construction congress*, Apr 13-16, New York, N.Y., USA, 342-347.
- Zalka, K.A. (2000). *Global structural analysis of buildings*. London ; New York : E & F Spon
- Zienkiewicz, O. C. and Cheung, Y. K., (1964). The Finite Element Method for Analysis of Elastic Isotropic and Orthotropic Slabs, *Institution of Civil Engineers - Proceedings*, **28**, 471–488, August 1964.
- Zou, X.K., and Chan, C.M. (2005). Optimal resizing technique for seismic drift design of concrete buildings subjected to response spectrum and time history loadings. *Computers and Structures*, **83**, pp 1689-1704.
- Zwillinger, D. e. a., ed., (2000). *Standard Mathematical Tables and Formulae*. Washington, D.C.: Chapman & Hall / CRC Press LLC, 31 ed.